Oklahoma Geological Survey
Charles J. Mankin, *Director*

Circular 108
ISSN 0078-4397

Finding and Producing Cherokee Reservoirs in the Southern Midcontinent, 2002 Symposium

DAN T. BOYD, *Editor*

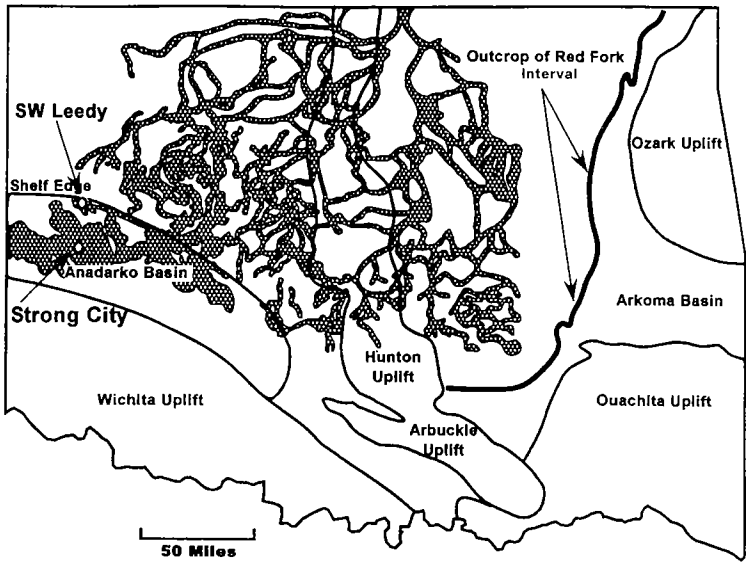

Proceedings of a symposium held May 14–15, 2002, in Oklahoma City, Oklahoma.

Co-sponsored by:

Oklahoma Geological Survey

and

National Petroleum Technology Office,
U.S. Department of Energy

The University of Oklahoma
Norman

2002

OKLAHOMA GEOLOGICAL SURVEY

CHARLES J. MANKIN, *Director*

SURVEY STAFF

JAMES H. ANDERSON, *Manager of Cartography*
RICHARD D. ANDREWS, *Geologist IV*
LARRY T. AUSTIN, *Core and Sample Library Assistant*
BETTY D. BELLIS, *Word-Processing Operator II / Technical Typist*
MITZI G. BLACKMON, *Clerk-Typist I*
DAN T. BOYD, *Geologist III*
JERLENE A. BRIGHT, *Technical Project Specialist*
RAYMON L. BROWN, *Geophysicist III*
RUTH E. BROWN, *Assistant to the Director*
JOCK A. CAMPBELL, *Geologist IV*
BRIAN J. CARDOTT, *Geologist IV*
JAMES R. CHAPLIN, *Geologist IV*
JANISE L. COLEMAN, *Office Assistant IV*
CHRISTIE L. COOPER, *Managing Editor*
TAMMIE K. CREEL-WILLIAMS, *Secretary II*
JIMMY G. DENTON, *Manager, Tulsa Core Library*
CHARLES R. DYER III, *Drilling Technician*
WALTER C. ESRY, *Manager, Core and Sample Library*
ROBERT O. FAY, *Geologist IV*
AMIE R. FRIEND, *Research Specialist I*
PRISCILLA A. JOHNSON, *Office Assistant IV*
JAMES W. KING, *Research Specialist II*
STANLEY T. KRUKOWSKI, *Geologist III*
EUGENE V. KULLMANN, *X-Ray / Imaging Technician*
JAMES E. LAWSON, JR., *Chief Geophysicist*
LAURIE A. LOLLIS, *Cartographic Technician II*
KENNETH V. LUZA, *Geologist IV*
MICHAEL J. MERCER, *Manager, Log Library*
GALEN W. MILLER, *Research Associate*
RICHARD G. MURRAY, *Copy Center Operator*
SUE M. PALMER, *Office Assistant II*
DAVID O. PENNINGTON, *Operations Assistant II*
CONNIE G. SMITH, *Promotion and Information Specialist*
PAUL E. SMITH, *Supervisor, Offset Press Copy Center*
G. RUSSELL STANDRIDGE, *Information Tech Analyst I*
THOMAS M. STANLEY, *Geologist III*
LLOYD N. START, *Assistant Drilling Technician*
JOYCE A. STIEHLER, *Chief Clerk*
MICHELLE J. SUMMERS, *Technical Project Coordinator*
NEIL H. SUNESON, *Assistant Director, Geological Programs*
JANE L. WEBER, *Publication and Database Coordinator*

Cover Picture

Tectonic provinces of Oklahoma and distribution of Red Fork Sandstone (from p. 120 of this volume).

This publication, printed by the Oklahoma Geological Survey, is issued by the Oklahoma Geological Survey as authorized by Title 70, Oklahoma Statutes, 1981, Sections 231–238. 1,050 copies have been prepared for distribution at a cost of $9,940 to the taxpayers of the State of Oklahoma. Copies have been deposited with the Publications Clearinghouse of the Oklahoma Department of Libraries.

PREFACE

A primary task of both the Oklahoma Geological Survey (OGS) and the U.S. Department of Energy, National Petroleum Technology Office (DOE–NPTO) involves assisting operators in their efforts to find and produce oil and gas in the southern Midcontinent. Towards this end, a series of two-day technology transfer symposia have been instituted, of which this is the 15th. Held on May 14–15, 2002, in Oklahoma City, Oklahoma, this year's topic was "Finding and Producing Cherokee Reservoirs in the Southern Midcontinent." It was designed to aid operators in identifying practical techniques and technology to both find additional fields, as well as efficiently produce the accumulations that already have been found in this prolific group of related geological formations. Efforts to review pitfalls and failed techniques, as well as those that succeed were one of the workshop's main goals.

This symposium was attended by a diverse group of geoscientists and other petroleum professionals who had the opportunity to see 20 oral and 10 poster presentations. These addressed almost every aspect of finding and producing Cherokee reservoirs, from the exploration phase, through development drilling, through secondary recovery, and finally enhanced recovery. They included stratigraphic correlation, environment of deposition determination, log interpretation, well completion-stimulation, and seismic stratigraphy, with an equal split between those that were field specific and regional. This meeting allowed operators to benefit from the experience of others, and provided an opportunity for smaller companies to see how their activity fits into the larger, regional picture. Because the technical challenges associated with this prolific group of related geological formations are often the same, successful practices in one area often succeed elsewhere. Technical interaction is critical to developing new insights into cost-effectively identifying and developing hydrocarbons in this complex set of reservoirs. Such cooperation is especially important in a business environment that has made it increasingly difficult for many operators to maintain long-term profitably.

Sandstones, granite washes, and coals of Cherokee age are among the most prolific petroleum reservoirs in the southern Midcontinent, and continue to rank as one of the area's most important exploration targets. They produce across the bulk of the region and are responsible in Oklahoma, where most Cherokee production is found, for approximately 15% of the gas and more than 50% of the oil that has been identified. The Bartlesville Sandstone, a prominent member of the Cherokee Group, accounts for most of the oil initially discovered in the State, and actually provided much of the impetus towards the granting of statehood in 1907.

Previous symposia have addressed other topics of major interest to the local petroleum industry. These are documented in OGS circulars and include: Anadarko Basin (Circular 90), Late Cambrian–Ordovician Geology of the Southern Midcontinent (Circular 92), Source Rocks in the Southern Midcontinent (Circular 93), Petroleum Reservoir Geology in the Southern Midcontinent (Circular 95), Structural Styles in the Southern Midcontinent (Circular 97), Fluvial-Dominated Deltaic Reservoirs in the Southern Midcontinent (Circular 98), Simpson and Viola Groups in the Southern Midcontinent (Circular 99), Ames Structure in Northwest Oklahoma and Similar Features: Origin and Petroleum Production (Circular 100), Platform Carbonates in the Southern Midcontinent (Circular 101), Marine Clastics in the Southern Midcontinent (Circular 103), Pennsylvanian and Permian Geology and Petroleum in the Southern Midcontinent (Circular 104), Silurian, Devonian, and Mississippian Geology and Petroleum in the Southern Midcontinent (Circular 105), Petroleum Systems of Sedimentary Basins in the Southern Midcontinent (Circular 106), and Revisiting Old and Assessing New Petroleum Plays in the Southern Midcontinent (Circular 107).

Persons involved in the organization and planning of this symposium include: Dan Boyd and Charles Mankin of the OGS and Bill Lawson of DOE–NPTO. Other contributors include: Michelle Summers, meeting coordinator; Neil Suneson, poster chair; Tammie Creel, registration chair; and Connie Smith, publicity chair, all from the OGS. Thanks are extended to OGS managing editor Christie Cooper, to Thomas W. Henry (Westminster, Colorado) for technical editing of this volume, and to Sandra Rush (Denver, Colorado) for layout and production. Special appreciation also is due the many authors that contributed to this symposium, who ultimately are responsible for the success of these programs.

DAN T. BOYD
General Chairman

CONTENTS

Red Fork Production in the Cherokita and Wakita Trends, North-Central Oklahoma—Fluvial Incised-Channel or Marine-Shoreline System?

Richard D. Andrews
Oklahoma Geological Survey
Norman, Oklahoma

ABSTRACT.—The Cherokita and Wakita Trends produce oil and gas from sandstone reservoirs of the middle Cherokee Red Fork sandstone. The two closely spaced trends are roughly parallel to each other, extend about 50 mi east–west across northern Grant and Alfalfa Counties in north-central Oklahoma, and then continue another 15–20 mi southwest into the Anadarko Basin in southern Woods and Major Counties.

The Cherokita and Wakita Trends were developed largely during the late 1950s and 1960s. The Cherokita Trend has produced ~23.7 MMBO (million barrels of oil) and 149 BCFG (billion cubic feet of gas), and the Wakita Trend to the north has produced ~10.2 MMBO and 152 BCFG.

Much speculation has existed about the depositional origin of sandstone in these trends. Some geologists interpreted the elongate sandstone trends to be shoreline deposits formed along the northern edge of the "Enid Embayment" of Swanson (1967) and Withrow (1968) as a result of eustatic sea-level changes during the time of Red Fork sandstone deposition. In contrast, the current investigation, as well as the opinion of most geologists, holds that the trends are erosional (incised) valleys that formed in response to lowering of eustatic sea level (falling stage). The predominant sandstone facies is fluvial—probably longitudinal bars, although estuarine deposits are also believed present. This conclusion is based on the evaluation of many well logs, regional mapping, literature review, core examinations, and personal correspondence.

The vast majority of well logs penetrating the Red Fork sandstone in the Cherokita and Wakita Trends show sandstone with a sharp basal contact with shale—and blocky to fining-upward textural profile typical of fluvial deposits. Basal scour has eroded below the underlying Inola Limestone marker bed in many places, and the distal extent of both trends terminate to the southwest in marine delta-front deposits characterized by a coarsening-upward textural profile as best seen on gamma-ray and resistivity logs. This latter facies is generally much thicker than the terrestrial channel deposits because accommodation space farther basinward is greater.

The implication of making a correct interpretation of the depositional origin of these sandstones is important in determining the logical extension of these and other similar trends. As in other parts of Oklahoma, the Red Fork has a tendency to form long, incised-channel complexes that terminate in a low-stand delta. The Wakita and Cherokita Trends are no exceptions, and, regionally, they too pass basinward into delta-front sequences that are exceptional producers of natural gas.

LOCATION

Significant quantities of oil and gas are produced from the middle Cherokee Red Fork Sandstone (Fig. 1) in the Cherokita and Wakita Trends of north-central Oklahoma (Fig. 2). The two trends form broadly arcuate bands that are roughly parallel, separated 2–6 mi from one another, extend roughly 50 mi in an east–west direction across northern Grant and Alfalfa Counties, and continue another 15–20 mi southwest into the Anadarko Basin in southern Woods and Major Counties. Both trends occupy slightly more than 30,000 acres. Andrews (1997), with the assistance of others, mapped the Cherokita and Wakita Trends separately as part of a fluvial-dominated deltaic-reservoir study.

Andrews, R. D., 2002, Red Fork production in the Cherokita and Wakita trends, north-central Oklahoma—fluvial incised-channel or marine-shoreline system?, *in* Boyd, D. T. (ed.), Finding and producing Cherokee reservoirs in the southern Midcontinent, 2002 symposium: Oklahoma Geological Survey Circular 108, p. 1–10.

	SUBSURFACE NAMES
	Oswego limestone
Cherokee Group	Prue sandstone interval (shale)
	Verdigris Limestone
	Skinner sandstone interval (mostly shale)
	Pink limestone
	Red Fork sandstone interval
	Inola Limestone
	Bartlesville interval (shale)
	Mississippian limestone (locally "chat")

Figure 1. Chart showing stratigraphy of principal Cherokee Group rock units in the Cherokita and Wakita Trend areas, north-central Oklahoma. See Figure 2 for location.

PRODUCTION

The Cherokita and Wakita Trends were discovered in the mid-1950s and largely developed during the late 1950s and 1960s. The Cherokita Trend has produced ~23.7 MMBO (million barrels of oil) and 149 BCFG (billion cubic feet of gas), and the more gas-prone Wakita Trend to the north has produced ~10.2 MMBO and 152 BCFG. On a production map (Fig. 2), the Cherokita and Wakita Trends look like ribbons of oil and gas wells with relatively few offset wells immediately north or south of each trend. Oil production dominates on the east and west limbs of both trends, and gas and oil production dominate in the central parts of each trend. The reason for this is not certain; however, as both trends turn south into the basin, the thermal maturity of the source sediments increases with depth, and production largely consists of gas.

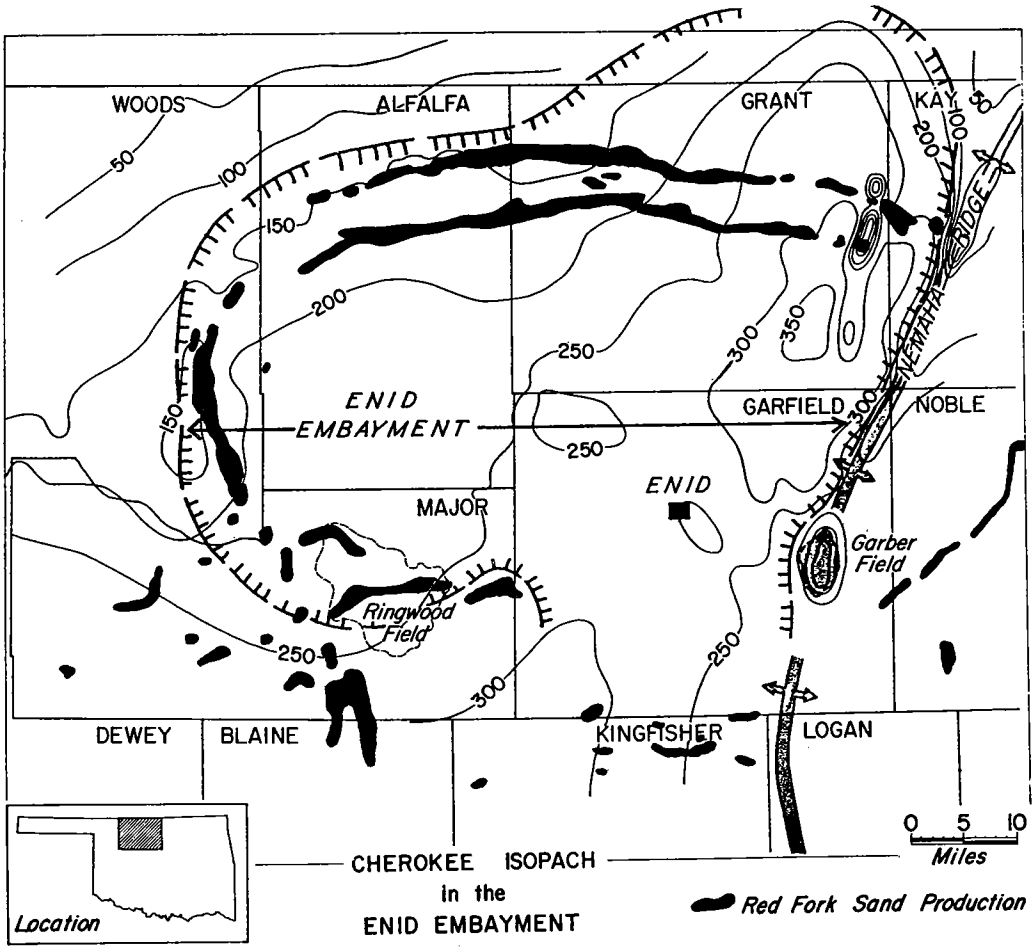

Figure 2. Isopach map showing configuration of the "Enid Embayment" during time of deposition of Cherokee Group. Contour interval = 50 ft. From Withrow (1968, fig. 3).

STRATIGRAPHY

The Red Fork sandstone is the lowest sandstone of the Cherokee Group (Fig. 1) in the study area. The older Bartlesville sandstone is absent in this area, although shale underlying the Inola Limestone is presumed to be in part, or predominantly equivalent to the Bartlesville. Likewise, the younger Skinner and Prue intervals are also present but consist mostly of shale.

Mississippian carbonate "basement" sediments underlie the lower Cherokee shale (i.e., Bartlesville or older clastic sediments). Locally, the Mississippian is productive when "chat" develops on the upper, eroded, unconformable surface. The Mississippian is very near the lower boundary of the Red Fork along the western extent of the Cherokita and Wakita Trends, where less than 20 ft of shale separate the two units. More than 100 ft of shale, however, separate the Red Fork from the Mississippian in the eastern part of the trends.

Locally, the Inola Limestone, which underlies the Red Fork interval (Fig. 1), is absent either because it was never deposited (in areas where the Mississippian closely underlies the Red Fork) or is absent due to erosion. Fluvial scouring in incised valleys during periods of falling sea level caused the latter.

METHODS OF INVESTIGATION

The interpretations resulting from this study are based on the evaluation of many well logs, literature review, personal correspondence, core examinations, and regional mapping. The vast majority of well logs penetrating the Red Fork sandstone in the Cherokita and Wakita Trends show sandstone having a sharp basal contact with shale and blocky to fining-upward textural profile typical of fluvial deposits. Basal scour has eroded below the underlying Inola Limestone marker bed in many places, and the distal extent of both trends terminate to the southwest in marine delta-front deposits characterized by a coarsening-upward textural profile as seen on most log traces. This later facies is generally much thicker than the terrestrial channel deposits because accommodation space farther basinward is greater.

LITERATURE REVIEW

Several investigations regarding all or parts of the Cherokita and Wakita Trends are present in the literature. The first major interpretation comes from Withrow (1968), who mapped the subsurface Cherokee Group in north-central Oklahoma and engrained the term "Enid Embayment," as used previously by Swanson (1967). Withrow's marine "Enid Embayment" was characterized by a thick sequence of sediments encompassing the entire Cherokee Group west of the Nemaha Uplift and south of the Cherokita Trend (Fig. 2). The embayment was used to justify the existence of a marine environment extending basinward to the south during Red Fork time. Withrow also constructed short cross sections across parts of the trends and interpreted the depositional environment of the Red Fork as off shore marine bars. However, he interpreted the north–south extension of the trends in Woods County farther to the southwest (Oakdale Field area) as channels. In both areas, well logs showed sandstone sequences with a sharp basal contact (with shale) and fining-upward textural profile. One of Withrow's overwhelming considerations for determining depositional environments appeared to be the parallelism of the two east–west trends along the northern part of the "Enid Embayment." Despite contradicting evidence, this interpretation is still engrained in people's minds today.

In 1981, Glass studied the area encompassing both trends as part of his Oklahoma State University M.S. thesis. He interpreted cores and well logs and concluded that the trends consisted of channel deposits. A sequence of maps prepared by Glass showed the evolution of these channels. One of these maps is shown as Figure 3.

O'Reilly (1986) completed another study encompassing the same area as part of her University of Tulsa M.S. thesis. O'Reilly refuted the conclusions of Glass (1981) and concluded that the principal depositional environment of both trends was a transgressive barrier-bar system.

Subsequently, Al-Shaieb and others (1989) interpreted the trends to be alluvial-deltaic channels that were backfilled in response to subsequent transgressive events. A regional study updated by Masera (1994) also mapped the trends as channels. Andrews and others (1997) interpreted the trends at that time to be incised channels.

REGIONAL TREND ANALYSIS

The Cherokee isopach map of Withrow (1968) (Fig. 2) is not entirely relevant to depositional trends of the Red Fork, specifically considering basinward dip. In actuality, the Anadarko Shelf immediately west of the Nemaha Uplift sloped to the west or normal to the Nemaha Uplift during the time of deposition of the Red Fork. This is better illustrated by examining the isopach map of just the Red Fork interval as shown in Figure 4. This map shows that the Red Fork interval thickens immediately west of the Nemaha Uplift and then is very consistent in thickness farther west across Grant and Alfalfa Counties. The Red Fork interval begins to thicken appreciably to the southwest through most of Major County and reaches a hinge line slightly farther south in Blaine County.

FACIES ANALYSIS AND LOG CHARACTER: DETAILED CROSS SECTIONS

Three detailed stratigraphic cross sections were constructed for this paper to show different facies of the Red Fork interval across both trends and in a basinward direction. Specific Red Fork facies include marine bar (transgressive and/or delta front), open shelf, channel bar (probably longitudinal), abandoned channel, and channel margin.

Cross section A–A′ (Fig. 5) is farthest east and is oriented north to south along R. 4 W. The first well, at location 1, lies just north of the Wakita Trend and is out-

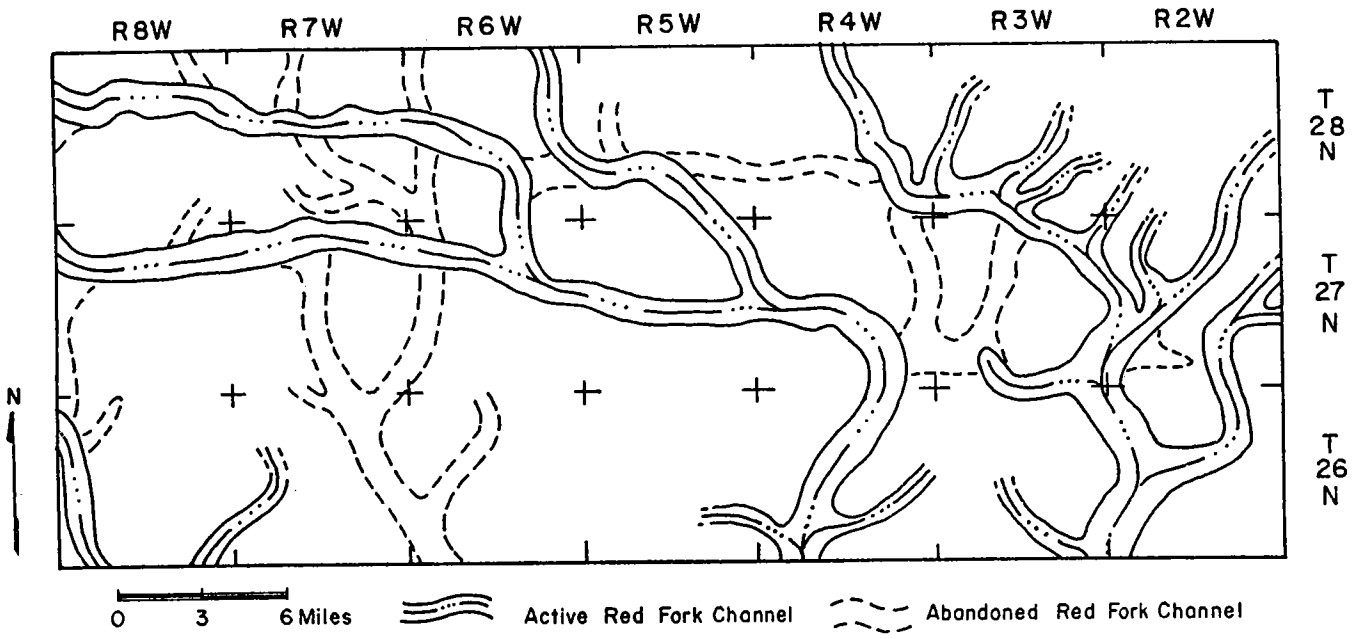

Figure 3. Diagram showing stage 1 in the development of Red Fork channel system. From Glass (1981, fig. 23a).

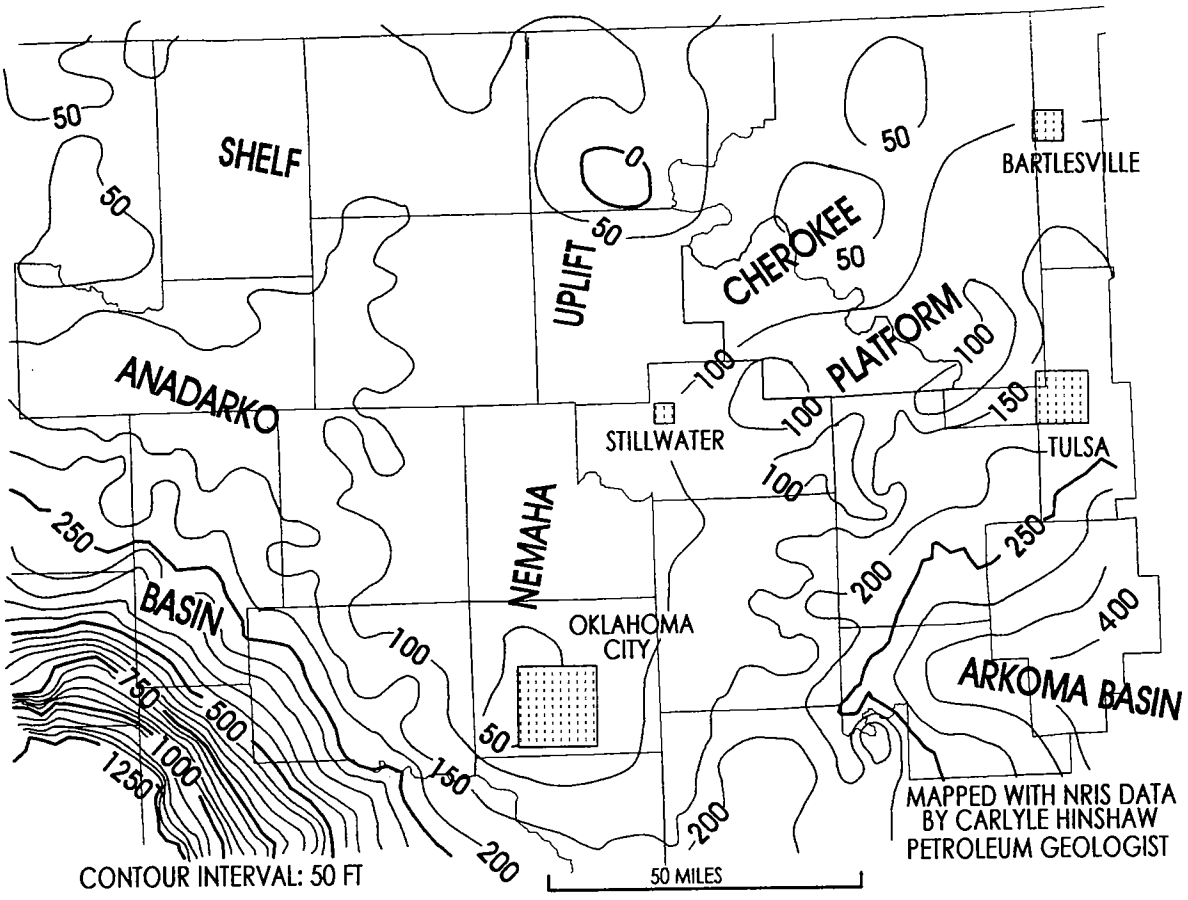

Figure 4. Regional isopach map of thickness of the interval from the top of the Pink lime to the top of the Inola Limestone (Red Fork interval plus the Pink lime), Oklahoma. Contour interval = 50 ft. From Andrews (1997, fig. 15).

side the limits of the field and channel. In this well, the log shows the Red Fork to consist entirely of shale and is believed to represent open-marine conditions (possibly pro-delta). Note that both the Pink and Inola Limestone are absent in this well—probably due to nondeposition. In well 2 (Fig. 5), The Red Fork sandstone is present in two benches that comprise the reservoir. The sandstone interval has an overall fining-upward textural profile and a sharp basal contact with shale as interpreted from resistivity, gamma-ray, and caliper logs. The Inola Limestone is believed to underlie the Red Fork, and immediately beneath the Inola may be Bartlesville shale or possibly pre-Cherokee limy sediments (Atoka?). Well 3 (Fig. 5) is in the center of the Cherokee Trend and has almost 60 ft of sandstone. The sandstone interval has a blocky textural profile with a sharp lower and upper contact that is consistent with a longitudinal bar deposited in an incised valley. The limy zone of the Inola is truncated by apparent downcutting of at least 25 ft, which is also indicative of erosional scour in a channel environment. Marine bars normally do not have erosional bases such as this. Half a mile to the south, in well 4, the Red Fork sandstone thins to less than 30 ft. Nonetheless, the log shape shows a sharp basal contact and a mostly blocky vertical profile in the lower half of the sandstone section. This deposit appears to lie on a valley bench along the southern edge of the channel because the Inola is not truncated as in well 3. The last well in cross section A–A′ at location 5 (Fig. 5) is about 5 mi south of the Cherokita Trend. There, the Red Fork consists mostly of shale with two sandy zones having a distinct coarsening-upward textural profile as seen best on the resistivity log trace. These strata may represent blanket marine deposits of sand and clay or possibly a distal delta-front.

Cross section B–B′ (Fig. 6) is also a north–south cross section in R. 10 W. The section begins with a well in the Wakita Trend having about 22 ft of sandstone. The sandstone has a very sharp basal contact with shale and a fining-upward textural profile as interpreted from the resistivity and gamma-ray logs. This textural profile is very indicative of a fluvial channel deposit in which abandonment occurred gradually. The SP-log trace has a simple harmonic curvature over the sandstone interval and is not a diagnostic indicator of facies. Well 2 (Fig. 6) is located about 5 mi south of the first well and lies between the Wakita and Cherokita Trends. The well log shows the Red Fork interval consisting of two coarsening-upward sandstone zones very similar to that seen 35 mi east in well 5, cross section A–A′ (Fig. 5). Again, the strata interpreted in well 2 (Fig. 6) are believed to be either distal delta-front deposits or blanket marine deposits. Well 3 (Fig. 6) is in the northern part of the Cherokita Trend and has an unusual log signature that is interpreted to represent strata consisting of finely interbedded shale and very fine grained sandstone common to abandoned-channel facies. This interpretation is based on log responses over the Red Fork interval—the conspicuous caliper log with its sharp basal contact, blocky upward shape, and shaly upper contact; gamma-ray values comparable to shale; and suppressed resistivity values. About a mile south of well 3 (Fig. 6), the same Red Fork interval has very different log characteristics that are indicative of a cleaner-sandstone interval. In well 4 (Fig. 6), the Red Fork is again identified on the caliper, gamma-ray, and resistivity logs, each showing a sharp basal contact and fining-upward textural profile. The sandstone interval consisting of channel sandstone occurs in two benches, whereas a higher sandstone layer probably represents transgresssive marine sandstone that is unrelated to the Cherokita Trend and is laterally extensive outside of the trend area. The last well in cross section B–B′ (Fig. 6) is located about 5 mi south of the Cherokita Trend. The log character is very similar to other wells outside both trends, as mentioned previously.

Cross section C–C′ (Fig. 7) is a north–south, shelf-to-basin section showing the character of the Red Fork sandstone interval at locations progressively farther south into the Anadarko Basin. Well 1 shows a Red Fork sequence consisting of basal sandstone overlain by shaly material. The sharp basal contact of the channel is noted from the resistivity log, whereas the same pick on the gamma-ray log appears slightly "hot," which is probably due to mud clasts and/or organic material in the channel base. The upper part of the channel fill turns shaly as noted from the gamma-ray log, whereas the resistivity logs still maintains higher values as compared to pure shale. This indicates a considerable amount of siliciclastics interbedded with shale. Nineteen miles to the south at location 2 (Fig. 7), a similar channel-fill sequence is noted immediately overlying the Inola Limestone. Ten miles farther south at location 3, the Red Fork consists of about 50 ft sandstone. The sharp lower and upper contacts are characteristic of a longitudinal bar in an incised valley that was abandoned suddenly. Sixteen miles to the southeast is well 4 (Fig. 7), where the well logs indicate that the Red Fork depositional system changes dramatically. At this location, two main depositional events occur, an upper and lower sequence, each having coarsening-upward textural profiles. This is very different than any of the channel environments previously described in the Cherokita and Wakita Trends. The lower sequence in well 4 consists of two coarsening-upward events, and the sandstone highest in the lower event contains the cleanest sandstone that is productive. This sequence may represent the subaqueous portion of a delta—the distributary-mouth bar. The highest sequence in well 4 that lies about 10 ft beneath the Pink limestone is thin and may represent the initial development of another marine bar. Farther basinward in well 5 (Fig. 7), it thickens and contains relatively clean sandstone that is undoubtedly prospective for hydrocarbons nearby. The lower sequence in well 5 is mostly shaled-out and represents the distal edge of the distributary-mouth bar described in well 4. Farther basinward is the prodelta, the depositional limit of this specific event.

CORE ANALYSIS

Five cores were examined for this paper with the intent of observing distinguishing sedimentary structures and textures that are indicative of a particular

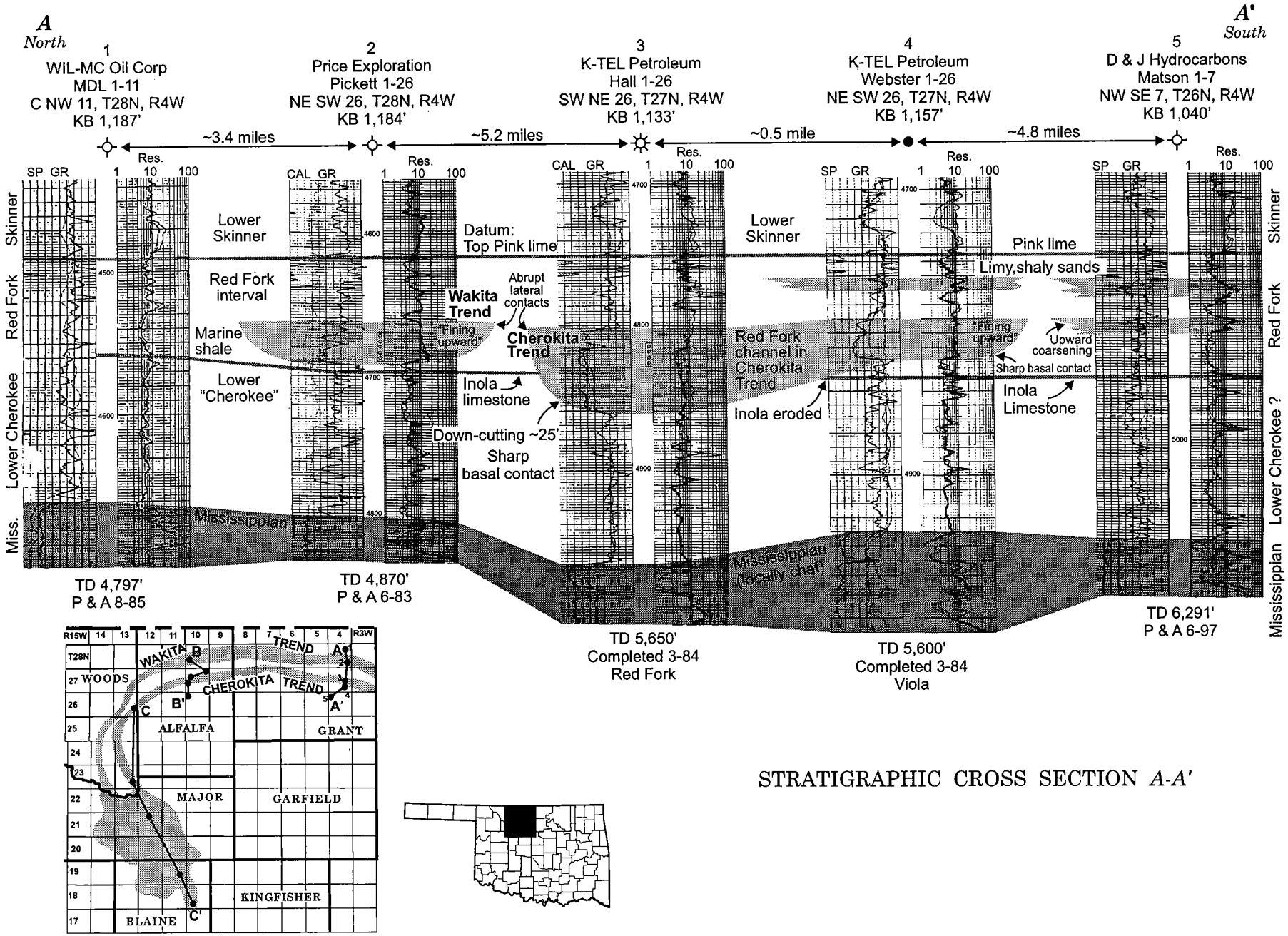

STRATIGRAPHIC CROSS SECTION *A-A'*

Figure 5. Stratigraphic cross section A–A′, north to south across the Wakita and Cherokita Trends. Location of cross section shown on inset map. *Abbreviations:* KB = Kelly bushing; P&A = plugged and abandoned; TD = total depth.

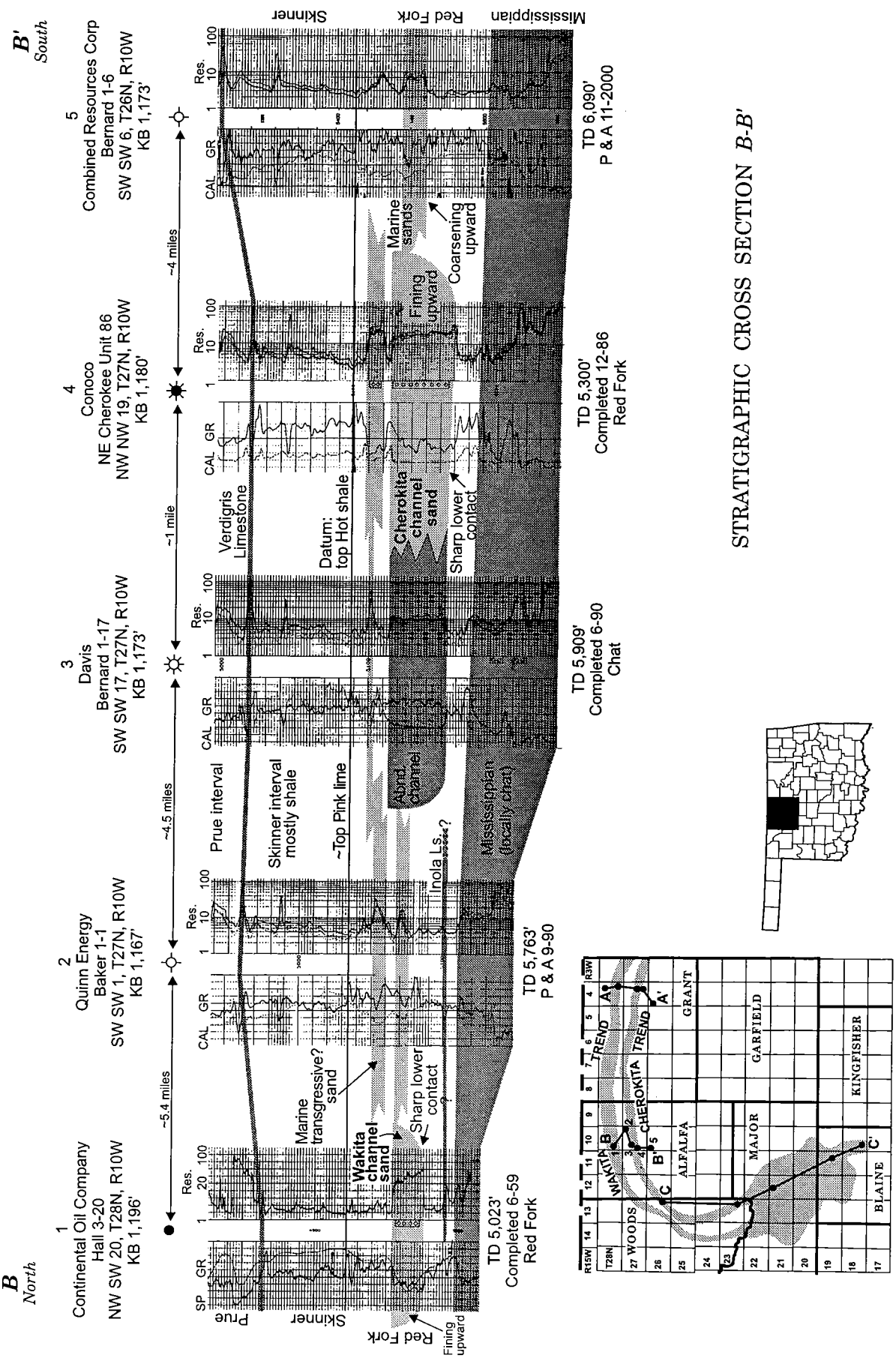

Figure 6. Stratigraphic cross section B–B', north to south across the Wakita and Cherokita Trends. Location of cross section shown on inset map.

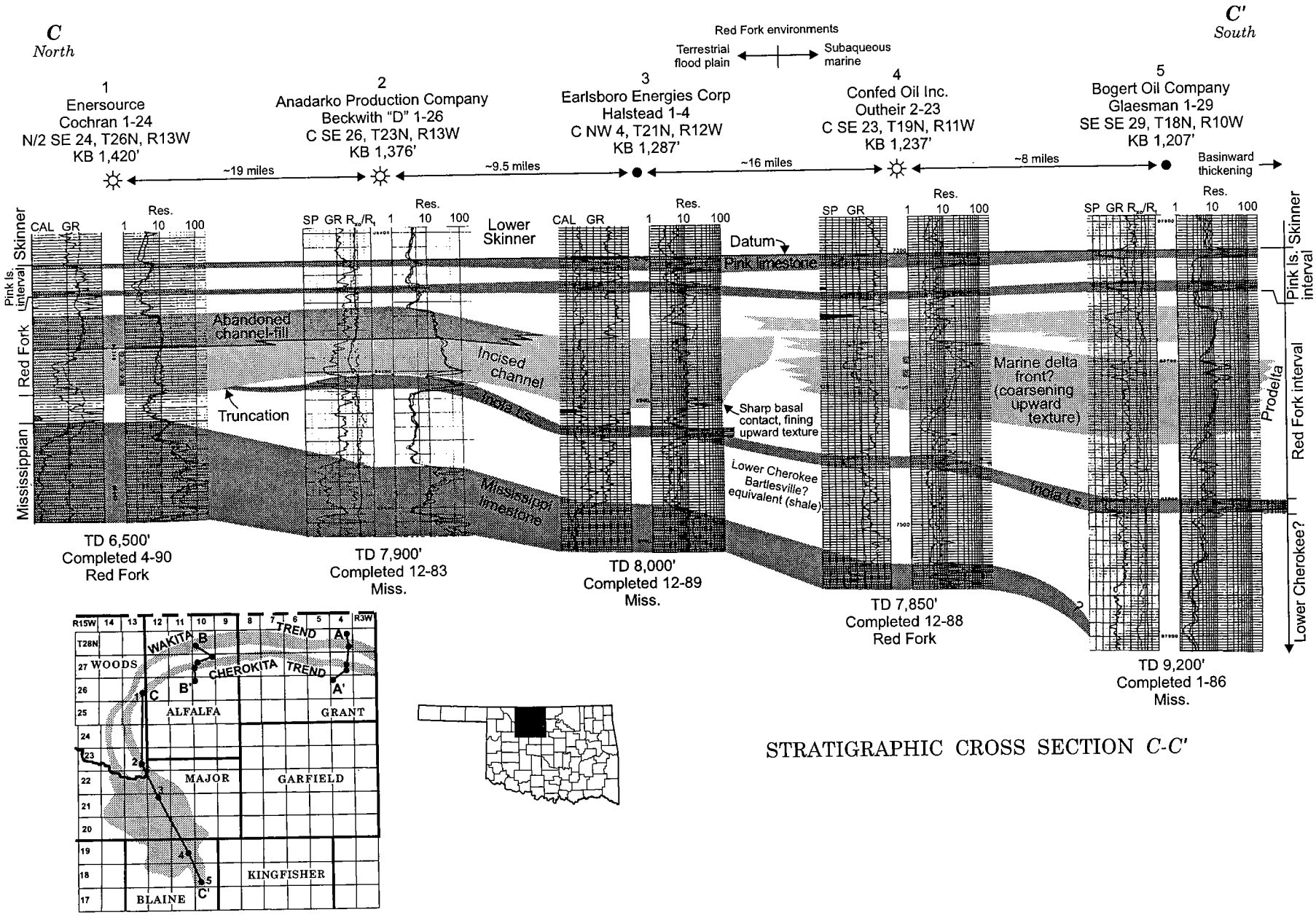

STRATIGRAPHIC CROSS SECTION *C-C'*

Figure 7. Stratigraphic cross section C–C′, shelf to basin. Location of cross section shown on inset map.

depositional environment. A consistent observation revealed high-angle and massive bedding in the bottom half of the sandstone sequence, whereas ripple or horizontal bedding occurred in the upper half (Fig. 8). Although these sedimentary structures are by themselves not unique to any one particular depositional environment, their stratigraphic position strongly indicates a fluvial interpretation rather than a marine-bar interpretation. Marine bars or shoreface deposits seldom have thick, well-developed basal sandstone having high-angle cross bedding. To the contrary, these deposits generally have a transition from shale to sandstone

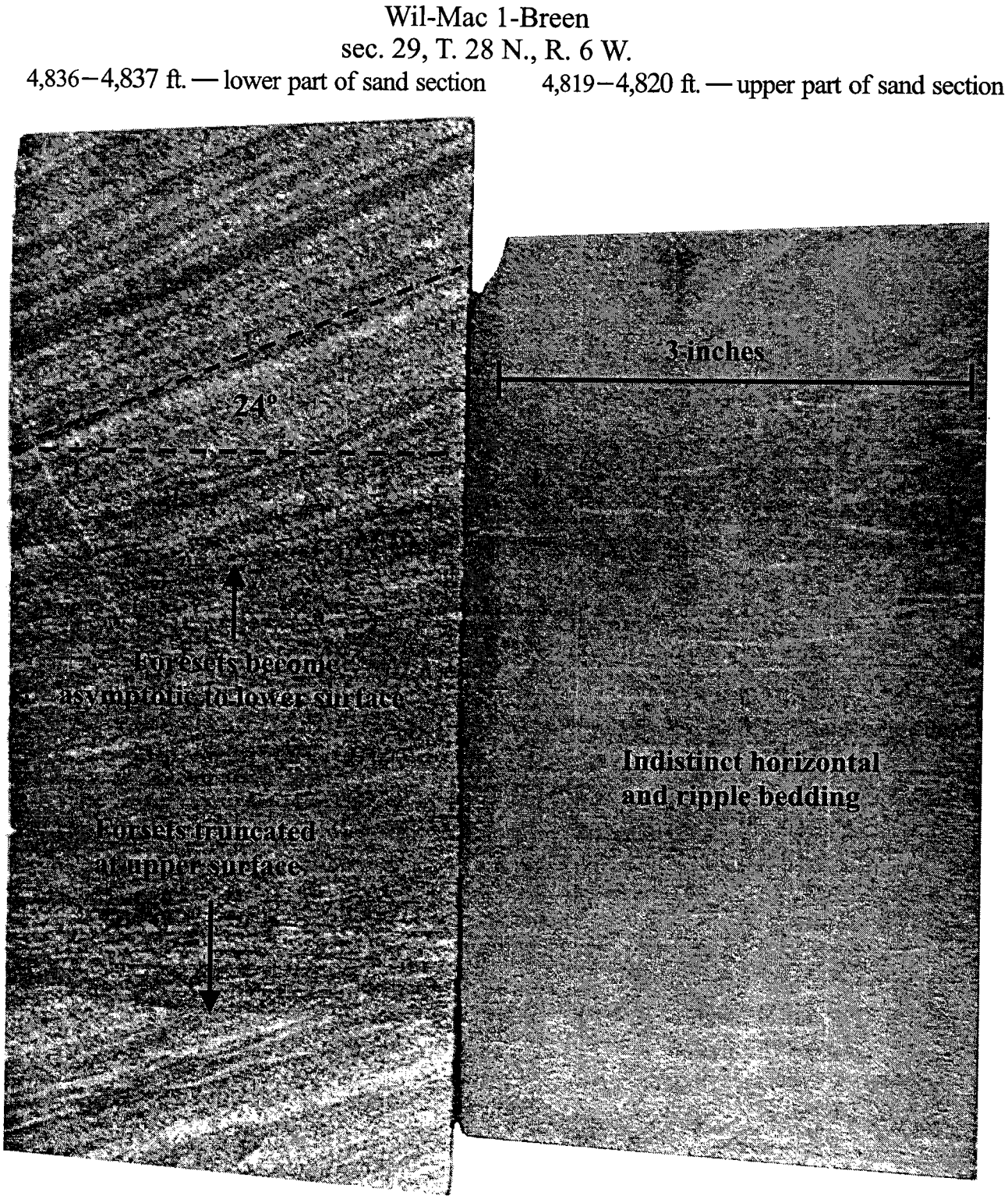

Figure 8. Bedding characteristics of Red Fork sandstone in cores of the Wakita and Cherokita Trends.

and gradually grade upward from interbedded shale and ripple-bedded sandstone into cleaner sandstone that may also be ripple bedded, horizontally bedded, or cross bedded. This sequence of sedimentary structures is the opposite of what normally occurs in channel deposits.

Another characteristic of the cores was the general lack of mud clasts or rip-up clasts. They are commonly found at the base of channel deposits and indicate bank erosion in a fluvial environment. Their absence may indicate overall low depositional energy, or more likely, straight-lined channels. The principal bar type is also believed to be longitudinal bars that characteristically do not meander from bank to bank, a feature characteristic of point bars.

CONCLUSIONS

The environment of deposition of sandstone within the Cherokita and Wakita Trends is an incised channel. The predominant facies is fluvial—probably longitudinal bars. The bases for this conclusion include the following.

- Consistent log character of sandstone with a sharp basal contact and blocky or fining-upward textural profile.
- Common associated channel facies, including abandoned-channel and channel-margin deposits.
- Regional Red Fork strata outside of channels consisting of two thin sandstone intervals, each having a coarsening-upward textural profile as seen on well logs. This is generally indicative of marine strata.
- Moderate to severe downcutting.
- Consistent core sedimentary structures most common in fluvial environments (i.e., massive to high-angle cross bedding in the bottom part of the sandstone sequence and ripple bedding in the upper half of the sandstone sequence).
- Regional sandstone trends extending basinward to the south and terminating in a subaqueous marine environment (delta front?). The marine bars have distinctive and repetitive log patterns indicating a coarsening-upward textural profile.

WHO CARES?

Although both the Wakita and Cherokita Trends are mature fields, numerous opportunities for discovering compartmentalized reservoirs immediately north and south of the trends undoubtedly exist. Therefore, it is very important to arrive at the correct interpretations of depositional environments, because this will guide future drilling and quantify expectations. Those who are correct will have the most effective strategies in finding new reserves. Those who are incorrect will only have serendipity in avoiding failure.

In the interpretation proposed in this paper, the most probable exploration and development targets are expected to be (1) small channel tributaries leading into the main channels, and (2) breakout or subordinate fluvial channels branching away from the main trends. These may also include overbank or splay-type sand deposits. Contrasting with the fluvial interpretation, those interpreting the trends as marine bars are hoping to find major north–south channels normal to the orientation of the trends.

REFERENCES CITED

Al-Shaieb, Zuhair; Shelton, J. W.; and Puckette, J. O., 1989, Sandstone reservoirs of the Mid-Continent: Syllabus for short course sponsored by the American Association of Petroleum Geologists Mid-Continent Section: Oklahoma City Geological Society, 33 p.

Andrews, R. D., 1997, Fluvial-dominated deltaic (FDD) oil reservoirs in Oklahoma: the Red Fork play: Oklahoma Geological Survey Special Publication 97-1, 90 p. [Numerous other geologists contributed to this study.]

Glass, J. L., 1981, Depositional environments, reservoir trends, and diagenesis of the Red Fork sandstone in Grant and eastern Kay Counties, Oklahoma: Oklahoma State University unpublished M.S. thesis, 99 p.

Masera Corporation, 1994, Red Fork sandstone of Oklahoma: Masera Corporation [formerly], unpublished document, Tulsa, Oklahoma.

O'Reilly, K. O., 1986, Diagenesis and depositional environments of the Red Fork sandstone (Des Moinesian) in the Wakita Trend, Grant County, Oklahoma: University of Tulsa unpublished M.S. thesis, 41 p.

Swanson, D. C., 1967, Some major factors controlling the accumulation of hydrocarbons in the Anadarko Basin: Shale Shaker, v. 17, no. 6, p. 106–114.

Withrow, P. C., 1968, Depositional environments of Pennsylvanian Red Fork sandstone in northeastern Anadarko Basin, Oklahoma: American Association of Petroleum Geologists Bulletin, v. 52, p. 1638–1654.

A Deposition and Reservoir Model for the Prue Sandstone in the Southwest Oklahoma City Area

John R. Broker
Helmerich and Payne Inc.
Tulsa, Oklahoma

Les J. Broker and Thomas N. Capucille
Consultants
Edmond, Oklahoma

ABSTRACT.—The study area extends from the Oklahoma City Field to about 25 mi southwest and covers 10 townships. Combined with additional reservoir analysis, this work led to the drilling and completion of a significant Prue sandstone discovery in sec. 22, T. 10 N., R. 5 W., where additional wells are being drilled.

The Prue sandstone (Desmoinesian, Middle Pennsylvanian) was deposited around the western side of the Oklahoma City Field area as a highstand-delta sequence. A significant drop in sea level during deposition caused the incision of a valley through the delta complex, precipitating the deposition of a lowstand-delta sequence west of the study area. After this incision, sea level rose, backfilling the valleys with sands and shales forming a major incised-valley–fill complex. This complex has left Prue sandstone in the study area up to 80 ft thick.

Initial Prue completions date to the initial development of the Oklahoma City Field in the early 1930s, but no further discoveries were made until 1980. Since that time, several areas of Prue production in this incised-valley complex were identified west of the Oklahoma City Field area, some of which are being waterflooded. Completion procedures have changed radically over the last 30 years and have made previously marginal areas commercial, leading to an expansion of the Prue play. The integration of core and electric-log analysis, regional deposition modeling, sequence stratigraphy, and completion technology has led to a valuable exploration tool that can be applied to Cherokee sands throughout the southeastern Anadarko Basin.

INTRODUCTION

The Prue is the youngest clastic interval of the Desmoinesian "Cherokee Group". The sandstone was first described in 1921 by White and Green, who worked in the Prue Field, in Osage County, Oklahoma (Jordan, 1957).

In spite of a long productive history, the Prue sandstone is still being targeted today. This study integrated subsurface mapping with core analysis to provide a better understanding of depositional environments, aerial extent, and paleotopography of Prue "channels" for exploration purposes. Sequence stratigraphic principles were applied to the data to test this methodology in better defining facies and stratigraphic relationships within the Prue. No high-resolution sequence stratigraphic interpretation was attempted due to lack of complete core data through the entire section.

Location

The study area is in the southeastern part of the Anadarko Basin, including 10 townships and more than 1,000 wells in parts of Oklahoma, Canadian, and Cleveland Counties, Oklahoma. The 10 townships included are: T. 9 N., R. 5–6 W.; T. 10 N., R. 3–6 W.; and T. 11 N., R. 3–6 W. (Fig. 1). This area was chosen for its abundance of data and continued exploration activity. In addition, the Prue sandstone has not been extensively studied using core data.

Purpose and Scope

The purpose of this study was to substantiate prior work on Prue depositional environments and to extend previous mapping of this interval. Objectives include: (1) mapping the distribution of the Prue sandstone; (2) determining the lithofacies and depositional environments associated with this interval; (3) documenting

Broker, J. R.; Broker, L. J.; and Capucille, T. N., 2002, A deposition and reservoir model for the Prue sandstone in the southwest Oklahoma City area, *in* Boyd, D. T. (ed.), Finding and producing Cherokee reservoirs in the southern Midcontinent, 2002 symposium: Oklahoma Geological Survey Circular 108, p. 11–36.

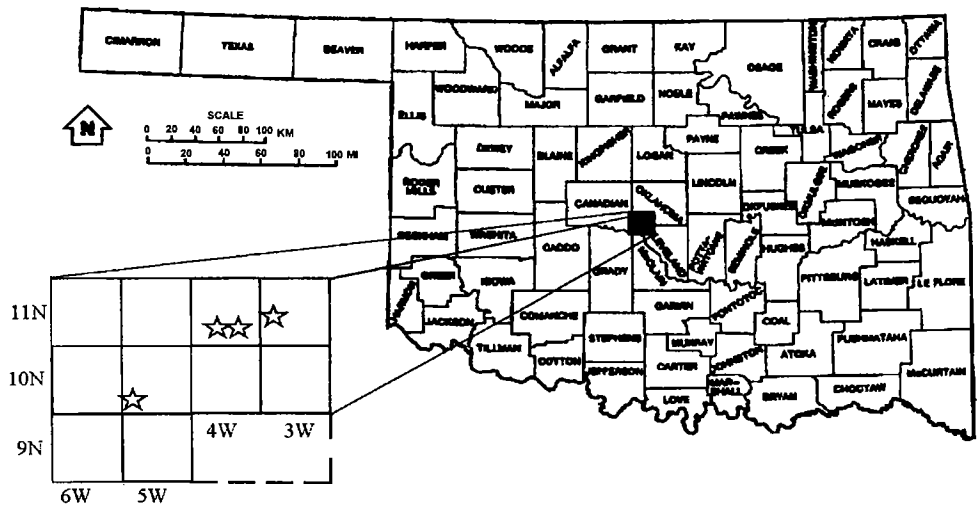

Figure 1. Map showing location of study area and core locations (stars), southwest Oklahoma City area; parts of Oklahoma, Canadian, and Cleveland Counties, Oklahoma. From Broker (2001).

channel incisions of the Prue sandstone into underlying units; (4) establishing the value of sequence stratigraphic concepts in the interpretation of Prue deposition; (5) determining the geometry and distribution of the Prue reservoirs; (6) investigating various Prue wireline-log responses and comparing them with core data; and (7) demonstrating how various sedimentary facies trap hydrocarbons in the Prue channel system and showing their associated production.

Methods of Investigation

An extensive literature search was conducted not only for this area, but also on associated topics such as incised-valley–fill (IVF) models. Contacts were made with the numerous companies that have drilled in the study area to access core analysis, waterflood data, and unitization reports.

Data were gathered from well scout tickets, wireline logs, and production reports for almost 1,000 wells. A series of preliminary east–west and north–south stratigraphic cross sections were made to ensure consistent correlation. Formation tops were taken from the gamma-ray curve, but other logs, such as combination neutron-density, were used to verify these picks. The classification for sandstone was based on a 50% "clean" line that was placed between the shale base line and a "clean" limestone value on the gamma-ray log. Net sandstone was classified as sand with porosity over 8%. Wireline logs showing typical formation tops and net sand determination are presented in Figures 2 and 3.

Cores were analyzed for sedimentary structures, textures, and mineralogical constituents to substantiate theories about depositional environments. Core and wireline-log data were used together in order to make paleo-environmental interpretations, especially regarding the criteria necessary to be considered incised-valley fill. Van Wagoner and others (1990) list of fundamental characteristics include: (1) the valley is a negative or erosional paleographic feature; (2) the base of the valley truncates underlying strata; (3) the base and the walls of the incised-valley–fill system represent a sequence boundary that may correlate to an unconformity in interfluvial areas; (4) the base of the valley fill exhibits a basinward shift in facies; and (5) depositional markers within the fill will onlap onto the valley walls.

Previous Investigations

Numerous investigations of the Pennsylvanian Desmoinesian rocks have been conducted throughout Oklahoma; however, only those that examined upper Cherokee sandstones, or that involved the study area are cited. The following listing of previous work is designed to trace the history of the stratigraphic nomenclature in the area as well as provide a reference list from which additional work can begin.

Oakes (1953) divided the informal "Cherokee Group" into the Krebs and Cabaniss Groups. The uppermost sandstone of the Cabaniss Group is informally known as the Prue sandstone. Before Oakes, White and Green (1921) first used the term Prue sandstone from its occurrence in the Prue field in Osage County, Oklahoma (Jordan, 1957).

McGee and Clawson (1932) were the first to describe the subsurface geology of the Oklahoma City Field, examining numerous formations and mapping the regional structure of the area. Jacobsen (1949) described the structural features on the east flank of the Anadarko Basin in Cleveland and McClain Counties. His work discussed the general stratigraphy and structural features of the area but focused primarily on the McClain County fault zone. Burkett (1957) also reported on the subsurface geology of western McClain County.

Ahmeduddin (1968) studied the geology of the Wheatland area, of McClain, Canadian, Grady, Cleve-

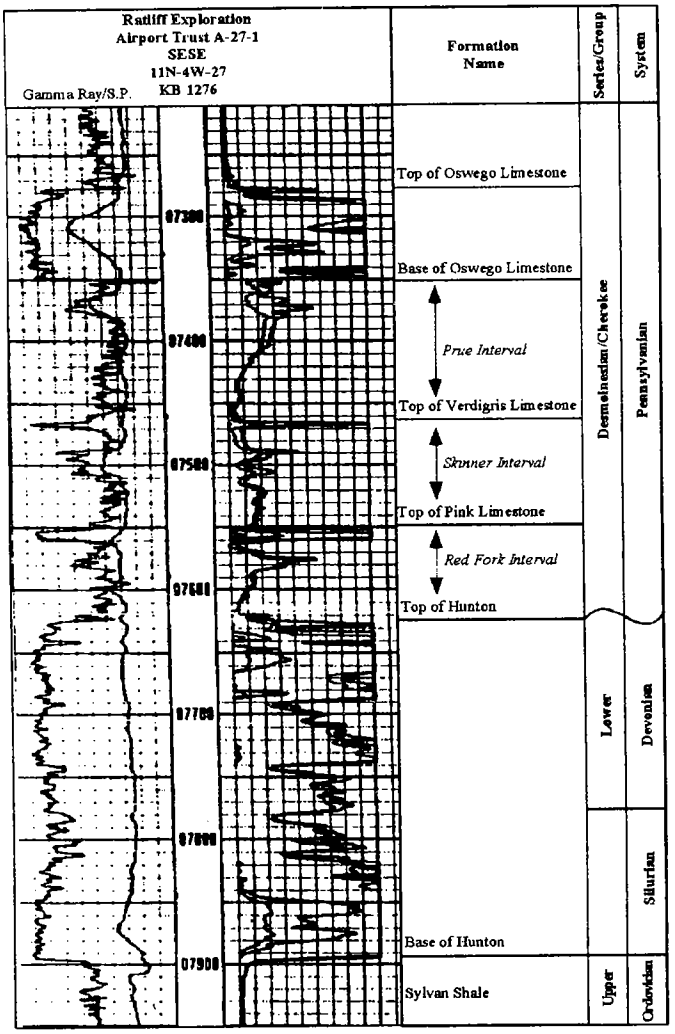

Figure 2. Type electric log for the southwest Oklahoma City area; parts of Oklahoma, Canadian, and Cleveland Counties, Oklahoma. Type log is Airport Trust A-27-1 well (SE¼SE¼ sec. 27, T. 11 N., R. 4 W.) From Broker (2001).

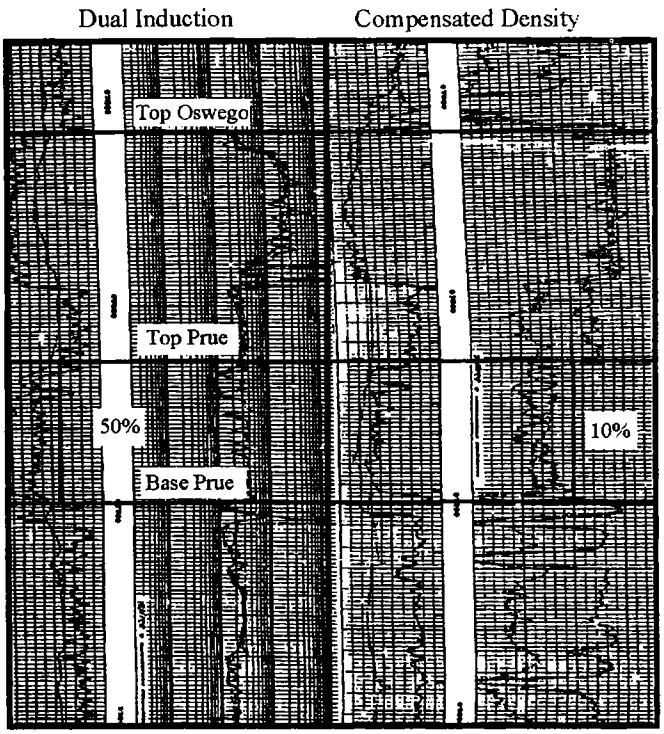

Figure 3. Electric log of the Prue sandstone interval in the Thomason No. 1 well (sec. 32, T. 11 N., R. 4 W.) showing the criteria for determination of clean (gross) and porous (net) sand; southwest Oklahoma City area; parts of Oklahoma, Canadian, and Cleveland Counties, Oklahoma. Log shows 40 ft of clean (>50% gamma-ray count) and net (>8 % porosity) Prue sandstone. From Broker (2001).

land, and Oklahoma Counties. He presented a detailed stratigraphic correlation of the Desmoinesian rocks, researched the geologic history, and assessed the influence of the pre-Desmoinesian erosional surface on "Cherokee" deposition. Contained within Ahmeduddin's research are structure maps that show the likely Pennsylvanian paleo-drainage pattern.

Berg (1969) conducted a large regional study of the "Cherokee Group" on the west flank of the Nemaha Ridge, matching a study performed by Cole (1969) on the eastern flank. Dahlgreen (1968) and Gatewood (1970) furnished studies on the history and development of the Oklahoma City Field. Albano (1973) did a subsurface stratigraphic analysis of the "Cherokee Group" in northeastern Cleveland County, east of this study area. His objectives were to determine the degree to which the pre-Pennsylvanian unconformity influenced "Cherokee" deposition, to interpret the clastic depositional environments, and to investigate the significance of both structural, and stratigraphic trapping. Albano mapped the Prue sandstone in T. 8–10 N., R. 1 E. through R. 2 W.

Andrews and others (1996) prepared a publication on the Prue entitled "Fluvial-Dominated Deltaic Oil Reservoirs in Oklahoma: The Skinner and Prue Plays." This special publication by the Oklahoma Geological Survey contains an overview of the Prue distribution, stratigraphy, and depositional models appropriate to the unit, and includes case studies for producing Prue fields. This paper is an excellent starting point for regional information relating to the Prue sandstone.

STRATIGRAPHY

Introduction

The three rock units studied here are, from top to bottom, the Oswego Limestone, Prue sandstone, and the Verdigris Limestone (Fig. 4). These three stratigraphic units are part of the Desmoinesian Stage of the Pennsylvanian System. This interval represents a period in the Paleozoic Era of 5–7 million years that began about 305 million years before the present and lasted until about 310–312 million years before present.

The Oswego limestone is part of the Marmaton

SYSTEM	STAGE	GROUP	FORMATION	SURFACE NAMES	SUBSURFACE NAMES
PENNSYLVANIAN	DESMOINESIAN	MARMATON	FT. SCOTT	FT. SCOTT LIMESTONE	OSWEGO LIME
		"CHEROKEE"	SENORA	LAGONDA SANDSTONE	PRUE SAND
				VERDIGRIS LIMESTONE	VERDIGRIS LIMESTONE
		CABANISS		OOWALA SAND	SKINNER SAND -Upper,Middle, Lower
				PINK LIMESTONE	PINK LIMESTONE

Figure 4. Stratigraphic nomenclature of the "Cherokee" Group, Anadarko Basin, Oklahoma. Prue Sand shown in gray-shaded area. From Broker (2001).

Group, whereas the older Prue and Verdigris are included in the Cabaniss Group. The Cabaniss and underlying Krebs are known informally as the "Cherokee Group." The two carbonate units, Oswego and Verdigris, were only used to define the boundaries of the Prue clastic interval. These carbonates are useful markers in dividing cyclic Cherokee clastics into genetic units and are used as stratigraphic guideposts throughout the Anadarko Basin. Examples include the Skinner clastic interval bounded by the Verdigris Limestone and underlying Pink limestone, and the Red Fork interval bounded by the Pink and Inola Limestone.

Cabaniss Group

The Verdigris Limestone, according to Jordan (1957), was named in 1914 from an outcrop along the Verdigris River near Claremore, Oklahoma. The Verdigris was cored in the Booth 9D-2 well, and is described later in this study. The Verdigris is mottled gray, microcrystalline limestone with dispersed crinoid and fossil debris. Wireline log characteristics include a "clean" gamma response with high resistivity (Fig. 2).

The Prue sandstone, located between the Oswego limestone and the Verdigris Limestone, is reported by Jordan (1957) to have been named in 1921 based on its occurrence in the Prue Field, in Osage County, Oklahoma. Sandstones within the Prue are primarily fluvial, although they become more marine southward (Andrews and others, 1996). The sandstone is present on the Cherokee Platform and in the eastern part of the Anadarko Basin. The volume of sand within the Prue is variable and can exceed 100 ft. The sand itself has a fine- to very fine grain size with abundant interbedded muscovite mica and clay. The micas are seen easily with a hand lens and appear mostly in thin shale interbeds.

Marmaton Group

The Oswego limestone, also seen in the core of the Booth 9D-2 well, is mottled gray microcrystalline limestone that varies in thickness in the study area. According to Jordan (1957), Hayworth and Kirk first named the formation in 1894 from an outcrop near Oswego, Kansas. However, the Stratigraphic Committee did not accept this name and the unit was named formally the Fort Scott Limestone, making the Oswego limestone an informal, subsurface equivalent of the Fort Scott Limestone. The Oswego changes facies from north to south in the study area from backreef, to reef, to forereef. The reef core is 1–2 mi wide and is part of a much larger system that continues northeastward toward Tulsa. Reef thickness in the study area can be as much as 80 ft, with 15–20 ft of this interval containing porosity. However, only minor, scattered production can be found on the Oklahoma City Uplift. North of the reef, the limestone thins into a backreef facies, and seaward becomes mainly shale with only a thin limestone marker bed. The gamma-ray–log characteristics of the Oswego make it identifiable throughout the study area. However, identifying its top is difficult in the southern part of the study area because of the development of two aerially restricted limestones.

DEPOSITIONAL FRAMEWORK

Tectonic Setting

The southwest Oklahoma City area lies in central Oklahoma and includes parts of Canadian, Oklahoma, and Cleveland Counties. It is on the eastern edge of the Anadarko Basin at the southern end of the Nemaha Ridge (Fig. 5). This area has been called a zone of transition that involves four major tectonic elements. These elements include: (1) the Central Oklahoma Platform, (2) the McClain County fault zone, (3) the Oklahoma City Uplift (Nemaha Ridge), and (4) the Anadarko Basin.

Gatewood (1969) described the structure of the Oklahoma City Uplift (Fig. 6) as a faulted anticlinal fold located at the southern end of the Nemaha Ridge. The history of the structure includes at least five stages of structural uplift with intervening periods of complete or partial submergence. The adjoining Anadarko Basin deepens southwest of the study area and contains up to 40,000 ft of sediment in its axis (Fig. 7). The basin is bounded on the south by the Wichita and Amarillo Uplifts, on the east by the Nemaha Uplift, and on the west

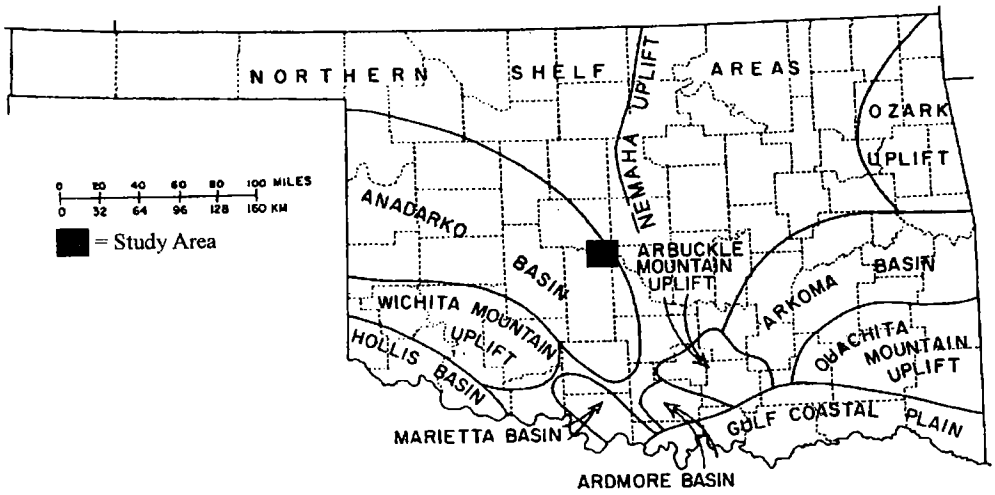

Figure 5. Map of the major geologic provinces of Oklahoma showing the location of the southwest Oklahoma City area (in black); parts of Oklahoma, Canadian, and Cleveland Counties, Oklahoma. From Johnson (1971).

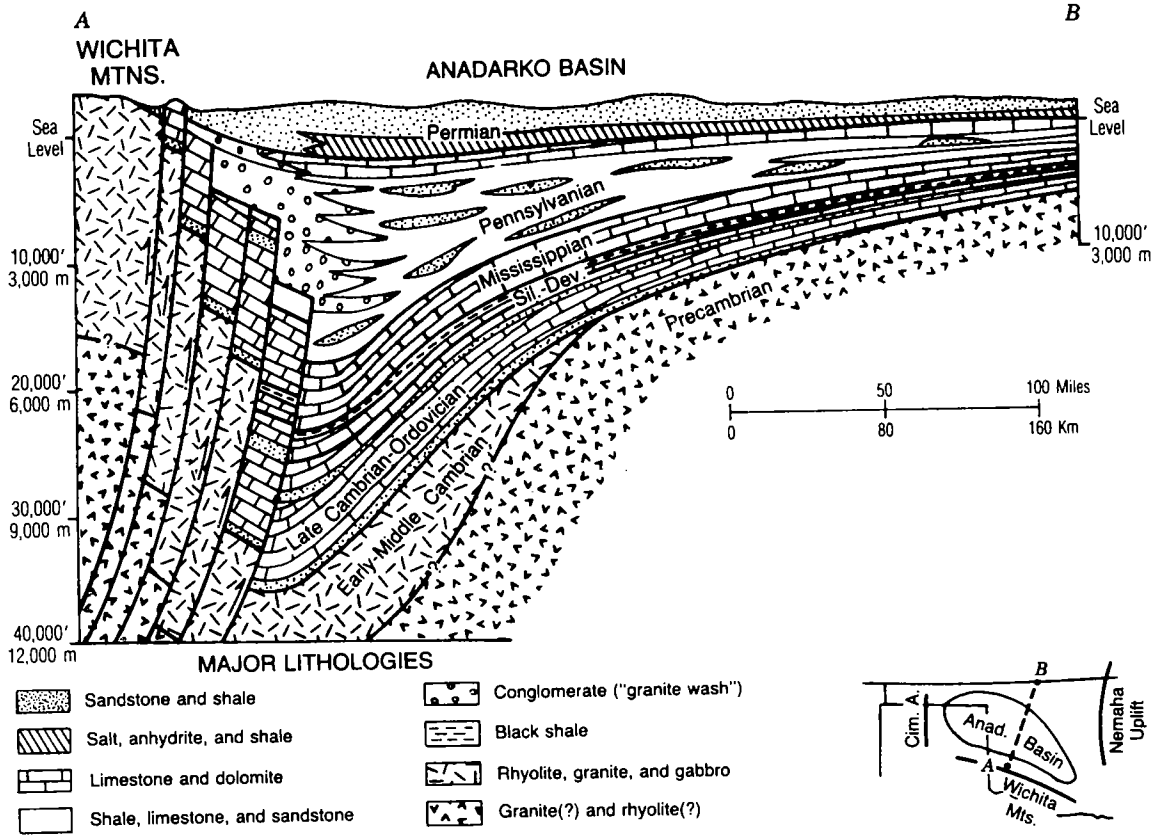

Figure 6. Generalized north–south structural cross section (A–B) through the Anadarko Basin of western Oklahoma. From Johnson (1989).

by the Cimarron Arch. The northern shelf of the basin extends across parts of western Kansas.

The Pennsylvanian Period was an active time geologically in Oklahoma. It was during the Early Pennsylvanian that the Wichita–Amarillo block was uplifted along a series of west–northwest-trending reverse faults. The Anadarko Basin began active subsidence during the late Morrowan, and subsidence continued through the end of the Virgilian. As much as 18,000 ft of sediment were deposited in the basin during the

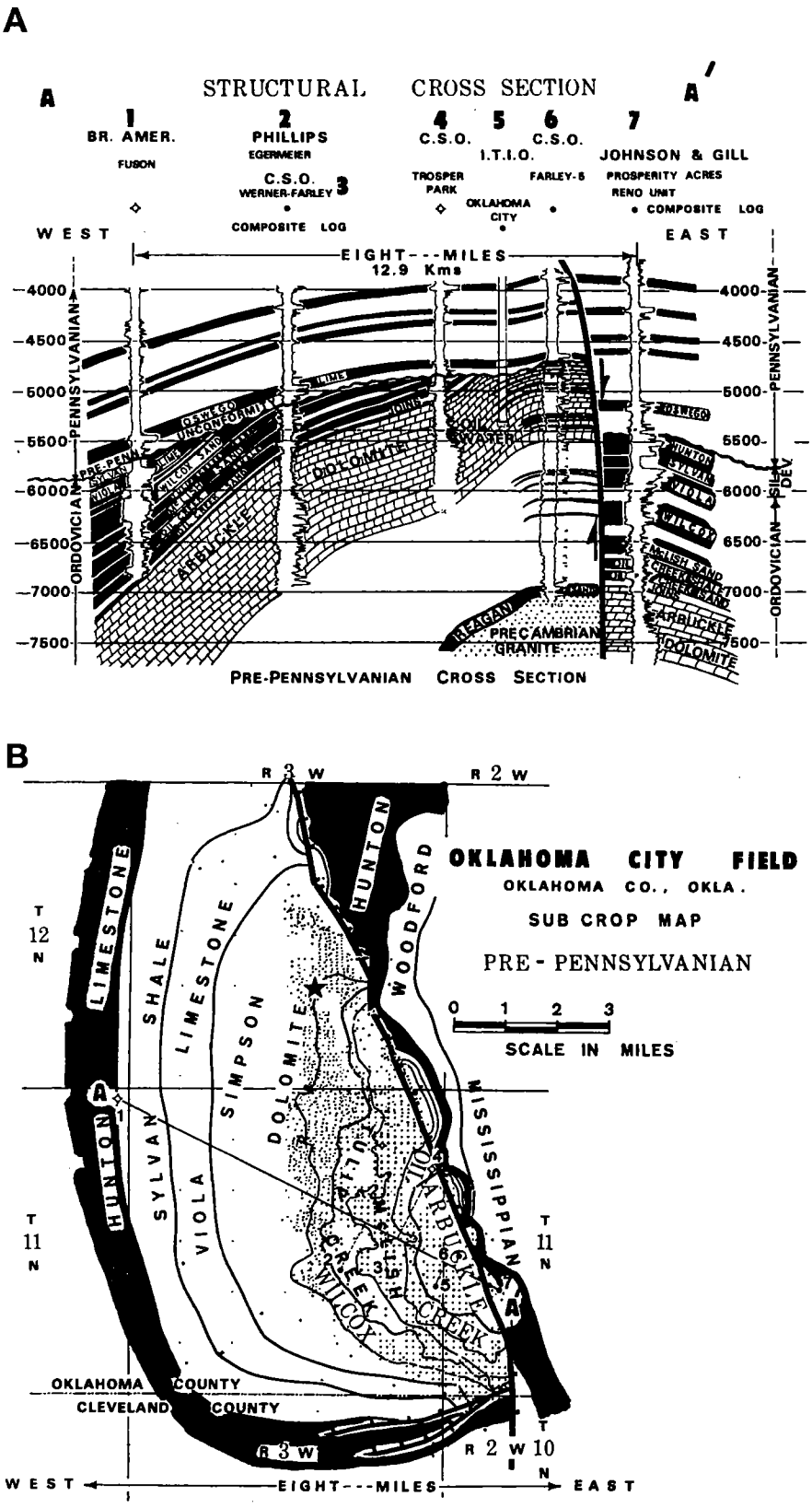

Figure 7. (A) West–east structural cross-section (A–A′) through the Oklahoma City field showing location of control wells (bold numbers). Depths in feet. (B) Pre-Pennsylvanian subcrop map of the Oklahoma City Field illustrating erosion and truncation onto the Nemaha Ridge. From Gatewood (1969). From AAPG (1969), reprinted by permission of AAPG whose permission is required for further use.

Pennsylvanian (Johnson, 1989) consisting of a mixture of conglomerates, limestones, shales, and sandstones. The Desmoinesian rocks of the Pennsylvanian consist of cyclic, interbedded marine limestones and shales, during periods of eustatic sea-level change, with marine and non-marine clastics. In the study area, the interbedded sands of interest are interpreted as channel-fill, distributary, and mouth-bar sands.

Source Area

The Prue sandstones in the eastern Anadarko Basin are fine- to very fine grained, subrounded quartzarenites with abundant muscovite as an accessory mineral. They originated from fluvial advances that progressed across the Cherokee Platform, southwest over the Nemaha Ridge and into the Anadarko Basin (Fig. 8). Sediment provenance was most likely the Canadian Shield or Wisconsin Arch. The fine-grained, subrounded nature of the sediment can be indicative of long transport or recycled sedimentary rock.

Andrews and others (1996) presented a regional isopach map of the interval from the top of the Verdigris to the top of the Pink limestone across most of Oklahoma. They concluded that the Prue's areal distribution was a result of the orientation of the Cherokee Platform and the fault zone of the Nemaha Ridge. Because the Nemaha was a positive feature at this time, the Prue sediment likely was redirected to the south, around the east side of the Nemaha Ridge. This concept is used to explain the west-trending channel complexes that are found in the study area.

SUBSURFACE ANALYSIS

Mapping

Many maps and cross sections were constructed, of which four maps and three cross sections are presented below. Where Prue channels are present or production was available, well logs were analyzed for sand content and log character. Typical electric-log signatures are shown in Figure 9. In other areas, a well log from each quarter section

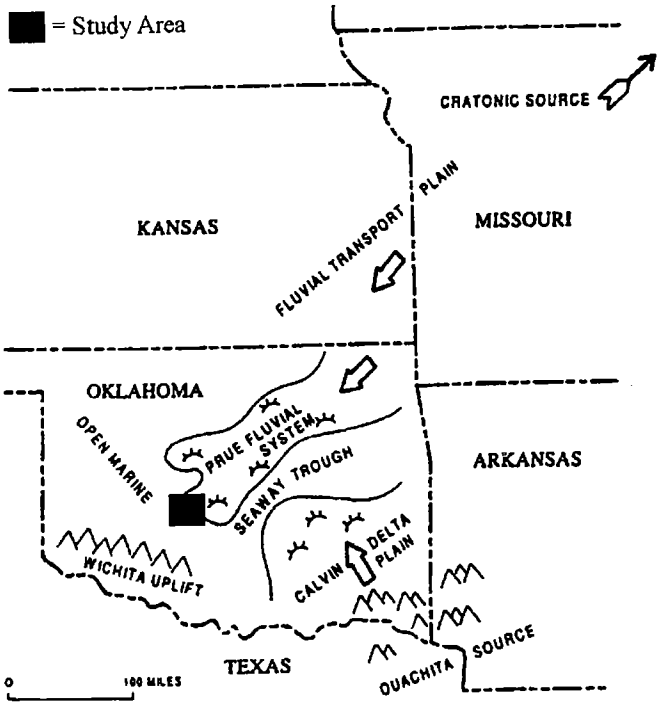

Figure 8. Map of the paleogeography of the central Midcontinent region during deposition of the Prue sandstone. Study area shown in black. Modified from Krumme (1981).

was included to improve lateral control and to validate mapping interpretations.

Verdigris Limestone Structure Map

The structure map on the Verdigris Limestone (Fig. 10) shows the strike of the basin here as northwest–southeast, with southwest dip averaging 190 ft/mi (3.2°). The Verdigris structure map indicates an area of slight reduction in dip, trending northwest–southeast, along strike, from T. 11 N., R. 6 W., into T. 10 N., R. 5 W., and the southern edge of T. 10 N., R. 4 W. Immediately southwest of this area, normal dip rate resumes. This feature probably reflects a minor hinge-line of the Anadarko Basin during Prue deposition. In several areas, the Verdigris Limestone has been eroded by Prue incision. In these areas, an estimate of the original top of the Verdigris Limestone was used. No specific structural anomalies are apparent on this map (Fig. 10) except the Oklahoma City Uplift.

Gross Prue Sandstone Isolith Map

The isolith map of the Prue sandstone (Fig. 11) shows the gross thickness of the sand calculated by placing a line halfway between the shale baseline and the clean limestone/sandstone value on the gamma-ray log. Jim Logsdon (personal communication, 2000) supplied data used here for many of the wells in the area of Oklahoma City Field that were otherwise unavailable.

Sand-body shapes and thicknesses as well as log character indicate that Prue sands in this area were deposited in a variety of depositional environments. The elongate, southwest-trending sandstone representing a large channel fill dominates the map. Smaller, irregularly shaped pods of thin sand in T. 11 N., R. 5 W., and T. 11 N., R. 6 W., possibly represent minor delta-front sands. These would have been deposited prior to the incisement and filling of the valley that would have occurred during a highstand event. This highstand delta appears to have prograded from the southeast corner of T. 11 N., R. 3 W., where it seems to have been eroded during subsequent incisement. The maximum thickness of the delta-front sands is 30 ft, and they seldom appear very clean. Completion attempts in these sands indicate that they are poor permeability, water-bearing sands.

The incised-valley sandstone mapped in the study area originated from the east, is up to 2 mi wide, and contains a maximum of 88 ft of clean sandstone. The sandstone trends northwest but makes a sharp southwestern turn in the northwest corner of T. 11 N., R. 3 W. The channel becomes remarkably linear in a southwest direction for 25 mi, and exits the study area in the southwest corner of T. 9 N., R. 6 W. A secondary channel is seen branching to the west in T. 10 N., R. 6 W.; however, it does not show the deep incision observed in the main channel.

Net Prue Sandstone Isolith Map

The isolith map of the net Prue sandstone shows net thickness based on gross sand with at least 8% porosity (Fig. 12). Where porosity logs were unavailable, net sand was estimated from the spontaneous-potential (SP) curve. Where micrologs were present, they were used to assist in net sandstone determination. The delta-front complex in T. 10 N., R. 3–4 W., was severely reduced in aerial extent when qualified with an 8% porosity cutoff, illustrating the poor reservoir quality of this sand. However, the incised-valley channel fill still reaches a maximum of 82 ft and closely mimics the character of the gross sand isolith.

Base Prue Channel Incision to Top Verdigris Limestone Isopach Map

The isopach map from the base of the Prue channel incision to the top of the Verdigris Limestone further delineates the incised valley and shows Prue thickness from the erosional channel base, regardless of channel lithology, to the top of the limestone (Fig. 13). Areas of maximum incision are shaded, and these areas correspond to where the Verdigris is absent. With the interval thickness decreasing toward the channel axis, this isopach aids in defining the location of the channel, even in areas where it is not sand filled. The map shows that the incised valley cuts through the Verdigris as far south as sec. 20, T. 10 N., R. 5 W., but does not incise deeply enough westward from that point to remove the Verdigris. Solid lines indicate the limits of gross channel sand. These limits are widened with wavy lines where channel incision extends beyond the limits of the sand, thus providing a more complete picture of channel width.

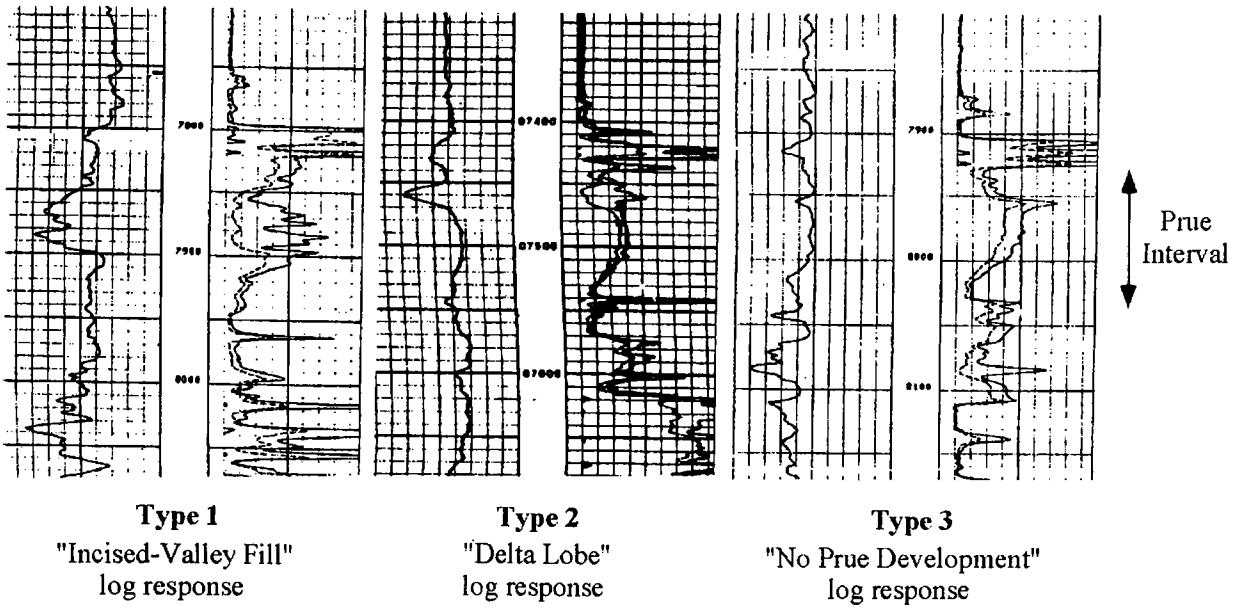

Figure 9. Electric-log signatures of the Prue interval for the southwest Oklahoma City area; parts of Oklahoma, Canadian, and Cleveland Counties, Oklahoma. From Broker (2001).

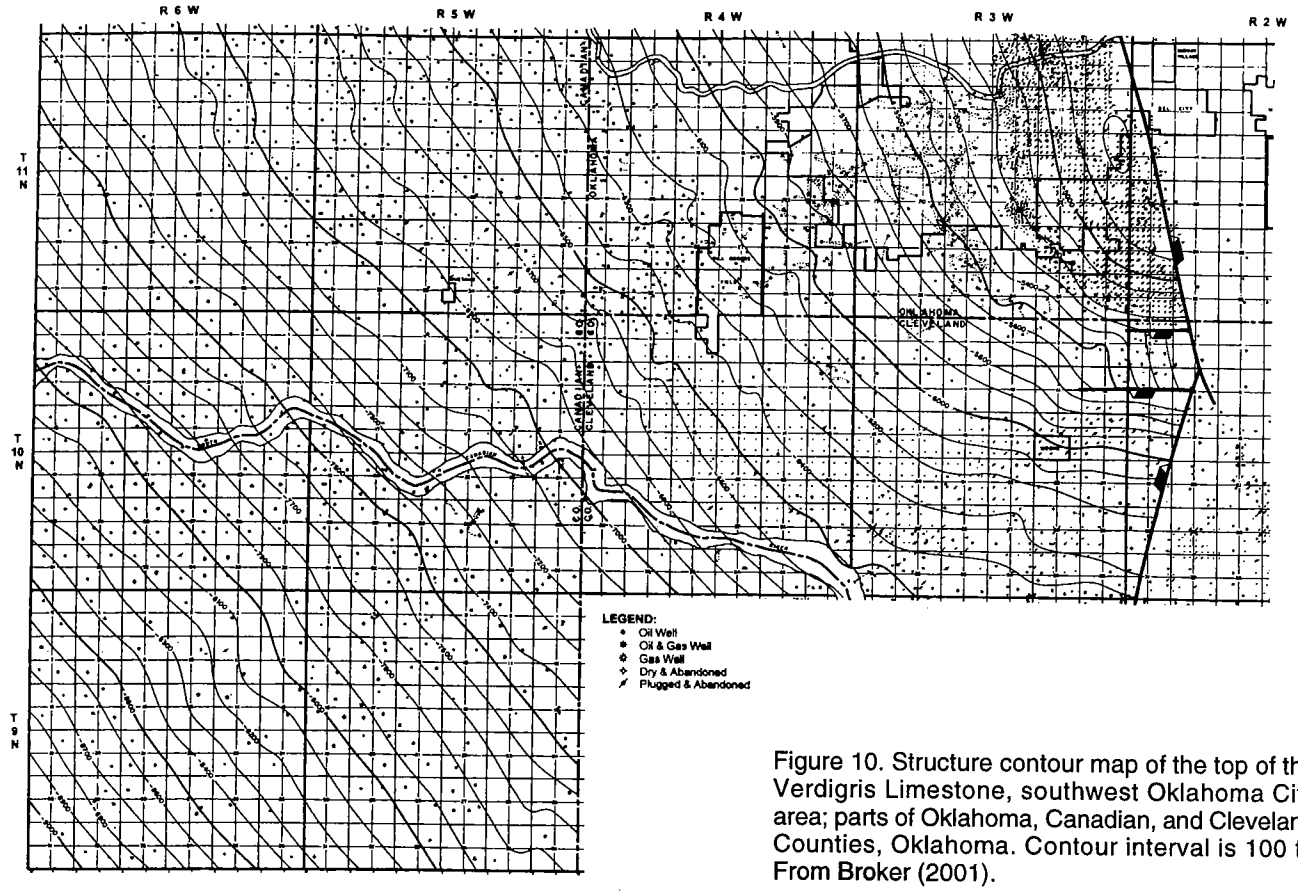

Figure 10. Structure contour map of the top of the Verdigris Limestone, southwest Oklahoma City area; parts of Oklahoma, Canadian, and Cleveland Counties, Oklahoma. Contour interval is 100 ft. From Broker (2001).

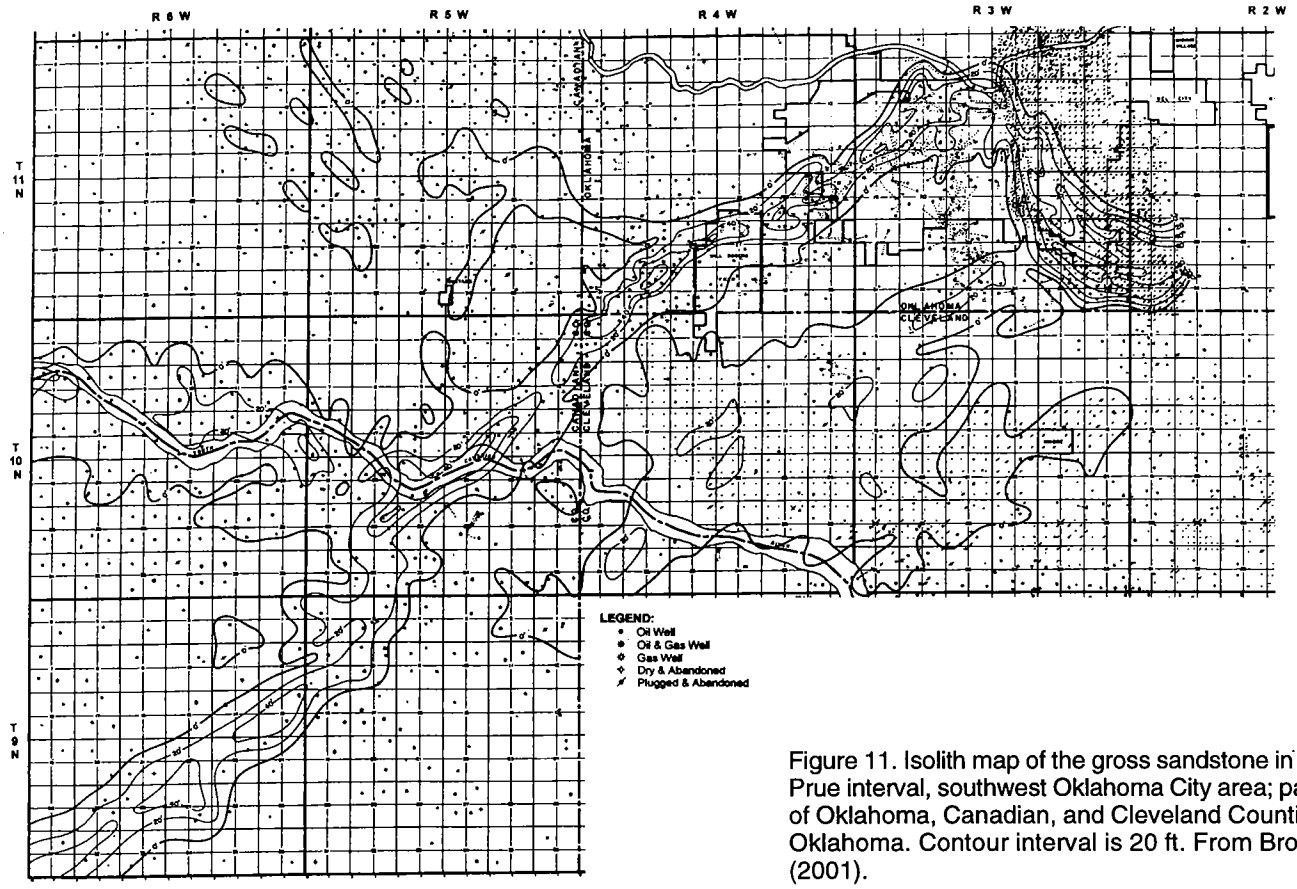

Figure 11. Isolith map of the gross sandstone in the Prue interval, southwest Oklahoma City area; parts of Oklahoma, Canadian, and Cleveland Counties, Oklahoma. Contour interval is 20 ft. From Broker (2001).

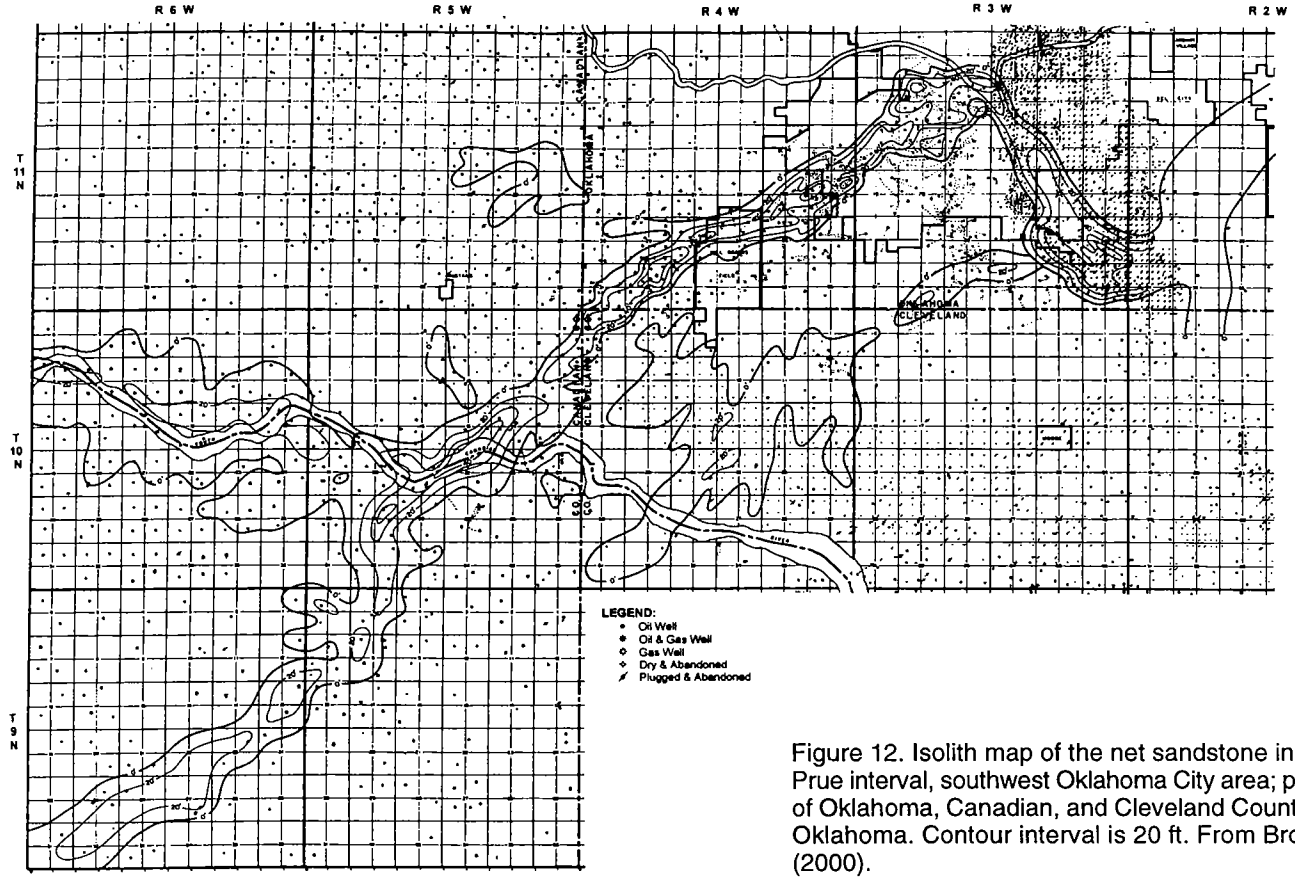

Figure 12. Isolith map of the net sandstone in the Prue interval, southwest Oklahoma City area; parts of Oklahoma, Canadian, and Cleveland Counties, Oklahoma. Contour interval is 20 ft. From Broker (2000).

Core Descriptions

Four cores of the Prue Sandstone were sampled and described, of which one is described (Fig. 14). The cores were examined for lithology, grain size, sedimentary structures, and mineralogical constituents. Electric logs were used in conjunction with the cores to link specific log signatures to depositional facies and environments. Although additional core from this area is available, it has not been included here. The core selected was chosen based on its location, the interval cut, and its gamma-ray signature. More detailed data on this and other cores examined can be found in Broker (2000).

The cored interval of the Booth 9D-2 well is from 6,644 to 6,750 ft (Figs. 15–20) and was cut from the base of the Oswego, through the Prue and Verdigris, and into the top of the Skinner shale.

The Oswego is mottled-gray, microcrystalline limestone with small amounts of fossil debris. At the top of the Prue sandstone is a 2-ft-thick calcareous mudstone. Below this is the Prue sandstone, which is light-gray, fine- to very fine grained micaceous sand, with varying degrees of sorting. The sandstone itself is well sorted, but abundant shale partings give the overall sorting a moderate to poor rating. For this well, this overall sorting rating is more a reflection of reservoir heterogeneity than sand quality. Sedimentary structures are minimal throughout the Prue section. Porosity values for the Prue sand range between 6% and 17 %. The base of the sandstone shows an erosional contact with the Verdigris Limestone. Immediately above the erosional contact (at 6,738 ft) are a large number of mud rip-up clasts. These shale clasts increase the average gamma-ray reading for this interval, in spite the sand itself being quite clean. The Verdigris is a mottled, gray limestone with dispersed crinoid fragments. At its base is a thin bed of coal, which rests on the Skinner shale. This shale is probably marginal marine in origin and is indistinctly laminated and contains some fossil hash.

Stratigraphic Cross Sections

The locations of the eight cross sections constructed in this study are shown in Figure 21, although only three are included here. Cross section A–A′ is a regional dip-section extending across the length of the study area from the southwest to northeast. The other two cross sections (B–B′, C–C′) are perpendicular to the regional trend of the channel. The datum for all of the sections is the top of the Oswego Limestone. Solid lines indicate conformable contacts and dashed, erosional

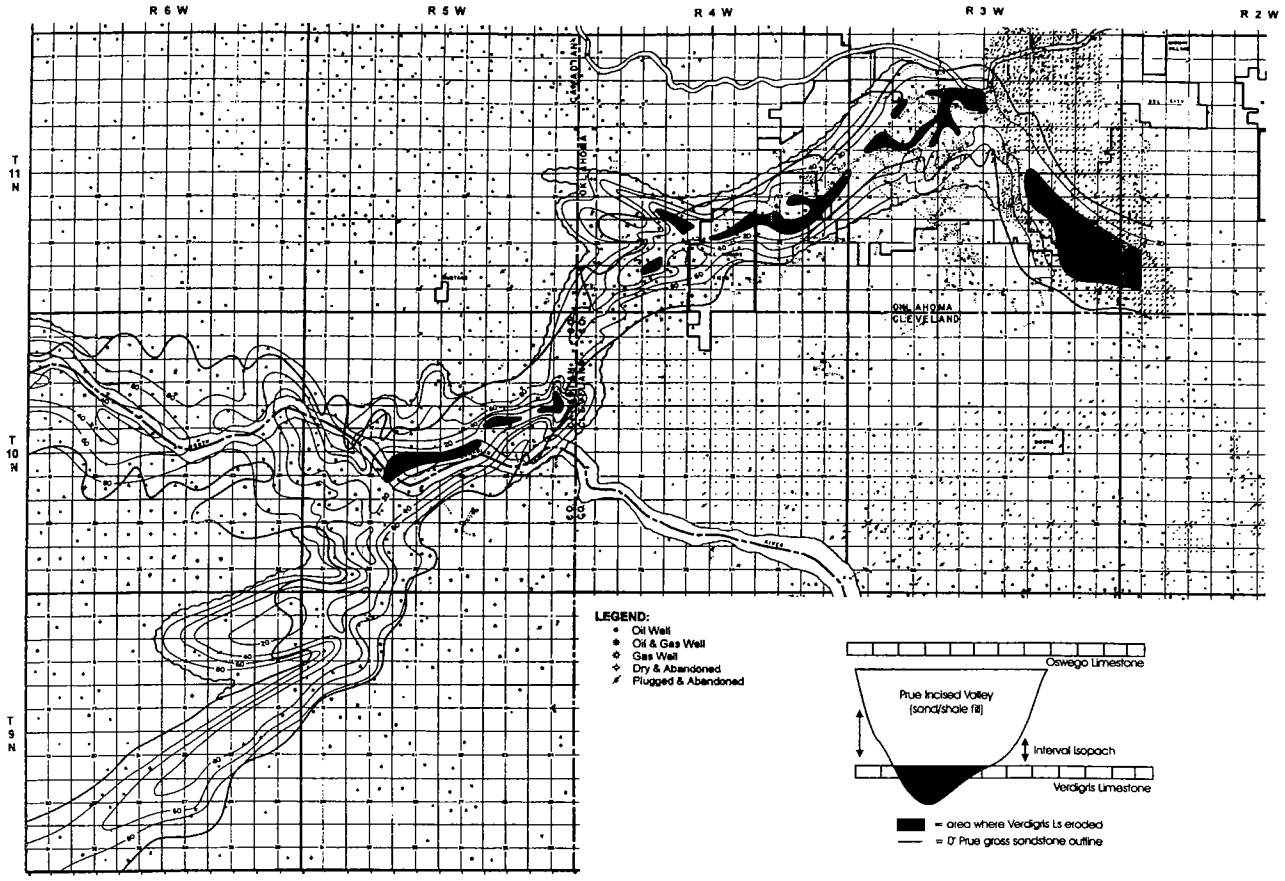

Figure 13. Isopach map of the interval from the base of the Prue channel incision to the top of the Verdigris Limestone in the southwest Oklahoma City area; parts of Oklahoma, Canadian, and Cleveland Counties, Oklahoma. Contour interval is 10 ft; solid areas denote areas of erosion of Verdigris Limestone. From Broker (2001).

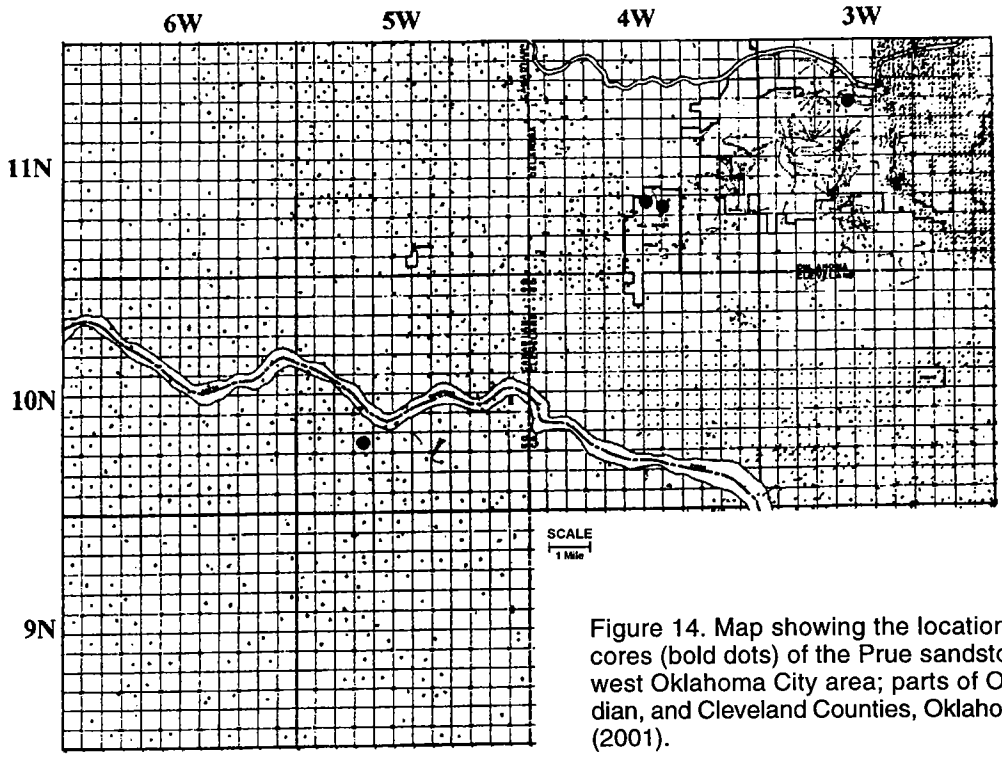

Figure 14. Map showing the location of the sampled cores (bold dots) of the Prue sandstone in the southwest Oklahoma City area; parts of Oklahoma, Canadian, and Cleveland Counties, Oklahoma. From Broker (2001).

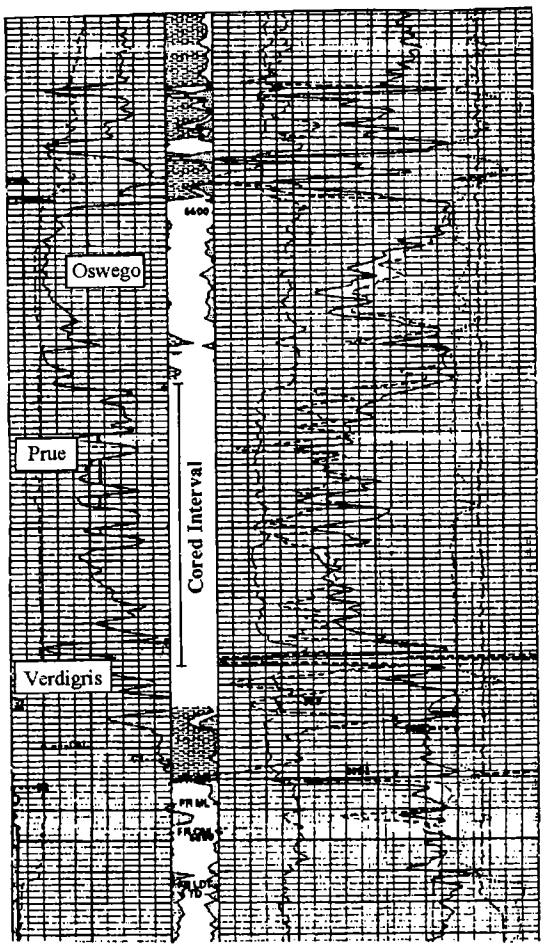

Figure 15. Neutron-density log of the Petrocorp Booth No. 9D-2, sec. 9, T. 11 N., R. 3 W., showing the cored interval of the Prue sandstone. From Broker (2001).

(unconformable). As a result of their wide separation, the Prue interval varies significantly in log character and in thickness in these cross sections. Their placement was selected to show channel geometry and the depth of incision.

Cross Section A–A′

Cross section A–A′ (Fig. 22) extends from the southwestern corner of the study area to the western edge of the Oklahoma City Uplift. Covering a larger stratigraphic interval than the other cross sections, its datum is the top of the Oswego limestone, and this cross section shows thinning of the entire stratigraphic section below the Oswego as the Oklahoma City Uplift is approached. This thinning is also illustrated in Gatewood's pre-Pennsylvanian subcrop map and cross section seen in Figure 6.

Cross Section B–B′

Cross section B–B′ is perpendicular to the Prue channel in the central part of T. 10 N., R. 5 W. (Fig. 23). This cross section includes North Mustang Field, where all wells are productive in the underlying Hunton Formation. Erosion of the Verdigris Limestone is seen in the Robberson 15-2 and 14-6 wells. The non-channel wells on this cross section indicate poorly developed Prue sands occurring near the top of the Prue interval. These were most likely deposited in the marginal-marine delta-front system shown on the gross Prue sand maps (Fig. 11). It is believed that this delta was deposited prior to the valley incision. Maximum sand thickness is found in the Robberson 15-2, where 60 ft of net and gross sand was deposited with porosities of 12% and 14%. The Robberson log shows stacked channel sands separated by 15 ft of shale.

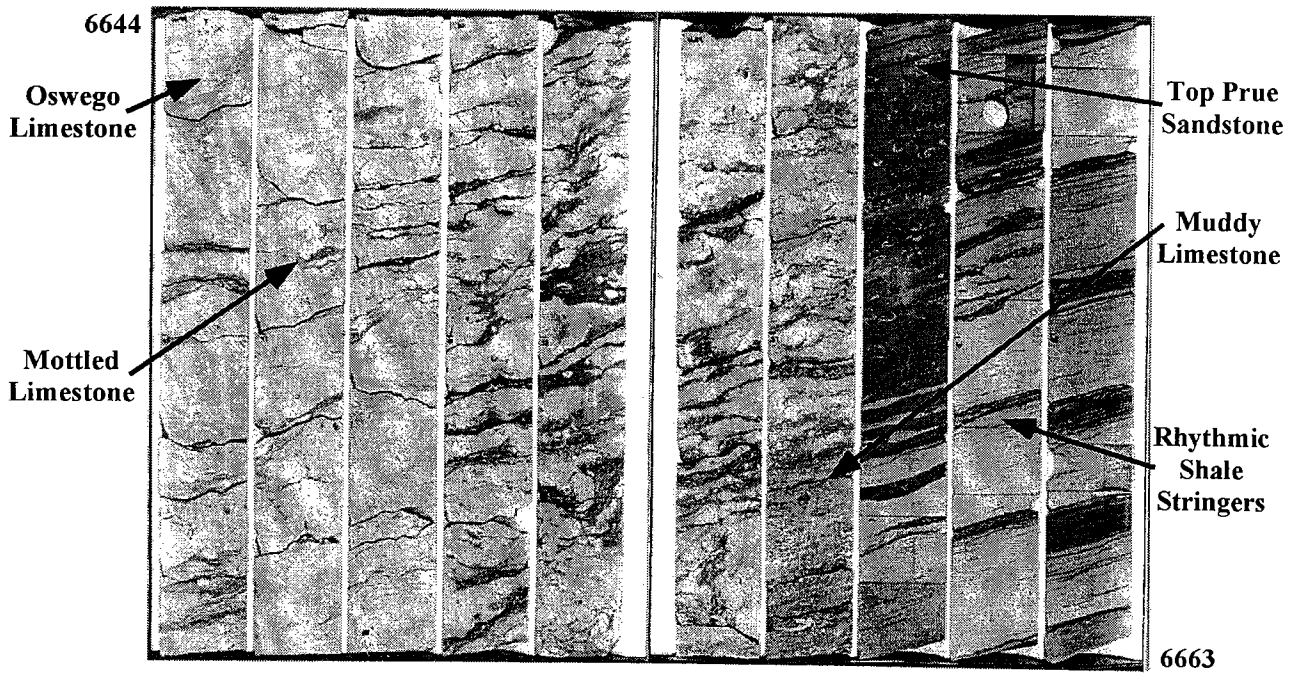

Figure 16. Photograph of the core interval from 6,644–6,663 ft of the Petrocorp Booth No. 9D-2, sec. 9, T. 11 N., R. 3 W. From Broker (2001).

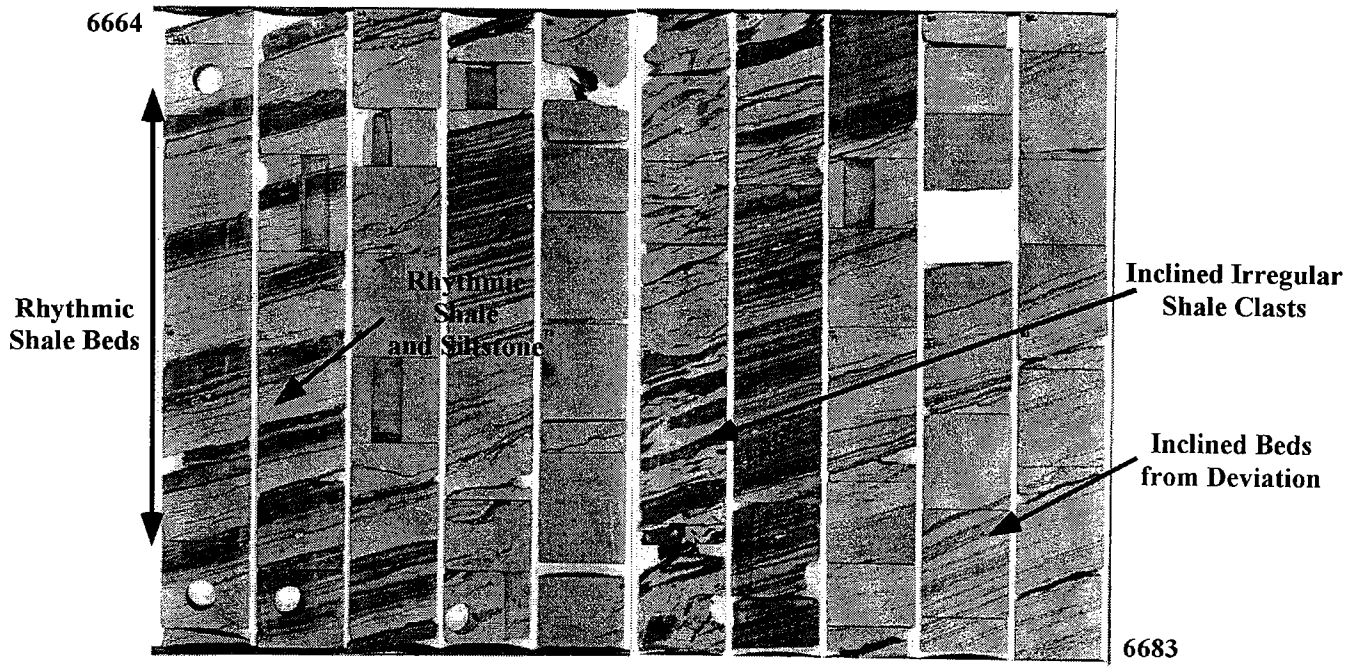

Figure 17. Photograph of the core interval from 6,664–6,683 ft of the Petrocorp Booth No. 9D-2, sec. 9, T. 11 N., R. 3 W. From Broker (2001).

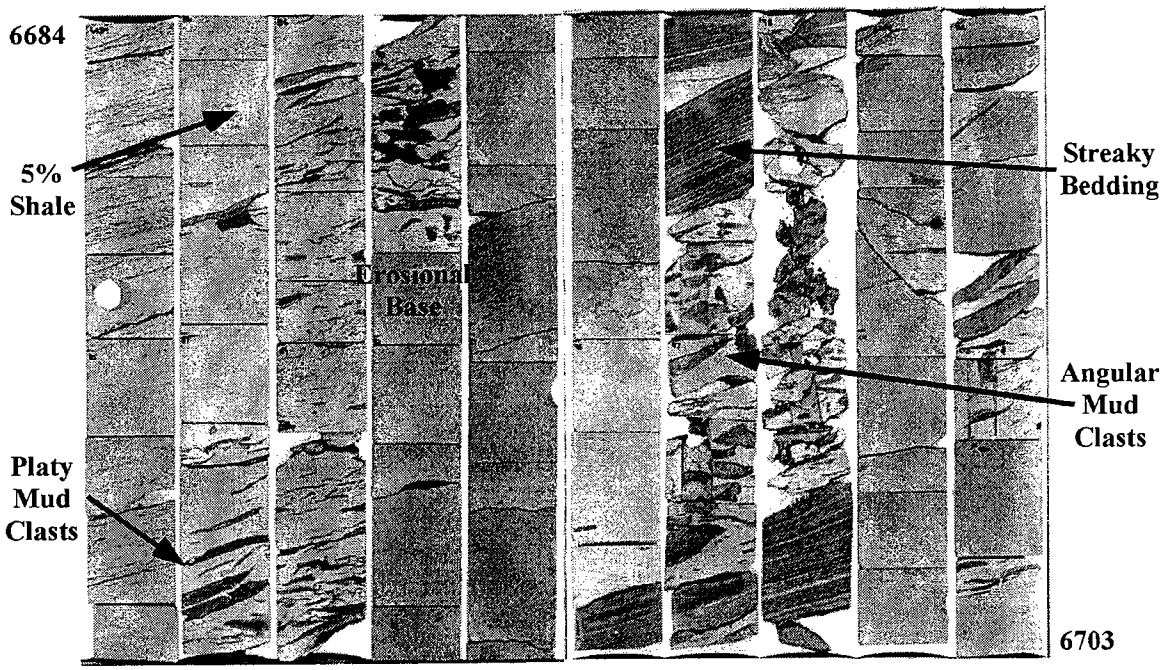

Figure 18. Photograph of the core interval from 6,684–6,703 ft of the Petrocorp Booth No. 9D-2, sec. 9, T. 11 N., R. 3 W. From Broker (2001).

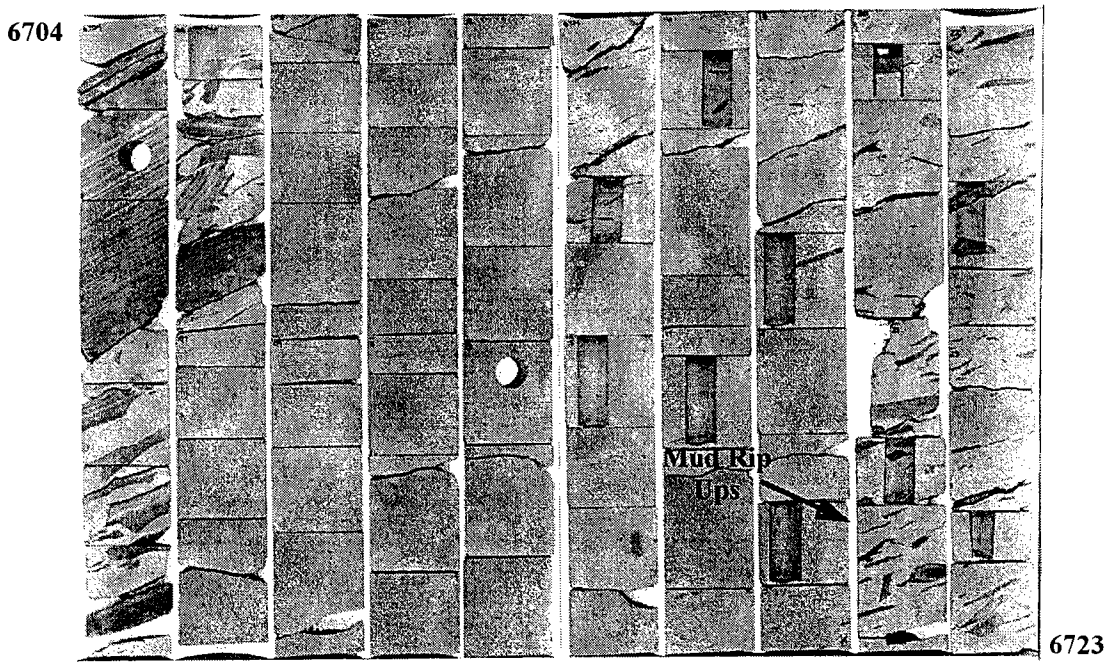

Figure 19. Photograph of the core interval from 6,704–6,723 ft of the Petrocorp Booth No. 9D-2, sec. 9, T. 11 N., R. 3 W. From Broker (2001).

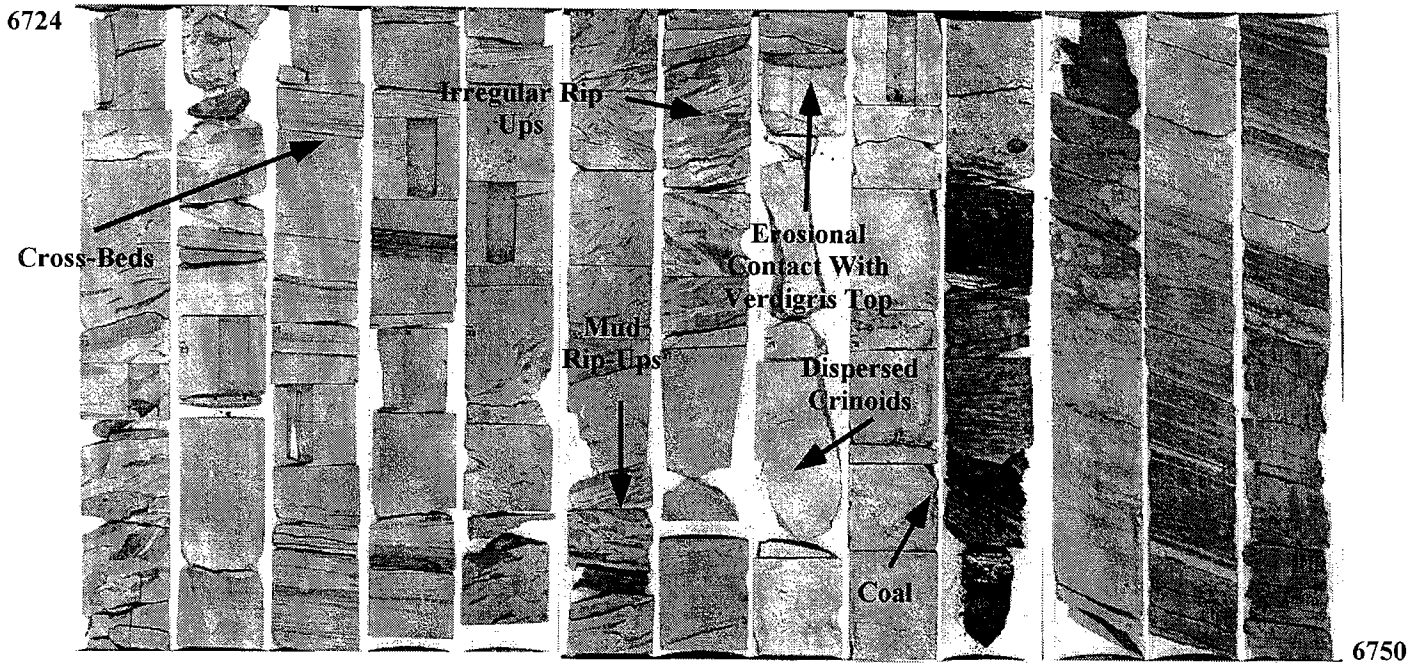

Figure 20. Photograph of the core interval from 6,724–6,750 ft of the Petrocorp Booth No. 9D-2, sec. 9, T. 11 N., R. 3 W. Note erosional contact on top of Verdigris limestone at 6,738 ft with rip-up clasts in overlying beds. From Broker (2001).

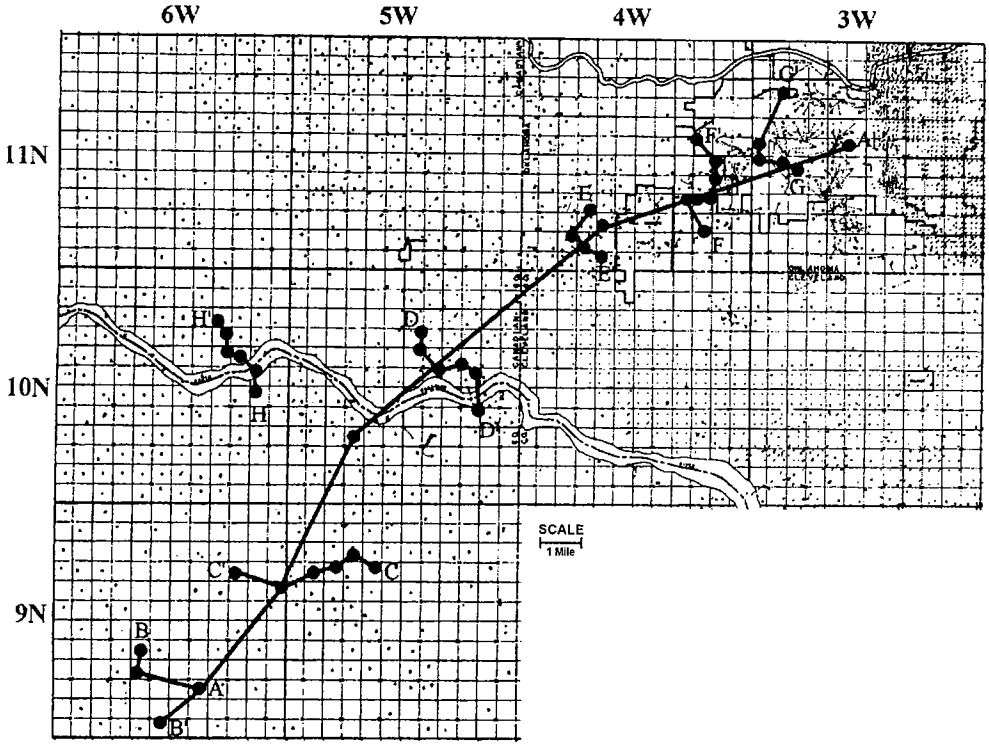

Figure 21. Map showing the locations of the stratigraphic cross sections in the southwest Oklahoma City area; parts of Oklahoma, Canadian, and Cleveland Counties, Oklahoma. Only cross sections A–A′, B–B′, and C–C′ are presented herein. From Broker (2001).

Cross Section C–C′

Cross section C–C′ (Fig. 24) is located in the northeast corner of the study area where the Prue sand crosses the western edge of the Oklahoma City Field. The overall thinning of the Prue interval is evident on this cross section, whereas the interval has thinned to less than 20 ft in the USF&G 20B-2 well (Well #1). This may indicate the presence of the previously discussed paleo-high. The incised valley cuts through the Verdigris in the USF&G 19B-2 and Rowland 1-13 wells. The USF&G 19B-2 well penetrates an excellent example of a mud-filled channel. There, the channel contains a 10 ft non-porous sand at its base and a thick shale sequence through the rest of the channel. The adjacent well, the Rowland 1, contains 56 ft of net and gross sand with 15–16% porosity that fills the entire interval from the top of the Verdigris to the base of the Oswego.

INCISED-VALLEY–FILL DEPOSITIONAL MODEL

The study of incised valleys has a history dating back more than 50 years, although no clear understanding of how they formed and were later filled was known at that time. Van Wagoner and others (1990) defined incised-valley fills as entrenched fluvial systems that extended and deepened their valleys as a result of a fall in sea level. Landward extension occurred through headward (upstream) erosion and basinward extension through downcutting into unconsolidated marine sediments. (Fig. 25). Zaitlin and others (1994, p. 1) defined the term "incised valley" as a "fluvial-eroded, elongate topographic low that is typically larger than a single channel form, and is characterized by an abrupt seaward shift of depositional facies across a regionally mappable sequence boundary at its base." According to these authors, the fill typically begins to accumulate in the eroded valley during the next base-level rise, and may contain deposits of the following highstand and subsequent sea-level cycles. Zaitlan and others (1994, p. 167) summarized their study by saying, "the fill of an incised valley may be extremely complex, no single facies succession (upward-coarsening, blocky, etc.) occurs along the entire length of the system" (Fig. 26).

Prue Valley-Fill System

Based on the evidence presented previously herein, parts of the Prue in the study area meet the requirements to be classified as an incised-valley–fill system. As described previously, the Prue truncates a regional marker, the Verdigris Limestone. The valley is also a negative, erosional paleogeographic feature. This can be clearly seen from the cross sections that were constructed across the channel. The Booth 9D-2 core also shows the erosional characteristics within the Prue interval, based on the presence of numerous rip-up clasts that were eroded from the underlying sediment or rock. This complex is also clearly larger than a single channel, which is seen on both the net and gross Prue sand maps. Finally, the base of the valley is a surface of regional extent that can be traced throughout the study area.

Prue sand deposition here shows the characteristics of a simple coastal-plain–fill system. The sediment present is fine grained and mature and was deposited on a low to moderate gradient with no evidence of a rapid break in elevation ("fall line") between upland and lowland. The presence of stacked (multi-storied) sand bodies indicates multiple incisions, but, with no evidence of sea-level changes, it is assumed that this is a simple fill system.

PETROLEUM GEOLOGY

The depositional model developed above was combined with regional reservoir analysis and developments in completion technology to reevaluate previously drilled Prue sandstone reservoirs (Broker, 2001). The successful drilling of six wells and recompletion of three more has delineated a 1,500,000 BO (barrels of oil) reservoir in a mature area located a scant 3 mi southwest of Will Rogers World Airport (Fig. 27).

Prue Development History

The Prue sandstone was first recognized as productive by McGee and Clawson (1932) as the giant Oklahoma City field was being developed. The open-hole–completion techniques used in the 1930s probably allowed Prue oil to be produced commingled with Simpson sands.

In 1965, Cities Service initiated a waterflood project for the Prue in the southern part of Oklahoma City Field. No further development of the Prue sandstone took place until 1981, when a Mississippian objective well was drilled at Will Rogers World Airport, 10 mi west of Oklahoma City Field. The well encountered 60 ft of productive Prue sandstone with 14–16% porosity. Development of the discovery eventually tied a Prue incised-valley–fill (IVF) sandstone eastward into the old Oklahoma City Field production first described by McGee and Slawson (1932) (see Fig. 27).

Three waterflood units are currently producing Prue reserves. Primary production from these units was 8,000,000 BO and 47 billion cubic feet of gas (BCFG). Waterflooding has recovered an additional 3,000,000 BO with ultimate waterflood recovery expected to be equivalent to that produced during primary production. Most of the wells in these three units were initially completed with "state of the art" diesel- or oil-fracture treatments and had good to excellent results. Initial production per well was occasionally >1,000 barrels of oil per day (BOPD) and some wells had cumulative production of >200,000 BO during primary recovery.

Recent Prue Developments

Downdip and southwest of these significant reservoirs, the Prue was recognized as hydrocarbon bearing in the early 1970s by companies operating in the southern part of North Mustang Field (Fig. 27) in Canadian County. The North Mustang Field is primarily a Hunton Limestone producer (Kirk, 1974).

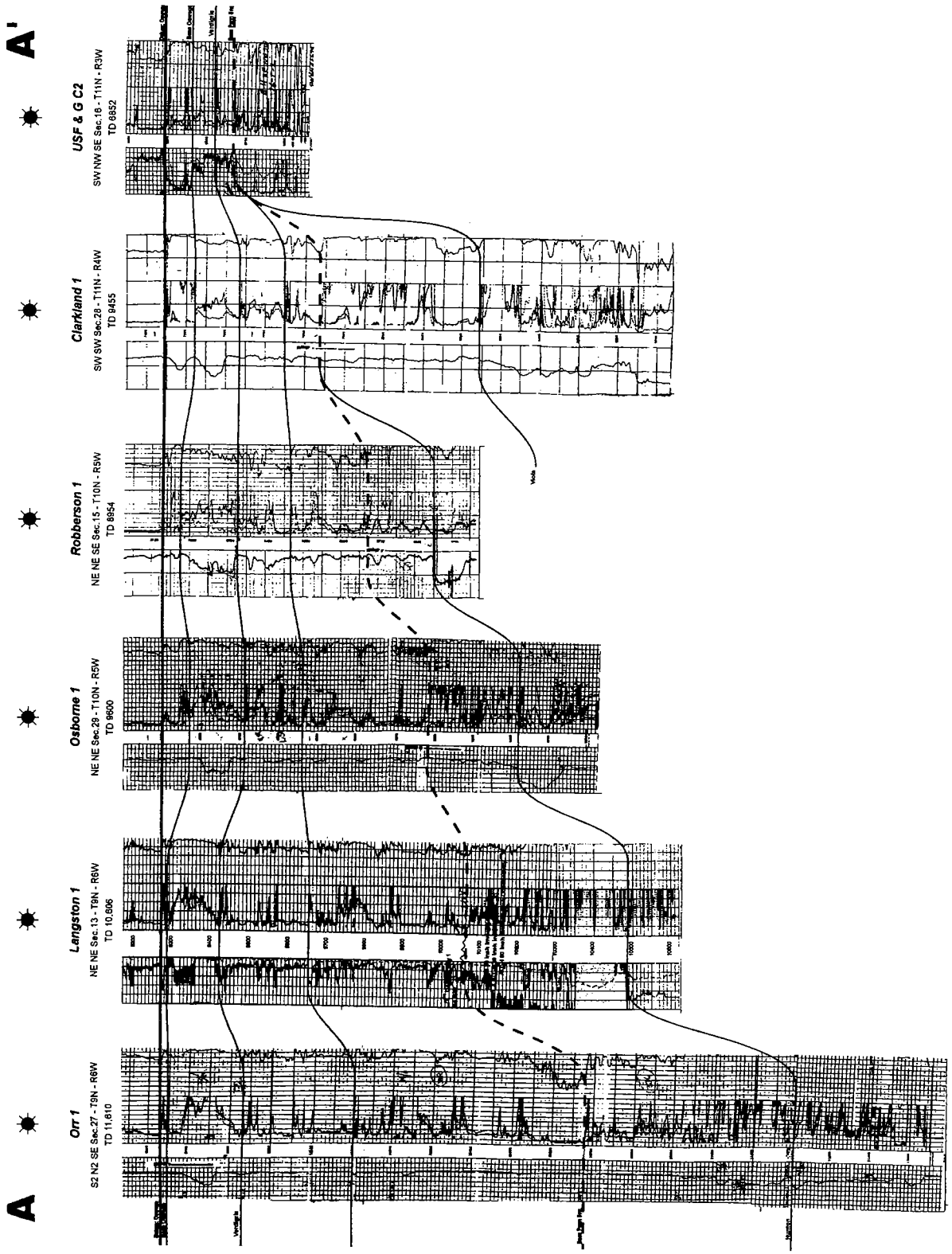

Figure 22. Stratigraphic cross section A–A' from southwest to northeast across the southwest Oklahoma City area; parts of Oklahoma, Canadian, and Cleveland Counties, Oklahoma. Datum is the top of the Oswego limestone. No vertical or horizontal scale. See Figure 21 for location of cross section. Modified from Broker (2001).

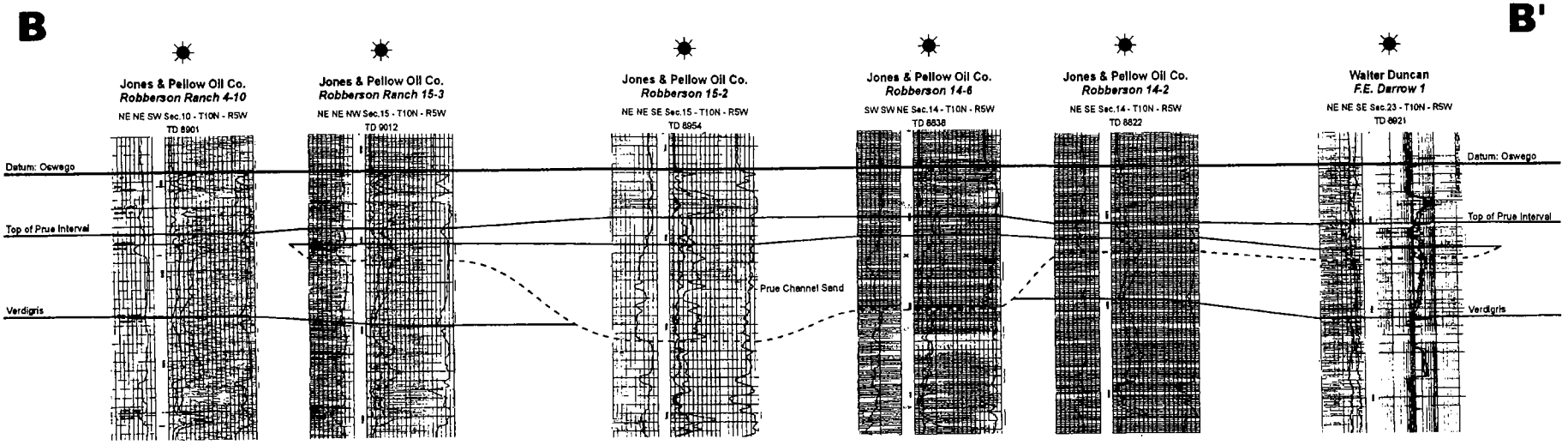

Figure 23. Stratigraphic cross section B–B′ across the Prue channel in T. 10 N., R. 5 W., southwest Oklahoma City area; parts of Oklahoma, Canadian, and Cleveland Counties, Oklahoma. Datum is the top of the Oswego limestone. No vertical or horizontal scale. See Figure 21 for location of cross section. Modified from Broker (2000).

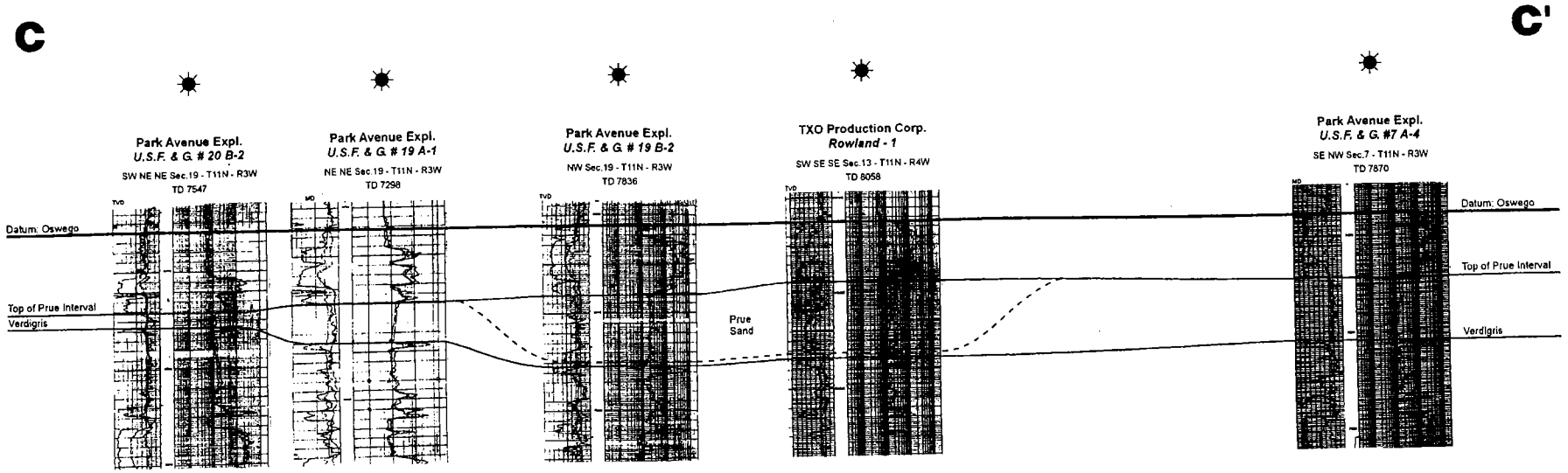

Figure 24. Stratigraphic cross section C–C′ across the Prue channel in T. 11 N., R. 3 W., southwest Oklahoma City area; parts of Oklahoma, Canadian, and Cleveland Counties, Oklahoma. Datum is the Oswego limestone. No vertical or horizontal scale. See Figure 21 for location of cross section. Modified from Broker (2000).

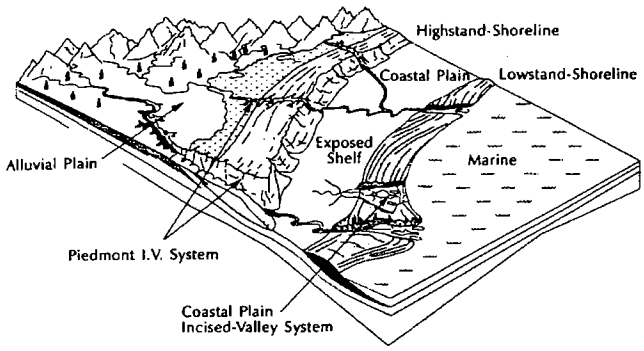

Figure 25. Schematic view of a coastal zone showing the distinction between piedmont and coastal-plain incised-valley systems. From Zaitlin and others (1994, p. 51).

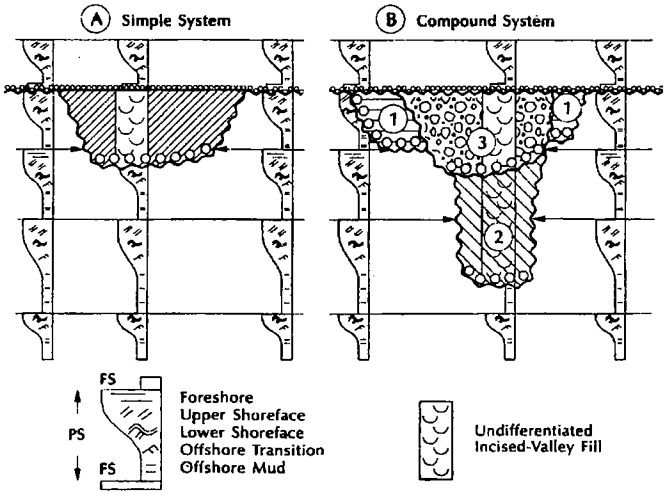

Figure 26. (A) Simple incised-valley fill. (B) Compound incised-valley fill (circled numbers 1, 2, and 3 represent different incised-valley fills, with 1 the oldest). From Zaitlin and others (1994, p. 52).

The Prue sandstone in the Robberson Ranch area, located on the southern end of the North Mustang field, has channel characteristics and a sand thickness in excess of 75 ft (Fig. 28). From 1973 through 1975, three wells drill stem tested the Prue sandstone in the Robberson Ranch area, and all recovering free oil. The well in the NE¼ sec. 15, T. 10 N., R. 5 W., recovered only 200 cc of oil- and gas-cut mud in 1973. In 1983 the well was reentered and dually completed in the Red Fork and Prue sands with an initial rate of 60 BO and 10 barrels of water per day (BWPD). The second well that tested the Prue, located in the NE¼ sec. 14, T. 10 N., R. 5 W., on a drill-stem test in 1974 recovered 1,000 cc of oil with a shut-in pressure of 3,004 psi.

The following year, the Jones and Pellow Robberson Ranch No.15-2, NE¼NE¼SE¼ sec. 15, T. 10 N., R. 5 W., recovered 6,000 ft of free oil on a drill-stem test with shut-in pressure of 3,254 psi from 75 ft of net sand (Fig. 29). A completion in the deeper Hunton was not successful and the well was completed from the Prue. The Prue was fracture treated with 13,000 lbs of sand and 476 bbl of 3% acid water, a treatment that was then considered "state of the art." The Prue was then commingled with the Skinner and Red Fork sandstones for a combined initial production rate of 55 BOPD. Cumulative production from these three zones is 47,740 BO and 90 million cubic feet of gas (MMCFG).

The Prue sandstone in the Robberson Ranch area was recognized in 1982 as the basinward equivalent of the IVF system that was productive to the northeast under the Will Rogers World Airport (Fig. 27). In that same year, Czar Resources drilled the Osborn No. 1-29 well in the NE¼SW¼NE¼ sec. 29, T. 10 N., R. 5 W. specifically for the Prue sandstone (Fig. 30). The well was cored and encountered 70 ft of clean Prue sandstone with 9–12% porosity. The well was completed with a "state of the art" diesel-fracture treatment and initially produced 38 BOPD but was soon pumping only 5 BOPD. The well has a cumulative production of 5,662 BO and 100 MMCFG in 16 years of production.

Between 1982 and 2000, several additional wells were drilled for completions in the Prue sandstone in the Robberson Ranch area but with minimal success. Fracture treatments were with water or diesel gel and small volumes of sand. In the 1990s, foam-fracture treatments of the Lower Pennsylvanian sands in Grady County, Oklahoma, south of the Robberson Ranch area, became the standard. Initial production and the ultimate reserves for these wells were significantly greater than that seen from wells fractured with diesel gel. Also, a factor was the fact that the amount of sand used during the treatments was increased substantially.

In 2001, the Louis Dreyfus Natural Gas Co. (now Dominion E & P) completed the Turnpike Federal No. 1-22, SW¼NE¼NW¼ sec. 22, T. 10 N., R. 5 W., in the Robberson Ranch area from three formations (Fig. 31). Given the fracturing success in Grady County area, the Prue and Skinner sands were individually fracture treated with foam and sand during one continuous operation and immediately commingled for testing. The Prue was fracture treated with 152,000 lbs of 20/40 sand and 794 bbls of 65 quality Binary foam at 25 barrels per minute (BPM) through 4½-in. casing. The well flowed through casing for 16 days, averaging 279 BOPD and 211 MCFGD before being commingled with the Mississippian. One year's production indicated a greatly improved productivity relative to the older-style Pennsylvanian sand completions.

A development-drilling program was commenced to exploit these Pennsylvanian reserves, with special attention given to the Prue. Reserves for the Prue reservoir, based on 80-acre spacing, are anticipated to be >100,000 BO per well. Six successful Prue development wells have now been completed and drilling continues. Several older Hunton wells also have been recompleted in the Prue using these stimulation procedures. Initial estimates for total field reserves are over 1,500,000 BO during primary recovery. The Prue will likely be water flooded in the future.

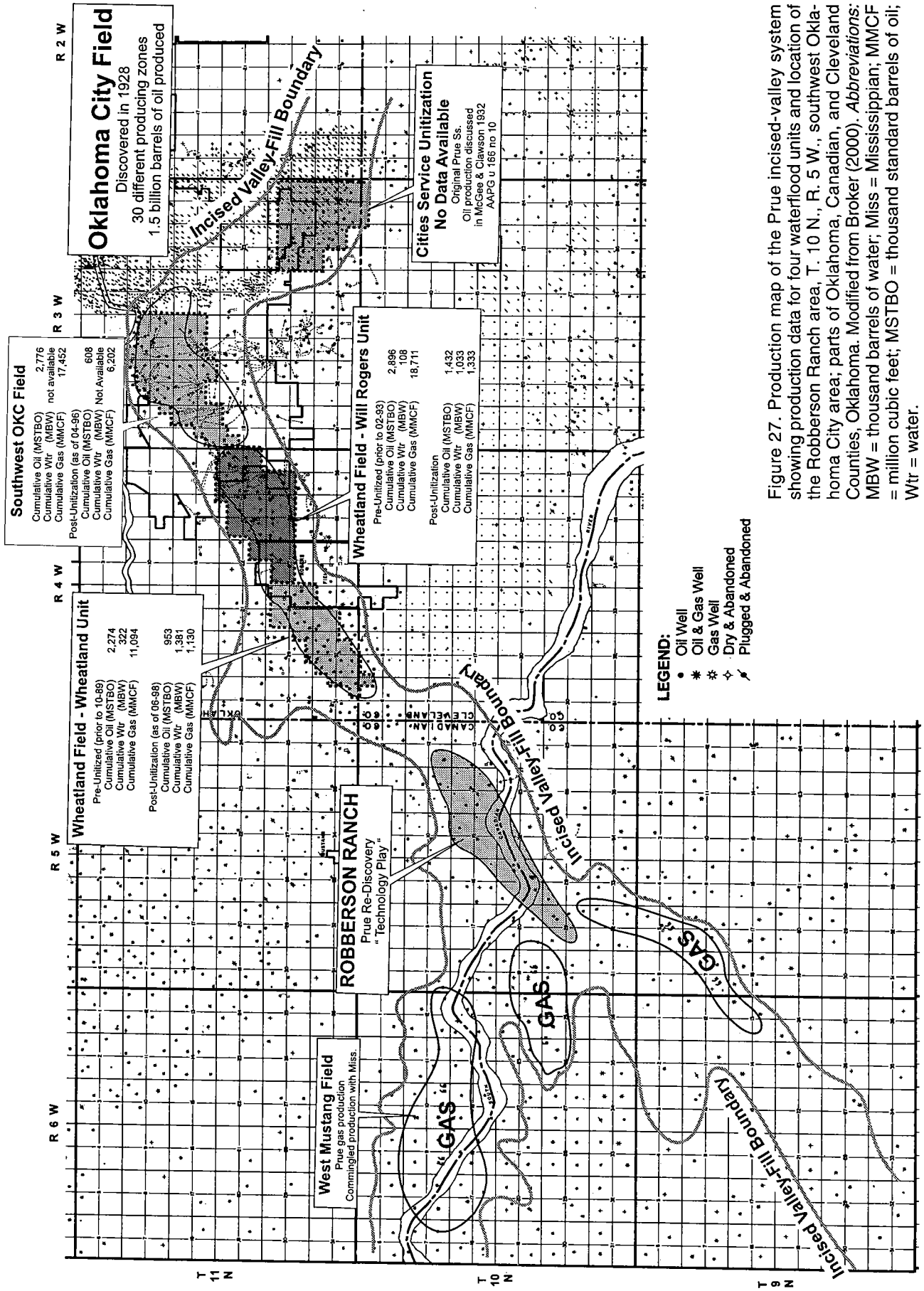

Figure 27. Production map of the Prue incised-valley system showing production data for four waterflood units and location of the Robberson Ranch area, T. 10 N., R. 5 W., southwest Oklahoma City area; parts of Oklahoma, Canadian, and Cleveland Counties, Oklahoma. Modified from Broker (2000). *Abbreviations:* MBW = thousand barrels of water; Miss = Mississippian; MMCF = million cubic feet; MSTBO = thousand standard barrels of oil; Wtr = water.

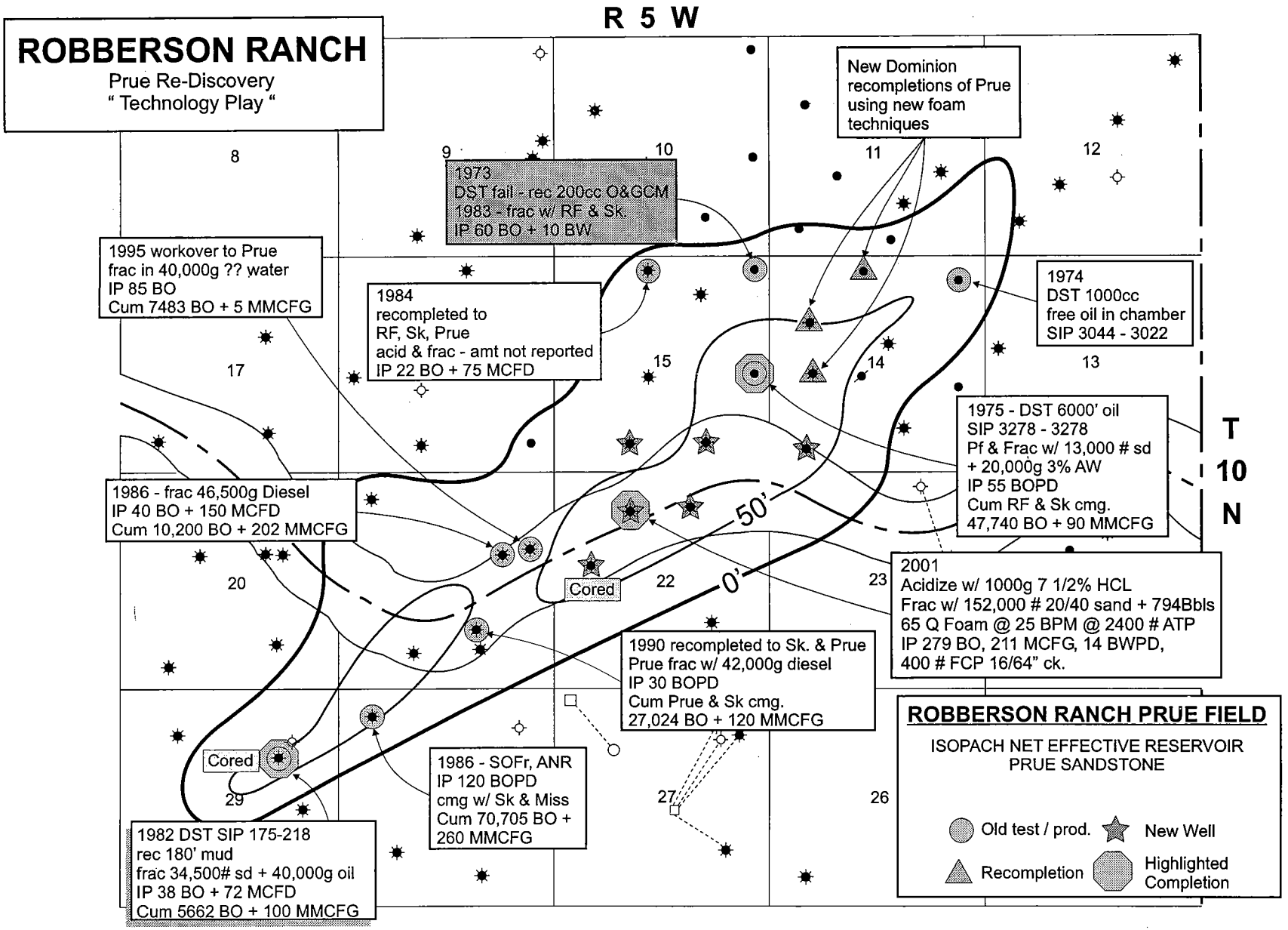

Figure 28. Isopach map showing selected Prue well completions and net effective Prue sand reservoir, Robberson Ranch area, North Mustang Field, southwest Oklahoma City area; parts of Oklahoma, Canadian, and Cleveland Counties, Oklahoma. Contour interval is 50 ft. *Abbreviations:* BO = barrels of oil; BWPD = barrels of water per day; Cgm = commingled; ck = choke; Cum = cumulative; DST = drill-stem test; frac = fractured; IP = initial production; MCFD = thousand cubic feet per day; MCFG = thousand cubic feet of gas; Miss = Mississippian; MMCFG = million cubic feet of gas; O&GCM = oil- and gas-cut mud; Pf = perforated; rec = recovered; RF = Red Fork; sd = sand; SIP = shut-in pressure; sk = Skinner.

Jones & Pellow
Robberson 15-2
NE NE SE sec. 15 - 10N - 5W
TD 8,954 ft
1974

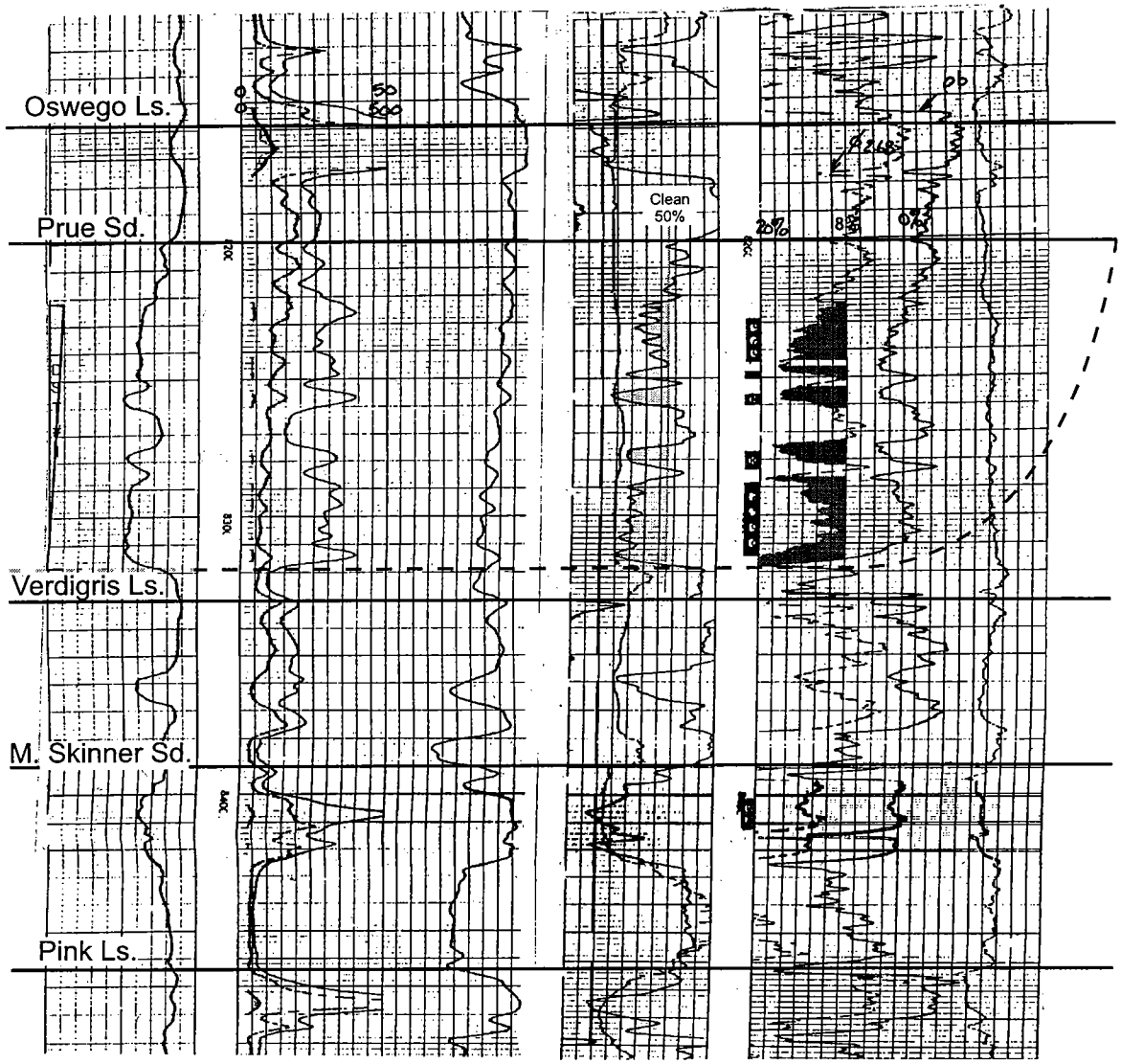

DST Prue Ss. 8222 - 8318 30/60/60/120
Rec. 6000' oil, 468' HO&GCM
FP 142 - 254 # SIP 3278 - 3278 #

Perf 8229 - 8314 OA acid 3000g 7 ½%
Frac 13,000# sand + 20,000g (476 bbl)
3% AW

Commingled w/ Redfork & Skinner
IP 55 BOPD

Cum. Prod. 47,740BO + 90 MMCFG

Figure 29. Electric log of the Prue interval, Jones and Pellow Robberson No. 15-2, NE¼NE¼SE¼ sec. 15, T. 10 N., R. 5 W., showing the log characteristics, testing, completion, and production data for the Prue sandstone, Robberson Ranch area. *Abbreviations:* bbl = barrels; BOPD = barrels of oil per day; DST = drill-stem test; FP = flow pressure; Frac = fractured; HO&GCM = heavy-oil- and gas-cut mud; IP = initial production; MMCGG = million cubic feet of gas; SIP = shut-in pressure.

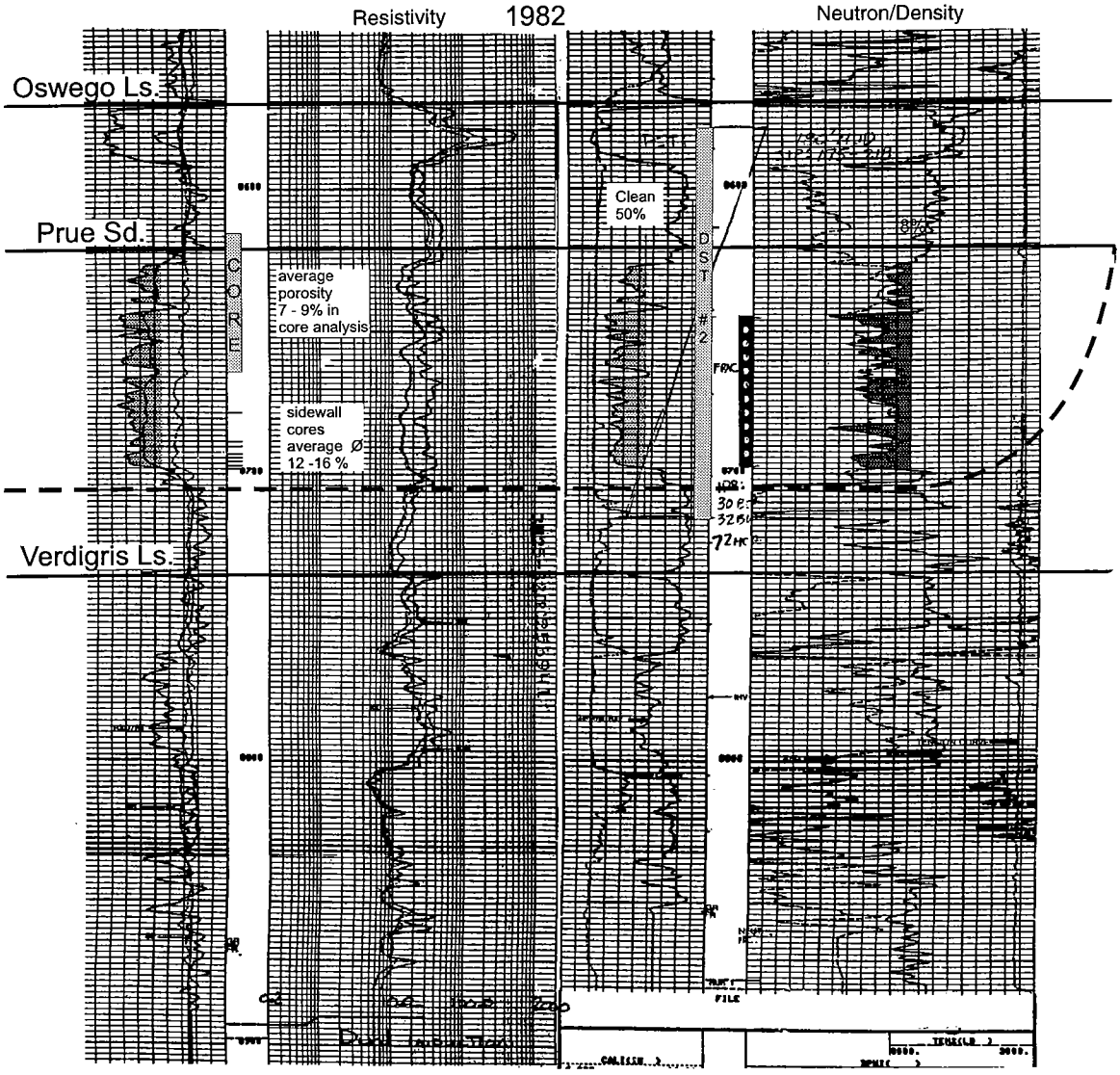

Core 8615 - 8666' primarily tight clean sand
Sidewall cores 8678 - 8697 12 - 16% porosity 8-21 MD perm.
DST #2 8580 - 8715' 30/60/60/120
FP 51 - 74 SIP 175 - 218
rec. 180' mud
Perfs 8645 - 8697 OA 18 holes, breakdown pfs with
4000g diesel & balls
Frac w/ 34,500 # 20/40 sand & 40,000g (952 bbls)
diesel oil @ 37 BPM @ 3590 # down 5 ½"csg.

IP 38 BO + 32 BW + 72 MCFD
Cum. Prod. 5662 BO + 100 MMCFG

Figure 30. Electric log of the Prue interval, Czar Resources Osborn No. 1-29, NE¼SW¼NE¼ sec. 29, T. 10 N., R. 5 W., showing the log characteristics, testing, completion, and production data for the Prue sandstone, Robberson Ranch area. *Abbreviations:* bbls = barrels; BO = barrels of oil; BW = barrels of water; csg = casing; Cum Prod = cumulative production; DST = drill-stem test; FP = flow pressure; Frac = fractured; IP = initial production; MCFD = thousand cubic feet per day; MD = millidarcies; MMCGG = million cubic feet of gas; perm = permeability; SIP = shut-in pressure.

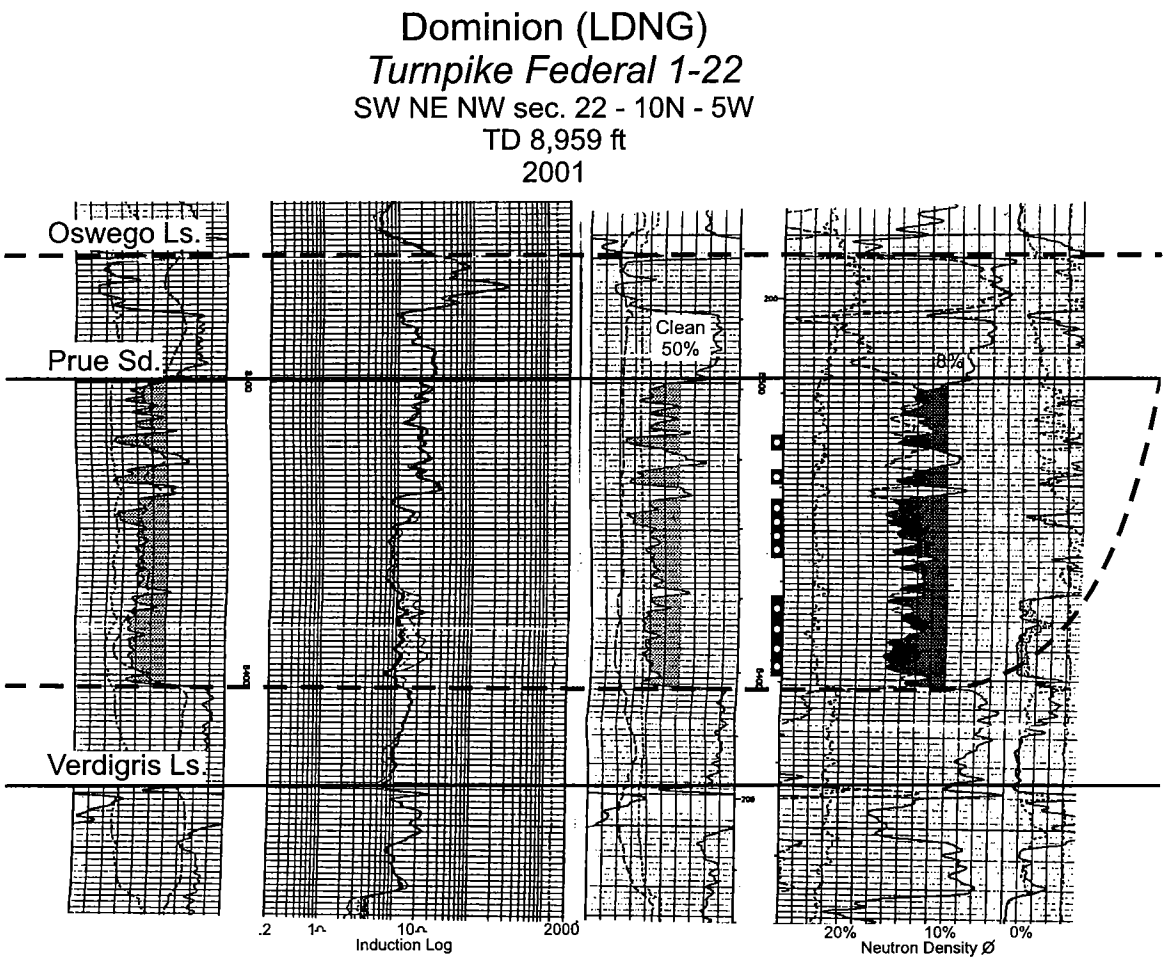

Perf: Prue 8317 - 8398 OA
Acidize 1000g 7 1/2% HCL,
Frac w/ 152,000 # 20/40 sand & 794 Bbls 65 Quality
Binary Foam @ 25BPM @ 2400 # ATP down 4 ½"csg.

IP 279 BO, 211 MCFD, 14 BWPD w/ 400 # FCP 16/64" ck.
Flowed up csing for 16 days, snub tbg in hole.
Commingled w/ Mississippian

Figure 31. Electric log of the Prue interval, Dominion (LDNG) Turnpike Federal No. 1-22, SW¼NE¼NW¼ sec. 22, T. 10 N., R. 5 W., showing the log characteristics, testing, completion, and production data for the Prue sandstone, Robberson Ranch area. *Abbreviations:* Bbls = barrels; BO = barrels of oil; BPM = barrels per minute; ck = choke; csg = casing; Frac = fractured; IP = initial production; MCFD = thousand cubic feet per day; tbg = tubing.

Completion Treatments

Fracture treatments in this area became much more effective with the use of foams. The progression from very small fracture treatments using gelled acid water and glass beads, to diesel and 40,000 lbs of sand, to foam and 150,000 lbs of sand, has all taken place in the last 30 years. The Prue sandstone in the Robberson Ranch area was recognized as potentially productive during early development of the Hunton reserves, but fracture technology was not adequate to make commercial completions. Another factor in the evolution of fracture treatments in this area is the decreasing porosity. In the Oklahoma City Field porosity varies from 16 to 18%, but in the distal and downdip area of Robberson Ranch, porosity varies from only 10 to 12%. This decrease in porosity is sufficient to cause water blockage with fluid-based fracture treatments. The use of foam as a component during fracture treatments has turned a bypassed reservoir into a significant producer. As stimulation technologies continue to advance, geologists and reservoir engineers must revisit mature areas searching for bypassed reserves. As tighter reservoirs are drilled, it must be recognized that fluid blockages created during the completion procedures (stimulation and tripping) can greatly reduce or completely inhibit

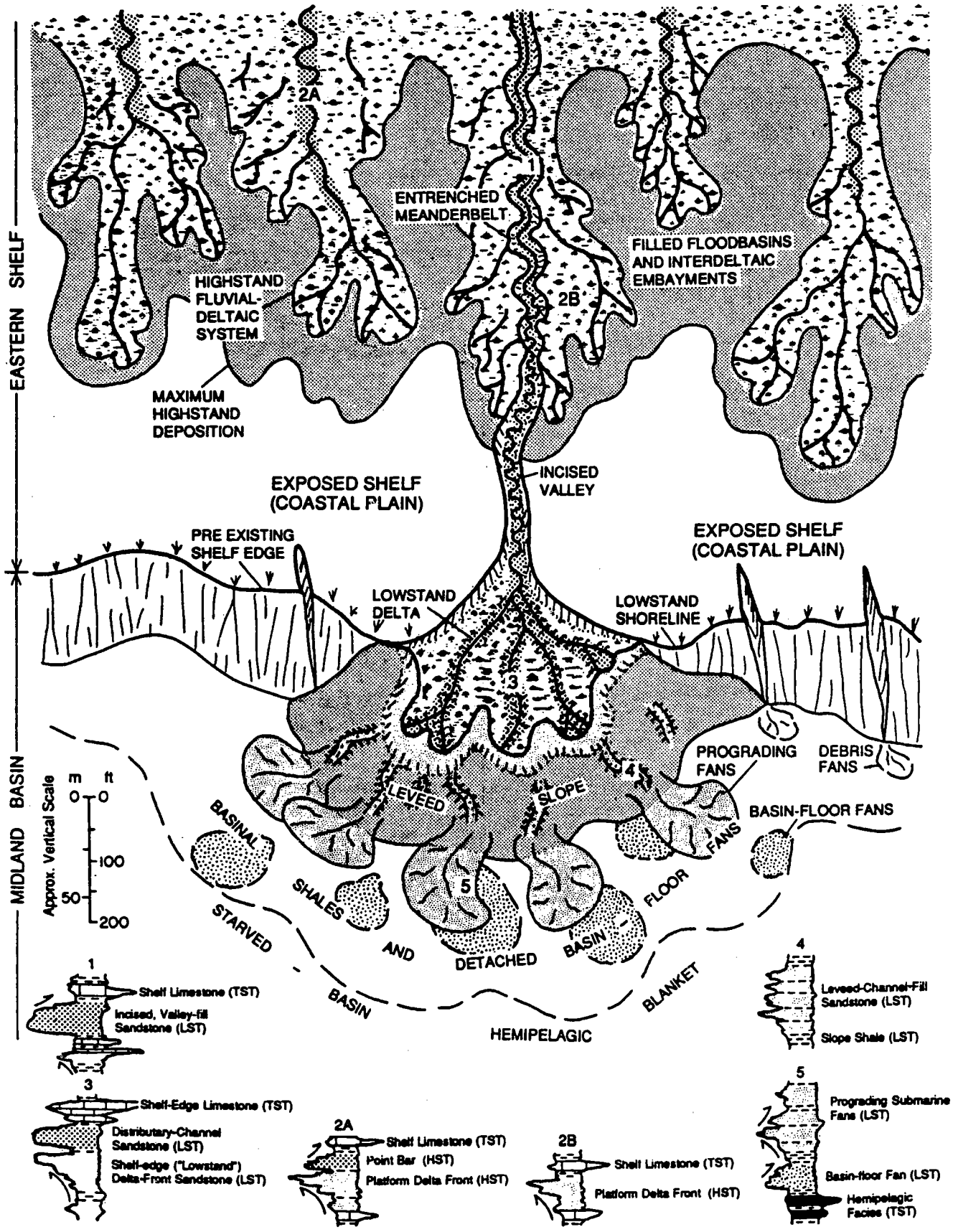

Figure 32. Schematic diagram showing the depositional systems tracts. *Abbreviations:* HST = highstand systems tract; LST = lowstand system tract; TST = transgressive systems tract, at maximum progradation of terrigenous classic systems. Representative logs illustrate facies within tracts. From Brown and others (1990, p. 47).

production. Techniques in which foam is used have been proven to increase productivity.

SUMMARY AND CONCLUSIONS

The Prue shows two distinctly different lithofacies within the study area. The combined use of well logs—and more importantly the use of cores—greatly assisted this determination. The study indicates that the basal part of the Prue interval was deposited around the Oklahoma City area in a highstand delta-front sequence (Fig. 32). A subsequent sea-level drop allowed for the development of a major incised valley from the northeast to the southwest corners of the study area. The formation of this valley eroded the underlying highstand deltaic sequence along the channel trend, with erosion deep enough in places to remove the Verdigris Limestone. A later rise in sea level backfilled the incised-valley with sands and shales. Some of these sands are as much as 80 ft thick and have porosity as high as 18%. The porosity of the Prue increases in an updip (northeasterly) direction, possibly indicating a higher-energy environment. A map that was useful in defining the channel's aerial extent was the Base Incision-Top Verdigris map, which was able to show the channel cut, even where it is filled with mud.

Although the Prue is productive in many fields within the study area, it is still a viable exploration target. The incised-valley–fill model outlined here may be applied to other similar sandstone intervals in the Pennsylvanian System (Fig. 33). With the use of improved foam-fracturing techniques, those Prue and Prue-like reservoirs that are found are much more likely to become significant producers.

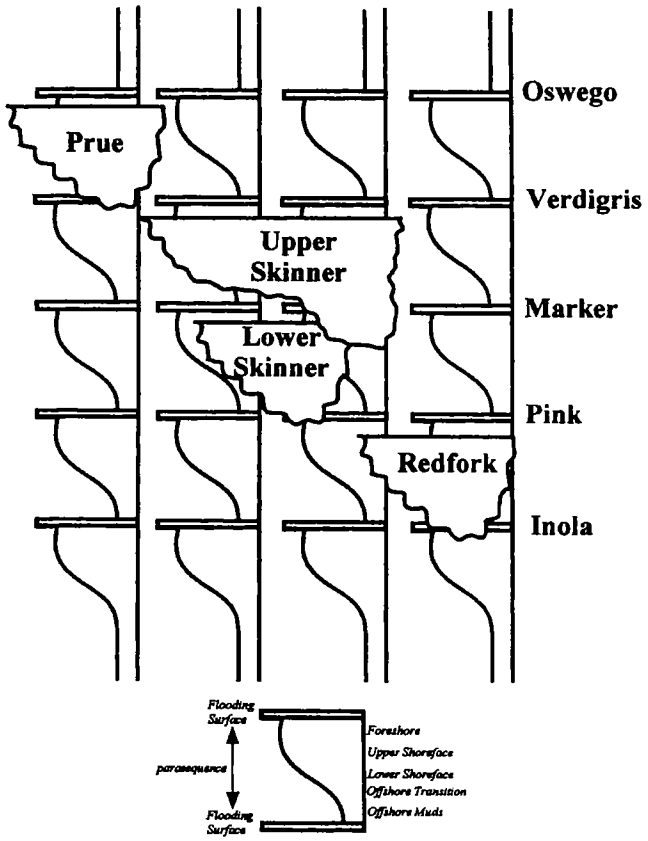

Figure 33. Schematic diagram illustrating incised-valley systems using Oklahoma subsurface stratigraphic nomenclature. Modified from Zaitlin and others (1994, p. 50).

ACKNOWLEDGMENTS

The authors wish to thank Sam Roark, Dominion Exploration and Production, Inc., for his cooperation and assistance in providing data on wells in the Robberson Ranch area and to Dominion Exploration and Production, Inc., and Ernie Knirk, for granting permission to use the data in this article. They also wish to express their gratitude to Robert A. Northcutt, consulting geologist, for his critical review and editing of the text and illustrations in this article.

REFERENCES CITED

Ahmeduddin, M., 1968, Subsurface geology of the Wheatland area, Cleveland, McClain, Grady, Canadian, and Oklahoma Counties, Oklahoma: Shale Shaker, v. 19, no. 1, p. 2–19.

Albano, M. A., 1973, Subsurface stratigraphic analysis "Cherokee" Group (Pennsylvanian), northeast Cleveland County, Oklahoma: Shale Shaker, v. 25, nos. 5, 6, 7, p. 94–103, 114–123, 134–143.

Andrews, R. D.; and others, 1996, Fluvial-dominated deltaic (FDD) oil reservoirs in Oklahoma: the Skinner and Prue plays: Oklahoma Geological Survey Special Publication 96-2, 106 p.

Berg, O. R., 1969, Cherokee Group west flank of the Nemaha Ridge: Shale Shaker, v. 19, no. 8, p. 134–146.

Broker, J. R., 2000, Subsurface stratigraphic analysis of the Prue sandstone interval in south-central Oklahoma: Oklahoma State University M.S. thesis, 114 p.

_____ 2001, Subsurface stratigraphic analysis of the Prue sandstone interval in south-central Oklahoma: Shale Shaker, v. 51, nos. 4, 5, p. 39–50, 63–76.

Brown, L. F., Jr.; Solis-Iriarte, R. F.; and Johns, D. A., 1990, Regional depositional systems tracts, paleogeography, and sequence stratigraphy, Upper Pennsylvanian and Lower Permian strata, north- and west-central Texas: Bureau of Economic Geology, University of Texas at Austin, Report of Investigation 197, 116 p.

Burkett, G. G., 1957, A subsurface study of the Middle Pennsylvanian rocks of western McClain County, Oklahoma: University of Oklahoma unpublished M.S. thesis, 49 p.

Cole, J. G., 1969, Cherokee Group east flank of the Nemaha Ridge: Shale Shaker, v. 19, nos. 8, 9, p. 134–146, 150–161.

Dahlgreen, E. G., 1968, Discovery of a giant, the Oklahoma City Oil Field: Shale Shaker, v. 19, no. 3, p. 53–55.

Gatewood, L. E., 1969, Oklahoma City Field—anatomy of a giant, *in* Geology of giant petroleum fields: American

Association of Petroleum Geologists Memoir 14, p. 223–254.

Jacobsen, L., 1949, Structural relations on the eastern flank of the Anadarko Basin in Cleveland and McClain Counties, Oklahoma: American Association of Petroleum Geologists Bulletin, v. 33, p. 695–719.

Johnson, K. S., 1971, Guidebook for geologic field trips in Oklahoma: Oklahoma Geological Survey Educational Publication 2, 15 p.

_____ 1989, Geologic evolution of the Anadarko Basin, *in* Johnson, K. S. (ed.), Anadarko Basin symposium, 1988: Oklahoma Geological Survey Circular 90, p. 3–12.

Jordan, Louise, 1957, Subsurface stratigraphic names of Oklahoma: Oklahoma Geological Survey Guidebook 6, 220 p.

Kirk, M. S., 1974, Mustang Field, *in* Berg, O. R. (ed.), Oil and gas fields of Oklahoma, reference report, supplement 1: Oklahoma City Geological Society, p. 16.

Krumme, G. W., 1981, Stratigraphic significance of limestones of the Marmaton Group (Pennsylvanian, Desmoinesian) in eastern, Oklahoma: Oklahoma Geological Survey Bulletin 131, 67 p.

McGee, D. A.; and Clawson, W. W., Jr., 1932, Geology and development of Oklahoma City Field, Oklahoma County, Oklahoma: American Association of Petroleum Geologists Bulletin, v. 16, p. 957–1020.

Oakes, M. C., 1953, Krebs and Cabaniss Groups of Pennsylvanian age in Oklahoma: American Association of Petroleum Geologists Bulletin, v. 37, p. 1523–1526.

Van Wagoner, J. C.; Mitchum, R. M.; Campion, K. M.; and Rahmanian, V. D., 1990, Siliciclastic sequence stratigraphy in well logs, cores, and outcrops: American Association of Petroleum Geologists Methods in Exploration Series No. 7, Tulsa, Oklahoma, 55 p.

Zaitlin, B. A.; Dalryrmple, R. W.; and Boyd, R., 1994, The stratigraphic organizations of incised-valley fill systems associated with relative sea level changes, *in* Dalrymple, R. W.; and Zaitlin, B. A. (eds.), Incised-valley systems: origin and sedimentary sequences: Society for Sedimentary Geology Special Publication 51, p. 45–62.

Dipmeter Navigation of the Location and Orientation of a Cherokee Sandstone Reservoir: A Kansas Case Study

John H. Doveton
Kansas Geological Survey
Lawrence, Kansas

ABSTRACT.—The Pennsylvanian Cherokee sandstones of southeastern Kansas are commonly elongate "shoestring" bodies with shapes that reflect their origin in alluvial channels and bars. It is commonly difficult to use traditional exploration methods to efficiently locate and determine the position and orientation of sandstone units to optimize a drilling program. Dipmeter surveys can provide orientation data for bedding structures within the sandstone bodies and are particularly useful in characterizing compactional drape in the shales immediately above the sandstone. The orientation of the drape reveals the local strike of the sandstone body. The direction of potential sandstone thickening can also be deduced, but this depends on whether the upper surface is convex or concave, so that interpretation should be guided by a realistic sedimentological model.

In this study, dipmeters were run in wells drilled during a productive-development program of the Bartlesville Sandstone in the Bronson Field of Bourbon County, Kansas. Dipmeter orientation data were used as "navigation" aids in the location of successive development wells in a feedback-learning process that modified the interpretation of the geometry and orientation of the sandstone.

INTRODUCTION

Exploration for productive Cherokee sandstones in southeast Kansas in the early part of the 20th century marked a radical change in philosophy from traditional methods that had relied on structural mapping. Initial exploratory boreholes on structural highs were dry, whereas successful wells were found to have no link with structural features. The first production appeared to be located away from structural highs, oriented in a north–northwesterly direction. This observation was temporarily adopted as an exploration key until disproved by later drilling (Miner, 1987).

Ultimately, Cadman (1927) concluded that the sandstone bodies originated mostly in narrow, meandering stream channels and that the key to success was to follow the "golden lanes," named because of their rich production combined with their great length and relatively narrow width. However, Bass (1936) concluded that the more prominent "shoestring" sandstones were most likely to have originated as marine offshore bar sands. Although the role of tectonically driven structure was muted, explorationists such as Rich (1938) pointed out that structural draping features were quite common above Cherokee sandstones. He speculated that this was caused by the ability of shales to compact to a much greater degree than sands after deposition. More recent authors, including Van Dyke (1976), Hulse (1978), and Boquet (1984) also noted the structural draping of limestone and black-shale markers over Cherokee sandstones.

Rich (1923) observed that the shape of the upper surface of the sandstone body varied from convex to flat to concave, and hypothesized that the morphology probably was linked with the depositional origin of the sandstone. In urging explorationists to apply principles of sedimentation in their search for shoestring sands, Rich (1923) made one of the earliest endorsements of sedimentology as an oil-exploration tool. Rich (1926) anticipated the modern interpretation of many of these Cherokee sandstones by suggesting that they originated in incised valleys that were silted up, using mild tectonic uplift as the mechanism for the incision. In more recent times, the relatively shallow depths and low drilling costs associated with reaching the Kansas Cherokee sandstones have ruled against utilizing expensive exploration technology. Instead, the siting of Cherokee wells has been made from the experience of the seasoned explorationist and a straight-edge ruler or pediction by the enterprising oil-witch.

A typical strategy, once the initial productive well has been drilled, is to establish the trend from a geological interpretation of the sand present in the borehole. This is then combined with careful mapping of

Doveton, J. H., 2002, Dipmeter navigation of the location and orientation of a Cherokee sandstone reservoir: a Kansas case study, *in* Boyd, D. T. (ed.), Finding and producing Cherokee reservoirs in the southern Midcontinent, 2002 symposium: Oklahoma Geological Survey Circular 108, p. 37–41.

sandstone isopachs, with an eye for potential draping features. Dry holes showing where the sand is not present are commonly as critical in following a productive trend as those that penetrate thick sand.

In the 1960s dipmeter logs were run in several Cherokee fields in southeast Kansas as part of a strategy to optimize development well location. Dipmeters are still relevant to contemporary Cherokee sandstone studies, particularly in the context of their technological descendant, the borehole electrical-imaging tool.

THE DIPMETER

The dipmeter was introduced as a logging tool to measure dips and strikes of features on borehole walls in the 1930s (Allaud and Martin, 1977). Originally a spontaneous potential (SP) device, the design concept moved to a multi-armed microresistivity tool, where the correlation of microresistivity-log traces across a borehole could be analyzed in terms of the orientation of planar features. The vertical resolution of the earlier tools was adequate for measurements of structural dip, but the recognition of sedimentary features, such as cross bedding, was only possible for large cross-bed sets, as are seen in eolian dunes. Because the trigonometric calculations necessary to establish strikes and dips are time consuming, the shift to computer processing must mark one of the earliest applications of computer technology to geology (e.g., Moran and others, 1962). As the tool design evolved over time, the number of arms and electrode buttons was increased and log-processing software became increasingly sophisticated. High-resolution dipmeters could now routinely discriminate small-scale sedimentary-bedding features (Nurmi, 1984). Eventually, vertical resolution progressed to the point where detailed electrical images of the borehole wall could be generated (Ekstrom and others, 1986).

Although the measurements of the dipmeter tool are microresistivity profiles of the borehole wall, the results are commonly presented as vector plots of dip and strike of planar features. The vertical axis is matched with depth and the horizontal axis is scaled for dip magnitude. At incremental depths, "tadpoles" are marked where successful correlations of microresistivity segments were possible between the measurements at the arms. The correlation quality is shown by the symbol of the tadpole head. The direction of dip is shown by the orientation of the tadpole tail as related to a conventional compass circle. The "tadpole plot" can then be searched for clustered vectors with systematic trend that are color-coded to aid in the geological interpretation. The standard color-coding scheme equates green with trends of constant dip and azimuth, red with increasing dip with depth and constant azimuth, and blue with decreasing dip with depth and constant azimuth. Dip patterns are attributed to structure, faults, compactional drape, and internal sedimentary features such as cross bedding.

In the 1960s, when dipmeters were run in the Cherokee Group of Kansas, the available tool was a three-armed device in which dip vectors were computed from microresistivity traces by batch runs on IBM mainframe computers. The resolution of the vectors was sufficient to measure tectonic structure and compactional draping, but commonly was insufficient to resolve sedimentary-bedding features.

The ability to measure draping over Cherokee sandstone bodies was a major factor in the decision to run dipmeters as part of the logging program. Whereas green tadpole patterns of relatively constant dip and azimuth would reflect regional tectonic dip, red patterns of increasing dip with depth immediately above the sandstone body would indicate the draping of shales over the sandstone. Although the strike of these vectors would be diagnostic of the local orientation of the long axis of the sandstone, a diametrically opposite interpretation was possible, depending on whether the top of the sandstone was convex or concave upward. Two basic geological models were suggested to match these alternatives: (1) an offshore-bar with a convex upper surface, or (2) a channel-fill sandstone with a concave top. If bedding structure could be identified by dips within the sandstone, the correct model could be determined from the assumption that bedding will be at right angles to the long axis for a bar and parallel to the axis for a channel (Campbell, 1968). Such a geological interpretation applied to dipmeter logs can be part of a successful Cherokee sandstone navigation strategy, as is outlined in the following case study.

CASE STUDY

In 1965–66, a Bartlesville Sandstone reservoir in Bourbon County, Kansas, was developed for oil production as the Bronson SE Field. Dipmeters were run in some of the wells (and dry holes) as part of the field-development program, with a good example being the Woodward #CH-4 well (Fig. 1). There, the gamma-ray log shows a section that is primarily shale with a development of the Bartlesville Sandstone toward the base. The shallow dips of the tadpole plot are characteristic of many Midcontinent stratigraphic sequences where regional structure is fairly subdued. It should be noted that structure that appears obvious from the mapping of correlated marker horizons might be subtle on the dipmeter log. A dip of only one degree is equivalent to a change in elevation of more than 92 ft in a mile. However, well spacing commonly is too broad to identify localized features, such as surface draping immediately above a sandstone, which can be measured by the dipmeter.

Schmidt nets are shown for subdivisions of the section. These polar projections are used commonly in the analysis of fold and fault geometry in structural geology, and, thus, their use with dipmeter data is a useful extension of traditional geological methods. The highest shales show very minor dips with no discernible preferred orientation, that grade downward to a zone with small dips with an eastern orientation. These sets may match local dip associated with the broad drape of overlying limestones and other markers that have been observed by workers over many of the Kansas Cherokee fields. As already discussed, this style of drape com-

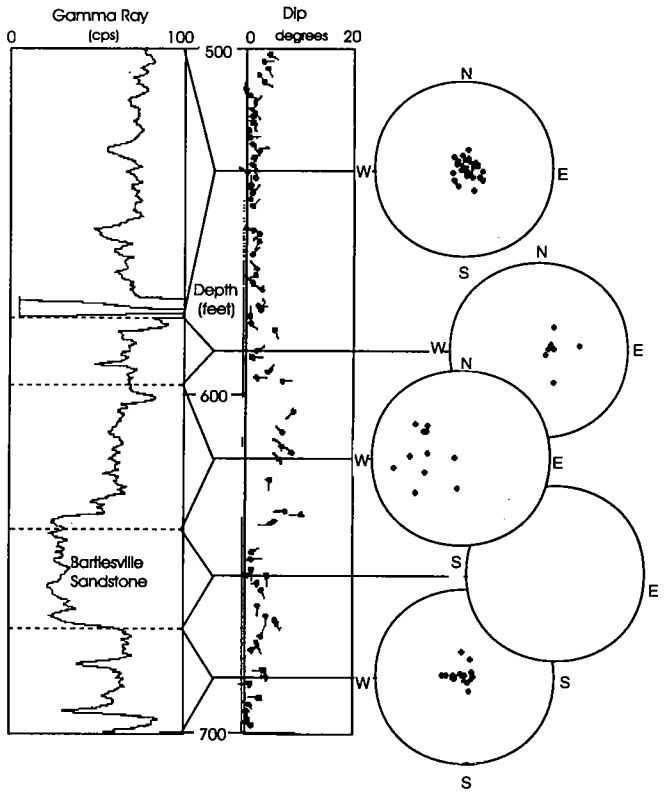

Figure 1. Gamma-ray and dipmeter tadpole logs from the Cherokee Group in C.R.A. Woodward #4 well, sec. 12, T. 25 S., R. 21 E., Bourbon County, Kansas. The Schmidt net plots of tadpole vectors have a perimeter of 15° dip and are referenced to section subdivisions. *Abbreviation:* CPS = counts per second.

monly can be mapped by correlation between wells, but its magnitude is matched by very small dips.

In the zone immediately above the Bartlesville Sandstone, there is a marked increase in dip, with a general western orientation that probably represents localized drape of the shale immediately over the upper surface of the sandstone. These data suggest that the long-axis of the sandstone is oriented north-south, and, if the upper surface of the sandstone is convex, that the central axis lies to the east of the well. The dips within the sandstone show an abrupt contrast, with dips strongly aligned to the south. If the dips discriminate the surfaces of cross-bedding sets, then the cross-bedding direction is aligned with the axis of the sandstone body. This interpretation would suggest a current flow from north to south and the depositional origin of the sandstone body as a channel. (The most likely alternatives of a marine bar or a strandline deposit would be expected to have cross-bed orientations at right angles to the long axis.) The gamma-ray profile of the sandstone is also consistent with a channel interpretation.

The illustrative well was the fourth in the development series, and a map of the field well locations (Fig. 2) graphically summarizes the progressive understanding of the limits of the field. The wells are numbered in

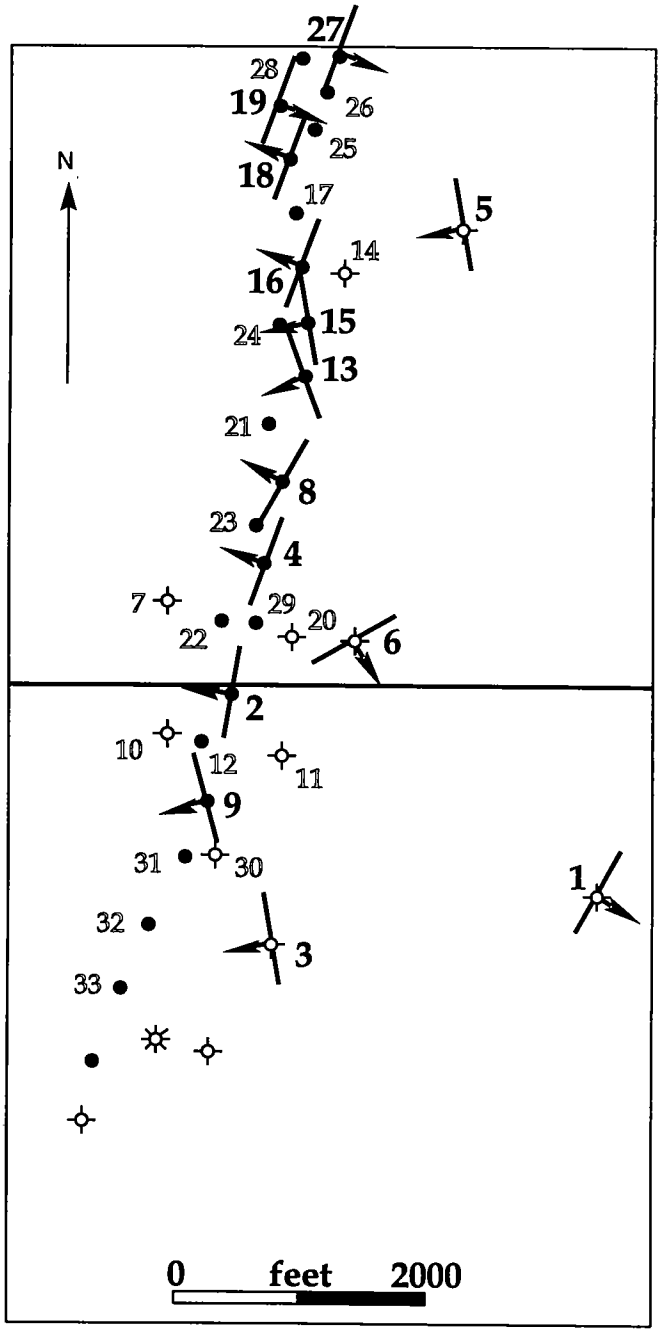

Figure 2. Drilling development of the Bronson SE Field, Bourbon County, Kansas, from October 1965 to July 1966. The holes are numbered in order of drilling, and solid numbers signify holes that were logged by dipmeter; hollow numbers reference holes that had no dipmeter logging. Each bar and arrow represents the strike and dip of draping in the shales immediately overlying the Bartlesville Sandstone as interpreted from dip vectors at the time of logging.

order of drilling and span a period between October 1, 1965, and July 18, 1966. Initially (wells 1 to 9), the Bartlesville Sandstone was interpreted to be a bar sand, but the model was later revised to that of a channel sandstone. As understood at the time, a change in

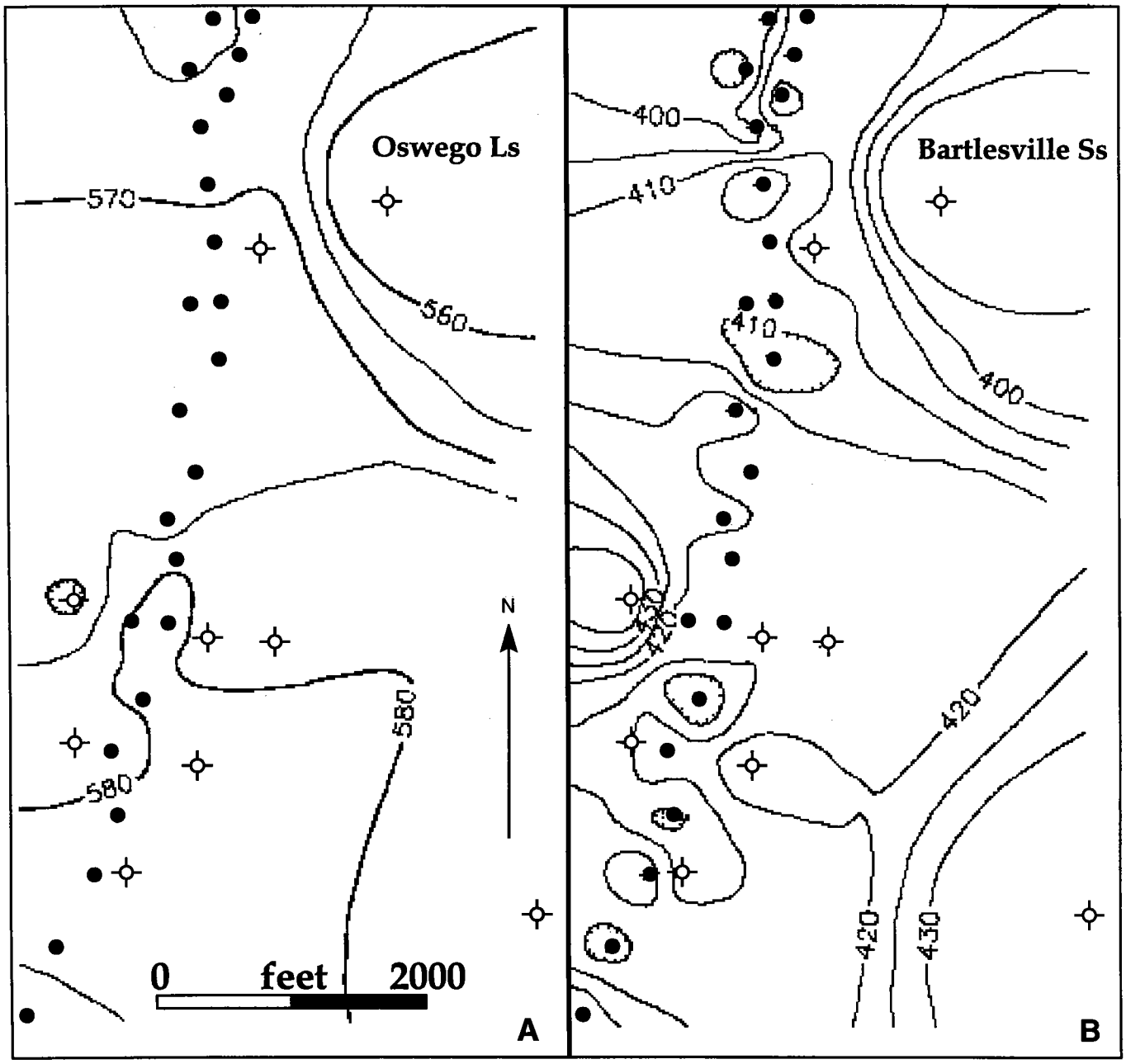

Figure 3. Structure-contour maps of (A) the Oswego Limestone and (B) the top of the Bartlesville Sandstone in the Bronson SE Field, Bourbon County, Kansas. Contours are in feet above sea level, with an interval of 5 ft.

the model made no difference to the interpretation of the sandstone log-axis orientation, but it did alter ideas on the direction of the sandstone axis (and thicker sandstone development) relative to the borehole location.

As can be seen on the map (Fig. 2), dipmeters were not run in all the wells, but only at times when the dip information was needed as an aid to interpretations drawn from core observations, correlation, and mapping. Overall, the siting of development wells was very successful and quickly established a classic "golden lane" Cherokee production pattern—that is, a sandstone body with a relatively narrow width but substantial long axis. This geometry makes it difficult to verify the detailed structure of the field even after it was developed fully, because the well control is so tightly constrained to this narrow trend.

Some useful observations can be drawn, nonetheless, from structure maps made on the Oswego Limestone and the top of the Bartlesville Sandstone (Fig. 3). The overlying Oswego Limestone shows a distinctive but gentle structural nose that reflects a broad compactional drape over the Bartlesville Sandstone. In contrast, the top of the Bartlesville Sandstone has a more complex configuration, whose features represent real local variability compounded by artifacts caused by

poor well control. Interestingly, it appears that the interpretation of a convex versus concave upper surface may be simplistic, as the shape of this surface seems to be variable along the length of this Bartlesville Sandstone body. However, this is no way diminishes the value of the dipmeter in establishing sandstone strike.

A CONTEMPORARY PERSPECTIVE

The old debate concerning the origin of individual Cherokee sandstones as deposits of either alluvial channels, deltaic distributaries, offshore bars or other environments has been superceded more recently by an incised-paleovalley model rooted in sequence stratigraphy. Demonstrated convincingly by detailed geological studies and 3-D seismic in the older Morrow and Chester sandstones of western Kansas (e.g., Sonnenberg and others, 1990; Montgomery and Morrison, 1999), the incised valley paradigm has been documented to describe both the Tonganoxie Sandstone in the younger Douglas Group of eastern Kansas (Archer and Feldman, 1995) and the Cherokee sandstones of southeastern Kansas (Brenner, 1995; Walton, 1996). In this model, a vertical facies sequence of alluvial, estuarine, tidal, and marine deposits are commonly observed in incised-valley–sandstone cores. Tadpole plots from dipmeters run through the Morrow sandstones of western Kansas show unidirectional cross bedding in the alluvial-sandstone facies and bidirectional dips in the overlying tidal facies (Luchtel, 1999). High costs inhibit the use of modern dipmeters in the Cherokee sandstones of eastern Kansas. However, it has been found that data from similar sandstones elsewhere in Kansas (and neighboring states) continue to offer fresh insights into the interpretation of older Cherokee data. These can improve not only the quality of the geological interpretation but also the future commerciality of these older areas.

REFERENCES CITED

Allaud, L.; and Martin, M., 1977, Schlumberger, the history of a technique: Wiley-Interscience, New York, 333 p.

Archer, A. W.; and Feldman, H. R., 1995, Incised valleys and estuarine facies of the Douglas Group (Virgilian): implications for similar Pennsylvanian sequences in the U.S. Mid-continent, *in* Hyne, N. J. (ed.), Sequence stratigraphy of the Mid-Continent: Tulsa Geological Society Special Publication 4, p. 119–140.

Bass, N. W., 1936, Origin of the shoestring sands of Greenwood and Butler Counties, Kansas: Kansas Geological Survey Bulletin 23, 126 p.

Boquet, D. J., 1984, Depositional environment, diagenesis, reservoir quality, and enhanced oil-recovery potential of a reservoir in the Skinner Sandstone (Desmoinesian), Crawford, Labette, and Neosho Counties, Kansas: University of Kansas unpublished M.S. thesis, 129 p.

Brenner, R. L., 1995, Sequences and cyclothems in upper portion of Cherokee Group (Middle Pennsylvanian, Desmoinesian), Mid-Continent, U.S.A., *in* Hyne, N. J. (ed.), Sequence stratigraphy of the Mid-Continent: Tulsa Geological Society Special Publication 4, p. 193–216.

Cadman, W. K., 1927, The Golden lanes of Greenwood County [Kansas]: American Association of Petroleum Geologists Bulletin, v. 11, p. 1151–1172.

Campbell, R. L., 1968, Stratigraphic applications of dipmeter data in the Mid-Continent: American Association of Geologists Bulletin, v. 52, p. 1700–1719.

Doveton, J. H., 1994, Geologic log interpretation: Society of Economic Paleontologists and Mineralogists Short Course Notes, 169 p.

Ekstrom, M. P.; Dahan, C. A.; Chen, Min-Yi; Lloyd, P. M.; and Rossi, D. J., 1986, Formation imaging with microelectrical scanning arrays: Society of Professional Well Log Analysts 27th Annual Logging Symposium, Paper BB, 12 p.

Hulse, W. J., 1978, A geologic study of the Sallyards field area, Greenwood County, Kansas: University of Kansas unpublished M.S. thesis, 152 p.

Luchtel, K. L., 1999, Sequence stratigraphy and reservoir analysis of the upper Kearny Formation (Morrowan Series, Lower Pennsylvanian System) within three Kansas fields: University of Kansas unpublished M.S. thesis, 149 p.

Miner, C., 1987, Discovery!: cycles of change in the Kansas oil and gas industry, 1860–1987: Kansas Independent Oil and Gas Association, Wichita, 239 p.

Montgomery, S. L.; and Morrison, E., 1999, South Eubank Field, Haskell County, Kansas: a case of field redevelopment using subsurface mapping and 3-D seismic data: American Association of Petroleum Geologists Bulletin, v. 83, p. 393–409.

Moran, J. H.; Coufleau, M. A.; Miller, G. K.;and Timmons, J. P., 1962, Automatic computation of dipmeter logs digitally recorded on magnetic tapes: Journal of Petroleum Technology, v. 14, no. 7, p. 771–782.

Nurmi, R. D., 1984, Geological evaluation of high resolution dipmeter data: Society of Professional Well Log Analysts 25th Annual Logging Symposium, Paper YY, 24 p.

Rich, J. L., 1923, Shoestring sands of eastern Kansas: American Association of Petroleum Geologists Bulletin, v. 7, p. 103–113.

_____ 1926, Further observations on shoestring oil pools of eastern Kansas: American Association of Petroleum Geologists Bulletin, v. 10, p. 568–580.

_____ 1938, Application of differential settling to tracing of lenticular sand bodies: American Association of Petroleum Geologists Bulletin, v. 22, p. 823–833.

Sonnenberg, S. A.; Shannon, L. T.; Rader, K.; and von Drehle, W. F., 1990, Regional structure and stratigraphy of the Morrowan Series, southeast Colorado and adjacent areas, *in* Sonnenberg, S. A. (ed.), Morrow sandstones of southeast Colorado and adjacent areas: Rocky Mountain Association of Geologists, Denver, Colorado, p. 1–8.

Van Dyke, R. J., 1976, Geology and depositional environments of the reservoir sandstone, Kincaid Oil Field, Anderson County, Kansas: University of Kansas unpublished M.S. thesis, 80 p.

Walton, A. W., 1996, Depositional framework and representative oil reservoirs of the Cherokee Group (Atokan–Desmoinesian, Middle Pennsylvanian), eastern Kansas, *in* Johnson, K. S. (ed.), Deltaic reservoirs in the southern Midcontinent, 1993 symposium: Oklahoma Geological Survey Circular 98, p. 168–187.

Cherokee Paleoenvironments, Long Branch Field, Payne County, Oklahoma

Greg A. Riepl
Independent Geologist
Oklahoma City, Oklahoma

INTRODUCTION

Discovery and development of the Long Branch Field, T. 18 N., R. 4 E., Payne County, Oklahoma, has provided a unique opportunity to delineate a variety of productive Cherokee depositional environments within the confines of one small field (Fig. 1). The lower Skinner, Red Fork, and Bartlesville sands of this field have a complex history of sedimentation that has created problems in the development of the reserves as well as secondary-recovery efforts. Understanding and recognizing these paleoenvironments and the reservoir architecture that they produce can enhance the ability to find and develop reserves in Cherokee sands.

STRUCTURE

Present-day regional structure consists of monoclinal west–southwest dip into the Anadarko Basin, with anticlinal features controlled by deep-seated–fault trends running subparallel to the north–northeast-trending Nemaha Ridge. There are also smaller structural elements controlled by differential compaction over large sand bodies encased in Cherokee shale.

The paleostructural environment in Payne County was in a state of flux during Cherokee time. During the period of deposition of the Bartlesville and Red Fork, the Nemaha Ridge to the west was still a positive influence on sedimentation, as can be seen in the east–southeast trends of the sands in those systems. However, by the time of deposition of the lower Skinner, regional tilting into the Anadarko Basin had eliminated the Nemaha Ridge as a positive influence and the lower Skinner was "captured" by the developing basin to the west, as can be seen in the south–southwest sand trends.

The structural geology of the Long Branch Field is dominated by the presence of a west-trending, anticlinal nose, which was detected through regional subsurface mapping. This was confirmed by common depth-point (CDP) seismic data, otherwise known as two-dimensional (2-D) analysis. The axis of this anticline runs generally east–west through the center of sec. 10 and provides the necessary structural support for entrapment in the Long Branch Field (Fig. 2).

LOWER SKINNER SANDSTONE

The lower Skinner sand of this area is composed primarily of fluvio-deltaic channel-mouth–bar sandstones that generally trend to the south–southwest. Within the field, the sand complex consists of a central main channel with two bifurcating arms that form a classic "birdfoot" deltaic pattern (Fig. 3). Fine-grained sands with thin, shaley laminations characterize the lower Skinner reservoir. Reservoir quality is generally good in the main channel with clay-rich, lower porosity sands in the bifurcating arms. The reservoir sand is characterized by a distinct "coarsening-upward" porosity profile, which grades laterally to nonreservoir-quality prodelta silt and clay. Reservoir-quality sand is generally considered to be any sand in excess of 15% porosity. Permeability can range from 10 to 400 millidarcies (md). The structural gradient during deposition of the Skinner was very low, which allowed for a highly mobile shoreline environment. Even slight changes in sea level caused shoreline shifts of several miles. Because of this mobile environment, Skinner deltaic sequences generally do not have much areal extent or attain much thickness. This low gradient also allowed an extensive tidal/estuarine environment to develop after deposition of the deltaic sequence. Considerable channeling and reworking of sands occurred within the tidal system.

The McFarland #1-10 well in the SE¼SE¼NW¼ sec. 10 was the discovery well for the field. It flowed 1,700 MCFPD (thousand cubic feet per day) from 4 ft of pay in the lower Skinner. Two subsequent offset wells found Skinner sand of very limited quality, but were successfully completed in Red Fork pay zones. The fourth and fifth wells, the Clemons #1-10 and Aletha #1-10, found 13 and 11 ft of lower Skinner sand, which flowed 148 and 169 BOPD (barrels of oil per day), respectively. In the last delineation well drilled on this side of the field, the Aletha #2-10, the reservoir sand was truncated by a shale- and silt-filled tidal channel (Fig. 4).

Regional mapping of the lower Skinner in central Payne County has revealed that a slow marine transgression created a broad, tidal-drainage environment across the area following the deposition of the Skinner

Riepl, G. A., 2002, Cherokee paleoenvironments, Long Branch Field, Payne County, Oklahoma, *in* Boyd, D. T. (ed.), Finding and producing Cherokee reservoirs in the southern Midcontinent, 2002 symposium: Oklahoma Geological Survey Circular 108, p. 43–59.

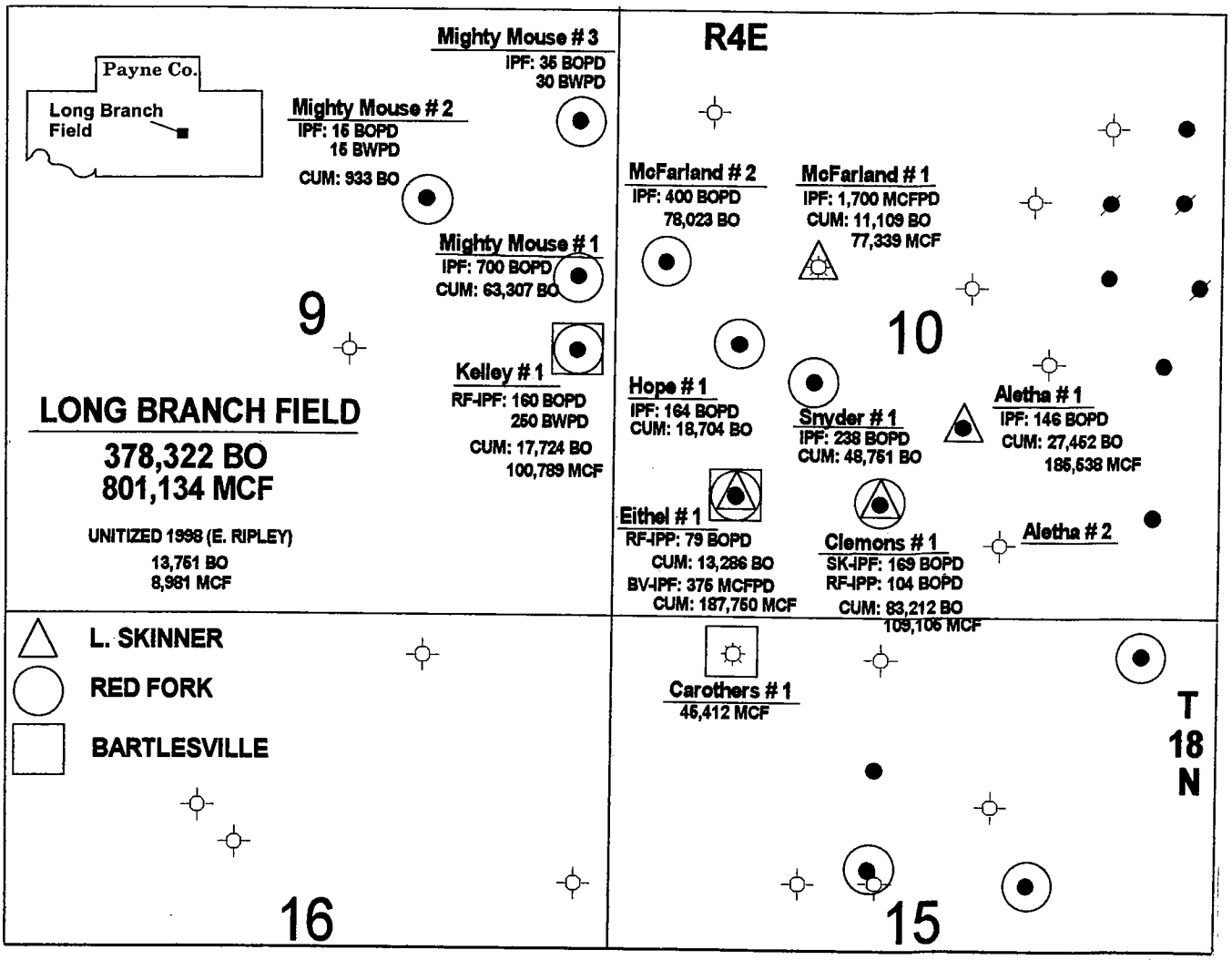

Figure 1. Cherokee production map, Long Branch Field, Payne County, Oklahoma. *Abbreviations:* BOPD = barrels of oil per day; BWPD = barrels of water per day; CUM = cumulative; IPF = initial-production flow; MCFPD = thousand cubic feet (of gas) per day; RF = Red Fork.

deltaic sequence. The focal point of the drainage was a north–south-trending synclinal valley associated with the downthrown side of a regional fault located just west of the city of Stillwater (see Fig. 5). This fault is part of a fault system that runs subparallel to the Nemaha Ridge, which is located about 15–20 mi to the west, and it is related tectonically to the Nemaha. The Stillwater feature was a fault-bounded anticline during pre-Pennsylvanian time but was only a broad fold during the Pennsylvanian. During the deposition of the lower Skinner, it was merely a slightly positive feature, with just enough relief to influence drainage.

The so-called "Stillwater Skinner channel complex" truncates the underlying lower Skinner, Pink limestone, and Red Fork sand and commonly contains more than 100 ft of reworked sand. Figure 5 illustrates that a series of dendritic drainage channels radiate to the east for several miles from the Stillwater channel, and it is one of these channels that has truncated the lower Skinner deltaic sand that was originally in the Aletha #2-10.

Detailed mapping of the Long Branch Field shows that the tidal channel truncating the sand is actually the trap for the lower Skinner part of the field (Fig. 6). In 1955, Mohawk Drilling drilled a dry hole that is a 20-acre northeast offset to the high-flowing Aletha #1-10. This well was 24 ft updip to the Aletha #1, had good reservoir quality sand in the lower Skinner, but recovered 370 ft of saltwater on a drill-stem test from that sand. The shale-filled tidal channel must run between those two wells and is probably no more that a few hundred feet wide (Fig. 7). Regional analysis of the area indicates that tidal-channel truncation of lower Skinner deltaic sands is common in many fields in Payne County and may be an important factor in other areas of the Cherokee Platform.

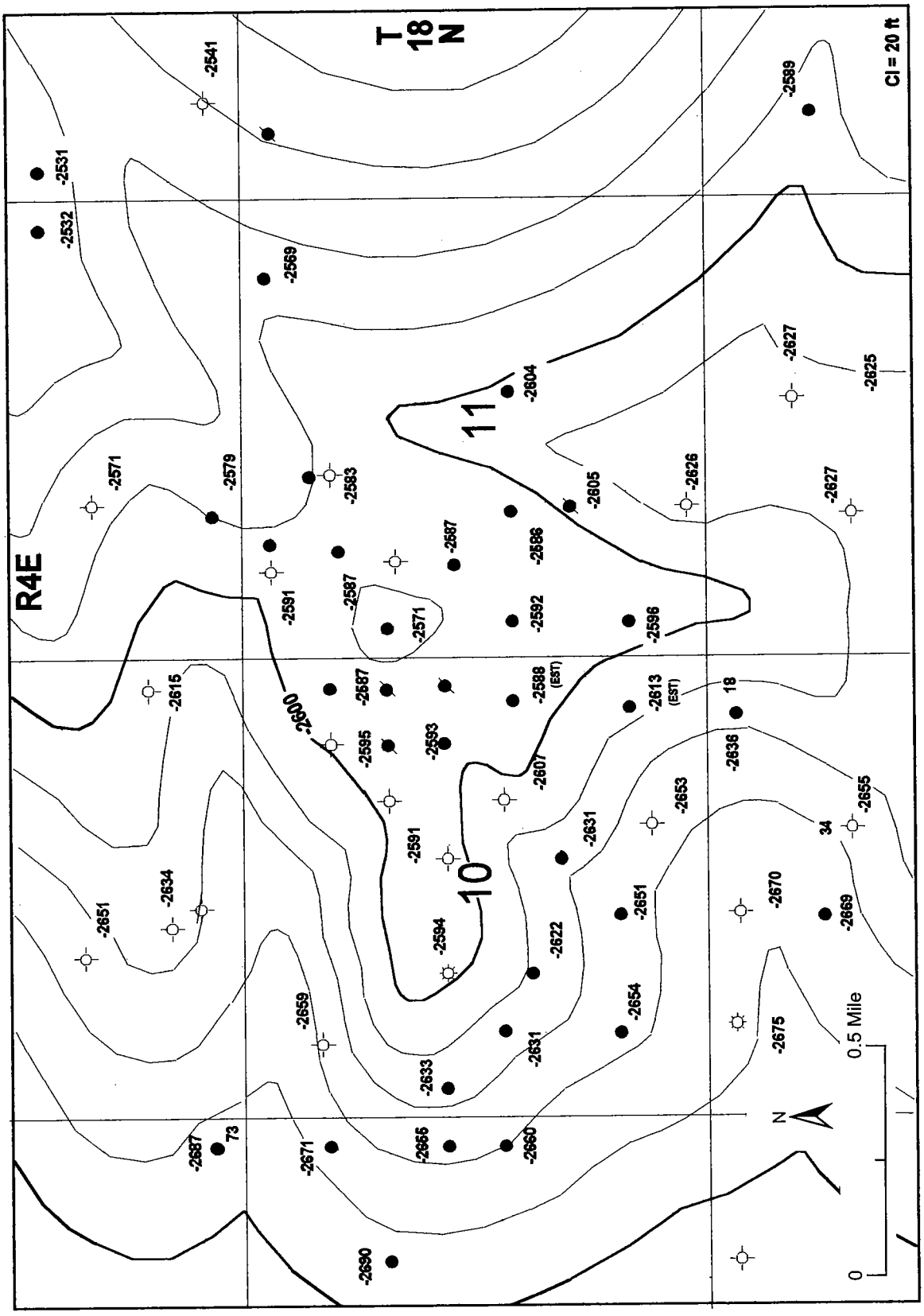

Figure 2. Structure-contour map on Pink limestone, Long Branch Field, Payne County, Oklahoma. Contour interval (CI) = 20 ft. Datum is mean sea level.

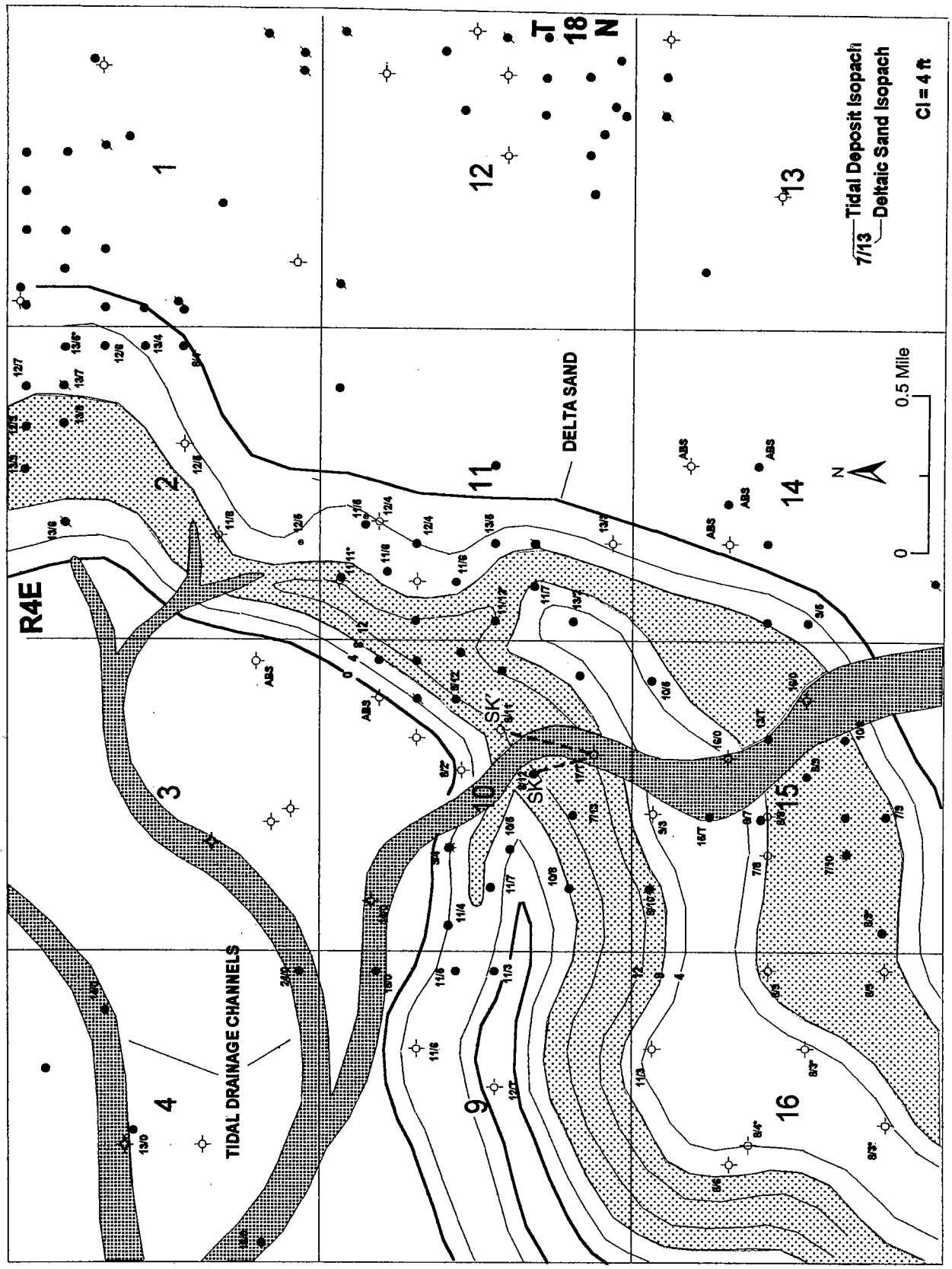

Figure 3. Depositional environments of lower Skinner sand, Long Branch Field, Payne County, Oklahoma. Location of cross section SK–SK′ (Fig. 4) shown by darker lines in sec. 10. Ratios shown are thickness of tidal deposits to thickness of deltaic sand. Contour interval (CI) = 4 ft. *Abbreviation:* ABS = absent. Ratios shown are thickness of tidal deposits to thickness of deltaic-sand deposits.

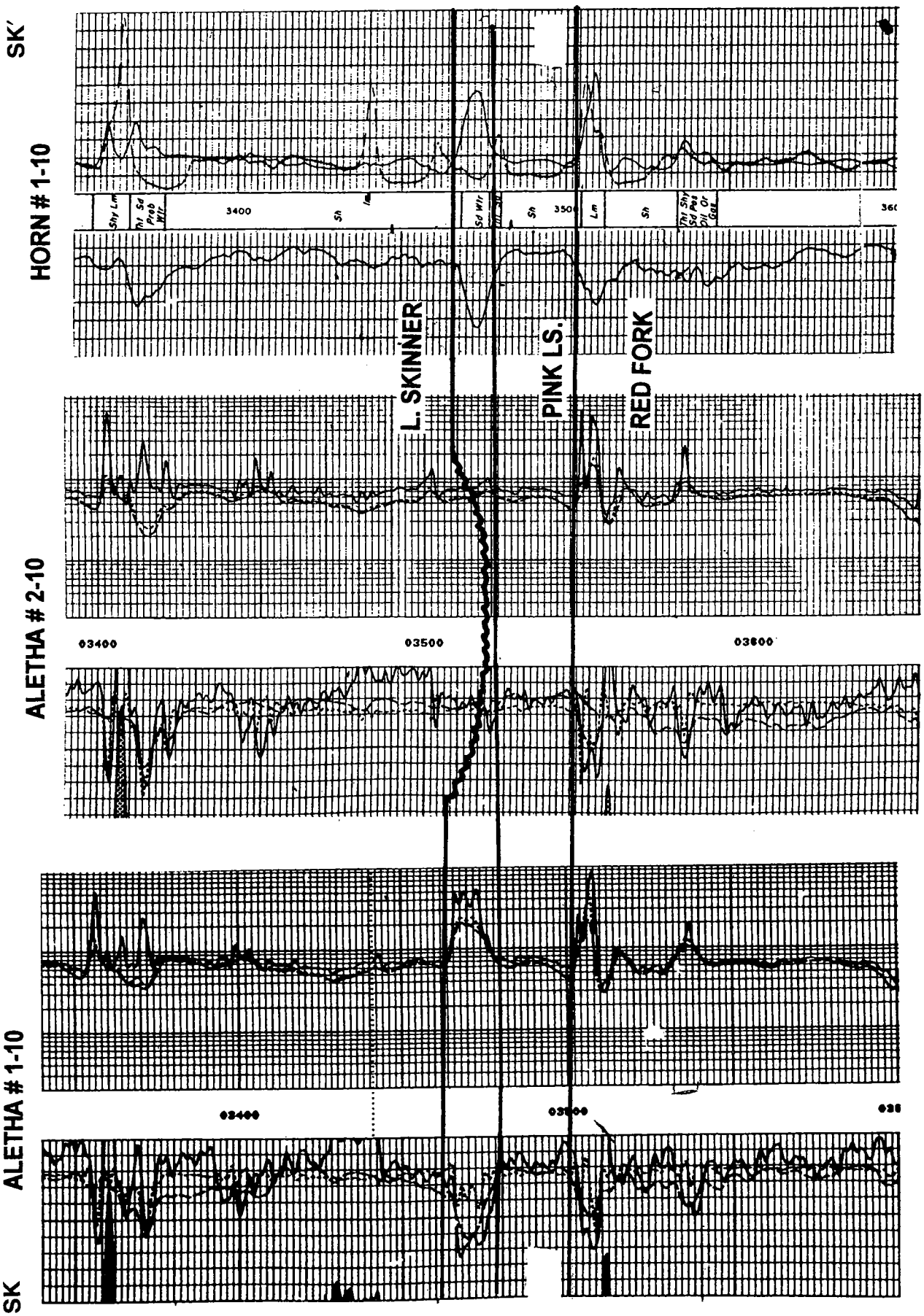

Figure 4. Stratigraphic cross section SK–SK'. See Figure 3 for location.

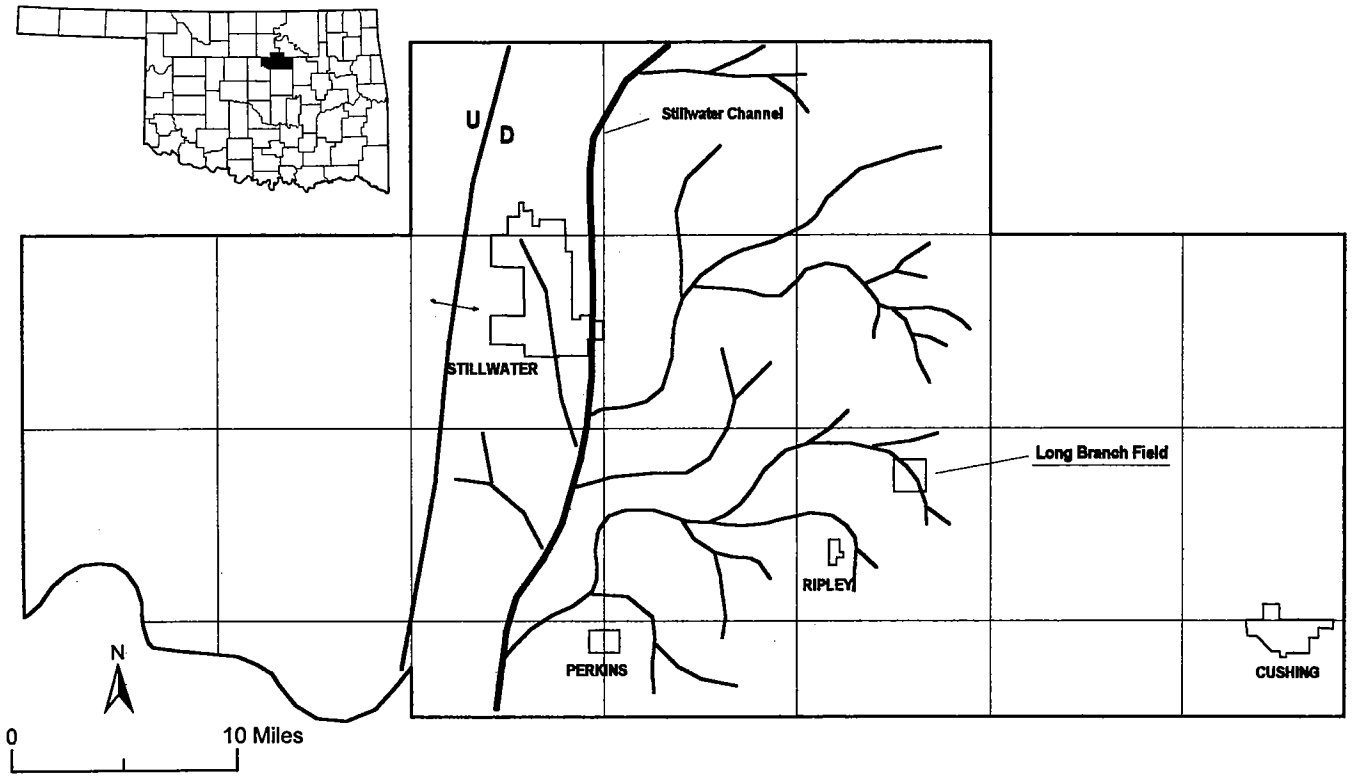

Figure 5. Lower Skinner tidal estuaries, including "Stillwater Skinner channel complex." Location of Long Branch Field, Payne County, Oklahoma, to these tidal estuaries shown. See text for explanation of structural feature mapped as a fault/anticline.

RED FORK SANDSTONE

The Red Fork sandstone in the Long Branch Field is part of an extensive deltaic complex that covers much of north-central Oklahoma. The general trend of sands is to the southeast. The Red Fork system of this area is composed of primarily shale- and silt-filled distributary channels containing interbedded longitudinal bars. Some deltaic channel-mouth bars and splay deposits are interspersed throughout the system tract. The channel deposits are identified by their diagnostic fining-upward log profile, whereas the channel-mouth bars and splays exhibit a distinct coarsening-upward log profile (Fig. 8). Just north of the Long Branch Field is a large distributory channel filled with silt, clay, and some sand. In secs. 3 and 4, a smaller channel splits off to the south and extends through secs. 9 and 10. From this smaller channel, an apparent crevasse splay extends to the east and southeast across the eastern part of sec. 10 and into sec. 15 (Fig. 9).

The original Red Fork discovery was made in November 1983 at the Snyder #1-10 well, which flowed 238 BOPD from 6 ft of splay sand. Subsequent offset wells also established production from the splay sand in the SW¼ sec. 10. All of the splay sands generally begin to develop 25 ft below the Pink limestone marker and exhibit a diagnostic coarsening-upward log profile. These sands produced a black, 35-gravity crude oil.

In July 1984, the Mighty Mouse #1-9 well was drilled in the SE¼SE¼NE¼ sec. 9. The well encountered approximately 25 ft of productive Red Fork sand, which flowed over 700 BOPD. The sand sits in a lower stratigraphic position than is seen in other productive wells (35 ft below the Pink limestone). It also exhibits a fining-upward log profile, and produced a distinct greenish-brown, 42-gravity crude oil. These physical differences made it obvious that this sand was in a separate compartment from the wells in sec. 10. The difference in crude oils is attributed to separate source and capture areas for each compartment. Since the splay deposit is totally isolated from the rest of the system, it is believed that it was sourced entirely from the local shales, which are not as thermally mature. The channel systems cover a much larger area and had more opportunity to capture higher-gravity crude oils generated deeper in the basin. The McFarland #2 and Hope #1 wells are just over 900 ft apart and are producing different types of oils.

Another key aspect to the Red Fork distributary system is the presence of shale-filled channels found between the longitudinal bar sands. These are natural permeability barriers and quite commonly can create secondary traps within a field that are normally overlooked. From structural cross-section RF–RF′ (Fig. 10), the oil/water contact in the Kelley #1 well can be seen distinctly. Yet, the Mighty Mouse #2 well produced oil

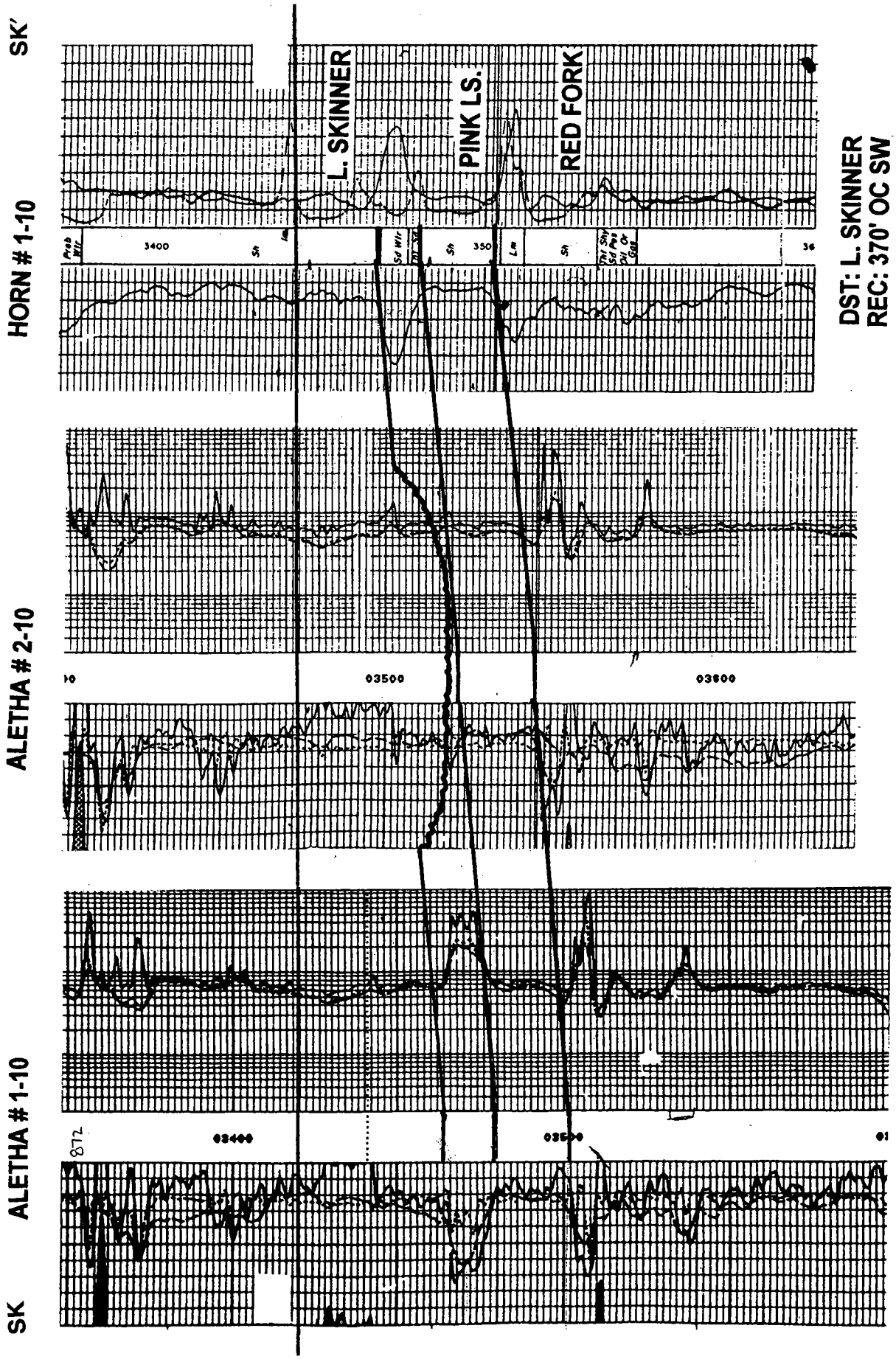

Figure 6. Structural cross section SK–SK', using top of lower Skinner sand as datum. See Figure 3 for location. *Abbreviations*: BOPD = barrels of oil per day; DST = drill-stem test; IPF = initial-production flow; OC SW = oil-cut saltwater.

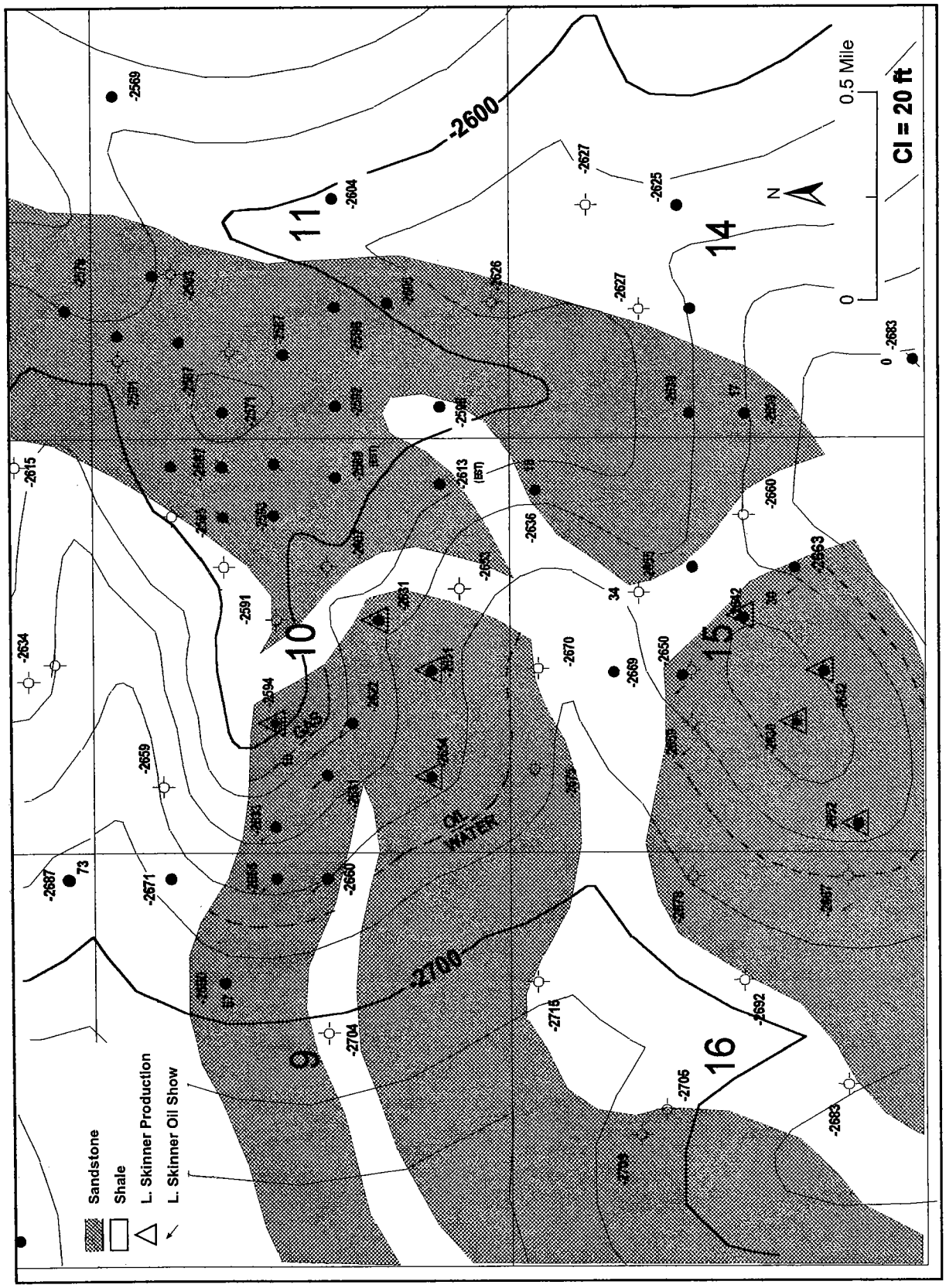

Figure 7. Map of lithology of lower Skinner sand superimposed on structure of Pink limestone. Contour interval (CI) = 20 ft. Datum is mean sea level.

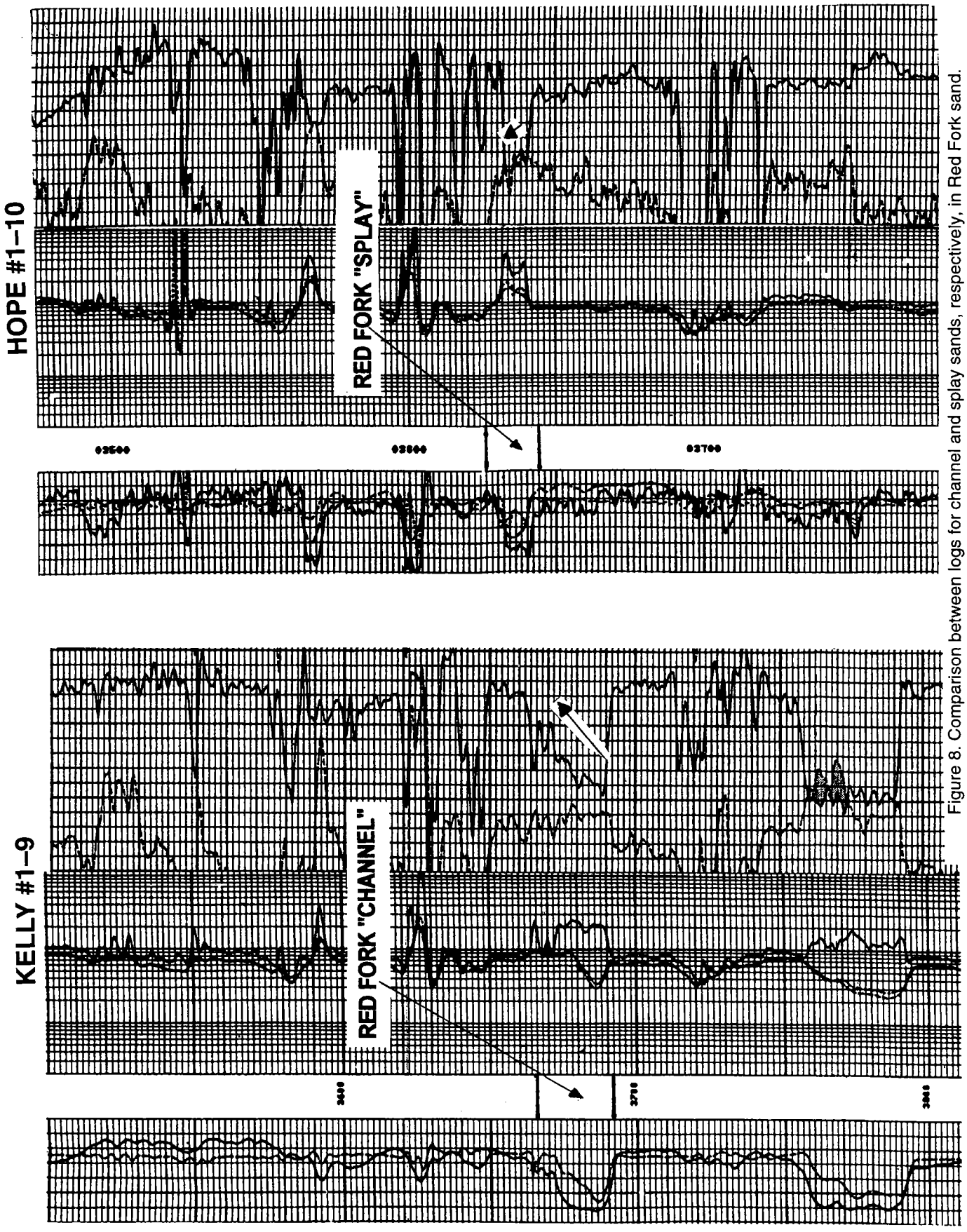

Figure 8. Comparison between logs for channel and splay sands, respectively, in Red Fork sand.

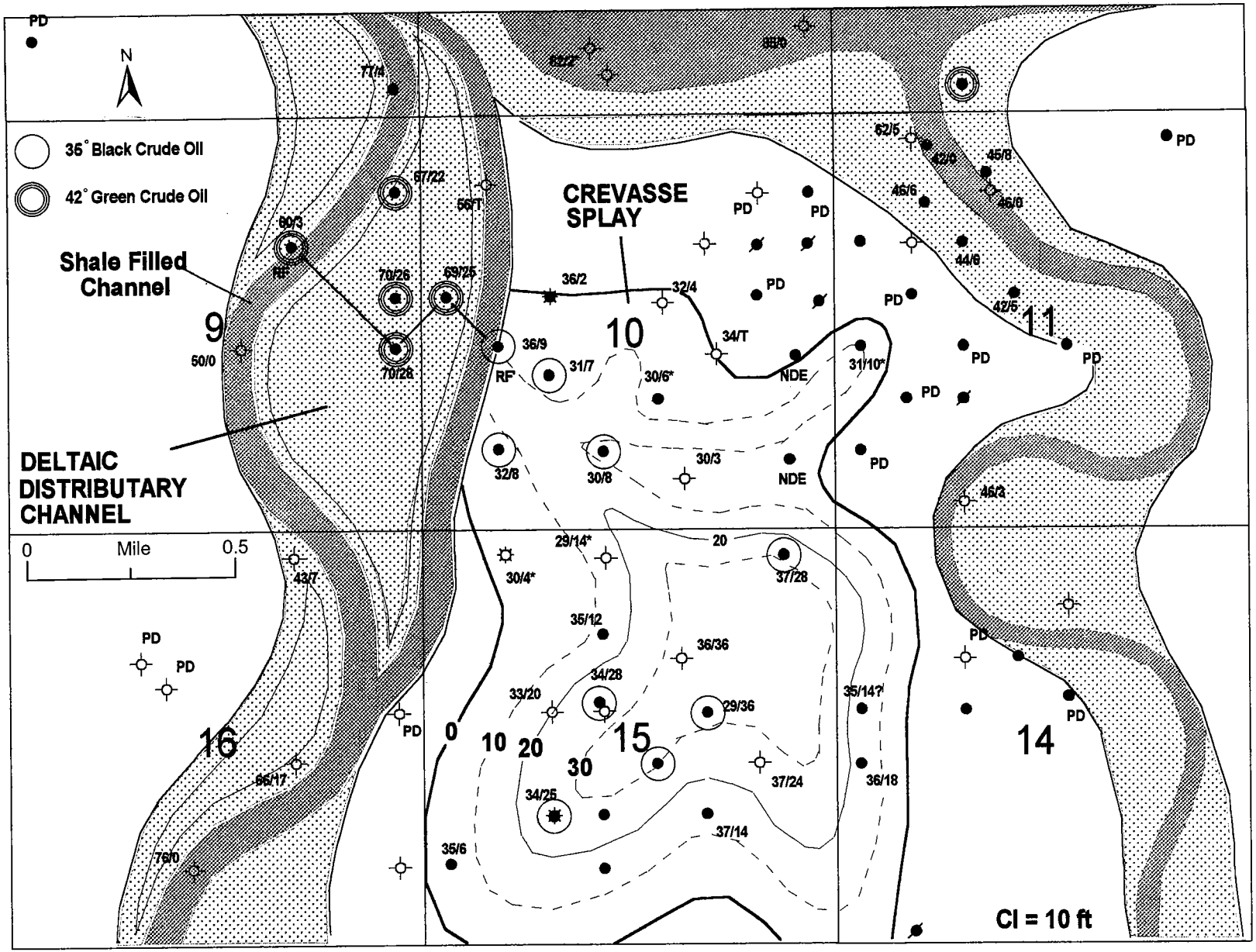

Figure 9. Depositional environments of Red Fork sand. Location of cross section RF–RF′ (see Fig. 10) shown by bold black line. Within the splay deposit, ratios (e.g., 37/28) represents the thickness of the interval from the Pink limestone to the base of the channel (in this case 37 ft), and the second number is the gross amount of sand in the channel (28 ft). Contour interval (CI) = 10 ft. *Abbreviations:* NDE = not deep enough; PD = pro-delta

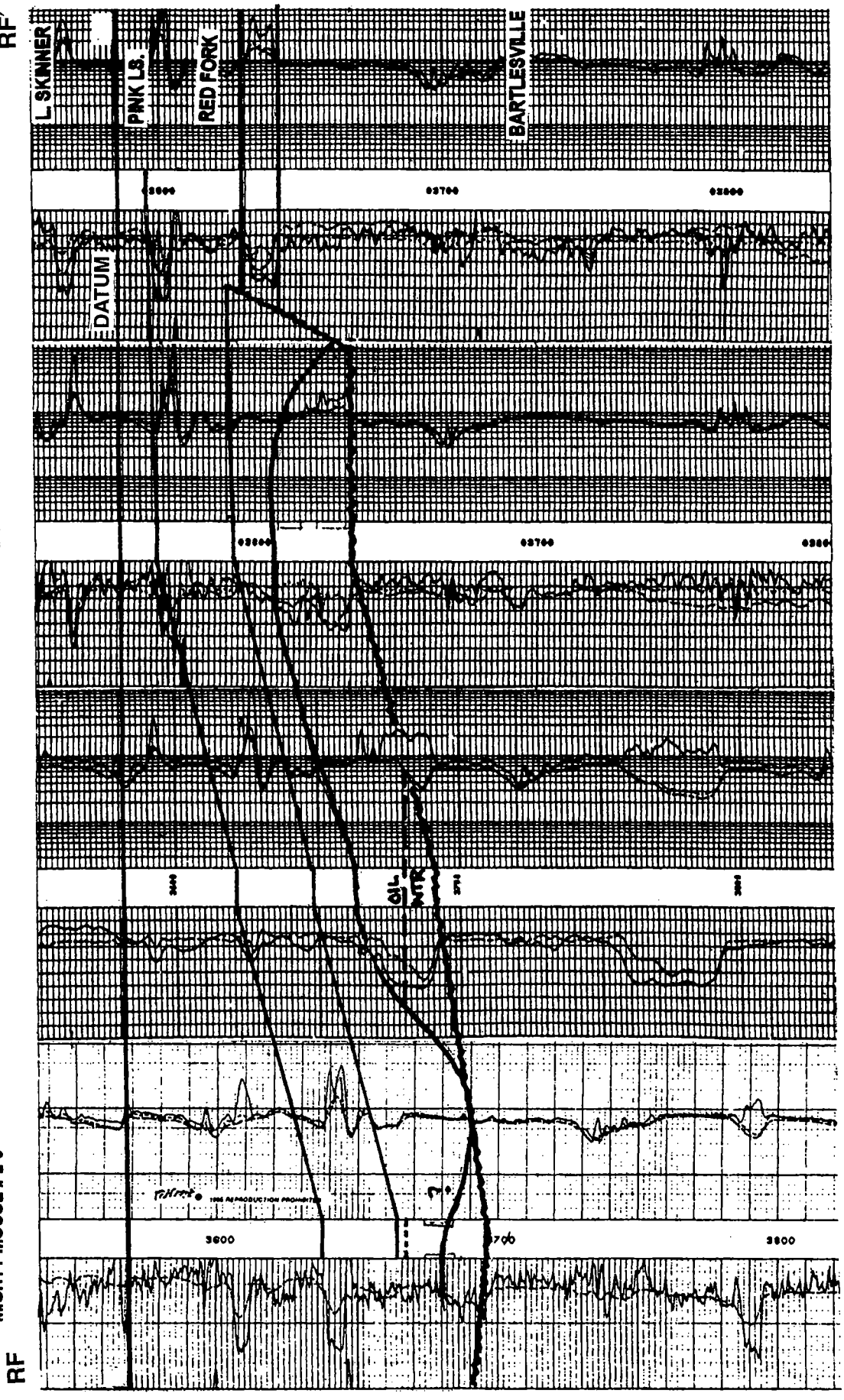

Figure 10. Structural cross section RF–RF′, drawn on top of Pink limestone. See Figure 9 for location. *Abbreviations:* BOPD = barrels of oil per day; BWPD = barrels of water per day; IPF = initial-production flow.

from sand that is 20 ft below the identified oil/water contact. A secondary trap was apparently present in the Long Branch Field, with a different oil/water contact than the rest of the field.

Several wells in and around the field have encountered the shale-filled channel, and, when anticipated, it is easily mapped rather than the sand. Many Cherokee sand fields in north-central Oklahoma have been underdeveloped because exploitation drilling was terminated when the shale-filled channel was drilled and misidentified as the sand boundary. When looked at in this way, zero edges of sands take on a new meaning and also will affect how the sand is mapped. When this type of deposit is encountered, it is highly suggestive of reservoir compartmentalization. Sand isopachs that are segregated by paleoenvironment can identify the component parts of these sand bodies. This can lead to additional reserves as well as understanding the intraformational boundaries that can complicate secondary-recovery efforts.

BARTLESVILLE SANDSTONE

The Bartlesville sand in this area is part of a long, linear trend of sand that begins in western Payne County and extends eastward into Creek County. Here it intersects the main Bartlesville trend extending southward out of Kansas. This trend of sand is rarely more than a mile in width, but is clearly complex in its architecture and contains many of the lithologic components already discussed in this paper. Two primary reservoir sand bodies are present within the system. The first is a deltaic sand with well-defined, shale- and silt-filled distributary channels. Superimposed on the deltaic sequence is an extensive tidal-estuary system. The channels within the tidal system truncate the underlying deltaic sequence and rework the sand, which is then deposited as point bars. The deltaic sequence has sand with a distinct coarsening-upward log profile and a persistent coal at the top of the interval, which is especially well developed in the shale-filled distributary channels. The tidal sandstones exhibit a distinct fining-upward log profile and contain *no* coal. The presence of the coal is extremely useful in separating deltaic channels from tidal channels when making paleoenvironmental interpretations.

In the Long Branch Field, it is primarily the deltaic sequence that is present. Figure 11 is a stratigraphic cross section illustrating the lithology of the Bartlesville. The sand found in the Fairway #1-16 well is representative of a full and unaltered section of deltaic channel-mouth–bar sandstone. The Kelley #1-9 contains a large section of sand, but the upper 8–10 ft is missing as the sequence grades into the distributary channel. The Mighty Mouse #1-9 is almost fully into the channel and only has 8 ft of basal sand remaining. Note the increasing presence of coal in this well versus the previous two wells (Fig. 11). Finally, the Hope #1-10 well illustrates an entirely shale-filled channel with no sand, but a well-developed coal.

Figure 12 is an interval isopach of the distributary-channel system in the Long Branch Field, which maps the interval from the top of the Inola Limestone to the top of the sand. In essence, it is a reconstruction of the channel that does not include sand thickness. The channel is the updip boundary for the system, and no sand is found north or east of it. The entrapment is caused by the intersection of this "zero edge" with the west-trending anticlinal nose. Because the top of the sand is a three-dimensional surface, it can affect where the structural "high" ultimately occurs.

A useful technique in arriving at a meaningful structure map on the sand utilizes detailed sand isopachs for each depositional package combined with a conventional structure map on the Inola Limestone. The map shown as Figure 13 uses the Inola as a datum, so that any intersection of a structural contour line with an isopach contour will result in a pseudo-structural point based on the geologic interpretation. Utilizing these pseudo-data points with actual well-data points, a more detailed structure map on top of the sand can be constructed that takes into account the shape of the sand body.

Figure 14 is such a map for the Bartlesville sand in the Long Branch Field. It shows quite clearly that the actual "high" for the trap was never drilled and may be as much as 10–15 ft higher than any of the wells that were drilled. Since the best reservoir quality found in this system occurs only in the upper part of the "full and complete" section of sand, it is likely that the "best" Bartlesville reservoir in this field was never drilled. If this were a water-driven oil reservoir rather than gas-driven, this location might still have potential for undrained "attic" reserves.

Another aspect to be considered is what this trap might look like in an area of less structural relief. If the structural slope within the area of entrapment is less than the stratigraphic slope of the sand body, the area of maximum closure will shift away from the structural "high" to the stratigraphic "high." This stratigraphic "high" is also commonly augmented by differential compaction over the thicker part of the sand body. The Cherokee Platform has numerous examples of "drilling updip from the show" type of prospects that failed. In many cases, the prospect was actually regionally "downdip" from the show well because of the shape of the sand body.

CONCLUSIONS

The following four conclusions can be drawn from this study.

(1) Almost all Cherokee sands have undergone some type of modification due to tidal action during marine transgressions following deposition of the primary deltaic sequence. This includes truncation of underlying sands that can create traps, as well as the reworking and deposition of sand into point bars capable of hosting hydrocarbons.

(2) Reservoir compartmentalization due to complex sand architecture in the Red Fork has resulted in distinctly different oils being produced, as well as different oil/water contacts within a very localized area of the Long Branch Field. These conspicuous inconsistencies

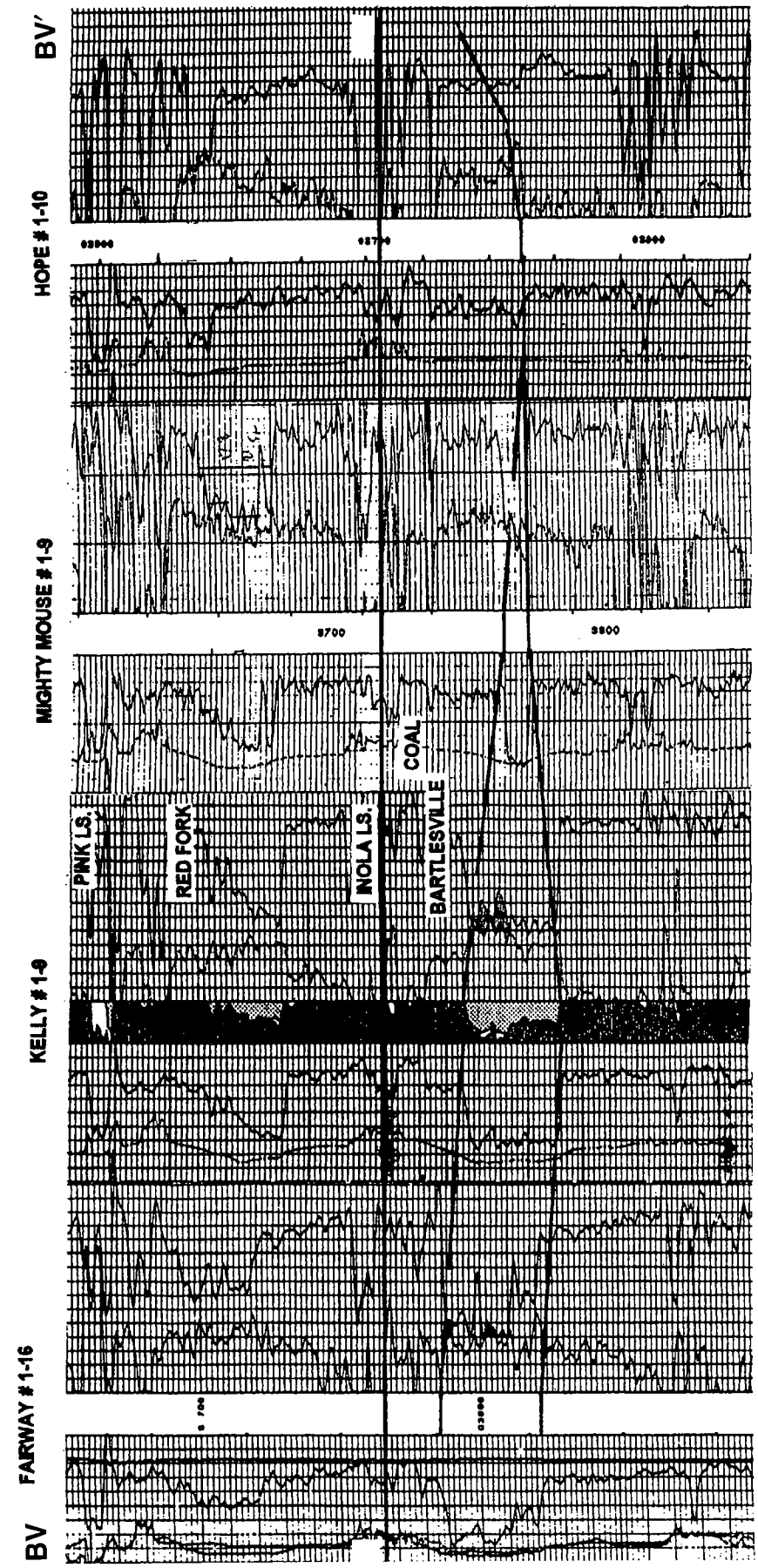

Figure 11. Stratigraphic cross section BV–BV'. See Figure 12 for location. Datum is base of Inola Limestone.

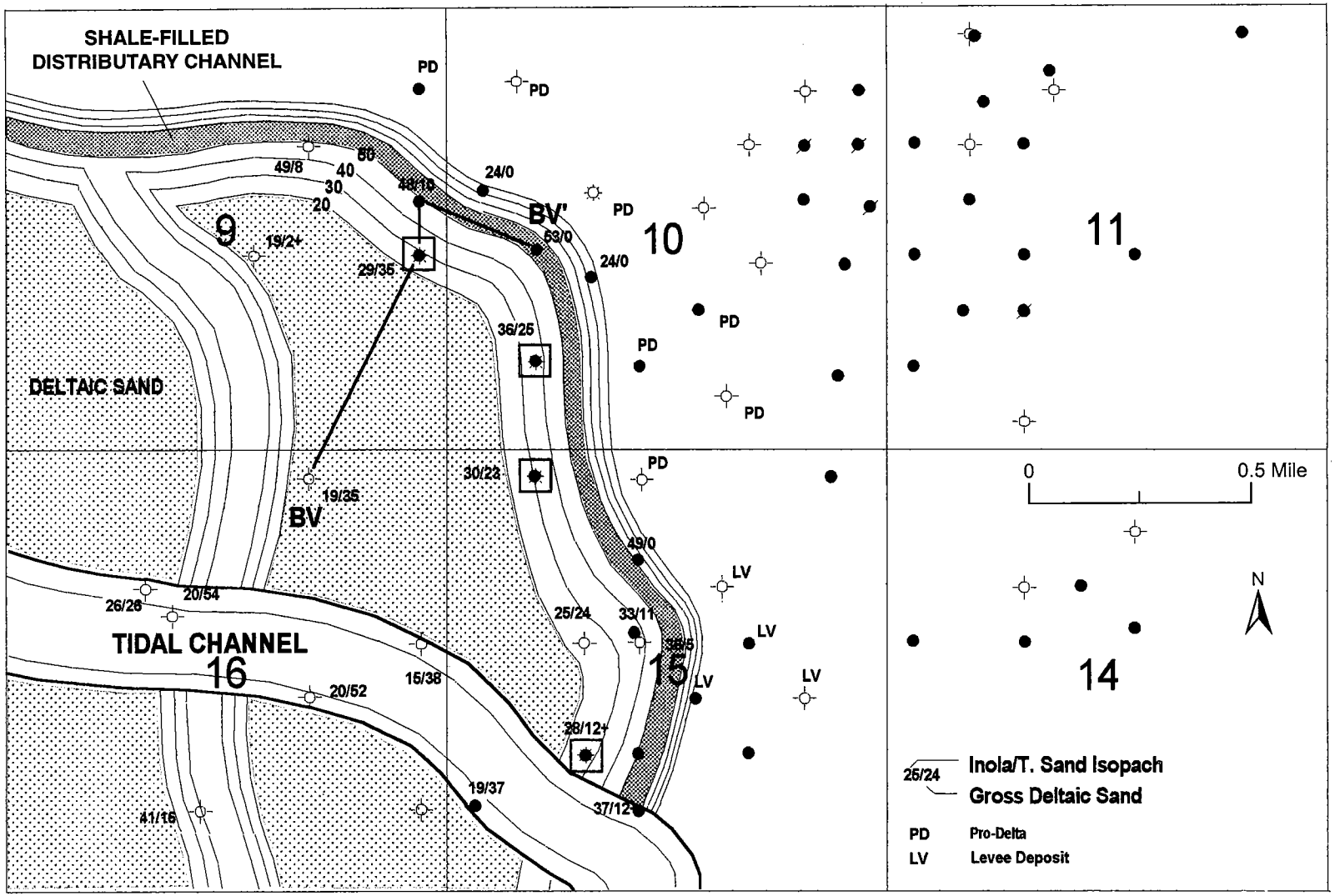

Figure 12. Environment of deposition of Bartlesville sand. Contours are a reconstruction of the distributary channel using thickness of interval from Inola Limestone to top of sand. Location of cross section BV–BV′ (Fig. 11) shown by bold lines. Ratios (e.g., 35/22) represents the thickness of the interval from the Inola Limestone to the top of the sand (35 ft), and the second number (22 ft) is the thickness of the gross deltaic sand. Contour interval = 10 ft. *Abbreviations:* PD = pro-delta; LV = levee deposit.

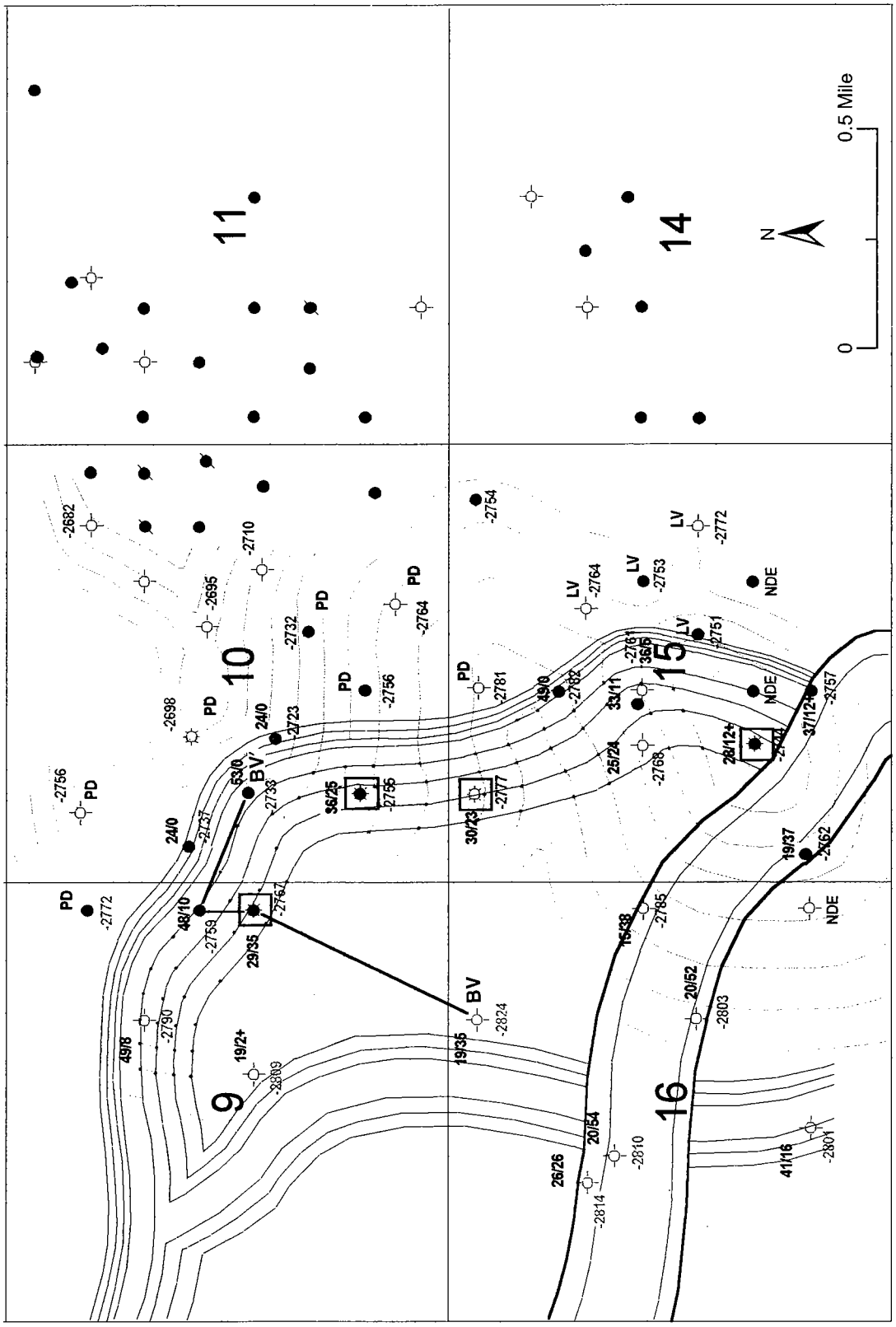

Figure 13. Isopachous map of thickness of Bartlesville sandstone with structural overlay of Inola Limestone (light-gray lines). Isopachous map based on interval from Inola Limestone to top of Bartlesville sand. Location of cross section BV– BV′ shown by old lines. Datum for structural-contour map is mean sea level. Contour interval = 10 ft. *Abbreviations:* LV = levee deposit; NDE = not deep enough; PD = pro-delta.

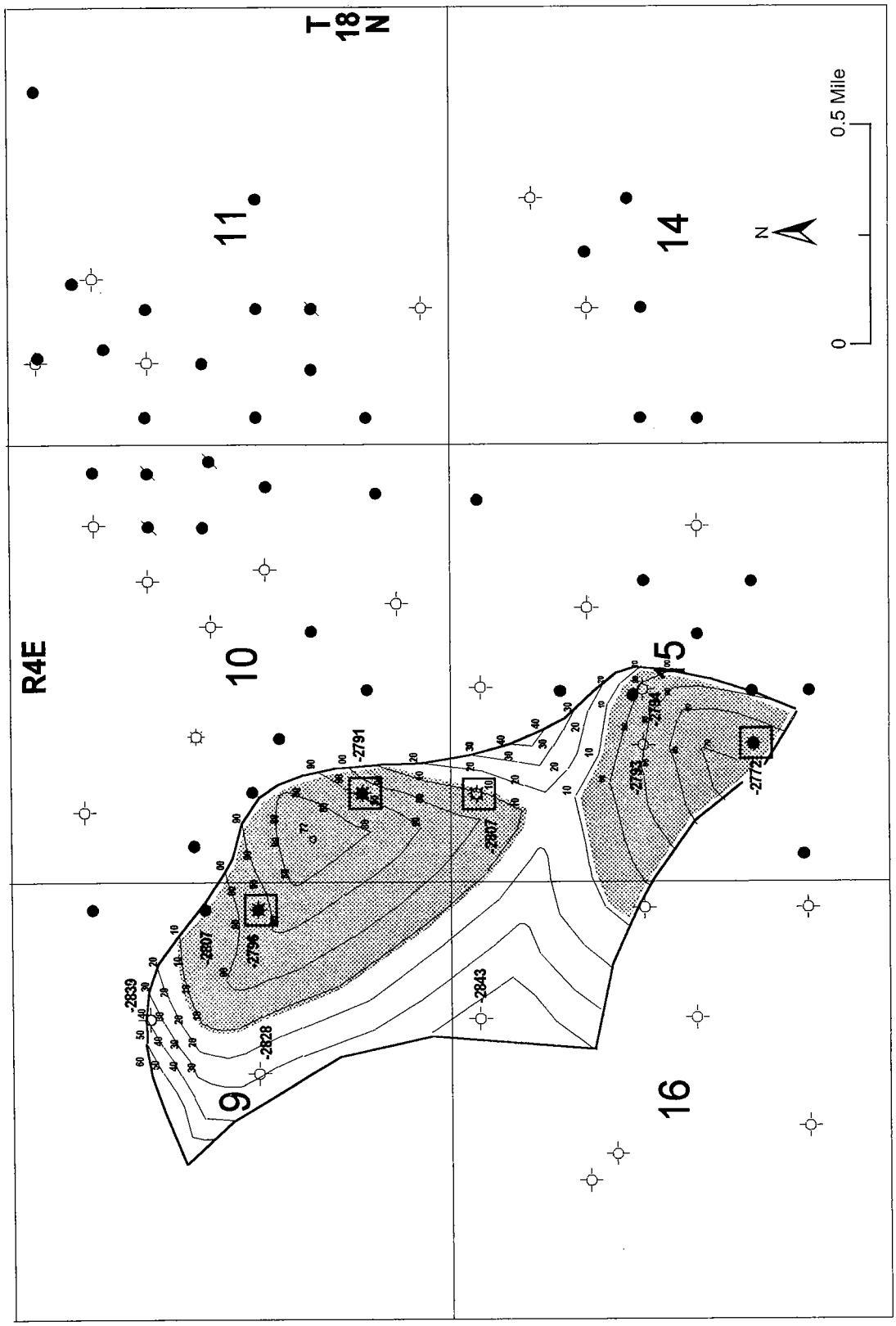

Figure 14. Structure-contour map of Bartlesville sand showing areas of production (stippled pattern). Contour interval is 10 ft. Datum is mean sea level.

are commonly evidence of reservoir barriers that need to be accurately identified in order to fully develop the reserves and to efficiently engineer secondary-recovery projects.

(3) Recognizing and mapping of the channel components of a sand sequence will dramatically increase the ability to visualize the three-dimensional aspects of a sand body. These techniques can more accurately depict the most prospective areas of the oil and gas trap.

(4) All aspects of the paleoenvironment of a sand trend should be mapped regionally in order to successfully prospect for oil and gas in the Cherokee sands of Oklahoma.

Development of Transition-Zone Reserves Around Abandoned Production: Case Study of Mount Vernon Field, Lincoln County, Oklahoma

David Chernicky and Scott T. Schad
New Dominion, L.L.C
Tulsa, Oklahoma

ABSTRACT.—The Mount Vernon Field in Lincoln County, Oklahoma, represents a typical Red Fork Sand body depleted of oil by conventional production methods and abandoned. Subsequent development of the thicker oil/water-transition zone underlying the original Red Fork oil sand, coupled with aggressive dewatering of the reservoir, recovered an additional 1,260,858 bbl of oil, 18,555,429 MCF (thousand cubic feet) of gas, and an estimated 1,767,184 bbl of natural-gas liquids, from a 4,960-acre area that previously contained 75 depleted oil wells and 42 dry holes.

HISTORY OF DEVELOPMENT AND PRODUCTION

J. R. McLean discovered the Mount Vernon Field (Fig. 1) in February 1952 with the completion of the Alberta Mingus No. 1, located in the NW¼NW¼ sec. 1, T. 15 N., R. 3 E., Lincoln County, Oklahoma. Producing from the Pennsylvanian Red Fork Sandstone, this well pumped 36 bbl of oil per day from an open-hole completion in just 8 ft of sand. The type log for this field is shown as Figure 2. Subsequent drilling over the next

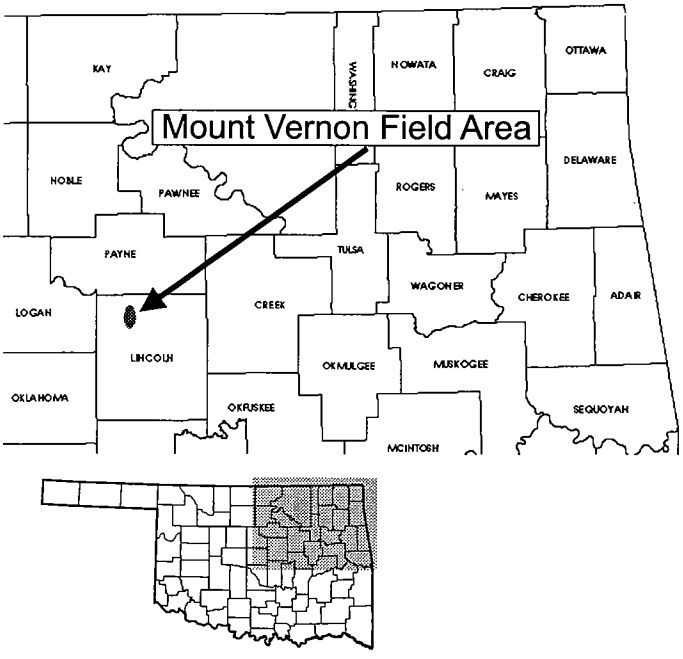

Figure 1. Location map of Mount Vernon Field, Lincoln County, Oklahoma

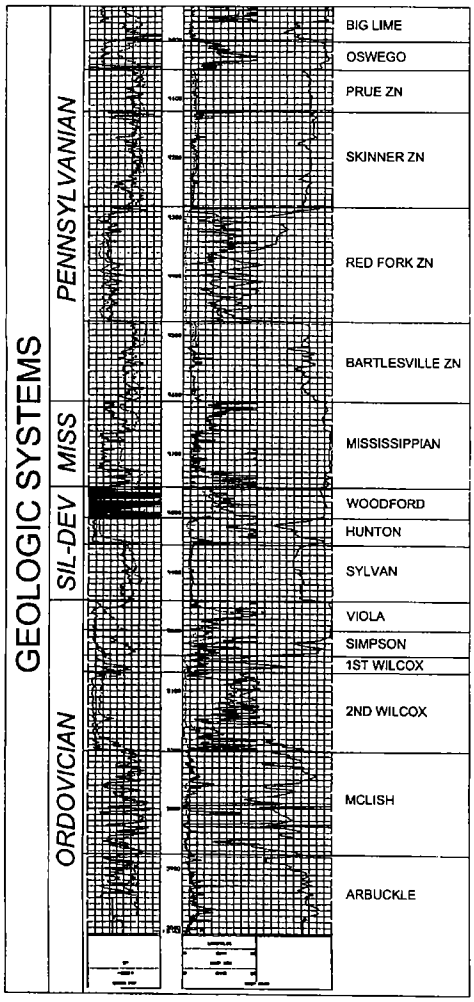

Figure 2. Type log for Mount Vernon Field.

Chernicky, David; and Schad, S. T., 2002, Development of transition-zone reserves around abandoned production: case study of Mount Vernon Field, Lincoln County, Oklahoma, *in* Boyd, D. T. (ed.), Finding and producing Cherokee reservoirs in the southern Midcontinent, 2002 symposium: Oklahoma Geological Survey Circular 108, p. 61–72.

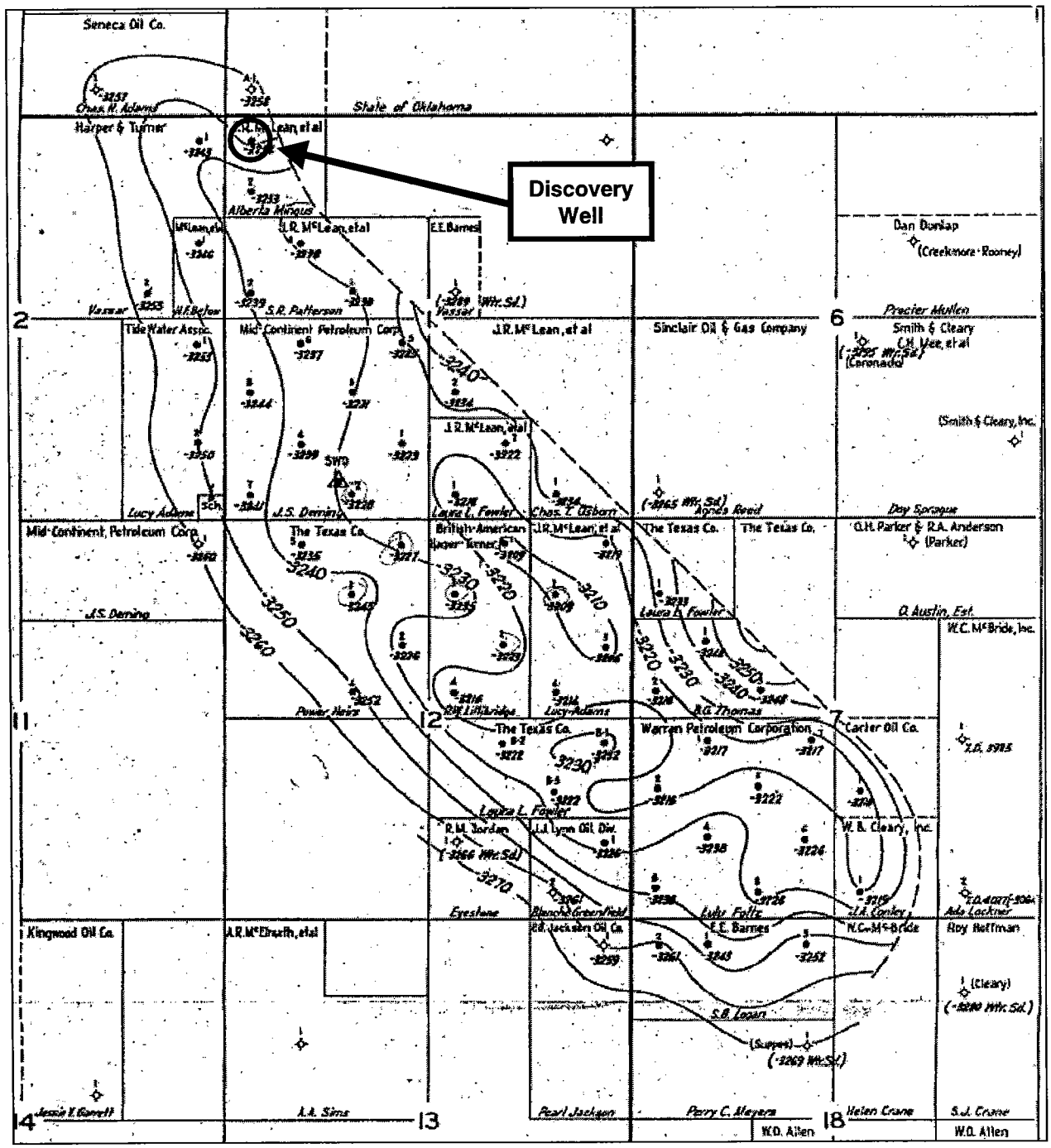

Figure 3. Structure-contour map on Red Fork "oil sand," Mount Vernon Field, T. 15–16 N., R. 3–4 E., Lincoln County, Oklahoma. Contour interval = 10 ft.

two years by additional operators like E. E. Barnes, British American Oil Producing Company, Carter Oil, W. B. Cleary, Harper-Turner, Mid-Continent Petroleum, the Texas Company, Tide Water Associated Oil, and Warren Petroleum, followed a 20-acre spacing pattern and rapidly delineated the field's extent. By the end of 1954 the field contained 57 producing wells and operators considered it completely defined (Fig. 3).

Most operators completed the Red Fork in an open hole in an average of 12 ft of sand. Operators typically used small fracture treatments of 1,000–2,000 gal of oil with 1,000–2,000 lb of sand, although E. E. Barnes, Carter Oil, and W. B. Cleary tried larger fracs with up to 20,000 gal of oil and 20,000 lb of sand. Cumulative data from the late 1950s shows that the field produced 5,625,270 bbl of oil by December 1956, for an average of

98,688 bbl of oil per well. Unitized for a pressure maintenance water flood (see Earlougher, 1955) in January 1957, the field produced an additional 2,193,236 bbl of oil through 1989, pushing the total production to 7,818,506 bbl of oil for an average-per-well recovery of 137,166 bbl. In 1987, two Red Fork wells were still active in the 1,890-acre unit, producing 7–9 bbl of oil per day, 500 bbl of water, and enough gas to run the pumping units.

DEVELOPMENT OF DOWNDIP SANDSTONES

Few wells in the Mount Vernon Field penetrated more than the top 30 ft of Red Fork Sandstone. Geologists assumed the field represented an isolated Red Fork channel, but subsequent drilling by Danube Oil and Tripledee, beginning in the 1970s, established the presence of a second sand body downdip to the west, trending in a similar direction. In 1973 Danube Oil Company drilled their Nelson No. 1 well, located in the SW¼ NE¼NE¼ sec. 14, T. 15 N., R. 3 E. On a drill-stem test in the Red Fork, this well recovered 600 ft of free oil and flowed 600 MCFGD (thousand cubic feet of gas per day). Tipledee Drilling Company assumed operation of the well and successfully completed it, flowing 142 BOPD (barrels of oil per day) and 600 MCFGD from 8 ft of sand completed open hole. Although never treated, this well produced 49,193 bbl of oil from 1973 through 1985 and vented an estimated 250 million cubic feet of gas. In following years, Tripledee drilled seven additional wells to delineate the downdip Red Fork channel, completing four of them.

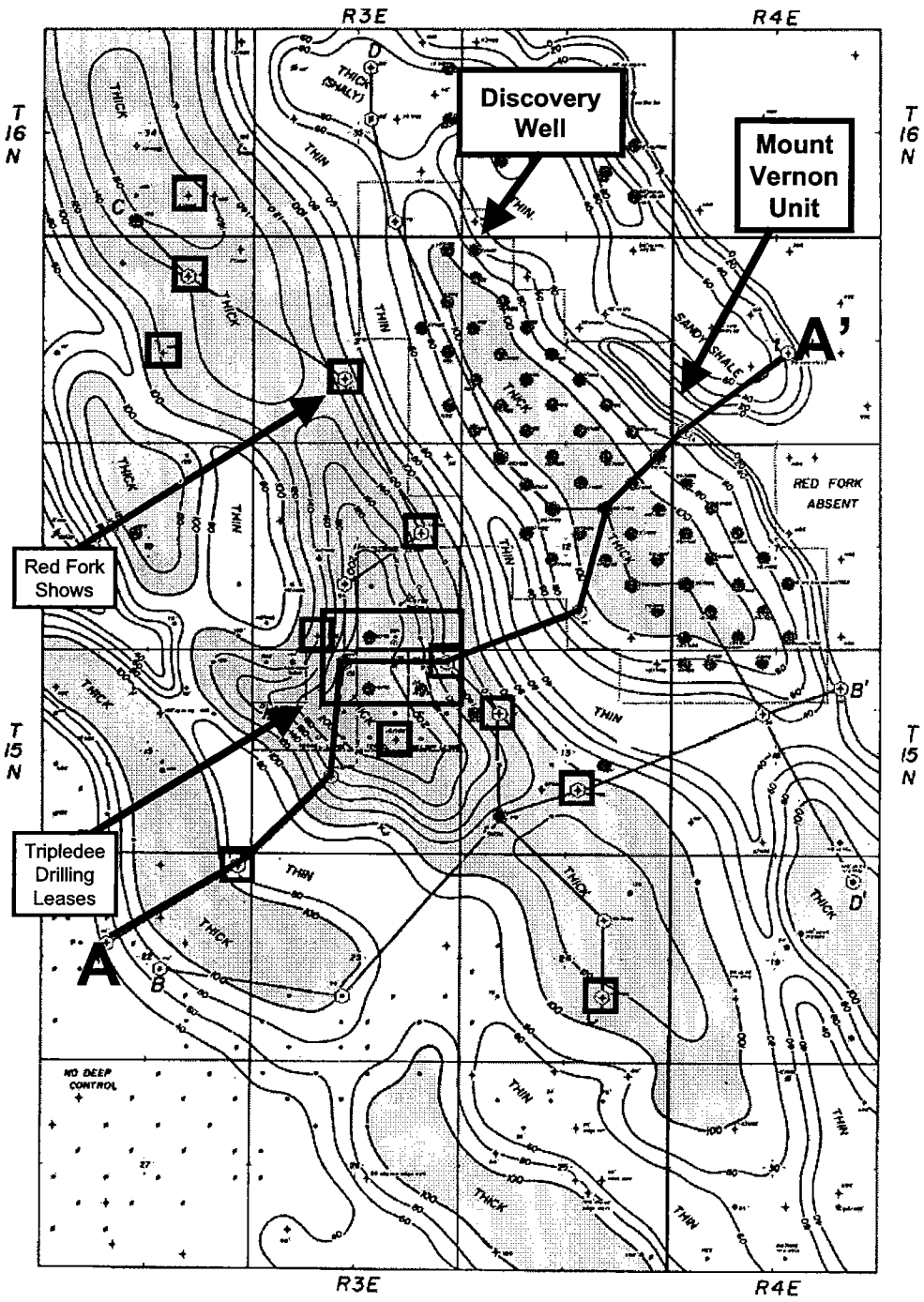

Figure 4. Mount Vernon Field area, gross Red Fork Sand isopach map (including Bartlesville equivalent) showing downdip sand bodies (gray-shaded areas) and location of cross-section A–A′ (Fig. 5). Contour interval = 20 ft.

An isopach map of the gross Red Fork sand interval made in the early 1990s (Fig. 4) shows a downdip sand body thicker and larger than Mount Vernon Field. In places, the Red Fork cuts into Bartlesville Sand, creating a sand package more than 200 ft thick (Fig. 5, cross-section A–A′). Structure on the Pink Lime (Fig. 6), which overlies the Red Fork Sandstone, shows regional dip to the southwest, interrupted by differential compaction effects over the sand "thicks." The Red Fork pay interval, termed the "free oil" sand, develops just below the Pink Lime and reaches a maximum thickness of 40 ft in the Mount Vernon Field, but only 8 ft in the downdip channel. The "free oil" sand sits atop a thicker oil and water "transition zone" with 40–80% water saturations that reaches 50 ft in thickness. The

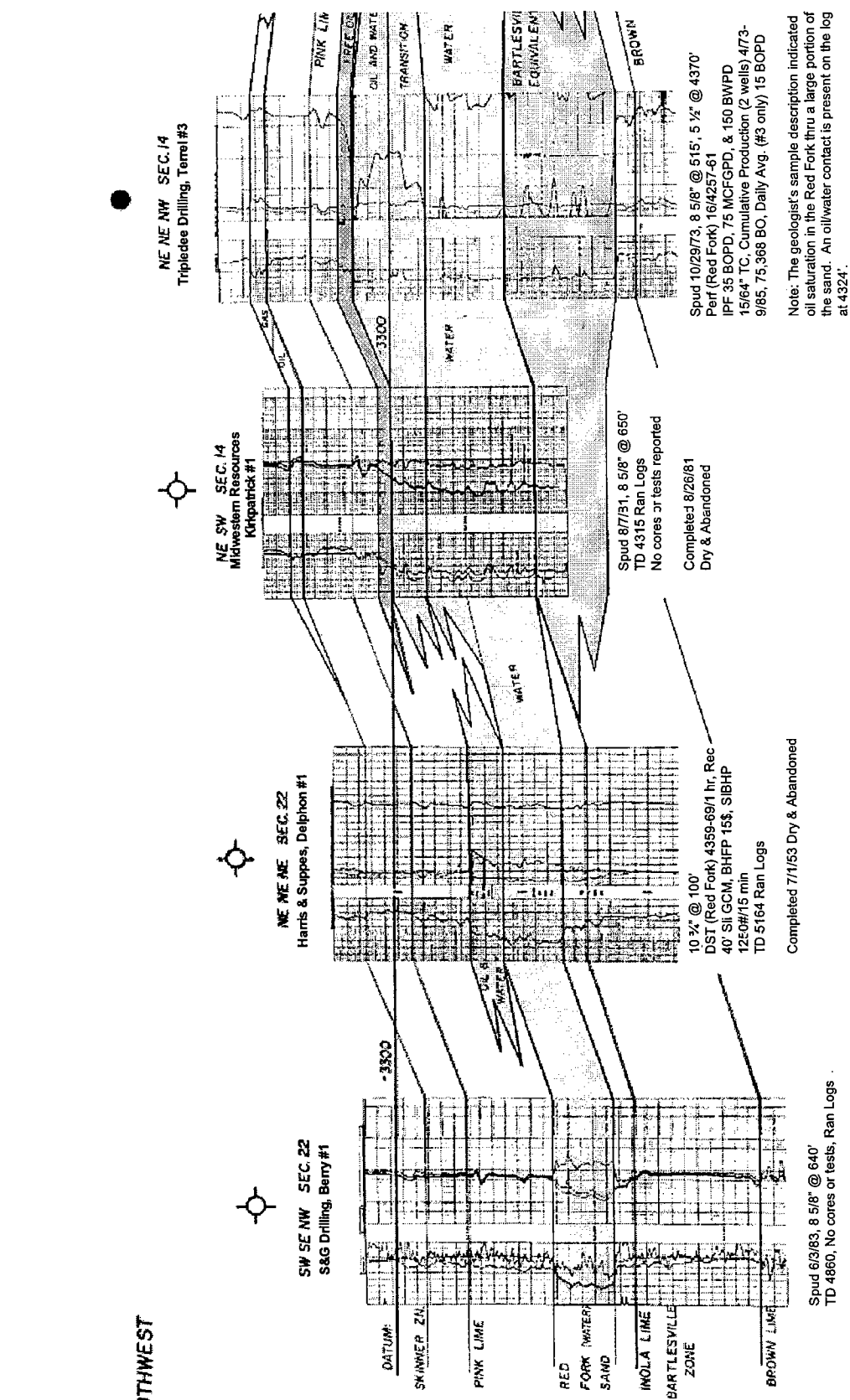

Figure 5 *(above and following pages)*. Regional structural cross-section A–A'. Line of section shown in Figure 4.

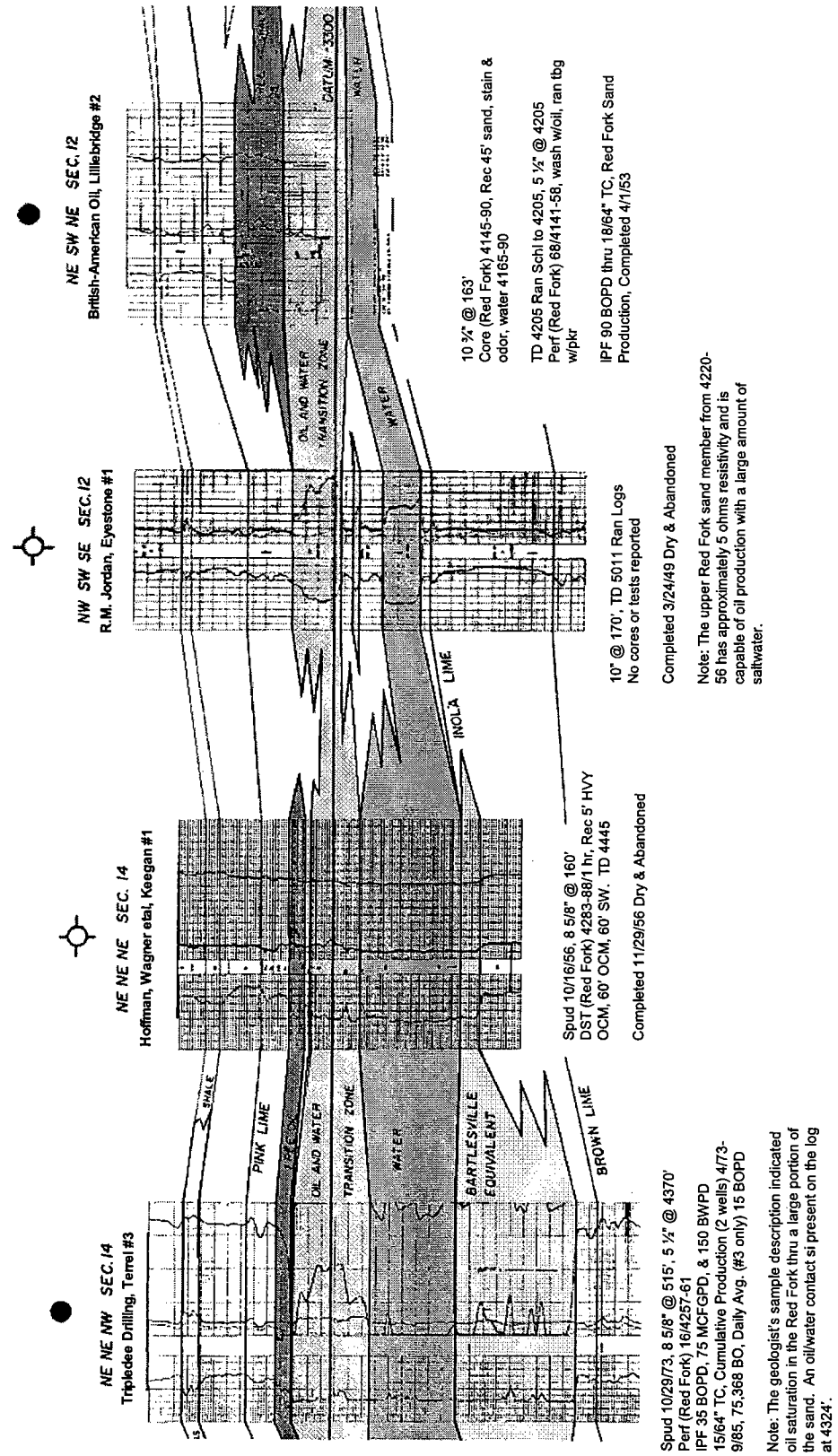

Figure 5 *(continued)*.

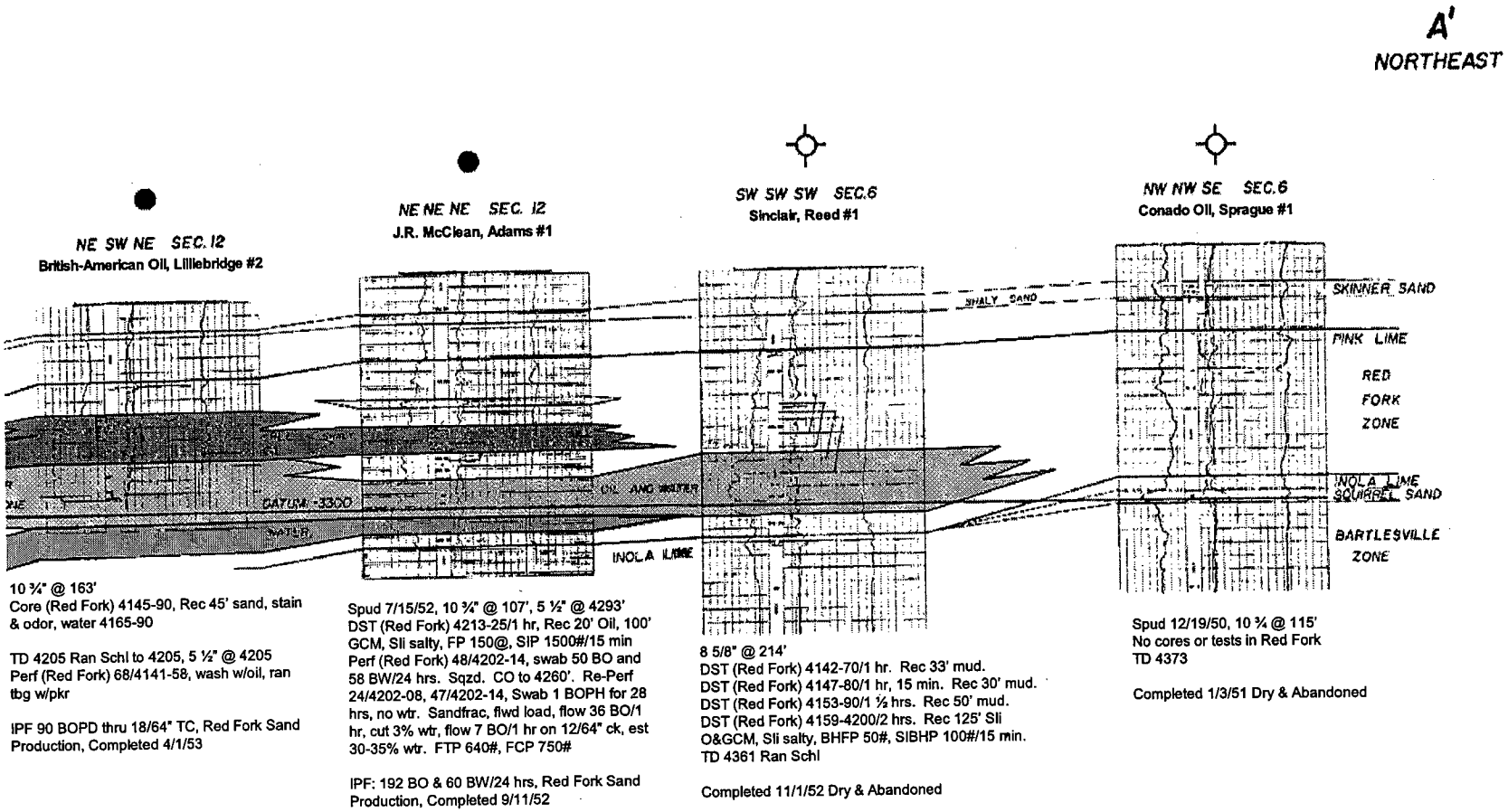

Figure 5 *(continued).*

transition zone in turn overlies 100% wet sand. Porosity is relatively constant at 18–20% throughout the Red Fork, so resistivity varies primarily with oil saturation. The water-bearing sand exhibits ≤1 ohm resistivity, the transition zone exhibits ≥2 ohms, and the oil zone ≥5 ohms.

Transition zones form in response to capillary attraction. Water rises in the reservoir rock-pore throats until the weight of the imbibed fluid column balances the upward pull of capillary attraction. As this water displaces oil, it creates a mixed-phase transition zone. In the diagram depicting a theoretical reservoir pore throat (Fig. 7), the important terms appear in the denominator of the equation for transition zone height, *h*. As the pore throat radius, *r*, increases, the supported transition-zone height decreases. The height also drops as the difference between the two fluid densities increases. For example, transition zones are common in fine-grained Midcontinent sandstones carrying oil and water but not in high-porosity Gulf Coast sandstones carrying only gas and water.

To produce the oil that is present in a transition zone, large volumes of water must be moved to drop the reservoir pressure. As bottom-hole pressure falls with sustained production, gas expansion is initiated, pushing imbibed oil out of the transition-zone porosity. Other mechanisms, such as gravity drainage, also come into play as the water level drops, letting oil move into larger pore systems and fracture networks that ultimately feed the production stream.

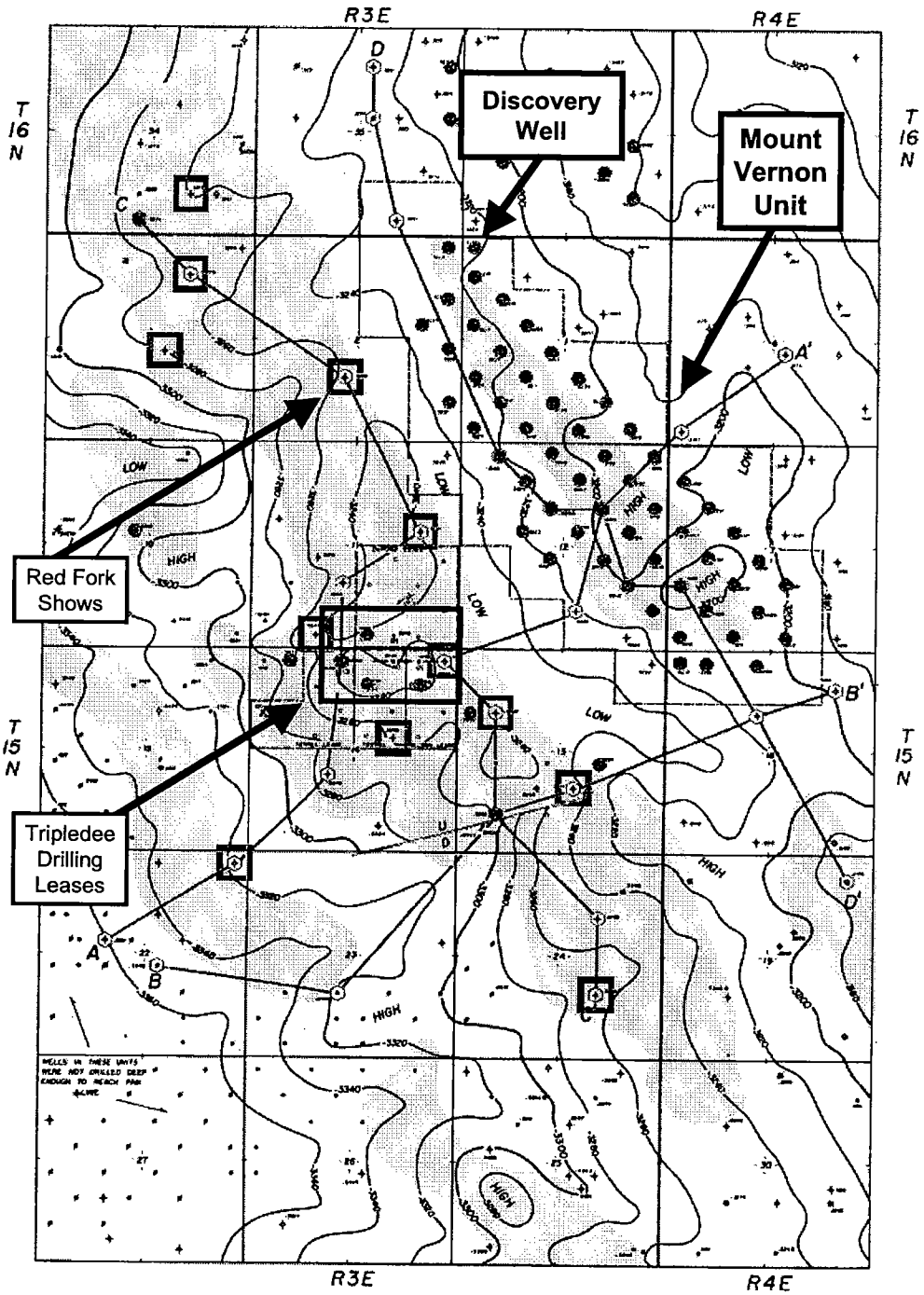

Figure 6. Mount Vernon Field area, structure map on Pink Lime; same area as Figure 4. Downdip sand bodies shown as gray-shaded areas. Contour interval = 20 ft.

In 1985, following their success in the Pawnee Lake Red Fork Field in Payne County, Oklahoma, Ames Oil and Gas decided to target the Red Fork transition zone in the Mount Vernon area. Their Miller No. 1 well, located in the NE¼SW¼SW¼ sec. 13, T. 15 N., R. 3 E., became the first Red Fork transition-zone producer. Completed for an initial potential of 12 BOPD and 1,400 BWPD (barrels of water per day), the well quickly climbed to 68 BOPD. ST Industries and Benson Mineral Group also completed transition-zone wells before the collapse of oil prices in 1986 halted drilling. This left most wells plugged or temporarily abandoned.

Altex Resources took over operations of the unit and surrounding acreage in 1990. They successfully drilled and completed 69 wells and re-completed 12 old unit wells in the Red Fork transition zone over a six-year period. The operator immediately put each new transition-zone well on submersible pump for 12–15 months

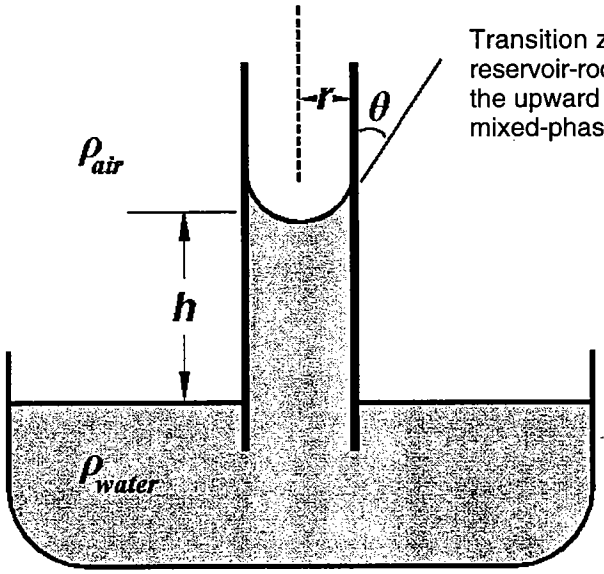

Transition zones form in response to capillary attraction. Water rises in the reservoir-rock pore throats until the weight of the imbibed fluid column balances the upward pull of capillary attraction. As this water displaces oil, it creates a mixed-phase transition zone.

$$Force = Pressure \times Area$$

$$2\pi rT\cos\theta = (\rho_w - \rho_a)h \times \pi r^2$$

$$h = \frac{2T\cos\theta}{r(\rho_w - \rho_a)}$$

h = height of water column in capillary tube
T = interfacial tension between the two phases
θ = contact angle between wetting fluid and the rock
r = radius of pore throats
$\rho_w - \rho_a$ = density difference between water and air

Figure 7. Diagram of theoretical reservoir pore-throat illustrating capillary attraction.

to dewater the formation, after which they converted to a beam pump. Produced water went into disposal wells drilled to the Arbuckle. Initial produced oil cuts ranged from 1% to 10% and averaged 2% to 3%. Established oil cuts remained relatively constant over the life of each well. As fluid volumes declined, gas volumes inclined, peaking after oil production.

TYPICAL TRANSITION-ZONE PRODUCER

The Altex No. 1 Goodbary, located 660 ft from the south line and 1,880 ft from the west line SW¼ sec. 2, T. 15 N., R. 3 E., represents a typical Red Fork transition-zone producer in the Mount Vernon Field area (Fig. 8). The dual-induction and compensated neutron-density logs for this well show 4 ft of Red Fork "oil sand" above 80 ft of transition zone, followed by 80 ft of wet sand. The operator fracture-treated 46 ft of the transition zone to complete the well pumping for 52 BOPD + 210 MCFGPD + 1,700 BWPD.

Given the resistivity cutoffs mentioned previously, the upper 20 ft of the transition zone in this well show anomalously low values. This results from averaging that occurs when the layer thickness of a finely laminated sand/shale sequence falls below the resolution of the logging tool. Thomas and Stieber (1975)[1] developed an analysis technique that shows promise for identifying the complete transition-zone section in such thinly bedded formations. This technique is effective if sandstone composition honors the following five assumptions: (1) detrital clay largely controls sand-layer porosity; (2) detrital clays come from the same provenance as the sand (so that offset shale beds reflect similar clay properties); (3) the gamma-ray tool responds to high cation-exchange–capacity clays; (4) both sand and shale show similar grain densities; and (5) the volumetric distribution of sand and shale controls the gamma-ray response.

Data from this well, plotted on a Thomas-Stieber chart of total porosity versus gamma-ray value (Fig. 9), support the assumption of fine laminations. End points of the sand/shale-model triangle represent 100% sand, 100% shale, and sand with porosity completely filled with dispersed shale. Dashed lines that intersect the top side of the triangle indicate increasing values of net-to-gross ratio, whereas dashed lines that intersect the right side of the triangle represent the measured porosity of the sandstone as a function of the scaled porosity of the clean sand. Sandstones with laminated shale tend to cluster along the top side of the triangle, whereas sandstones with dispersed shale cluster along the right side. Data for this well concentrate along the top, and most points fall within a region bounded by 60–90% net-to-gross ratio and sandstone porosities of 80–100% of the clean-sand porosity. This indicates the possibility of more Red Fork oil pay present than is perforated in the well. Based on this analysis the 35-ft section below the lowest perforation represents a good candidate.

TRANSITION-ZONE PRODUCTION STATUS

A recent Red Fork isopach map (Fig. 10) shows the extent of the transition zone that subsequently proved productive. Since 1987, the Red Fork transition zone produced an additional 1,260,858 bbl of oil, 18,555,429 MCF of gas, and an estimated 1,767,184 bbl of natural-gas liquids (Fig. 11) from a 4,960-acre area that previously contained 75 depleted oil wells and 42 dry holes (Oil-Law Records, 2000). The field currently produces at stripper levels.

[1] A web site created by Pedersen and Nordahl (1999) includes a detailed presentation of the Thomas-Stieber (1975) approach and a downloadable Excel spreadsheet for making the calculations.

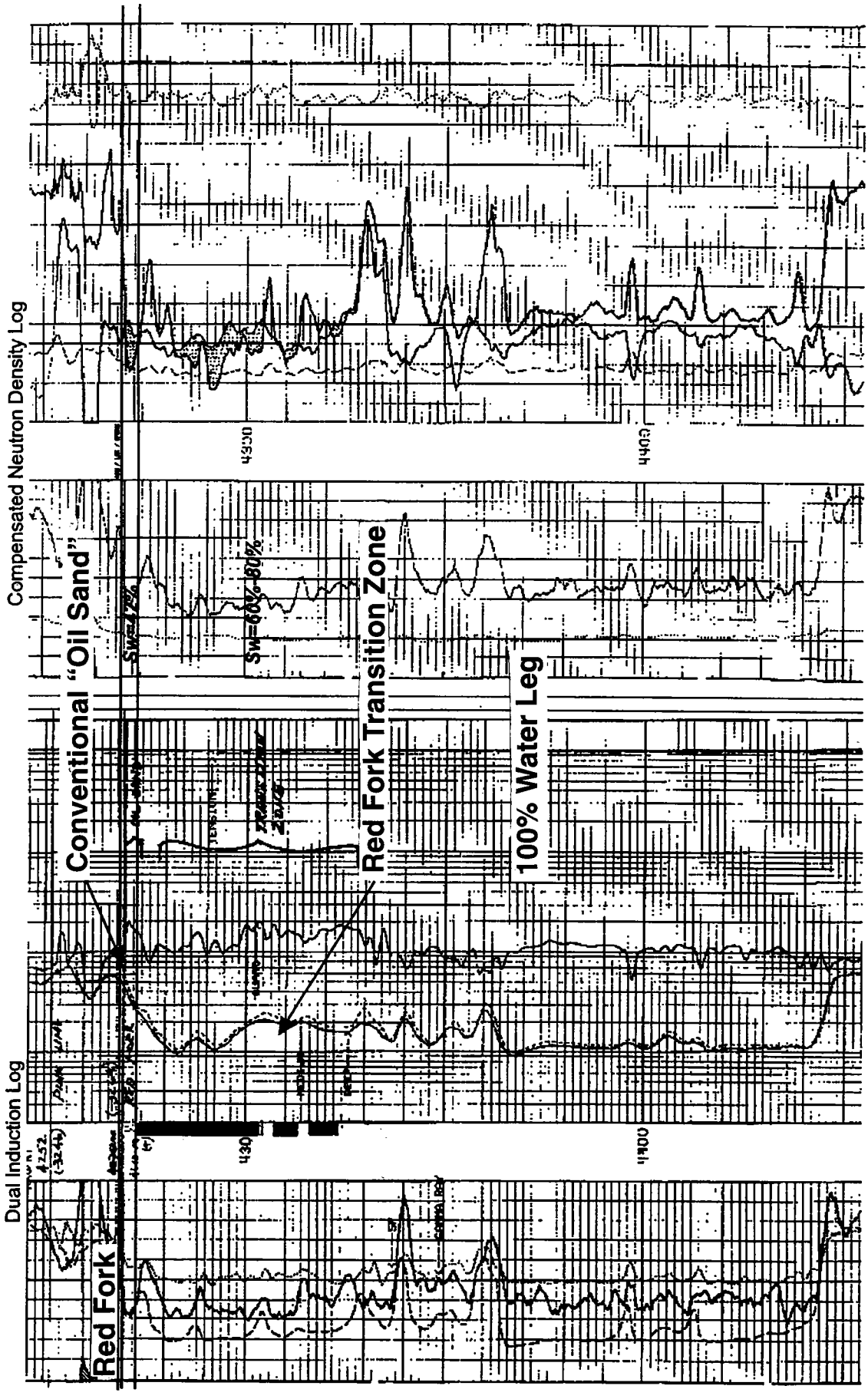

Figure 8. Altex #1 Goodbary Red Fork Sandstone, illustrating typical transition zone log response. 660 ft from south line, 1,880 ft from west line, SW¼ sec. 2, T. 15 N., R. 3 E. Depth in feet. The Red Fork was perforated from 4,270–4,316 ft in depth, was acidized and fraced, and the initial potential production was 52 barrels of oil per day + 210 thousand cubic feet of gas per day, and 1,700 barrels of water per day. *Abbreviation: Sw* = connate-water saturation.

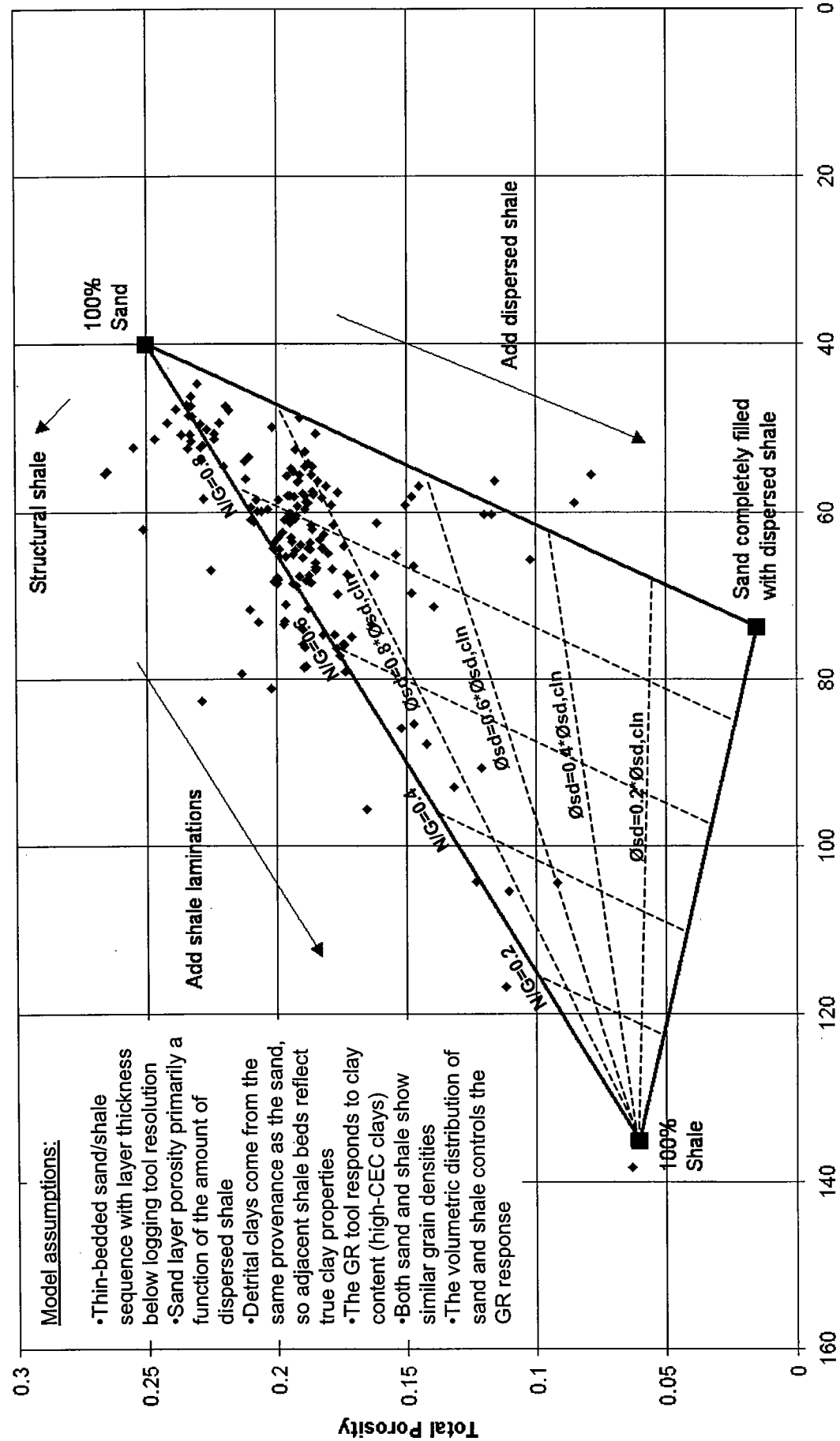

Figure 9. Thomas-Stieber sand/shale model triangle of Red Fork Sandstone in Altex #1 Goodbary well, located 660 ft from south line, 1,800 ft from west line, SW¼ sec. 2, T. 15 N., R. 3 E. Triangular plot of total porosity (in millidarcies) versus gravity (GR) in degrees API; grain size in ϕ units. *Abbreviations:* CEC = cation-exchange–capacity clays; cln = clean; G = GR = gamma-ray log; N = neutron log; sd = sand.

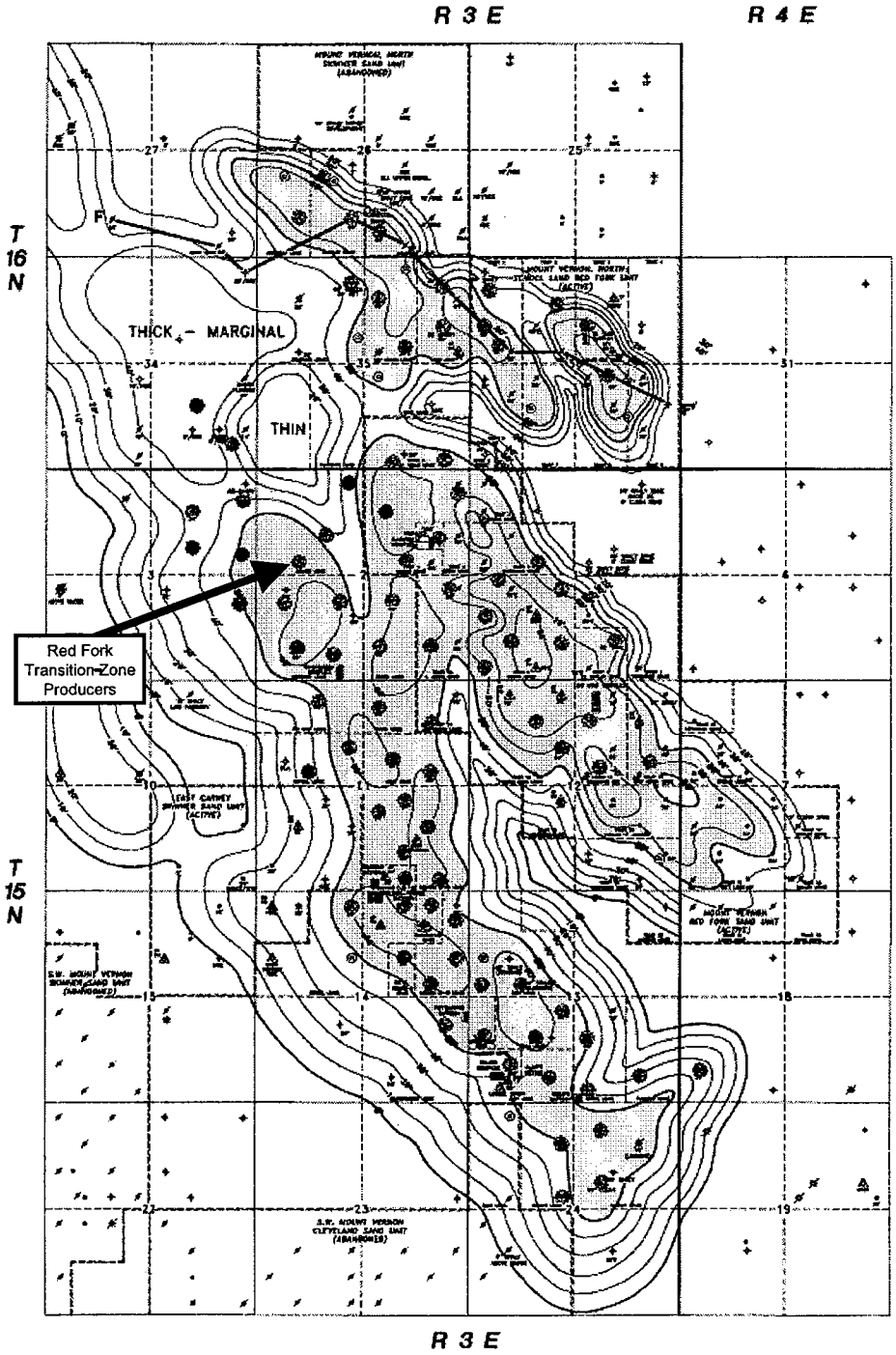

Figure 10. Gross Red Fork transition-zone isopach map (contour interval = 10 ft) in Mount Vernon Field area showing transition-zone production. Thick sand areas shown by gray-shaded pattern.

CONCLUSION

The authors believe additional Pennsylvanian sandstones in Oklahoma with significant oil/water transition zones are prime candidates for the aggressive types of dewatering of the reservoir described here.

ACKNOWLEDGMENTS

We thank John Ames and Altex Resources for access to original well files and permission to publish proprietary information.

REFERENCES CITED

Earlougher, R. C., 1955, Report for operators of the Mt. Vernon Pool, Lincoln County, Oklahoma, on pressure maintenance possibilities of the Red Fork Sand: Earlougher Engineering Professional Report, Tulsa, Oklahoma, 97 p.

Oil-Law Records, 2000, Recent production data from Oil-Law Records online data repository: http://welldata.oil-law.com.

Pedersen, B. K.; and Nordahl, Kjetil, 1999, Petrophysical evaluation of thin beds: a review of the Thomas-Stieber

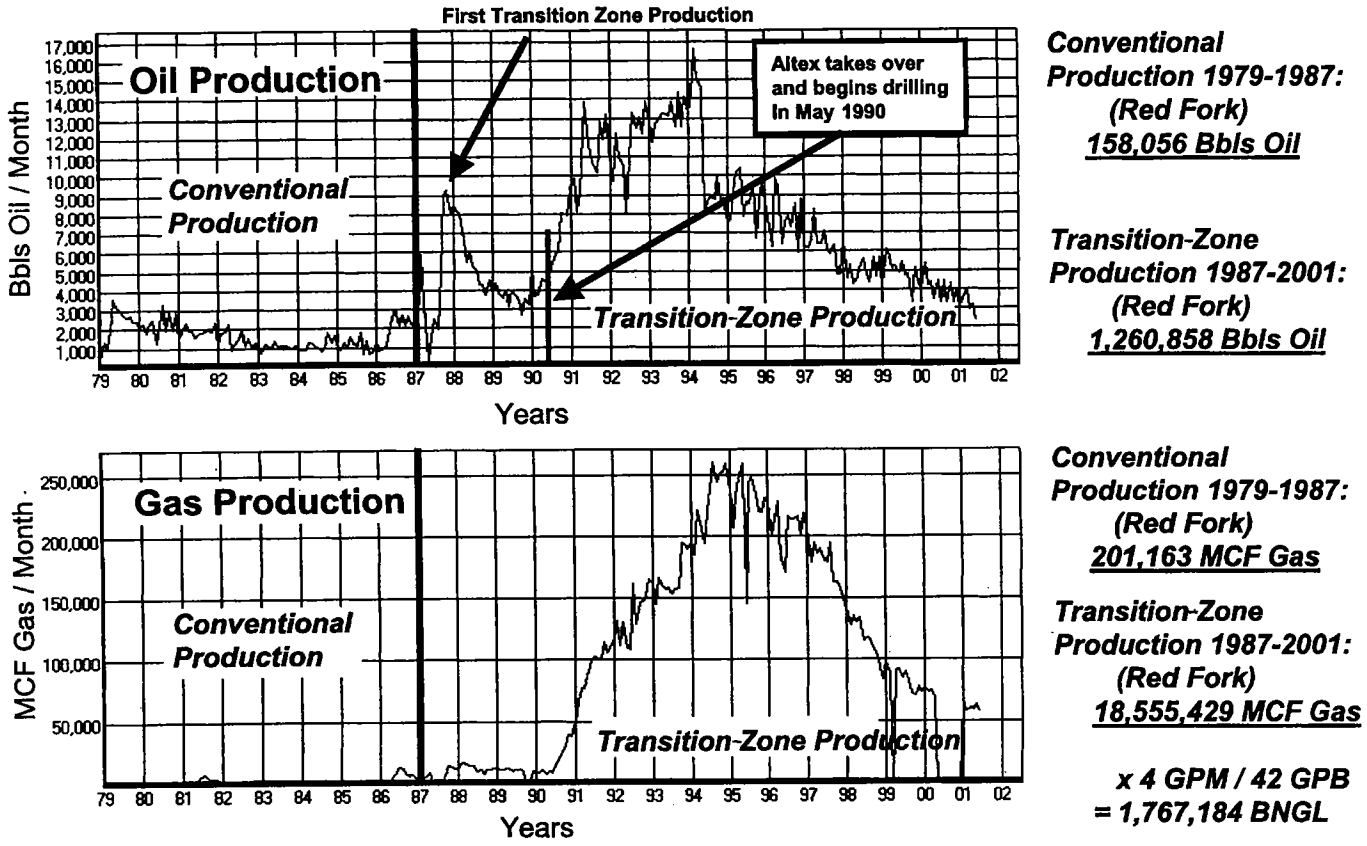

Figure 11. Oil and gas production of Red Fork Sand in Mountain Vernon Field, from 1979 through 2002, showing increase of production due to addition of transition-zone production, beginning in 1987.

approach: A semester report for Formation Evaluation, Norwegian University of Science and Technology, Fall 1999. Web site: http://www.ipt.ntnu.no/~bengtkp/thomasstieber.html.

Thomas, E. C.; and Stieber, S. J., 1975, The distribution of shale in sandstones and its effect upon porosity: Transactions of the 16th Annual Logging Symposium of the Society of Professional Well Log Analysts, paper T, 16 p.

History of the East Clinton Gas Field, Custer County, Oklahoma: A Seismic-Stratigraphic Case Study

Richard E. Schneider
Schneider Strata Science, Inc.
Oklahoma City, Oklahoma

William A. Clement
Stone Canyon Exploration
Edmond, Oklahoma

ABSTRACT.—The Fort Cobb Anticline near Clinton, Oklahoma, was recognized as a Pennsylvanian structural development in the 1960s. Cherokee gas sands were encountered in numerous wells in the 1970s with fair production seen. The thick Red Fork sand package was discovered to the north of the Fort Cobb Anticline in the early 1980s, which touched off a major gas play known as the East Clinton Channel. The regional seismic lines were shot concurrently with the development. A depositional history of this unique gas reservoir has been documented in this paper using both geology and geophysics to define the area.

EARLY HISTORY

Reconnaissance seismic shooting done in the 1950s by Conoco, Gulf, and Phillips sparked initial interest in this area. This single-fold (100%) data showed an anticlinal structural trend, at what was first considered to be the top of the Mississippian in the vicinity of the town of Corn. This structure trends to the southeast through Eakly and Fort Cobb and is now known as the Fort Cobb Anticline, a compressional fold having its roots in the Wichita Mountain Uplift.

Conoco purchased acreage along the Fort Cobb Anticline in the late 1950s and early 1960s, acquiring 10-year leases and some of the mineral interests that were available. They spudded the No. 1 North Corn Unit (sec. 19, T. 11 N., R. 14 W.) in 1963, encountering gas shows in the Skinner and Red Fork Sands. When they did not penetrate the Mississippian (Parvin) by 13,500 ft, the well was abandoned in the upper Morrow. The Phillips No. 1 Flaming "A" (sec. 24, T. 11 N., R. 15 W.) was drilled a year later northwest of the Corn Unit. It was also dry, but it had gas shows in the Red Fork. This area became the hotbed of the deep Pennsylvanian gas play of the late 1970s and 1980–81 (Fig. 1). Both major oil companies and contractors shot a series of regional seismic lines as group shoots in the late 1970s (Fig. 2).

Another key well in this area was the Gulf No. 1 Burgtorf (sec. 6, T. 13 N., R. 15 W.), which was drilled to 16,000 ft in 1959–60. It encountered productive sands in the Springer and an uphole velocity checkshot survey was run. This well and the 1969–71 Roden Oil, which was drilled on the Indianapolis Nose in the southeastern part of T. 13 N., R. 16 W., helped set up the play in the East Clinton Field.

A discussion of the historical development of oil and gas production in the Clinton area follows, specifically in the area north of the Fort Cobb Anticline.

CLINTON AREA DEVELOPMENT

The Clinton area in southeastern Custer County has long been one of Oklahoma's most active gas areas. Reaching a peak in the 1980s, several Pennsylvanian sands were proved to be economic targets, including the Red Fork, Atoka, and the Springer.

The gas potential of the area was first indicated in 1959 at Southeast Custer City's Gulf Oil No. 1 Burgtorf discovery in the Springer. The Burgtorf well was located in the SE¼NW¼ sec. 6, T. 13 N., R. 15 W. and was completed in 16 net feet of sand between 13,365 and 13,425 ft flowing 2,716 Mcf (thousand cubic feet) of gas daily. It was connected to a pipeline in April 1960 producing nearly 5 Bcf (billion cubic feet) of gas. However, this discovery came at the same time as a Hunton play (Fig. 1) 9 mi north near North Custer City. For this reason, it was 22 years before the Burgtorf discovery was confirmed by the Andover Oil No. 5-1 Manson in October 1981.

Roden Oil discovered a second and more prolific Springer reservoir in 1970, 5.5 mi southwest of the Gulf discovery. The Roden No. 35-1 Henry Nickel (sec. 35,

Schneider, R. E.; and Clement, W. A., 2002, History of the East Clinton gas field, Custer County, Oklahoma: a seismic-stratigraphic case study, *in* Boyd, D. T. (ed.), Finding and producing Cherokee reservoirs in the southern Midcontinent, 2002 symposium: Oklahoma Geological Survey Circular 108, p. 73–110.

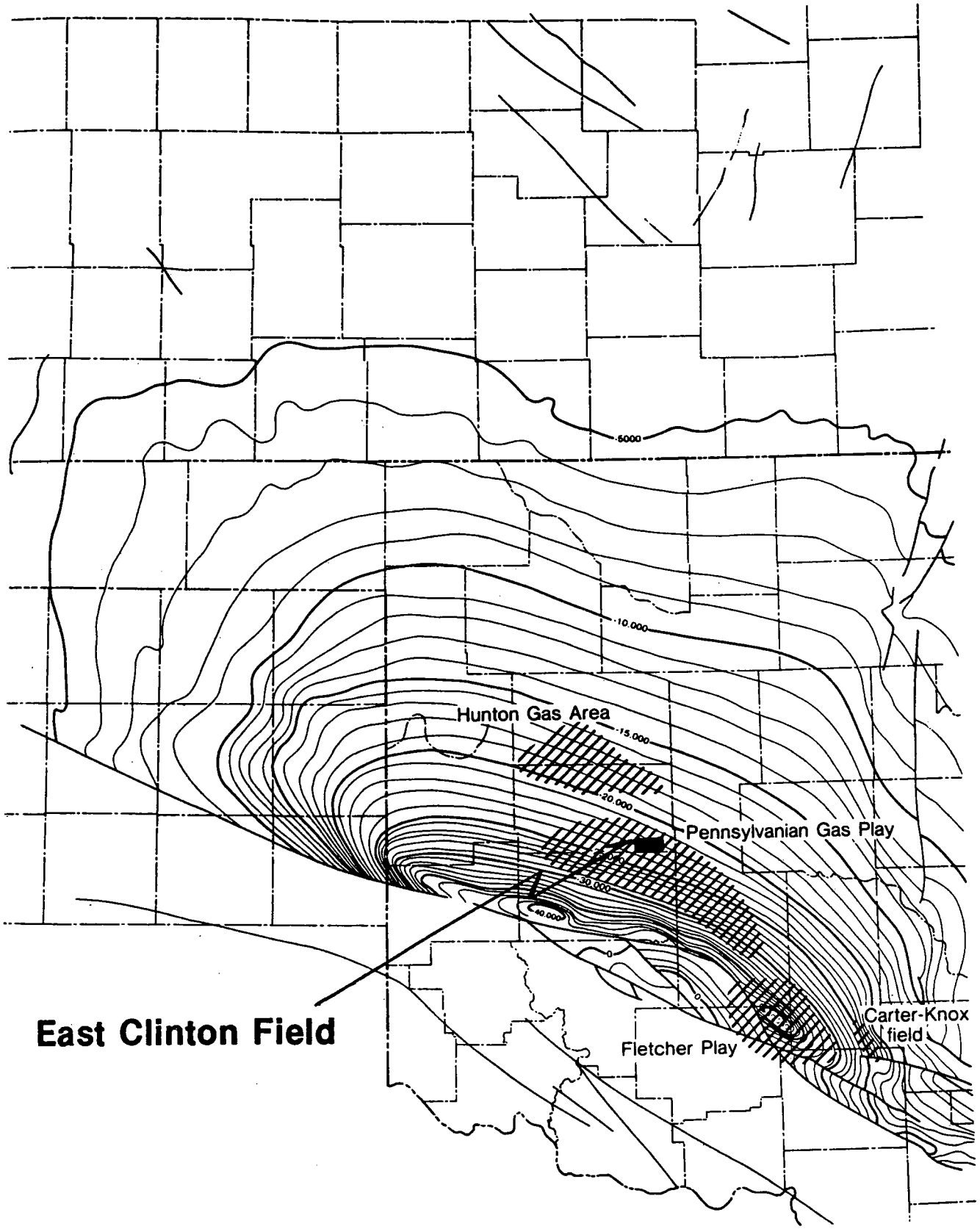

Figure 1. Regional trend map on base of the Arbuckle Group western in the deep part of the Anadarko Basin (contour interval = 1,000 ft). Locations shown for East Clinton Field, Pennsylvanian Gas Play area, Hunton Gas Area, Carter-Knox Field, and Fletcher Play.

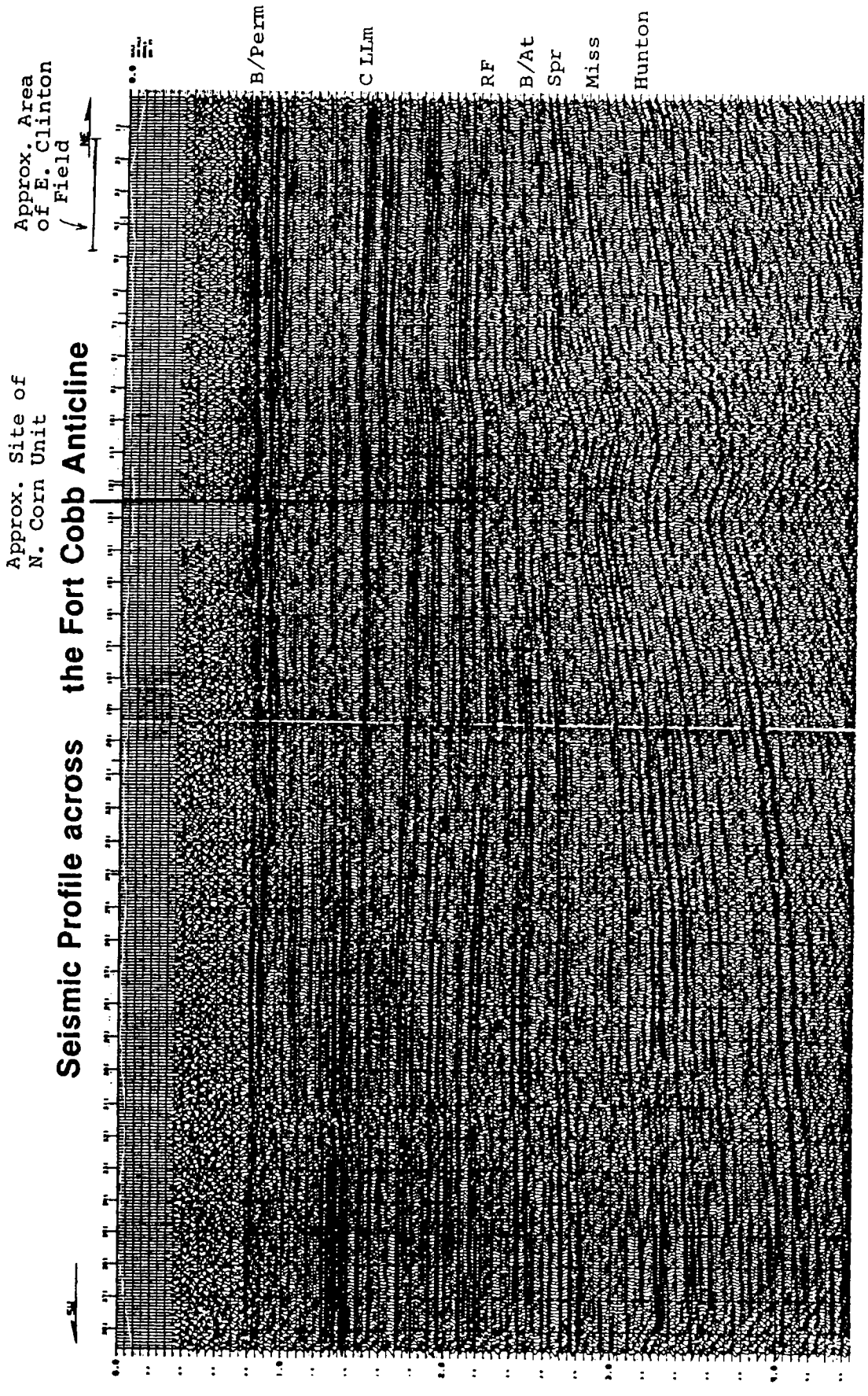

Figure 2. Typical regional seismic profile over Ft. Cobb Anticline and onto the Cherokee (Red Fork) depositional zone; profile southwest to northeast. Approximate site of North Corn Unit shown by dark vertical line and area of East Clinton Field shown by horizontal line at top of right (northeast) side of figure. *Abbreviations:* B/Perm = base of Permian; C L Lm = County Line Lime; RF = Red Fork; B/At = base of Atoka; Spr = Springer; Miss = Mississippian.

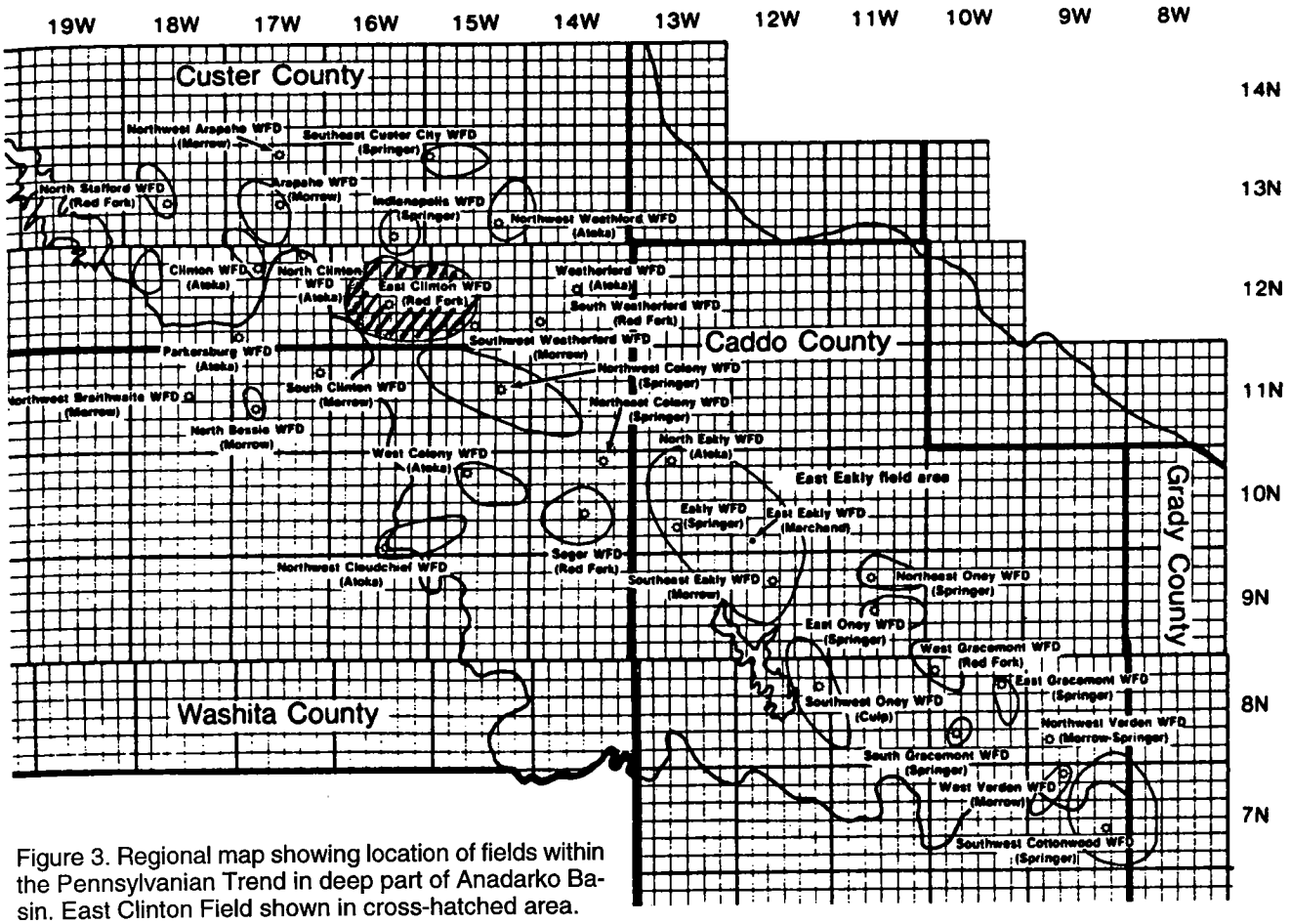

Figure 3. Regional map showing location of fields within the Pennsylvanian Trend in deep part of Anadarko Basin. East Clinton Field shown in cross-hatched area.

T. 13 N., R. 16 W.) had an open flow of 48 MMcfpd from the Springer at 14,872–14,880 ft, with >90 bbl of condensate. Gas shows were seen in the upper Red Fork, but not tested. This well was confirmed by the Roden No. 1-36 Friesen (sec. 36, T. 13 N., R. 16 W.) that tested 1.5 MMcf (million cubic feet) from 14,598–14,606 and 14,665–14,670 ft. After acidizing, the flow rate decreased, and the well was plugged back and completed in the Red Fork at 12,246–12,275 ft for 1.2 MMcf and 52 bbls of condensate. This was the beginning of Indianapolis Field.

Three new pays were added to the field in the late 1970s, as eight wells were successfully completed in a northwest–southeast trend. In 1978, Woods Petroleum found Morrow gas in their No. 34-1 Taylor-Haynes well in a 14-ft net zone starting at 14,308 ft. The initial production (IP) was 1.8 MMcf on an 8/64-in. choke on this test in sec. 34, T. 13 N., R. 16 W. In 1979, Woods drilled the No. 1 Sawatzky well in sec. 3, T. 12 N., R. 16 W. It tested gas in both the Skinner and Cottage Grove, producing 830 Mcf from Skinner at 11,592–11,606 ft. The Indianapolis area was growing.

West of the Indianapolis area, North Stafford Field was added as a new local Red Fork producer in 1971, when the discovery well (No. 1-21 Beauchamp) was drilled by Arkla Exploration in sec. 21, T. 13 N., R. 18 W. This test was drilled to the Hunton at a total depth of 20,898 ft. After flowing non-commercial quantities of gas from the Hunton, it was plugged back and completed in the Red Fork at 12,310–12326 ft. This zone flowed 1.35 MMcf through a 24/64-in. choke. Woods Petroleum drilled the confirmation well at the No. 16-1 Walther in 1978. The third and fourth Red Fork wells were completed in 1981 and 1982 by Woods and Sun Oil.

In July 1979, An-Son Petroleum opened Atoka production in the Indianapolis Field at the No. 1-21 Stehr well in sec. 21, T. 13 N., R. 16 W. During a 17-hour production test at 13,217–13,222 ft, gas flowed at a daily rate of 7.1 MMcf with 36 bbl of condensate.

The Pennsylvanian sands were proving to be successful targets in the Red Fork, Atoka, and the Springer. Other discoveries in the late 1970s and early 1980s are shown in Figures 1 (labeled "Pennsylvanian Gas Play") and Figure 3.

EAST CLINTON FIELD HISTORY

Early Development

The Roden No. 35-1 Nickel (sec. 35, T. 13 N., R. 16 W.) was the key well in the area. Its productive Springer section and shows uphole in the Red Fork and downhole in the Hunton led Conoco to continue exploring this area (Figs. 3 and 4). It was noted that strong-

amplitude events were associated with the basal Pennsylvanian sands and also with the top of the Red Fork zone in this area. An early common-depth–point (CDP) line near the Roden Nickel displayed this seismic effect quite well (Fig. 5). Additional seismic control was obtained in this area that showed the strong structural expression of the Indianapolis Nose (later called the Custer City Nose) and led to the acquisition of acreage on the flank of this feature. A "thin" seen on a 1975 isotime map of the interval from the 13-Finger Lime to the Mississippian (Parvin) Lime shows this structure (Roden-Nickel Structure on Fig. 6) expressed strongly. This structure was later called the Indianapolis or South Custer City Nose.

By 1978 the acreage was in place and the proposal was approved to drill the Conoco No. 1 Snider as a 17,000-ft Springer test in the NE¼ of sec. 22, T. 12 N., R. 16 W. Based on the increasing number of amplitude anomalies seen on the seismic data and the two-dimensional computer models run from the Roden well southward, this well appeared to have better Springer sand development than the Roden Nickel well. The Red Fork sand was considered a secondary objective, based on the results of the Roden Friesen well (sec. 36, T. 13 N., R. 16 W.) and the seismic indicators at the top of the zone. Based on prevailing geological literature and the shape of the basin, it was presumed that both the Springer and the Red Fork were deposited in a nearly north–south fluvial/deltaic trend.

Late Development

The Conoco No. 1 Snider (sec. 22, T. 12 N., R. 16 W.) was staked in late 1978, and the rig was in

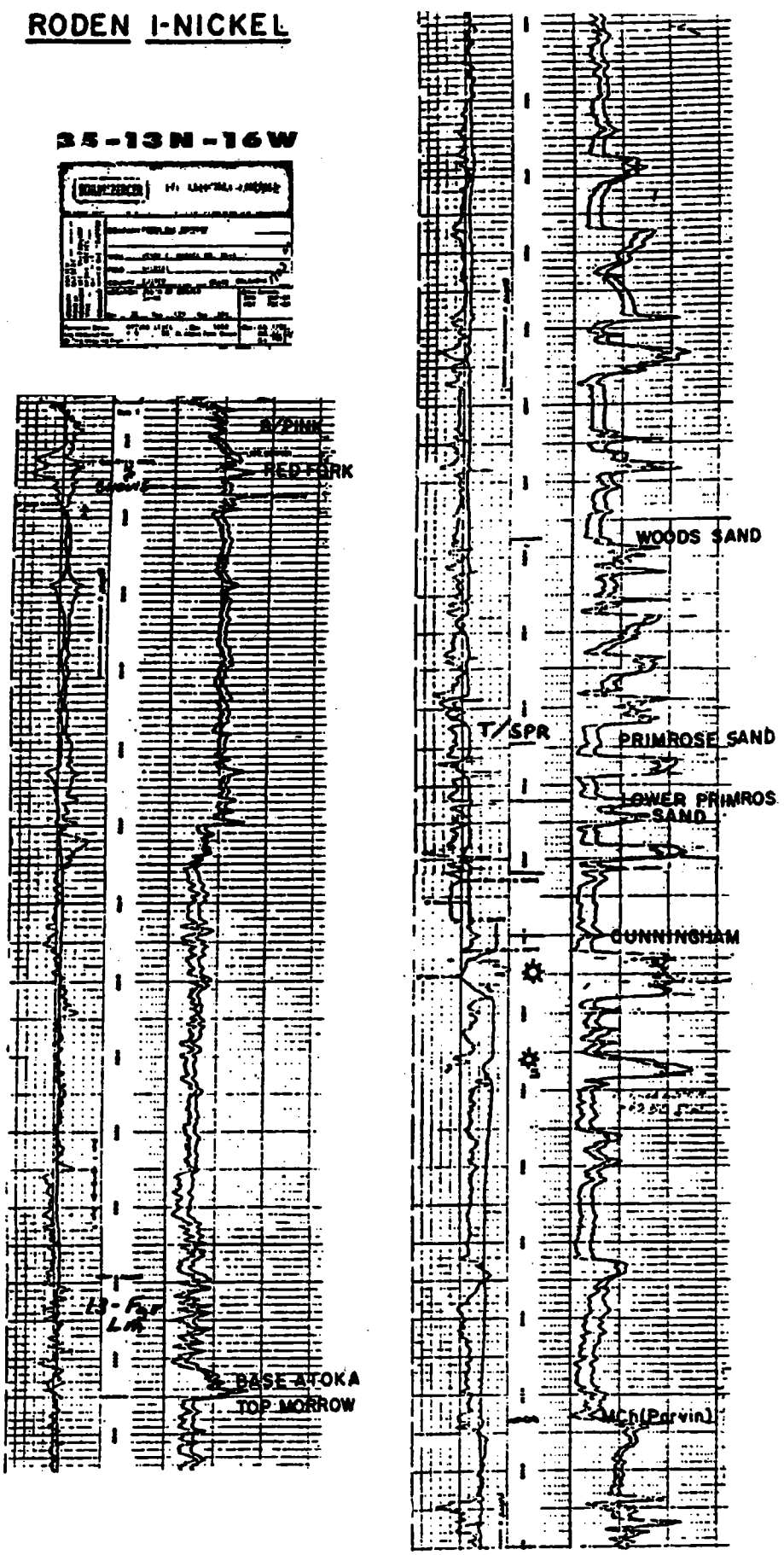

Figure 4. Resistivity and spontaneous-potential logs for Roden No. 1 Nickel well, from base of Pink Limestone (B/PINK) through Parvin in Mississippian sequence (includes all of Morrow and Springer). *Abbreviations:* 13-Fgr Lm = Thirteen Finger Limestone; T/SPR = top of Springer.

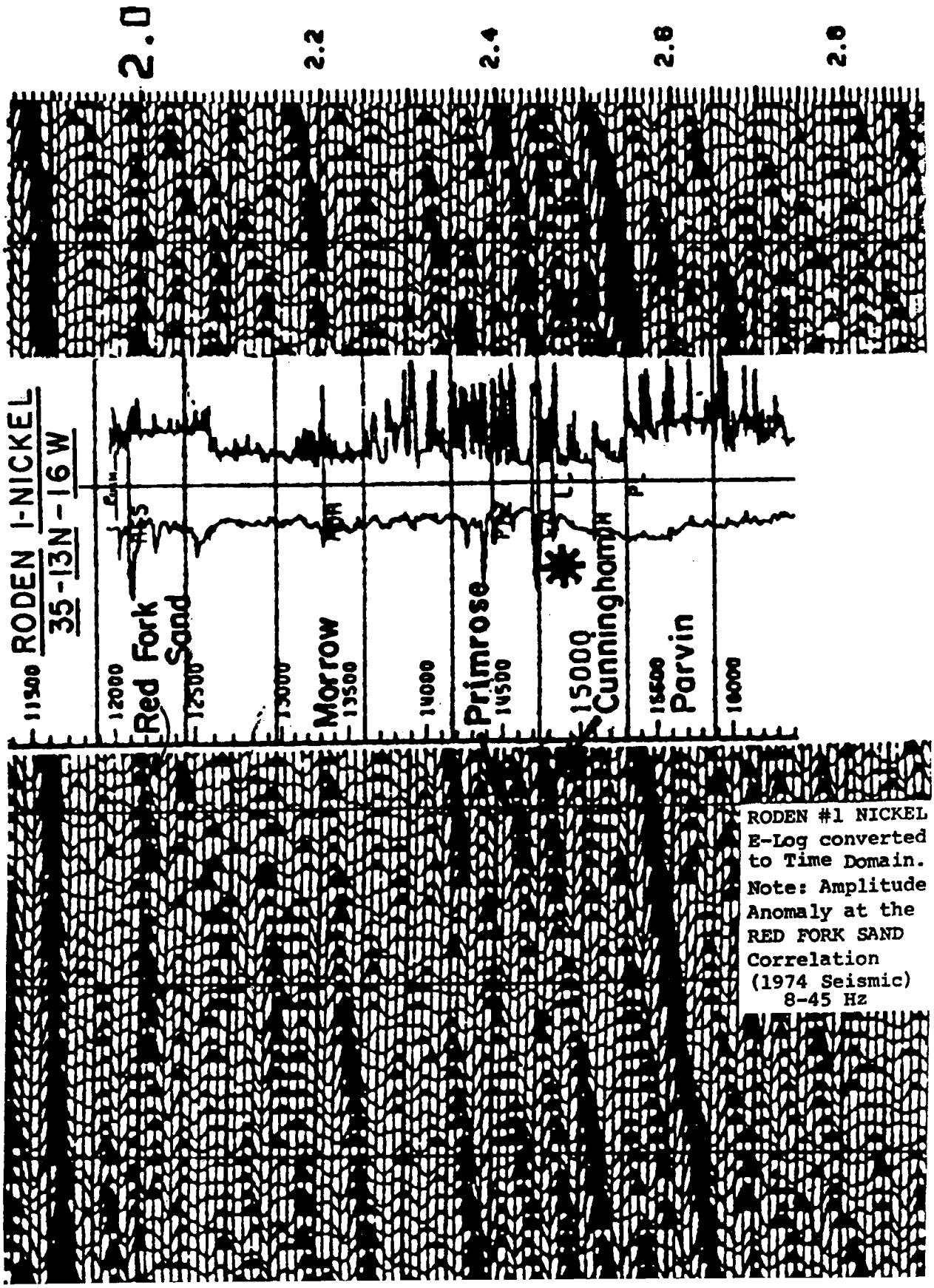

Figure 5. Electric log converted to time domain for Rodgen No. 1 Nickel well, and correlated with 1974 seismic line through area. Note the amplitude anomaly at the correlation with the Red Fork Sand. Depth in feet; travel time in seconds.

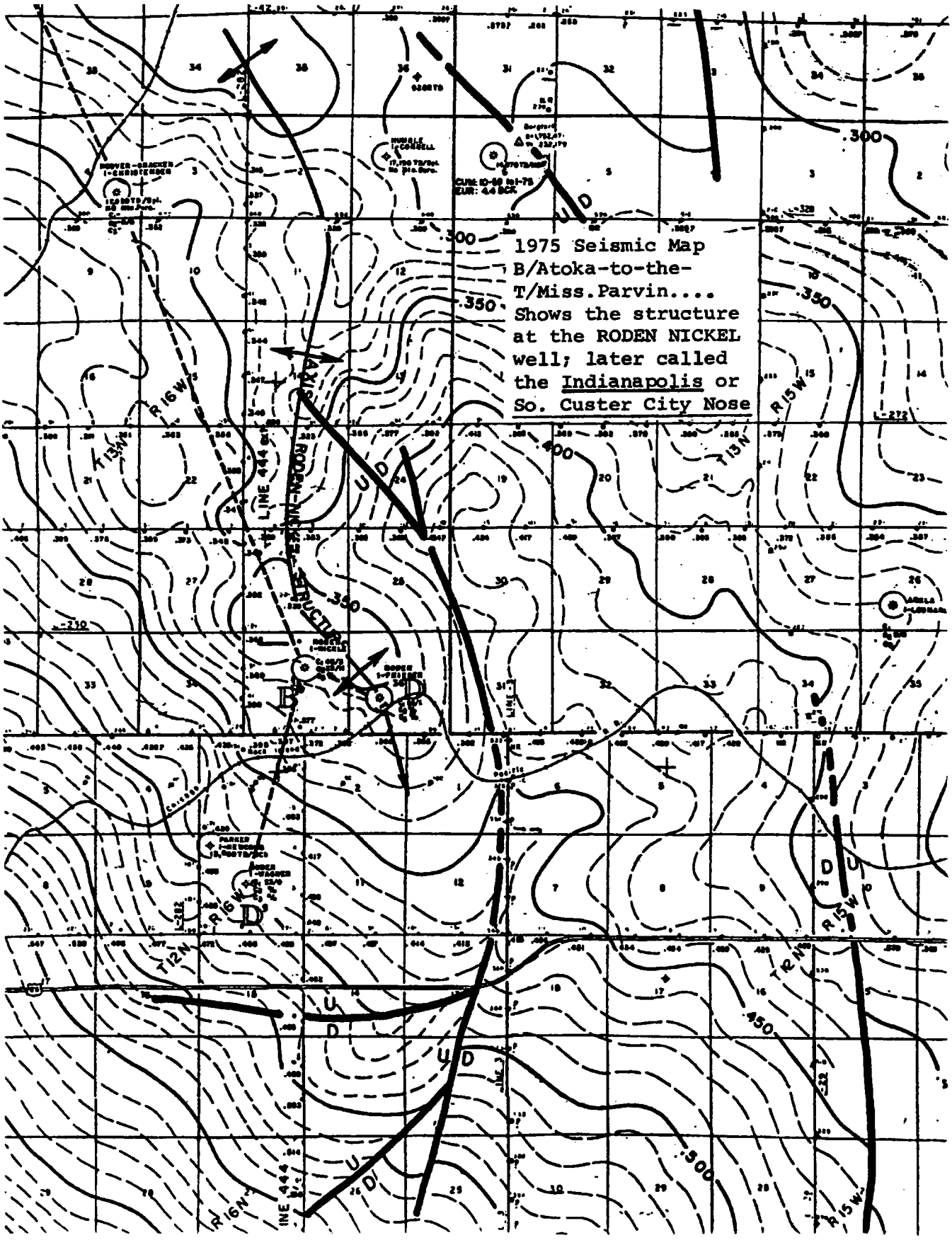

Figure 6. Seismic map (1975) from base of Atoka to top of Mississippian Parvin. Note structure just east of the Roden-Nickel No. 1 well.

place by early 1979. Spring brought more than May showers, however. While drilling at 12,200 ft, the well kicked and blew out in the Red Fork, and the hole was lost unlogged. The rig was moved 1,000 ft south, and drilling on the Snider No. 1-A well was commenced. The anticipated Middle Pennsylvanian section at this well is shown in Figure 7. To prevent a repetition of the previous drilling problems, this well was drilled with higher mud weight when the Skinner zone was penetrated. The well successfully reached the Red Fork in October 1979 and was logged. The porosity log showed the upper Red Fork to have 76 ft of gross sand with a net total of 64 ft with greater than 7% porosity.

In spite of the excellent Red Fork log and gas shows while drilling the Snider No. 1-A well, it was decided to drill deeper to test the Springer. While this deeper drilling continued, another rig was moved onto the adjacent Conoco No. 1 Agan well, located in sec. 23, T. 12 N., R. 16 W.

The Snider No. 1-A tested the Springer in 1980, but was plugged back to produce from the Red Fork with an initial production of 8 MMCFGPD under choke (Fig. 8). The No. 1-23 Agan well was logged to a total depth of 13,000 ft in March 1980 with good Red Fork Sand development. Although this well had 56 ft of gross sand, it was shaly with indications of channel-bank development and showed only 21 ft of net sand porosity greater than 7%. Based on these results it was decided to drill this area only to the Red Fork and another rig was added to test this play. The resulting Hoffman well was spotted in the SW¼ of sec. 15, T. 12 N., R. 16 W. to test persistent amplitude anomalies that trend east–west across T. 12 N., R. 16 W. Because the well had to be spudded north of the best reflectors, however, it was dry.

Meanwhile, An-Son Corporation had participated in the group shoot performed by Digicon Geophysical. Using a combination of geology and seismic they moved in two rigs east of the Snider well. The An-Son No. 1 Meacham (sec. 13, T. 12 N., R. 16 W.) and the No. 1 Goldie (sec. 19, T. 12 N., R. 15 W.) both reached the Red Fork in June 1980. Both wells showed channel-sand development in the Upper Red Fork, with the Goldie having 95 ft of gross sand and 89 net ft of porous sand, which was the thickest section yet seen. An-Son wasted no time and had the Murphy (sec. 18, T. 12 N., R. 15 W.) and the Palmer (sec. 17, T. 12 N., R. 15 W.)

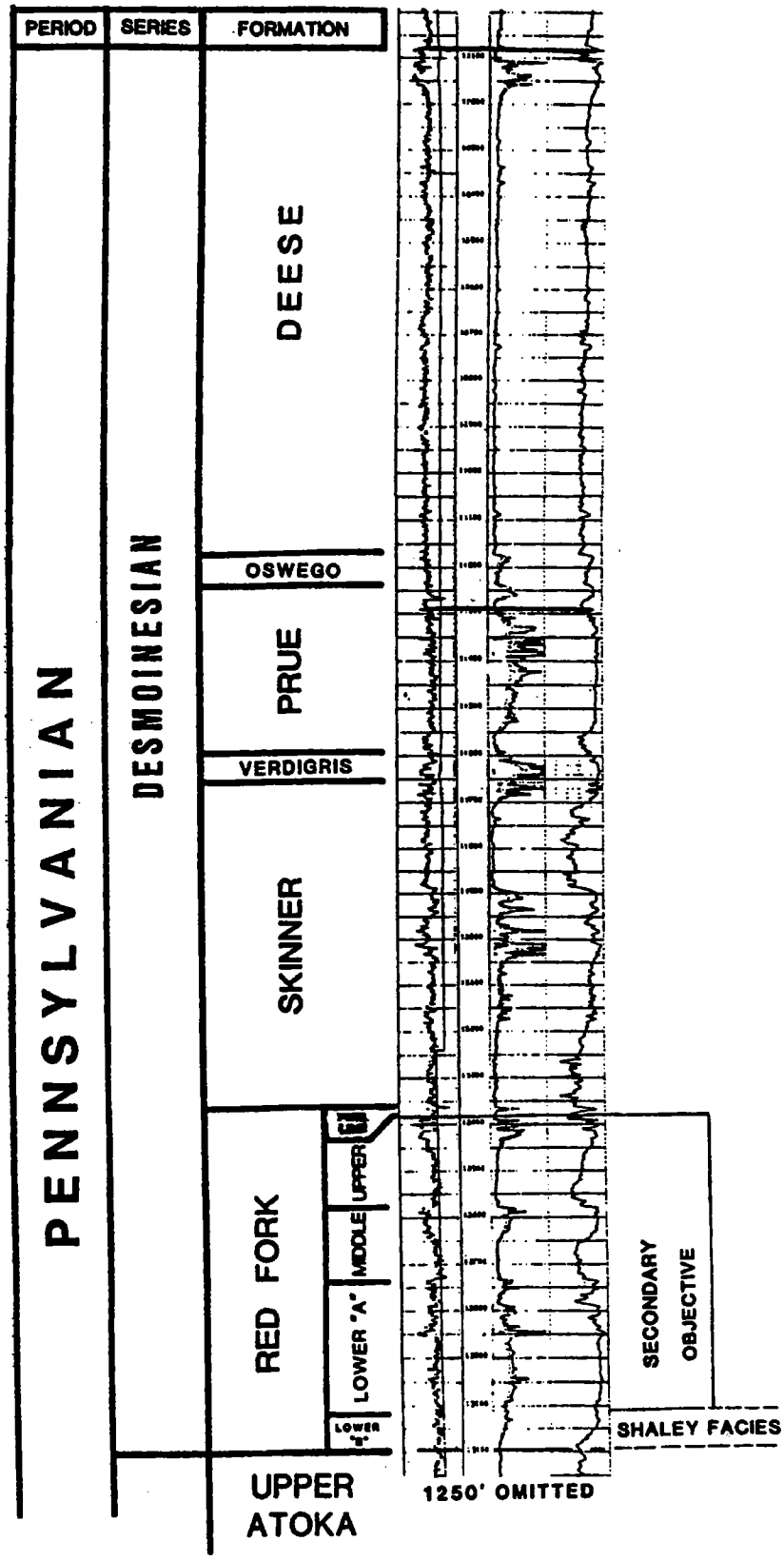

Figure 7. Anticipated Middle Pennsylvanian section at location of Conoco No. 1-A well. Depth in feet. The primary objective was the Springer Formation. The modified sand estimations were based on seismic-stratigraphic evaluations.

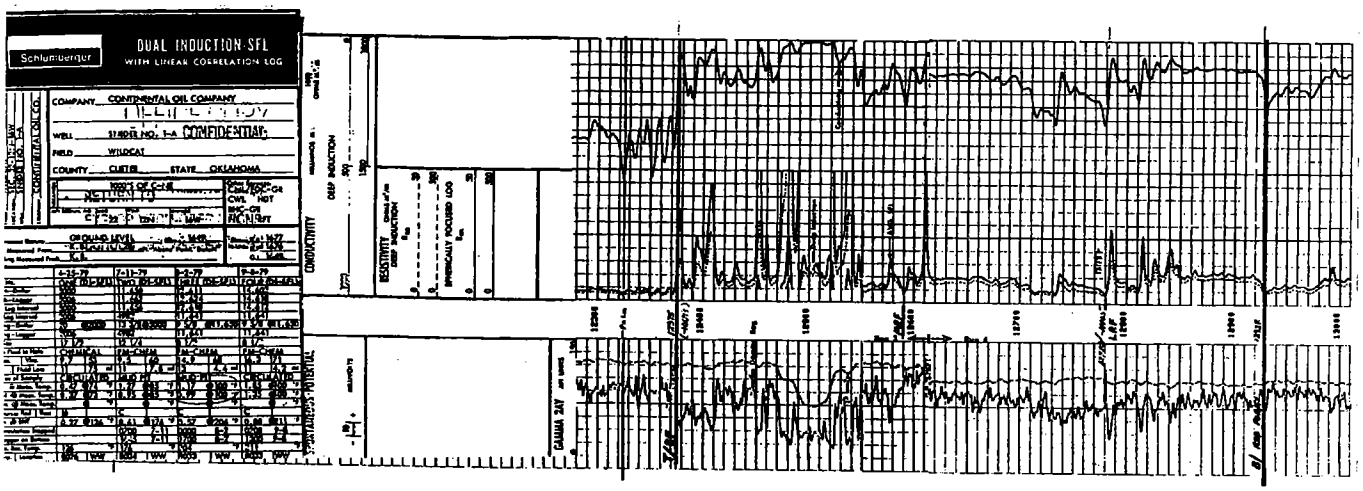

Figure 8. Gamma-ray and resistivity logs from Conoco No. 1-A Snider well, through the Red Fork pay zone. Note the upper Red Fork sands from 12,375 to 12,595 ft. The sand from 12,450 to 12,525 was opened to flow (8+ million cubic feet of gas) under a 0.25-in. choke. *Abbreviations:* T/RF = top of Red Fork; MRF = middle Red Fork; B/Red Fork = base of Red Fork.

wells down and logged by September 1980. Both encountered good, albeit thinner channel sands.

Conoco was now drilling the northeast and southwest offset sections to the Snider No. 1-A. The No. 14-1 Meacham (sec. 14, T. 12 N., R. 16 W.) had 41 ft of channel sand in the Upper Red Fork, whereas the No. 28-1 Fransen (sec. 28, T. 12 N., R. 16 W.) caught the channel edge with only 12 ft of shaly sand present. Both wells were tested in December 1980. The Conoco No. 27-1 Fransen (sec. 27, T. 12 N., R. 16 W.) and the No. 26-1 Sawatzky (sec. 26, T. 12 N., R. 16 W.) were spudded that same month. An-Son completed the No. 1 Stidham (sec. 20, T., 12 N., R. 15 W.) in January 1981 and gained a farmout from Conoco to redrill the Hoffman section. The No. 1 Downing well, located in the SE¼ of sec. 15, T. 12 N., R. 16 W., caught the northern edge of the channel and logged 47 ft of gross sand. Conoco retained a large back-in interest in the test.

The race was on. This trend developed rapidly, not as a northeast–southwest fluvial trend as thought prior to development, nor as a north–south deltaic trend as described in Red Fork literature, but as an elongate east–west channel system—a near look-alike to the Cherokee Trends on the north shelf of the basin.

EVALUATING THE TREND WITH WELLS, MODELS, AND SEISMIC

In this study, we are limiting our comments to the three townships in the main East Clinton Field play—i.e., T. 12 N., R. 15–17 W (see Fig. 3). The overall trend is now more than 30 mi in length and has more than 200 wells bracketing the channel.

Eastern Trend

Profile A–A′ (Fig. 9) was constructed along Digicon seismic line D-20-4 in a northeast–southwest direction. The line started at the Amoco No. 1 Kirtland well (sec. 28, T. 12 N., R. 15 W.), went to the Nova No. 1-27 Reiman, to the No. 1-22 Reiman, to the Amoco No. 1-23 Sauer, and then to the Amoco No. 1 Bauer in sec. 14. The Upper Red Fork is productive only in the Nova No. 1-22 Reiman, although other formations produce in other wells. The Sauer well had a sonic curve that was modified to generate pseudo-sonics for each of the other wells. Models were made, flattened on the base of the Pink Lime, and convolved with a 12–60 Hz pulse. When the resulting 2-D models were compared with the actual seismic data, excellent matches can be seen in the Red Fork zone (compare Figs. 10–13).

The second profile, cross section B–B′ (Fig. 14), was constructed along Digicon seismic line A-14-4, also in a northeast–southwest direction, paralleling the first profile to the east. This profile was started at the Lobar No. 1 Susanna (sec. 30, T. 12 N., R. 15 W.), to the An-Son No. 1 Stidham, to the No. 1-19 Goldie, to the No. 1-17 Palmer, and ending at the An-Son No. 1-8 Newman. The Stidham, Goldie, and Palmer wells all had upper Red Fork sand production, the Goldie being the best. This Goldie well also had sonic control that enabled the creation of pseudo-sonic curves for all of the wells without sonic data, with the exception of the Lobar. Again the resulting 2-D model was remarkably similar to the actual seismic data (Figs. 15–18).

Middle Trend

In contrast to cross sections A–A′ and B–B′ (Figs. 9 and 14, respectively), cross section C–C′ (Fig. 19) was constructed in a north–south direction along Digicon seismic line T-80A. The starting point was the Andover No. 34-1 Harms well (sec. 34, T. 12 N., R. 16 W.), then to the Conoco No. 28-1 Fransen, to the No. 21-1 Deputy, to the No. 1-15 Hoffman, to the Huber No. 1 Wagner, and finally to the Parker No. 1 Newcombe in the NW¼ of sec. 10. The three Conoco wells had sonic curves, and, thus, pseudo-sonics created from E-logs were only

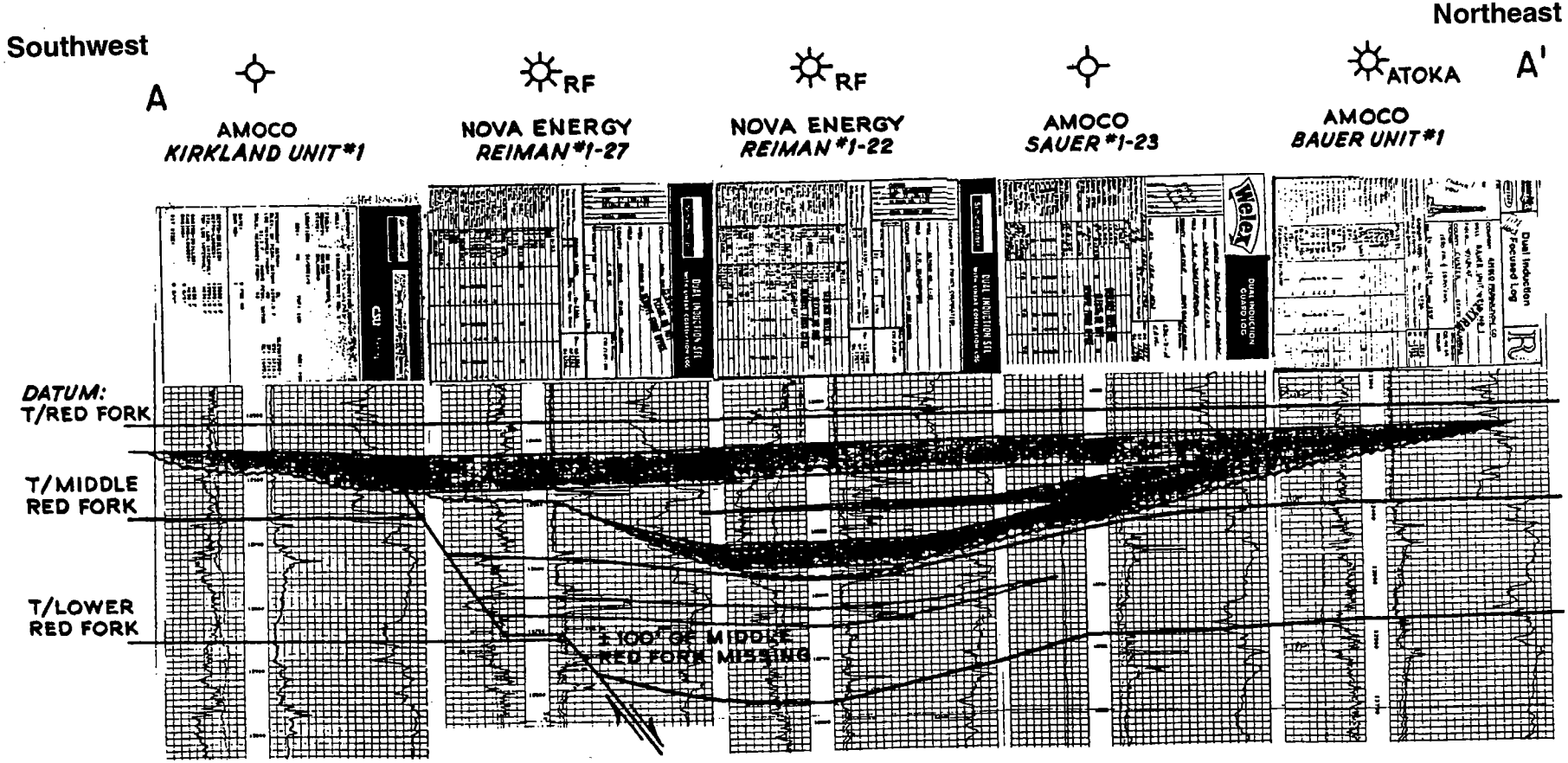

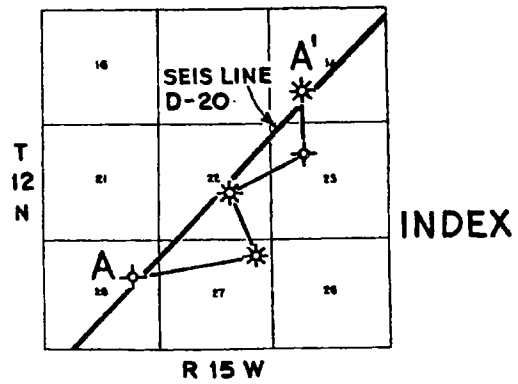

Figure 9. Geologic cross section A–A′ through part of East Clinton Field from southwest to northeast in proximity of part of Digicon seismic line D-20. Location of wells and seismic line shown on index map. Note that approximately 100 ft of middle Red Fork is missing on southwest side of cross section due to faulting. Datum is top (T/) of Red Fork.

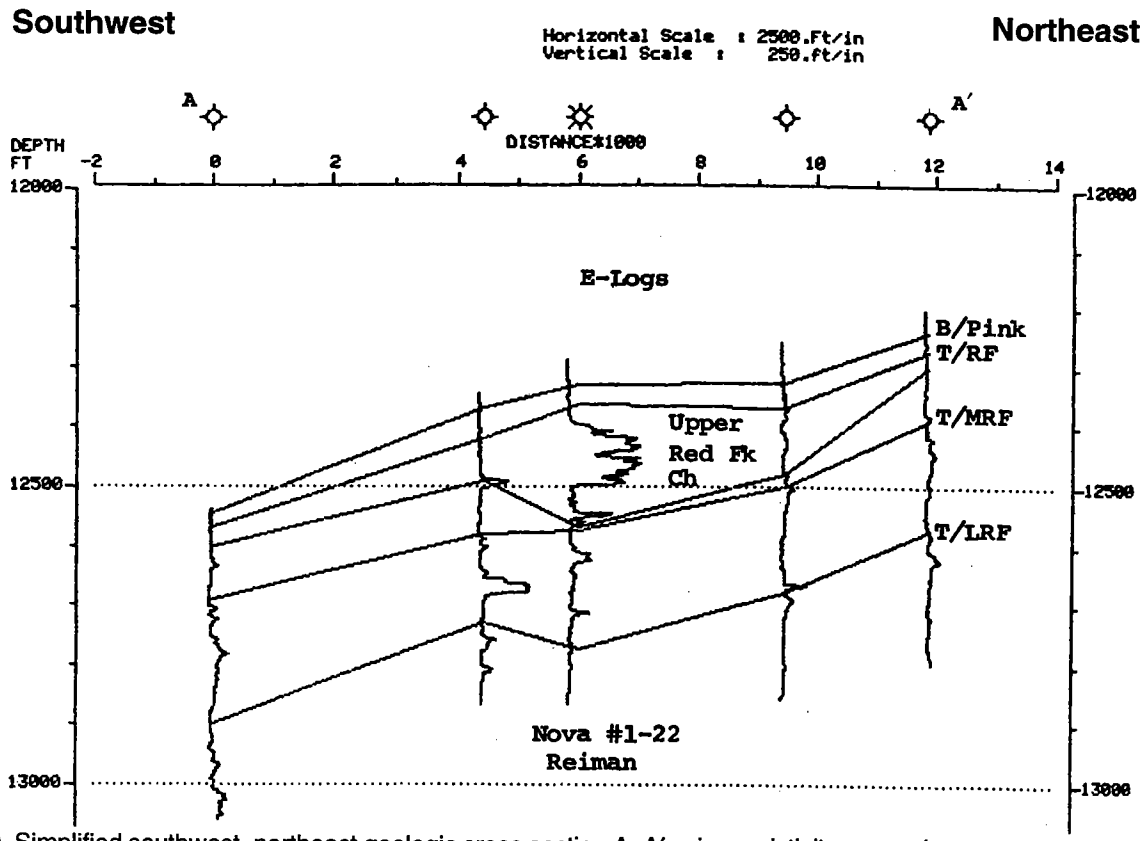

Figure 10. Simplified southwest–northeast geologic cross section A–A′ using resistivity curves hung on sea level through part of East Clinton Field. Wells are those used in Figure 9. Depth in feet and distance in feet × 1,000. *Abbreviations:* B/Pink = base of Pink Limestone; T/RF = top of Red Fork; T/MRF = top of middle Red Fork; T/LRF = top of lower Red Fork.

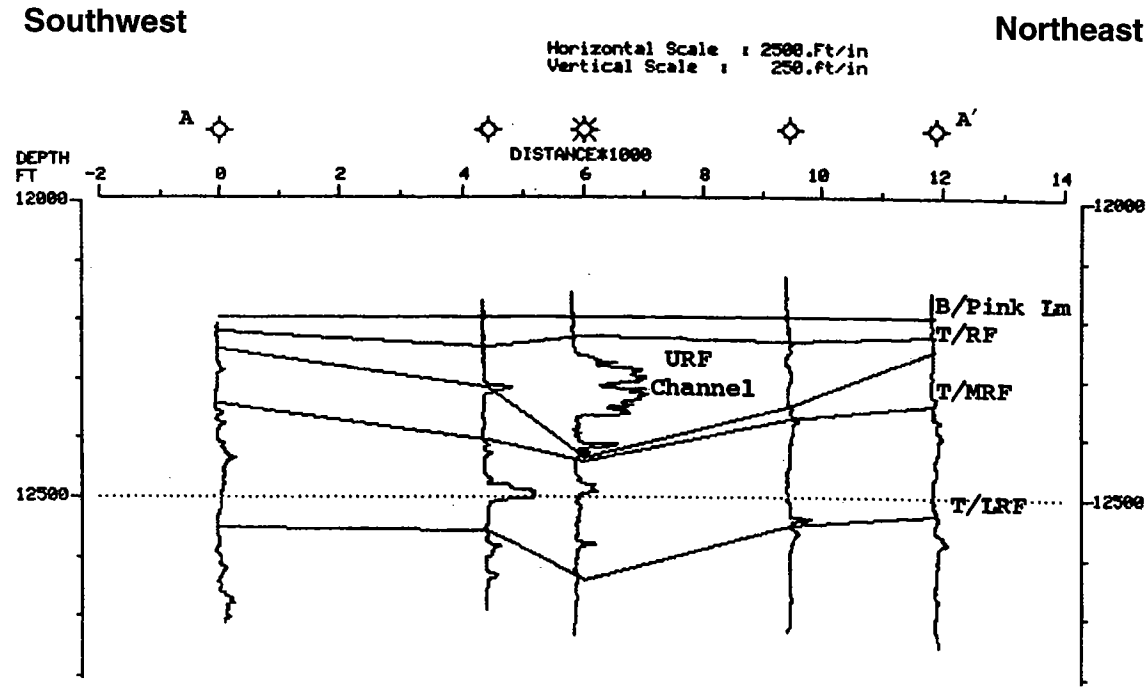

Figure 11. Simplified southwest–northeast geologic cross section A–A′ using resistivity curves hung on Pink Limestone through part of East Clinton Field. Note upper Red Fork (URF) sand-filled channel in middle two wells. Wells are those used in Figure 9. Depth in feet and distance in feet × 1,000. *Abbreviations:* B/Pink = base of Pink Limestone; T/RF = top of Red Fork; T/MRF = top of middle Red Fork; T/LRF = top of lower Red Fork.

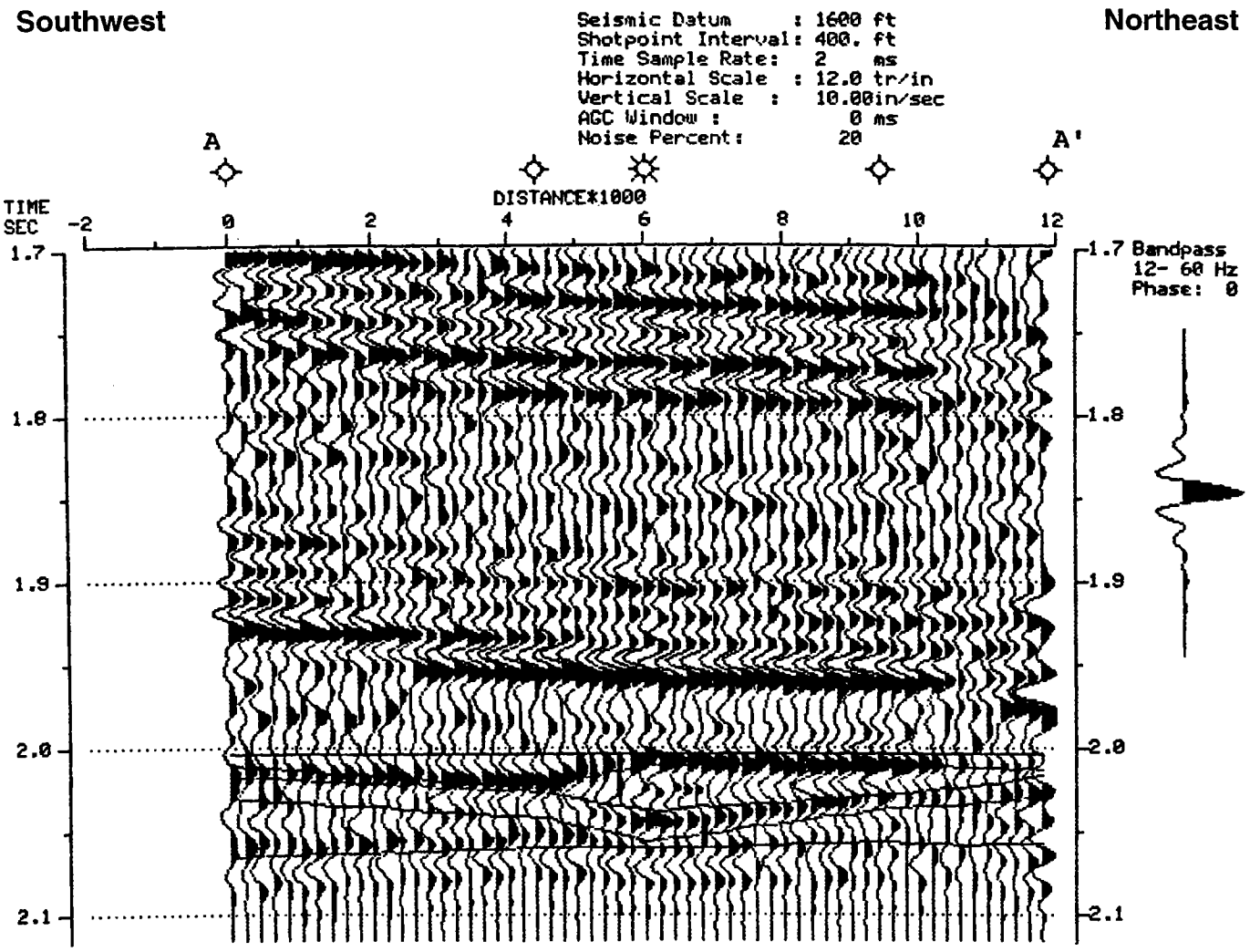

Figure 12. Two-dimensional southwest–northeast cross section generated by computer from log curves between the five control logs shown in Figure 11 and used for cross section A–A′ (Fig. 9). Logs and traces are flattened on base of Pink Limestone at 2,003 ms and interpolated between wells. *Abbreviations:* B/Pink = base of Pink Limestone; B/UpRF = base of upper Red Fork; T/UpRF = top of upper Red Fork; T/MidRF = top of middle Red Fork; T/LRF = top of lower Red Fork.

necessary for the remaining three wells. Only the Conoco No. 21-1 Deputy penetrated productive upper Red Fork channel sand. As in other profiles, the flattened model was convolved with a 12–60-hz band-pass pulse and then displayed as a 2-dimensional seismic model (Figs. 20–23). Note the similarity of the model to the actual seismic at the Deputy well and the loss of the upper reflector as the line nears the Hoffman location.

Western Trend

Profile D–D′ (Fig. 24) was constructed southwest–northeast along Digicon seismic line D-22-5. The starting point for this cross-channel section was the Woods No. 24-1 Meacham Farms well (SE¼ sec. 24, T. 12 N., R. 17 W.), then to the No. 24-2 Meacham, to the An-Son No. 2 Soar, to the Woods No. 1 King, and ending at the An-Son No. 1 Herrald-Lacey in sec. 7, T. 12 N., R. 16 W. Only the King well had a sonic curve, and thus pseudo-sonics were interpolated from nearby channel-well velocities. Note the large shale section ("shale plug") within the channel in the An-Son Soar well (Fig. 24). Although both the 2-D model and the actual seismic data show diminished amplitude at the top of the Red Fork in this location, this would still have been most difficult to predict (Figs. 25–28).

Figure 29 is cross section E–E′, a south–north line paralleling An-Son's seismic line WC-4. The starting point is the TXO No. 1-20 Meacham (sec. 20, T. 12 N., R. 17 W.), then to the An-Son No. 2-20 Moore, to the Woods No. 17-3 Hogan, to the No. 17-1 Meacham, and ending at the Woods No. 1-8 Lewis in sec. 8. The TXO Meacham, An-Son Moore, and Woods Lewis wells had sonic curves, and, thus, only two pseudo-sonics were necessary. Note that the thickest channel sand in the trend is seen at the An-Son Moore. This 200+ ft zone causes a de-tuning effect on the data and forms a secondary peak within the Red Fork interval. Again the 2-D model indicators compare favorably with the seismic lines (Figs. 30–33).

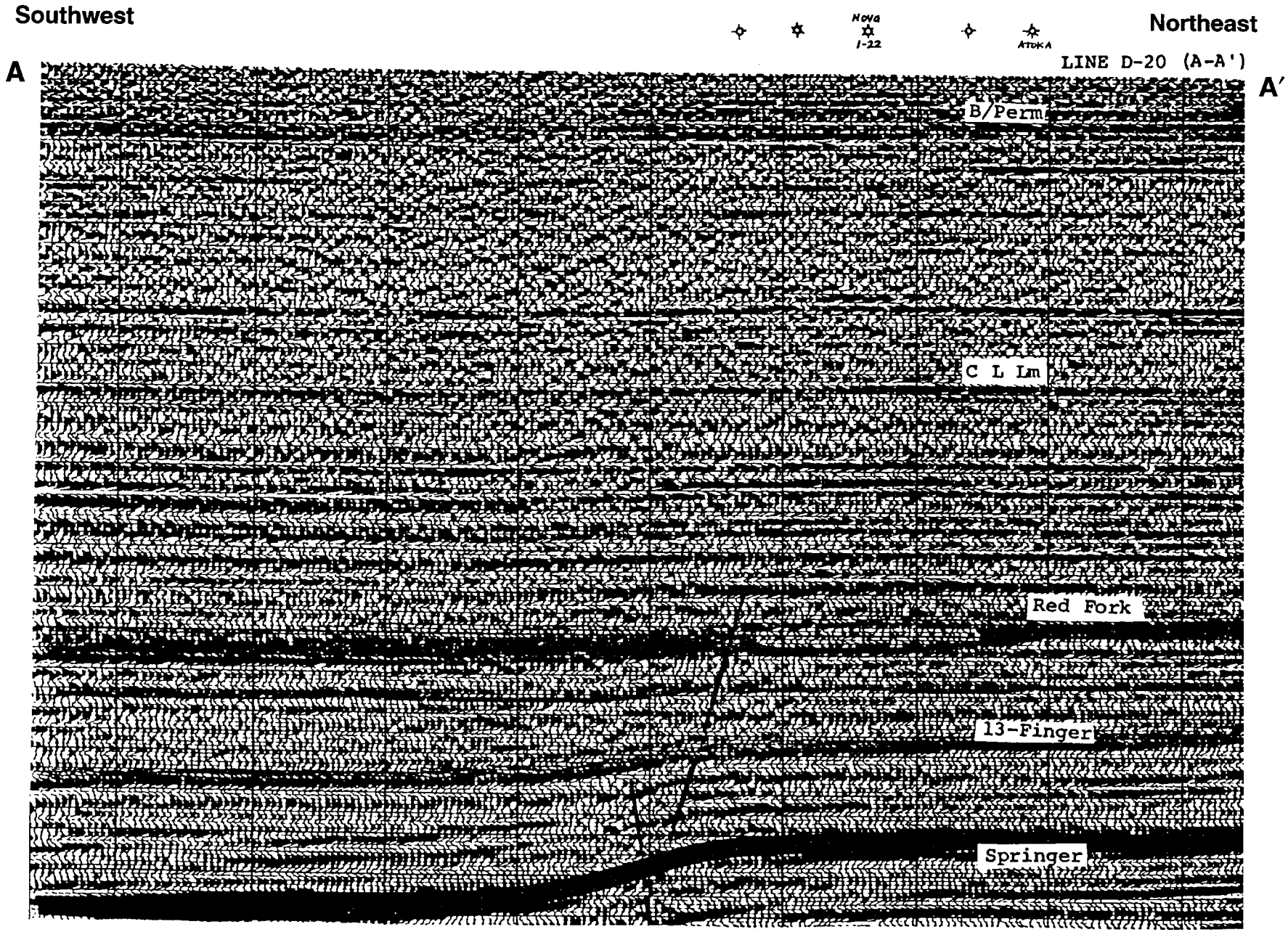

Figure 13. Actual seismic data from part (A–A′) of Digicon seismic line D-20 shot across the five wells shown in Figures 9–12; locations of those wells shown at top-right side of figure. *Abbreviations:* B/Perm = base of Permian; C L Lm = County Line Lime.

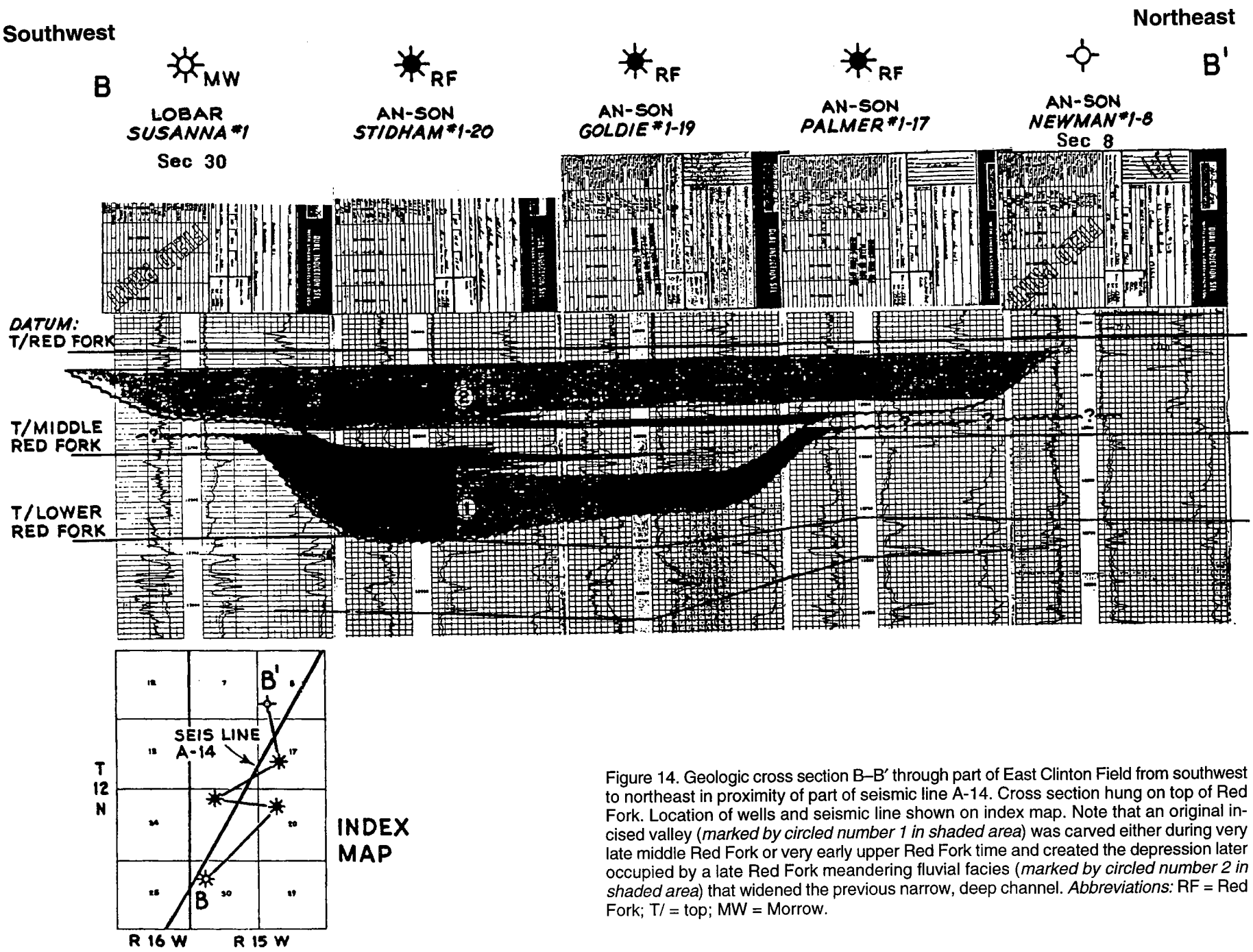

Figure 14. Geologic cross section B–B′ through part of East Clinton Field from southwest to northeast in proximity of part of seismic line A-14. Cross section hung on top of Red Fork. Location of wells and seismic line shown on index map. Note that an original incised valley (*marked by circled number 1 in shaded area*) was carved either during very late middle Red Fork or very early upper Red Fork time and created the depression later occupied by a late Red Fork meandering fluvial facies (*marked by circled number 2 in shaded area*) that widened the previous narrow, deep channel. *Abbreviations:* RF = Red Fork; T/ = top; MW = Morrow.

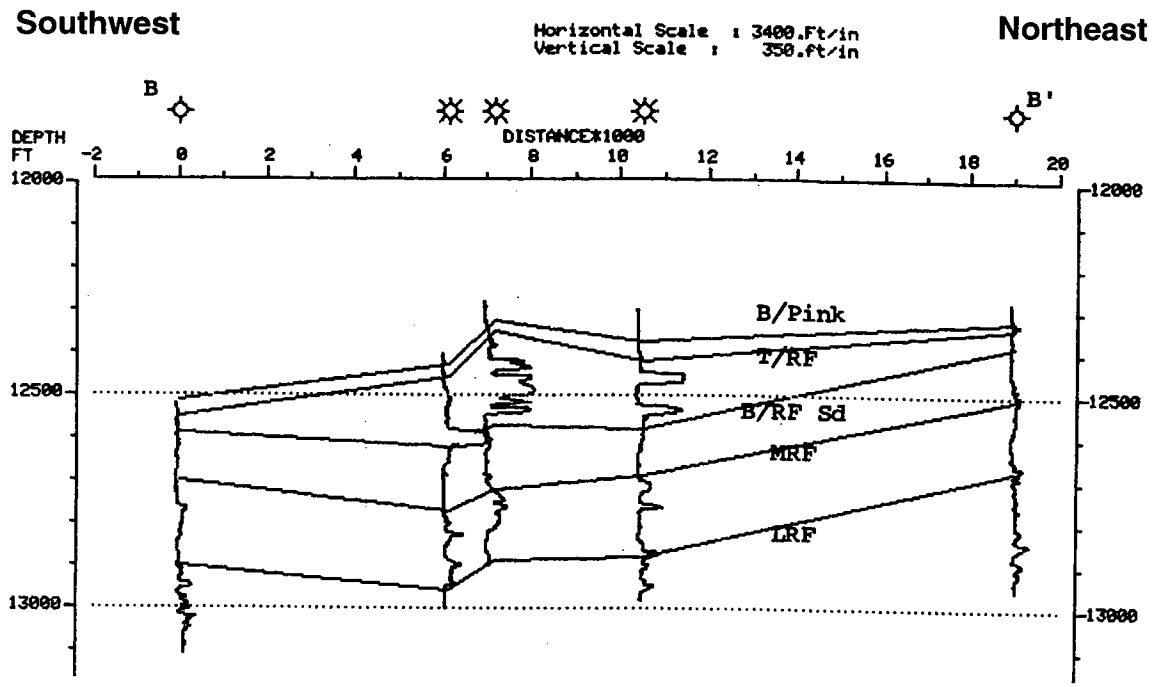

Figure 15. Simplified southwest–northeast geologic cross section B–B′ using resistivity curves hung on sea level through part of East Clinton Field. Wells are those used in Figure 14. Depth in feet and distance in feet × 1,000. *Abbreviations:* B/Pink = base of Pink Limestone; T/RF = top of Red Fork; MRF = middle Red Fork; LRF = lower Red Fork.

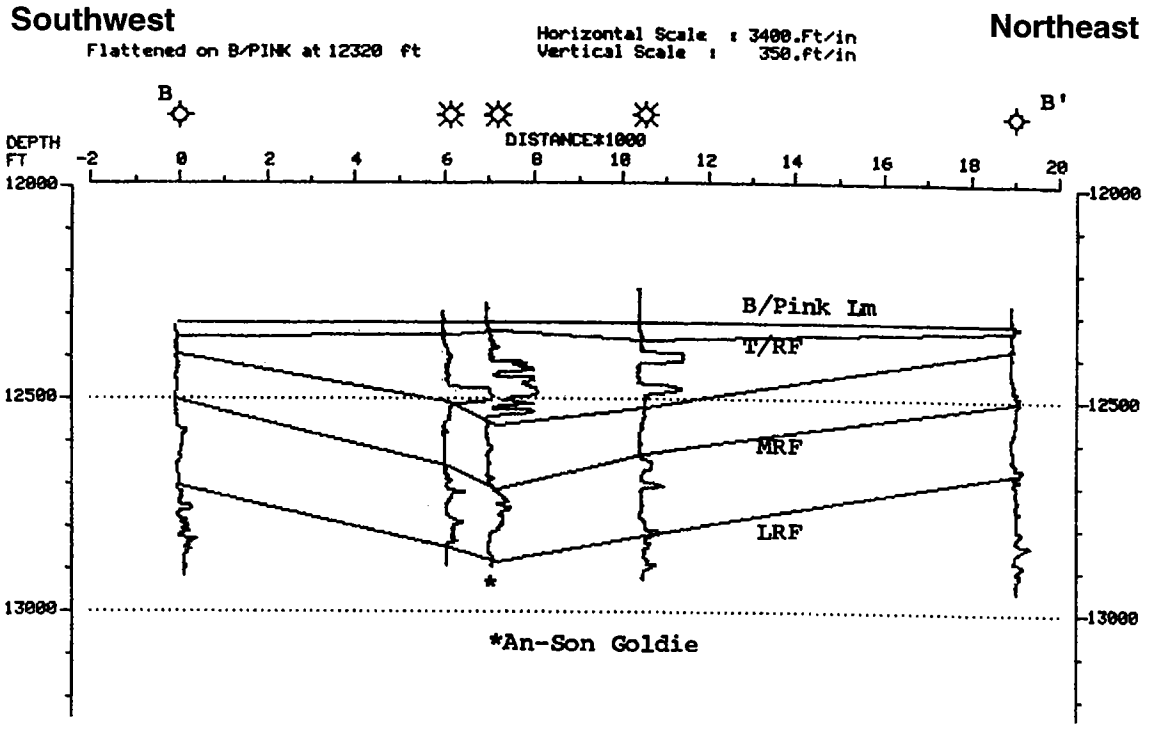

Figure 16. Simplified southwest–northeast geologic cross section B–B′ using resistivity curves hung on Pink Limestone through part of East Clinton Field. Note upper Red Fork (URF) sand-filled channel in middle two wells. Wells are those used in Figure 14. Depth in feet and distance in feet × 1,000. *Abbreviations:* B/Pink = base of Pink Limestone; T/RF = top of Red Fork; MRF = middle Red Fork; LRF = lower Red Fork.

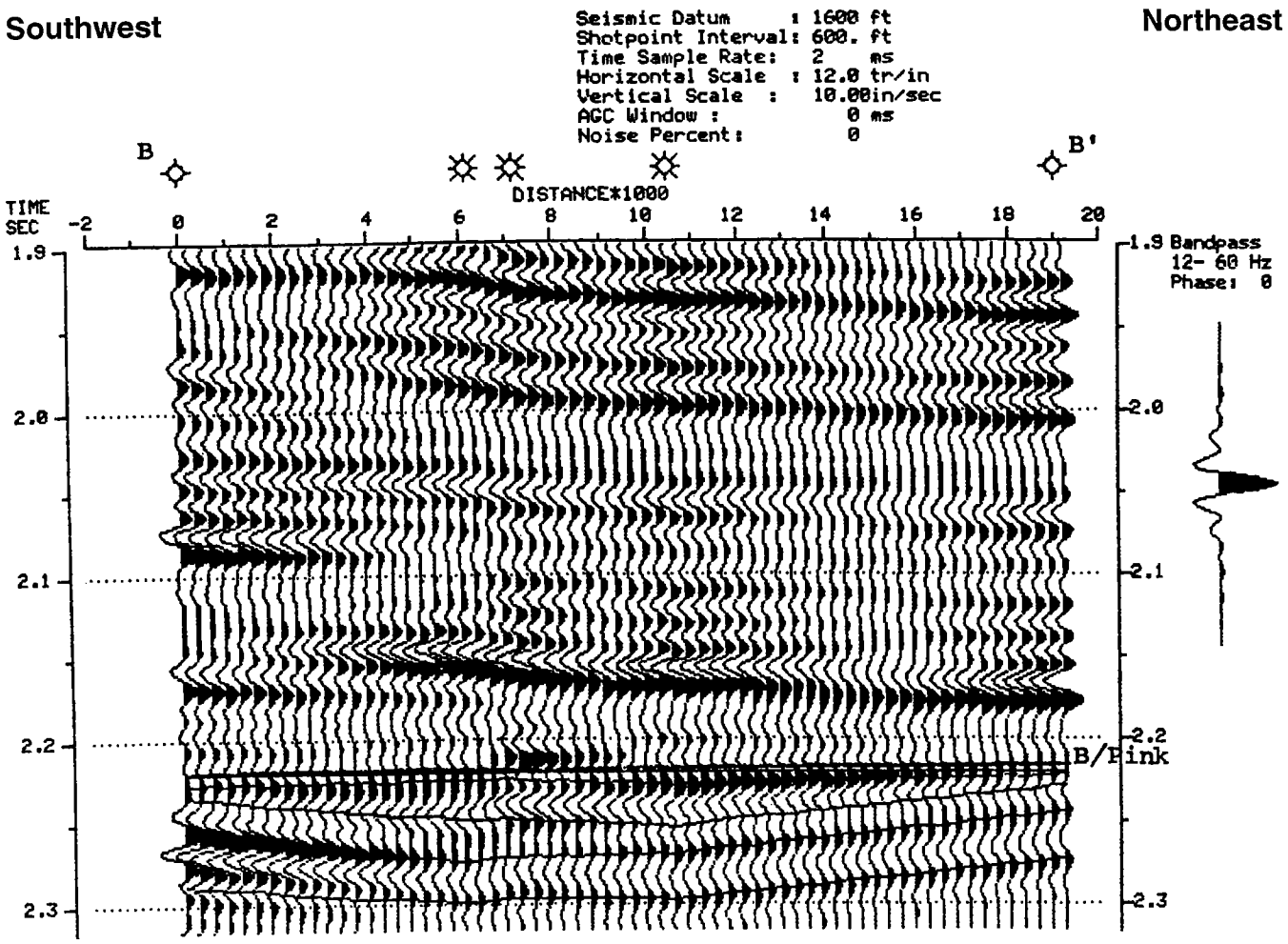

Figure 17. Two-dimensional southwest–northeast cross section generated by computer from log curves between the five control logs shown in Figure 14 and used for cross section B–B′. Logs and traces flattened on base of Pink Limestone at 2,220 ms and interpolated between wells. *Abbreviations:* B/Pink = base of Pink Limestone; B/UpRF = base of upper Red Fork; T/UpRF = top of upper Red Fork; T/MidRF = top of middle Red Fork; T/LRF = top of lower Red Fork.

A Closer Examination of the Snider Area

The wells offsetting the Conoco No. 1-A Snider were examined in detail, and a series of connecting lines were shot by Conoco in order to evaluate the seismic/stratigraphic relationships seen on the data sets. These wells had full sonic curves run. In addition, the Snider had a 60-ft core taken from the base of the Pink Limestone Lime downward.

Profile F–F′ (Fig. 34) is a detailed cross section that was constructed from northwest–southeast along Conoco Line 556, starting at the Conoco No. 1-15 Hoffman dry hole, across the No. 1-A Snider, to the No. 1-23 Agan, and terminating at the Conoco No. 26-1 Sawatzky. Because all wells had sonic control, the logs could be directly converted into reflection-coefficient curves and displayed flattened on the Pink Lime. Note how the sand in each of the last three wells becomes thinner and more shaley as the channel edge is approached. In addition to the electric logs, the sonic curves were included as the 2-D model was built. The computer model is nearly an exact match to what is seen on the field seismic—i.e., a strong relationship to the sand distribution and seismic bed tuning across the Red Fork channel (Figs. 35–38).

Detailed cross-section G–G′ (Fig. 39) crosses the Snider well in a southwest–northeast direction. This line starts at the Conoco No. 1-28 Fransen, across the No. 1-A Snider, to the No. 1-14 Meacham, and ends at the Andover No. 1 Rainey well (dry in the Red Fork) in the SE¼ of sec. 12. This line was displayed first as an E-log section (Fig. 40), then flattened on the Pink Lime (Figs. 41–42), then as sonic curves, and finally as a series of synthetic seismograms constructed from the interpolated sonics (Fig. 43). A near-perfect match is achieved in a comparison of the profile to the seismic line shot across these wells. See Conoco Line 567 (Fig. 44) displayed with a larger vertical time scale and the inset 2-D computer model generated from interpolated sonic data.

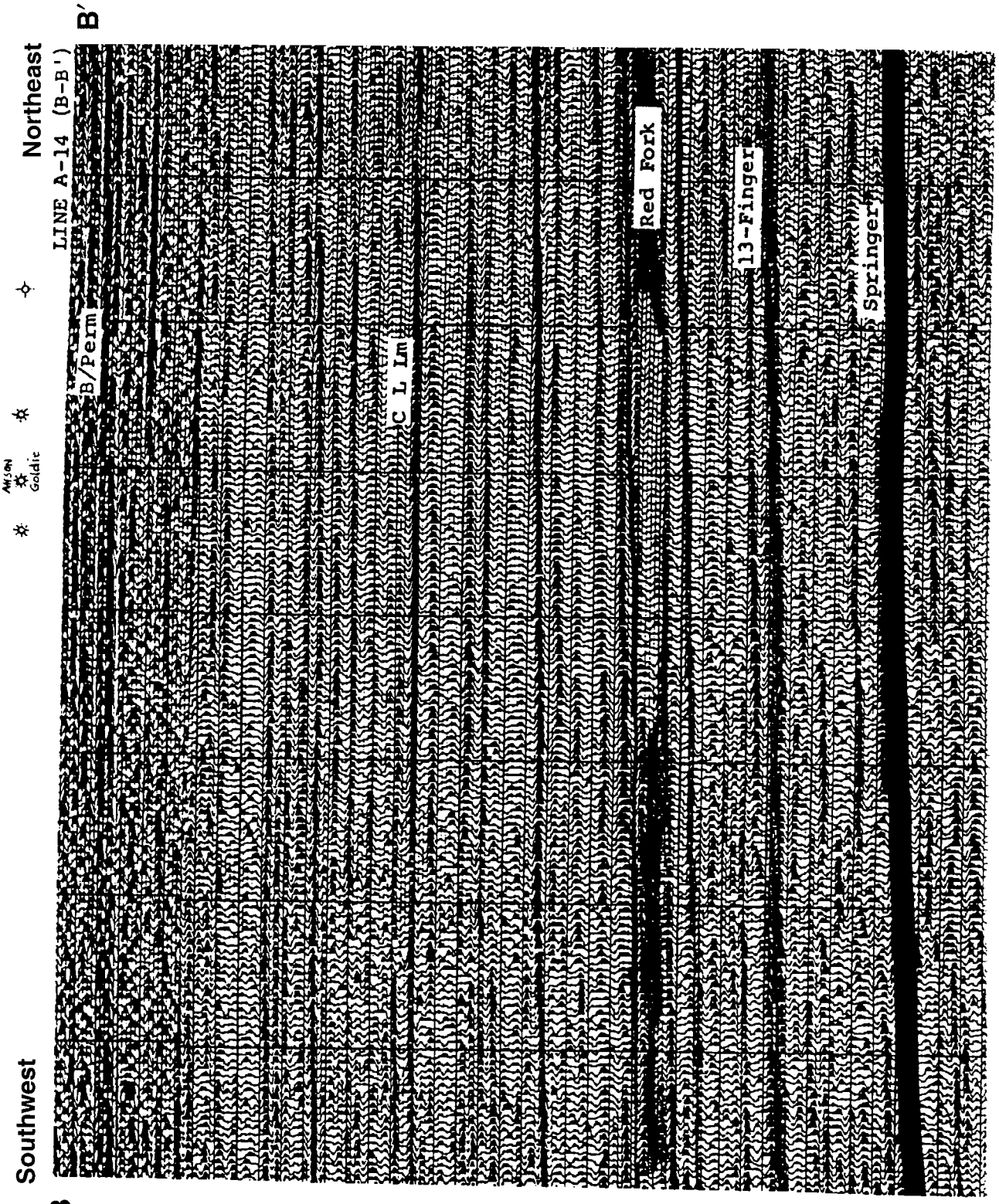

Figure 18. Actual seismic data from part (B–B') of Digicon seismic line A-14 shot across the five wells shown in Figures 14–17; locations of those wells shown at top of figure. *Abbreviations:* B/Perm = base of Permian; C L Lm = County Line Lime.

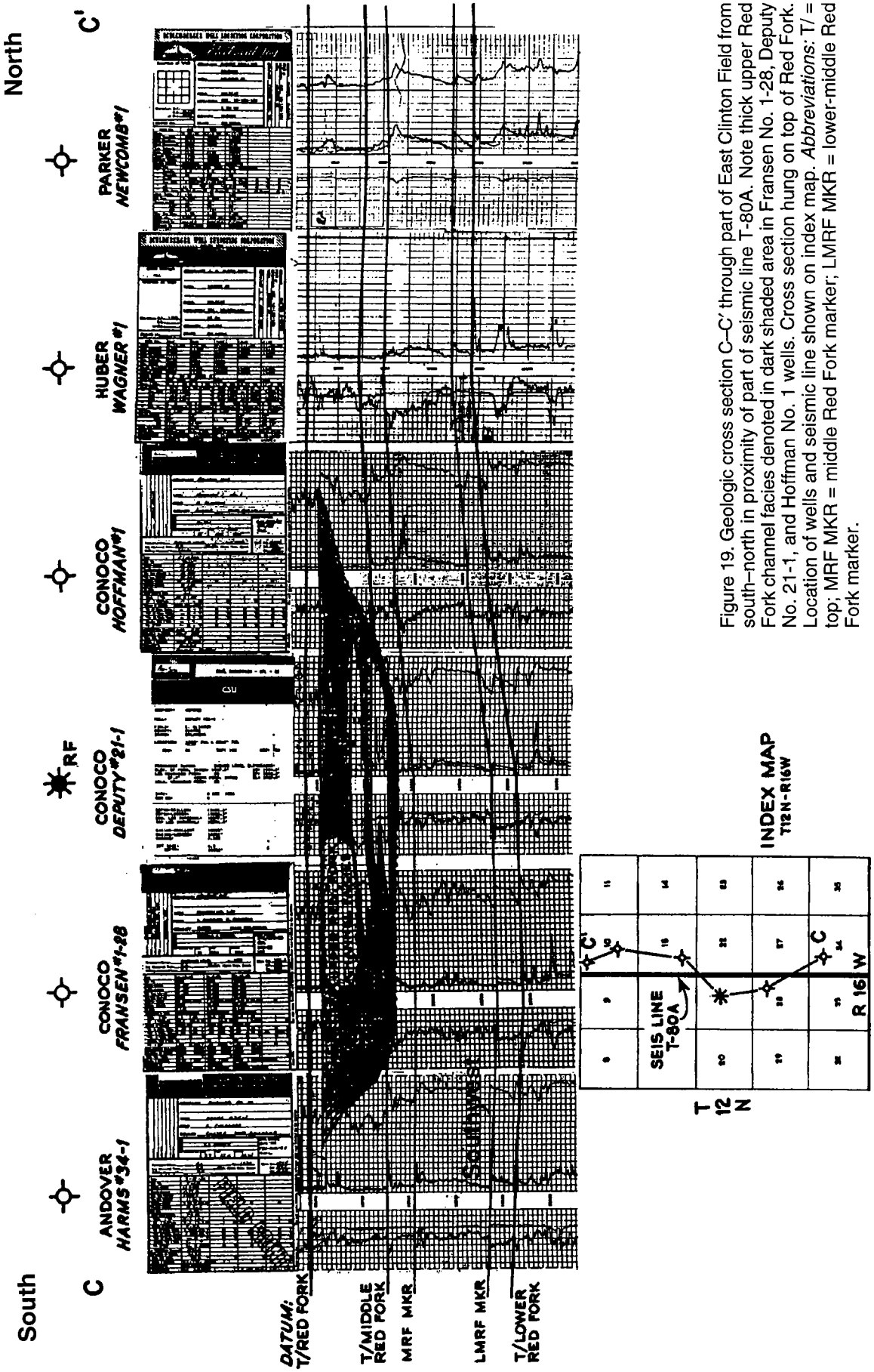

Figure 19. Geologic cross section C–C' through part of East Clinton Field from south–north in proximity of part of seismic line T-80A. Note thick upper Red Fork channel facies denoted in dark shaded area in Fransen No. 1-28, Deputy No. 21-1, and Hoffman No. 1 wells. Cross section hung on top of Red Fork. Location of wells and seismic line shown on index map. *Abbreviations:* T/ = top; MRF MKR = middle Red Fork marker; LMRF MKR = lower-middle Red Fork marker.

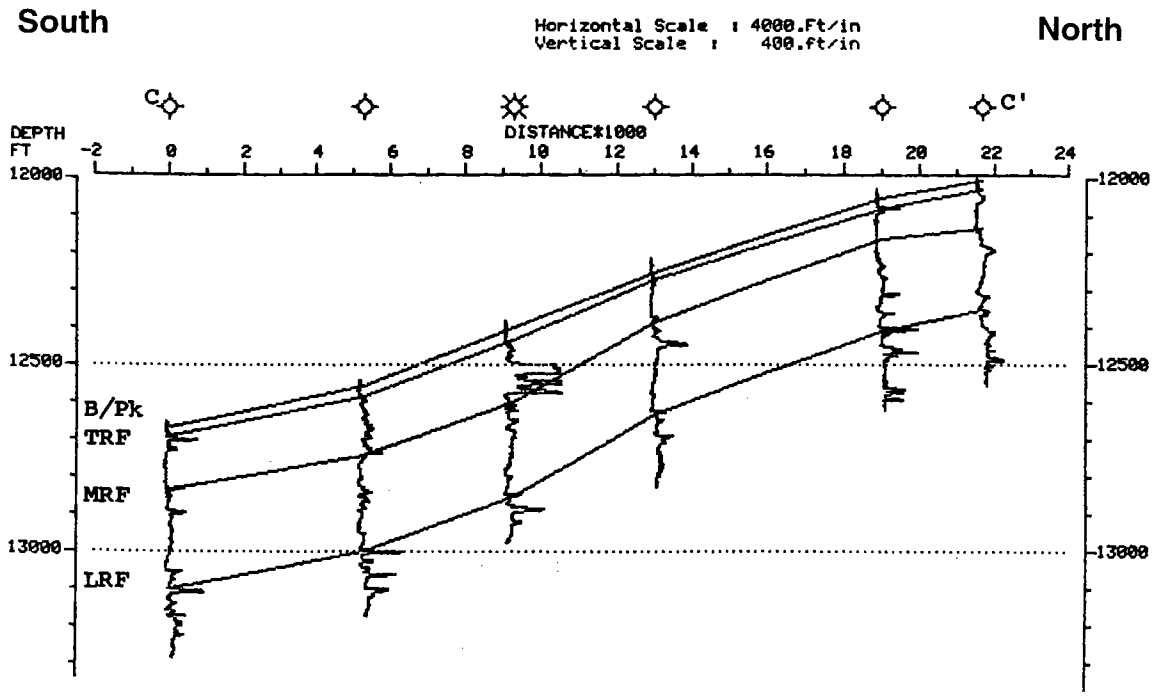

Figure 20. Simplified south–north geologic cross section C–C′ using resistivity curves hung on sea level through part of East Clinton Field. Six wells are those used in Figure 19. Depth in feet and distance in feet × 1,000. *Abbreviations:* B/Pk = base of Pink Limestone; T/RF = top of Red Fork; MRF = middle Red Fork; LRF = lower Red Fork.

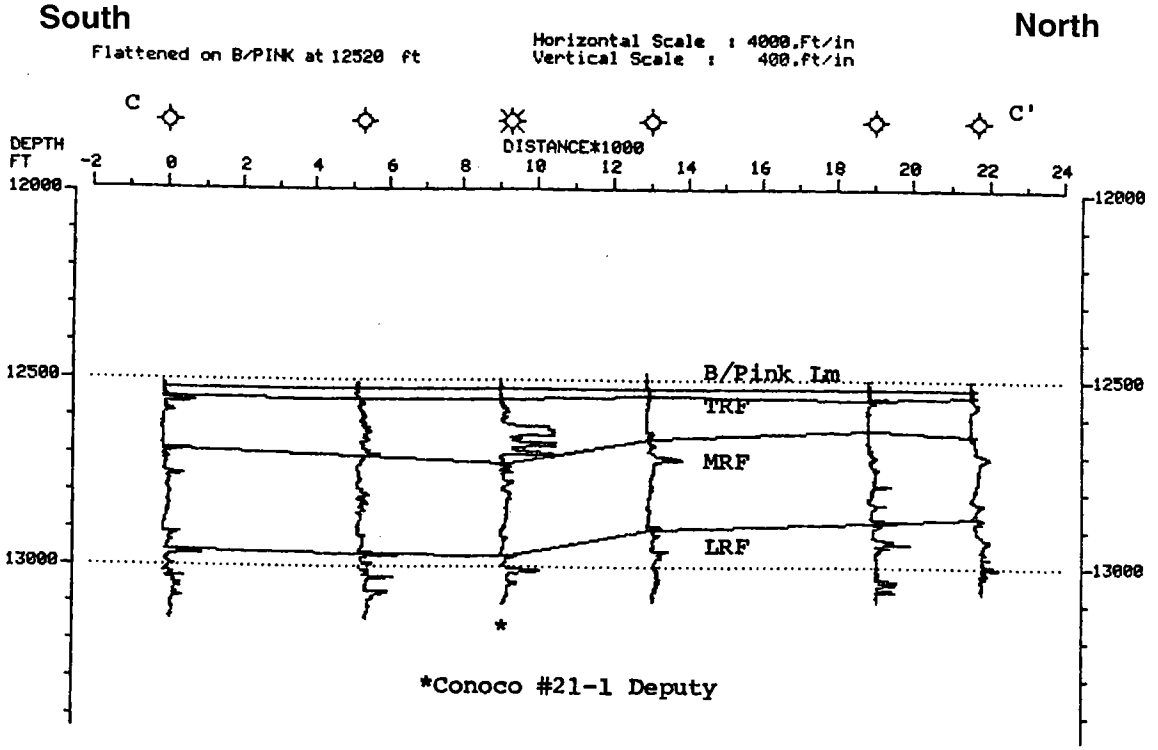

Figure 21. Simplified southwest-northeast geologic cross section C–C′ using resistivity curves flattened on base of Pink Limestone at 12,520 ft through part of East Clinton Field; log curves are hung on top of Red Fork. Wells are those used in Figure 19. Depth in feet and distance in feet x 1,000. *Abbreviations:* B/Pink Lm = base of Pink Limestone; T/RF = top of Red Fork; MRF = middle Red Fork; LRF = lower Red Fork.

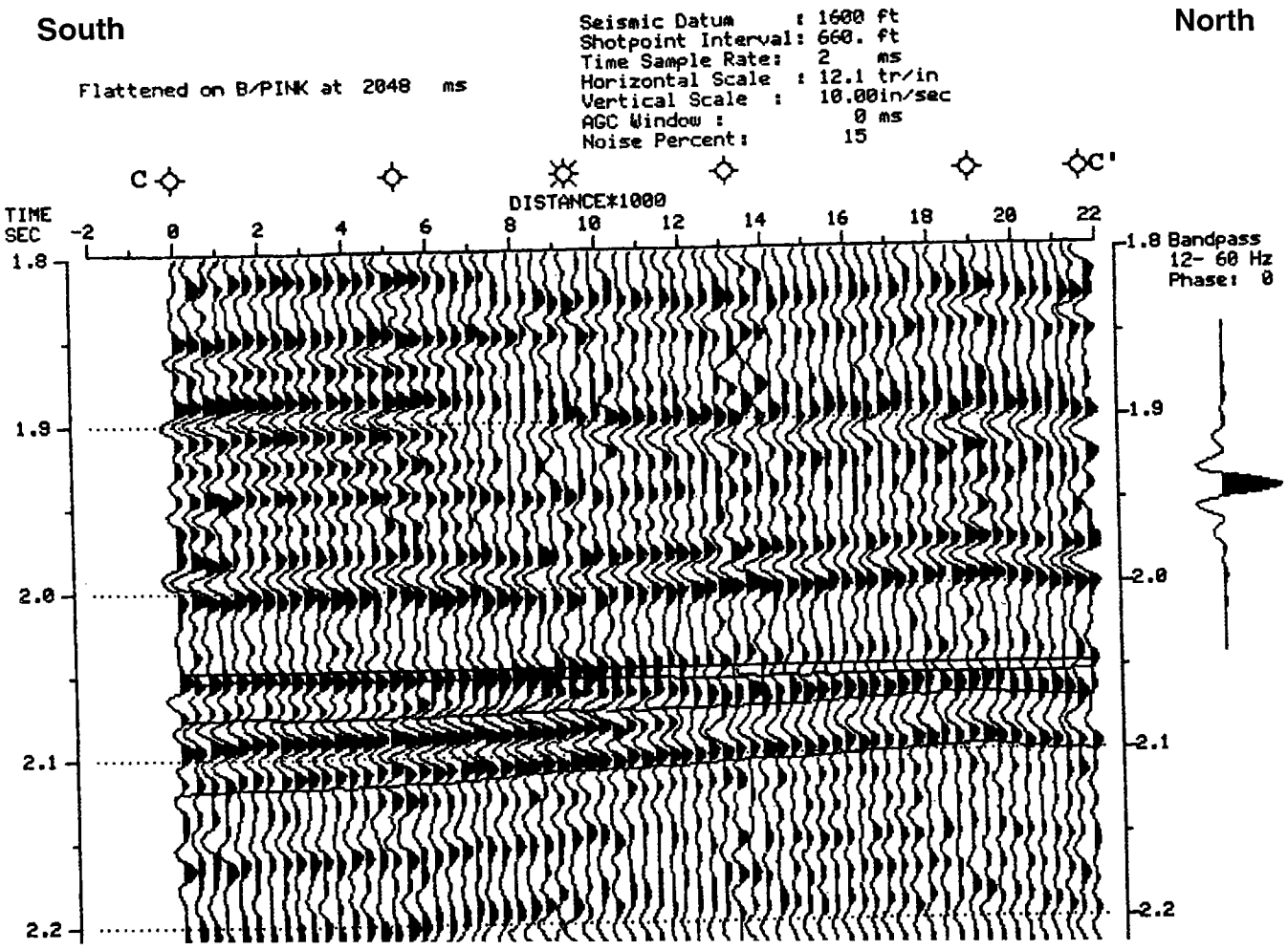

Figure 22. Two-dimensional south–north cross section generated by computer from log curves between the six control logs shown in Figure 19 and used for cross section C–C′. Logs flattened on base of Pink Limestone at 2 ms, and traces between wells are interpolated. Depth in seconds and distance in feet x 1,000. *Abbreviations:* T/RF = top of Red Fork; T/MidR = top of middle Red Fork; T/LRF = top of lower Red Fork.

CONCLUSIONS

The East Clinton Field was an excellent area in which to conduct seismic/stratigraphic analyses. The seismic data are relatively free of noise and destructive multiples. Few problems with near-surface statics were present, although these exist and become more severe to the west. Excellent separation between high- and low-velocity events is due to the relatively simple stratigraphy in the Desmoinesian section in the study area. Significant channel sands are present at depths of 12,000 ft or greater, with nearly 60-Hz high frequency being returned and recorded at the surface. The core data proved the presence of the Red Fork channel. The seismic data and subsequent drilling showed it to be in an east–west lineation in the East Clinton Field (Fig. 45), and production has proven economically robust.

The trend now has more than 200 wells within the currently defined channel boundaries and is still expanding. However, only 100 wells were examined in this study and many of the seismic lines were not available (Fig. 45).

Although Amoco drilling dominates the east part of the trend, An-Son drilled 26 wells within the study area. Because of good exploration techniques, only eight of these An-Son wells were dry holes. Conoco contributed 12 tests in the channel, and by using key seismic/geologic relationships, drilled eight producers, three dry holes, and a single lost hole. Woods Petroleum was another active participant in this trend with nine tests, but had only three productive wells in the channel.

Keys to seismic interpretation in this area include the following:

(1) If the Red Fork Sand is developed at the top of the Red Fork interval, an amplitude anomaly (peak) could be seen, even with only 20 ft of sand.

(2) Where the upper Red Fork and middle Red Fork were 165–200 ft apart, a strong tuning effect was noted as the 50-Hz dominant high frequency was reinforced. Note the strong peak-trough-peak relationship in the Conoco No. 1-14 Meacham well (see Fig. 43).

(3) The upper Red Fork can become de-tuned with a

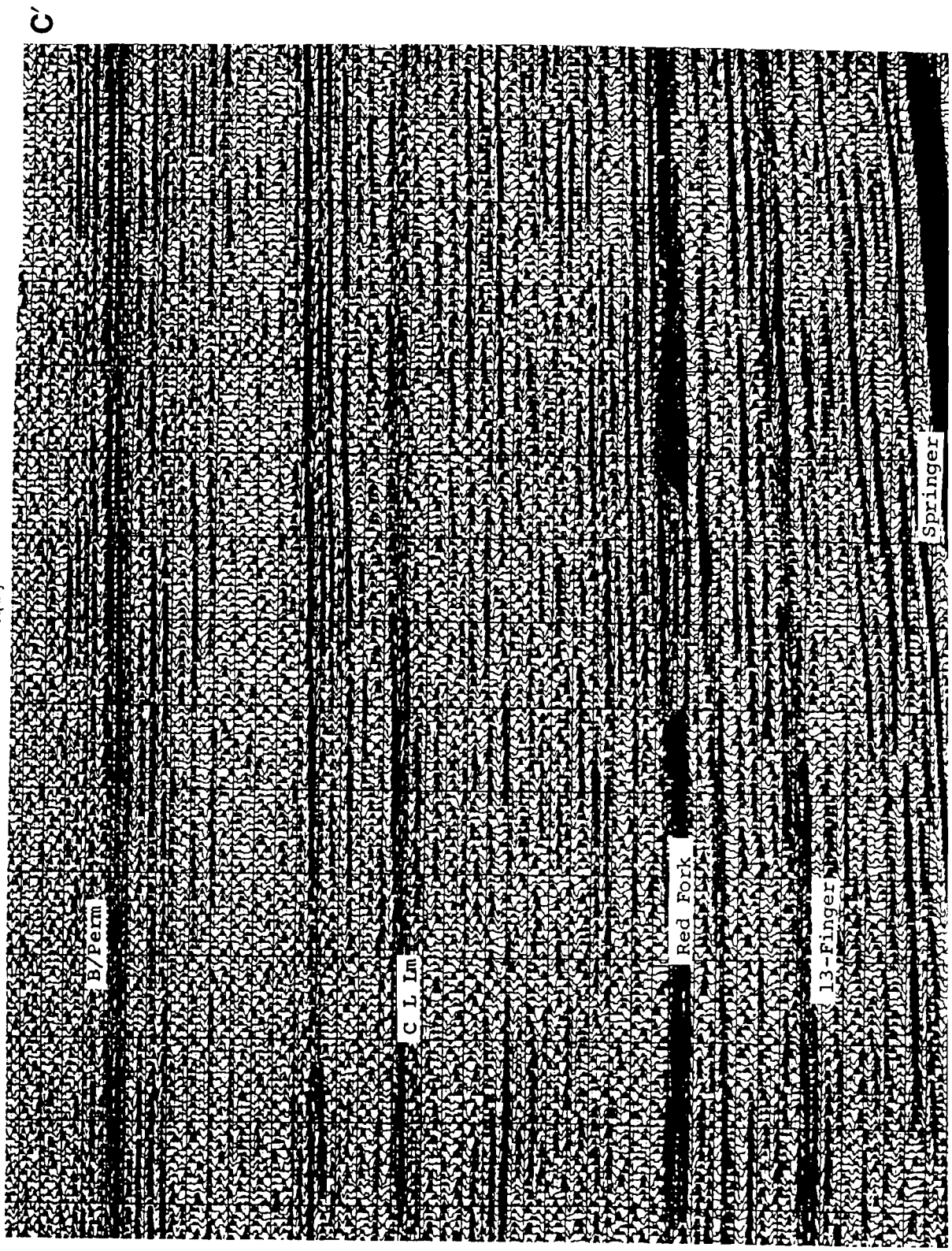

Figure 23. Actual seismic data from part (C–C') of Digicon seismic line T-80A shot across the five wells shown in Figures 19–22; locations of those six wells shown at top of figure. *Abbreviations:* B/Perm = base of Permian; C L Lm = County Line Lime.

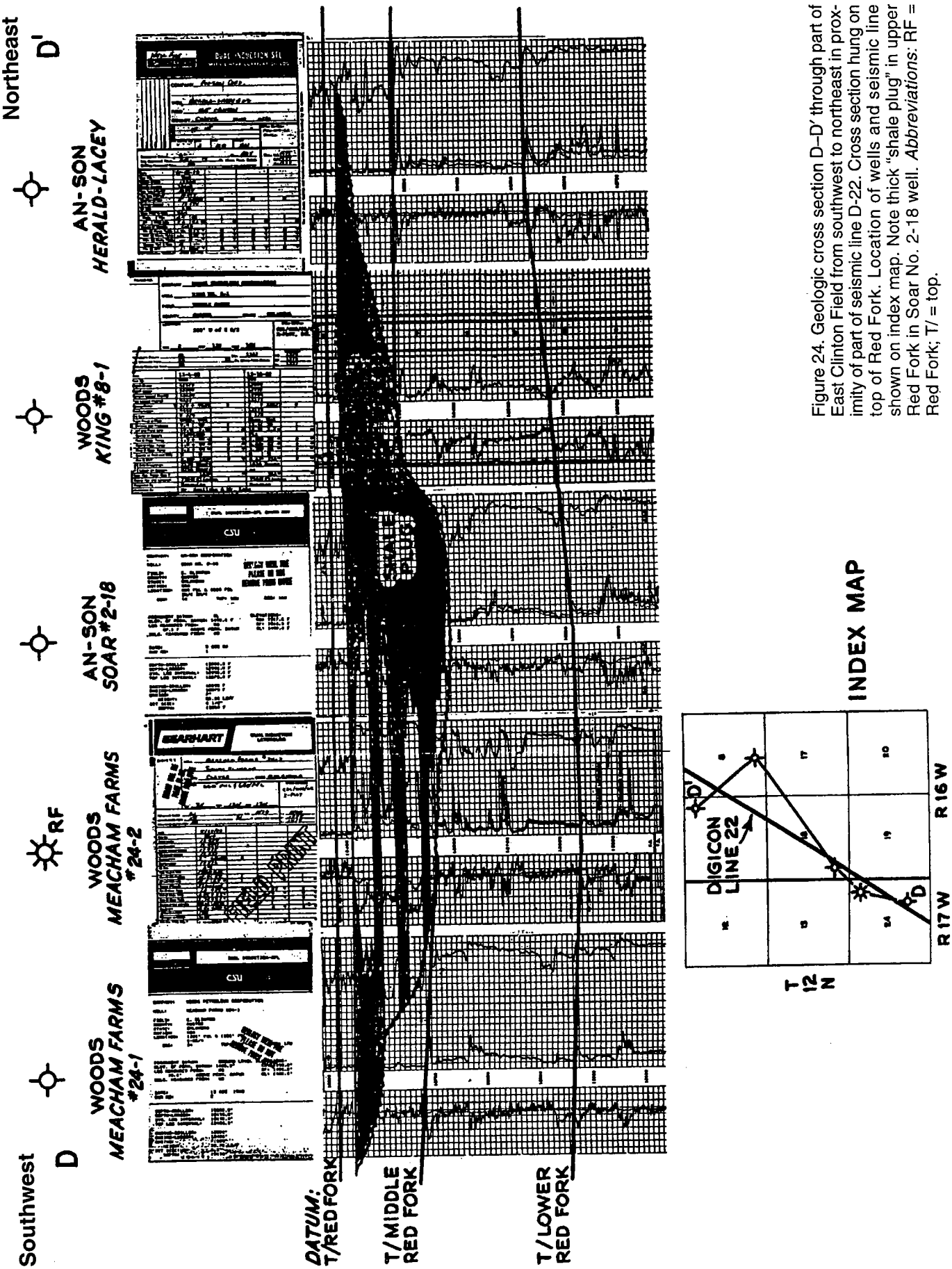

Figure 24. Geologic cross section D–D′ through part of East Clinton Field from southwest to northeast in proximity of part of seismic line D-22. Cross section hung on top of Red Fork. Location of wells and seismic line shown on index map. Note thick "shale plug" in upper Red Fork in Soar No. 2-18 well. *Abbreviations:* RF = Red Fork; T/ = top.

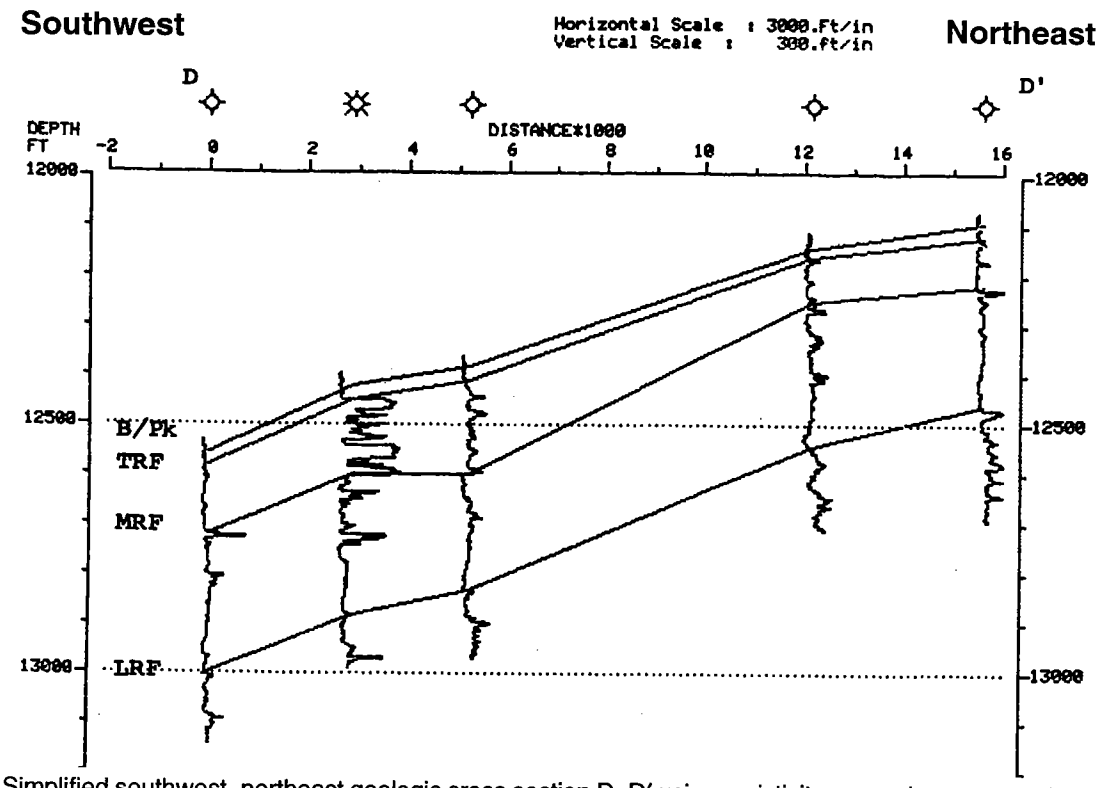

Figure 25. Simplified southwest–northeast geologic cross section D–D′ using resistivity curves hung on sea level through part of East Clinton Field. Wells are those used in Figure 24. Depth in feet and distance in feet × 1,000. *Abbreviations:* B/Pk = base of Pink Limestone; T/RF = top of Red Fork; MRF = middle Red Fork; LRF = lower Red Fork.

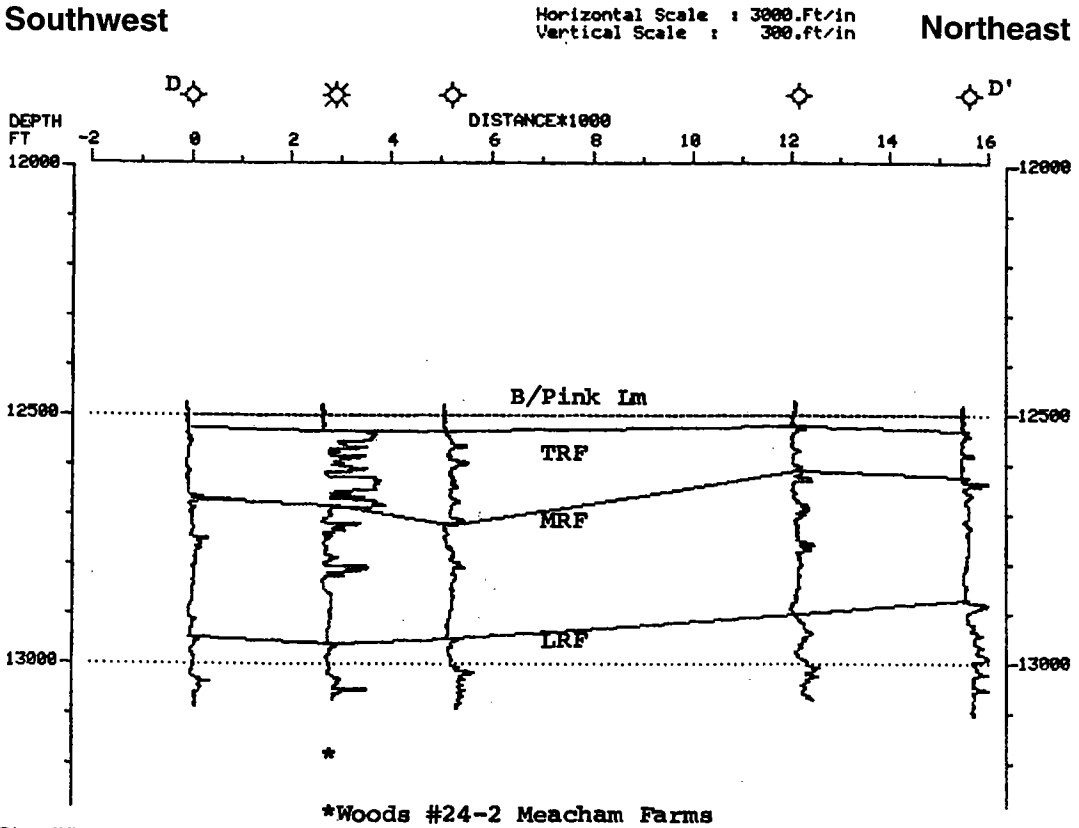

Figure 26. Simplified southwest–northeast geologic cross section D–D′ using resistivity curves through part of East Clinton Field. Wells flattened on base of Pink Limestone at 12,500 ft and log curves hung on top of Red Fork. Wells are those used in Figure 24. Depth in feet and distance in feet × 1,000. *Abbreviations:* B/Pink Lm = base of Pink Limestone; T/RF = top of Red Fork; MRF = middle Red Fork; LRF = lower Red Fork.

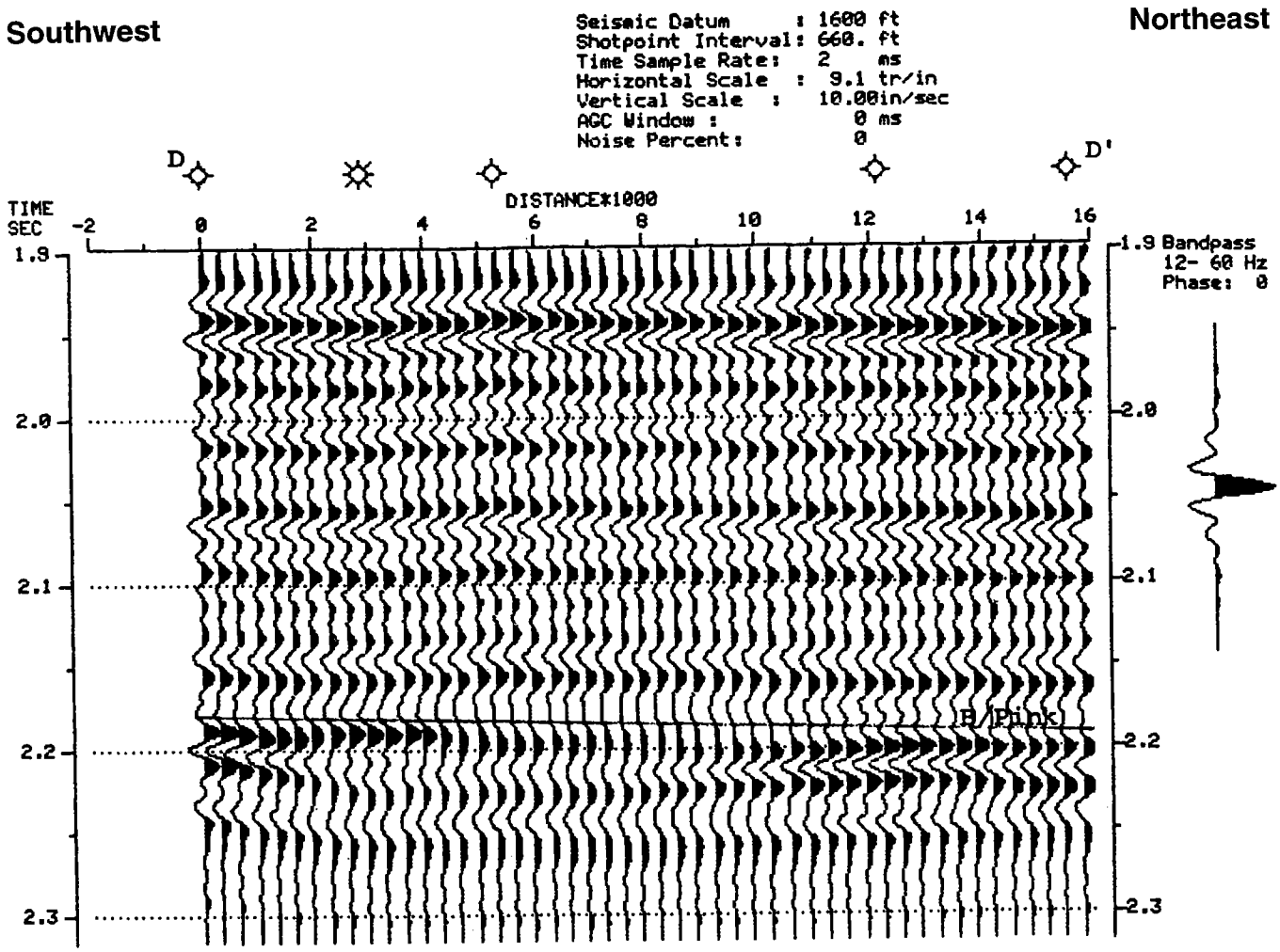

Figure 27. Two-dimensional southwest–northeast cross section generated by computer from log curves between the five control logs shown in Figure 24 and used for cross section D-D′. Logs flattened on base of Pink Limestone at 2,184 ms and traces are interpolated between wells. Depth in seconds and distance in feet × 1,000. *Abbreviations:* T/RF = top of Red Fork; T/MidRF = top of middle Red Fork; T/LRF = top of lower Red Fork.

corresponding loss of amplitude when the sands become too thick. In the frequency range present, the destructive effects could be seen at thicknesses over 150 ft. An example is the result seen at the An-Son No. 2 Moore well on Profile E–E′ (Fig. 32).

(4) The iso-time thickness seen on the first two Red Fork reflectors are critical. They mirror the channel thickness if both the Upper and Middle zones have high velocity rocks present.

(5) Anomalous "slope breaks" are important because they can help explain lithology changes.

(6) Using all available well data, create computer models, synthetic seismograms, and learn as much as possible about the "cause and effect" relationship of the borehole geology to the seismic data. If one plays the "what if" game, the success ratio can be improved.

ACKNOWLEDGMENTS

A special thanks to Anson Corporation and Conoco, Inc., for allowing us to use their data in putting this paper together. Without their willingness to share their information, this study could not have been completed. Additional thanks are due Digicon Geophysical Corp. for releasing parts of their group shoot data for presentation in this paper. Thanks also to Oklahoma Seismic Corp. for the free use of their facilities in creating the models and synthetic seismograms seen in the data sets presented here.

A very special thanks to Bill Rigsby (Conoco, retired) for the drafting and help in slide preparation. This study would have been impossible unless Bill had given us first call on his services.

REFERENCES CITED

Barrett, Ed, 1963, The geologic history of Oklahoma—an outline; oil and gas fields of Oklahoma: Oklahoma City Geological Society Reference Report, v. 1, p. 1–31.

Berg, O. R., 1969, The Cherokee Group, west flank of the Nemaha Ridge: Oklahoma City Geological Society Shale Shaker, v. 19, no. 6, p. 94–110.

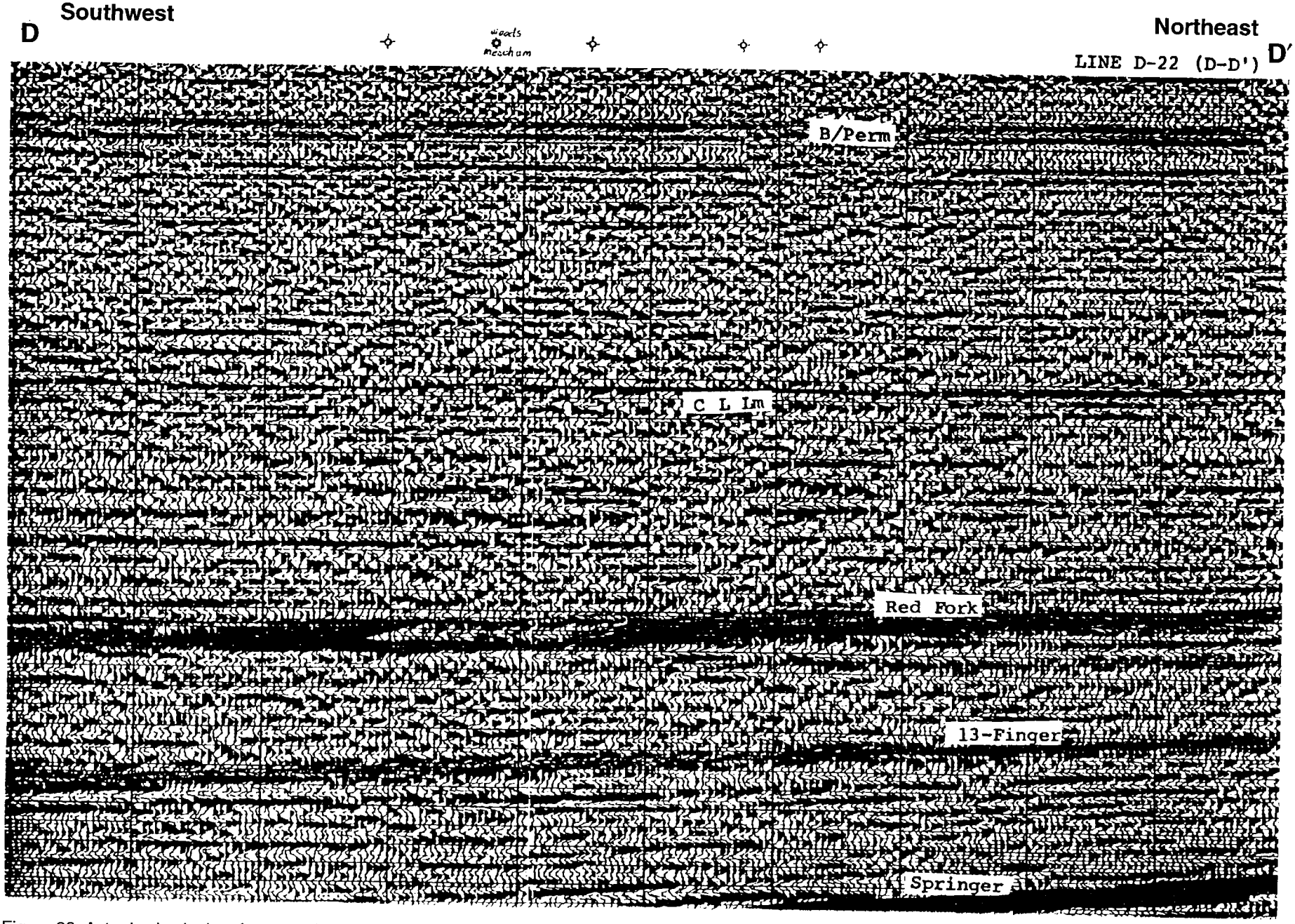

Figure 28. Actual seismic data from part (D–D′) of Digicon seismic line D-22 shot across the five wells shown in Figures 24–27; locations of those wells shown at top of figure. *Abbreviations:* B/Perm = base of Permian; C L Lm = County Line Lime.

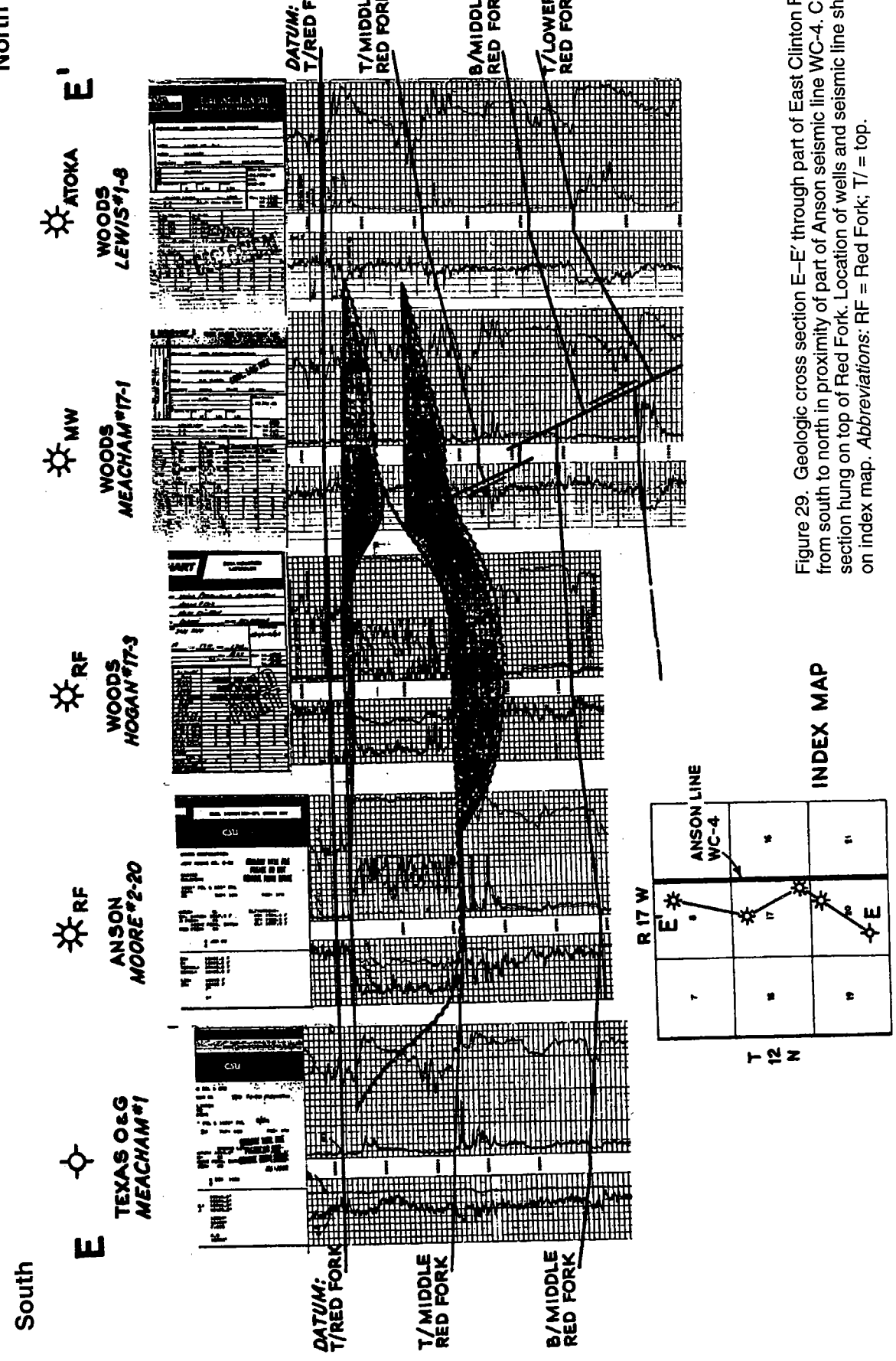

Figure 29. Geologic cross section E–E′ through part of East Clinton Field from south to north in proximity of part of Anson seismic line WC-4. Cross section hung on top of Red Fork. Location of wells and seismic line shown on index map. *Abbreviations:* RF = Red Fork; T/ = top.

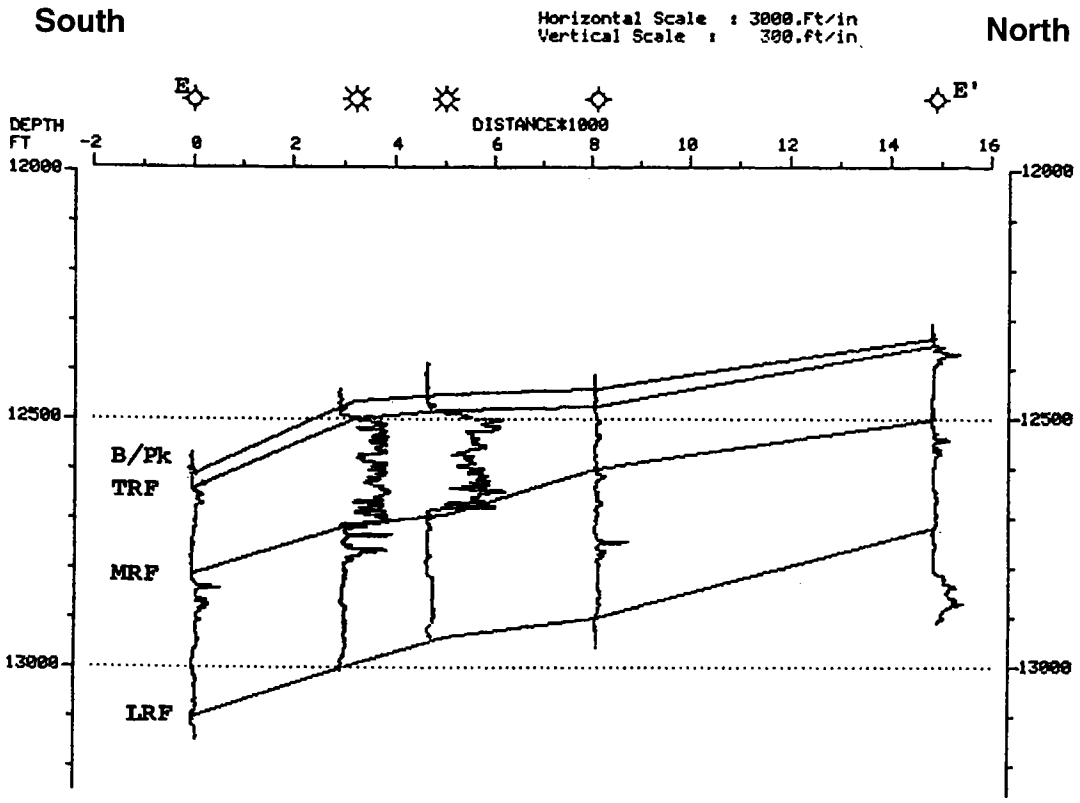

Figure 30. Simplified southwest–northeast geologic cross section E–E′ using resistivity curves hung on sea level through part of East Clinton Field. Wells are those in Figure 29. Depth in feet and distance in feet × 1,000. *Abbreviations:* B/Pk = base of Pink Limestone; T/RF = top of Red Fork; MRF = middle Red Fork; LRF = lower Red Fork.

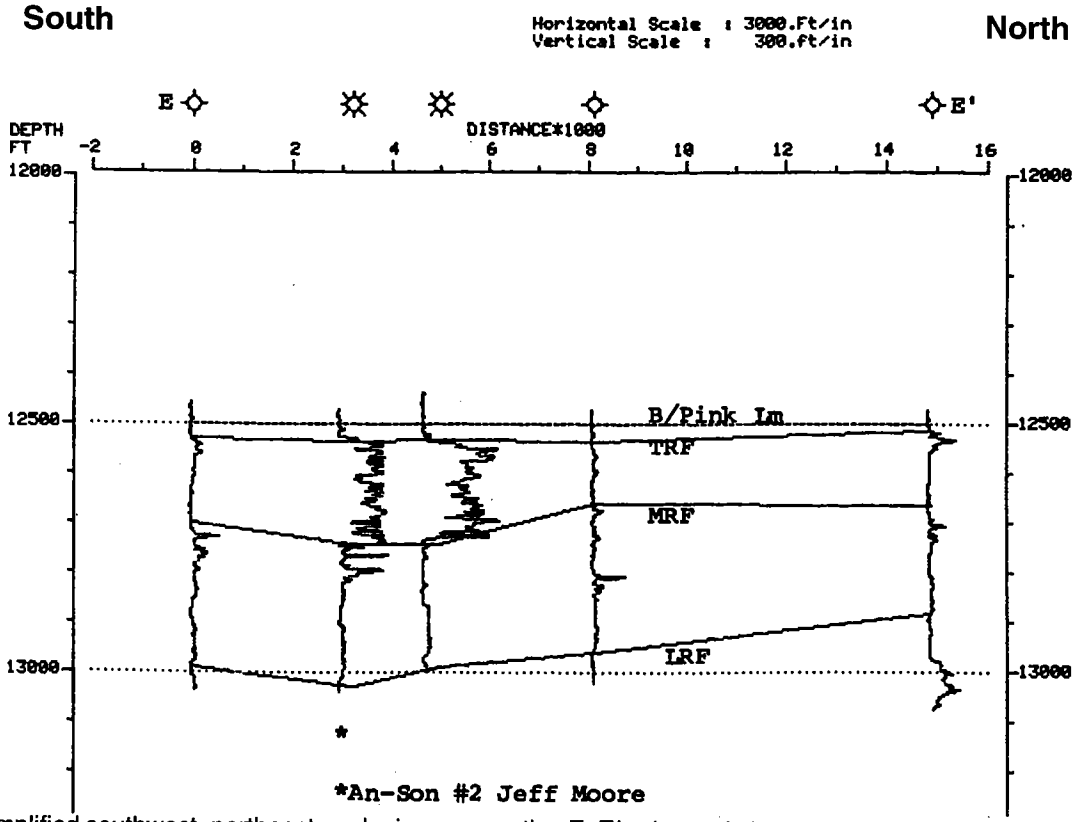

Figure 31. Simplified southwest–northeast geologic cross section E–E′ using resistivity curves flattened on base of Pink Limestone at 12,500 ft through part of East Clinton Field. Note upper Red Fork sand-filled channel in middle two wells. Wells are those in Figure 29. Depth in feet and distance in feet × 1,000. *Abbreviations:* B/Pink Lm = base of Pink Limestone; T/RF = top of Red Fork; MRF = middle Red Fork; LRF = lower Red Fork.

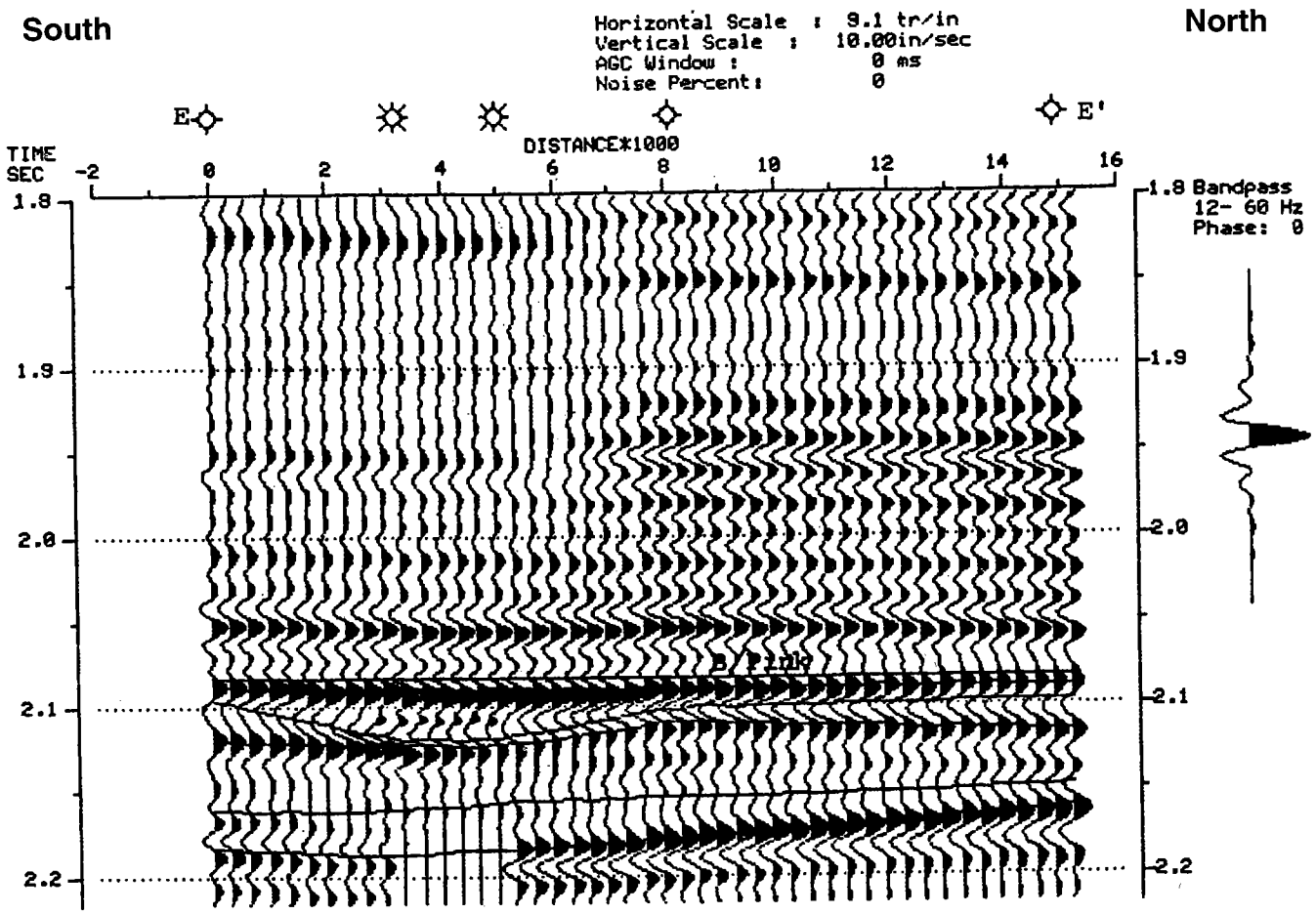

Figure 32. Two-dimensional (2-D) southwest–northeast cross section generated by computer from log curves between the five control logs shown in Figure 29 and used for cross section E–E′. Logs flattened on base of Pink Limestone at 2,083 ms, and traces are interpolated between wells. Depth in seconds and distance in feet × 1,000. *Abbreviations:* B/Pink = base of Pink Limestone; B/UpRF = base of upper Red Fork; T/UpRF = top of upper Red Fork; T/MidRF = top of middle Red Fork; T/LRF = top of lower Red Fork.

Brown, L. F., Jr., 1979, Deltaic sandstone facies of the Mid-Continent, *in* Hyne, N. J. (ed.), Pennsylvanian sandstones of the Mid-continent: Tulsa Geological Society Special Publication 1, p. 35–64.

Edwards, A. R., 1959, Facies changes in the Penn rocks along the north flank of the Wichita Mountains, *in* Petroleum geology of southern Oklahoma, a symposium: American Association of Petroleum Geologists, Tulsa, Oklahoma, v. 2, no. 3, p. 142–155.

Hawthorne, H. W., 1985, The Red Fork Sandstone, Cherokee Group (Penn) of the Southeast Thomas Field, Custer County, OK: Oklahoma City Geological Society Shale Shaker, v. 35, no. 3, p. 50–57.

Johnson, C. L., 1984, Depositional environment, reservoir trends and diagenesis of the Red Fork Sandstone in Blaine, Caddo, and Custer Counties, OK: Oklahoma City Geological Society Shale Shaker, v. 35, no. 2, p. 30–46.

Jordan, Louise, 1967, Geology of Oklahoma, a summary: Oklahoma Geology Notes, v. 96, p. 319–325.

Levine, S. D., 1984, Provenance and diagenesis of the Cherokee SS, Deep Anadarko Basin, western Oklahoma: Oklahoma City Geological Society Shale Shaker, v. 34, no. 10, p. 120–144.

Moore, G. E., 1979, Pennsylvanian paleography of the southern Mid-Continent, *in* Hyne, N. J. (ed.), Pennsylvanian sandstones of the Mid-continent: Tulsa Geological Society Special Publication 1, p. 2–9.

McElroy, M. N., 1961, Isopach and lithofacies study of the Desmoinesian Series of north-central Oklahoma: Oklahoma City Geological Society Shale Shaker, v. 12, no. 1, p. 1–18.

Swanson, D. C., 1980, Handbook of deltaic facies, Penn sandstones of the Mid-Continent: Lafayette Geological Society Special Workshop, p. 80–82.

Whiting, P. H., 1984, Depositional environment of the Red Fork Sandstones, Anadarko Basin, western Oklahoma: Oklahoma City Geological Society Shale Shaker, v. 34, no. 9, p. 104–119.

Zeliff, C. W., 1975, Subsurface analysis of the Cherokee Group (Penn), northern Kingfisher County, Oklahoma: Oklahoma City Geological Society Shale Shaker, v. 27, no. 1, 2, 3, p. 4–6, 22–32, 44–56.

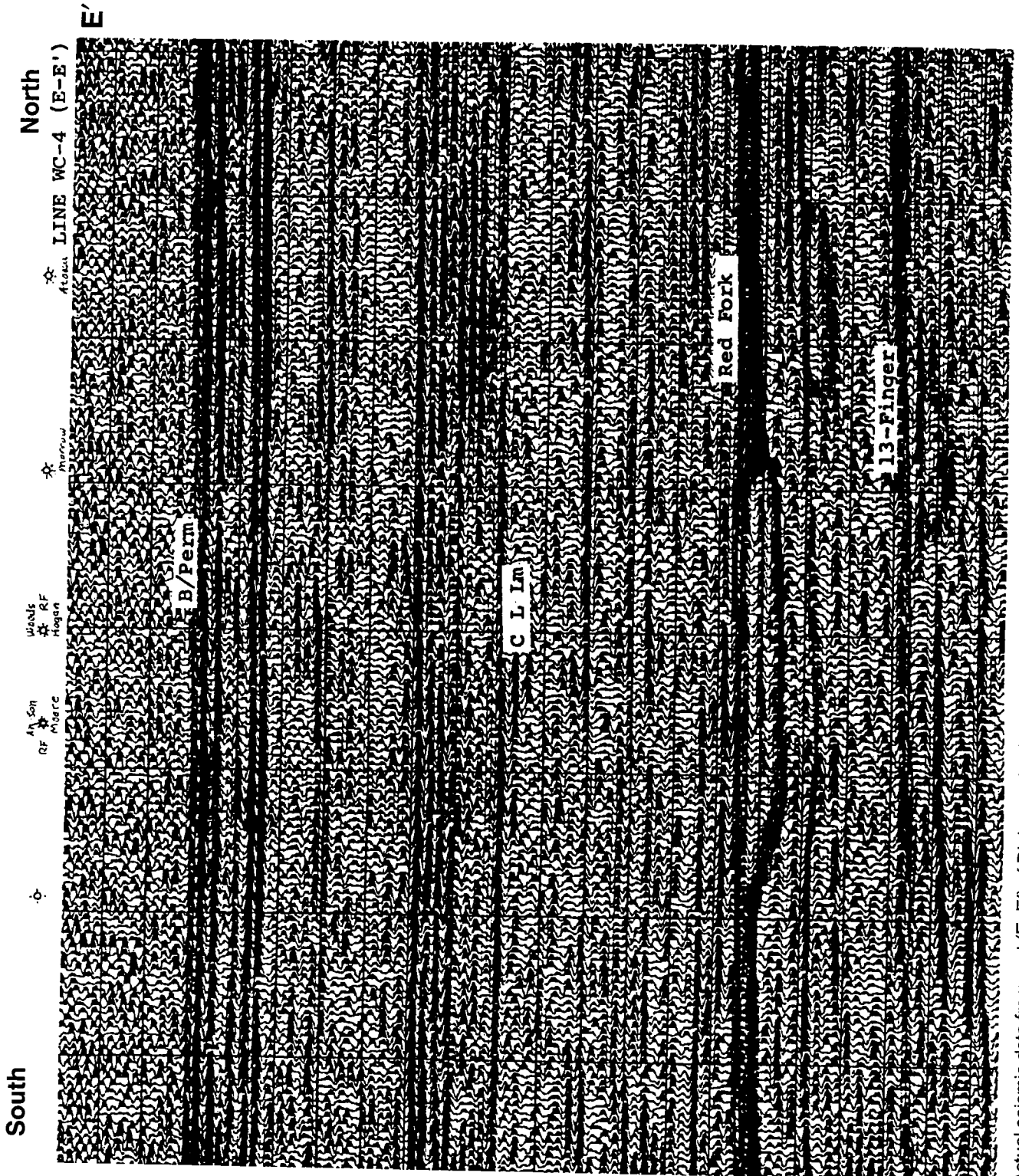

Figure 33. Actual seismic data from part (E–E') of Digicon seismic line WC-4 shot across the five wells shown in Figures 29–32; locations of those wells shown at top of figure. *Abbreviations:* B/Perm = base of Permian; C L Lm = County Line Lime.

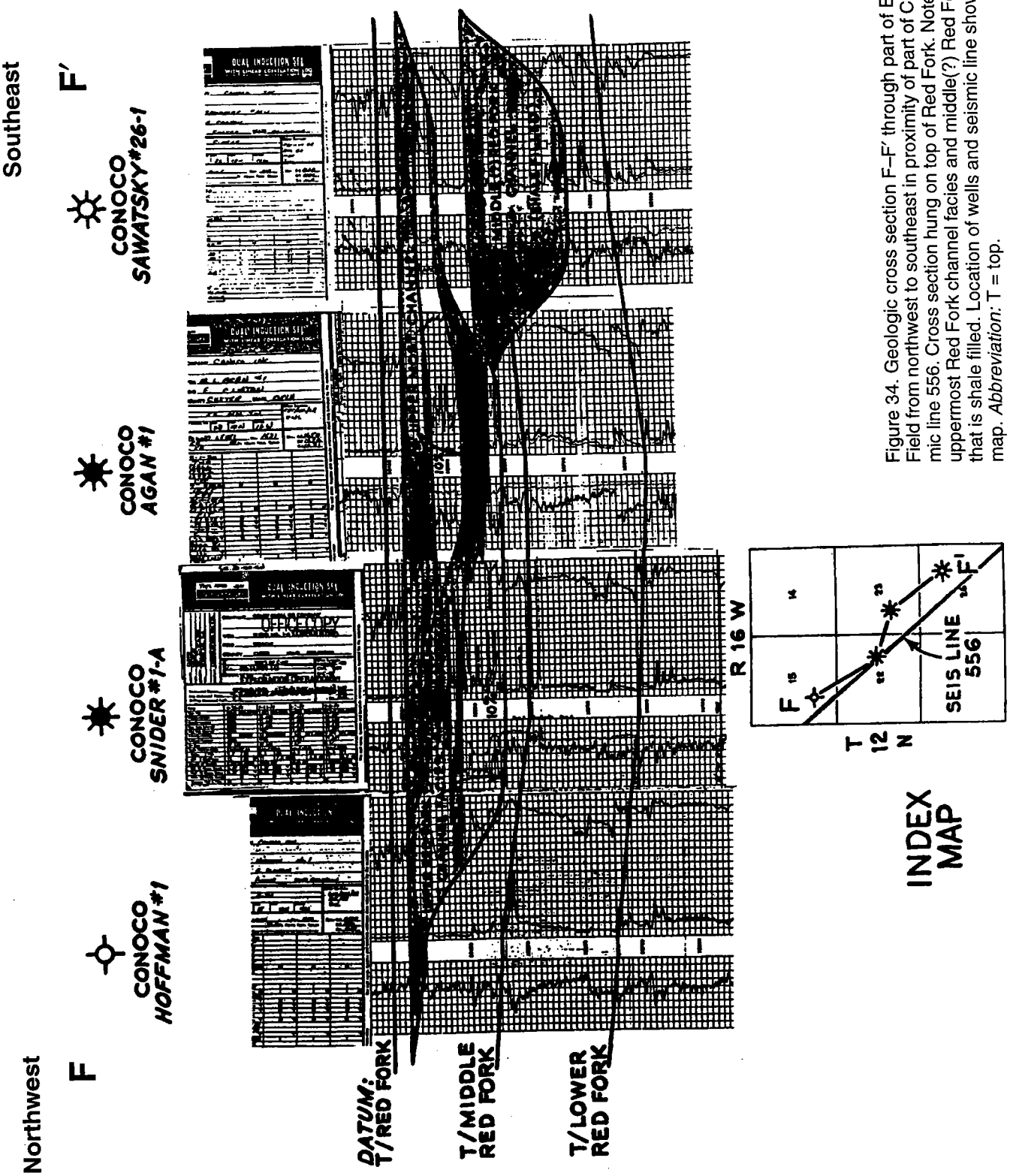

Figure 34. Geologic cross section F–F′ through part of East Clinton Field from northwest to southeast in proximity of part of Conoco seismic line 556. Cross section hung on top of Red Fork. Note upper and uppermost Red Fork channel facies and middle(?) Red Fork channel that is shale filled. Location of wells and seismic line shown on index map. *Abbreviation:* T = top.

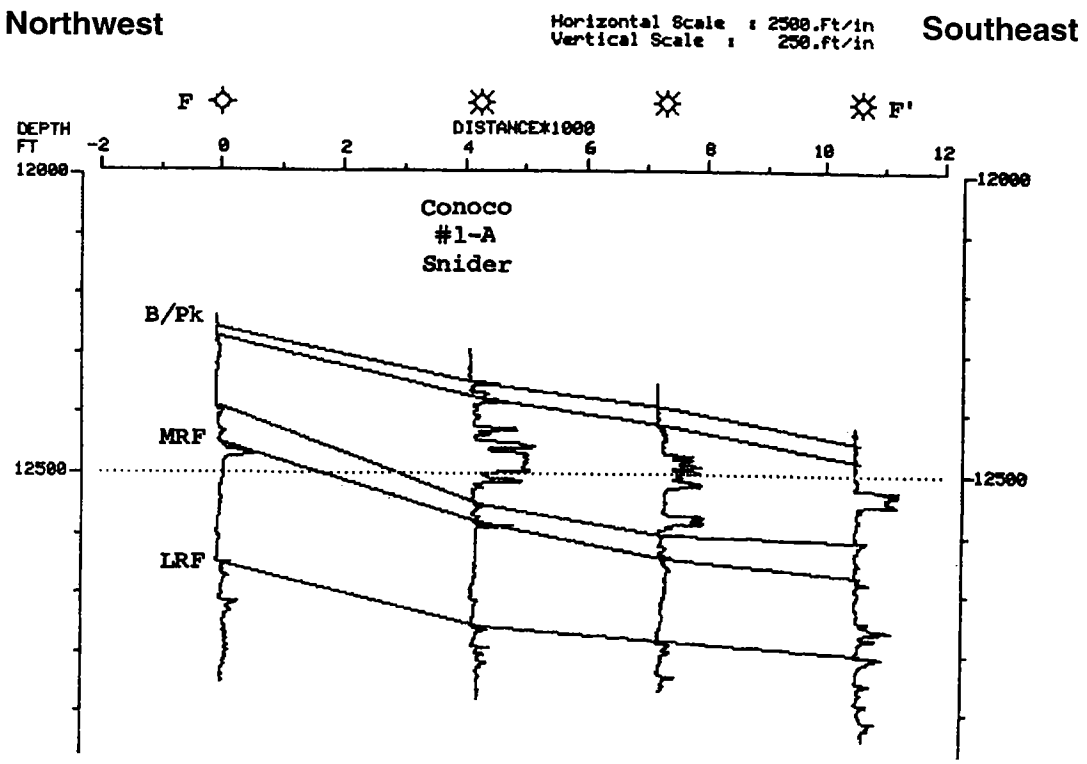

Figure 35. Simplified northwest–southeast geologic cross section F–F′ using resistivity curves hung on sea level through part of East Clinton Field. Wells are those in Figure 34. Depth in feet and distance in feet × 1,000. *Abbreviations:* B/Pk = base of Pink Limestone; T/RF = top of Red Fork; MRF = middle Red Fork; LRF = lower Red Fork.

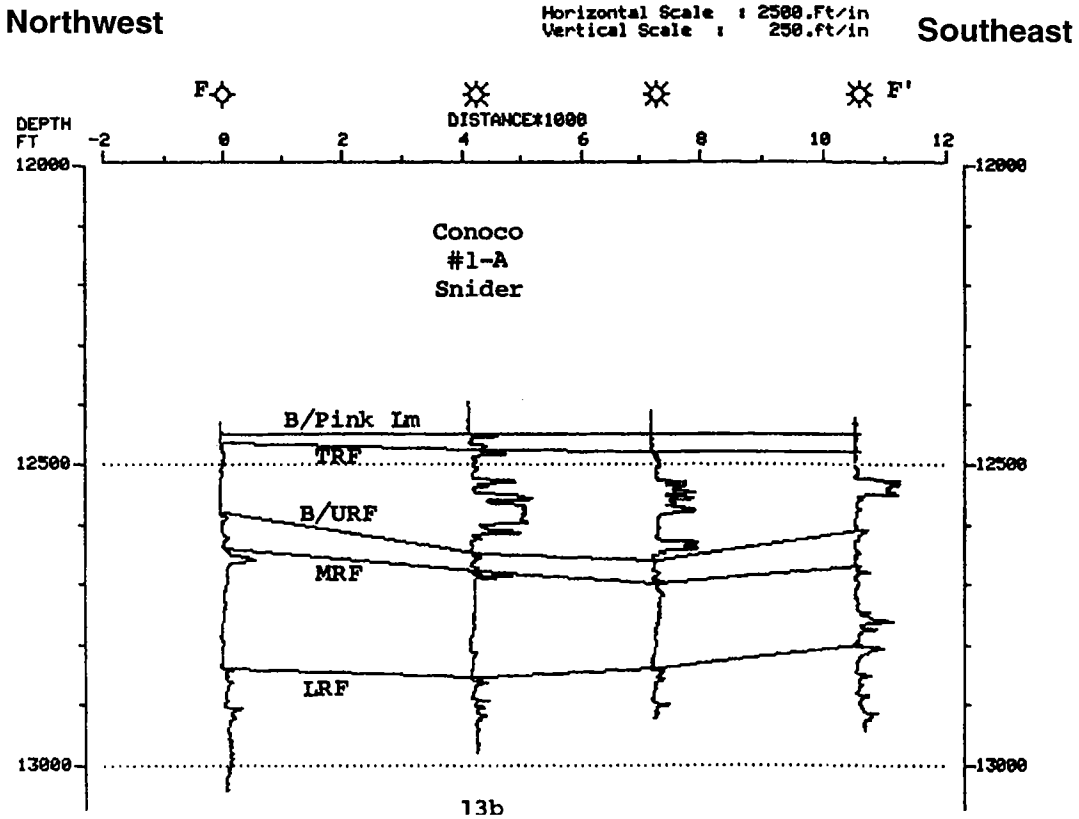

13b

Figure 36. Simplified southwest–northeast geologic cross section F–F′ using resistivity curves flattened on base of Pink Limestone at 12,450 ft through part of East Clinton Field. Curves hung on top of the Red Fork. Note upper Red Fork sand-filled channel in middle two wells. Wells are those in Figure 34. Depth in feet and distance in feet × 1,000. *Abbreviations:* B/Pink Lm = base of Pink Limestone; TRF = top of Red Fork; B/URF = base of upper Red Fork; MRF = middle Red Fork; LRF = lower Red Fork.

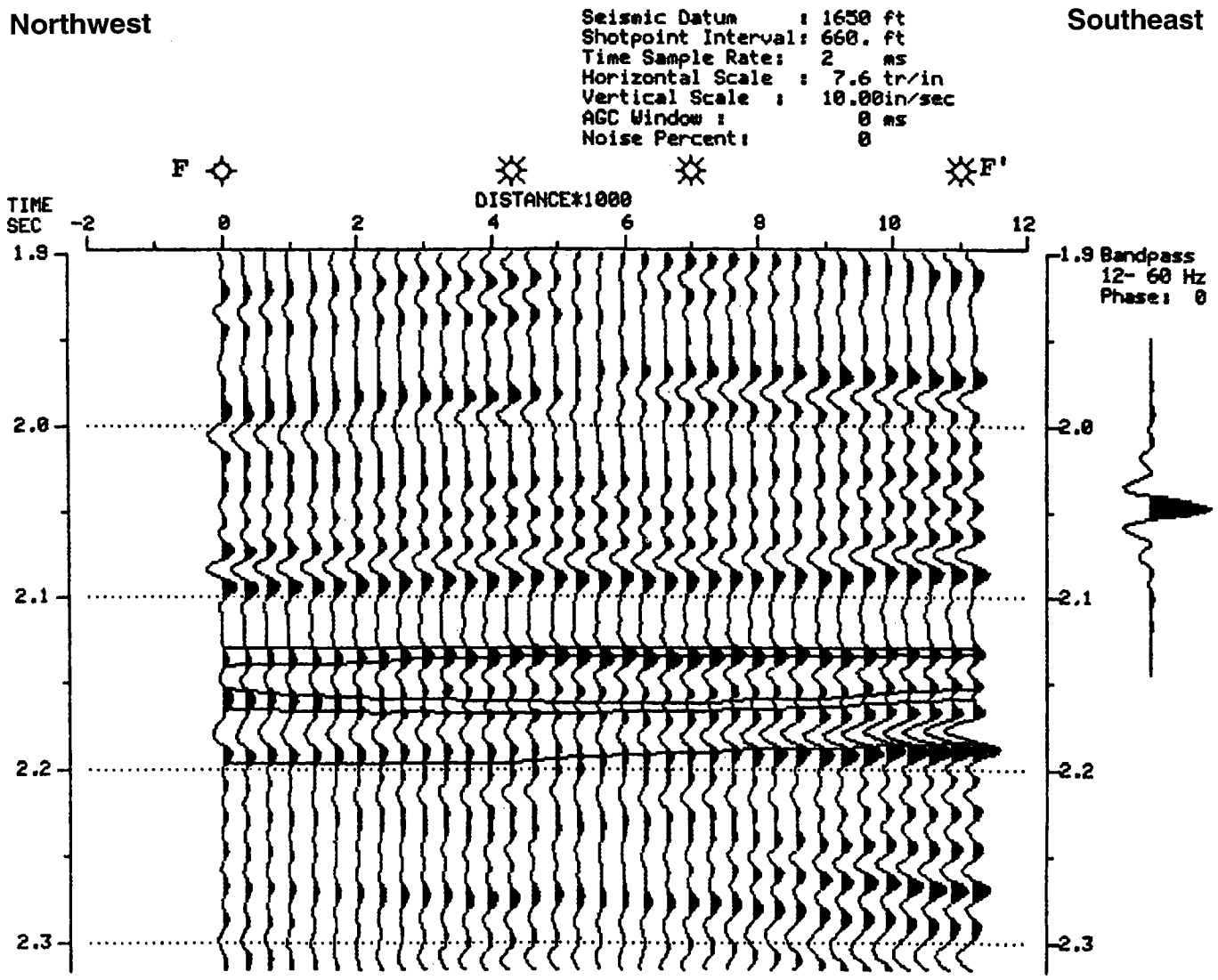

Figure 37. Two-dimensional (2-D) southwest–northeast cross section generated by computer from log curves between the four control logs shown in Figure 34 and used for cross section F–F′. Logs flattened on base of Pink Limestone at 2,083 ms, and traces are interpolated between wells. Depth in seconds and distance in feet × 1,000. *Abbreviations:* T/RF = top of Red Fork; T/MRF = top of middle Red Fork; T/LRF = top of lower Red Fork.

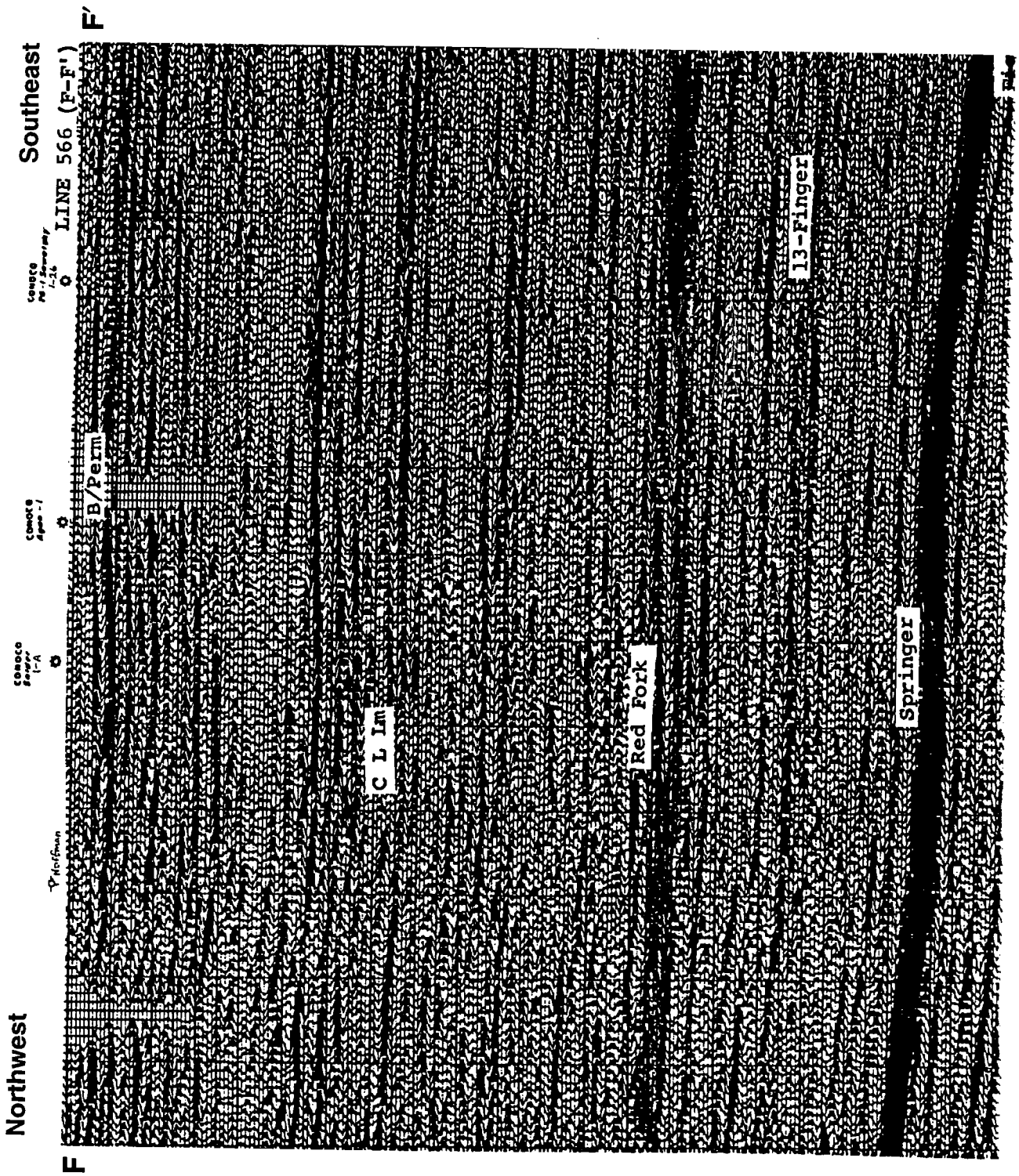

Figure 38. Actual seismic data from part (F–F') of Conoco seismic line 566 shot across the four wells shown in Figures 34–37; locations of those wells shown at top of figure. *Abbreviations:* B/Perm = base of Permian; C L Lm = County Line Lime.

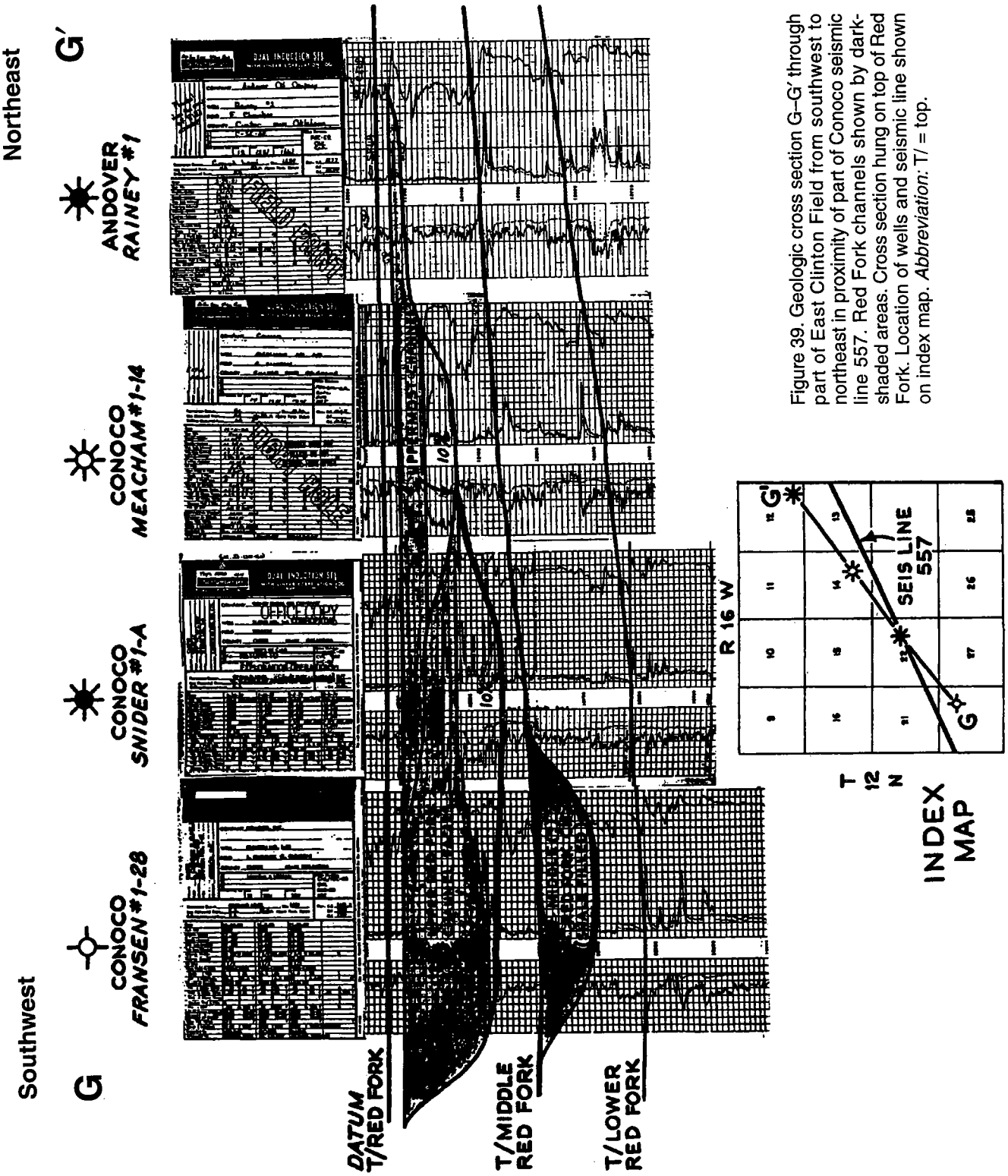

Figure 39. Geologic cross section G–G' through part of East Clinton Field from southwest to northeast in proximity of part of Conoco seismic line 557. Red Fork channels shown by dark-shaded areas. Cross section hung on top of Red Fork. Location of wells and seismic line shown on index map. *Abbreviation:* T/ = top.

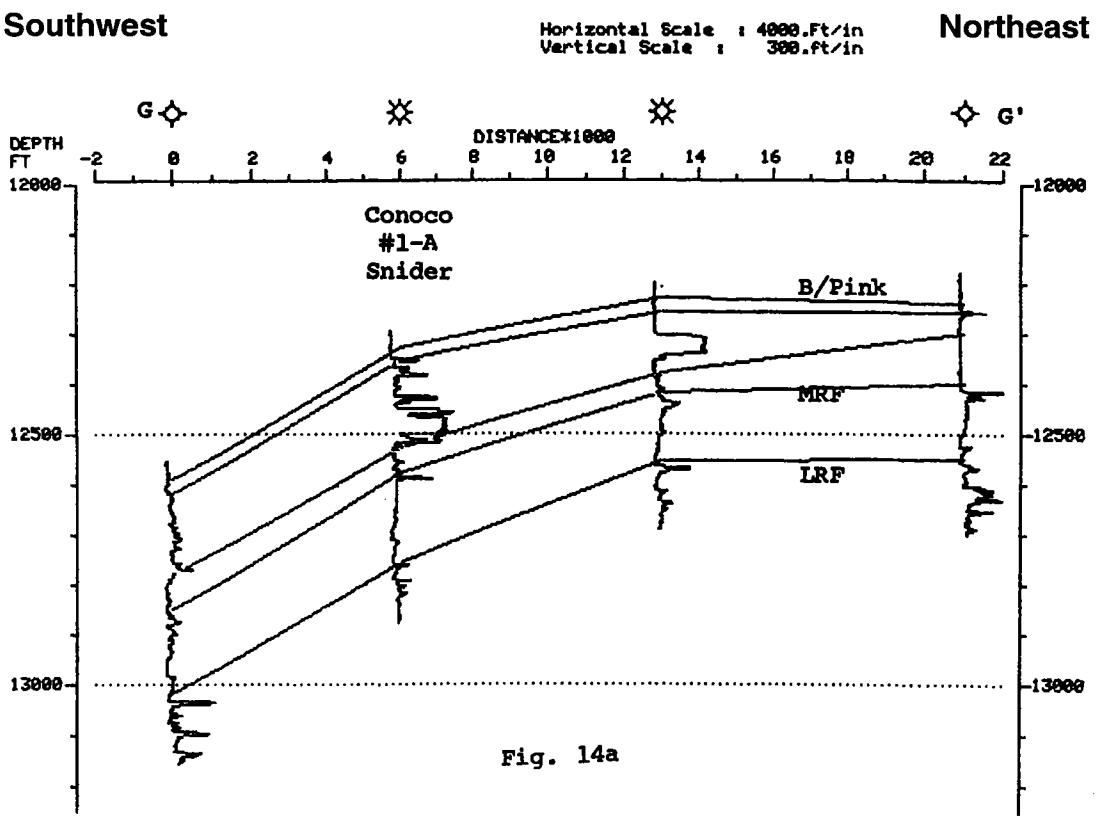

Figure 40. Simplified southwest–northeast geologic cross section G–G′ using resistivity curves hung on sea level through part of East Clinton Field. Wells are those in Figure 39. Depth in feet and distance in feet × 1,000. *Abbreviations:* B/Pink = base of Pink Limestone; T/RF = top of Red Fork; MRF = middle Red Fork; LRF = lower Red Fork.

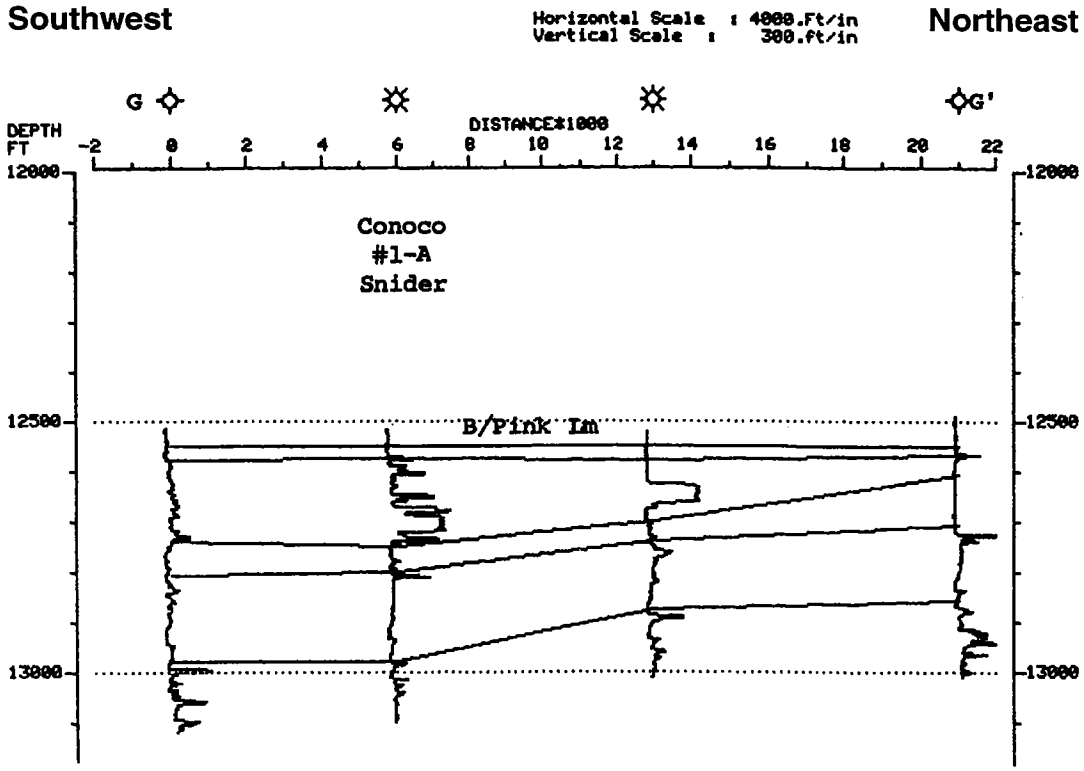

Figure 41. Simplified southwest–northeast geologic cross section G–G′ using resistivity curves flattened on base of Pink Limestone at 12,550 ft through part of East Clinton Field. Well curves hung on top of Red Fork. Note upper Red Fork sand-filled channel in middle two wells. Wells are those in Figure 39. Depth in feet and distance in feet × 1,000. *Abbreviations:* B/Pink Lm = base of Pink Limestone; T/RF = top of Red Fork; MRF = middle Red Fork; LRF = lower Red Fork.

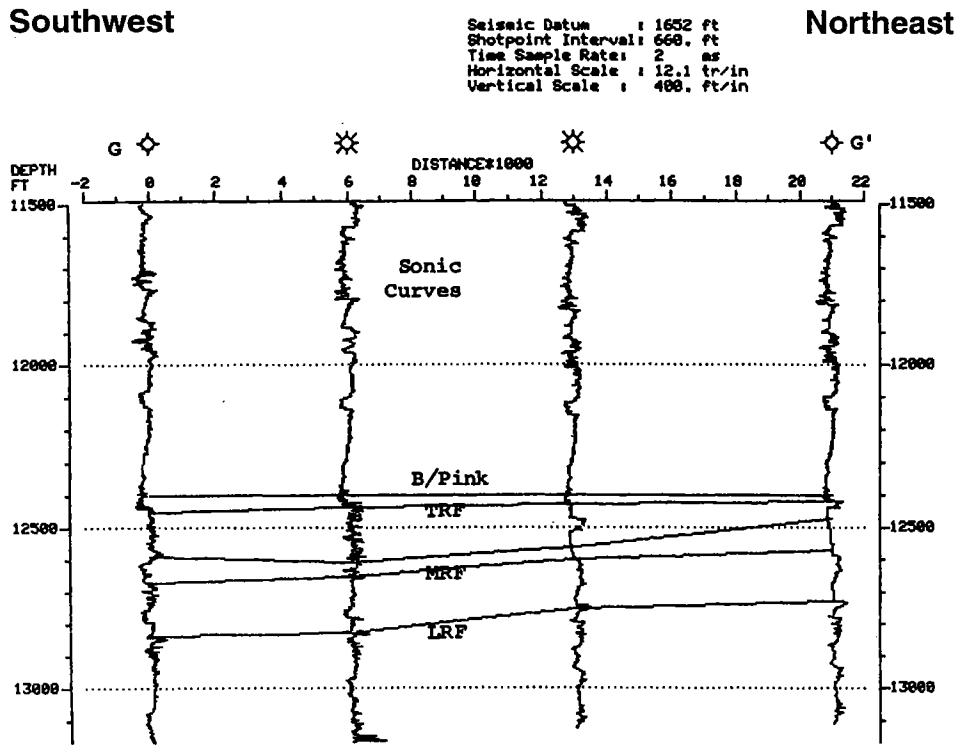

Figure 42. Cross section from southwest to northeast, showing data and interpolation for sonic curves for all four wells shown in cross-section G–G′ (Fig. 39) for part of East Clinton Field. All curves flattened on base of Pink Limestone at 12,400 ft and hung on top of Red Fork. Depth in feet and distance in feet × 1,000. *Abbreviations:* B/Pink = base of Pink Limestone; TRF = top of Red Fork; MRF = middle Red Fork; LRf = lower Red Fork.

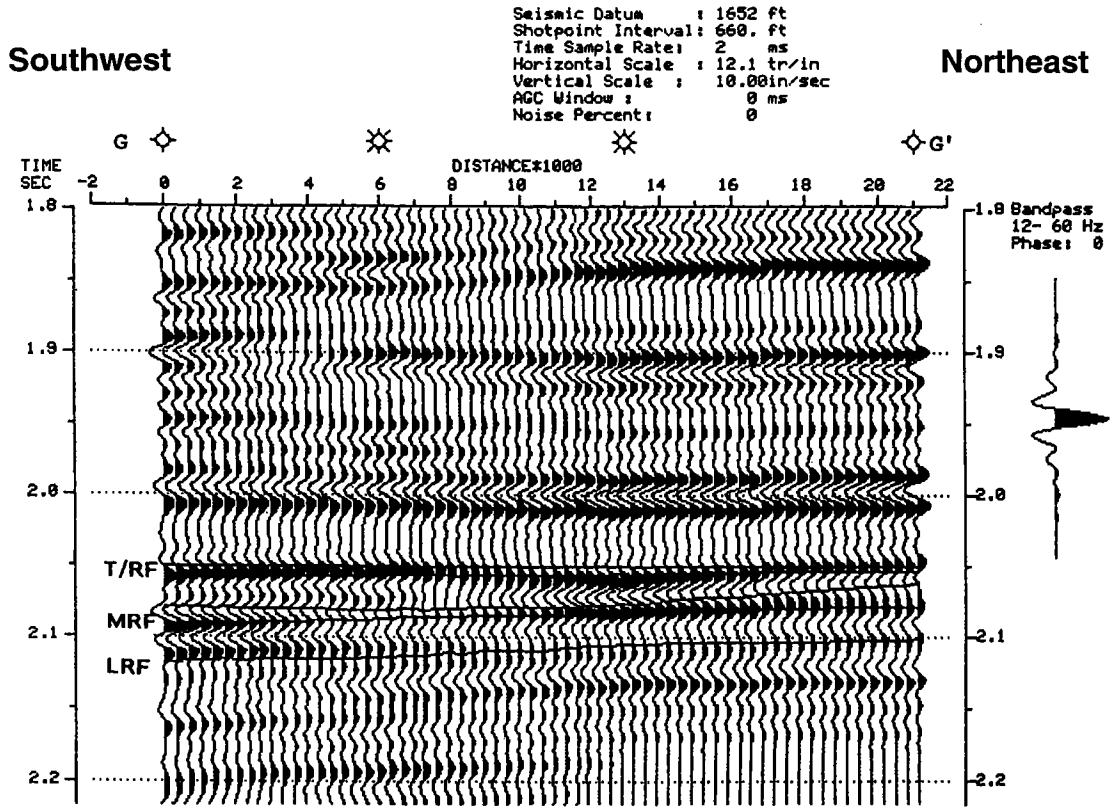

Figure 43. Two-dimensional (2-D) southwest–northeast cross section generated by computer from sonic-well log curves between the four control logs shown in Figure 39 and used for cross section G–G′. Logs flattened on base of Pink Limestone at 2,050 ms, and traces are interpolated between wells. Depth in seconds and distance in feet × 1,000. *Abbreviations:* B/Pink = base of Pink Limestone; T/RF = top of Red Fork; MRF = middle Red Fork; LRF = lower Red Fork.

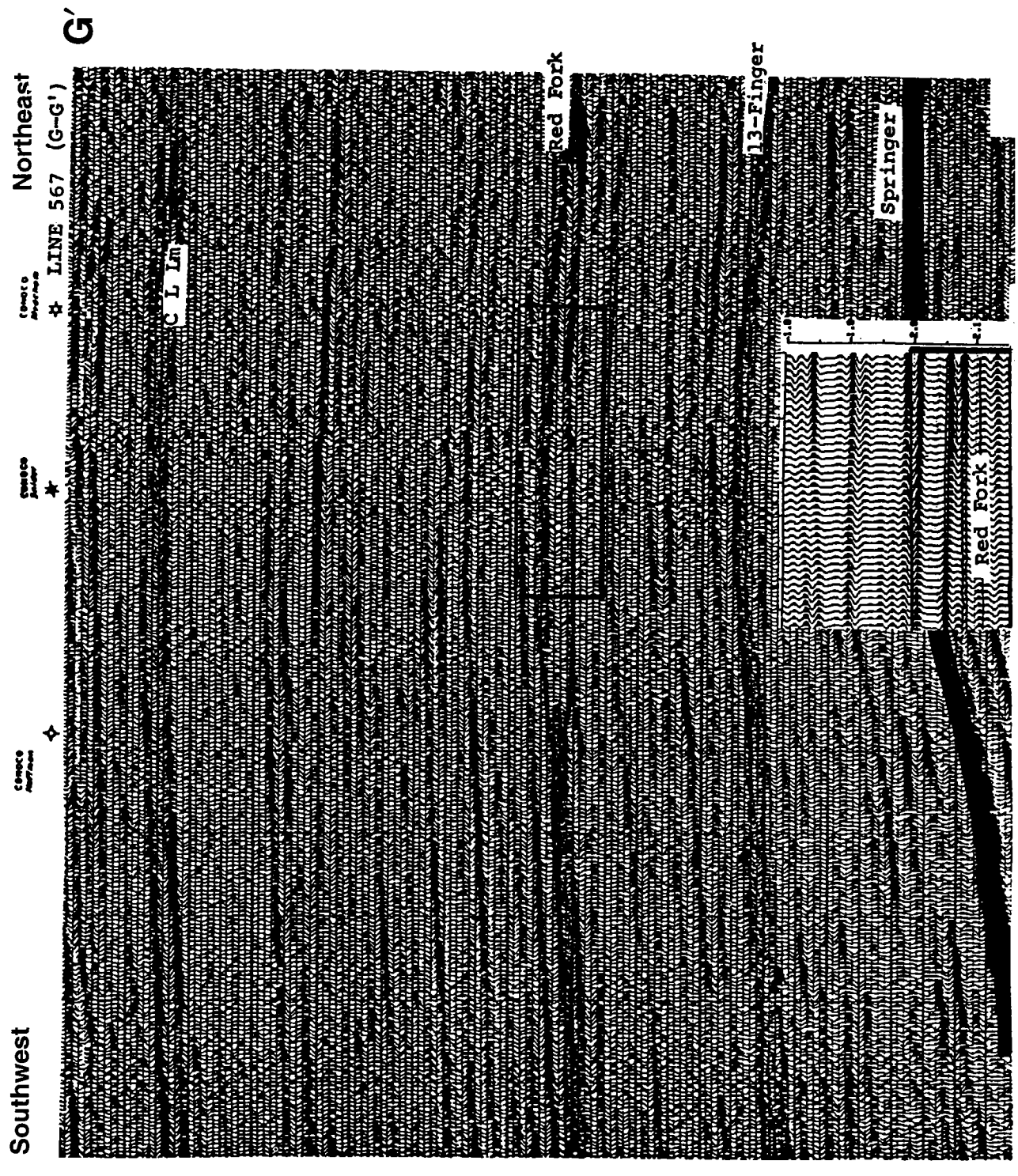

Figure 44. Actual seismic data from part (G–G') of Conoco seismic line 567 shot across the five wells shown on Figure 39; locations of those wells shown at top of figure. Inset is 2-D computer model generated from sonic-log data (Fig. 43).

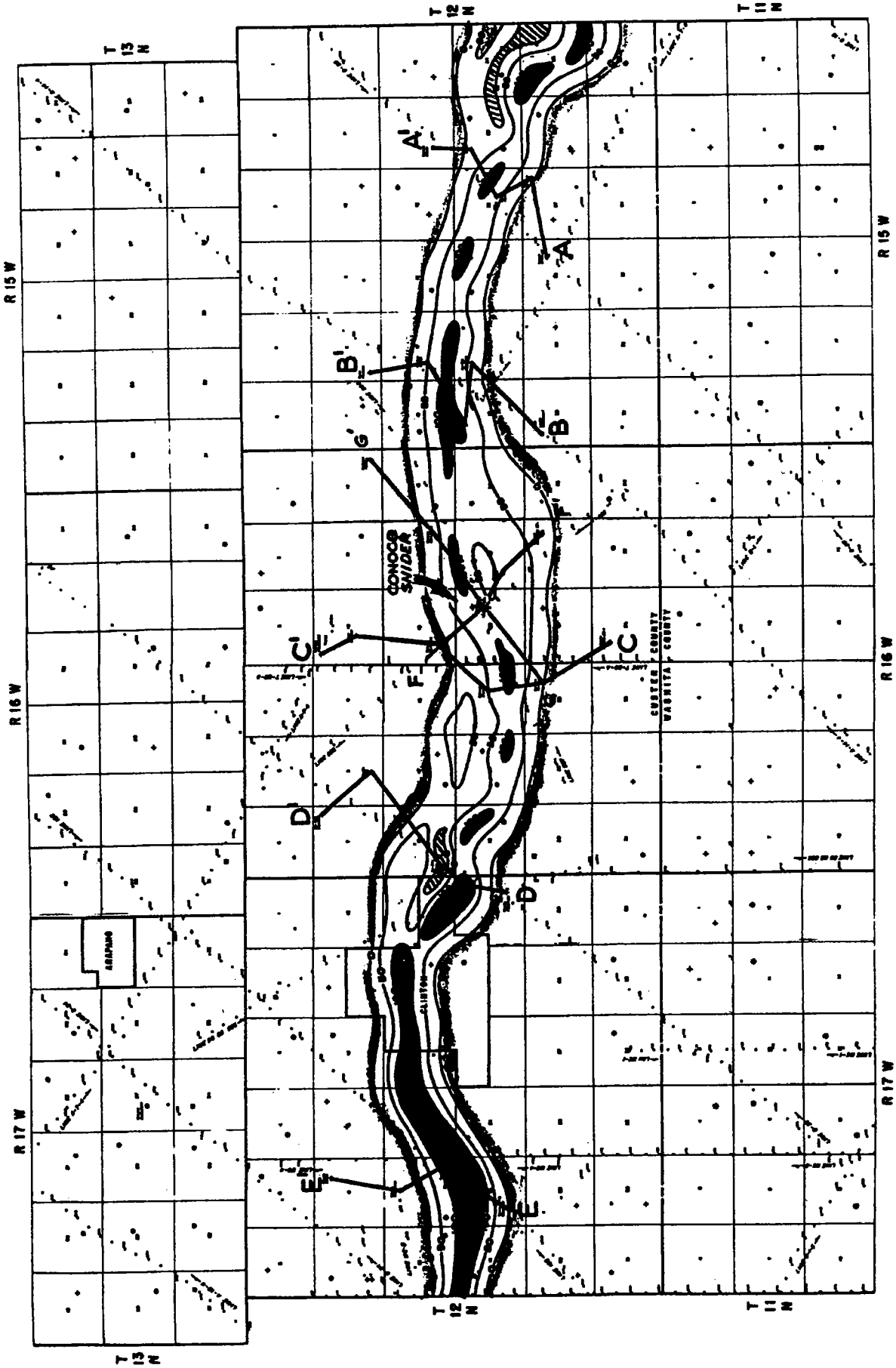

Figure 45. Map of part of East Clinton Field showing orientation of east–west oriented Red Fork channel. Isopach map of thickness of Red Fork channel given in feet (50-ft contour interval); with areas within channel margins of no Red Fork Sand shown as cross-hatched area, and areas of 100 ft or greater thickness of sand shown as blackened area. Cross sections A–A′ (Figs. 9–13), B–B′ (Figs. 14–18), C–C′ (Figs. 19–23), D–D′ (Figs. 24–28), E–E′ (Figs. 29–33), F–F′ (Figs. 34–38) and G–G′ (Figs. 39–44) shown on map.

Gas in an Incised Valley, Upper Cherokee, Southeastern Kansas

William T. Stoeckinger
Geological Consultant
Bartlesville, Oklahoma

ABSTRACT.—Buried gassy coals in southeastern Kansas, at depths of 600–800 ft, continue to expel methane gas into fluvial sands occupying an incised valley (channel) carved completely through the Cabaniss Formation of Desmoinesian age. In the early 1900s, cable-tool operators discovered shallow gas in thick sandstones called the Squirrel/Cattleman. It is now known that these sands were deposited in a north–south-trending channel extending the entire breath of Kansas. Channel splaying is evident in Montgomery County, Kansas, and south of the Kansas-Oklahoma border.

Pressure drawdown during gas production in the 1900s forced juxtaposed coals to desorb their gas, which migrated into the channel, thus explaining the observation that some sands seemed to rejuvenate themselves. It is not a coincidence that this steep-sided, flat-bottomed, incised and refilled valley bisects the most productive portion of the 1920s shale-gas industry, which sought gas from the overlying Mulky-Excello coals/shales. Anticlinal doming as well as fracture-enhanced permeability in rocks overlying thick sands in the channel are the expected result of differential compaction of sands versus coal/shales. New gas opportunities include the coals themselves and domed rocks overlying sand in the channel.

INTRODUCTION

Southeastern Kansas has a long history of oil and gas production. Shallow wells drilled into sands of the Cherokee Group (Desmoinesian Stage, Middle Pennsylvanian Series) delivered copious amounts of both oil and gas at the turn of the century. It is now realized that much of the gas is associated with sands deposited in one long, meandering, incised, and refilled valley. See Figure 1 for approximate location.

The Krebs Formation (Fig. 2) is dominated by both marine and deltaic sands. Correlating individual sands is difficult, and all but impossible on a regional basis. On the contrary, the cyclic nature of the black radioactive shales and coals of the overlying Cabaniss Formation lend themselves to regionally reliable correlations. Thick sands found in the Cabaniss Formation are locally called the Cattleman and Squirrel, and are found at the drilled depth of about 750 ft. For the first time, both of these thick sands are proven to be part of a narrow, north–south-trending, incised valley. The main channel is generally less than 2 mi wide, about 130 ft deep, flat-bottomed, and at least 90 mi long. Based on the techniques presented herein, future work will extend the channel into northeastern Kansas and south of the border into Oklahoma where extensive splaying occurs.

The channel's presence is easily recognized on the geophysical logs by the notable absence of several depositional packages or cyclothems that are replaced by either sand or shale. Once recognized, stratigraphic traps should be sought within the channel on eastward-facing meander loops, which are composed of porous, point-bar sand.

The greater compaction with burial of both cyclic shales and coals relative to sand causes structural doming to occur in rock units overlying thick sand within the channel. This draping or doming creates both early anticlinal closure as well as fracture permeability in younger rock units such as the Mulky-Excello and Summit coals and the Fort Scott Limestones.

CHANNEL STRATIGRAPHY

Past workers in eastern Kansas recognized the vast number of sand-filled channels in the Krebs Formation of the lower Cherokee Group (see Walton, 1996; Staton, 1987). Denesen (1985) correctly identified fluvial channel sands in the upper part of the Cabaniss Formation in northeastern Oklahoma. Brenner (1989) also referred to fluvial sands in the upper part of the Cabaniss Formation, even though only a few of the 1,293 wells he studied actually cut this incised valley. It was not until 1990, while mapping coals of the Cabaniss Formation, that the author recognized the existence and scope of this new channel.

The channel is present where the coals abruptly disappear (Fig. 2). The absence of Cabaniss-aged

Stoeckinger, W. T., 2002, Gas in an incised valley, upper Cherokee, southeastern Kansas, *in* Boyd, D. T. (ed.), Finding and producing Cherokee reservoirs in the southern Midcontinent, 2002 symposium: Oklahoma Geological Survey Circular 108, p. 111–118.

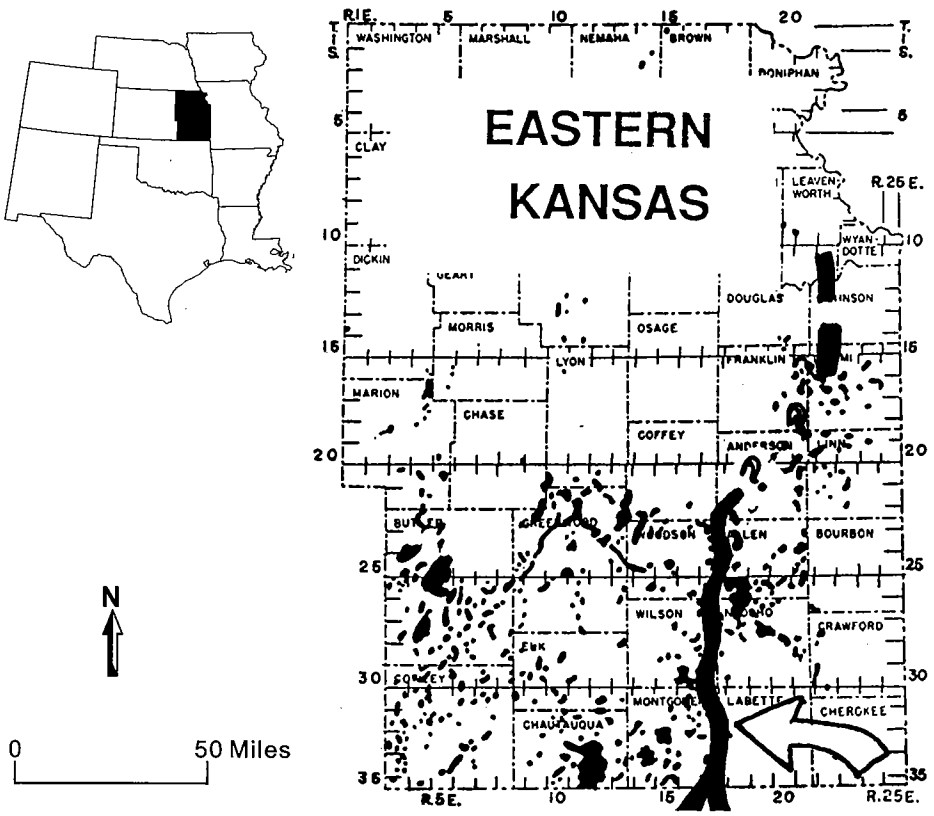

Figure 1. Map of eastern Kansas showing oil producing areas and location of the newly recognized channel in the Cabaniss Formation. Channel width exaggerated.

coals and the presence of the channel can only be recognized using geophysical logs. However, once the channel's limits are established in both a vertical and horizontal sense, it is possible to organize what fills the channel (shale, sands, limes, etc.) by using the sample description from drillers' logs.

Abundant subsurface data convincingly show that the Cabaniss Formation consists of a half dozen cyclothems of varying thickness occurring over a gross interval of about 130 ft. Individual cycles caused by sea-level drop and rise resulting from continental glaciation and deglaciation are remarkably persistent and correlate reliably for miles. In the simplest terms, from bottom to top, each cycle begins with a marine transgression that caused the deposition of thin, black, fissile, highly radioactive shale in oxygen-poor seas. Subsequently, as the seas retreated, dark-gray shales were deposited followed by silts and limes, and the sequence was covered by vast coastal swamps in which coals developed. Put another way, each cycle is capped by a coal that is immediately overlain by a thin, marine, radioactive shale, which represents the beginning of the next cycle. This coal–radioactive-shale combination provides exceptional markers of regional extent. The only reason that a group of these markers could be missing locally is for a later event, such as an erosional valley, to downcut and erode these soft, black, poorly consolidated muds, silts, and thick peats.

CHANNEL EXTENT

The first successful effort to pinpoint and define this undocumented channel occurred in the Altoona Gas Field area of Wilson County, Kansas (T. 29 S., R. 16 E.) (Fig. 3). From there, work was extended northward into Woodson County and southward into Montgomery County. Based on a cursory review of logs in northeastern Kansas, this same channel will most certainly be identified there, where it is the reservoir for shallow, very gassy oil pools. At the Kansas-Oklahoma border this narrow Cabaniss channel widens, begins to splay, and abruptly turns to the southwest toward the town of Wann, Oklahoma.

As mapping of this Cabaniss channel proceeded, it became apparent that major gas accumulations such as (1) the Vilas Gas Field in T. 27 S., R. 17 E., (2) the Cherryvale Gas accumulation in T. 31 S., R. 17 E., and (3) the Liberty Gas Field (now converted to storage) in T. 33 S., R. 17 E., were all nestled in the channel where it meanders slightly to the east (Fig. 3). The combination of regional westward dip away from the Ozark Mountains and subtle, eastward-pointing meander loops created perfect updip stratigraphic traps in point bars.

Figure 4 shows detail in the Altoona area of Wilson County, Kansas. Once the limits of the main channel are determined using geophysical logs, the vast num-

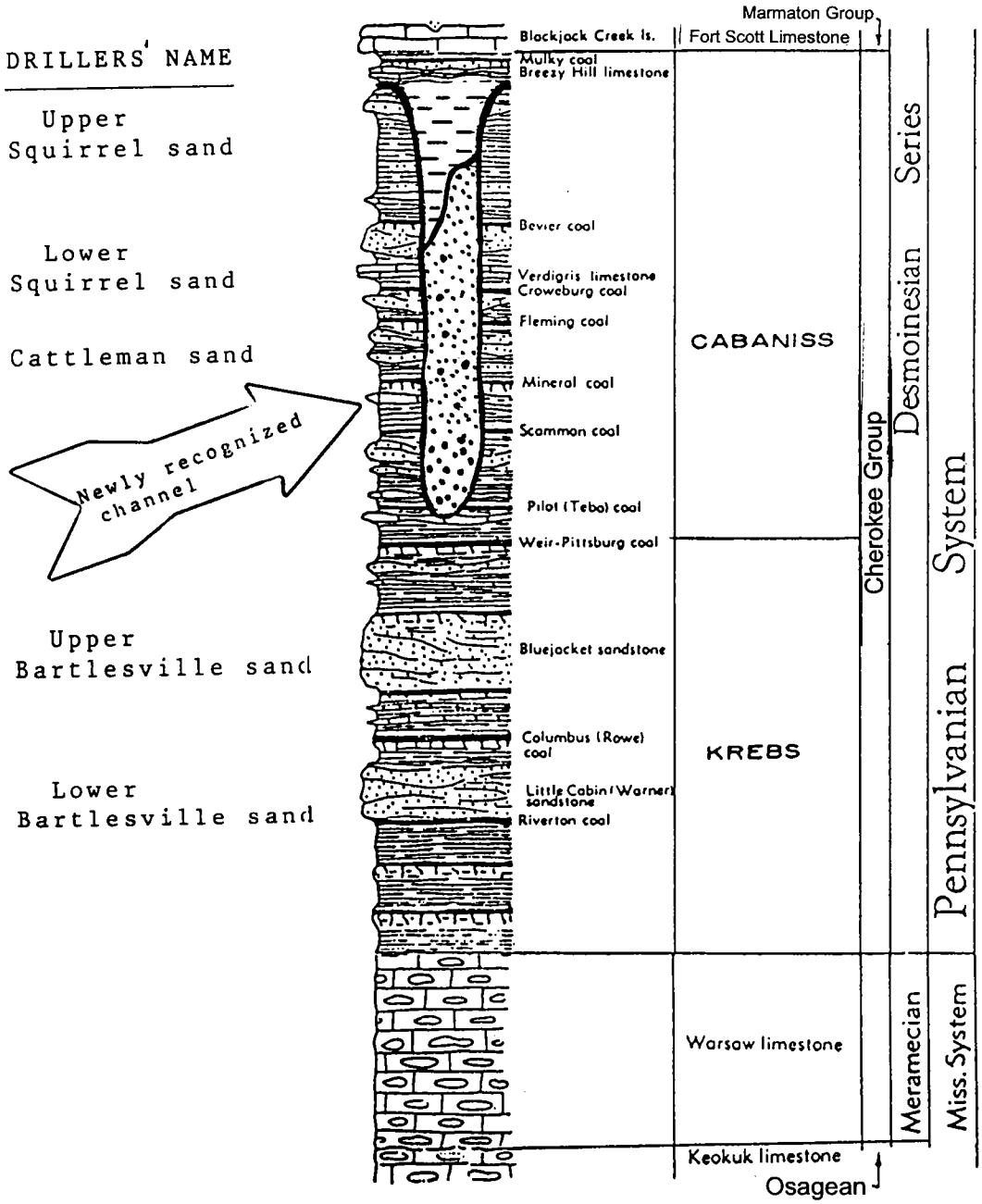

Figure 2. Generalized section of outcropping Cherokee and Mississippi rocks in eastern Kansas, showing the newly recognized channel in the Cabaniss Formation.

ber of drillers' logs becomes invaluable in identifying the best and thickest sand in the channel itself. This map shows thicker sand is restricted to narrow tongues and meander loops. Where sand is absent, the channel is still flat-bottomed, >100 ft deep, but clay filled. Wagner (1961), in his mapping of the Altoona Quadrangle, was aware of the unique nature of the sand buildup in the Cabaniss Formation (Fig. 5). He did not pursue its nature or extent, however.

THE CHANNEL AS SEEN ON GEOPHYSICAL LOGS

The Gamma Ray-Density Neutron logs from wells 1 mi apart are shown on Figure 6. The log on the right captures the cyclic sequences, cyclothems, in the Cabaniss Formation above a regional marker bed. The log at the left depicts the absence of these cycles and the presence of a thick, upward-fining sand. Based on the

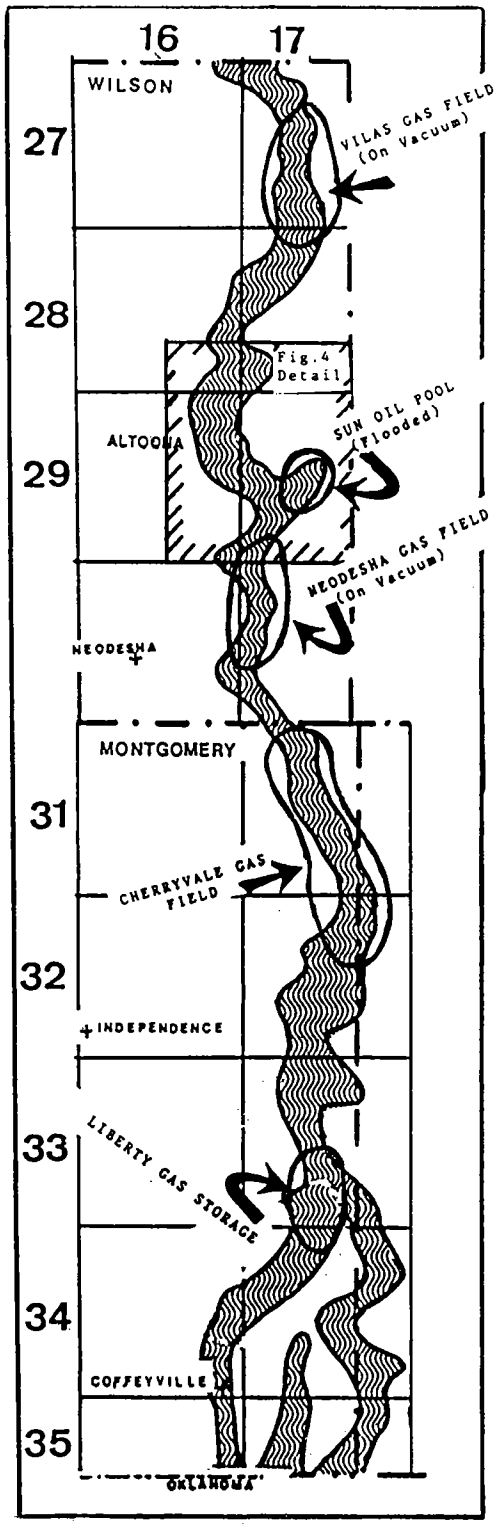

Figure 3. Trace of the channel cut into the Cabaniss Formation showing associated oil and gas fields.

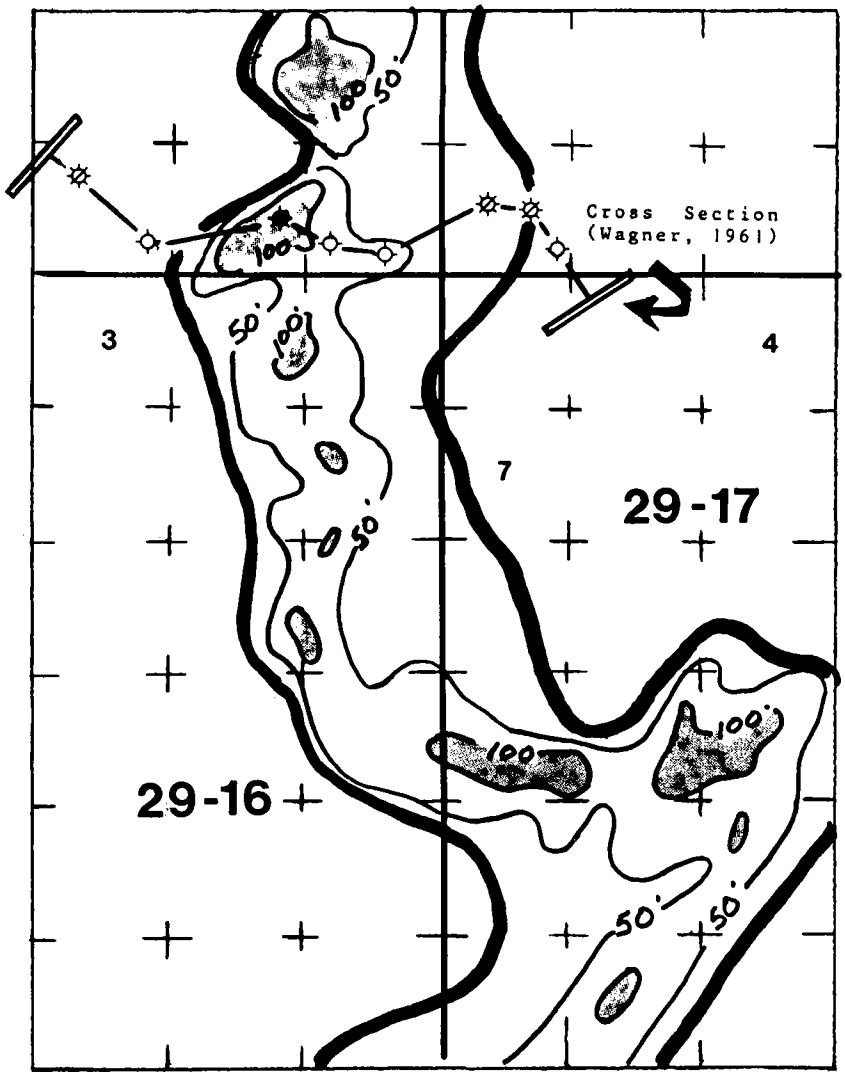

Figure 4. Detail of Cabaniss channel showing net sand thickness in the Altoona area. Contour interval = 50 ft. Areas where sand thickness exceeds 100 ft are shaded. Location of cross section by Wagner (1961) shown across northern end of map (see Fig. 5). See Figure 3 for location.

density-neutron crossover effect, the sand is clearly gas bearing, and part of the severely depleted Neodesha Gas Field (Fig. 3). Prodigious, but unknown amounts of gas were sold from the Neodesha Field in the early 1900s. Gas is still commercially produced, free of water, using compression.

Local, third-generation operators, claimed formation pressures in some of these old gas pools have actually increased over the years. Such claims were discounted until coalbed-methane production flashed into vogue in the mid-1980s. As these channel gas sands produced and became depleted, the drop in pressures caused juxtaposed coals to desorb their gas, which migrated into and recharged the channel sand with coalbed methane. Some support for this argument came when a well in sec. 14, T. 32 S., R. 16 E., encountered a thick (4 ft) Bevier coal bed. The coal was sampled and desorbed of its gas in a sealed canister. It proved to have very little gas, and was both under-pressured and depleted. The well is about 3 mi west and downdip from the Cabaniss channel sand that was reportedly being repressurized. Was sand in the channel rejuvenated by gas migrating out of the Bevier coal?

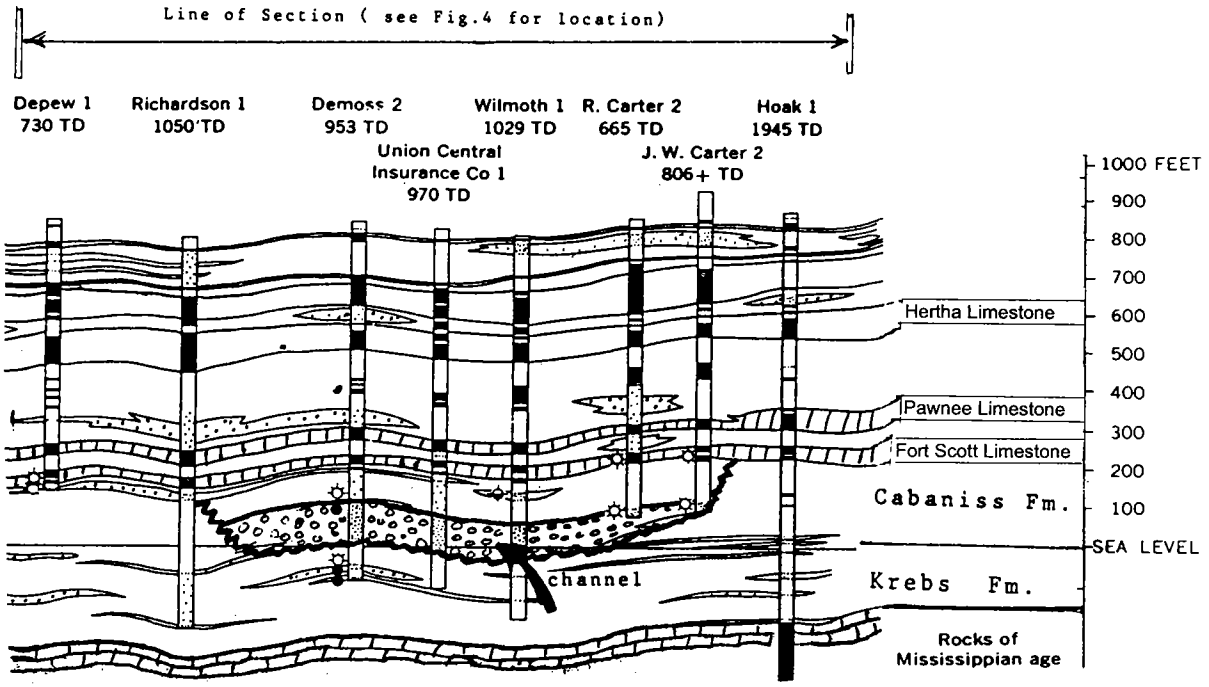

Figure 5. Cross section of Cabaniss channel system in the Altoona area. Modified after Wagner (1961). See Figure 4 for location.

Figure 7 shows another example using cased-hole gamma-ray–neutron logs. The well on the right is from the Liberty Gas Storage Field. Its upward-fining sand is typical of the channel sands that replace the cyclic sequences depicted on the left.

In both Figures 6 and 7, sand (probably fluvial) replaces thin cyclic coals and shale. As these sediments were buried by several thousand feet of younger Pennsylvanian material, the cyclic coals and shales compacted more than the sands within the channel. The result is doming of the overlying Mulky-Excello coal/shale, and the Fort Scott Limestone.

Identifying the precise top of this refilled incised valley, or in effect its geological age, is difficult because of log quality and number. At this time, the top of the channel appears to be within a few feet of the stratigraphic level of the Breezy Hill Limestone, perhaps slightly earlier. Certainly the channel was cut and refilled before the Breezy Hill was deposited, because this limestone is present throughout the area.

STRUCTURE IN THE VICINITY OF THE CHANNEL

Most subsurface workers in eastern Kansas select the top of the Fort Scott Limestone (Oswego lime of Oklahoma) as the primary mapping horizon. This is because these limes are easily recognized and identified by most drillers.

It has become axiomatic that gas accumulations in southeastern Kansas are restricted to anticlinal features. East dip seems essential. However, as mentioned above, where thick sands in the Cabaniss channel come into play, the Fort Scott Limestone may drape anticlinally. Drilling wells on the crest of drape features will find gas in the Squirrel/Cattleman sands only where the doming due to drape is associated with sand deposited as a point bar on an eastward-facing meander. Because a stratigraphic trap is formed there, structure is only coincidental. Where the Fort Scott Limestone domes over a point bar at a westward-facing meander, the chances of finding Squirrel/Cattleman gas sands are poor.

Mississippi gas potential below domes that have been produced by drape does not exist. However, any doming of the Fort Scott Limestone where the Cabaniss channel is absent should be productive at multiple levels.

Another favorable aspect of doming of the Mulky coal/shale over thick channel sands was touched upon by Charles and Page (1929). They wrote that it was because conventional gas produced from sand was gone that the shale-gas industry was born. This production consisted of non-conventional gas from the Mulky-Excello coal/shale interval at the base of the Fort Scott Limestone. As reported by Charles and Page (1929), the better shale-gas wells were on anticlinal highs where the shale was coalier. If anticlinal doming is important, then it should not come as a surprise that the best shale-gas area of the 1920s was on top of the thick sands in this north–south-trending Cabaniss channel (Fig. 8). Operators quit drilling for the Mulky-Excello coal/shale in about 1924 because of the Great Depression, not because the gas played out. Today, because of

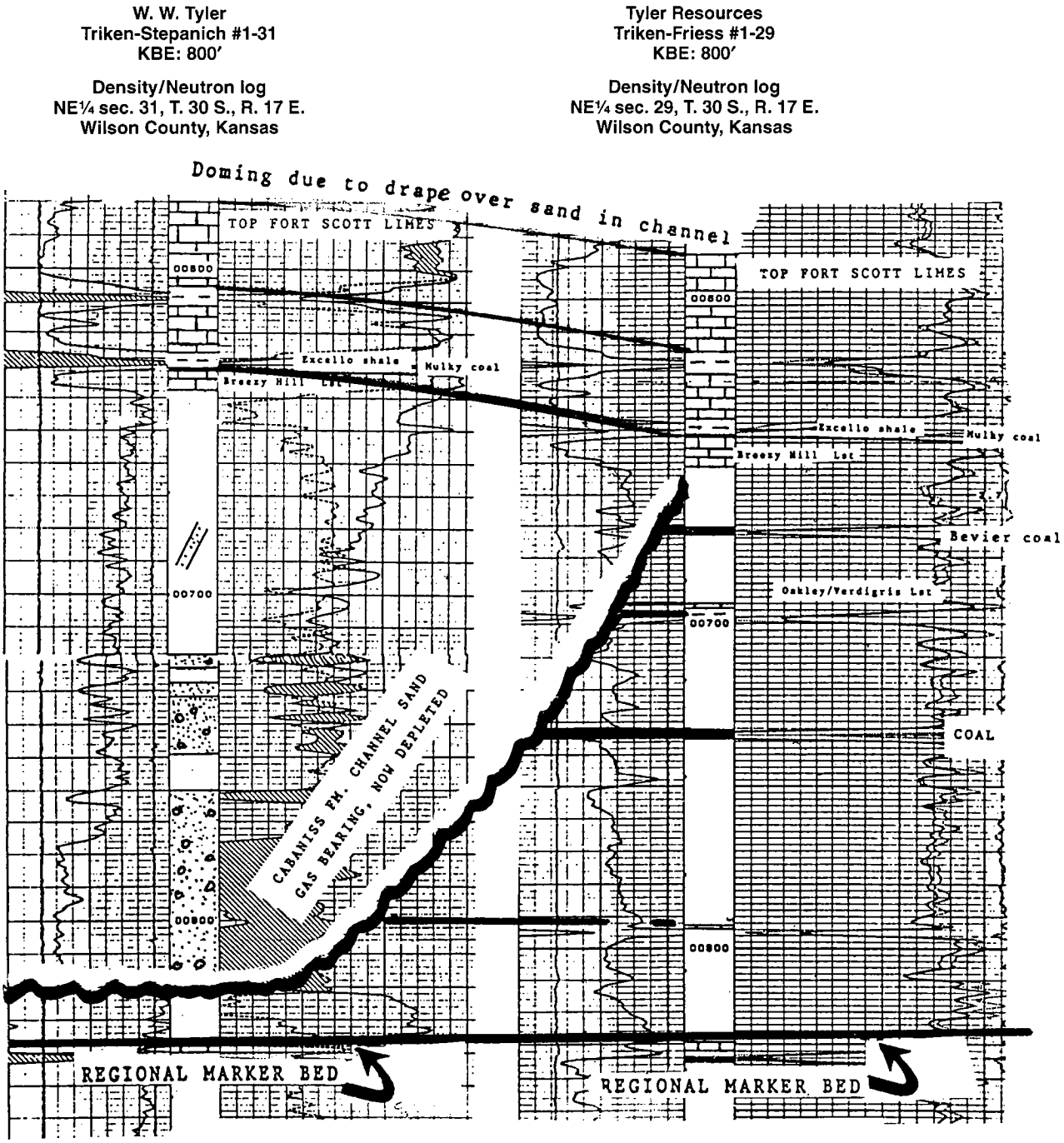

Figure 6. Stratigraphic cross section using density-neutron logs from the Neodesha area. Normal cyclic sequences are seen on the right and the typical channel sand on the left. Compactional doming of rock units over thick sand in the channel is common.

better gas prices, the shale-gas industry of the 1920s has been reborn, only now it is called coalbed-methane production.

CONCLUSIONS

A narrow, long, north–south-trending incised and refilled valley slices through most of the Cabaniss Formation in eastern Montgomery, Wilson, and Woodson Counties of southeastern Kansas. The channel extends into northeastern Kansas and southward into Oklahoma, where it begins to splay and turn in a southwesterly direction. The channel is generally less than 2 mi wide, about 130 ft deep, and flat-bottomed. Sand dominates in the channel where point bars fill meander loops. Elsewhere, the channel can be 100% clay filled.

Westward dip off the Ozark Mountains, combined

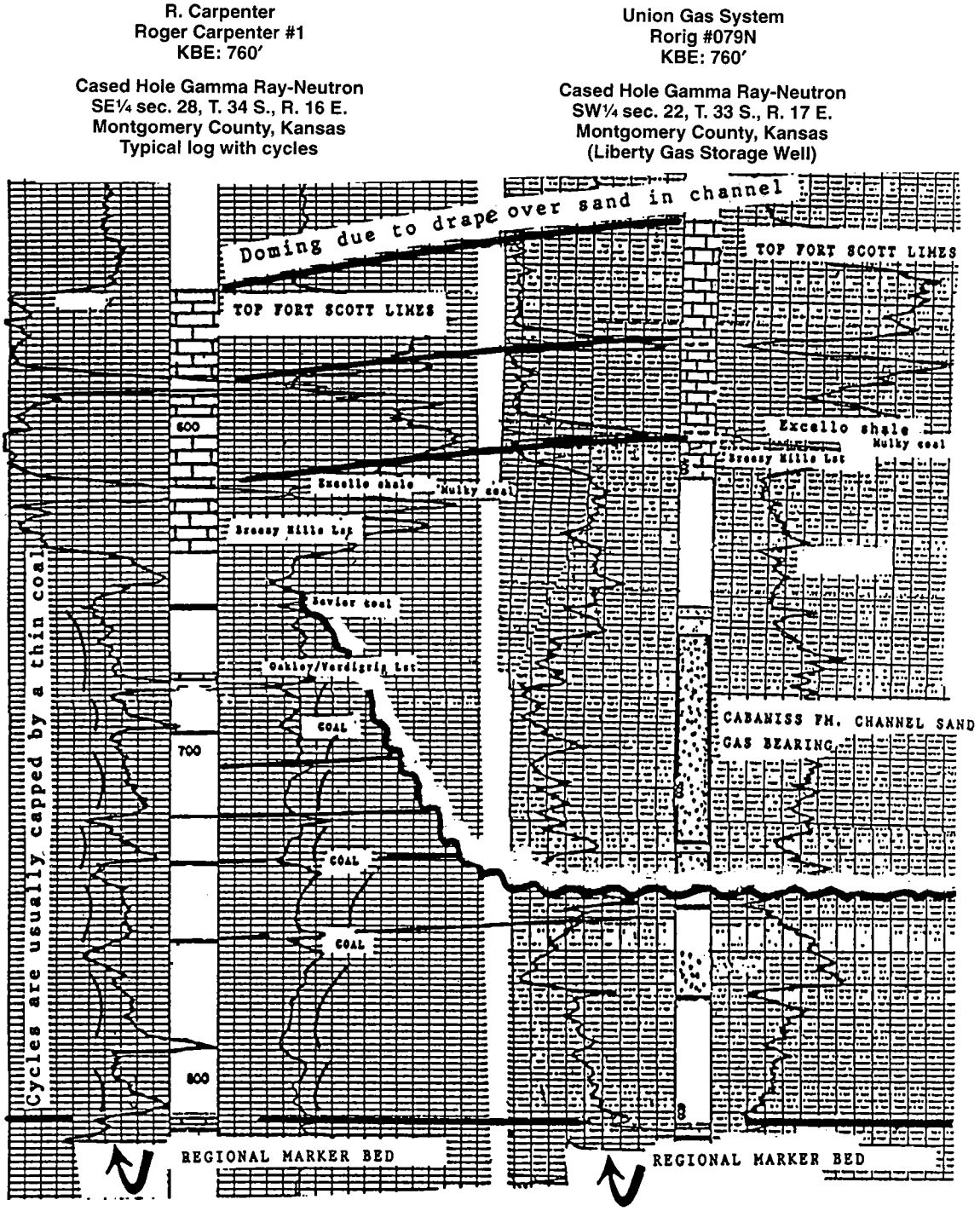

Figure 7. Stratigraphic cross section using cased-hole gamma-ray–neutron logs from the Liberty Gas Storage Area. Normal cyclic sequences are seen on the left versus channel sand on the right. Compactional doming over thick sand in the channel is common.

with east-facing meander-loop point bars, provides the perfect stratigraphic trap. Timing of the last migration of gas appears to be after the uplift of the Ozark Mountains, which the writer believes is a relatively recent (late Tertiary) event. Compactional doming of younger rocks over thicker sands within the channel should create a fairway for the better shale-gas (Mulky coal/shale) wells by providing both doming and fracture permeability.

The channel is easily recognized on geophysical logs where at least a half dozen, regionally extensive, cyclothems are absent, and replaced by shale or fluvial sand. The top of the channel, which determines its geological age, is just below the Breezy Hill Limestone Member

of the upper part of the Cherokee Group. Channel recognition will facilitate the reinterpretation and reconstruction of the paleogeographic maps of the Cabaniss Formation.

Significant, new conventional gas discoveries in this mature area are unlikely. For the most part, however, the coalbed-methane potential remains intact.

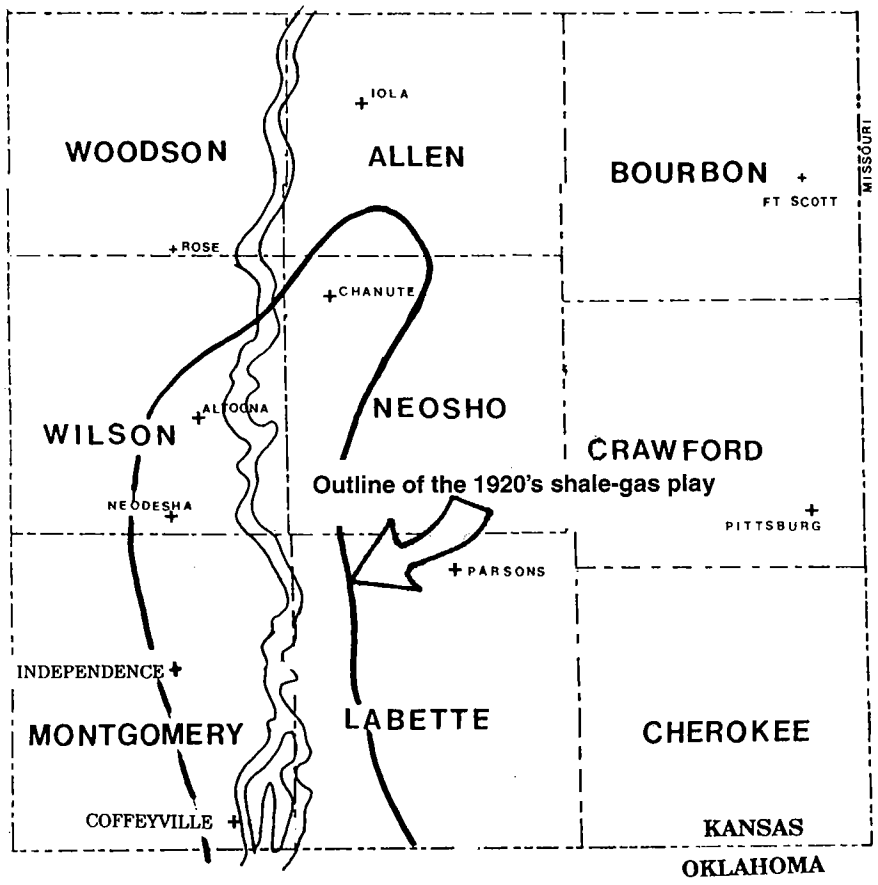

Figure 8. Map of southeastern Kansas showing the outline of the shale-gas industry of the 1920s and the location of the channel cut into the Cabaniss Formation.

REFERENCES CITED

Abernathy, G. E., 1940, Oil and gas in Montgomery County, Kansas: Kansas Geological Survey Bulletin 31, p. 1–29.

Brenner, R. L., 1989, Stratigraphy, petrology and paleogeography of the upper portion of the Cherokee Group (Middle Pennsylvanian), eastern Kansas and northeastern Oklahoma: Kansas Geological Survey Geology Series 3, 69 p.

Charles, H. H.; and Page, J. H., 1929, Shale-gas industry in eastern Kansas: American Association Petroleum Geologists Bulletin, v. 13, p. 367–381.

Denesen, S. L., 1985, Stratigraphy, petrography and depositional environment of the Banzet formation (Middle Pennsylvanian) in southeastern Kansas and northern Oklahoma: University of Iowa unpublished M.S. thesis, 141 p.

Heckel, P. H., 1977, Origin of the phosphatic black shale facies in the Pennsylvanian cyclothems of Mid-continent North America: American Association Petroleum Geologists Bulletin, v. 61, p. 1045–1068.

Jewett, J. M., with 25-year update by Oros, Margaret, 1979, Oil and gas in eastern Kansas: Kansas Geological Survey Bulletin 104, 397 p.

Moore, R. C.; and Boughton, C. W., 1921, Oil and gas resources of Kansas; Wilson and Montgomery Counties: Kansas Geological Survey Bulletin 6, part 6, 32 p.

Rascoe, Bailey, Jr.; and Adler, F. J., 1983, Permo–Carboniferous hydrocarbon accumulations, Mid-continent, USA: American Association Petroleum Geologists Bulletin, v. 67, p. 979–1001.

Staton, M. D., 1987, Stratigraphy and depositional environments of the Cherokee Group (Middle Pennsylvanian), central Cherokee basin, southeastern Kansas: University of Kansas unpublished M.S. thesis, 102 p.

Stoeckinger, W. T., 1997, A newly recognized upper Cherokee channel sand complex meanders through southeastern Kansas, *in* McMahan, Greg (ed.), Transactions of the 1997 American Association Petroleum Geologists Mid-continent Section meeting, Sept. 14–16, Oklahoma City: Oklahoma City Geological Society, Oklahoma City, p. 198–206.

Swanson, D. C., 1993, The importance of fluvial processes and related reservoir deposits: Journal of Petroleum Technology, April, p. 368–377.

Visher, G. S.; Saitta, B. S.; and Phares, R. S., 1971, Pennsylvanian delta patterns and petroleum occurrences in eastern Oklahoma: American Association Petroleum Geologists Bulletin, v. 55, p. 1206–1230.

Wagner, H. C., 1961, Geologic map Altoona Quadrangle, Kansas: U.S. Geological Survey, Map GQ-149, scale 1:62,500.

_____ 1962, A summary of the geology of Wilson County, Kansas: Kansas Geological Society 27th Field Conference Guidebook, p. 138–148.

Walton, A. W., 1996, Sequences in the Cherokee Group (Desmoinesian Middle Pennsylvanian) of southeastern Kansas, *in* Swindler, D. L.; and others (eds.), Transactions of the 1995 American Association Petroleum Geologists Mid-continent Section meeting, Oct. 8–10, Tulsa, Oklahoma: Tulsa Geological Society, Tulsa, Oklahoma, p. 336–348.

Ye, H.; and others, 1996, Late Paleozoic deformation of the interior North America: the greater ancestral Rocky Mountains: American Association Petroleum Geologists Bulletin, v. 80, p. 1397–1432.

Zeller, D. E. (ed.), 1969, The stratigraphic succession in Kansas: Kansas Geological Survey Bulletin 189, 81 p.

The Red Fork Sandstone: Overview of Marine and Deep-Marine Reservoirs

Jim Puckette and Zuhair Al-Shaieb
Oklahoma State University
Stillwater, Oklahoma

ABSTRACT.—Red Fork submarine sandstones in the Anadarko Basin are major gas-producing reservoirs. Gas production from over-pressured Red Fork marine sandstones in the Strong City District and SW Leedey Fields exceeds 1 TCF (trillion cubic feet). Sandstones in these two fields have very different geometries, distribution patterns, and production histories.

The Red Fork was deposited during the Middle Pennsylvanian (Desmoinesian) as part of a large southerly flowing sediment-dispersal system. This large fluvial-deltaic complex formed as deltas prograded southward toward the Anadarko and Arkoma Basins. At the same time, Desmoinesian "wash" fan-deltas prograded northward into the Anadarko Basin from the Wichita Mountain Uplift. During sea-level lowstands, Red Fork sediments were transported beyond the Anadarko shelf margin and deposited on the basin floor. Consequently, an upper Red Fork submarine-fan complex formed on the basin floor that became the Strong City District. Concurrently, sand accumulated on the shelf margin as a shallow-marine bar. This deposit became the SW Leedey Field.

Core data, wireline-log signatures, and sandstone-distribution patterns were integrated to reconstruct depositional facies and to characterize reservoirs in these fields. The Strong City District is composed of multiple facies with different productivities. Most cores contain incomplete Bouma turbidite sequences and sedimentary structures typical of fan facies. Large gas reserves are found in channel-fills. Many channels are narrow (2,600 ft wide) but contain thick (>150 ft) sandstones. Productivity decreases as shale content increases. The stacking and coalescing of fans complicates channel-trend delineation, and detailed correlation and mapping are necessary to identify individual reservoirs. Pressure data confirm the highly compartmentalized nature of the Red Fork in this area.

The SW Leedey Field contains Red Fork Sandstone that is similar across the field. It is an interlaminated to interbedded, coarsening-upward interval that is capped by a relatively shale-free sandstone. Sandstone thickness across the field changes gradually and thins toward the margins. Pressure data indicate the reservoir is remarkably well connected and heterogeneity is minimal. Sandstone composition and reservoir evolution are similar for both fields. Porosity is predominantly secondary and resulted from the dissolution of labile grains and matrix.

INTRODUCTION

The Red Fork Sandstone is one of the more active exploration plays in the Anadarko Basin and Midcontinent region. Fields comprising the greater Strong City District contain over 800 wells with a total cumulative production in excess of 900 billion cubic feet (BCF) of gas. The nearby, but separate, SW Leedey Field has produced nearly 200 BCF of gas from approximately 50 wells (International Oil Scouts Association, 2000). These sandstones are different from other Red Fork reservoirs in the region. Sandstones in the Strong City District display a variety of features associated with submarine-fan deposits. They occupy a low paleogeographic position beyond a well-defined shelf edge and represent deposition at the basinal termination of the Red Fork sediment-dispersal system. The SW Leedey Field is located on the shelf edge and produces from a sandstone interval with features associated with shallow-marine shelf deposits.

GEOLOGIC SETTING

The Red Fork was deposited during the Middle Pennsylvanian (Desmoinesian). Most sediment was transported southward via a large fluvial-deltaic distributary system. It formed a complex pattern of linear trends (Fig. 1) delineated by channels that filled with

Puckette, Jim; and Al-Shaieb, Zuhair, 2002, The Red Fork sandstone: overview of marine and deep-marine reservoirs, *in* Boyd, D. T. (ed.), Finding and producing Cherokee reservoirs in the southern Midcontinent, 2002 symposium: Oklahoma Geological Survey Circular 108, p. 119–133.

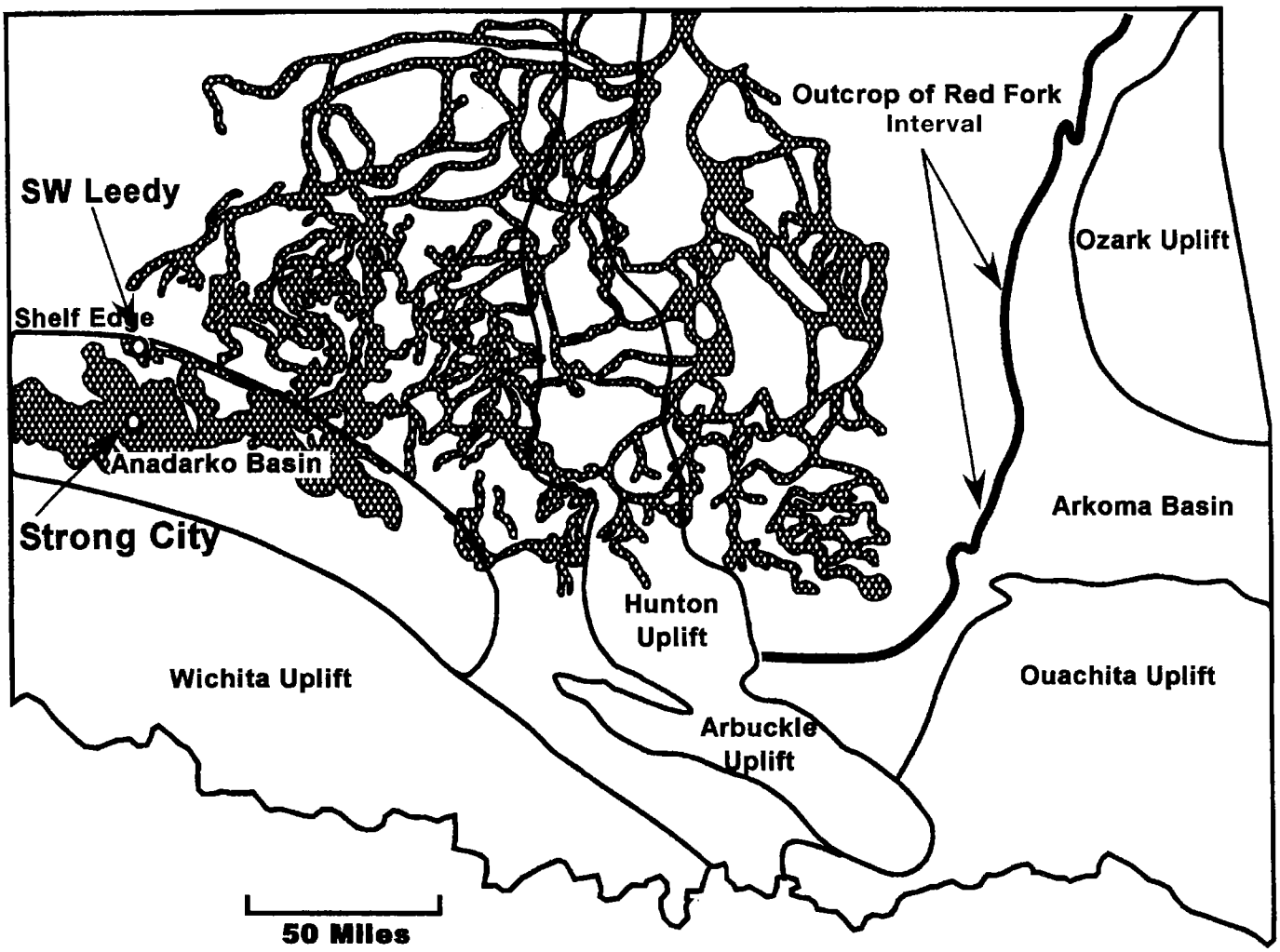

Figure 1. Tectonic provinces of Oklahoma and distribution of Red Fork Sandstone. Red Fork sediments were dispersed by a southerly prograding fluvial-deltaic complex that extended to the shelf edge in the Anadarko Basin. Locations of the SW Leedey Field, Strong City District, and shelf edge are identified; outcrop of Red Fork Interval shown by bold line. After Al-Shaieb and others (1995).

sand. These channels were conduits for sediment transport toward the Arkoma and Anadarko depocenters. In the Anadarko Basin, the Clinton-Weatherford channel was the largest conduit and supplied most sediment for the basin-floor deposit containing reservoirs of the Strong City District (Fig. 2).

PREVIOUS STUDIES

The Red Fork has generated considerable interest in industry and academia. Studies of the Anadarko Basin include Glass (1981), Whiting (1982), Johnson (1984), Udayashankar (1985), Schneider and Clement (1986), and Anderson (1992, 1993). These studies established the stratigraphic framework and interpretations of depositional facies critical to reconstructing the basin architecture. Johnson (1984) recognized the lower Red Fork hinge line and described rock features that suggested deeper-water depositional environments, including submarine-channel–fill and submarine fan. Schneider and Clement (1986) defined the trend and provided evidence that the Clinton–Weatherford channel was incised. Anderson (1992) examined basinal upper Red Fork lithofacies and proposed the submarine-fan–complex model. Anderson (1993) used integrated seismic and conventional mapping to predict the location of higher-quality channel reservoirs within fan lobes.

STRATIGRAPHIC FRAMEWORK

The Red Fork interval includes all strata between the Inola Limestone and Pink Limestone marker beds. Johnson (1984) subdivided this interval into upper Red Fork and lower Red Fork using the "hot" shale marker (Fig. 3). A scarcity of data limited study of the lower Red Fork in the western Anadarko Basin. Anderson (1992) mapped the thickness of the upper Red Fork, establishing the location of the shelf edge and basin depocenter. The shelf-break is marked by an increase

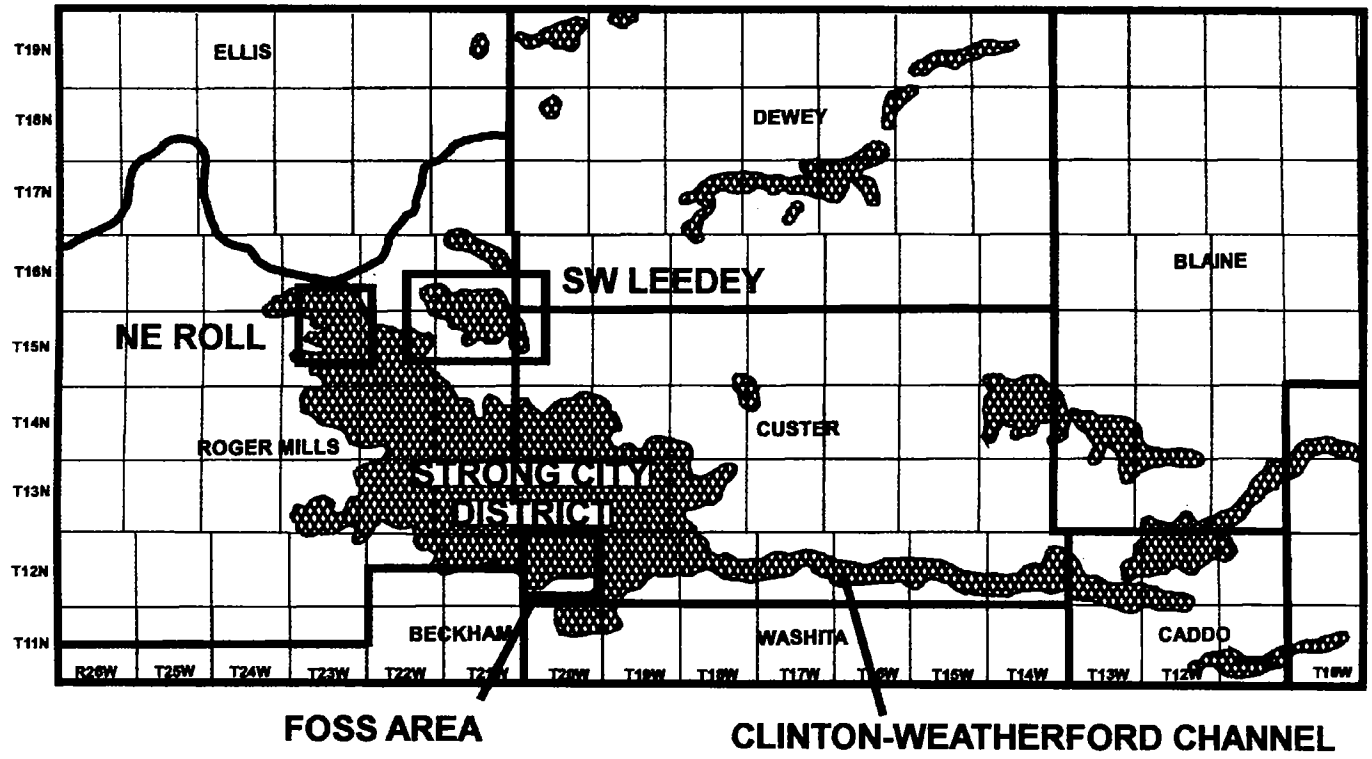

Figure 2. Locations of NE Roll and Foss Areas within the Strong City District, as well as SW Leedey Field, and Clinton–Weatherford Channel. See Figure 1 for generalized location.

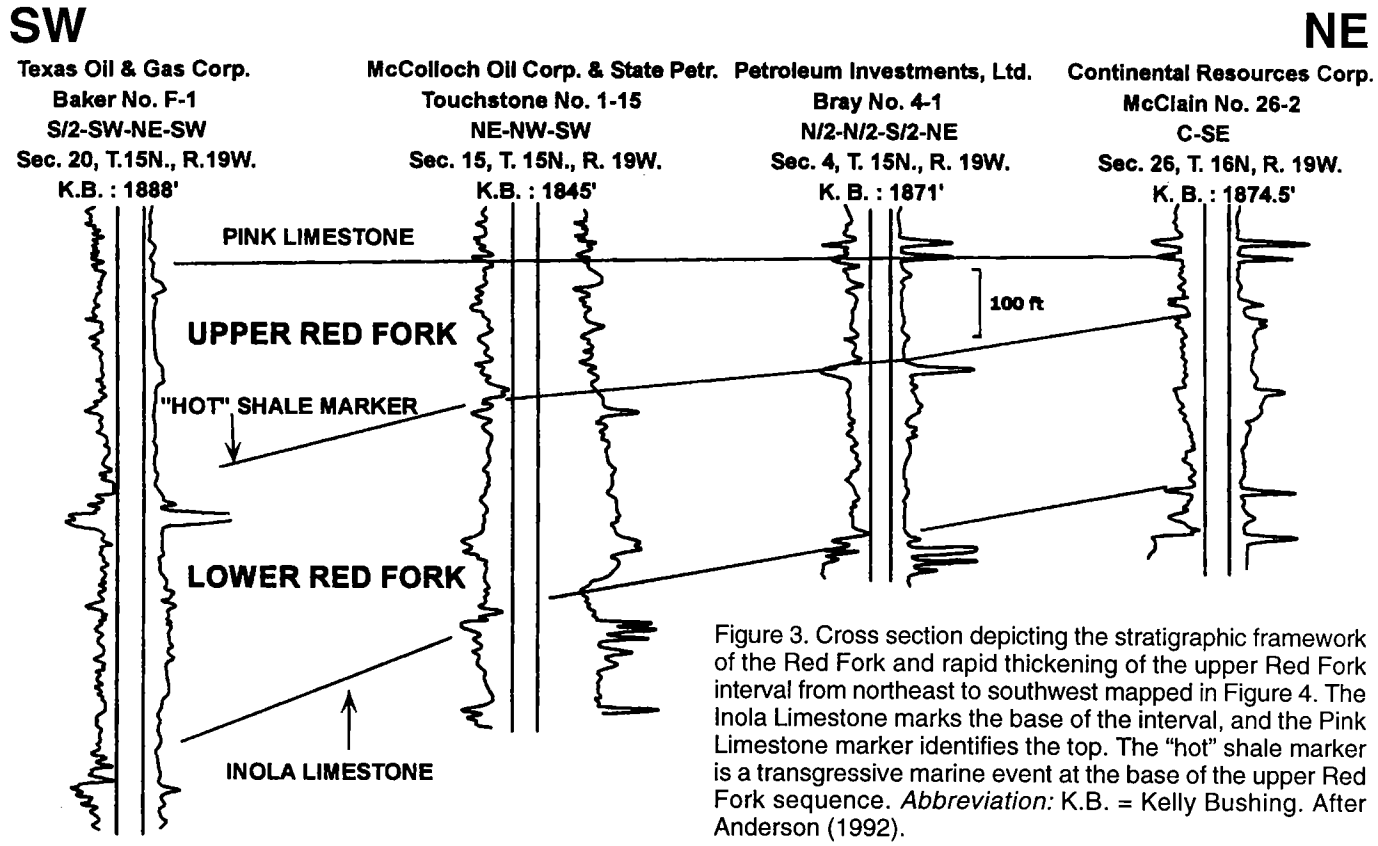

Figure 3. Cross section depicting the stratigraphic framework of the Red Fork and rapid thickening of the upper Red Fork interval from northeast to southwest mapped in Figure 4. The Inola Limestone marks the base of the interval, and the Pink Limestone marker identifies the top. The "hot" shale marker is a transgressive marine event at the base of the upper Red Fork sequence. *Abbreviation:* K.B. = Kelly Bushing. After Anderson (1992).

in the rate of thickening from <10 ft/mi to 50 ft/mi. As a result, upper Red Fork thickens from 150 ft in T. 16 N., R. 19 W., to approximately 1,000 ft in T. 12 N., R. 22 W. (Fig. 4). The shelf break represents the transition from dominantly deltaic to marine lithofacies. These facies were the basis for interpreting upper Red Fork depositional settings.

FACIES ANALYSIS

Eleven cores of the upper Red Fork interval were examined to determine sedimentary features, petrology, and diagenetic history. Those cores located in the central part of the depocenter and productive area of the Strong City District contained a wide variety of sedimentary and biogenic features associated with marine deposition. Anderson (1992) described these features in detail. In addition, most cores contained incomplete Bouma (1962) turbidite sequences (Fig. 5) and sedimentary features similar to those reported by Mutti and Ricci Lucchi (1972). Examples of incomplete cored Bouma (1962) sequences are shown in Figure 6. The core contains dark shale that is overlain by massive sandstone (T_a) at 13,082 ft that grades into horizontally laminated sandstone (T_b) at 13,080.8 ft. Above this sandstone is ripple and wavy-laminated sandstone (T_c) from 13,080.4 to 13,073 ft. The upper parallel-laminated shale (T_d) is located from 13,073 to 13,072 ft. An upward increase in clay content suggests a possible transition to pelagic or low-density–turbidite (T_e) phase, which was not preserved. The core (Fig. 6) contains additional incomplete T_{ab}, T_{abcd}, and T_{ab} sequences. Other cores contain incomplete Bouma sequences T_{bcde} and T_{cde}. Examples of these sequences and a comparison of cored sedimentary features to facies of the Mutti and Ricci Lucchi (1972) model are found in Anderson (1992).

The core from the SW Leedey Field contains features associated with shallow-marine sand deposits. It exhibits a cleaning-upward (coarsening-upward) character, with increasing sand and current indicators toward the top. Wireline logs have a similar cleaning-upward signature, supporting this interpretation.

Strong City District: Upper Red Fork Sandstone

Geometry and distribution of upper Red Fork lithofacies in the Strong City District were compared to that in published fan models. None of the analogues in the literature provided an ideal fit to the upper Red Fork, but the Mutti and Ricci Lucchi (1972) and Walker (1978) models exhibited striking similarities. A modified (for grain size) Walker (1978) facies model was used to predict lithofacies distribution; facies described by Mutti and Ricci Lucchi (1972) reinforced this model. The primary elements of the model are: (1) a feeder channel that supplies sediment, (2) a leveed-channel upper fan that transports sediment across older deposits, (3) a middle-fan composed of supra-fan lobes that grade outward from non-leveed, shallow, braided channels to smooth turbidity deposits, and (4) a lower fan and basin plain with smooth relief, parallel bedding, and distal turbidites (Fig. 7).

After wireline logs were calibrated to cores, log signatures were used to infer lithofacies and the position of individual wells within the fan model. The hypothetical stratigraphic profile of Walker (1978), that was modified for grain size (Fig. 8) and vertical stacking patterns published by Mutti and Ricci Lucchi (1972)

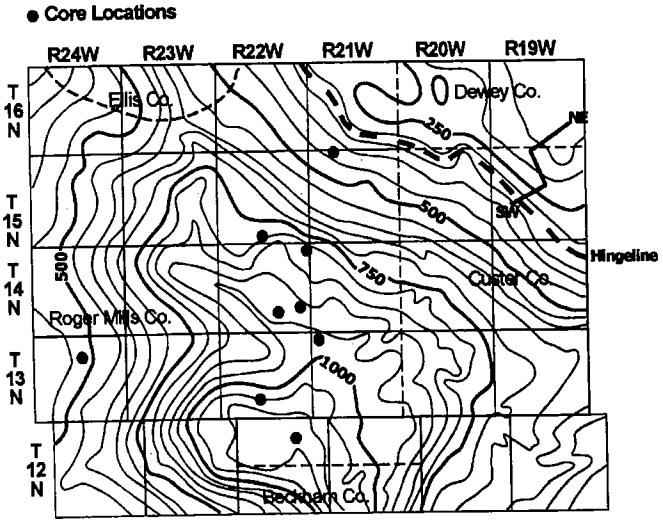

Figure 4. Thickness map of the upper Red Fork sandstone interval (contour interval = 50 ft) showing the trend of the upper Red Fork hingeline (thick dashed line); locations of wells in which the upper Red Fork was cored, and position of southwest–northeast cross section (Fig. 3) shown. After Anderson (1992).

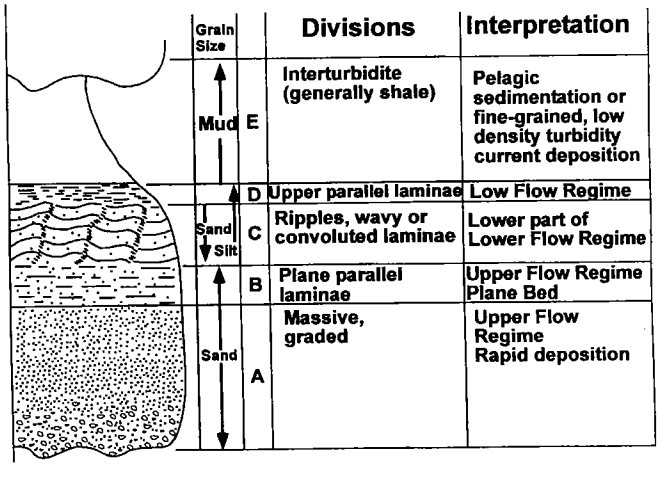

Figure 5. Complete, classical Bouma (1962) sequence (T_a–T_e). Incomplete Bouma sequences are characteristic of submarine-fan deposition. Deposition of T_{ab} occurs in higher-energy, upper- and middle-fan channels, and T_{cde} occurs in lower-energy levee, overbank, and distal-lobe deposits.

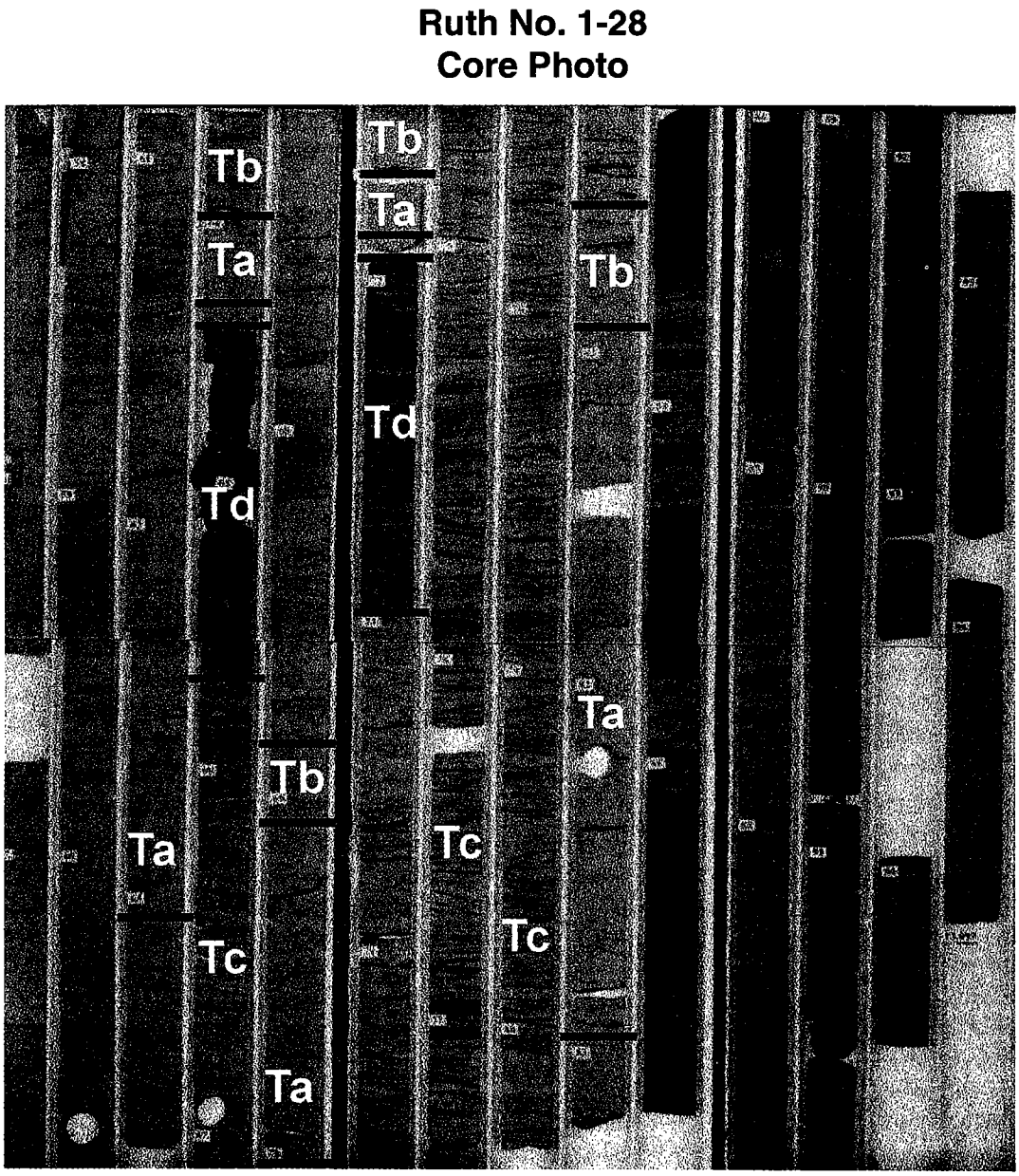

Figure 6. Incomplete Bouma sequences in core. The sand-rich, middle-fan channel contains T_{ab} to T_{abcd} partial sequences, taken from 13,055–13,097 ft depth. Louisiana Land and Exploration, Ruth No. 1-28, Sec. 28, T. 13 N., R. 22 W, Custer County, Oklahoma.

and Mutti and others (1999), served as patterns for electrofacies interpretation.

Upper-Fan Facies

Upper-fan lithofacies are dominantly channel-fill sandstones. The distinction between a coastal plain/deltaic-feeder channel (such as the Clinton–Weatherford trend), shelf break/slope submarine-feeder channel, and the channelized upper fan was based primarily on paleotopography and location. No cores were available, so interpretation of grain size (sand and clay/silt content) was based on log signatures. Thick graded/stratified fining-upward sandstone intervals in the Foss area are interpreted as upper-fan channels. The log signatures (Fig. 9) resemble those of fluvial-deltaic intervals, but T. 12 N., R. 19 W., is located basinward of the upper Red Fork shelf break. Channel bifurcation evident in Figure 10 is a feature of fan models (Fig. 7).

Middle-Fan Facies

Eight cores contain features associated with middle-fan deposits. Well-log signatures show serrate gamma-ray and resistivity profiles (Fig. 11). High gamma-ray response is the result of interbedded, dark, silty shale that may represent lower flow regime and suspension

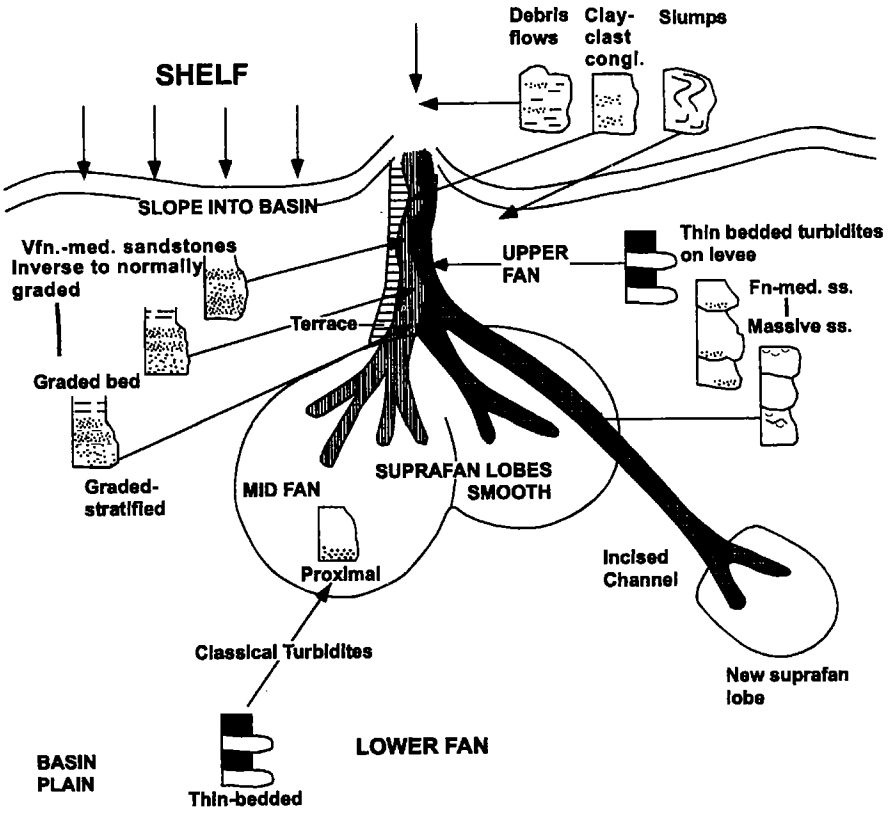

Figure 7. Submarine-fan model. Modified after Walker (1978). *Abbreviations:* congl = conglomerate; fn = fine grained; med = medium grained; ss = sandstone: vfn = very fine grained;

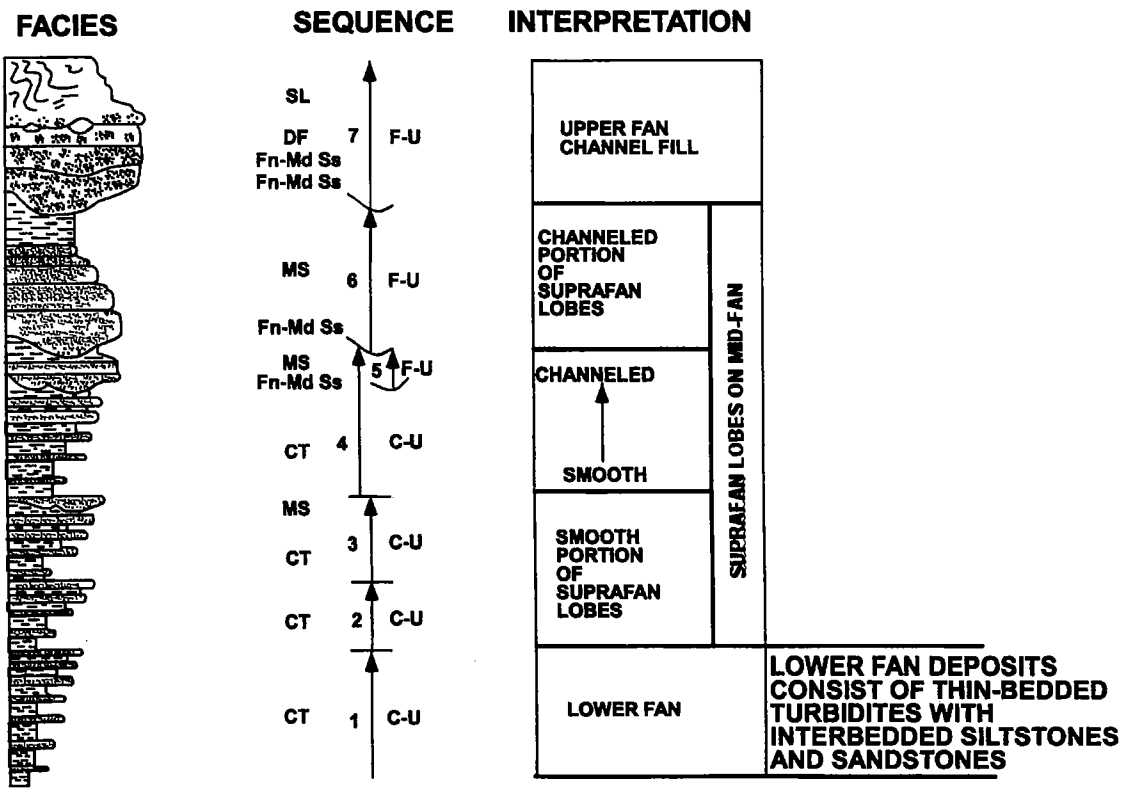

Figure 8. Hypothetical stratigraphic sequence developed by fan progradation. *Abbreviations:* F-U = fining- and thinning-upward sequence; C-U = coarsening- and thickening-upward sequence; CT = classical turbidite; MS = massive sandstone; DF = debris flow; SL = slump; fn = fine grained; md = medium grained; ss = sandstone. Modified after Walker (1978).

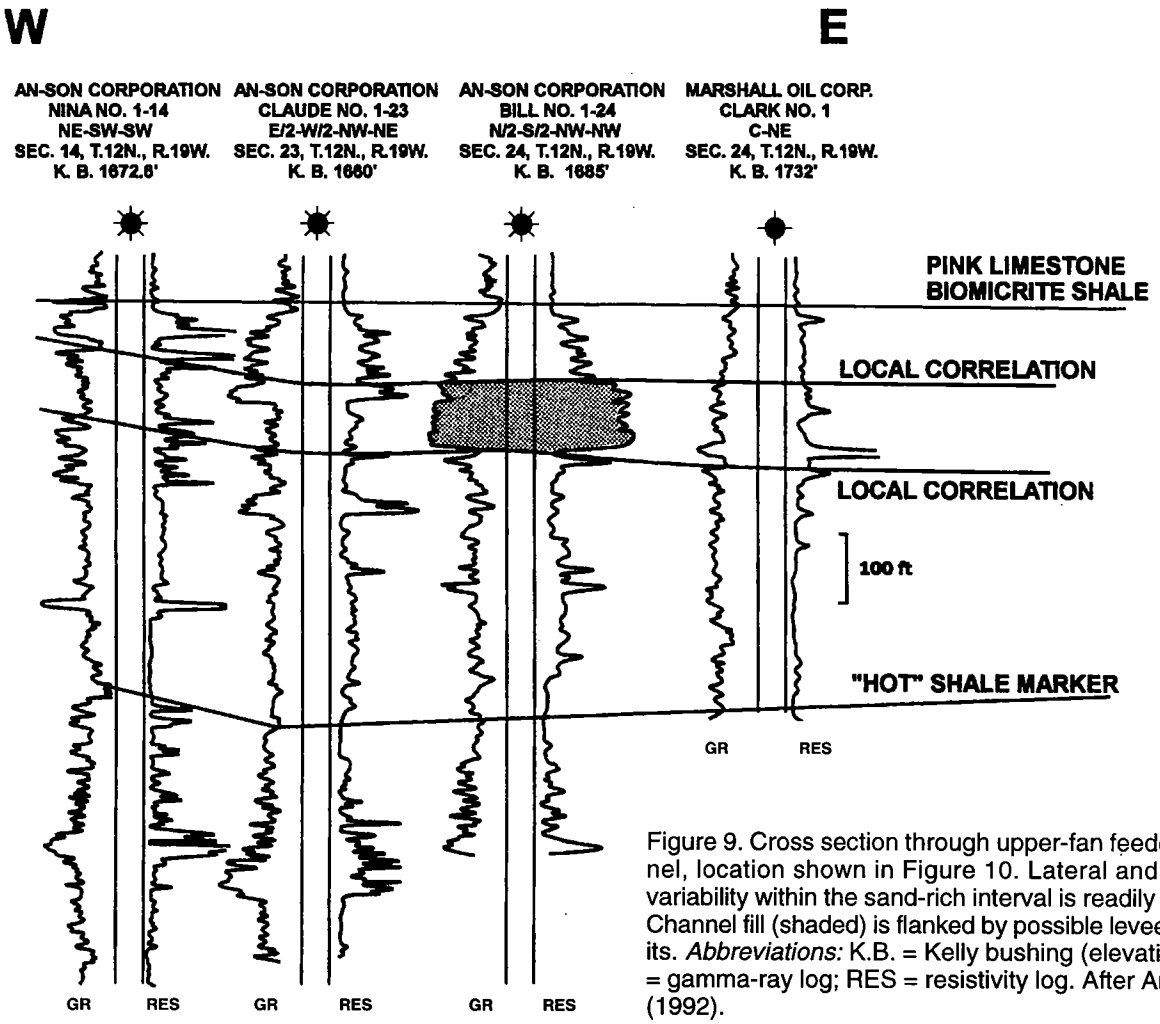

Figure 9. Cross section through upper-fan feeder channel, location shown in Figure 10. Lateral and vertical variability within the sand-rich interval is readily evident. Channel fill (shaded) is flanked by possible levee deposits. *Abbreviations:* K.B. = Kelly bushing (elevation); GR = gamma-ray log; RES = resistivity log. After Anderson (1992).

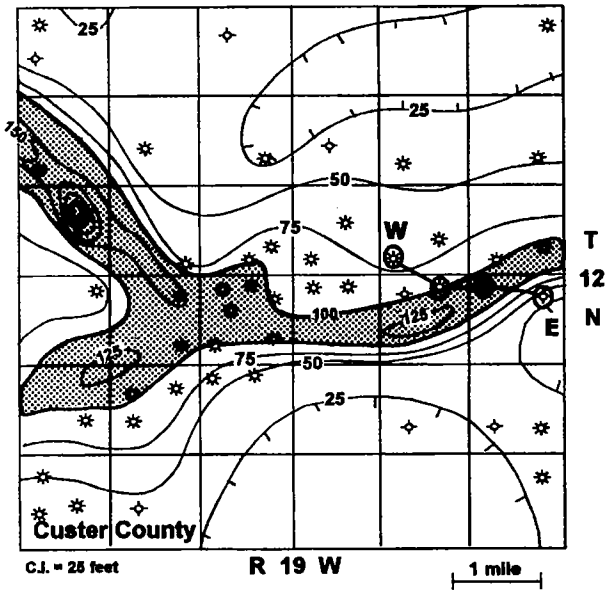

Figure 10. Net sandstone thickness (contour interval = 25 ft) and interpreted upper-fan feeder channel in the Foss Area, eastern Strong City District. Location of cross section (Fig. 9) is shown by circled well symbols.

settling, low-density turbidity flow, or clay/silt-rich intervals within Bouma (1962) sequences. Ripple laminae are common in cores of middle-fan sandstones, as are dish structures and other indicators of fluidized flow. Wireline-log patterns indicate multiple, stacked, sandstone-shale packages. They represent turbidites of the upper middle fan. Localized deposition in areas such as NE Roll resulted in several hundred feet of total sandstone accumulation (Fig. 12). A cross section through these thick accumulations illustrates their complexity (Fig. 13).

Lower-Fan Facies

Lower-fan deposits are composed of parallel, thin-bedded turbidites (Mutti and Ricci Lucchi, 1972; Walker, 1978). Characteristic electrofacies are coarsening-upward, shale-rich intervals, containing thin sandstones (Fig. 14). Lower-fan facies were cored in the Southport Exploration, 1-10 Merrick well in T. 12 N., R. 22 W. They consist of thin-bedded to laminar siltstones and shales, as well as shale with soft-sediment deformation features and microfaulting. These intervals are interpreted as deposits of low-density turbidity flows and suspension settling.

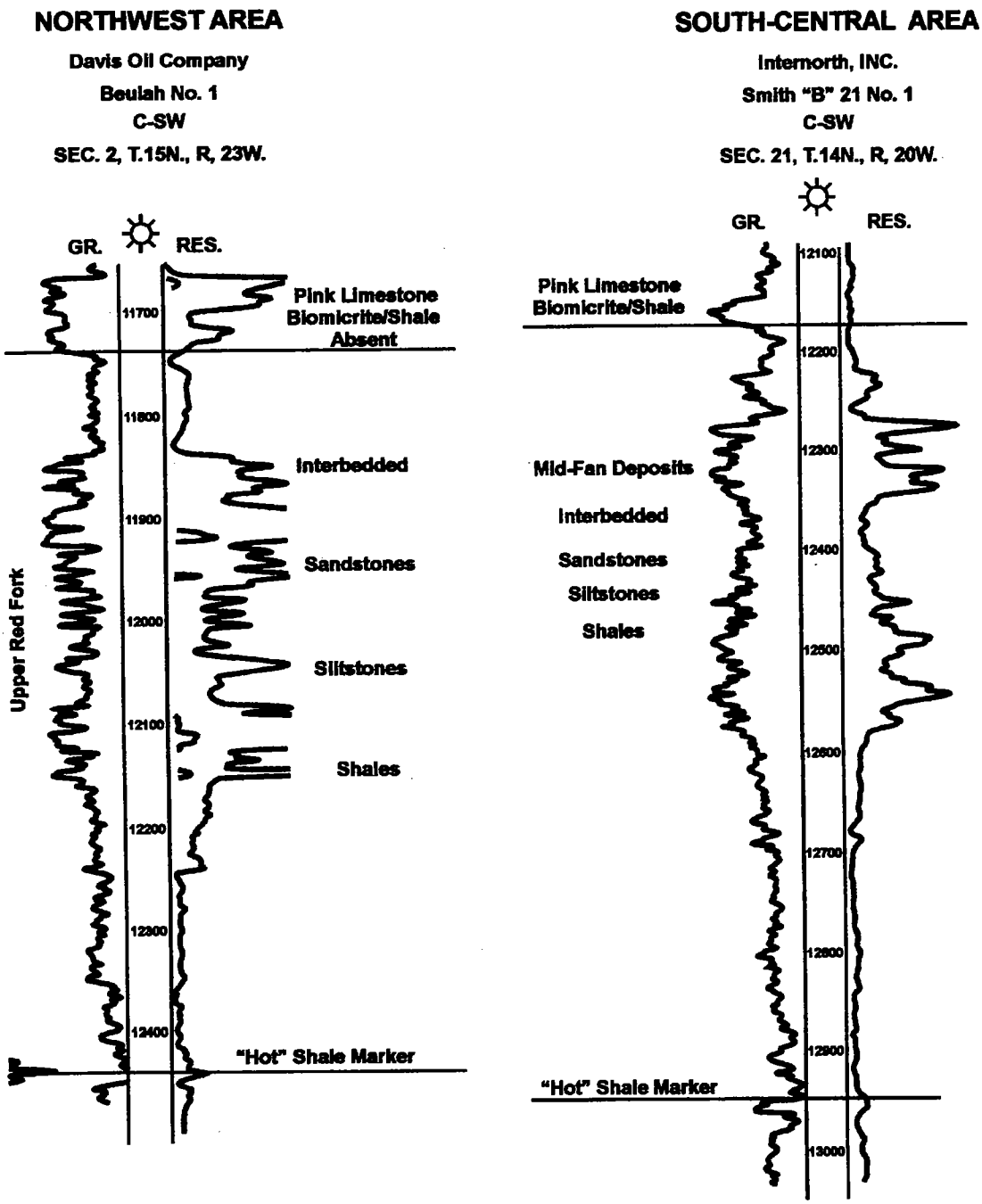

Figure 11. Middle-fan channel fill with serrated, wireline-log signatures. Depths in feet. *Abbreviations:* GR = gamma-ray log; RES = resistivity log. From Anderson (1992).

Basin-Plain Facies

Basin-plain facies are very similar to lower-fan facies and are difficult to distinguish. Wire-line log signatures (Fig. 14) indicate shale with minor amounts of sandstone. Plane-parallel bedding with hemipelagic sediment dominates basin-plain facies. Turbidity flows are minor (Mutti and Ricci Lucchi, 1972). Cored basin-plain interval contains interbedded brown and dark-gray shale with lighter-colored, thin siltstones and sandstones. Soft-sediment deformation features are common and include flowage, slump structures, and microfaulting (Anderson, 1992). Thin beds of very fine grained sandstone contain ripples that are attributed to traction currents (Mutti and Ricci Lucchi, 1972). The basin-plain facies is the most abundant in the basin depocenter and a likely source bed for gas and oil in adjacent sandstone reservoirs (Puckette and others, 2000).

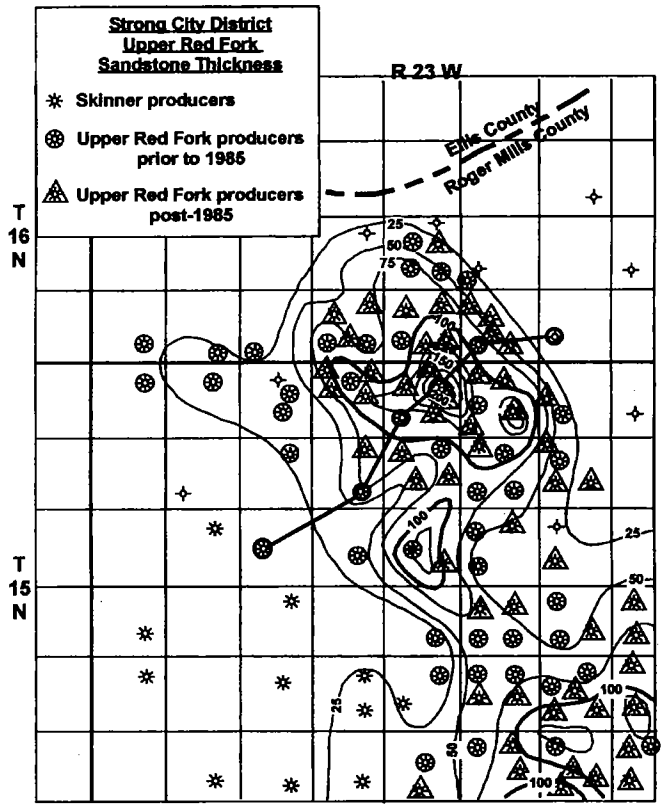

Figure 12. Net sandstone thickness (contour interval = 25 ft), NE Roll Area, Strong City District. Stacking of middle-fan channels results in sand accumulation that exceeds 200 ft. Position of cross section (Fig. 13) is shown by circled wells and bold line.

SW Leedey Field: Upper Red Fork Sandstone

The distribution and geometry of upper Red Fork lithofacies in the SW Leedey Field were compared with those in a variety of depositional models. The overall coarsening-upward character, upward increase in current features, and concurrent decrease in burrowing suggest a regressive, shallowing-upward marine environment (Leckie and Rosenthal, 1987). The distribution of sandstone (Fig. 15) subparallel to depositional strike and funnel-shaped log signatures (Fig. 16) support this interpretation.

Within the SW Leedey Field, wireline logs across the upper Red Fork sandstone have a cleaning-upward signature. Gamma-ray curves are an inverted bell shape (Fig. 17), indicating a reduction in clay content toward the top of the sandstone. Shallow-resistivity curves are similarly shaped with increasing resistivity toward the top (Fig. 16). Beyond the limits of the SW Leedey Field, gamma-ray, resistivity and porosity signatures indicate shale.

RESERVOIR CHARACTERISTICS

Porosity in upper Red Fork sandstones is predominantly secondary. It results mainly from the dissolution of metastable grains such as metamorphic-rock fragments and feldspars (Anderson, 1992; Johnson, 1984; Udayashankar, 1985). Primary porosity provided a conduit for corrosive fluids to reach these grains. In intervals where primary porosity is occluded by early cement, secondary porosity is negligible. For example, a low porosity, clean zone (low gamma-ray reading)

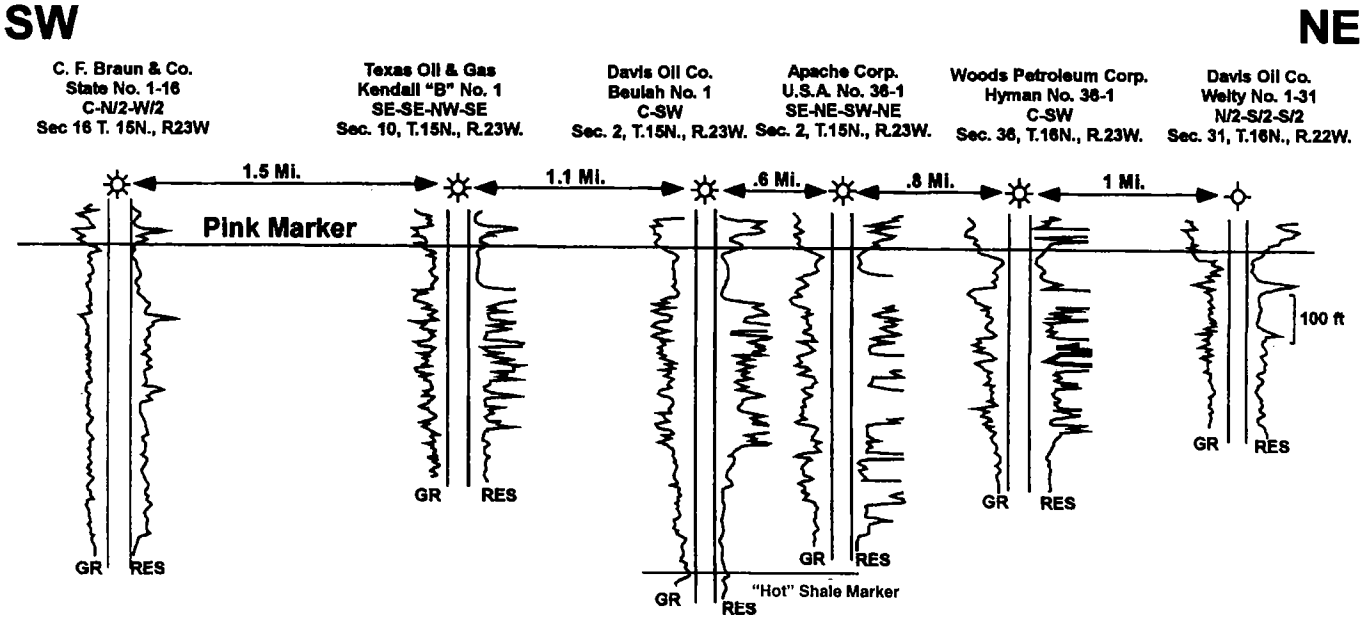

Figure 13. Local southwest–northeast cross section illustrating lateral and vertical changes in log signature that indicate heterogeneity in the middle-fan deposit mapped in Figure 12. *Abbreviations:* GR = gamma-ray log; RES = resistivity log.

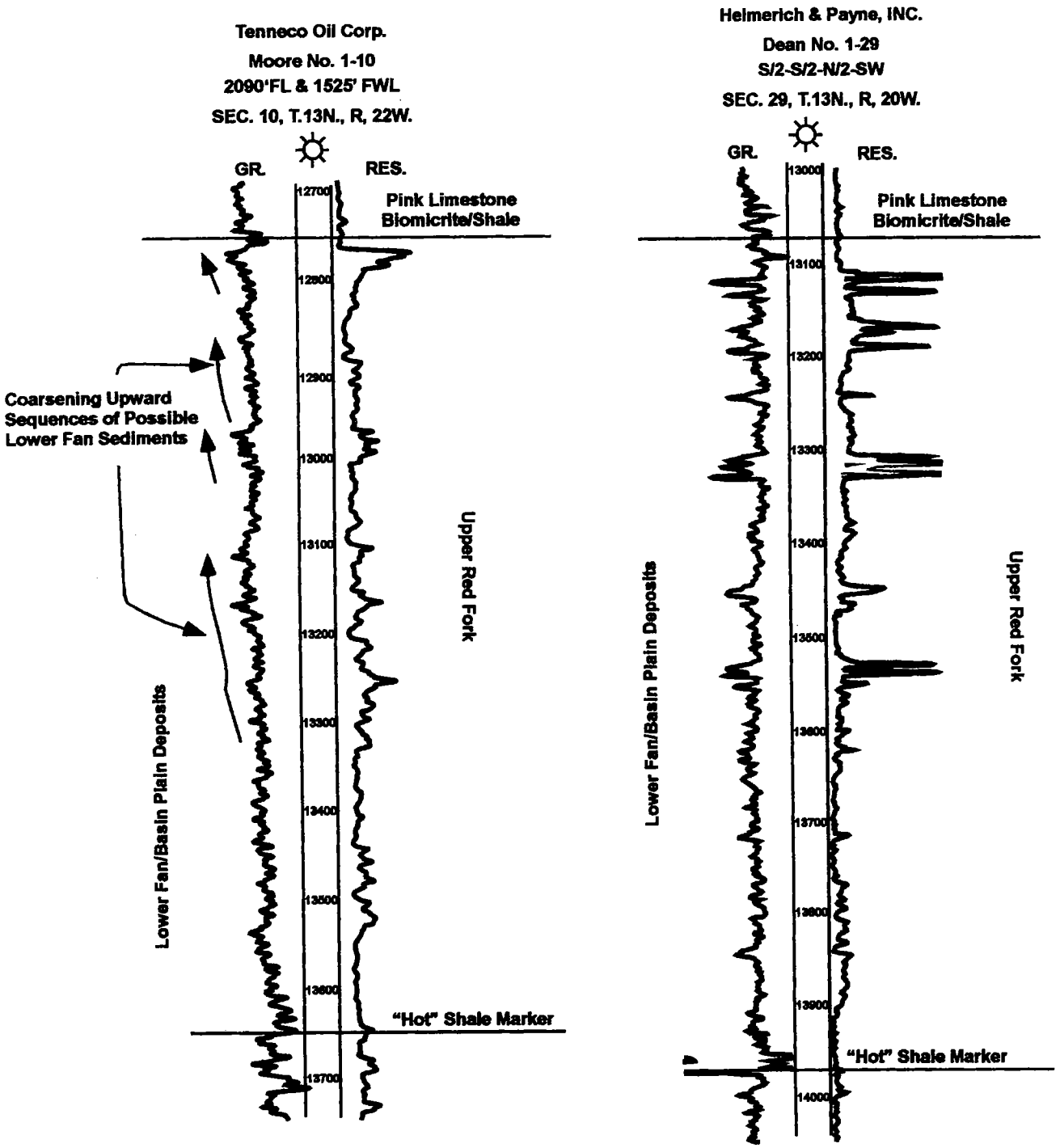

Figure 14. Wireline-log signatures illustrating lower-fan and basin-plain deposits. A scarcity of core resulted in a reliance on electrofacies in interpreting these deposits. Depth in feet. *Abbreviations:* GR = gamma-ray log; RES = resistivity log; FSL = from south line; FWL = from west line.

with high resistivity occurs at the top of the upper Red Fork sandstone in the Woods, Switzer 1-5 well, SW Leedey Field (Figs. 16, 17). This low-porosity zone (2–6% density porosity) likely resulted from early cement that precipitated in the cleaner, coarser-grained sand. This phenomenon is evident in other shallow-marine sandstones (Al-Shaieb and others, 2001; B. Carpenter, personal communication, 2002). In the Switzer 1-5 well, highest density porosity (16–18%) occurs below the cemented zone in an interval with increased clay content (Fig. 17).

Pressure measurements indicate that the upper Red Fork sandstone is a common reservoir throughout the SW Leedey Field. Decline curves for wells completed

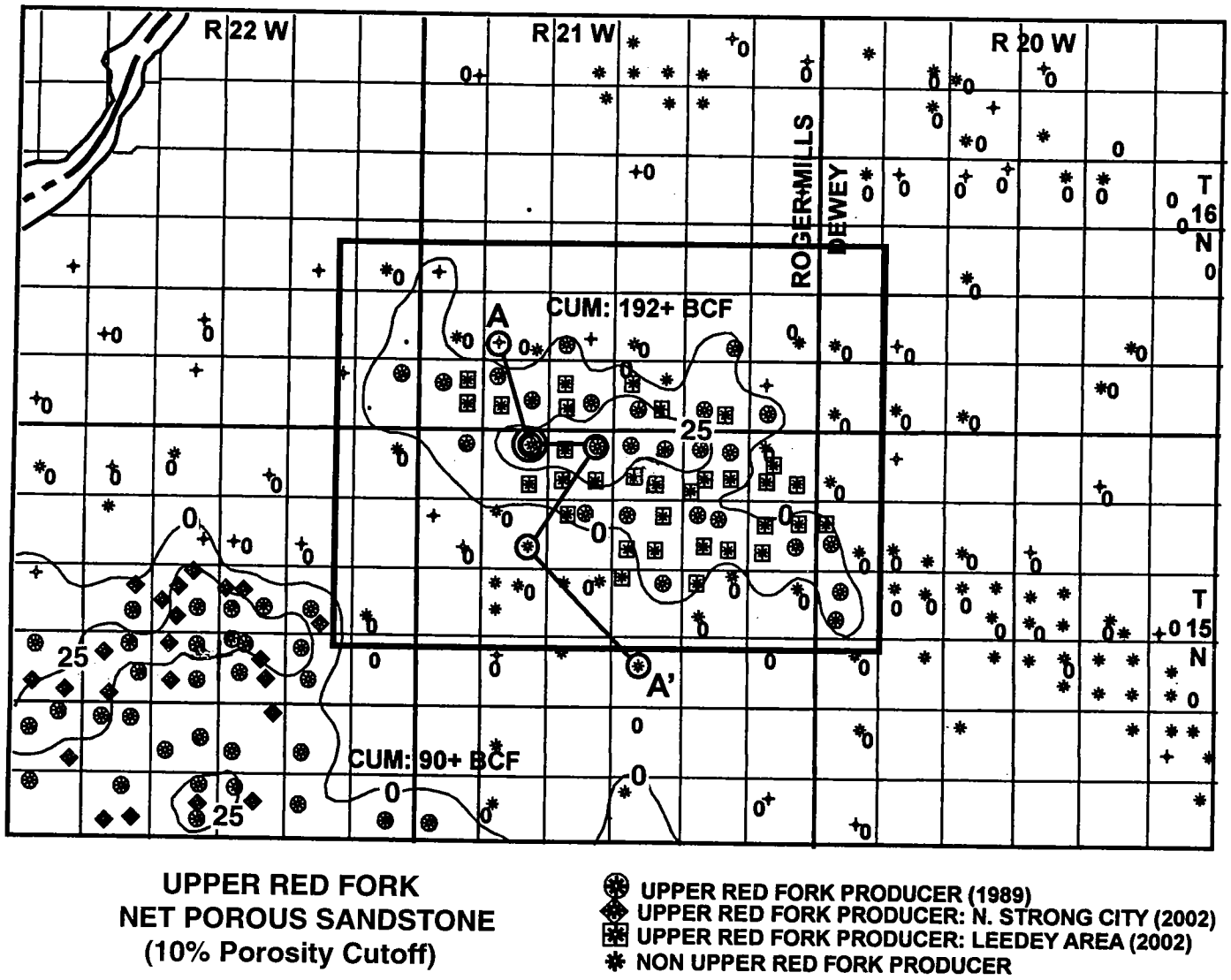

Figure 15. Net sandstone thickness map (contour interval = 25 ft), SW Leedey Field and portion of NE Roll Field. Upper Red Fork sand in SW Leedey is interpreted as a shallow-marine bar; NE Roll as middle-fan channel complex. Position of cross section (Fig. 16) is shown by circled well symbols; cored well by double circle. *Abbreviations:* BCF = billion cubic feet (of gas); Ma = grain density of formation matrix (gm/cm^3).

during the initial-development phase indicate a reduction in reservoir pressure with time and a clustering of reservoir pressures (Fig. 18). This reservoir homogeneity helps explain high-volume gas production in the field.

The complexity of coalescing-fan deposits contributed to the variability in production volumes that are evident in the Strong City District. Better reservoirs are found in the narrow channels of the middle-fan supra-fan lobes and upper-fan feeder channels (Anderson, 1992, 1993). Considerable variation in the position of individual sandstones is evident in cross sections of the Roll and Foss areas (Figs. 9, 13). Detailed correlation, however, can identify reservoirs common to multiple wells. Lateral and vertical variability has resulted in extensive reservoir compartmentalization. Although this reduces the ultimate recovery for individual wells, it creates potential for finding additional reserves between existing producers.

DEPOSITIONAL HISTORY

Red Fork marine sands and mud represent the most distal deposition along the sediment-dispersal system. Submarine fans formed as a result of sea-level drop and an absence of accommodation space on the shelf. During deposition of the upper Red Fork, the Clinton–Weatherford incised channel was a primary conduit for sediments. Sand and mud were transported to the shelf edge and carried into the basin, forming the Strong City fan complex. During the deposition of the lower Red Fork, channels in the vicinity of the S Thomas Field (T. 13 N., R. 13 and 14 W.) were sources of sediment for submarine fans identified by Johnson (1985)

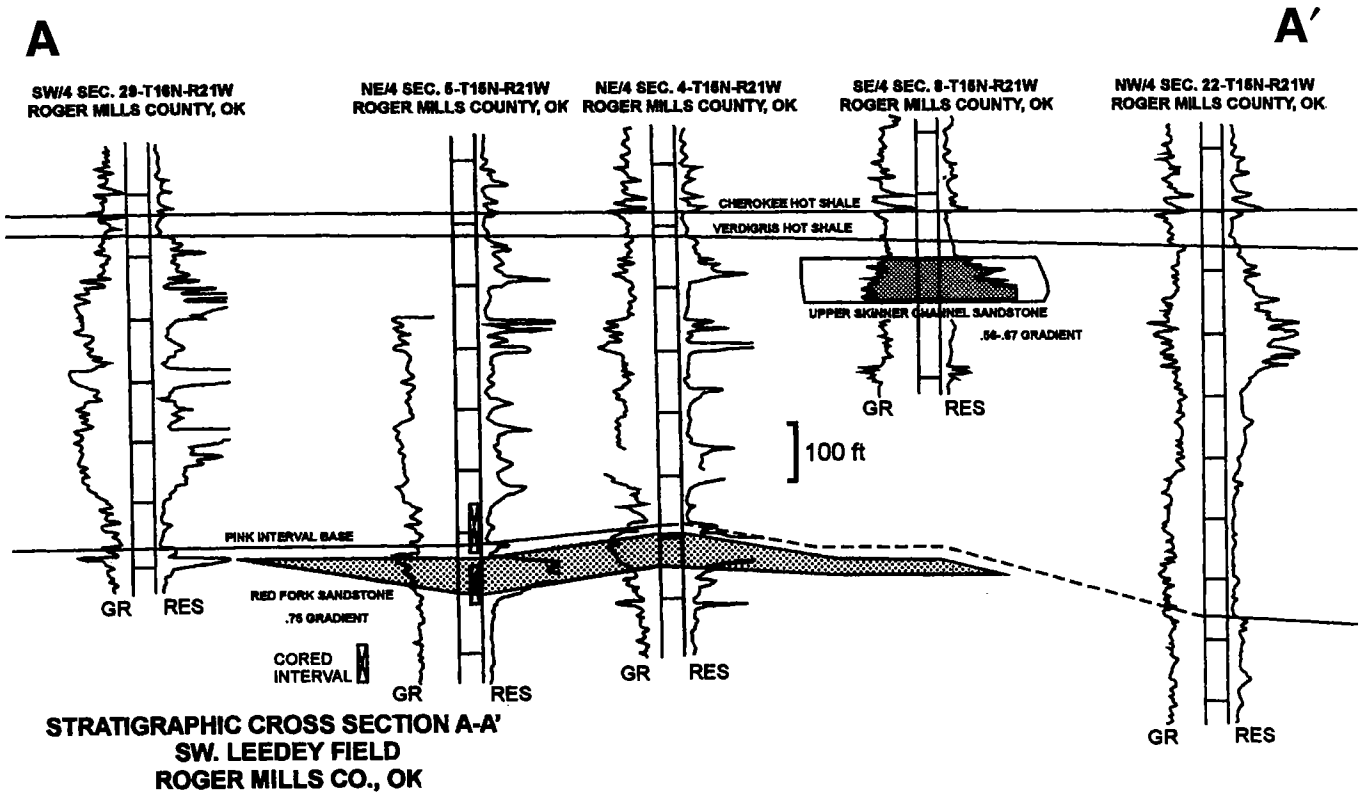

Figure 16. Cross section through shallow-marine bar mapped in Figure 15. Wireline logs across the upper Red Fork exhibit funnel-shaped character typical of coarsening-upward sequences. In contrast, the upper Skinner channel-fill sandstone has a bell-shaped, fining-upward signature. *Abbreviations:* GR = gamma-ray log; RES = resistivity log.

in T. 12 N., R. 16 W. Mud accumulated in the Strong City/Leedey area, where the lower Red Fork is predominantly shale.

The upper Red Fork sandstone in the SW Leedey Field may have formed from sand transported by longshore currents. Potential sediment sources include the Clinton-Weatherford channel, or as yet undiscovered feeder channels located nearby.

A generalized sequence-stratigraphic model was developed for the upper Red Fork. This sequence began with a transgression and flooding of the underlying lower Red Fork deltaic and marine sediments. The "hot" shale marker represents this flooding event, which is traceable across much of the deep basin and shelf. Following this transgression, the upper Red Fork (highstand) fluvial-deltaic complex prograded basinward. A subsequent drop in sea level (regression) forced the Clinton–Weatherford channel to incise underlying deltaic and shelf deposits. During this lowstand, most sediment was transported beyond the shelf edge and deposited on the basin floor. A rise in sea level and transgression followed. As sea level rose, deposition beyond the shelf edge ceased as sand accumulated in the feeder channel(s), and the basin became starved. The silt- and sand-rich muds at the top of the Red Fork interval (Fig. 19) were deposited during this transgression.

The upper Red Fork silty shale is overlain by dark-colored (deeper) marine shale of the Pink interval. This shale represents a significant rise in sea level and correlates with limestone on the shelf (Puckette, 1990).

The upper Red Fork sequence is punctuated by higher-frequency cycles. On the shelf, cored marine shales identify transgressions, whereas coal, rootlets, and caliche indicate subaerial exposure (Johnson, 1985; Udayashankar, 1985). In the basinal study area, where coring is limited and a thicker upper Red Fork interval exists, these higher-frequency cycles are difficult to identify.

IMPLICATIONS

The complexity of submarine-fan deposits in the Strong City District contributes to reservoir heterogeneity and, in some cases, reduces reserves for individual wells. However, this highly compartmentalized, heterogeneous nature creates potential for finding additional reserves close to existing wells. Upper- and middle-fan channel-fill sandstones offer the best reservoir quality. The complex patterns generated by fan-lobe switching may be resolved by detailed mapping using wireline-log and seismic data.

In contrast, the high production volumes of the SW Leedey Field are a manifestation of reservoir homogeneity. Exploration targets in this area may include similar, but likely smaller, marine bars or the feeder channels that supplied their sediment.

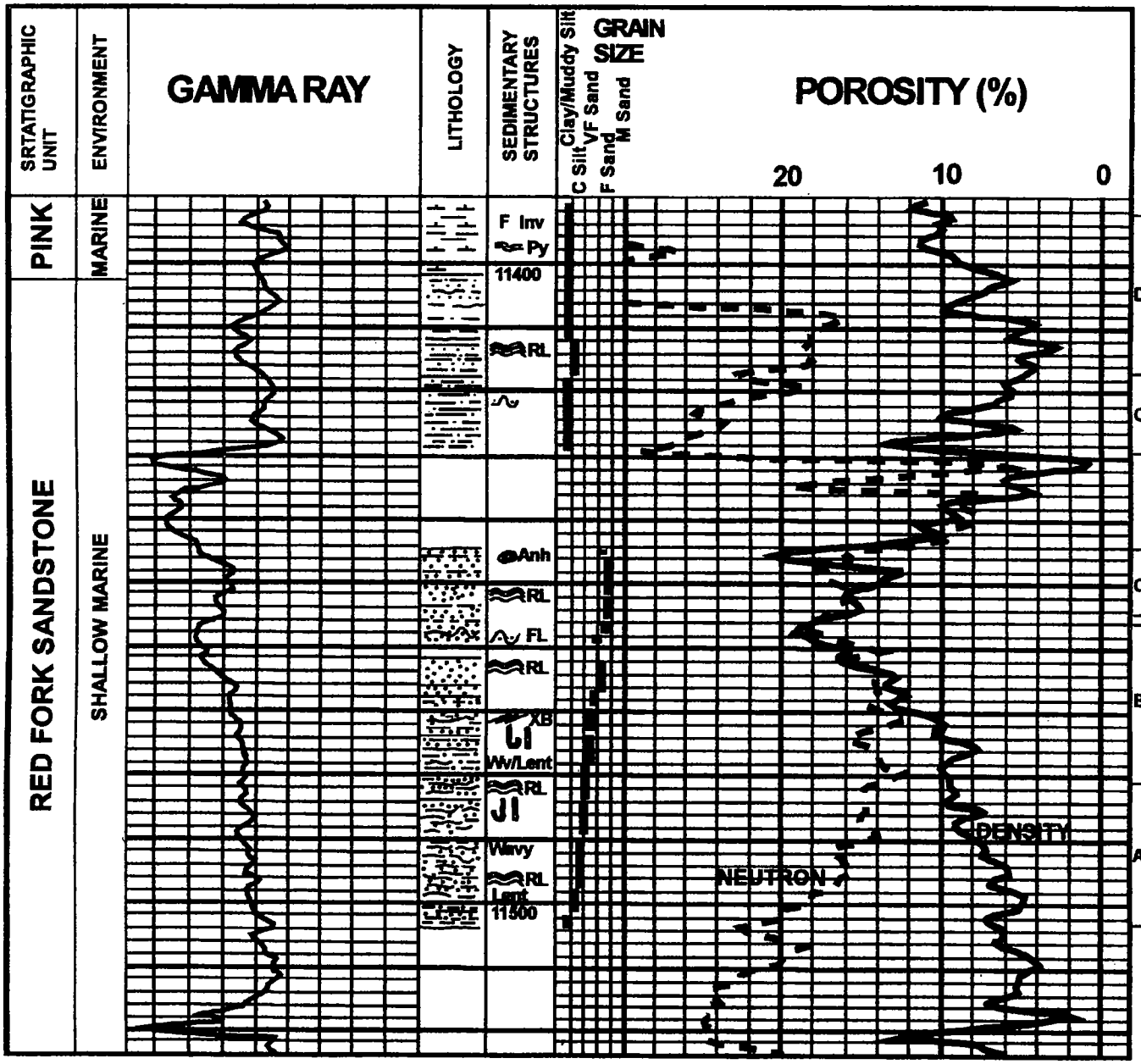

Key to Symbols

- Burrowing
- Cross beds
- Ripple Laminae
- Soft-Sediment Flowage

Figure 17. Petrolog of Woods, Switzer 1-5 well illustrating gamma-ray and porosity-log signatures and rock data for parts of upper Red Fork and Pink Limestone intervals. Depths in feet. Gamma-ray curve across the Red Fork exhibits a cleaning-upward (shallowing) signature. Porosity curves identify the cemented zone at the top of the sandstone and a general cleaning-upward character that coincides with increasing average grain size. *Abbreviations:* Lent = lenticular bedding; RL = ripple laminae; Wavy = wavy bedding; X = cross beds; FL = flowage feature; Anh = anhydrite nodule; Py = pyrite; and F Inv = fossil invertebrates.

ACKNOWLEDGMENTS

The authors thank Eric Anderson and Charles Anderson for their valuable contributions. We also thank Ken Rechlin, Chris Armistead, Erin VanEvera, and Chris Wiggers for their help in preparing this paper. We also acknowledge Walter Esry and Larry Austin of the Oklahoma Geological Survey Core Library for providing cores critical to this research.

REFERENCES CITED

Al-Shaieb, Z.; Shelton, J. W.; Puckette, J.; and Boardman, D. B. II, 1995, Sandstone and carbonate reservoirs of the Mid-Continent: Syllabus for a short course sponsored by the Oklahoma City Geological Society, 195 p.

Al-Shaieb, Z.; Puckette, J.; Patchett, J.; Deyhim, P.; Li, H.; Close, A.; and Birkenfeld, R., 2000, Identification

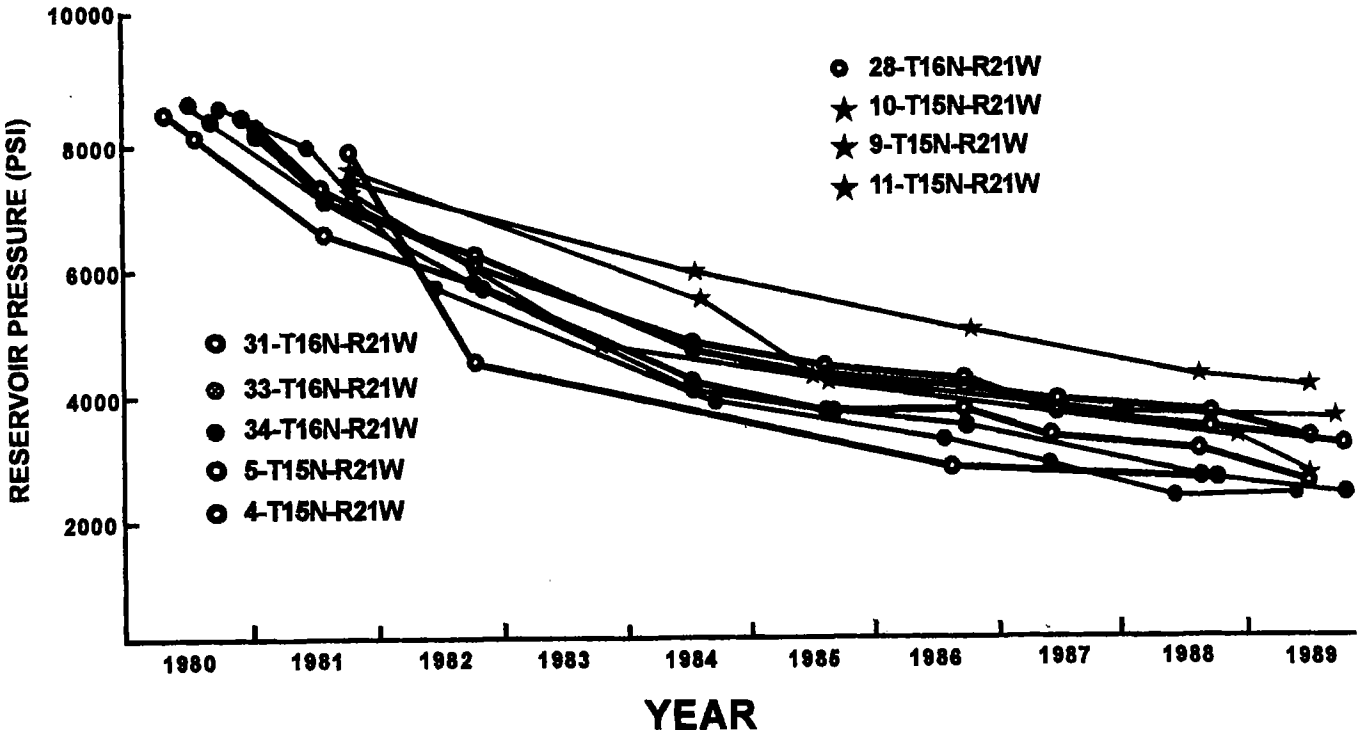

Figure 18. Partial decline curves (reservoir pressure in psi) from 1980–1989 for wells drilled during the initial development phase of the SW Leedey Field.

and characterization of reservoirs and seals in the Vicksburg Formation, TCB Field, Kleberg County, Texas: Search and Discovery, American Association of Petroleum Geologists/Datapages Inc., http://www.searchanddiscovery.net/.

Anderson, C. J., Jr., 1992, Distribution of submarine fan facies of the upper Red Fork interval in the Anadarko Basin, western Oklahoma: Oklahoma State University unpublished M.S. thesis, 275 p.

Anderson, E., 1993, Submarine-fan delta depositional environment of the Pennsylvanian Red Fork Sandstone [abstract]: American Association of Petroleum Geologists Bulletin, v. 77, p. 1570.

Bouma, A. H., 1962, Sedimentology of some flysch deposits: a graphic approach to facies interpretation: Elsevier, Amsterdam, 168 p.

Glass, J. L., 1981, Depositional environments, reservoir trends, and diagenesis of the Red Fork Sandstone in Grant and Kay Counties, Oklahoma: Oklahoma State University unpublished M.S. thesis, 99 p.

International Oil Scouts Association, 2000, International oil and gas development: International Oil Scouts Association, Austin, Texas, v. 69, p. 1057.

Johnson, C. L., 1984, Depositional environments, reservoir trends, and diagenesis of the Red Fork sandstones in portions of Blaine, Caddo, and Custer Counties, Oklahoma: Oklahoma State University unpublished M.S. thesis, 122 p.

Leckie, D.; and Rosenthal, L., 1987, Sedimentology of sandstone reservoirs course notes: Geological Survey of Canada Contribution No. 22487, 160 p.

Mutti, E.; and Ricci Lucchi, F., 1972, Le torbiditi dell' Appennino settentrionale: Introduzione all'analisi di facies: Society Geologia Italiana Memoir, v. 11, p. 161–199.

Mutti, E.; Tinterri, R.; Remacha, E.; Mavilla, N.; and Angella, S.; and Fava, L., 1999, An introduction to the analysis of ancient turbidite basins from an outcrop perspective: American Association of Petroleum Geologists, Continuing Education Course Note Series, no. 39, 61 p.

Puckette, J. O.; Anderson, C.; and Al-Shaieb, Z., 2000, The deep-marine Red Fork sandstone: a submarine-fan complex, *in* Johnson, K. S. (ed.), Marine clastics in the southern Midcontinent, 1997 symposium: Oklahoma Geological Survey Circular 103, p. 177–184.

Schneider, R. E.; and Clement, W. A., 1986, The East Clinton gas field, Custer County, Oklahoma: a seismic-stratigraphic case history: Oklahoma Geological Society, Shale Shaker Digest, v. 12, p. 63–67.

Udayashankar, K. V., 1985, Depositional environment, petrology and diagenesis of the Red Fork Sandstone in central Dewey County, Oklahoma: Oklahoma State University unpublished M.S. thesis, 188 p.

Walker, R. G., 1978, Deep-water sandstone facies and ancient submarine fans: models for exploration for stratigraphic traps: American Association of Petroleum Geologists Bulletin, v. 62, p. 932–966.

Whiting, P. H., 1982, Depositional environment of Red Fork sandstones, deep Anadarko Basin, western Oklahoma: Oklahoma City Geological Society, Shale Shaker Digest, v. 11, p. 104–119.

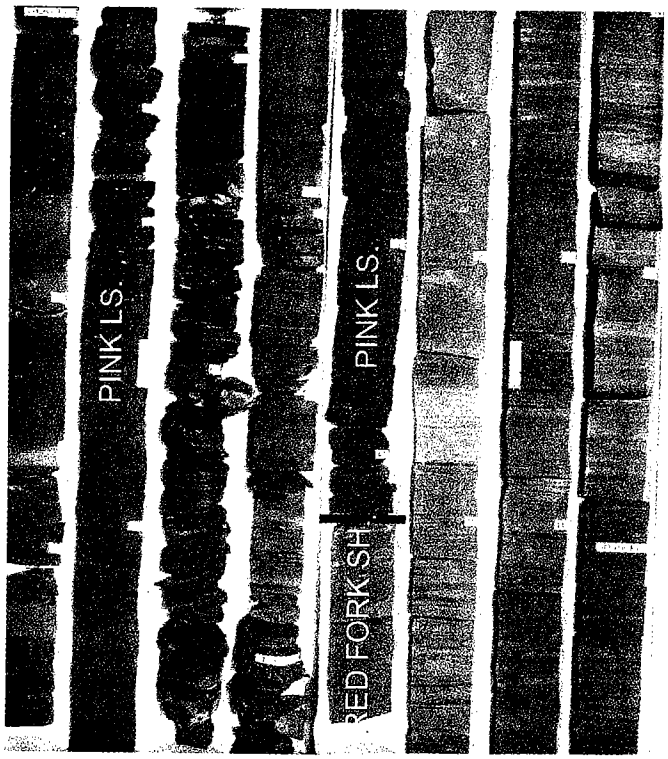

D Switzer "C" No. 1–5
Core Photo 11,393–11,417 ft

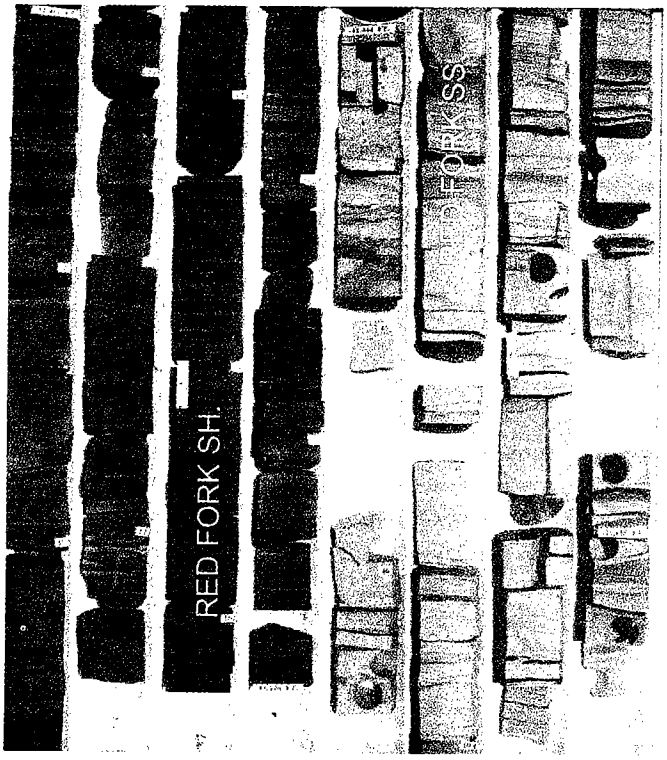

C Switzer "C" No. 1–5
Core Photo 11,417–11,455.7 ft

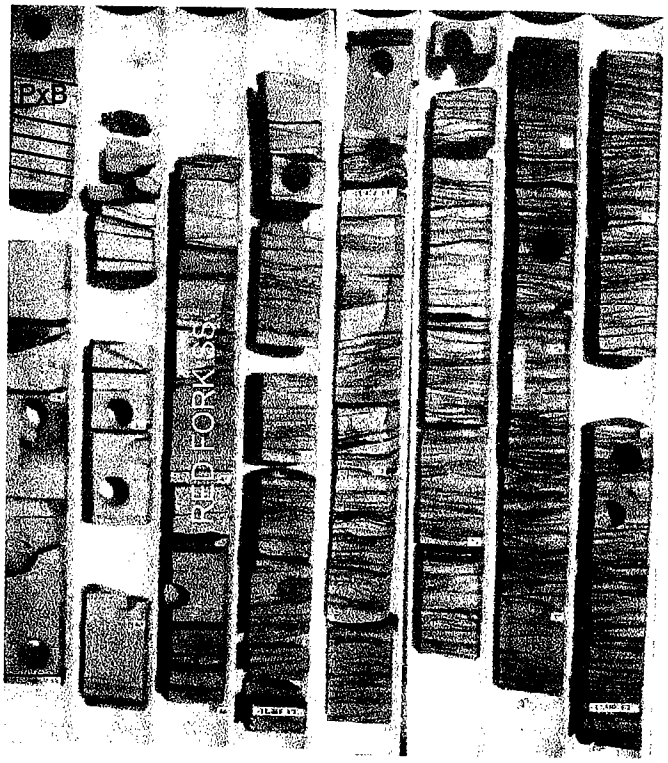

B Switzer "C" No. 1–5
Core Photo 11,456.5–11,480.4 ft

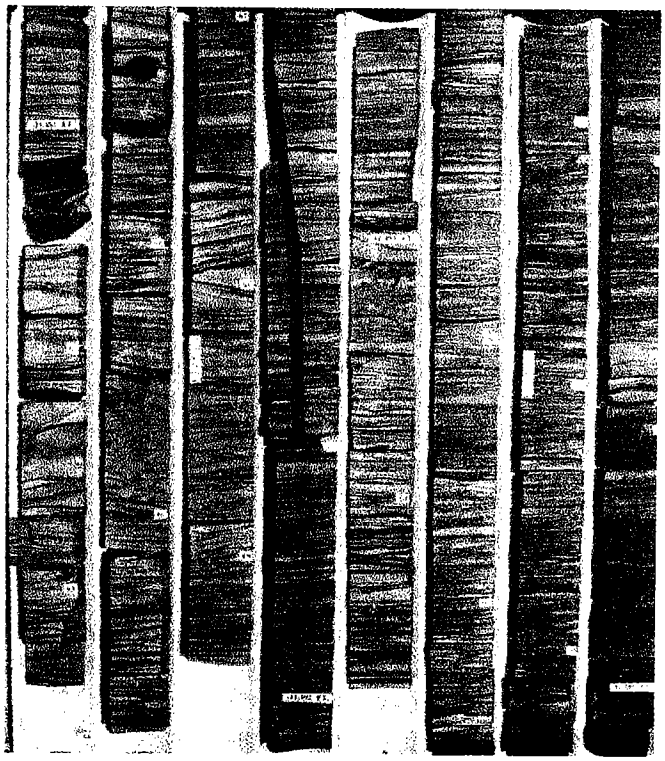

A Switzer "C" No. 1–5
Core Photo 11,480.4–11,503.3 ft

Figure 19. Core photographs of rocks representing the upper Red Fork and Pink sequences. Positions of photographs are shown in Figure 17. Depths (in feet) of cores shown below each core set. (A) Transition from shale to thinly bedded sandstone and shale. (B) Coarsening- or shallowing-upward character of the marine bar. (C) Contrast between the sandstone interval and overlying siltstone and shale zone. (D) Contact between dark, deeper-marine shale of the Pink interval and upper Red Fork sandy siltstone and shale.

Petrophysical Study of the Prue Sands in Washita County, Oklahoma: A Multiple-Parameter Approach to Log Analysis

George A. Anderson III, George B. Asquith, and Scott M. Frailey
Texas Tech University
Lubbock, Texas

ABSTRACT.—A petrophysical study was conducted on the Prue Sands in western Washita County in southwestern Oklahoma. The study used data from a standard wireline-logging suite and a petrophysical-analysis program developed on a personal computer using the spreadsheet program Microsoft Excel. Results were extracted from the program and a series of charts generated in Excel were used to display and interpret the results.

The Prue Sands are stratigraphically a part of the Middle Pennsylvanian (Desmoinesian) Cherokee Group. Geologically, the study area is located near the main basin-bounding–fault system that separates the sediment-supply terrain of the Wichita–Amarillo Uplift from the southern margin of the Anadarko Basin. The sediments there are a part of the granite-wash depositional environment. Granite-wash reservoirs exhibit mineralogical and textural characteristics that complicate standard petrophysical analysis. This most applies to the identification of clean reservoir and the determination of useful water-saturation values.

In this study, a suite of petrophysical parameters is applied to reservoir identification, hydrocarbon detection, and assessment of hydrocarbon movability. Spontaneous-potential– (SP–) log data in combination with mudlog data (where available) provide initial indications of permeable beds, and porosity and gas-effect are determined using a density-neutron–log combination. Data from a dual-induction/shallow-resistivity–log suite, which included deep-induction and medium-induction logs and a shallow-resistivity log, consisting of either a laterolog or spherically focused log (SFL), provide many of the key analytical parameters used to identify clean, productive hydrocarbon zones in the granite-wash facies of the Prue in this area of the basin.

Resistivity characteristics of a reservoir are a function of several rock-fluid properties that include geometric character of the pore system, conductivity, and volume of electrolytic brine contained in the pore system, and conductive properties of the rock matrix. Porosity and connate-water resistivity (inverse conductivity) and formation resistivity are applied in standard Archie water-saturation analysis. In this study, additional analytical parameters based on reservoir-resistivity characteristics are developed from the formation-resistivity factor, resistivity porosity, moved-hydrocarbon index, and ratio water saturation. Interpretation of these parameters is based on the effects of invasion in a reservoir, and they are used to broaden the analysis to provide further indications of hydrocarbon presence and transmissibility properties of reservoir rock-fluid systems. An amplified form of bulk-volume water is used to assess grain-size and textural variability across a reservoir zone.

The SP log is used in this study to examine the resistivity characteristics of the connate water in the reservoir in addition to the initial identification of permeable beds. Using this application, the SP has shown that connate-water resistivity (*Rw*) can vary significantly among stacked sands within the Prue in a single well. Assuming a constant, saline *Rw* across the stratigraphic extent of the Prue can lead to erroneous Archie water-saturation calculations and result in failed completions.

The determination of the shale content ("shaliness") in granite-wash reservoirs is a common problem, because the gamma-ray response of shales is similar to that of the feldspar and mica grains commonly found in the framework mode of these sands. The potential for a disproportionate gas effect on the density and neutron logs reduces the usefulness of this potential shale-volume indicator. In this study, excess conductivity—a condition where shallow-resistivity porosity exceeds formation porosity derived from neutron-density logs— has been correlated with failed production attempts and is interpreted here as a potential shaliness indicator.

Results of all the methods applied in the analysis are ranked statistically and grouped based on the initial potential (IP) of the specific zone. This provides a rapid and objective means of comparing and ranking the hydrocarbon-productive characteristics among several zones being considered for completion in a well. These page-size summaries can be completed for zones beyond the main objective and readily filed and can be used to identify behind-pipe potential when initial completions are depleted. The statistical ranking is based on logical arguments developed in Excel that can be established by the operator. It is intended to systematize an interpreter's experience with critical rock-fluid–system properties to evaluate a developing field or exploration play.

Anderson, G. A. III; Asquith, G. B.; and Frailey, S. M., 2002, Petrophysical study of the Prue Sands in Washita County, Oklahoma: a multiple-parameter approach to log analysis, *in* Boyd, D. T. (ed.), Finding and producing Cherokee reservoirs in the southern Midcontinent, 2002 symposium: Oklahoma Geological Survey Circular 108, p. 135–159.

INTRODUCTION

A suite of petrophysical methods has been applied to analysis of the hydrocarbon potential of Prue Sands in Washita County, Oklahoma, using logs from wells in T. 9–10 N., R. 19–20 W. (Fig. 1). The wells examined exhibit a wide range of production-test results. Outcomes from all the petrophysical methods are interpreted in terms of these test results to develop a system of petrophysical interpretation that provides a ranked assessment of the hydrocarbon potential of Prue Sands.

The study area lies in the deepest part of the asymmetrical Anadarko Basin in southwestern Oklahoma, 6–7 mi north of the fault system that brought the granitic source rocks in the Wichita Mountains to the surface (Fig. 1). The Amarillo Uplift is a buried mountain range that continues this uplifted-basement trend west into the Texas Panhandle. Together, the faults on the northeastern margin of these uplifts constitute the southern border of the Anadarko Basin. These fault-bounded uplifts are elements of the Early Pennsylvanian Ancestral Rockies, a system of intracratonic, fault-bounded, basement uplifts and adjacent basins found throughout the western Midcontinent and adjoining Rocky Mountain region (Ver Weibe, 1930; Dutton, 1982; Rascoe and Adler, 1983).

Edwards (1959) indicated that igneous-rock fragments eroded from exposed basement rocks of the Wichita Mountains were transported from the highlands into a fringing marine environment, resulting in a broad front of coalescing alluvial fans, deltas, and interfingering shallow-marine deposits in the southern Anadarko Basin. According to Edwards (1959), deposition of the immature (gravelly-sandy-silty) sediments derived from the adjacent granitic highlands led to the development of mineralogically and texturally complex granite-wash system that we know today. The results of a sedimentological study by Dutton (1982) supported Edwards' conclusion and indicated that Atokan through Wolfcampian granite wash accumulated as thick fan-delta wedges along the fault-bounded uplifts that form the southern border the Anadarko Basin. For this reason, the terrigenous sediments of the upper Desmoinesian, upper Cherokee Prue Sands (Fig. 2) in this setting would be expected to exhibit characteristics typical of granite-wash clastics deposited in a fan-delta environment.

STATEMENT OF PROBLEM

The Prue is 800–900 ft thick in the study area. Eight or more discreet permeability streaks (sands) are recognized in the Prue based on spontaneous-potential (SP) logs, drilling breaks, and sample descriptions. Well cuttings in these intervals are described as granite wash, conglomerate wash, quartz wash, and sandstone,

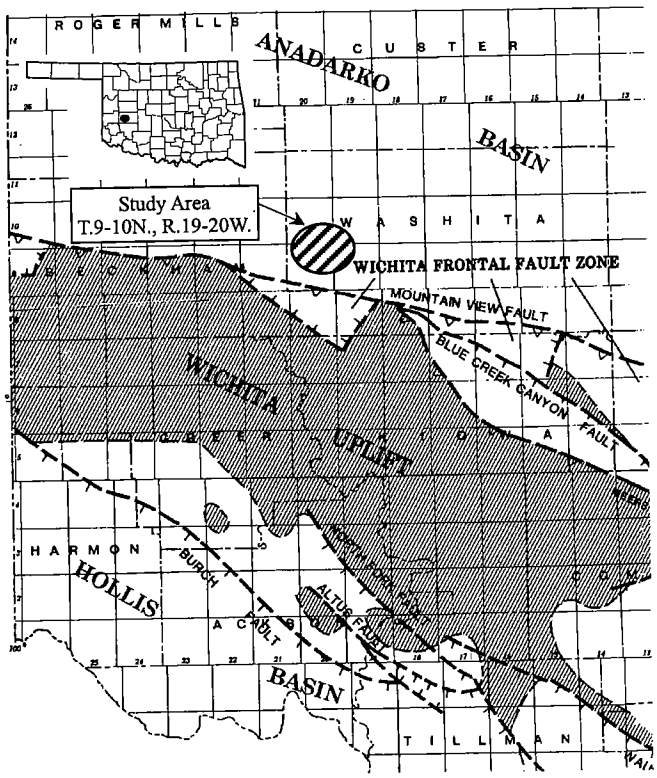

Figure 1. Map of study area in southern part of Anadarko Basin (adapted from Andrews and others, 1996).

System	Series	Group		Formation
Permian	Wolfcampian	Chase / Council Grove		Brown Dolomite
Pennsylvanian	Virgilian	Cisco	Wabaunsee	
			Shawnee	Heebner Sh.
			Douglas	Douglas
				Tonkawa
	Missourian	Hoxbar	Ochelata	Avant
				Cottage Grove
			Skiatook	Hogshooter
				Checkerboard
				Cleveland Ss.
	Desmoinesian	Deese	Marmaton Group	Big Lime
				Oswego
			Cherokee Group	**Prue Ss.**
				Verdigris Ls.
				Skinner Ss.
				Pink Lime
				Red Fork Ss.
	Atokan			Atoka
				Clinton Lake
				13 Fingers Lime
	Morrowan			Upper Morrow
				Lower Morrow
				Primrose
	Springeran			Cunningham
				Springer

Figure 2. Stratigraphic column for study area.

and they commonly exhibit gas shows. Commercial gas production has been established in several of the sands encountered in the Prue in the study area.

Although Prue Sands have demonstrated productive potential in the study area, completing these sands requires expensive hydraulic fracturing. For this reason, the reliable identification of potentially productive zones is critical in avoiding the expense of unnecessary testing. Effective petrophysical analysis and interpretation are critical toward achieving this end. Unfortunately, no Prue cores are available in the study area to provide the opportunity for rock-log calibration.

Textural and Mineralogical Complexity versus Log Data

The log suite typically available for each well in this study includes density-neutron logs, gamma-ray logs, and dual-induction laterologs or spherically focused logs (SFL), and spontaneous-potential (SP) logs. Frost and others (1982) indicated that granite-wash reservoirs throughout the southwestern United States are complex reservoirs that standard logging suites cannot reliably evaluate due to the complexity of their mineralogy. Mineral groups represented include feldspar and mica (as grains and in rock fragments) and commonly a significant clay volume. Potassium in the radioactive feldspar and mica framework grains deprives the petrophysicist of a key shaliness indicator, the conventional gamma-ray log. In addition, that these Prue Sands are gas reservoirs disproportionately affects the density and neutron logs, negating their value as reliable shale-volume indicators. Taken together this makes the identification of a clean reservoir difficult in granite wash.

Garber (1999) described the Pennsylvanian granite washes of North America's Midcontinent as exhibiting tremendous textural variance, with diverse mineralogical composition. Evaluating its reservoir potential is a daunting challenge, according to Garber, that requires combined technologies to properly address the analytical difficulties. He recommended a combination of formation-imaging and magnetic-resonance tools as the solution for improved interpretation of productive zones in granite-wash reservoirs. Frost and others (1982) previously had concluded that interpretation in granite-wash formations does not yield satisfying results when approached with conventional techniques and that natural gamma-ray spectral logs are critical to successful petrophysical interpretation in granite wash.

The combination of formation-imaging and magnetic-resonance tools could add useful information to petrophysical interpretation in granite wash, but these types of data are not routinely gathered in this study area. However, the basic strategy noted by Garber (1999) and by Frost and others (1982) is sound in recommending reliance on a variety of petrophysical measurements to produce better interpretations. The current study has shown that the complete analysis of all the important information contained in a standard logging suite is an effective method in granite-wash evaluation, leading to the development of multiple petrophysical parameters that provide more information pertinent to evaluating Prue hydrocarbon-productive potential than just calculated water saturation.

Potential for Variable Connate-Water Resistivity

In one well analyzed early in the study, the SP-deflection amplitude varies considerably among separate Prue Sands over a 300-ft interval. The mudlog, in contrast, showed that the rate of penetration (ROP) in those same sands is quite uniform, with little to no clay noted in the samples. If all the sands are reasonably clean, then something else is influencing SP development in the Prue Sands in this well. Analysis of connate-water resistivity (Rw) from SP showed that calculated Rw varied by a factor of two in different sands over that 300-ft interval. This indicated that Rw variability could be a critical issue in petrophysical analysis in Prue Sands in the study area and that simply assuming a constant Rw in all calculations for the entire interval could render misleading results. Connate-water–resistivity values published for granite-wash reservoirs in the general study area show a range of values from 0.04 to 0.4 at 100°F.

Zanier and Timko (1970) reported significant differences in connate-water salinity in Morrow sands in the Anadarko Basin east and north of the study area. In the 27 wells examined, the ratio of water-salinity values in two vertically adjacent Morrow sands ranged from 1.25 to 5.88. Zanier and Timko attributed the salinity changes to the effect of overpressuring. Al-Shaieb and others (1994) documented the presence of overpressure, not only in the Morrow but also in the Atokan and Desmoinesian intervals in this area of the Anadarko Basin.

An example of significant differences in connate-water salinity comes from the Minnelusa in the Powder River Basin (Patchett and Rausch, 1967, table 1). They reported that the salinity varied from 3,500 ppm to 35,000 ppm between two sands with about 50-ft vertical separation in one well. They also noted a change from 35,000 ppm to 200,000 ppm between two wells with about 6-mi lateral separation. Wichmann (1986) reported on a petrophysical interpretation that failed to distinguish productive from nonproductive Minnelusa sands because such changes in connate-water salinity had not been taken into account. Although this was unknown before his study, Wichmann (1986) stated that the salinity differences in adjacent sands were a result of their different environments of deposition and their consequent effect on connate-water chemistry and Rw. The Minnelusa in the Powder River Basin was deposited in cyclically alternating marine and nonmarine environments (Desmond and others, 1984).

Dutton and Land (1985) used isotopic and diagenetic evidence to propose that connate-water composition of Pennsylvanian granite-wash sands in Mobeetie Field in the Texas Panhandle might have been influenced by the inflow of meteoric water along recharge conduits adjacent to the fault-bounded highlands of the Amarillo

Uplift. The salinity of connate water in the affected beds certainly would be altered by meteoric inflow and large variations in connate-water salinity can be explained by differing sand permeability and varying access to active recharge conduits. Dutton and Land noted additional compositional changes in connate water resulting from diagenetic reactions in the sands.

Three separate processes have been recognized that could potentially lead to the development of variable salinity in granite-wash sediments in the Anadarko Basin. These include fluid transfer associated with the development of overpressure, the interfingering of marine and nonmarine depositional environments, and meteoric recharge along the adjacent Wichita–Amarillo Uplift. Variable connate-water salinity, causing variable *Rw*, must be considered a key challenge in obtaining a reliable petrophysical analysis of the Prue in the study area.

Purpose of Study

Prue Sands are viable objectives in the study area, but the identification of Prue test candidates can confound routine petrophysical analysis. The purpose of this study is to determine how to recognize producible hydrocarbon accumulations in the Prue from a standard logging suite. This must be performed in a rock-fluid system with common gas shows, complex mineralogy, textural variability, and the potential for variable *Rw* in stacked sands.

METHOD OF INVESTIGATION

Log Data

The logging-data set most commonly available in the study area includes density-neutron–gamma-ray and dual-induction laterolog (or SFL) SP logs. Potential reservoirs were identified using negative SP deflection from the shale baseline, using the procedure described by Wyllie (1963, p. 37–39). Top and bottom reservoir-bed boundaries were picked at the points of maximum inflection on the SP curve, and these were fine-tuned using the resistivity and curves from the density-neutron–gamma-ray logs. If a mudlog was available, the rate-of-penetration (ROP) curve, sample descriptions, and gas shows were also used to help define reservoir bed boundaries. The ROP curves on the mudlogs in this study are commonly not "on-depth," and, therefore, must be adjusted in order to match the wireline-log interpretation.

Formation porosity in reservoir zones was calculated using a standard density-neutron cross-plot. Deep-resistivity data were invasion-corrected using the *Advisor* software program from The Logic Group, where medium-induction–log data were available in digital format. However, pertinent resistivity ratios in these reservoirs generally fall within the area of the tornado chart where little invasion correction is required. Values of flushed-zone resistivity (*Rxo*) used in the study were calculated for each zone using relationships from Schlumberger (1989a, p. 8–11). The calculated *Rxo* data are labeled *Rxoc* to denote that they are calculated data, not measured data. (A glossary of abbreviations or symbols used for log types and petrophysical terms is presented in the Appendix.)

Spreadsheet Application

Petrophysics is an analytical science. For complex granite-wash reservoirs, however, a promising analytical technique was not immediately obvious. Consequently, the study began with the progressive development of an analytical spreadsheet that was used to test the usefulness of a variety of petrophysical techniques to address the stated problem.

Two separate spreadsheets were developed for the study. The first is used to calculate a value for *Rw* from SP in each zone of interest. In wells with multiple zones, a simple chart or plot of depth versus *Rw* is also generated to document a trend for zonal comparison within and between wells. The second spreadsheet is used for basic log-data entry and formulas to permit the use of other petrophysical calculations. A series of charts are also developed from this spreadsheet in order to display and interpret results of the techniques used in the analysis.

Connate-Water Analysis

Connate-water–resistivity (*Rw*) values are simple but critical in petrophysical analysis. A spreadsheet was developed to determine *Rw* from SP in each zone analyzed in this study based on the conventional relationship of static SP to the ratio between mud-filtrate resistivity and connate-water resistivity [*Rmf* / *Rw*]. The procedure and relationships used are shown in Dresser Atlas (1983, p. 11–13) to complete the thin-bed correction for the SP, develop a value for *equivalent connate-water resistivity* (*Rwe*) and then calculate *Rw* from *Rwe*. Calculated *Rw* values are generated in this manner for each zone of interest.

Petrophysical-Analysis Methods

Petrophysical analysis and interpretation in granite wash has been recognized (Frost and others, 1982; Garber, 1999) as a problem that requires information beyond that contained in a standard approach. Additional data from non-standard tools have been recommended as one path to a better solution to the effects of complex mineralogy and variable texture in granite-wash reservoirs. However, faced with a database that generally lacks that extra information, it was necessary to find ways to apply standard petrophysical data in such a way that more information than simple water-saturation values calculated using the standard Archie method could be obtained. A strategy of combined methods was sought.

Figure 3 shows the suite of methods compiled in the petrophysical analysis spreadsheet developed for this study. The overall approach is three-fold. First, parameters representing different aspects of reservoir quality are evaluated. Next, additional parameters providing information on the presence and movability of hydrocarbons in a reservoir are analyzed that do not require an actual water saturation calculation. Information on

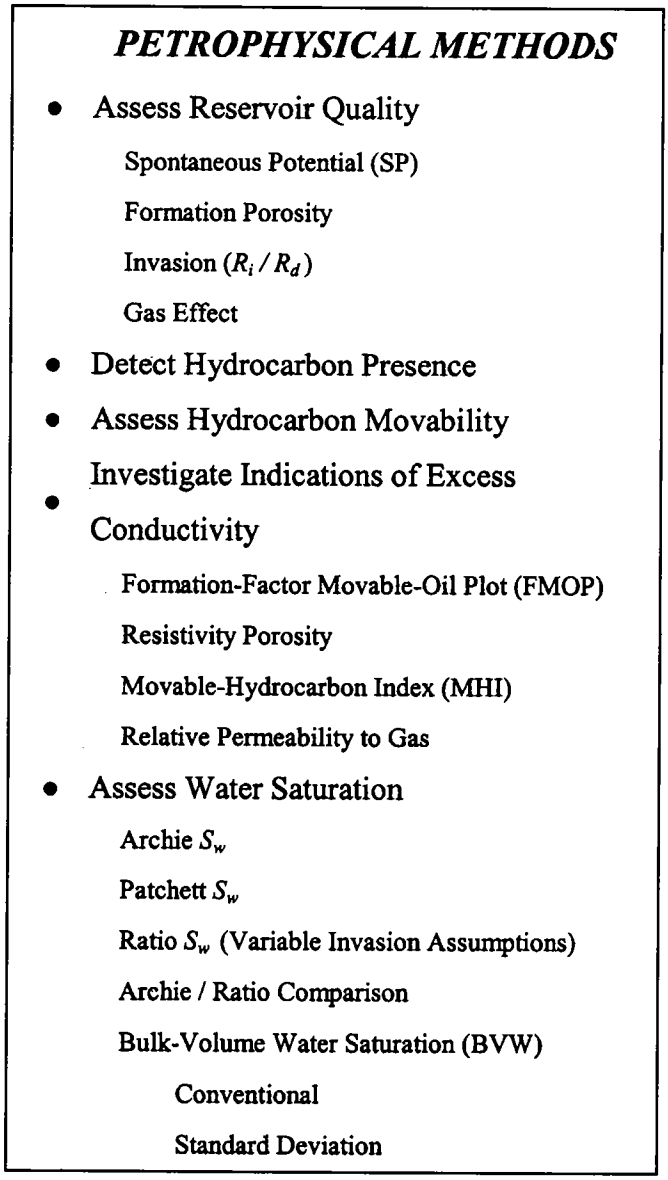

Figure 3. Petrophysical methods used in the multiple-parameter study of the hydrocarbon potential of granite-wash facies of the Prue Sands.

excess conductivity in a reservoir can also be extracted from several of these methods. Finally, the analysis includes several different methods to calculate water saturation, and each method requires different assumptions. It is useful to compare the water-saturation values from different methods. Are the resulting values comparable? And, how have the different assumptions influenced the results?

Assess Reservoir Quality

Spontaneous Potential

The first step in log analysis is to locate potentially permeable beds by distinguishing impermeable shales from non-shales (Dewan, 1983, p. 35). Generally, the gamma-ray and the spontaneous-potential logs are used for this. The presence of radioactive grains in non-shale facies renders the gamma-ray log less effective for this purpose in granite wash. However, the SP log measures electrical currents that flow naturally in borehole mud at the contact between shale and a permeable zone. Rate-of-penetration (ROP) curves and sample descriptions confirm that the SP is useful in recognizing permeable beds in Prue granite-wash sands in the study area.

One measure of reservoir quality used in this study is developed through a ratio of the amplitude of the SP deflection in any permeable zone to the maximum SP deflection across the entire Prue interval in that well. The SP development in the Prue in any given well is normalized against the maximum SP through this ratio, with values approaching 1.0 indicating a clean sand with minimum *Rw* values. Values less than 1.0 are either less clean or have a higher *Rw* and represent reservoirs with more risk for successful completion.

Formation Porosity

Formation porosity is calculated using density- and neutron-log data and the standard cross-plot relationship. Formation porosity is used as a reservoir quality indicator based on where individual reservoir porosity values fall in a range of values interpreted to represent poor to excellent Prue reservoir character.

Invasion

To prevent a blowout, standard drilling practice is to maintain hydrostatic pressure of the mud column above that of the formation pressure. The resulting "over-balance" pressure forces filtrate from the mud into permeable formations as the drill bit penetrates them. The invading filtrate replaces *in situ* formation fluids from around the wellbore, thereby creating an invaded zone that extends a few inches to a few feet into the reservoir (Dewan, 1983, p. 13).

The resistivity properties of the invading mud filtrate generally are distinct from those of the original formation fluids they replaced. A resistivity profile develops across the invaded zone that can be detected by comparing resistivity tools with different depths of investigation. Standard resistivity-logging tools are designed to measure formation resistivity in increments along the invasion profile using shallow-, medium-, and deep-reading tools.

All resistivity curves read about the same in shales because they are impermeable and therefore have not been invaded by mud filtrate during the drilling process (Dewan, 1983, p. 13, 28–29). In contrast, resistivity curves separate in permeable zones based on differences in filtrate- and formation-fluid–resistivity properties and the depth of invasion (Dewan, 1983, p. 28–29, fig. 2-4). Shallow- and deep-resistivity–curve separation, expressed as a ratio of the two measurements, has been evaluated as a reservoir-quality indicator in this study, with greater separation representing better reservoir quality.

Gas Effect

Gas effect refers to a characteristic curve crossover on density and neutron-porosity logs in gas-bearing reservoirs. The density tool measures the electron density of a formation, which is related directly to bulk density. Gas, as a low-density pore fluid, reduces formation bulk density to a greater extent than does liquid-filled porosity. The presence of gas in a reservoir, therefore, causes the density log to read lower formation bulk density and higher porosity than would be found in an equivalent liquid-filled reservoir.

The neutron tool measures the hydrogen content of a fluid-filled formation and relates that to formation porosity. Hydrogen concentration is much higher in water and in hydrocarbon liquids than in hydrocarbon gases; therefore, the neutron tool will measure less hydrogen and a much lower apparent porosity in a gas-filled reservoir than in an equivalent liquid-filled reservoir.

The classical gas-effect is caused by the opposing responses to gas seen by the combination of density and neutron-porosity logs. As density porosity increases in gas-bearing reservoirs, neutron porosity simultaneously decreases, and the two curves cross. The amount of curve separation, or crossover, is the difference between the neutron- and density-porosity readings. Shaliness will lessen this gas-effect, so that increased curve separation commonly is due to the presence of cleaner reservoir with greater gas saturation, and those zones with the larger gas-effect are considered the better candidates for economic gas production.

Detecting Hydrocarbons and Assessing Movability

The response of a reservoir rock-fluid system to the mud-filtrate–invasion process, as measured by formation-resistivity tools, provides an opportunity to detect the presence and movability of hydrocarbons in a reservoir. To augment the calculation of water saturation as the primary indicator of a hydrocarbon-productive reservoir, several additional petrophysical methods were applied to the task of detecting and assessing indications of movable hydrocarbons in the invaded zone. These methods are based on petrophysical fundamentals and provide a multiple-parameter interpretation to Prue granite-wash reservoirs.

Traditional shaliness indicators are of limited use in granite wash, as we have stated. Other studies have found certain resistivity characteristics in a reservoir can provide evidence that the rock matrix contributes to total reservoir conductivity. That characteristic is termed excess conductivity and is used in this study as a potential Prue shaliness indicator.

Formation-Factor Movable-Oil Plot

Bassiouni (1994, p. 255) described the formation-factor movable-oil plot (FMOP) as an effective method in locating movable hydrocarbons, whereas Schlumberger (1989a, p. 8–12) described it as a tool to show hydrocarbon saturation and movability. Dresser Atlas (1982, p. 161–164) reviewed the processes and relationships used to produce and evaluate the FMOP.

In the FMOP, three separate formation-resistivity–factor curves are generated and plotted across a reservoir interval. These are an *actual* formation-resistivity–factor curve and two *apparent* formation-resistivity–factor curves. The *actual* formation-resistivity–factor curve, labeled F(*DN*), is generated from the density-neutron–porosity data, using Archie's empirical correlation between the formation resistivity factor and porosity (Archie, 1942). Two *apparent* formation-resistivity–factor curves are generated, the first using resistivity data from the flushed zone (*Rxo*) and labeled the F(*Rxo*) curve, and the second using deep-resistivity data from the uninvaded zone (*Rd*) and labeled the F(*Rd*) curve.

In a wet zone, the two apparent formation-resistivity–factor curves on the FMOP, F(*Rxo*) and F(*Rd*), should overlay the third curve on the FMOP, the F(*DN*) curve. Where all three curves overlay, it indicates (1) that the apparent formation-resistivity factors for the invaded and uninvaded zones are identical to the actual wet-formation–resistivity factor and (2) that the reservoir is indeed wet.

The three curves on the FMOP will separate if a reservoir is hydrocarbon bearing, because a formation becomes more resistive where insulating hydrocarbons replace conducting brine in the reservoir pore system. The F(*Rxo*) curve increases above the wet F(*DN*) curve because of residual-oil saturation in the flushed zone. The F(*Rd*) curve increases above the F(*Rxo*) curve because of greater hydrocarbon saturation in the uninvaded zone. The amount of separation between the F(*DN*) and F(*Rd*) curves is directly related to Sw, whereas the separation between the F(*DN*) and F(*Rxo*) curves is related to the water saturation in the flushed zone (*Sxo*).

Examining the trends in the amount of separation among the curves on the FMOP across the extent of a reservoir can identify the presence of movable hydrocarbons in the reservoir, and its relationship to a producible accumulation of hydrocarbons can be assessed. The relationship among these curves provides the foundation for the method of interpretation of the FMOP data generated in this study.

Where the F(*Rxo*) curve plots as less than the F(*DN*) curve, it indicates the formation is less resistive than when its pore system is 100% water saturated, and conductivity in the rock-fluid system is in excess of that which can be accounted for by water-filled porosity. In this case, the rock matrix must contribute to electrical conductivity. This can be either through the presence of clay minerals—with their inherent property of electrical conductivity through cation-exchange capacity—or the presence of water-filled, microporous grains. Such a condition is termed "excess conductivity" (Schlumberger, 1989b, p. 43).

Resistivity Porosity

Porosity calculated from resistivity logs is not a new practice. Doll (1950) discussed the potential of the

microlog to provide a value of formation porosity using resistivity of the flushed zone (*Rxo*) and resistivity of the mud filtrate (*Rmf*) to determine the formation-resistivity factor. With a calculated value for the formation-resistivity factor, Doll applied Archie's empirical correlation of formation-resistivity factor with porosity to calculate formation porosity in the interval covered by microlog measurements. Schlumberger (1958, p. 111–116) discussed in detail the principle of porosity determination from resistivity logs.

Resistivity porosity represents water-filled porosity. Therefore, values for formation porosity calculated from resistivity data require a correction for the effects of any residual hydrocarbons in the flushed or invaded zone of the reservoir (Asquith, 1982, p. 44). Dresser Atlas (1982, p. 152–160) proposed that, if the hydrocarbon correction is not made, then conductivity-derived porosity can be used in combination with formation porosity from porosity logs as an indicator of the presence of hydrocarbons. According to Dresser, in a reservoir that is 100% wet, all the porosity is water-filled, and porosity values derived from porosity and resistivity logs should be the same. The porosity curves from each source, therefore, will overlay. However, where conductive connate water is replaced by insulating hydrocarbons in the pore system, the *resistivity porosity will be less than formation porosity* derived from porosity logs because the conductive pore volume has been reduced, and the porosity curves will separate.

In this study, values for resistivity porosity are calculated from shallow- and deep-resistivity data, each of which is compared with total formation porosity calculated from the density-neutron logs. The amount of separation of shallow-resistivity porosity from total formation porosity is a reflection of water-filled porosity in the invaded zone. The separation of deep-resistivity porosity and total formation porosity is related to water-filled porosity in the uninvaded zone.

As with the FMOP, examining the trends in the amount of separation among these curves provides the opportunity to identify the presence of movable hydrocarbons in the reservoir and assess its relationship to a producible accumulation of hydrocarbons. Again, the relationship among these curves underpins the method of interpretation of the resistivity-porosity data generated in this study.

Asquith and others (1992), in a petrophysical study of the shaly Tannehill Sandstone in Knox County, Texas, documented a case in which shallow resistivity porosity is greater than total formation porosity. This was determined to be the result of excess conductivity contributed to the reservoir rock-fluid system by the presence of illite-smectite clays. This current study of Prue Sands lacks the core data necessary to document a similar relationship. However, the condition in which shallow-resistivity porosity is greater than formation porosity is not uncommon in the Prue and is considered to represent excess conductivity, possibly due to shaliness. Asquith (1985, p. 29) indicated that excess conductivity also might be attributed to the presence of microporous grains in the reservoir.

Movable-Hydrocarbon Index

The movable-hydrocarbon index (MHI) is based on the ratio of water saturation in the uninvaded zone (*Sw*) to water saturation in the flushed (*Sxo*) or invaded zone (*Si*). In 100% water zones, $Sw = Sxo = 1.0$. If the ratio [Sw / Sxo] is less than 1.0, the value for *Sxo* must be greater than *Sw* . It then follows that residual-oil saturation (ROS) in the flushed zone is less than oil saturation (*So*) in the uninvaded zone because [$Sw + So = 1.0$] and [$Sxo + ROS = 1.0$]. Therefore, the underlying assumption is that oil originally present in the flushed zone of a reservoir was swept away from that near-wellbore region by invading mud during drilling. The ratio [*Sw / Sxo*] is, therefore, a function of the volume of hydrocarbons moved from the flushed or invaded zones during drilling. This is the *movable-hydrocarbon index* (MHI) (Asquith, 1982, p. 97). As the MHI value decreases, hydrocarbon movability increases, and the potential for a hydrocarbon-productive reservoir likewise increases.

Relative Permeability to Gas

Pirson and others (1963) developed two relationships to describe two-phase flow of gas and liquid in a reservoir. The two relationships are a function of calculated Archie water saturation and irreducible water saturation in the reservoir. The two relationships presented by Pirson and others (1963) were used to calculate values for relative permeability to gas (*Krg*) and relative permeability to water (*Krw*) in the reservoirs evaluated in this study.

Irreducible water saturation in this study is calculated using the method presented by Asquith (1982, p. 142), which assumes that each reservoir consists of medium- to coarse-grained sand. This grain-size assumption leads directly to a value for irreducible bulk-volume water (Asquith, 1982, p. 98, table 8). The referenced algorithm in Asquith was derived using this particular value of irreducible bulk-volume water and formation porosity as elements in the formation-resistivity–factor relationship. The algorithm was applied to calculate values for irreducible water saturation in the Prue reservoirs examined in this study.

If the reservoir under evaluation is not medium- to coarse-grained material, but is instead even finer grained, then the actual irreducible water saturation for the reservoir will be higher than the value calculated using this algorithm. Then, even at conditions of irreducible water saturation, the calculated relative permeability to gas in hydrocarbon-productive reservoirs will be less than 100%. It has been observed in this study, however, that the ratio of relative permeability to water to relative permeability to gas (*Krw / Krg*) will still be much less than 1.0, even in very fine grained reservoirs in hydrocarbon-productive Prue reservoirs. The relative permeability data generated in this study are interpreted in terms of this ratio. As the values of the ratio decrease, the likelihood of a Prue reservoir producing water-free gas is increased.

Assess Water Saturation

Archie Water Saturation

Archie water-saturation (*Swa*) values are calculated using density-neutron porosity and invasion-corrected deep resistivity in the Archie relationship for water saturation shown as follows (Asquith, 1982, p. 96):

$$S_w = \left(F_R \times \frac{R_w}{R_t} \right)^{\frac{1}{n}}, \text{ where } F_R = \frac{a}{\phi^m}$$

In this study, values for the *formation resistivity factor*, F_R, in Archie's water-saturation relationship are calculated based on the empirical correlation Archie developed between porosity and the formation resistivity factor (Archie, 1942). Archie's original correlation was simply [$F_R = \phi^{-m}$], where ϕ is the *porosity*, but that was expanded by later work to the more general relationship shown above. In the general correlation, the parameter a, the *tortuosity factor*, is divided by porosity, raised to the power of m. The exponent of porosity, m, is called the *cementation exponent*. The second empirical correlation developed by Archie (1942) related water saturation and the resistivity ratio of a hydrocarbon-bearing and water-saturated reservoir. In this relationship, an exponent n, called the *saturation exponent*, was presented. Standard assumptions for the values of the Archie empirical parameters, $a = 1.0$ and $m = n = 2.0$ are used to complete the formula.

Water-saturation values are interpreted based on where individual calculated water-saturation values fall in a range of values considered to represent poor to excellent hydrocarbon-productive potential in the Prue. As water-saturation values decrease, the potential for a hydrocarbon-productive Prue reservoir increases.

Patchett Water-Saturation

Patchett and Rausch (1967) examined shaly sands with variable water resistivity using a variety of input data. Their intent was to develop an improved calculated water-saturation value in shaly pay sands by incorporating the SP into Archie's standard water-saturation relationship. In this way, the effects of shaliness on SP development are intended to compensate for the effects of shaliness on the resistivity data used in the water-saturation calculation (Tixier and others, 1968, p. 19). Patchett's relationship is shown in the following equation:

$$S_w = \left[\left(F_R \times \frac{R_w}{R_t} \right) \times \left(\frac{R_{mf}}{R_{mf} - R_w} \right) \times \left(\frac{(x-1)}{x} \right) \right]^{\frac{1}{n}}$$

where $x = 10^{PSP/K}$. Patchett's relationship was used to calculate water saturation in the current study. The pseudostatic SP, called the *PSP*, represents the reduction in SP deflection from the shale baseline because of the effects of internal shale in sandstone, and K is a thermodynamic parameter in the fundamental SP equation (Dewan, 1983, p. 39; Schlumberger, 1989a, p. 4-1).

The value of water saturation from Patchett, *Swpat*, is compared with the Archie-derived value of water saturation (*Swa*) in the form of a ratio. The ratio is interpreted as a shaliness indicator—the closer this ratio is to unity, the cleaner the reservoir is considered.

The Patchett equation used in this study was examined by other authors, including Tixier and others (1968, p. 19), Fertl and Hammack (1972, p. 15–16), Dresser Atlas (1982, p.181), and Hilchie (1982, p. VII-17). These references provide useful insights into development and application of this equation.

Ratio Water Saturation

Ratio water saturation (*Swr*) is a method developed by Tixier (1949) to calculate a value for *Sw* when formation-porosity data are not available. The method is based on a ratio of Archie water saturation in the uninvaded zone (*Swa*) and the flushed zone (*Sxo*) or invaded zone (*Si*). The formation-resistivity factor is a variable used to calculate each of these water-saturation parameters and, therefore, would be cancelled-out of a ratio of the parameters. Removal of the formation-resistivity factor from the *Swr* calculation eliminates the need for porosity and the Archie empirical parameters (a and m) in the ratio water-saturation relationship. If a value for *Sxo* or *Si* is known or can be assumed in terms of *Swa*, then, with substitution, the *Swr* equation is reduced to just one unknown water-saturation value (Asquith, 1982, p. 96). Two separate relationships have appeared in the literature to address this need. Tixier (1949) examined a suite of logs from productive sands in the Rocky Mountains and developed the relationship, [$Si = Swa^{1/2}$], and Schlumberger (1989a, p. 8–7) reported a strictly empirical relationship, [$Sxo = Swa^{1/5}$].

The first relationship between the two water-saturation values, [$Si = Swa^{1/2}$], represents a reservoir condition with a smaller volume of movable hydrocarbons than does the second reported relationship, [$Sxo = Swa^{1/5}$]. Ratio water-saturation (*Swr*) calculations in this study are based on the ratio of the *Swa* and *Si* parameters, using both invasion-flushing assumptions noted above. Hence, two *Swr* values are calculated for each data-depth increment, labeled *Swr(1/2)* and *Swr(1/5)*, respectively.

Ratio water-saturation values are interpreted in analogous fashion to the Archie water-saturation values, based on where individual calculated water-saturation values fall in a range of values considered to represent poor to excellent hydrocarbon-productive potential. As ratio water-saturation values decrease, the potential for a hydrocarbon-productive reservoir increases.

Archie/Ratio Comparison

Similar results in calculated water saturation from two methods that rely on different assumptions provide confidence in the data and assumptions, as well as the results. Calculation of *Swa* values requires a value for formation porosity and assumptions concerning values for the empirical parameters, a, m, and n. Calculation of *Swr* requires neither formation porosity nor values

for a and m, but it does require an assumption concerning the volumetric relationship between water saturation in the invaded and uninvaded zones.

Archie water-saturation (Swa) values are compared with the range of ratio water-saturation values to assess the degree of similarity. If Swa values are close to $Swr(1/2)$ [where $Swr(1/2)$ = ratio water saturation using the assumption of $Si = Swa^{1/2}$], it gives confidence in the Archie water-saturation values, but suggests that any associated productive hydrocarbon pore fluids may be less movable because $Swr(1/2)$ represents less-moved hydrocarbons due to invasion. If Swa values are close to $Swr(1/5)$ [where $Swr(1/5)$ = ratio water saturation using $Si = Swa^{1/5}$], it promotes confidence in the Archie values and suggests that any associated productive hydrocarbons exhibit greater movability because $Swr(1/5)$ represents greater moved hydrocarbons due to invasion. A multiple-parameter approach to petrophysical analysis provides the opportunity to validate these possibilities through examination of other methods, such as the FMOP, resistivity porosity or MHI methods.

If Swa falls below $Swr(1/2)$, or above $Swr(1/5)$, a lower confidence in all calculated water-saturation values is indicated and should lead to inspection of the input data in both the Archie and ratio water-saturation calculations. Where Swa values are less than $Swr(1/2)$, it could indicate that the value of m used in the Swa calculation (and *not* in Swr) is too low, possibly due to the presence of vuggy porosity. Where Swa values are greater than $Swr(1/5)$, it could indicate that the value of m is too high, possibly because of excess conductivity associated with shale laminations or microporous grains in the reservoir. However, it also could indicate that the invasion assumptions used in the Swr calculations (and *not* in Swa) are not applicable to the reservoir being studied and that the Swr values are incorrect. The Archie-Ratio comparison promotes an examination of the analytical parameters used in calculating water saturation and the petrophysical character of the rock-fluid system.

Bulk-Volume Water

Morris and Biggs (1967) stated that porosity and water saturation are two essential values determined through log analysis because of their value in identifying pay thickness and in-place hydrocarbon volumes. However, by themselves, they cannot resolve whether productive hydrocarbons are present in a reservoir, so they must be augmented by parameters that will help to define the expected fluid production. Buckles (1965, p. 44–45, fig. 3c) demonstrated that a linear cross-plot of porosity and water saturation, through a reservoir at irreducible water saturation, will produce a locus of points that follows a hyperbolic trend line. The equation representing the plot is:

[Porosity × Irreducible Water Saturation = Constant]

Buckles called the constant in this equation the bulk-volume water (BVW) saturation. Buckles also reviewed studies that showed that irreducible water saturation is not fixed by porosity, but rather it varies based on particle size and the related grain surface area.

Morris and Biggs (1967) showed how a cross-plot of porosity and water saturation can be used to predict type and rate of fluid production from oil-bearing reservoirs. They demonstrated how increasing scatter in the BVW data reflects a fluid transition zone in the reservoir. The development of this scatter indicates that the product of porosity and water saturation is no longer a constant because the reservoir is not at irreducible-water saturation. Asquith (1982, p. 107, fig. 39) used three examples from the Ordovician Red River formation in North Dakota to document how increasing scatter in BVW data results in a range of decreasing oil-cut from 96% oil, to 68% oil, to 0% oil.

Bulk-volume water (BVW), the product of formation porosity and calculated Archie water saturation, has been determined through each reservoir examined in this study. A measure of the scatter in the BVW data, labeled BVW_SD, is determined by filtering the data through a standard-deviation screen. This screen was developed through standard-deviation–scatter tests on a series of computer-generated synthetic reservoirs with different porosity and water-saturation pairings. As noted in the references cited above, reservoirs at irreducible water saturation exhibit essentially constant values of BVW. Therefore, increasing scatter in the BVW data, as measured by the standard-deviation screen, represents increasing risk to the reservoir's hydrocarbon-productive capacity.

The value of irreducible water saturation depends on grain size, as noted by Buckles (1965). Therefore, *in a reservoir at irreducible water saturation*, the BVW values can be used to determine grain sizes. Calculated BVW values in this study are grouped into grain-size classes defined by Asquith (1982, p. 98, table 8), with the number of classes represented in a given reservoir reflecting the measured BVW scatter. The grain-size grouping can provide information not only on grain size, but also on the level of textural uniformity in a reservoir.

As was noted above, instead of grain-size variability, BVW data scatter can also indicate that *the reservoir is not at irreducible water saturation.* By plotting BVW values on the depth scale of the well log, the assessment can be made whether the apparent grain-size variability across a reservoir can be interpreted as a depositional artifact—such as graded bedding or variable lithologies at irreducible water saturation—or if the data are so heterogeneous that they are better explained by deviations from irreducible water saturation. On a Buckles-type porosity–water-saturation cross-plot, multiple grain-size populations and/or variable lithologies at irreducible water saturation are represented by multiple data clusters, with each cluster well defined by distinct hyperbolic trend lines.

Petrophysical-Method Plots

Four charts were developed in order to summarize the results calculated for the Prue sands using the petrophysical techniques described here. The petrophysi-

cal method charts are in standard log-data format, held so that the depth track is to the left and curve value scales are at the top and bottom of the chart. Examples from Well A in the study are included to provide an opportunity to review the informational layout and interpretational significance of the charts. Well A was perforated in a Prue Sand from 11,359 ft to 11,370 ft and completed with an initial potential of 4.9 million standard cubic ft of gas per day (mmscfpd) + 37 barrels of condensate per day (bcpd). Cumulative production for Well A is 2.9 billion cubic ft of gas (bcfg) over 78 months. The dark-gray bar along the depth axis of each chart marks the perforated interval in Well A.

It is important to understand the character of the basic log data before applying it to generate all the calculated curves on which the final interpretation will be based. The first chart (Fig. 4) is a plot of the standard log data acquired through the zone of interest. On this log-data chart, values of the GR curve are referenced to the chart-bottom scale and the values of all remaining curves are referenced to the chart-top scale. The only calculated curve on this plot is the BVW curve, which was generated by multiplying calculated BVW values by 1,000 to match the scale on this plot.

The two curves used to identify potential reservoir beds (Fig. 4) are the gamma-ray (GR) and spontaneous-potential (SP). The SP curve seems to indicate that the reservoir extends to about 11,385 ft, whereas the GR shows a marked change, from clean to hot, at about 11,372 ft. The density-neutron (DN) curves show uniform gas effect over the GR-clean interval, which ends at the GR-hot interval. Resistivity-curve separation is obvious across the GR-clean interval but is reduced across the GR-hot interval. The plotted BVW curve reads between 60 and 65 (0.060 to 0.065 × 1,000) across the GR-clean interval and climbs to about 90 across the GR-hot zone. These BVW numbers suggest the interval shown as potential reservoir by the SP is texturally bimodal, with much finer-grained rock (more grain surface area) at the bottom that grades into coarser, but clean, very fine grained sand at the top.

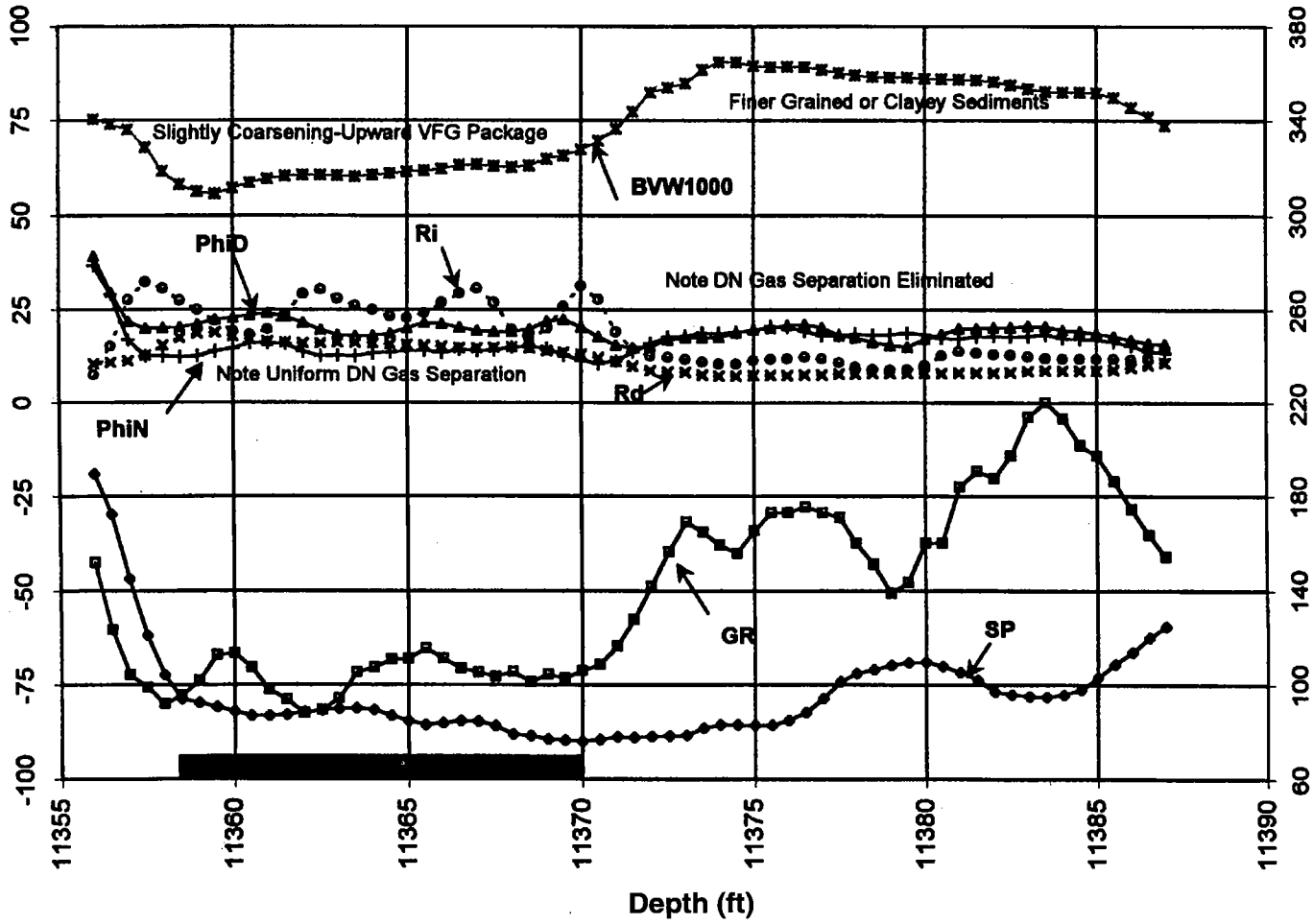

Figure 4. Well A petrophysical methods chart: plot of Prue basic log data and amplified Bulk-volume water (BVW) x 1,000 curve. *Abbreviations:* VFG = very fine grained; PhiN = neutron porosity; PhiD = density porosity; DN = density neutron log; GR = gamma-ray log; SP = spontaneous-potential log; *Ri* = resistivity of invaded zone; *Rd* = deep or formation resistivity. Depth of perforated interval shown by dark-gray bar at base of figure. Examine the chart holding the depth scale to the left; GR curve is referenced to chart-bottom scale, all other curves on this figure are referenced to chart-top scale.

Potential shaliness effects are seen on the basic log data through decreased gas effect on the density neutron (DN) curves, reduced separation of the shallow- and deep-resistivity curves, and increased GR curve radioactivity. If the reservoir is at irreducible water saturation, then the BVW curve indicates that the interval from 11,372 ft to 11,386 ft could be shaly, very fine-grained sand. It is not so shaly however, to cause the SP deflection to decrease significantly.

The standard-log curves and BVW curve provide a textural framework from which to examine the calculated data and demonstrate different reservoir-quality properties in the top half of the interval from those in the bottom half. The dark-gray bar along the depth axis shows the perforated interval, 11,359 ft to 11,370 ft. Although porosity is about the same across the entire zone (11,356 ft to 11,387 ft), the character of the standard-log data and the BVW data indicates that the perforated interval corresponds to apparently better reservoir quality than is found in the remainder of the interval.

Knowing that the zone was completed water-free indicates that it is at irreducible water saturation and that the textural information from the BVW curve is valid. However, even if this were a new well with no completion data, the textural trend with depth indicated by the BVW curve is sedimentologically reasonable and is supported by the depth trends in the standard-log data noted above. If sample descriptions also fit that analysis, it could provide important information in support of the petrophysical analysis of the zone.

The next chart (Fig. 5) is the FMOP for Well A. The SP-curve scale is at the chart top and the scale for the FMOP curves is at the bottom of the chart; the dark-gray bar along the depth axis shows the perforated interval. There are four formation resistivity factor curves on this FMOP chart, rather than three, because two curves were generated to represent change in saturation across the invaded zone: the apparent-resistivity factor from calculated flushed-zone–resistivity data, labeled F(*Rxoc*) and the apparent-resistivity factor from invaded-zone resistivity, labeled F(*Ri*).

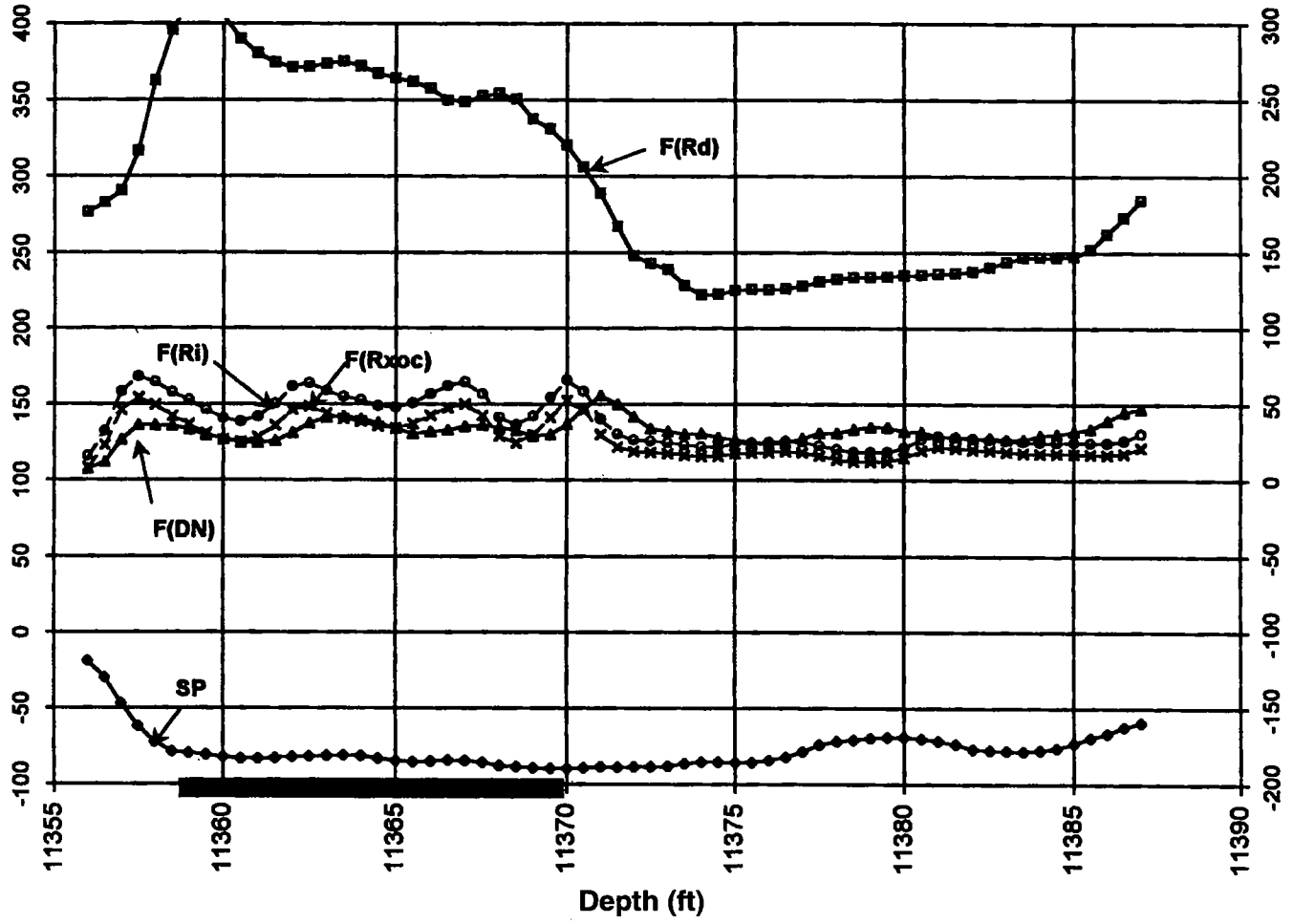

Figure 5. Well A petrophysical-methods chart: FMOP. *Abbreviations:* FMOP = FMOP = formation-factor movable-oil plot; F(*Ri*) = formation-resistivity–factor curve calculated from invaded-zone–resistivity data; F(*Rxoc*) = formation-resistivity–factor curve calculated from calculated flushed-zone–resisitivity data; F(*Rd*) = formation-resistivity–factor curve calculated from deep-resistivity data; F(*DN*) = formation- resistivity–factor curve calculated from density-neutron porosity; SP = spontaneous-potential log. Depth of perforated interval shown by dark-gray bar at base of figure. Examine the chart holding the depth scale to the left; the SP curve is referenced to the top scale and all other curves on this figure are referenced to the bottom scale of the chart.

The formation resistivity factor curves from the shallow resistivity, F(*Ri*), and calculated flushed-zone resistivity, F(*Rxoc*), nearly overlay the formation-resistivity–factor curve from formation porosity, the F(*DN*) curve. This means that the reservoir is either wet or flushed. Note the separation between the deep-formation-resistivity–factor curve, F(*Rd*), and the wet-formation–resistivity factor, F(*DN*), which indicates the presence of hydrocarbons in the uninvaded zone. The separation between F(*Rd*) and F(*Ri*), and between F(*Rd*) and F(*Rxoc*) indicates that this hydrocarbon saturation is highly movable.

The trend in the F(*Rd*) curve indicates a textural change across the SP-defined reservoir interval that supports the BVW curve on Figure 4. The perforated interval is reasonably uniform texturally with a slight gradational change from bottom to top in the perforated interval.

The dramatic decrease in the F(*Rd*) curve in the bottom half of the SP-defined reservoir indicates that the formation there is not as resistive as the top. However, the F(*Rd*) curve still maintains separation from F(*DN*), indicating that hydrocarbon saturation continues into the lower half of the SP-defined reservoir. Note that the flushed and invaded-zone formation-resistivity–factor curves, *F(Rxoc)* and *F(Ri)*, are less than the F(*DN*) curve, suggesting the presence of excess conductivity and possible shaliness in the lower half of the reservoir. All curves in Figures 4 and 5 support the idea that the SP-defined reservoir is clean in the top half (the perforated interval) and finer grained and possibly shaly in the bottom half.

Although only the top half of the reservoir was perforated, its completion using a hydraulic-fracture treatment probably means that the lower half of the reservoir is included in the completion. This is inferred because no barrier to downward fracture propagation is noted on the logs between the top and bottom of the SP-defined–reservoir zone. Initial water-free production suggests that, if the lower half of the reservoir is sufficiently permeable to contribute to production, then it too is at irreducible water saturation, although it holds more irreducible water because of its finer texture.

Figure 6 is the plot of resistivity porosity and movable-hydrocarbon–index data for Well A. The anchor curve on the plot is the total formation-porosity curve, Phi(*DN*), developed from the density-neutron–crossplot porosity. There are three resistivity-porosity curves on the plot: Phi(*Rxoc*) from calculated flushed-zone–resistivity data, Phi(*Ri*) from the invaded-zone–resistivity data, and Phi(*Rd*) from resistivity data in the uninvaded zone. There are also two MHI curves on the plot, one using the shallow-resistivity data and the other using the calculated *Rxoc* data. All four porosity curves are referenced to the top scale on the figure and the MHI curves are referenced to the bottom scale.

Resistivity-derived porosity represents water-filled porosity. The flushed- and invaded-zone–resistivity-porosity curves in the perforated interval nearly overlay total formation porosity. This indicates that formation porosity in the flushed and invaded zone is nearly all water-filled, meaning the reservoir is either wet or highly flushed. Note that the deep-resistivity–porosity curve is considerably less than the total–formation-porosity curve. Therefore, reservoir porosity in the uninvaded zone contains little water, and the reservoir is highly flushed and contains movable hydrocarbons. Separation of the Phi(*DN*) and Phi(*Rd*) curves relates directly to *Swa*, with the separation of Phi(*DN*) and Phi(*Ri*) relating to *Si* and the separation of Phi(*DN*) and Phi(*Rxoc*) relating to *Sxo*.

The MHI curves in the perforated interval are at values of about 0.4, considerably less than 1.0. This indicates moved hydrocarbons and supports the interpretation from the resistivity-porosity curves that the reservoir is saturated with movable hydrocarbons.

The flushed- and invaded-zone–resistivity-porosity curves increase to values greater than total-formation porosity in the bottom half of the reservoir, a condition similar to that noted by Asquith and others (1992). This indicates the presence of excess conductivity in the bottom half of the reservoir, once again suggesting that there could be clay (shale laminations) in the bottom of the reservoir that is not found in the perforated interval.

Figure 7 includes four water-saturation curves referenced to the chart top scale, calculated Archie water saturation (*Swa*), Patchett water saturation (*Swptcht*) and two ratio–water-saturation curves, *Swr*(1/2) and *Swr*(1/5), based on the two different invasion-flushing assumptions described above. The chart also includes two calculated relative-permeability curves referenced to the bottom scale on the figure—the relative permeability to gas (*Krg*) and the relative permeability to water (*Krw*).

Calculated Archie and Patchett water-saturation curves nearly overlay throughout the extent of the reservoir, reflecting the relatively stable SP across the reservoir. This apparently conflicts with the previously described shaliness in the bottom of the reservoir, and indicates why Archie (1950, p. 961) concluded that good sample descriptions are critical to petrophysical analysis. This result may indicate the presence of a small volume of clays with high-cation–exchange capacity in the bottom of the reservoir, and/or the presence of microporous framework grains.

Archie water saturation follows *Swr*(1/5) through the perforated interval. This gives confidence in the calculated value of *Swa* and indicates good hydrocarbon movability in the perforated interval.

In the bottom half of the reservoir, the *Swa* curve climbs above *Swr*(1/5), which raises concern about what the actual calculated water saturation is in this portion of the reservoir. Other petrophysical techniques indicate finer texture and excess conductivity in the bottom half of the reservoir. This could indicate that the value for the Archie empirical parameter (*m*) is too high and that the calculated value is wrong. Alternatively, the invasion-flushing assumptions used to calculate *Swr* could be incorrect, causing the calculated ratio water saturation to be wrong. In a new well, further effort would be required to properly characterize the bottom half of the reservoir, using guidance from the multiple-parameter interpretation. Initial

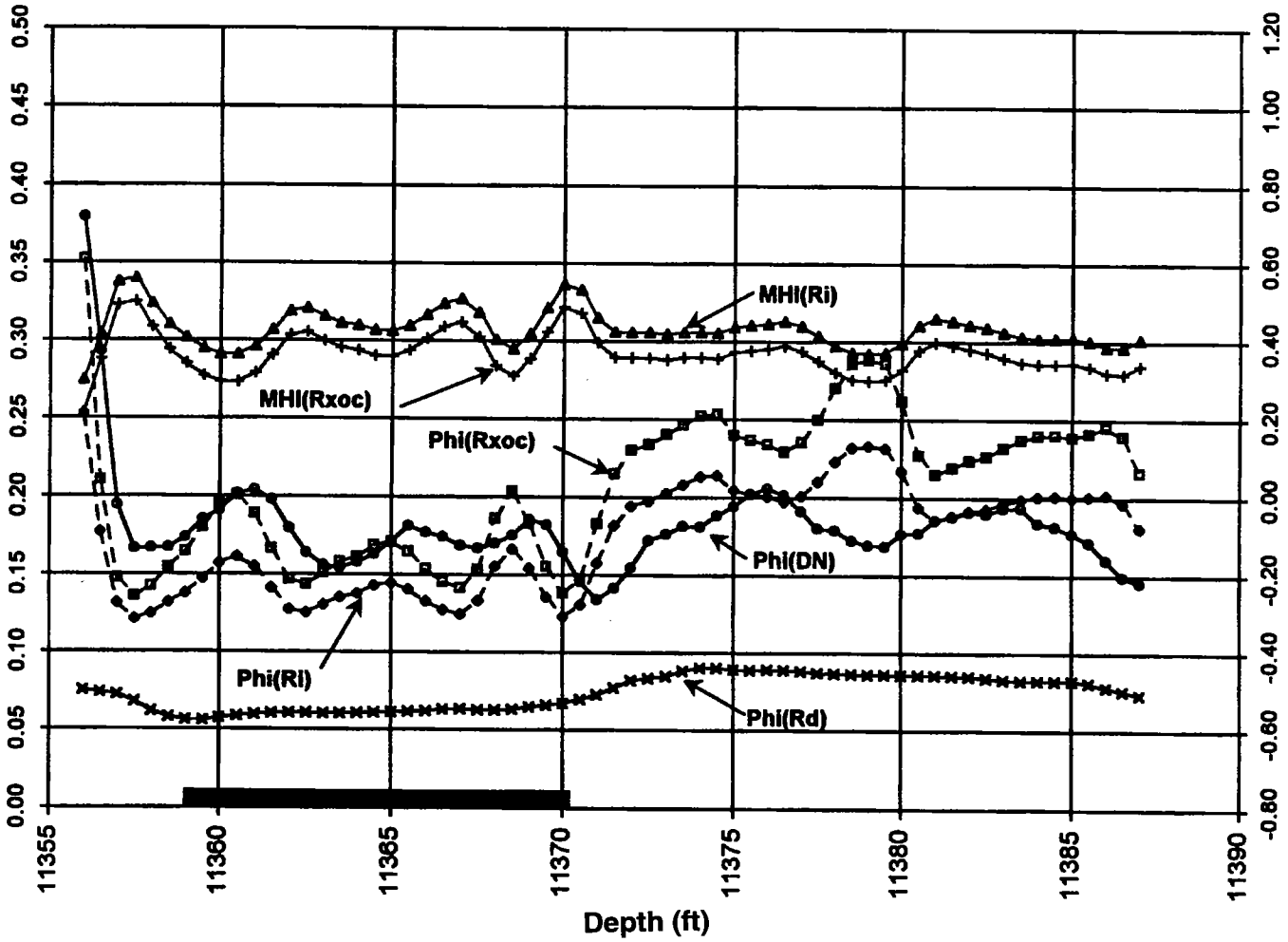

Figure 6. Well A petrophysical-methods chart. Plot of resistivity porosity and movable-hydrocarbon index. *Abbreviations:* MHI(*Ri*) = movable-hydrocarbon index calculated from resistivity of invaded zone; MHI(*Rxoc*) = movable-hydrocarbon index using resistivity of flushed zone; Phi(*DN*) = formation porosity from density-neutron cross-plot porosity; Phi(*Rxoc*) = resistivity porosity from calculated flushed-zone–resistivity data; Phi(*Ri*) = resistivity porosity from invaded zone resistivity data; Phi(*Rd*) = resistivity porosity from uninvaded zone resistivity data. Depth of perforated interval shown by dark-gray bar at base of figure. Examine the chart holding the depth scale to the left; all porosity curves are referenced to the top scale and the MHI curves are referenced to the bottom scale of the chart.

indications are that the bottom half of the reservoir contains movable hydrocarbons that could be contributing to the water-free production through hydraulic-fracture communication with the perforations in Well A.

The calculated relative permeability to water is virtually nil in the perforated interval, whereas the relative permeability to gas is about 60%. Because these are very fine-grained sands, and, as noted above, calculated *Krg* cannot be 100%, although the reservoir produces water-free. The ratio of *Krw* to *Krg* is good in the perforated interval. It remains encouraging even in the finer-textured lower half of the reservoir, where water saturations apparently increase above those in the upper half.

A thorough examination of the charts presented can lead to observations that permit a qualitative assessment of the petrophysical characteristics and hydrocarbon content of a reservoir. Using these data to develop a consistent, objective interpretation is the next step in evaluating the productive potential of a hydrocarbon reservoir.

Rank Multiple Petrophysical Parameters

Compiling the suite of petrophysical parameters effective in the evaluation of hydrocarbons in the granite-wash reservoirs of the Prue was the first critical step in this study. Ultimately, the results computed from all these parameters must be interpreted consistently and objectively.

To address the issue of consistent, objective interpretation, a ranking system was developed in this study that is intended to examine analytical results from each method through a series of logical arguments developed in Excel. Each argument is designed to examine the results of a particular petrophysical method and assign a score to the result based on how each value is

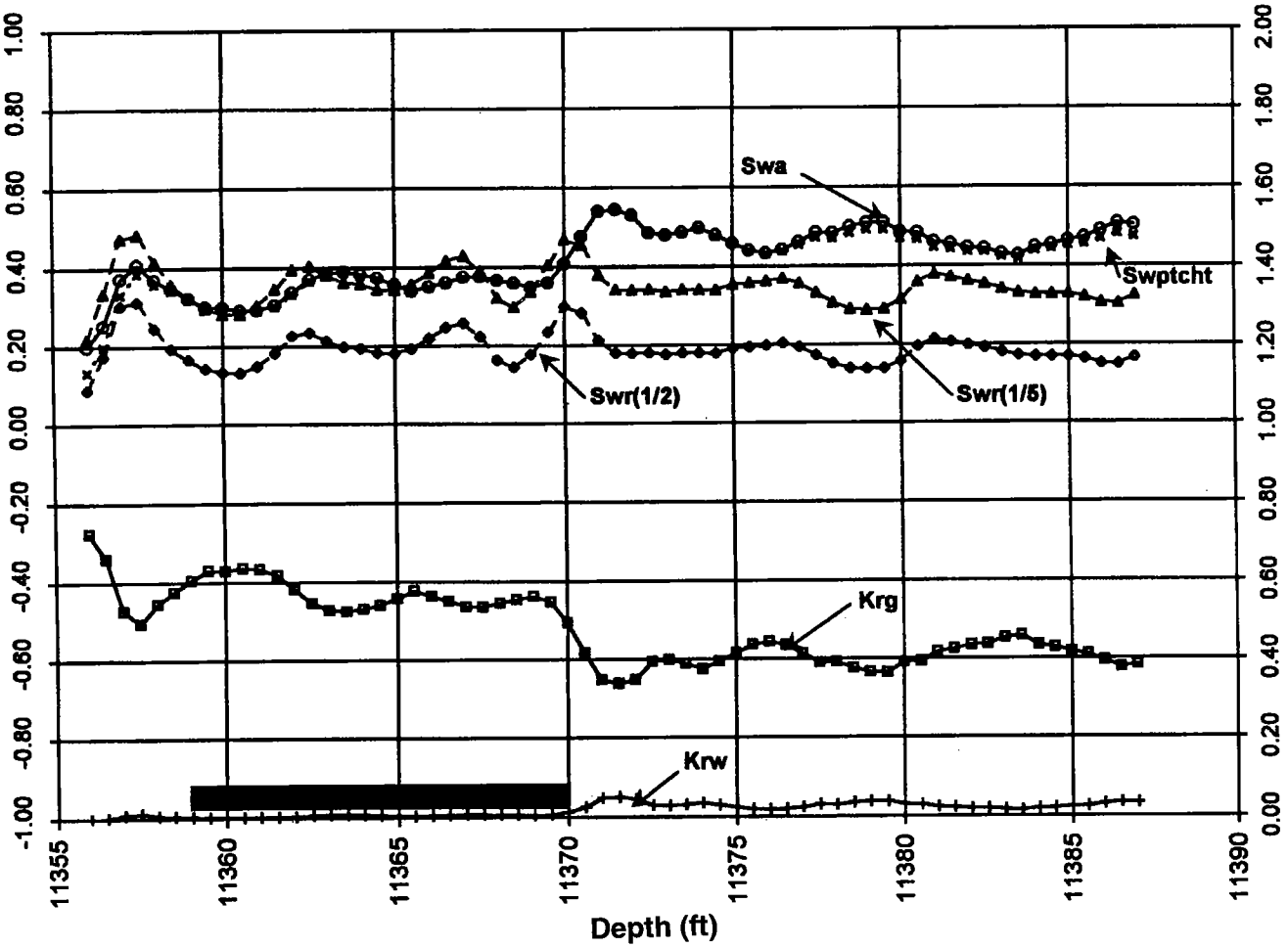

Figure 7. Well A petrophysical-methods chart. Plot of calculated water saturation values and relative permeability to gas and water. *Abbreviations: Swa* = Archie water saturation; *Swptcht* = Patchett water saturation; *Swr*(1/2) = ratio water saturation using assumption that ($Si = Swa^{1/2}$); *Swr*(1/5) = ratio water saturation using assumption that ($Swr = Swa^{1/5}$); *Krg* = relative permeability to gas; *Krw* = relative permeability to water. Depth of perforated interval shown by dark-gray bar at base of figure. Examine the chart holding the depth scale to the left; all water saturation curves are referenced to the top scale and relative permeability curves are referenced to the bottom scale of the chart.

interpreted to represent a producible volume of hydrocarbons.

Possible scores for the analytical ranking of a particular petrophysical method range from 5 to –1, with 5 the best score, representing high-rate, water-free production. A score of 1 represents a reservoir the least likely to produce water-free hydrocarbons because it is wet or tight. A zone with a score of 0 represents ambiguous petrophysical characteristics, such as possible excess conductivity or shaliness, and represents questionable potential. A score of –1 indicates that the results from one or more petrophysical methods fall outside the range considered possible. It may indicate poor data quality due to bad hole conditions, poor assumptions in the algorithms used in the method, or simply incorrect data entry.

Figure 8 is an example of the process in which analytical results from one particular petrophysical method, *movable-hydrocarbon index* (MHI), are grouped into a range of values that represents a scale for potential hydrocarbon producibility. Where the MHI ratio is about 1 (i.e., between 0.9 and 1.1), the reservoir is either wet or, alternatively, contains no moveable hydrocarbons (Schlumberger, 1989a, p. 8–7). As the value of the MHI ratio decreases from 1, it indicates that hydrocarbons are present in the reservoir with increasing movability. Where the ratio is <0.3, the values are considered to be unreasonably good for the Prue, and the input calculations should be examined. If the ratio values are >1.1, no hydrocarbons have been moved, and it is ranked 0.

In a similar fashion, every petrophysical method used in the study (see Fig. 3) was reviewed, and scores from 5 to –1 were assigned to an expected range of analytical outcomes. A logical argument was then developed in Excel for each method to properly apply these scores to the actual analytical outcomes from each method. In the Prue Sands evaluated in this study, a

$$MHI = [\, Rxo\ /Rt)/(Rmf/Rw)\,]^{0.5}$$

Score	Range
–1	MHI < 0.3
5	0.5 > = MHI > 0.3
4	0.6 > = MHI > 0.5
3	0.7 > = MHI > 0.6
2	0.9 > = MHI > 0.7
1	1.1 > = MHI > 0.9
0	MHI > 1.1

Figure 8. Movable-hydrocarbon index (MHI). Examples of ranked scores for an expected range of outcomes from a petrophysical method. *Abbreviations: Rxo* = resistivity of flushed zone; *Rt* = true formation resistivity; *Rmf* = resistivity of mud filtrate; *Rw* = resistivity of connate water.

score was generated for each analytical outcome of each petrophysical method for every 0.5 ft of depth. Under this process, a large number of score values are generated for each method across the vertical extent of a reservoir penetrated by a wellbore. To assess reservoir quality based on the scored results, the distribution of scores must be determined for each method. To accomplish this, a portion of the petrophysical-analysis spreadsheet is designed to compile the scores from each petrophysical method and calculate the relative frequency of each score. The results are displayed in a chart that includes a series of relative frequency histograms, with one histogram generated for each method.

Calibrate to Production

To develop a ranking system, the range of analytical values and respective scores in each method must be calibrated against some form of production results. The suite of petrophysical methods described here has been applied to wells that include data on perforation depths and production-test results. Final scores are compared to initial-potential (IP) results for the zone to determine how well the ranked scores represent the test results. The range of initial potential groupings used to calibrate production-test results is illustrated in Figure 9.

CALIBRATE TO PRODUCTION

Prue Initial-Potential Groupings

> 4 mmscfpd

2.0 – 4.0 mmscfpd

1.0 – 2.0 mmscfpd

< 1.0 mmscfpd

Tested and Non-Productive

Water Produced

No Production Reported (Not Completed)

Figure 9. Initial potential groupings used to calibrate production-test results in the Prue Sands examined in this study. *Abbreviation:* mmscfpd = million standard cubic feet per day.

The intent of the production-calibrated ranking system developed in this study is to provide an operator working in the Prue with more than two choices, yes or no, in test decisions. Using a ranked scoring system adds an element of risk for any zone that is considered for testing. Those that score 4s and 5s should be good test candidates. Zones that score 3s and 4s fair to good, and those with 2s and 3s risky. Calculated at 0.5-ft intervals, every reservoir will have some scatter in its scores. However, the overall ranking should be based on the score that predominates in the most methods.

Histograms for Production-Calibrated Ranking System

Examples of histograms for production-calibrated ranking systems from three wells are included to illustrate the effectiveness of this system. The reference key for each method used on the succeeding charts is identified on Figure 10. That figure is organized as follows: (1) reservoir-quality parameters are placed on the left side of the ranking histogram chart; (2) the petrophysical parameters designed to detect hydrocarbon presence, assess hydrocarbon movability, and provide indications of excess conductivity are in the central portion of the chart; and (3) the parameters used to assess water saturation are on the right side of the chart. A legend, illustrating the pattern identification for each score bar in the histogram, has been placed on the upper left of each of the succeeding charts (Figs. 11–18). On these charts, the arrangement of the vertical bars that represent the relative frequency of each score in the individual histograms on the chart proceed left to right, from 5 to –1.

Figure 11 is the ranking system histogram across the complete SP-defined reservoir interval in Well A,

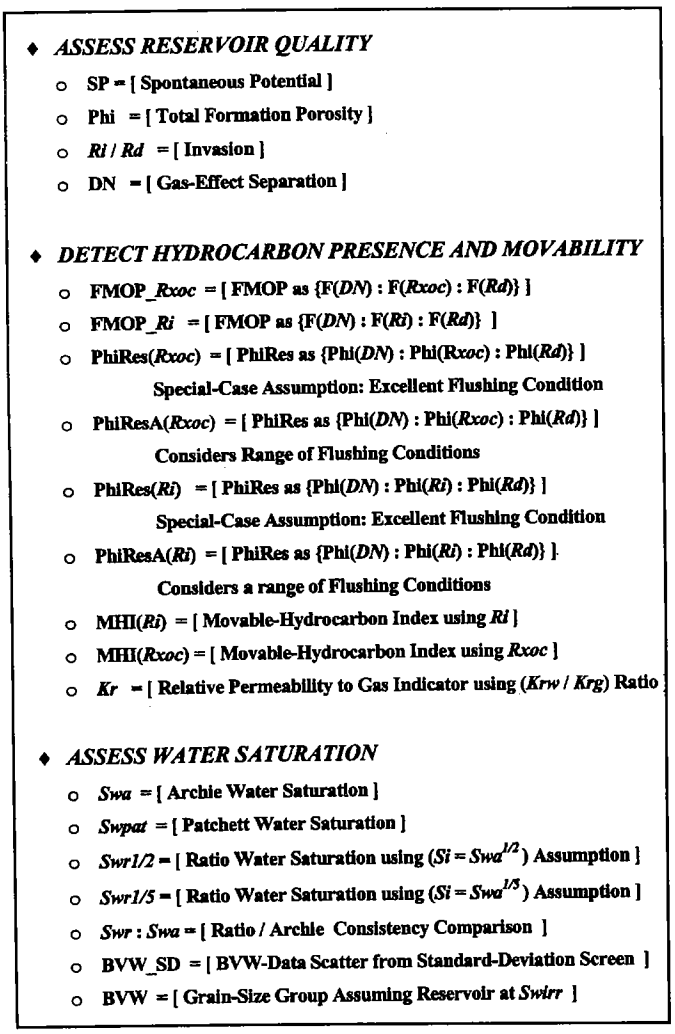

Figure 10. Legend for petrophysical methods listed along the bottom of the histograms of the production-calibrated ranking system (Figs. 11–18). See Appendix for explanation of abbreviations.

which was shown in the petrophysical methods charts in Figures 4–7. Figure 11 illustrates the relative frequency of the scores for analytical outcomes from the full suite of petrophysical methods from 11,356 ft to 11,387 ft. Reservoir-quality parameters for SP and formation porosity (Phi) are nearly all 4s and 5s. Movable hydrocarbons show some strength, with almost 40% of the scores being 5s for the FMOP and PhiResA parameters. These two parameters (FMOP and PhiResA*) also show some 0 scores, reflecting excess conductivity in the bottom half of the interval. The MHI and *Kr* parameters are very strong, as are the water-saturation values. The BVW_SD parameter shows high scatter with a score of 1, but the BVW parameter shows that this scatter is from two grain-size groups which, as can be seen on Figure 4, appear to represent graded bedding in the reservoir. This zone's scores are encouraging.

Figure 12 is the ranking histogram for the perforated interval in Well A. With an initial potential of 4.9 mmscfpd plus 37 bcpd and no water, this well falls into the highest IP-calibration group (>4 mmscfpd). Most of the petrophysical parameters have >75% of their scores as 5s. The *Swr:Swa* parameter indicates that about 80% of the Archie water-saturation values fall within the range of ratio water-saturation values. This gives confidence in the calculated values of *Swa*, which itself has a score of 100% (5s). The BVW_SD scatter measurement improved from a score of 1 to a score of 4 when the lower portion of the SP-defined zone was disregarded. Based on the BVW parameter, this portion of the reservoir has a uniform texture (one grain size). The scores match the test results well, indicating that the ranking system worked in this interval.

Two separate Prue Sands were tested in Well B. The shallower was perforated and tested from 11,237 ft to 11,251 ft, where its IP was 2.46 mmscfpd plus 30 bcpd (barrels of condensate per day) and no water and had a cumulative production of 1.45 bcfg over 112 months. Figure 13 is the ranking histogram for this interval in Well B. Score frequencies for the SP and Phi reservoir-quality parameters are predominantly 4s and 5s. The FMOP and PhiResA parameters show 5s and 4s, but included many 0s, indicating apparent excess conductivity in the reservoir. The movable-hydrocarbon index (MHI) and *Kr* parameters are encouraging, but *Swa* is showing a range in values from 2s to 5s. The values for *Swpatchett* show that the SP is stable and does not indicate a lot of shaliness in the reservoir, in contrast to the apparent excess conductivity indicated by the 0s in the FMOP and PhiRes parameters. The *Swr1/2* and *Swr1/5* parameters look good, but the agreement between *Swa* and *Swr*, as measured by the *Swr:Swa* parameter, is not good, indicating limited confidence in the calculated water-saturation values. The BVW parameters show a lot of scatter, but, because the well completed water-free, the zone is at irreducible water saturation, although the scatter probably indicates textural heterogeneity that could create treatment and production difficulties. There are encouraging scores in the zone, but the overall score frequencies indicate it should not be the quality of Well A.

Figure 14 is the ranking-system histogram that represents the interval 11,239–11,246 ft, a high-graded subzone within the overall perforated interval examined in Figure 13. Scores for the FMOP, PhiResA and *Swa* parameters in Figure 14 are predominantly 4s and 5s, with some 3s. The score for the *Swr:Swa* comparison almost doubled with the high-grading of the interval, bringing more confidence in calculated water-saturation values. The ranking histogram represented by Figure 14 contains scores of 3 through 5, suggesting

*The PhiResA is a reference analogous to the use of FMOP. It is a general petrophysical parameter on the ranking histogram. It is defined specifically on Figure 10, and is based on the analysis of results of the resistivity porosity calculations shown as curves on Figure 6, using the logical argument described above to assign scores to the results of the analysis of the resistivity-porosity data. We did not plan to review the method for all the petrophysical parameters, intending instead that the MHI example (Fig. 8) demonstrates the general analytical process.

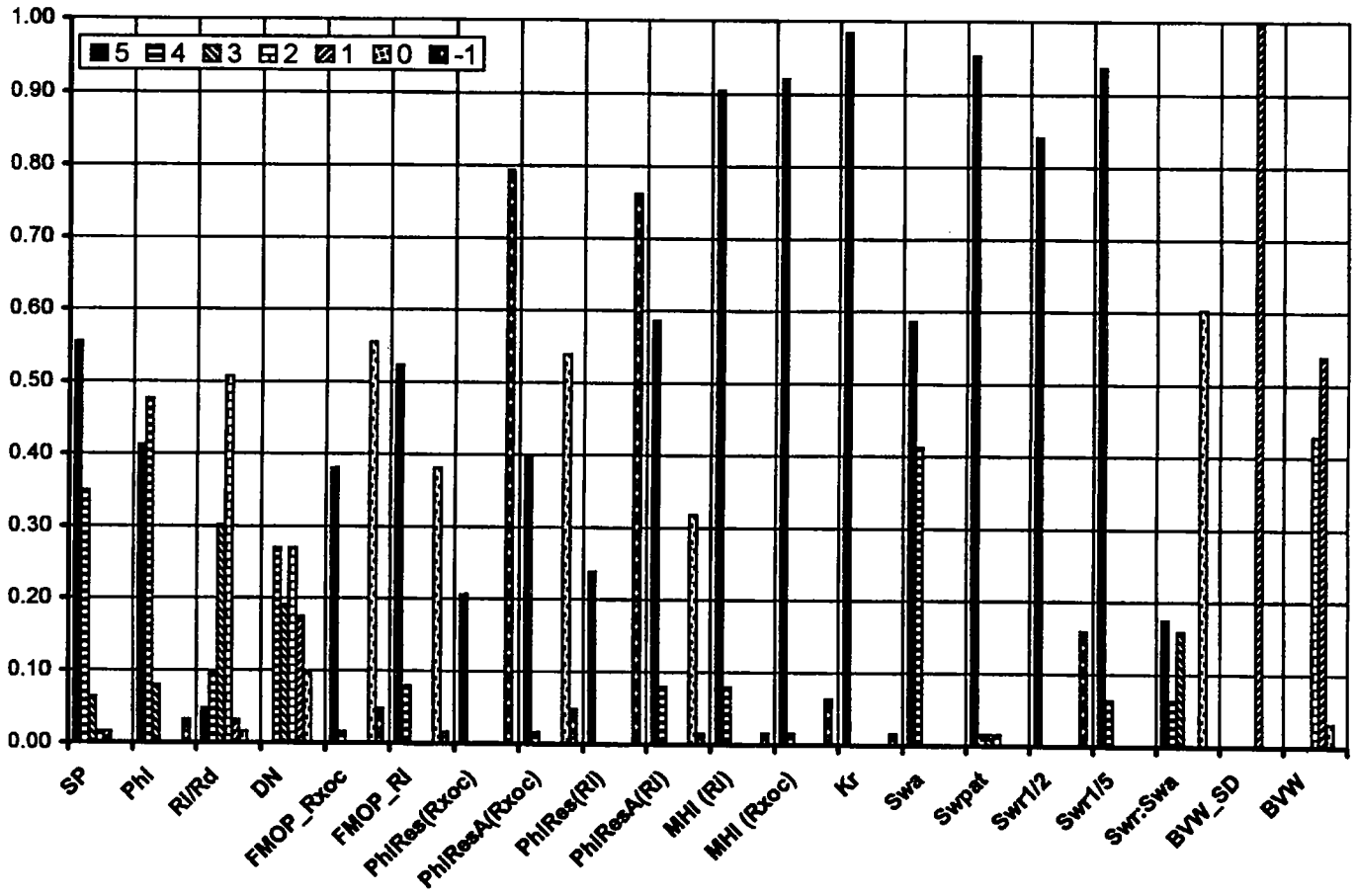

Figure 11. Well A: Histogram of production-calibrated–ranking system for the SP-defined reservoir interval (11,356–11,387 ft), that is represented by the petrophysical methods plots in Figures 4–7. Compare the range of scores with characteristics on the method plots. See Appendix for explanation of abbreviations.

that most of the production in the overall perforated interval is coming from this high-graded subzone. The overall interval is texturally heterogeneous, but the BVW parameter indicates that the subzone is more uniform and is composed primarily of one grain size. Although not in the class of Well A, the ranking histogram indicates this zone should be tested.

Figure 15 is the ranking histogram for the second (deeper) Prue Sand tested in Well B, from 11,552 to 11,578 ft. The zone flowed 0.353 mmscfpd plus 336 bw (barrels of water) and was not completed. The histogram shows that the SP, which exhibits a predominant score of 3, is not as well developed as much of the rest of the Prue in this well. The FMOP and PhiResA parameters have a predominance of 0s, indicating excess conductivity in the reservoir with very little indication of movable hydrocarbons in the sand. The *Kr* parameter indicates calculated relative permeability to gas is poor, and the *Swa* scores are predominantly 2s. The *Swa:Swr* parameter indicates little correlation between ratio and Archie saturation values, and the BVW_SD parameter has the most scatter seen in any of the zones examined. The predominance of 0s and dearth of 4s and 5s makes this sand too risky to contemplate completion.

Two separate Prue Sands were also tested in Well C, and the results provide a good example of the potential for a failed interpretation and unnecessary testing if a constant *Rw* is assumed. The shallower sand in Well C was perforated and tested from 11,098 to 11,114 ft. The initial potential was 3.7 mmscfpd plus 43 bcpd and no water. Cumulative production from this sand in Well C was 1.95 bcfg over 78 months.

Figure 16 is the ranking histogram for this Prue Sand in Well C. This shows a predominance of 4s and 5s. Scores for the FMOP and PhiResA parameters indicate that the sand is saturated with movable hydrocarbons, with the MHI parameters all 4s and 5s. Relative permeability to gas and the *Swa* parameters show scores of all 5s. Almost 80% of the *Swa* values fall within the range of ratio water-saturation values, adding confidence to the quality of the *Swa* values calculated in this sand. The BVW_SD parameter shows minimal scatter and BVW is scored a 3. Grain size in the reservoir indicated by the BVW grades from fine- to very fine grained. The recommendation based on this histogram would be for a test of this sand, with the expectation of strong production similar to that seen in Well A.

The second Prue Sand tested in Well C was perfo-

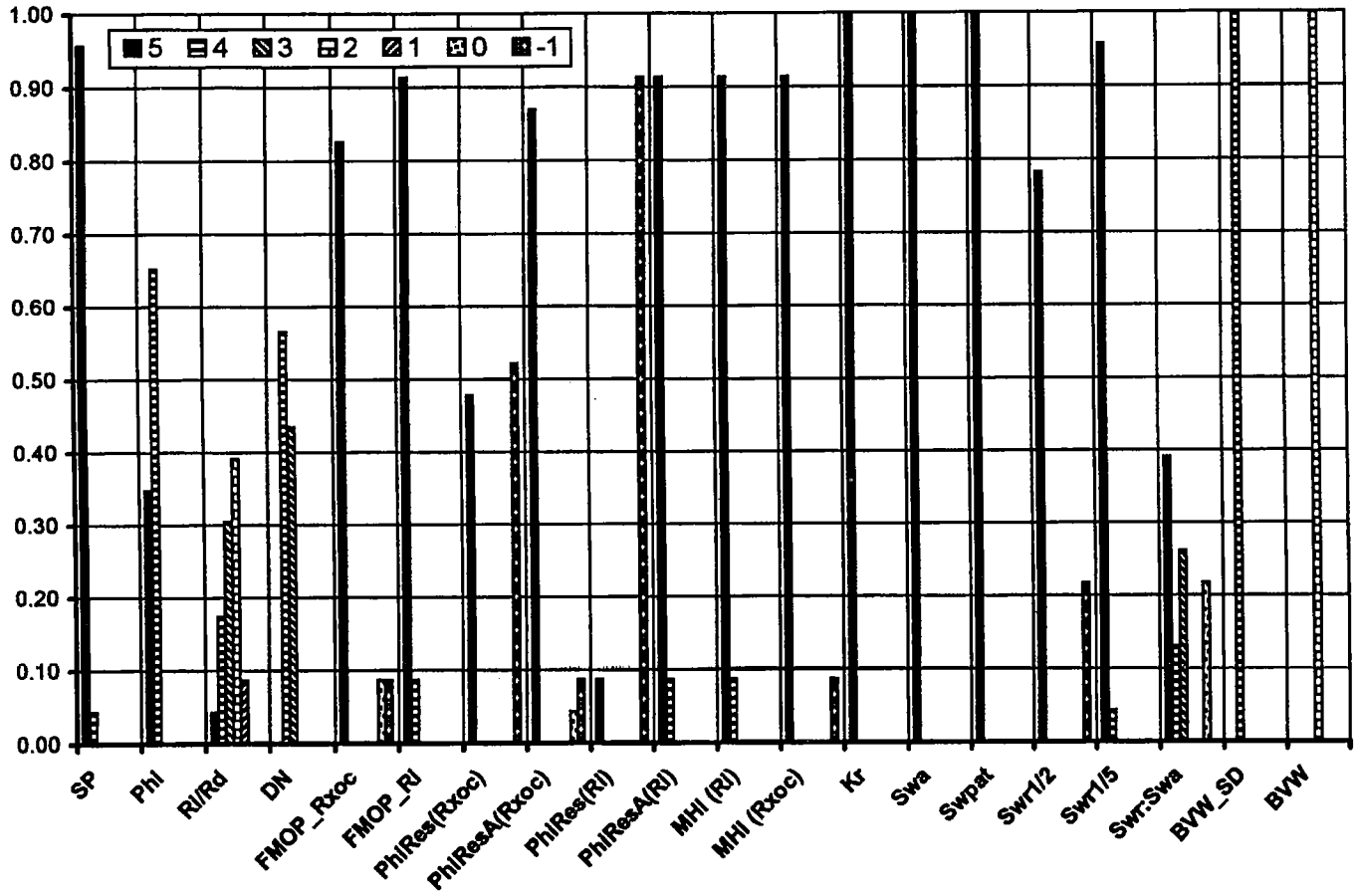

Figure 12. Well A: Histogram of production-calibrated–ranking system for the SP-defined reservoir interval, 11,359–11,370 ft. Initial production was 4.9 mmscfpd (million standard cubic feet per day) + 37 bcpd (barrels of condensate per day) and no water. Cumulative production was 2.9 bcfg (billion cubic feet of gas) over 78 months. See Appendix for explanation of abbreviations.

rated from 11,401 to 11,416 ft. It was production tested and swabbed unmeasured gas plus 41 barrels of water. The sand was not completed. Figure 17 is the ranking histogram for this sand. The scores are predominantly 5s for all the petrophysical parameters and BVW-data scatter is very low, apparently indicating the reservoir is at irreducible water saturation. However, this analysis contradicts the test results. Caution is indicated by the scores for the SP parameter and the *Swpat* (Patchett *Sw*), which are all 1s and 2s, respectively.

The value for *Rw* used in the analysis of this lower sand is 0.065, a value similar to the *Rw* used in the productive upper sand. The SP-parameter scores for the upper Prue Sand in Well C on Figure 16 are predominantly 4s and 5s. The SP deflection in the upper Prue Sand is as great as that in any other Prue Sand in Well C, whereas the scores in the lower sand indicate that its deflection is considerably less than other Prue Sands in Well C. This variable SP deflection between zones could be a result variable *Rw*. If that is the case, then the use of a similar *Rw* in the lower zone would be incorrect.

This interval was reanalyzed using a value for *Rw* that was calculated from its SP deflection rather a value that seemed to work in another Prue Sand in the same well. The new *Rw* value is 0.21, and the results from this new analysis are shown on Figure 18. Scores are now predominantly 2s, except those for the *Swpat* parameter, which are now 80% 5s. Patchett agrees with the higher values of Archie. Nothing on the ranking histogram shown in Figure 18, based on the new *Rw*, would indicate that this sand be tested.

Ranking-histogram examples from three productive Prue Sands were examined. These show a range of scores that provide a representation of the range in production results that were seen. Scores on the ranking histograms for the productive sands from Wells A and C (Figs. 12 and 16, respectively) indicate each of the sands to be valid test candidates with low risk and high expected-production rates. Well A scored better than Well C and produced better, although both had good results.

The initial-potential and cumulative-production values from the productive sand in Well B are about half that seen in Well A. The scores on the ranking histograms for the productive Well B sand (Figs. 13, 14) clearly indicate that it would represent a riskier test candidate, with lower production expectations. Had the

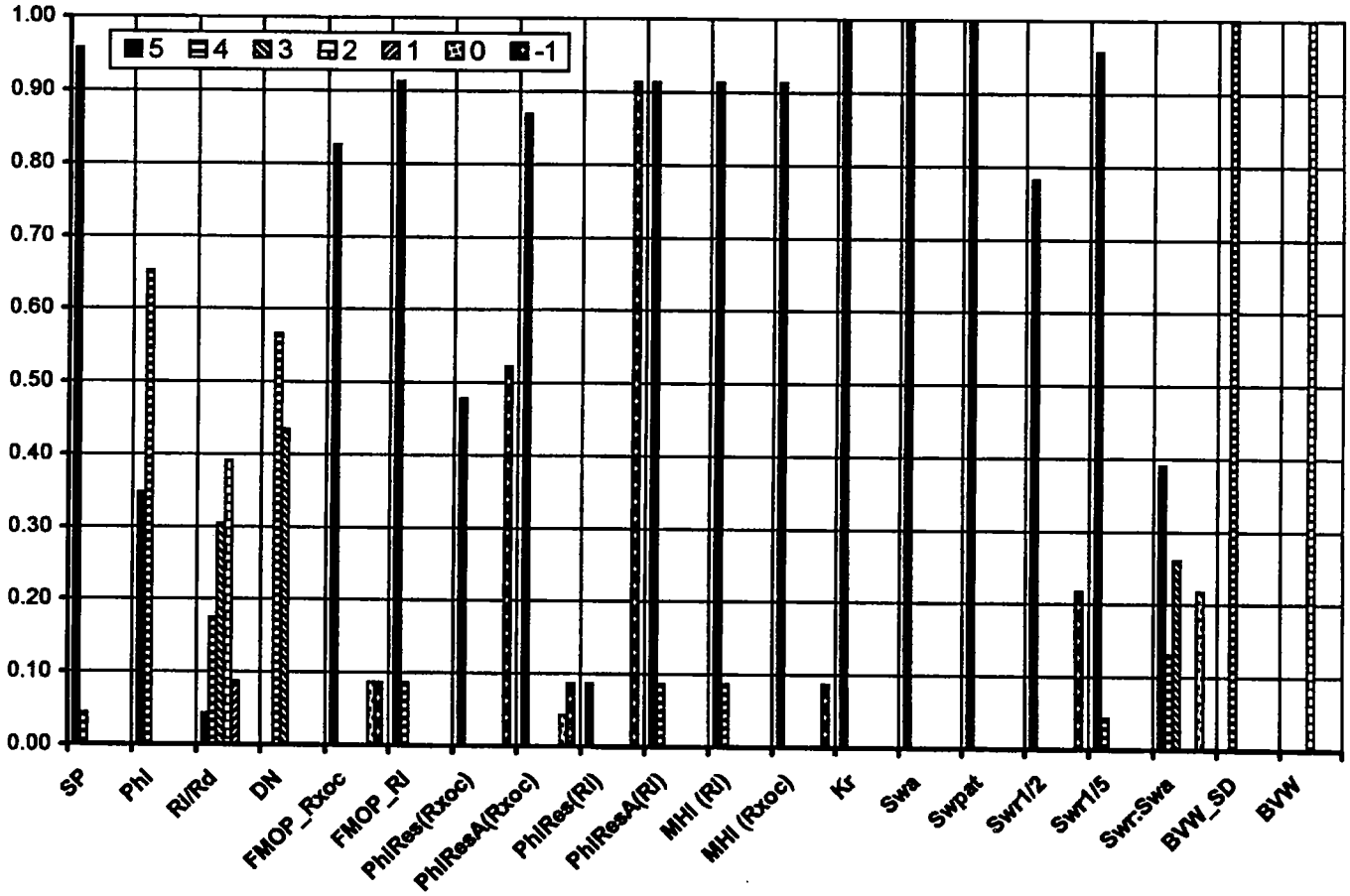

Figure 13. Well B: Histogram of production-calibrated–ranking system for the perforated interval, 11,237–11,251 ft. Initial production = 2.46 mmscfpd (million standard cubic feet per day) + 30 bcpd (barrels of condensate per day) and no water. Cumulative production = 1.45 bcfg (billion cubic feet of gas) over 112 months. See Appendix for explanation of abbreviations.

Prue Sand in Well A been in Well B, the ranking of the two sands would have been straightforward.

Two Prue Sands, the ranking histograms of which (Figs. 15, 18) indicated would be poor candidates, were tested. Field-test results on these zones were so poor that neither was completed. Figure 17 demonstrates the risk for failed completions in Prue Sands that can result from assuming a constant *Rw* in a petrophysical evaluation of stacked sands in the Prue.

BLIND TEST

This method of petrophysical evaluation through the analysis and interpretation of multiple petrophysical parameters was tested in two wells in which the test results were not known. One well was completed successfully whereas the other was tested wet and abandoned. Zones of interest in both wells had similar mudlog shows. The ranked multiple approach was able to distinguish productive from non-productive sands.

CONCLUSIONS

This study has shown that a ranked-multiple–parameter approach to petrophysical analysis and interpretation, using a standard suite of logging data, can be used to distinguish variation in production potential in Prue Sands in the study area. The recognition that the value of *Rw* can vary among the stacked Prue Sands was necessary to properly distinguish variation in production potential.

This method represents an Expert System approach to petrophysical analysis and interpretation, relying on ranking factors and methods selected in this study. However, the ranking factors and methods were selected through calibration to production in the zone of interest. This can be recalibrated by operators in other parts of the Anadarko Basin, separated both geographically and stratigraphically from the Prue in Washita County. Every operator should be an expert in calibrating his test results to the petrophysical analysis that led to the test. The ranked-multiple–parameter approach developed in this study provides one way to do that.

ACKNOWLEDGMENTS

Burlington Resources, Midland, Texas, provided generous funding to support this study and data to

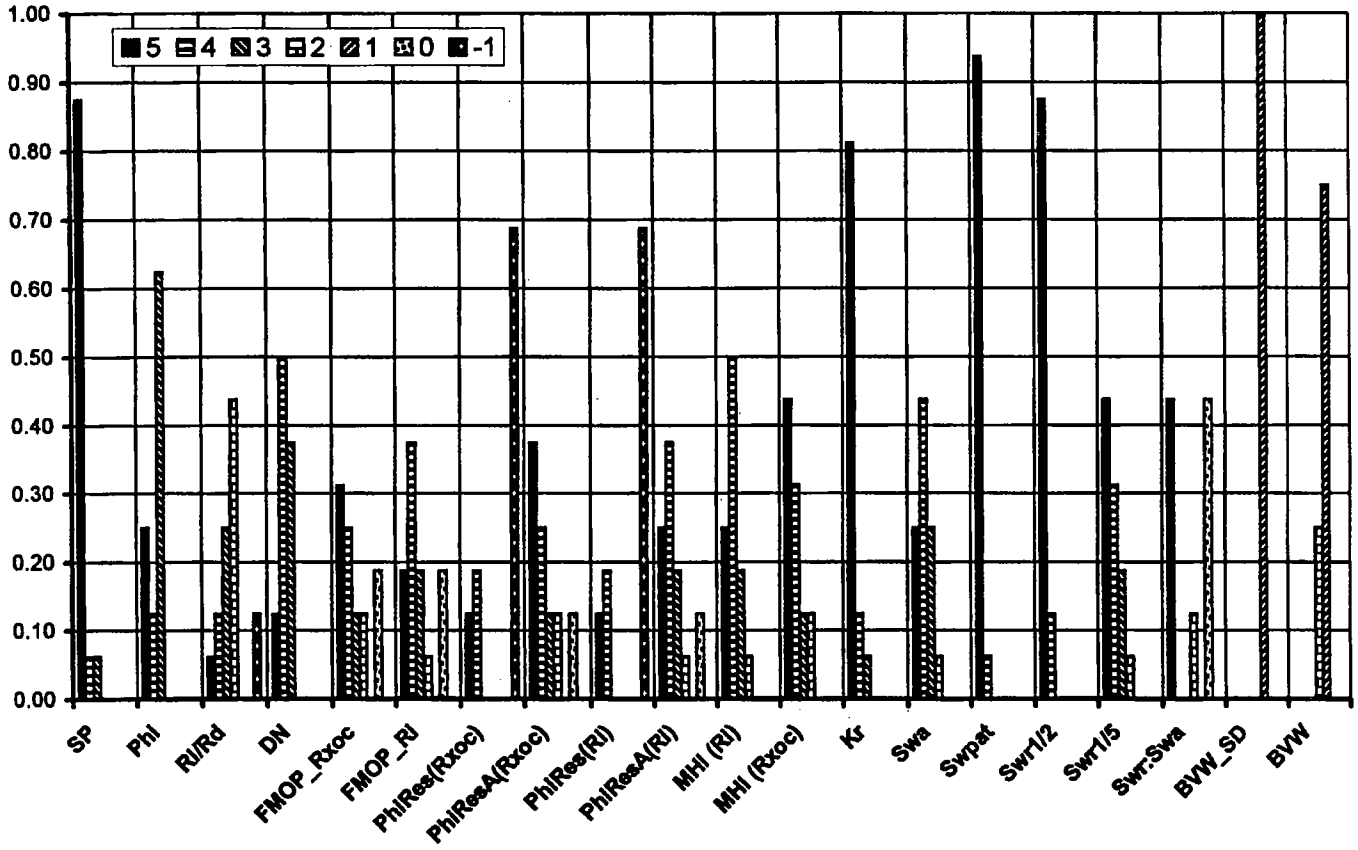

Figure 14. Well B: Histogram of production-calibrated–ranking system for high-graded subzone, 11,239–11,246 ft, of the perforated interval shown in Figure 13. Compare the scores on Figures 13 and 14 to assess if most of the production from the overall perforated interval in this Prue Sand, represented by Figure 13, may be coming from the subzone represented by Figure 14. See Appendix for explanation of abbreviations.

complete the study, and their personnel always were accessible to answer questions and helpful with additional data requests.

REFERENCES CITED

Al-Shaieb, Zuhair; Puckette, J. O.; Abdalla, A. A.; and Ely, P. B., 1994, Megacompartment complex in the Anadarko Basin: a completely sealed overpressured phenomenon, *in* Ortoleva, P. J. (ed.), Basin compartments and seals: American Association of Petroleum Geologists Memoir 61, p. 55–68.

Andrews, R. D.; and others, 1996, Fluvial-dominated deltaic (FDD) oil reservoirs in Oklahoma: the Skinner and Prue plays: Oklahoma Geological Survey Special Publication 96-2, 118 p.

Archie, G. E., 1942, The electrical resistivity log as an aid in determining some reservoir characteristics: Transactions of the American Institute of Mining and Metallurgical Engineers (AIME), v. 146, p. 54–62

_____ 1950, Introduction to petrophysics of reservoir rocks: American Association of Petroleum Geologists Bulletin, v. 34, p. 943–961

Asquith, G. B., 1985, Handbook of log evaluation techniques for carbonate reservoirs: American Association of Petroleum Geologists, Methods in Exploration Series No. 5, 47 p.

Asquith, G. B.; with Gibson, C., 1982, Basic well log analysis for geologists: American Association of Petroleum Geologists, Tulsa, Oklahoma, 216 p.

Asquith, G. B.; Thomerson, M. D.; and Saha, S., 1992, Petrophysical study of the Permian Tannehill Sandstone, Knox County, Texas, *in* Mruk, D. H.; and Curran, B. C. (eds.), Permian Basin exploration and production strategies: applications of sequence stratigraphic and reservoir characterization concepts: West Texas Geological Society Symposium, Publication 92-91, p. 123–133.

Bassiouni, Z., 1994, Theory, measurement, and interpretation of well logs: Society of Petroleum Engineers Textbook Series, v. 4, 372 p.

Buckles, R. S., 1965, Correlating and averaging connate water saturation data: The Journal of Canadian Petroleum Technology, January–March, p. 42–52.

Desmond, R. J.; Steidtmann, J. R.; and Cardinal, D. F., 1984, Stratigraphy and depositional environments of the Middle Member of the Minnelusa Formation, Central Powder River Basin, Wyoming, *in* Goolsby, J.; and Morton, D. (eds.), The Permian and Pennsylvanian geology of Wyoming: Wyoming Geological Association Guidebook, p. 213–239.

Dewan, J. T., 1983, Essentials of modern open-hole log interpretation: PennWell Books, Tulsa, Oklahoma, 361 p.

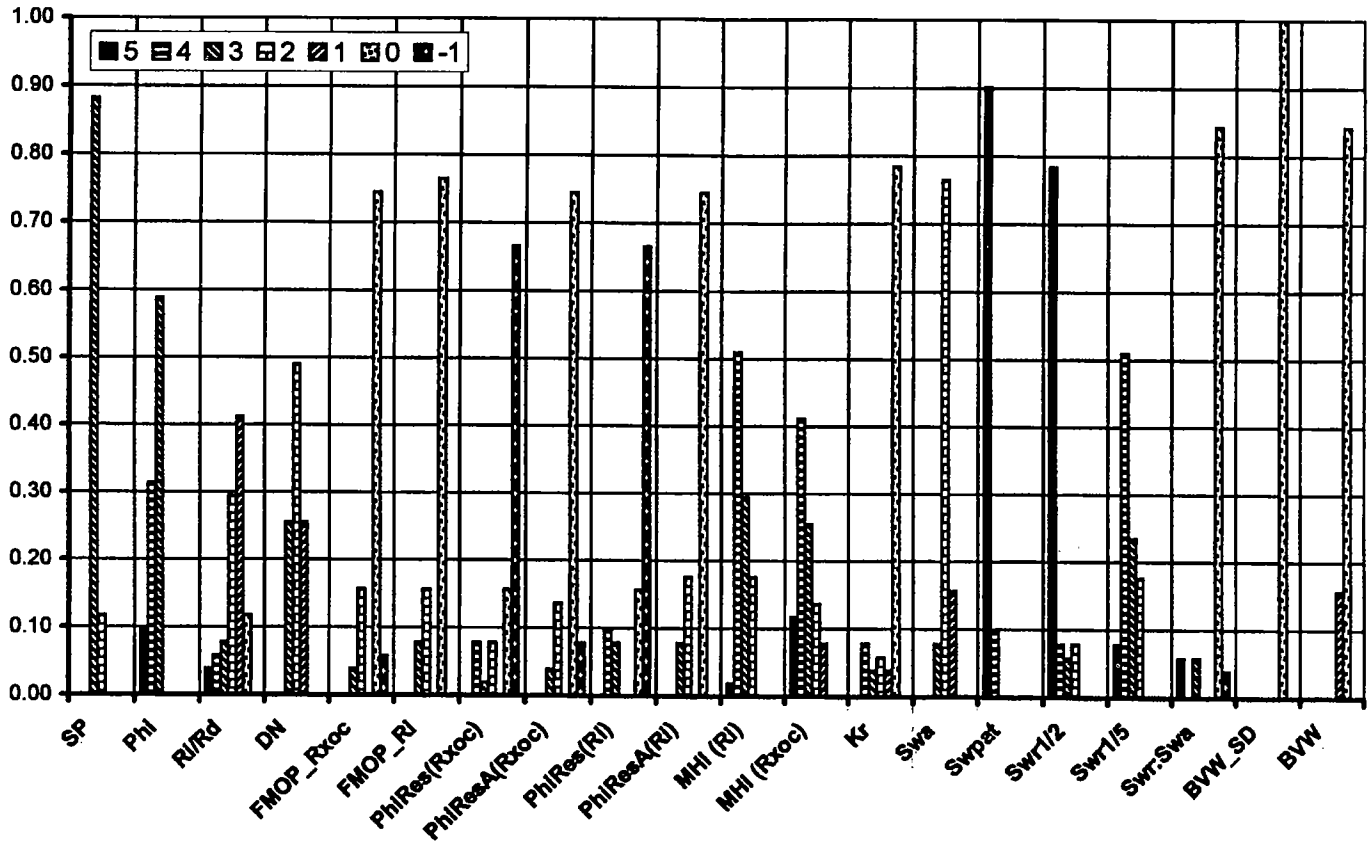

Figure 15. Well B: Histogram of production-calibrated–ranking system for the zone test from 11,552–11,578 ft. This Prue Sand interval was production tested and flowed 0.353 mmscfpd (million standard cubic feet per day) plus 336 barrels of water and was not completed. Note the lack of strong indication of presence of movable hydrocarbons and the very low rank of the BVW_SD parameter indicating a high degree of scatter in the BVW data and consequent risk of a high water-cut test. Using the ranking system histogram, it is likely that this zone would have been rejected as a test candidate. *Abbreviations:* BVW = bulk-volume water saturation; BVW_SD = scatter in BVW data from standard-deviation screen. See Appendix for explanation of abbreviations.

Doll, H. G., 1950, The Microlog—a new electrical logging method for detailed determination of permeable beds: Society of Petroleum Engineers Reprint Series No. 21, Openhole Well Logging, p. 74–83.

Dresser Atlas, 1982, Well logging and interpretation techniques: The Course for Home Study [3rd edition]: Dresser Atlas, Dresser Industries, Inc., 211 p.

_____ 1983, Log interpretation charts: Dresser Atlas, Dresser Industries, Inc., 149 p.

Dutton, S. P., 1982, Pennsylvanian fan-delta and carbonate deposition, Mobeetie Field, Texas Panhandle: American Association of Petroleum Geologists Bulletin, v. 66, p. 389–407.

Dutton, S. P.; and Land, L. S., 1985, Meteoric burial diagenesis of Pennsylvanian arkosic sandstones, southwestern Anadarko Basin, Texas: American Association of Petroleum Geologists Bulletin, v. 69, p. 22–38

Edwards, A. R., 1959, Facies changes in Pennsylvanian rocks along the north flank of Wichita Mountains, *in* Petroleum geology of southern Oklahoma, v. II: American Association of Petroleum Geologists, Tulsa, Oklahoma, p. 142–155.

Fertl, W. H.; and Hammack, G. W., 1972, A comparative look at water saturation computations in shaly pay sands: The Log Analyst, v. 13, no. 2, p. 12–20.

Frost, E., Jr.; Allen, T.; and Fertl, W. H., 1982, Formation evaluation in granite wash reservoirs: World Oil, September, p. 121–132.

Garber, M., 1999, Improved interpretation in the granite wash features combined measurements [abstract]: Presentation to Panhandle Geological Society, Amarillo, Texas, March, 31, 1999 (published as part of a 2-page meeting announcement).

Hilchie, D. W., 1982, Advanced well log interpretation: Douglas W. Hilchie, Inc., Golden, Colorado, p. I-1 to XI-14, 359 p.

Morris, R. L.; and Biggs, W. P., 1967, Using log-derived values of water saturation and porosity: Transactions of the Society of Professional Well Log Analysts Eighth Annual Logging Symposium, Paper X, 26 p.

Patchett, J. G.; and Rausch, R. W., 1967, An approach to determining water saturation in shaly sands: Journal of Petroleum Technology, October, p. 1395–1405.

Pirson, S. J.; Boatman, E. M.; Nettle, R. L., 1963, Prediction of relative permeability characteristics of intergranular reservoir rocks from electrical resistivity mea-

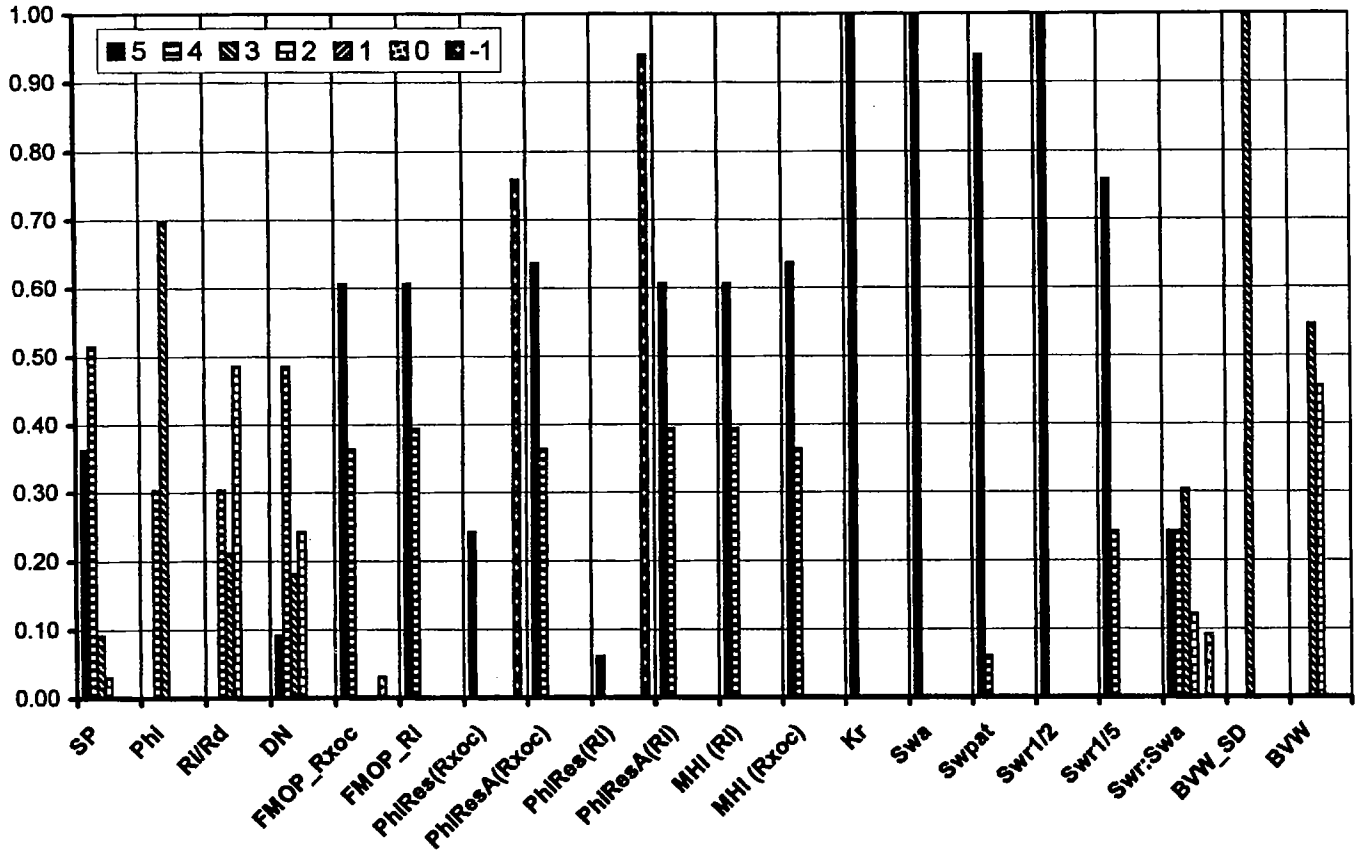

Figure 16. Well C: Histogram of production-calibrated–ranking system for the perforated interval, 11,098–11,114 ft. Initial production = 3.7 mmscfpd (million standard cubic feet per day) + 43 bcpd (barrels condensate per day) and no water. Cumulative production was 1.95 bcfg (billion cubic feet of gas) over 78 months. Note the overall preponderance of scores of (4s) and (5s), the strong evidence for the presence of movable hydrocarbons and excellent values of calculated water saturation from ratio and Archie that compare well to one another, adding further to the confidence in the strong productive potential of this zone. See Appendix for explanation of abbreviations.

surements: Transactions of Society of Professional Well Log Analysts Fourth Annual Logging Symposium, Paper VIII, 23 p.

Rascoe, Bailey, Jr.; and Adler, F. J., 1983, Permo–Carboniferous hydrocarbon accumulations, Mid-continent, U.S.A.: American Association of Petroleum Geologists Bulletin, v. 67, p. 979–1001.

Schlumberger, 1958, Introduction to Schlumberger well logging: Schlumberger Document Number 8, Schlumberger Well Surveying Corporation, 176 p.

_____ 1989a, Log interpretation principles/applications: Schlumberger Educational Services, Houston, Texas, 227 p.

_____ 1989b, Archie III: electrical conduction in shaly sands: Oilfield Review, v. 1, no. 3, p. 43–53.

Tixier, M. P., 1949, Electric log analysis in the Rocky Mountains: The Oil and Gas Journal, v. 48, no. 7, p. 143, 145, 146, 148, 217, 219.

Tixier, M. P.; Morris, R. L.; and Connell, 1968, Log evaluation of low resistivity pay sands in the Gulf Coast: The Log Analyst, v. 9, no. 6, p. 3–20.

Ver Wiebe, W., 1930, Ancestral Rocky Mountains: American Association of Petroleum Geologists Bulletin, v. 14, p. 765–788.

Wichmann, P. A., 1986, What's the real Rw?, *in* Problematic overview: a series of six studies on difficult log analysis: Transactions of the Society of Professional Well Log Analysts 27th Annual Logging Symposium, June 9–13, v. 2, Paper NNN, 25 p.

Wyllie, M. R. J., 1963, The fundamentals of log interpretation [3rd edition]: Academic Press, New York City, 238 p.

Zanier, A. M.; and Timko, D. J., 1970, Prediction of Morrow Sand performance and geological environment by well log salinity: API Mid-Continent District Spring Meeting, April 8–10, Wichita, Kansas; Mid-Continent Division of Production, American Petroleum Institute, Paper No. 851-44–B, 16 p.

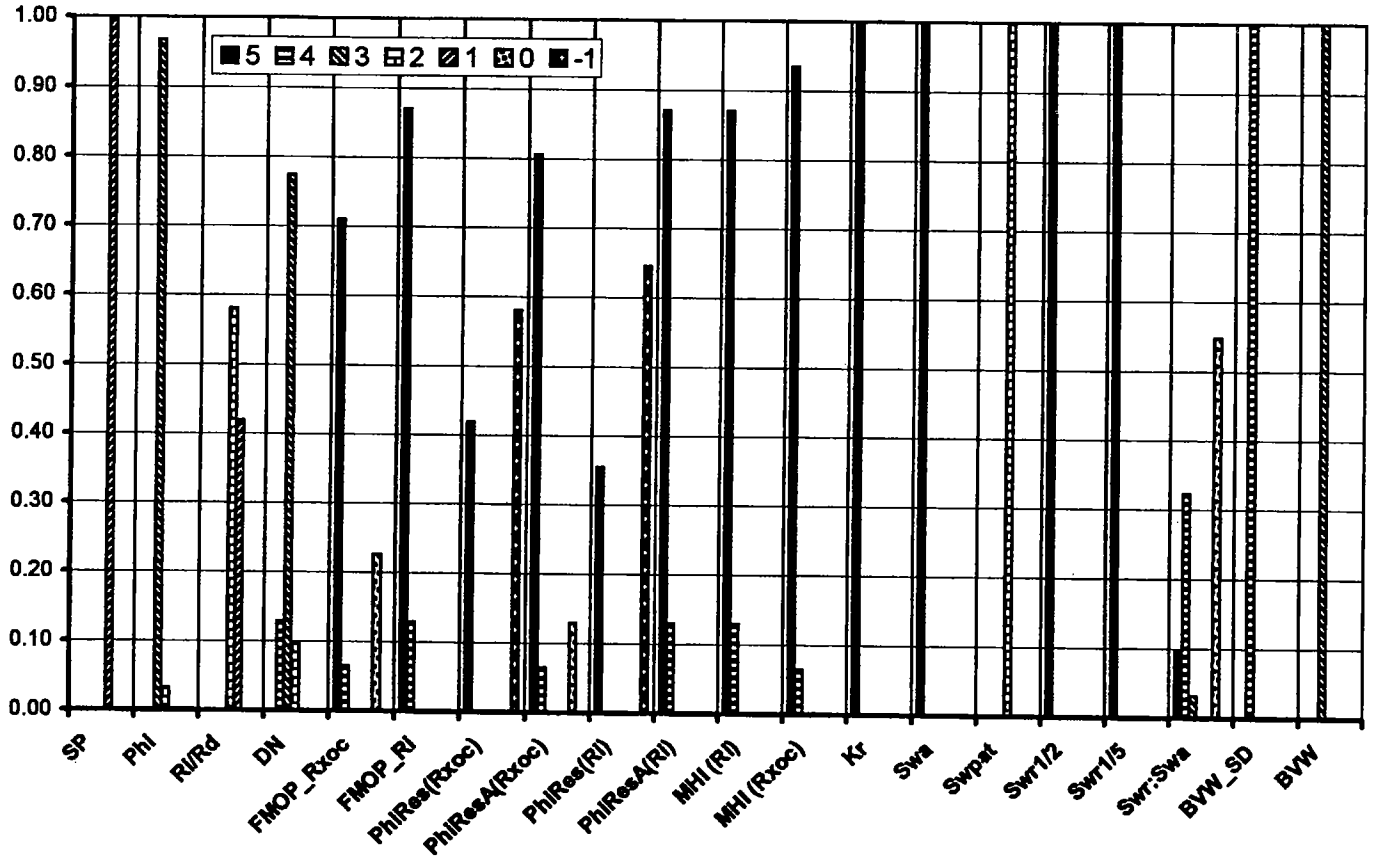

Figure 17. Well C: Histogram of production-calibrated–ranking system for the perforated interval, 11,401–11,416 ft. The zone was production tested and was swabbed for a recovery of unmeasured gas plus 41 bw (barrels of water). The ranking system histogram for this zone looks as good or better that on Figure 16, which represents a very successful test. Compare the SP scores between Figures 16 and 17 to note the culprit for the waste of time and money on this failed test. The dramatic difference in SP deflection between the two sands is a result of different values for resistivity of connate water (*Rw*) in the two sands. The analysis leading to the results plotted on Figure 17 are based on an erroneous *Rw*. See Appendix for explanation of abbreviations.

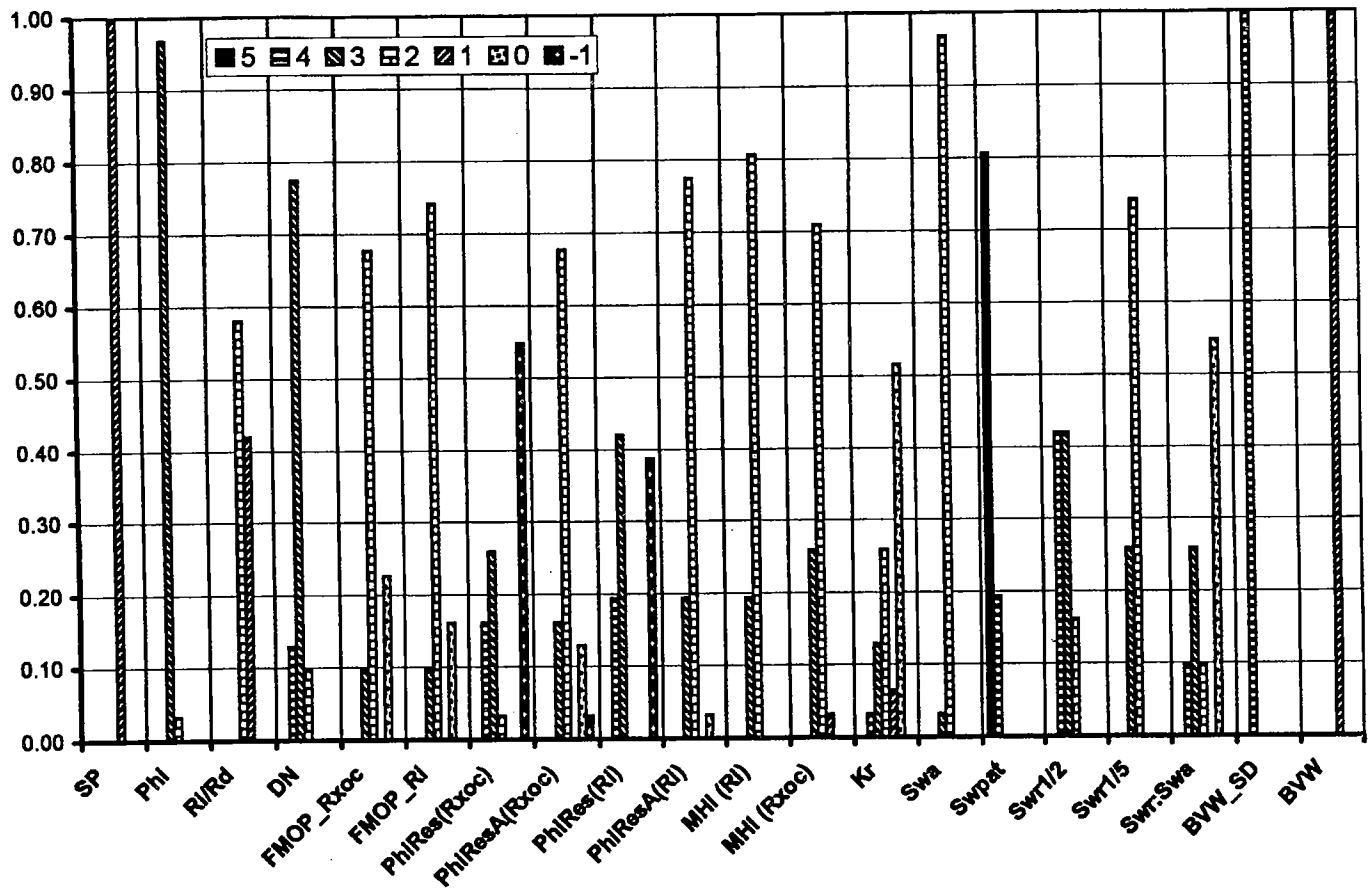

Figure 18. Well C: Histogram of production-calibrated–ranking system for the perforated interval, 11,401–11,416 ft. The zone was production tested and swabbed for a recovery of unmeasured gas plus 41 bw (barrels of water). The scored results of all the petrophysical methods indicate poor potential for movable hydrocarbons in the sand and it should not have been tested, and probably would not have been tested if the concept of variable resistivity of connate water (*Rw*) in Prue Sands had been applied to the analysis and interpretation in this well. See Appendix for explanation of abbreviations.

APPENDIX:

Abbreviations and Terminology

In the fields of petroleum geology and exploration and petrophysics, terminology and use of acronyms and abbreviations can be overwhelming. The following Appendix has been constructed for the benefit of the reader to more easily follow the text discussion.

BVW = bulk-volume water saturation
BVW_SD = scatter in BVW data from standard-deviation screen
bw = barrels of water
bcfg = billion cubic feet of gas
bcpd = barrels of condensate per day
DN = density-neutron log
dual-induction = deep- and medium-reading induction log
F(*DN*) = formation-resistivity-factor curve calculated from density-neutron cross-plot porosity; plotted on FMOP
F(*Rd*) = formation-resistivity-factor curve calculated from deep (formation) resistivity; plotted on FMOP
F(*Ri*) = formation-resistivity-factor curve calculated from resistivity of invaded zone; plotted on FMOP
F(*Rxo*) = formation-resistivity-factor curve calculated from resistivity of flushed zone; measured *Rxo* data not available in this study
F(*Rxoc*) = formation-resistivity-factor curve calculated from resistivity of flushed zone. Calculated *Rxoc* data used in this relationship; plotted on FMOP.
FMOP = formation-factor movable-oil plot
GR = gamma-ray log
IP = initial potential
Kr =petrophysical parameter based on [*Krw* / *Krg*] ratio
Krg = relative permeability to gas
Krw = relative permeability to water
laterolog = shallow-reading focused resistivity log
MHI = movable-hydrocarbon index
MHI(*Ri*) = movable hydrocarbon index using resistivity of invaded zone (*Ri*)
MHI(*Rxoc*) = movable hydrocarbon index using resistivity of flushed zone (*Rxoc*)
mmscfpd = million standard cubic feet (gas) per day
Phi = total formation porosity
Phi(*D*) = porosity developed from density log
Phi(*DN*), total formation-porosity curve developed from density-neutron–cross-plot porosity
Phi(*N*) = porosity developed from neutron log
Phi(*Rd*) = resistivity porosity from uninvaded zone
Phi(*Ri*) = resistivity-porosity from invaded zone
Phi(*Rxoc*) = resistivity-porosity from calculated flushed-zone resistivity
PhiRes = resistivity-porosity petrophysical-parameter–interpretation method
PhiRes(*Ri*) = resistivity porosity petrophysical parameter interpretation method based on Phi(*Ri*) in a case for excellent flushing conditions
PhiRes(*Rxoc*) = resistivity porosity petrophysical parameter interpretation method based on Phi(*Rxoc*) in a case for excellent flushing conditions
PhiResA = resistivity porosity petrophysical parameter interpretation method using a range of flushing conditions
PhiResA(*Ri*) = resistivity porosity petrophysical parameter interpretation method based on Phi(*Ri*) in a range of flushing conditions
PhiResA(*Rxoc*) = resistivity porosity petrophysical parameter interpretation method based on Phi(*Rxoc*) in a range of flushing conditions)
Rd = deep resistivity or formation resistivity
Ri = resistivity of invaded zone
Rmf = resistivity of mud fitrate
ROP = rate of penetration (mudlog curve)
ROS = residual-oil saturation
Rt = true formation resistivity based on invasion-corrected deep resistivity
Rw = (connate) water resistivity
Rwe = equivalent resistivity of water
Rxo = measured resistivity of flushed zone; not available in this study
Rxoc = calculated resistivity of the flushed zone
SD = standard deviation
Si = water saturation in the invaded zone.
SFL = shallow-reading spherically focused resistivity log
So = oil saturation
SP = spontaneous-potential log
Sw = water saturation in the uninvaded zone
Swa = Archie water saturation
Swirr = irreducible water saturation
Swpat = Patchett water saturation
Swr = ratio water saturation
Swr(1/2) = ratio water saturation using assumption of $Si = Swa^{1/2}$
Swr(1/5) = ratio water saturation using assumption of $Si = Swa^{1/5}$
Sxo = measured resistivity (water saturation) in the flushed zone

Facies Architecture of the Bartlesville and Skinner Intervals, Southwestern Rogers County, Oklahoma

Dennis R. Kerr and Alexander A. Aviantara
University of Tulsa
Tulsa, Oklahoma

ABSTRACT.—The Skinner and Bartlesville zones (middle Desmoinesian) were studied in a 1-mi^2 area around the former Amoco Catoosa Test Facility experimental drilling site northeast of Tulsa. Data from the DM21A well included whole core, a standard well-log suite, and borehole image. Standard well logs were also examined from ten offset wells.

A facies architecture hierarchy is established from well-log characteristics (calibrated by core) and well-log correlation. The discrete genetic interval (DGI) constitutes the largest-volume architectural element, and it is the basis for subsurface mapping. The upper Skinner interval is divided into five DGIs, and the Bartlesville interval is divided into two DGIs. A DGI is made up facies, which are volumetrically the next smaller element in the architectural hierarchy. Five facies are readily recognizable in core and well logs: channel-fill, splay, levee, floodplain mudstone, and carbonate; however, smaller-scale architectural elements can be discerned in the core and borehole image.

The channel-fill facies is characterized by fining-upward successions. The lower channel-fill subfacies consists of cross-stratified, moderately sorted, fine-grained sandstone. The middle channel-fill subfacies is represented by moderately sorted, very fine to fine-grained sandstone, with mud-draped lateral-accretion surfaces and chute channel-fill deposits. The upper channel-fill subfacies consists of low-angle parallel stratified, light- to dark-gray siltstone. Average channel-fill gross thickness in the Bartlesville reaches 24 ft, and that of the Skinner is 21 ft.

The splay facies is identified by coarsening-upward successions with sharp upper contacts. Each splay succession shows an upward change from interstratified floodplain mudstone and distal-splay lower very fine grained sandstone to upper very fine grained sandstone with cross stratification.

Levee and floodplain mudstone facies are both dominated by light- to dark-gray mudstone. Carbonaceous and mica debris are common. Starved, ripple laminated, lower very fine grained sandstones are also common. The levee facies are distinguished by coarsening-upward succession and low-angle parallel stratification with low-angle discordance and widely varying dip azimuths. The abundance and regularity of mudstone drapes in these two facies as well as the channel-fill and splay facies, suggests a tidal influence.

Analysis of the borehole image has provided information for facies architectural reconstruction in the vicinity of the DM21A well. Within the channel-fill facies, the vertical trends in dip azimuth and angle predict the location and evolution of lateral accretion. In the splay facies, vertical trends also identify the location, and hence the direction of net sandstone thickening of crevasse breaks.

INTRODUCTION

The Bartlesville and Skinner intervals of the Middle Pennsylvanian Krebs and Cabaniss Groups (also known informally as the "Cherokee Group") are prominent petroleum producers in northeastern Oklahoma. Oil production statistics for 1979–1995 show the Bartlesville producing 90 MMBO (million barrels of oil) and the Skinner 35 MMBO; total production is much higher where both zones are commingled with other producing zones (Andrews, 1996; Andrews and Northcutt, 1997). Production from reservoirs in the Bartles-

Kerr, D. R.; and Aviantara, A. A., 2002, Facies architecture of the Bartlesville and Skinner intervals, southwestern Rogers County, Oklahoma, *in* Boyd, D. T. (ed.), Finding and producing Cherokee reservoirs in the southern Midcontinent, 2002 symposium: Oklahoma Geological Survey Circular 108, p. 161–174.

ville and Skinner has been in decline for many decades, and many wells are near abandonment. A better understanding of facies architecture can assist in development of exploitation strategies for the remaining resources (e.g., Kerr and others, 1999).

Facies architectural analysis is possible from the rare opportunity to evaluate whole core and borehole images from a single well, the Amoco DM-21A. In addition, this well has several nearby offsets (Fig. 1). It is anticipated that greater insights from the facies architecture will lead to improved understanding of the production character of these intervals.

In this report, the informal subsurface stratigraphic names "Bartlesville" and "Skinner" are used. Both of these names are more familiar to those working the subsurface than the formal stratigraphic nomenclature. The lithostratigraphic nomenclature is reviewed later in this paper.

Paleogeographic Setting

The Bartlesville and Skinner intervals were deposited on a prominent Middle Pennsylvanian southern Midcontinent paleogeographic feature known as the Northeast Oklahoma Platform (the Cherokee Platform) (Fig. 1). The platform is situated between the Ozark Uplift to the east and the Nemaha Ridge to the west. The Krebs and Cabaniss (Cherokee) Groups, as well as units within these groups, expand in thickness southward into the Arkoma Basin (Visher and others, 1971). Southward increase in accommodation space records the response to the rapidly subsiding Arkoma Basin foreland deformation in front of the evolving Ouachita Fold–Thrust Belt (see review by Johnson and others, 1988).

The Bartlesville interval records the filling of an incised valley (Ye and Kerr, 2000). The axis of the main paleovalley is found about 18 mi west of the study area, which is located in a tributary to the main paleovalley. The Skinner interval also represents the filling of an incised valley; however, the details of the paleotopography have yet to be determined.

Study Area and Data Resources

The study area is located in southwestern Rogers County, Oklahoma (Fig. 1). The focus of the study is the Amoco DM21A well located at the experimental drilling site known as Catoosa Test Facility (SE¼SE¼ sec. 25, T. 21 N., R. 14 E.), formerly operated by Amoco. Well logs from within the same section and sections to the east and to the southeast were included in the study (Fig. 1).

Data from eleven wells were used in this study (Table 1). The Amoco DM21A well provided conventional well logs, whole core, and borehole image. Conventional 2-in. (2 in. = 100 ft) well logs from ten offset wells also were examined. A gamma-ray log was available from each well. Porosity logs, mainly cased-hole neutron, were evaluated from eight of the wells, and resistivity logs were used from the remaining three wells (Table 1). Wells typically are spaced about 1,000–1,500 ft apart. The Amoco Shads 1 well is located about 400 ft to the northeast of the Amoco DM21A well (Fig. 1).

Also of value were detailed lithologic descriptions of nearby shallow cores taken by the Oklahoma Geologic Survey. Descriptions from Hemish (1997) core holes 5, 6, and 7, which are located about 5 mi to the northeast (core 5; Fig. 1) of this study area and extending approximately 13 mi eastward. Hemish (1997) also described core from the Marathon Kelly 1 well, which is located 5 mi to the southwest (Fig. 1) of this study area.

Lithostratigraphic Nomenclature

The lithostratigraphic nomenclature for the Cherokee Group in northeastern Oklahoma and adjacent states of Kansas and Missouri has had a long history of study (see Ebanks, 1979, or Hemish, 1997, for review). The term Cherokee Group has not been widely used outside of the oil industry in many years to denote the Desmoinesian Series in Oklahoma. Instead, this section has been assigned formally to the Krebs, Cabaniss, and Marmaton Groups (Hemish, 1997). The subsurface intervals of interest in this study are included in the medial part of the Krebs Group (Bartlesville zone) and the lower Cabaniss Group (Skinner zone) (Fig. 2).

The subsurface Bartlesville zone, which at the surface includes the Bluejacket Sandstone, is the lowest member of the Boggy Formation, which, in turn, is the highest formation in the Krebs Group (Hemish, 1997) (Fig. 2). The "Bartlesville" comes from the first commercially productive oil reservoir discovered near the town of Bartlesville, Oklahoma, in 1897 (Andrews and Northcutt, 1997). Contact with the underlying Savanna Formation is a disconformity, a sequence boundary as recognized by Ye and Kerr (2000). Within the area covered in this report, the Bartlesville braided-fluvial lowstand systems tract (Ye and Kerr, 2000) is missing. Consequently, the transgressive systems tract rests directly on the sequence boundary. It is customary in subsurface correlation to extend the Bartlesville zone up to the base of the Inola Limestone, which includes a black phosphatic clay shale at the top (Fig. 2).

The Skinner zone was named from the Skinner lease in Lauderdale field, Pawnee County (Jordan, 1957). It resides stratigraphically between the overlying Verdigris Limestone and underlying subsurface Pink (surface Tiawah) limestones (Fig. 2) and is typically subdivided into upper and lower (in some instances includes middle) subunits. The Skinner is the subsurface equivalent to the Chelsea Sandstone Member of the Senora Formation of the Cabaniss Group at the surface. However, Hemish (1997) restricted the Chelsea Sandstone to the interval above the Tiawah Limestone and below the Mineral coal bed (Fig. 2), and he used the name Oowala Sandstone for the interval above the Croweburg coal bed and below the Verdigris Limestone. This study only considers the interval below the base of the Verdigris Limestone to above the top of the lower Skinner sandstone (Fig. 2).

Preliminary study indicates that the base of the Skinner is also a sequence boundary, a disconformity developed above the Red Fork zone. In Craig County

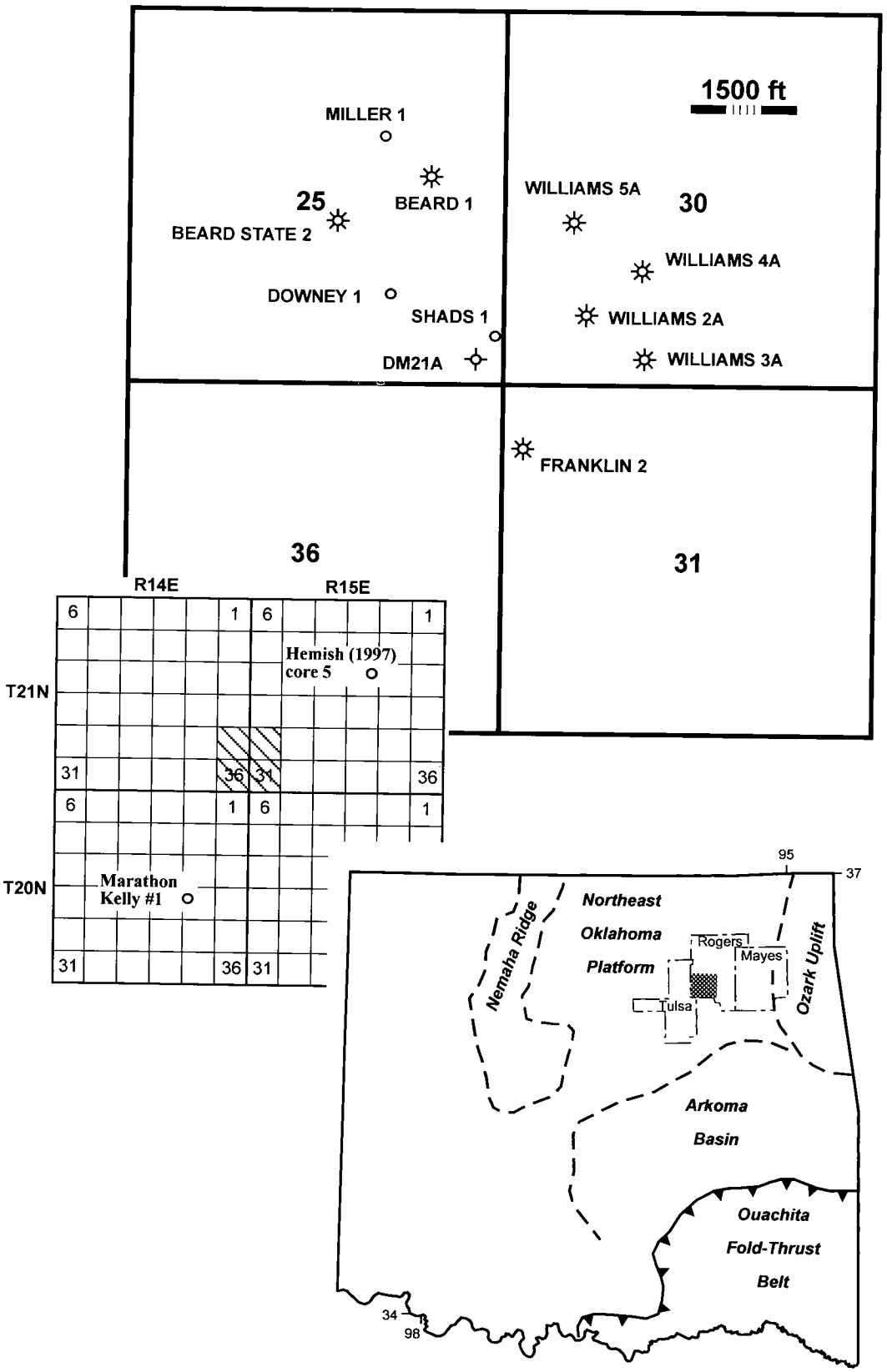

Figure 1. Index maps. Paleogeographic features for eastern Oklahoma during the Middle Pennsylvanian are shown in the lower map; also shown is the location of Rogers County (stipple pattern). The middle map illustrates the location of the study area (diagonal ruled) in southwestern Rogers County (T. 21 N., and R. 14–15 E.). The Marathon Kelly #1 well, which has a detailed core description, and OGS core 5 (Hemish, 1997) are also shown in the middle map. The upper map provides the location of wells used in this study. See Table 1 for listing of data used in this study.

TABLE 1. — Data Resources

Location	Operator / lease	Well	Gamma ray	Resistivity	Porosity log
NW¼SE¼NE¼ sec. 25, T. 21 N., R. 14 E.	MPC / Miller	1	✓		✓[1]
C SE¼NE¼ sec. 25, T. 21 N., R. 14 E.	Volant / Beard	1	✓		✓[2]
NW¼NW¼SE¼ sec. 25, T. 21 N., R. 14 E.	Volant / Beard State	2	✓		✓[2]
C SE¼ sec. 25, T. 21 N., R. 14 E.	Fields / Downey	1	✓	✓	
SE¼SE¼SE¼ sec. 25, T. 21 N., R. 14 E.	Amoco / Shads	1	✓	✓	
SE¼SE¼SE¼ sec. 25, T. 21 N., R. 14 E.	Amoco / CTF	DM21A[3]	✓	✓	
SW¼SW¼ sec. 30, T. 21 N., R. 15 E.	Volant / Williams	2A	✓		✓[2]
SE¼SW¼ sec. 30, T. 21 N., R. 15 E.	Volant / Williams	3A	✓		✓[2]
NE¼SW¼ sec. 30, T. 21 N., R. 15 E.	Volant / Williams	4A	✓		✓[2]
NW¼SW¼ sec. 30, T. 21 N., R. 15 E.	Volant / Williams	5A	✓		✓[2]
NW¼NW¼ sec. 31, T. 21 N., R. 15 E.	Volant / Franklin	2	✓		✓[2]

NOTE: Well locations are only general descriptions. See Figure 1 for map locations of wells.
[1]Open-hole density log.
[2]Cased-hole neutron porosity log.
[3]Includes whole core and borehole image (Schlumberger FMI).

(about 50 mi northeast of the study area), Hemish (1986) documented the erosional contact at the base of the Chelsea Sandstone that locally drops some 250 ft to the top of the Bluejacket (Bartlesville) Sandstone. In addition, the lower Skinner in the Amoco DM21A well has a blocky well-log profile (Fig. 2) and lithologic characteristics that are similar to the braided-fluvial lowstand systems tract found in the Bartlesville (Kerr and others, 1999; Ye and others, 1999; Ye and Kerr, 2000). The meandering fluvial deposits of the upper Skinner are also similar to the transgressive systems tract of the Bartlesville (Ye and Kerr, 2000).

FACIES ARCHITECTURE

Miall (1996) advanced the idea of facies architecture particularly as it applies to fluvial deposits. Facies architecture strives to classify the accumulation of sediment and development of strata surfaces through a hierarchy of elements. Each level within the hierarchy is, at least theoretically, related to sedimentary processes that operate through a spectrum of temporal and spatial scales. An example might progress from the accumulation of lamina, through the advance of bed forms and bar forms, through avulsion sedimentation of channel-fill deposits, and so on through larger and larger scale phenomena. The definition of levels and the elements contained within the levels is a logical approach to the analysis of sedimentary facies.

Application of facies architecture to the degree of detail envisioned by Miall (1996) to subsurface data, however, generally is not possible. In the analysis of gas reservoirs in fluvial deposits of the south Texas Gulf Coast, Kerr (1990) and Kerr and Jirik (1990) used a modified approach to defining facies architecture. A similar approach has been used in previous studies of the Bartlesville zone (Martinez, 1993; Kerr and others, 1999; Ye and others, 1999). This modification uses a discrete genetic interval (DGI) as the informal, fundamental subsurface-mapping unit. A DGI is defined as contiguous genetically related facies deposited during a limited interval of time. It is presumed that each discrete genetic interval represents paleo-landscape evolution toward conditions of stability (Figs. 3, 4). The advantage of using such an approach is that the correlation and mapping of discrete genetic intervals, as an architectural element, establishes lithostratigraphic units whose surfaces have chronostratigraphic significance; the same advantage is found in using the sequence stratigraphic approach (see Van Wagoner and others, 1990). The steps for using this approach are outlined later in the paper.

A tacit assumption is that relatively continuous fluvial aggradation has occurred. If this assumption is invalid, as, for example, in the case of repeated entrenchment of channel systems (e.g., Blum, 1994), then mistaken correlations are possible. Unfortunately, the evidence for entrenchment generally is not available from conventional subsurface data. It is, however, possible to demonstrate entrenchment in continuous outcrop exposures.

The accumulation of DGIs into different stacking patterns, including distribution within floodplain facies, is likely related to accommodation space development in a fluvial depositional system (Kerr and Jirik, 1990; Ye and Kerr, 2000), as has been discussed by Shanley and McCabe (1994).

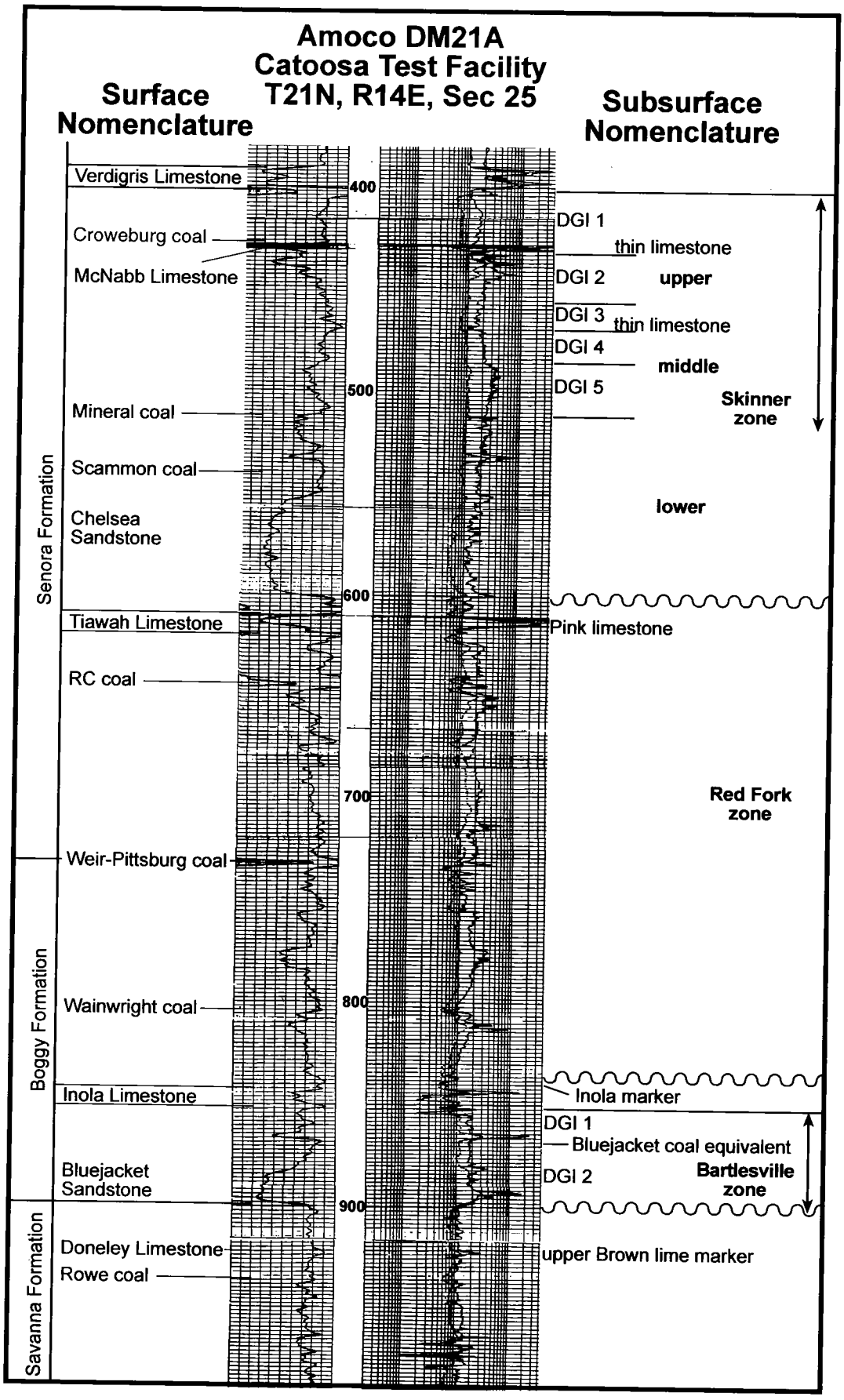

Figure 2. Stratigraphic nomenclature and study-area index log. Surface lithostratigraphic terms are from Hemish (1997). Subsurface lithostratigraphic terms are adapted from the Tulsa Geological Society Stratigraphy Committee, and include additional names and relationships recognized in this study. The well-log curve on the left is gamma ray, and curves on the right are resistivity. The double-arrow lines (right side of figure) bracket the study intervals. See Figure 1 for well location.

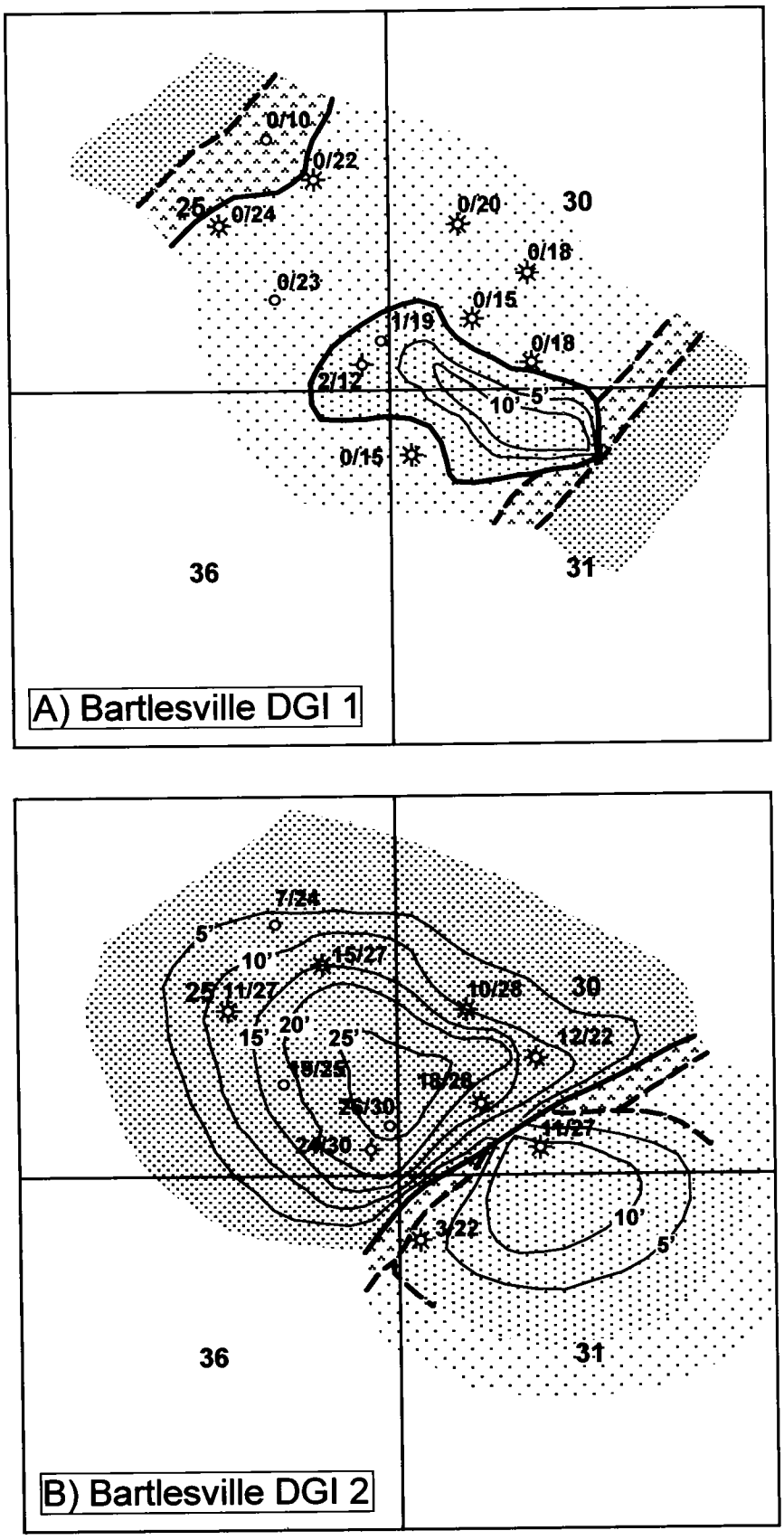

Figure 3. Combined facies and net-sand isopach maps for the Bartlesville zone for the discrete genetic intervals (DGIs) for (A) the Bartlesville DGI 1 and (B) the Bartlesville DGI 2. See Figure 2 for the depth range of each DGI in the Amoco DM21A well. See Figure 4 for legend and Figure 1 and Table 1 for well names and data resources.

In meandering fluvial depositional systems, the discrete genetic interval architectural element can be subdivided into facies architectural elements. The most common and readily recognizable facies from conventional subsurface data are the channel-fill, levee, splay, and floodplain mudstone facies. Where appropriate, a facies element can be further subdivided into subfacies architectural elements.

Channel-Fill Facies and Subfacies

For the Bartlesville and Skinner zones, the channel-fill facies is made up of interstratified sandstones and mudrocks. An upward reduction in texture, which is mainly the result of increasing mudrock content, and reduction in the scale of physical sedimentary structures are characteristic. The basal contact is sharp. The upper contact is either sharp or gradational. A gradational upper contact with floodplain facies being most common is likely caused by the gradual filling as a result of channel abandonment. The channel-fill facies is subdivided based on details of texture and sedimentary structures as observed in the Amoco DM21A core and borehole image.

Lower Channel-Fill Subfacies

The lower channel-fill subfacies consists of subrounded, moderately sorted, upper fine-grained sandstone. Mudstone intraclasts and large fragments of carbonaceous debris are found above the basal contact. Medium scale (1-ft-thick) trough cross stratification is common. Mudstone drapes and varying concentrations and size of carbonaceous debris and mica are developed on cross strata and between cross-strata sets.

Middle Channel-Fill Subfacies

The middle channel-fill subfacies is most noted for the occurrence of lateral-accretion strata. Interstratified subrounded, moderately sorted, fine-grained sandstone, siltstone, and mudstone are inclined at low angles (5° and 15° most common). Ripple cross-stratification is developed within some inclined strata. The apparent regularity of thin (0.1–0.2-ft-thick) sandstone-mudstone couplets suggests a regular fluctuation in flow competence, such as occurs in modern tidal-influenced fluvial settings (e.g., Smith, 1987).

One- to two-set thick, medium-scale trough cross-stratified cosets occur among the lateral accretion strata, the basal contact being erosional. The cross-strata are inclined at a low angle (<10°) and include numerous mudstone drapes as seen within the lateral-accretion strata. These deposits are regarded as chute-channel cuts and fills. Chute channels are secondary erosional features developed transverse to the migration direction of a lateral-accretion bar.

Upper Channel-Fill Subfacies

Upper channel-fill subfacies is dominated by gray to dark-gray siltstone. Ripple crossstratified, very fine grained sandstone also occurs. Mudstone drapes are common throughout. Indication of oxidation conditions (brown coloration) is also present.

The channel-fill subfacies described above are characteristic of meandering fluvial-channel fills (Miall, 1996). In addition, the abundance of mud drapes is evidence for tidal influence during deposition. It is not suggested, nor is there any indication, that these are tidal channels that experienced semi-diurnal or neap-spring tidal fluctuations. When combined with other hydrologic factors, tidal fluctuations are known to influence fluvial flow many miles inland (see examples cited in Dalrymple and others, 1992).

Well-log profiles exhibit the classic bell-shape (see Bartlesville DGI 2 in Fig. 2). The basal contact on the gamma-ray curve may appear gradational where mudstone intraclasts are present; the resistivity curve typically shows an abrupt deflection to higher values. The lower channel-fill subfacies gamma-ray response has the lowest values and has a minimal serrated character. The middle channel-fill subfacies well-log response is highly serrated, reflecting the abundance of interstratified sandstones and mudrocks. The upper channel-fill subfacies on the gamma-ray curve is gradational with the log response of other mud-rich lithologies. However, this subfacies is best recognized in the resistivity curve, being intermediate between the well log character of the upper channel filling and other facies.

Although the only example of channel-fill facies in the Amoco DM21A core is found in the Bartlesville zone, its distribution and thickness is established from the facies well-log profile (Fig. 3). In the Bartlesville, the channel-fill facies has an average gross thickness of 24 ft, with a minimum of 22 ft and maximum of 30 ft. The net-sand thickness, based on the one-third rule (i.e., the thickness measured by one-third the distance from the minimum to the maximum gamma-ray–log deflection), averages 16 ft, with a minimum of 7 ft and maximum of 26 ft. In the Skinner (Fig. 4), the channel-fill facies has an average gross thickness of 21 ft, with a minimum of 15 ft and a maximum of 32 ft. Its net-sand thickness averages 8 ft, with a minimum of 0 ft and a maximum of 17 ft. The higher average thickness values for the Bartlesville, compared to the Skinner, is evidence that Bartlesville channels were deeper than Skinner channels.

Splay Facies

The splay facies is made up of subrounded, moderately sorted, very fine grained sandstone interstratified with siltstone. Physical sedimentary structures in the sandstones include medium-scale, trough cross stratification, ripple cross lamination, and low-angle parallel stratification (<10° dip). Cross stratification (≥10° dip) occurs mainly in the upper levels of a splay facies interval. Contorted strata are developed at some levels. Siltstones occur as discrete strata near the base and progress upward to become discontinuous lenses within sandstones; thus, an upward-coarsening textural profile is developed. Upper contacts are sharp. Mudstone drapes occur throughout.

Well-log profiles are commonly serrated, funnel shaped, which reflect the upward-coarsening–texture

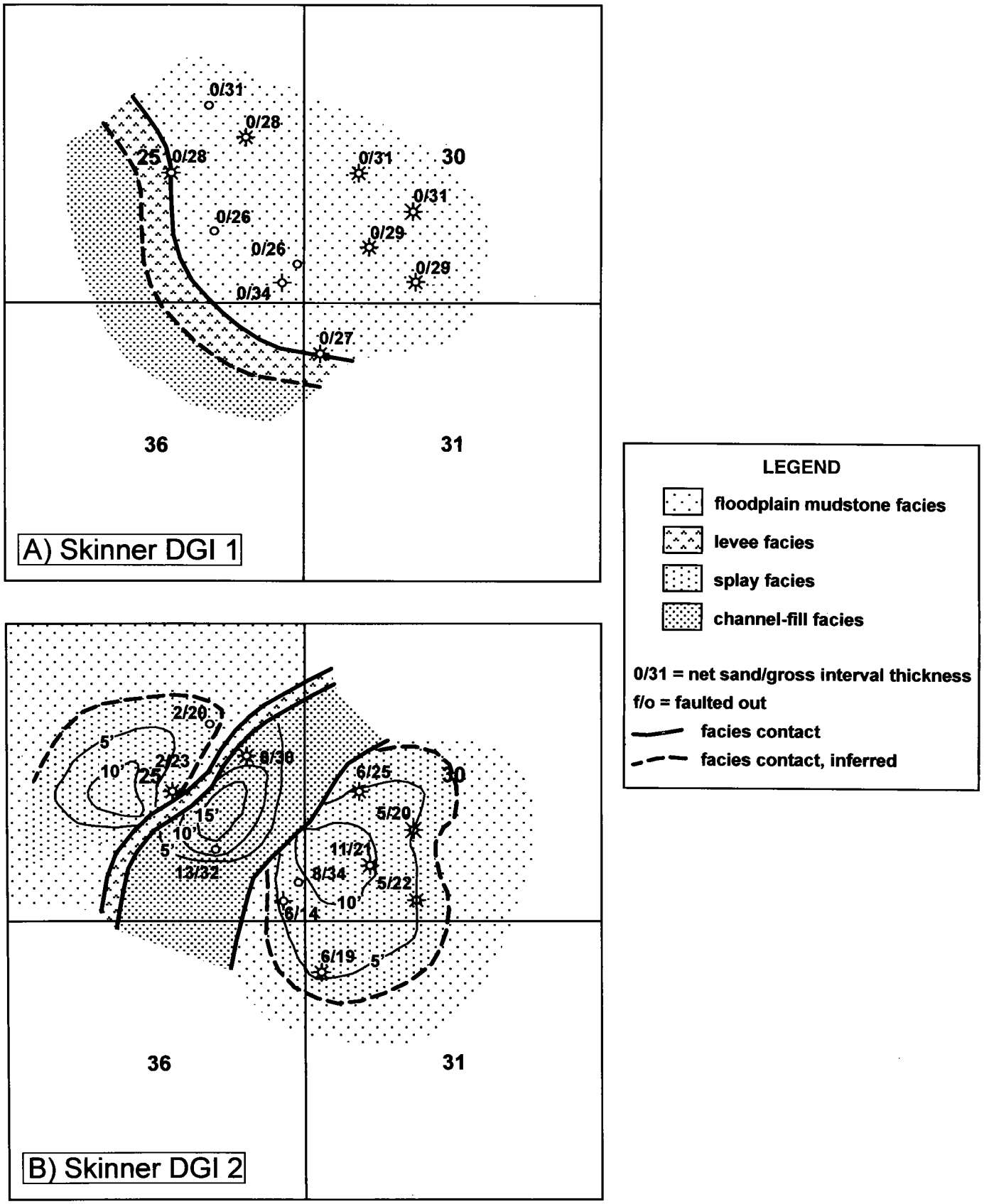

Figure 4 *(above and facing page).* Combined facies and net-sand isopach maps for the middle and upper Skinner zones. See Figure 2 for the depth range of each discrete genetic interval (DGI) in the Amoco DM21A well and Figure 1 and Table 1 for well names and data resources.

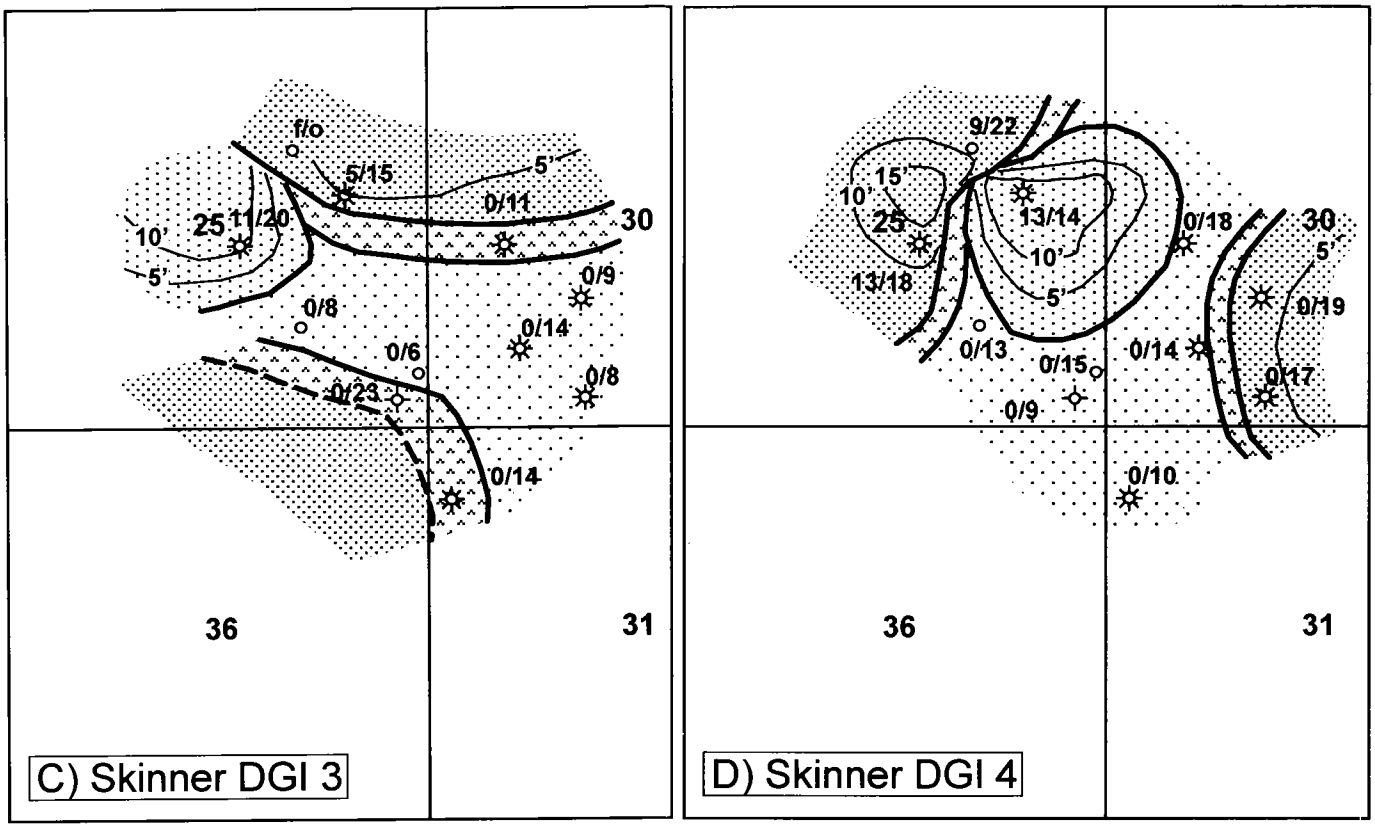

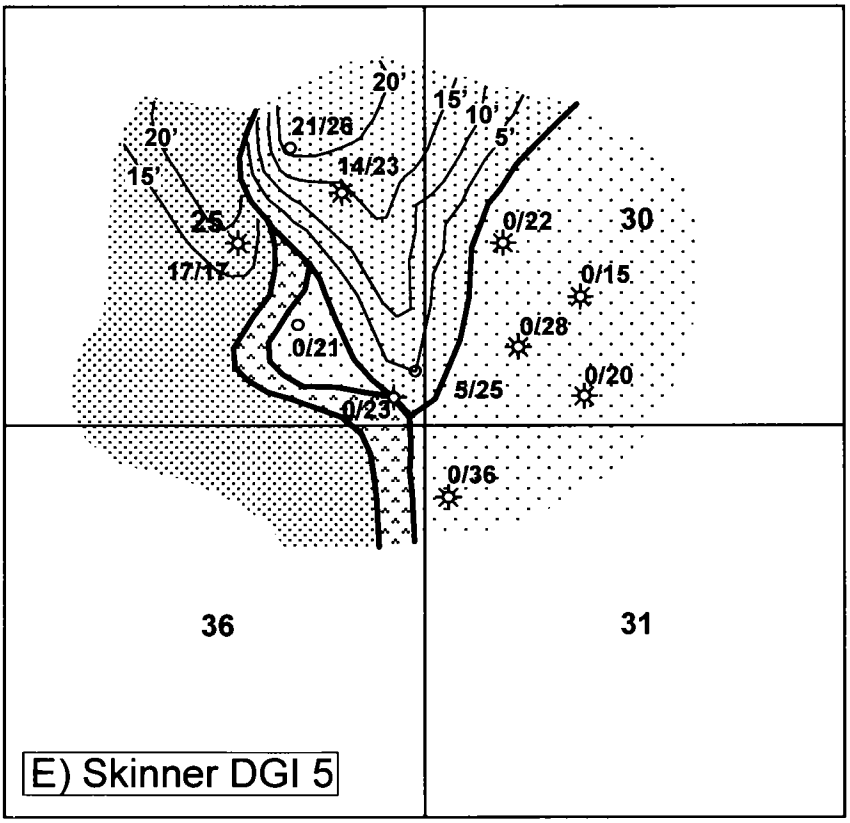

Figure 4 *(continued).*

profile (see Skinner DGI 2 in Fig. 2). However, isolated, symmetrical, low gamma-ray defections, typically a few feet thick, also characterize of the splay facies (e.g., Bartlesville DGI 1; Fig. 2).

Splays are deposited during flood events that bring relatively coarser-grained detritus to the floodplain. Where the levee is breached (i.e., crevasse break), sand is delivered to the floodplain with flow being unconfined, the result being a fanning-outward, prograding sand body. Where the levee is not breached, sand is deposited as a discrete, thin sheet. A splay complex is deposited where multiple crevasse breaks deliver sand to an area on the floodplain. Low-angle surfaces are produced by the advancing front of sand deposition. The upward increase in texture and indications of stronger current flow (cross stratification as deposits of dune bed forms) are expressions of the prograding nature of splay depositional events. Similar examples of splay deposits have been described from the rock record (Miall, 1996) as well as associated with the Mississippi River channel belt (Farrell, 1987).

The splay facies is recognized in all of the discrete genetic intervals (DGI) except the Skinner DGI 1 (Fig. 4A). Maximum net-sand thickness (using the one-third rule) and net to gross ratio occur near proximal locations within a splay deposit. Maximum thickness of between 15 and 10 ft are preserved or predicted for Skinner DGI 2, 3, and 4 (Fig. 4B–D), and Bartlesville DGI 1 and 2 (Fig. 3A,B). Measurements for the Skinner DGI 5 reach 21 ft (Fig. 4E). Maximum net-sand thickness is not expected to exceed the maximum gross-interval thickness of the contiguous channel-fill facies (Figs. 3, 4).

Levee Facies

In the Amoco DM21A core and borehole image, the levee facies is represented by 0.1-ft-thick inclined interstratified sandstone and carbonaceous mudrocks. Starved ripple lamination and climbing ripple stratification grading to contorted ripple stratification are common. Soft-sediment deformation is also present. Sand-filled root casts are prevalent in some intervals. Medium-scale hollows are inferred for mud-draped intervals that show an upward decrease in strata dip angles and minimal change in dip azimuth.

One of the distinctive aspects of the levee facies is noted in the wide variation of dip azimuths observed in the borehole image from the Amoco DM21A. Strata dip angles are typically between 1° and 5°, less commonly reaching 15°. In the Skinner DGI 3 example, dip azimuths occur in every compass quadrant. However, the azimuth distribution of higher strata dip angles is bimodal with dips to the east–southeast and to the west–northwest. A number of mechanisms or circumstances can explain the wide variation in dip azimuths: (1) the primary depositional surface sloping toward the floodplain; (2) filling of shallow depressions formed by erosion or fallen tree trunks; (3) draping of deeper scours of crevasse channels; and (4) slumping into the adjacent river channel, into crevasse channels, or toward the floodplain. Efforts to determine the record of these various explanations have yet to be attempted.

The recognition of levee facies in well logs is challenging and commonly overlooked. The levee facies has a serrated funnel-shaped profile in the gamma-ray and resistivity responses. The minimum gamma-ray value rarely reaches two-thirds the distance from the minimum to maximum deflection. Anomalously high-resistivity values are possible where carbonate cementation is abundant. The well-log profile for the levee facies might be mistaken for the distal-splay facies; however, the distal-splay facies does not have the strong gradational character at the thickness resolution commonly used in gamma-ray logging. The preceding description is characteristic of the few levee deposits documented in the literature (see Reineck and Singh, 1980; Miall, 1996).

The inclined, repeated, and thinly interstratified sandstones and mudrocks are thought to record regular flooding events. Levees are a part of the geomorphologic elements that confines the flow of rivers. Thus, the recognition of levee facies can be critical in the prediction of channel-fill facies where the latter has not been penetrated by a well in the immediate vicinity.

Floodplain Mudstone Facies

The floodplain mudstone facies is dominated by dark-gray, micaceous and carbonaceous mud and clay shale. Isolated occurrence of starved-ripple laminated and load casted rippled, very fine grained sandstone to siltstone was also noted in core. Also observed in core are small irregular pods of very fine grained sandstone and siltstone, which are possible casts of invertebrate burrows or plant roots. Coals, as well as associated underclays, are also included in this facies (Hemish has provided, through several Oklahoma Geological Survey publications, details of coal characteristics and distribution in the Boggy and Cabaniss Groups of northeastern Oklahoma).

The well log character of the floodplain mudstone is best expressed by high gamma-ray values. Resistivity responses are typically, but not always, low compared with other facies. Coal is readily identified by its anomalous response on porosity logs and its commonly low resistivity and high gamma-ray response. The vertical well-log profile is uniform with little variation.

The floodplain mudstone facies is regarded has having been deposited in low-lying areas that are sufficiently distant from sources of coarser clastic influx and low current strength to be dominated by suspension sedimentation. Although the presence of starved ripple laminations indicates that traction currents did develop, such currents were not the dominant process. The dark coloration and abundance of carbonaceous debris, including coal, indicates poorly drained, low oxygenation conditions. The absence of paleosol features further suggests this condition, as soil development is favored under conditions of good drainage and oxygenation.

In the Bartlesville and Skinner, the floodplain mudstone facies occurs in areas not occupied by deposition

of the other fluvial facies. It was encountered in the Amoco DM21A well in the Skinner DGI 1 and 4. Because the floodplain mudstone facies is laterally and vertically transitional to the splay and levee facies, finer-grained lithologies typical of the floodplain facies are interstratified with these facies in other discrete genetic intervals. Thickness of the floodplain mudstone has little meaning in the understanding of the depositional setting; however, the lateral and vertical distribution or thickness is important to establishing pore-fluid flow among reservoir compartments.

Carbonate Facies

Carbonate rocks are also present through the interval considered in this study. The Inola, Pink (Tiawah), and Verdigris Limestones have long been known for their regional surface and subsurface occurrence (Hemish, 1990a,b; 1997). Two additional thin limestones were encountered in the Amoco DM21A well—one at the base of Skinner DGI 1 (below the Croweburg coal bed) and the other in DGI 3 (Fig. 2). The limestone in the Skinner DGI 1 is at the same stratigraphic position as a limestone assigned by Hemish (1989) to the McNabb Limestone in a measured section 7 mi to the southeast of the study area. The limestone associated with Skinner DGI 3 is correlated with an unnamed limestone that Hemish (1997) called unit 42 in the Marathon Kelly 1 well.

The carbonate facies are not the focus of this study, and only general remarks are offered on their depositional setting. In addition, little published information is available for making detailed inferences. The more widely distributed units, such as the Inola and Pink (Tiawah) include limestone beds with abundant and diverse fossil faunas, as well as phosphatic black shales (Hemish, 1990a,b). These limestones are regarded as a record of major marine incursions onto the Northeastern Oklahoma Platform. By contrast, the thin limestones are sparsely fossiliferous and are limited in faunal diversity (e.g., core descriptions in Hemish, 1988). Moreover, these thin limestones are not associated with phosphatic black shale. It seems reasonable to consider that these thin limestones represent only limited marine incursions, or even perhaps brackish-water conditions.

Correlation and Mapping of Discrete Genetic Intervals

Correlation and mapping of discrete genetic interval facies architectural elements is a useful approach for defining reservoir-scale stratigraphic units as well as reservoir compartment barriers (e.g., Kerr, 1990; Kerr and others, 1999). Because the approach aims to establish lithostratigraphic units the contacts of which have chronostratigraphic significance, such units are more likely to be spatially correlative. By contrast, the conventional lithostratigraphic approach emphasizes lithologic (well-log) similarity and therefore may lead to miscorrelation.

Delineation of discrete genetic intervals proceeds through the eight steps that are discussed below.

Step 1. Establish a cross-section network using regional knowledge as a guide. For example, it is well known that the Northeastern Oklahoma Platform sloped southward into the Arkoma Basin, as demonstrated by the regional correlations of Visher and others (1971). A higher degree of facies contrast is expected in an east–west direction (parallel to basin depositional strike) for the fluvial facies of the Bartlesville and Skinner intervals. Thus, east–west cross-section views should reveal more readily fluvial facies contacts. Identify and correlate marker beds. Select one marker bed as the datum from which to hang the cross sections. In this study, the black shales (high gamma-ray and low-resistivity well-log response) associated with the Inola Limestone were used as a datum for correlating the Bartlesville zone, the Mineral coal was used for the middle Skinner, and the Croweburg coal was used for the upper Skinner (Fig. 2).

Step 2. Identify and correlate discrete genetic intervals. Correlation is done by comparing elevations of surfaces relative to one or more marker beds. In meandering fluvial depositional systems, a DGI is recognized as the top of a channel-filling episode with this surface extended across inferred lateral facies equivalents (e.g., top of the levee and splay facies). The base of a DGI is picked at the top of a coal bed or the base of a thin, discontinuous limestone; each is regarded as the record of base-level rise and is, in this case, comparable with a parasequence contact (Van Wagoner and others, 1990). Alternatively, the base of the succeeding DGI is the base of the overlying channel-fill facies and correlative base of an adjacent levee or splay facies. Presumably, this basal contact records the reoccupation of the channel-belt system as a result of upstream channel avulsion. The boundary of a DGI is difficult to define through the floodplain mudstone facies.

Step 3. Make a preliminary estimate of facies contacts within a discrete genetic interval throughout the cross-section network.

Step 4. Measure net-sand and gross-interval values. See the facies descriptions above for how these were defined for this study.

Step 5. Post facies and thickness values on a map for each discrete genetic interval.

Step 6. Map facies contacts and adjust contacts in Step 3 as needed.

Step 7. Evaluate the reasonableness of the map. This is an important step because the framework for isopach mapping is being established. If illogical facies relationships are present, then the most likely cause is a miscorrelation. Repeat Steps 2 through 6 if necessary.

Step 8. Map net-sand isopachs using expectations for facies geometries, as well as any other information, as a guide. Meandering fluvial-channel belts are expected to have "ribbon" geometry. Moreover, lateral-accretion bars are the traps for sand being transported through the channel. For this reason, local thick areas should exist along the trace of the ribbon ("beads on a ribbon"). Mapping the trace of the minimum net-to-gross ratio

within the channel-fill facies approximates the location of the channel thalweg at the time of channel abandonment. The local thick areas are expected on the inside bend of the thalweg trace. The splay facies geometry is expected to be a low-profile conical segment. Where several splays issuing from different crevasses have merged on the floodplain, the geometry is likely to be more complex. Careful, detailed correlation might be able to define the individual splay event deposits. In addition, the distal margins of a splay can be lobate. The levee facies has an expected geometry of a wedge-shaped prism that parallels the course of the channel belt.

Figures 3 and 4 show the combined facies and net-sand isopach map for each discrete genetic interval recognized for the Bartlesville and Skinner intervals. Although the channel-fill facies is not present in any wells for some discrete genetic intervals, the expected lateral association of facies predicts its presence. For the Bartlesville DGI 1 and Skinner DGI 1, no wells encountered channel-fill facies; however, the occurrence of channel-fill facies is predicted by the presence of levee facies in some wells (Figs. 3A, 4A). Similarly, the extension of channel-fill facies from the known occurrence of the facies is predicted by the occurrence of levee facies in Skinner DGI 3 and 5 (Fig. 4C,E). The prediction of channel-fill facies in the southeastern area for Bartlesville DGI 1 (Fig. 3A) is based on analysis of the borehole image. This shows an upward rotation of dip azimuth indicating the source of the splay (Fig. 5A).

Analysis of the Amoco DM21A borehole image helps to define the expected geometry of the lateral-accretion–bar deposit (middle channel-fill subfacies) that dominates Bartlesville DGI 2 (Fig. 5B). The well is located on the downstream side of the bar, as indicated by the opening obtuse dip azimuth from the lower channel-fill subfacies upward through most of the middle channel-fill subfacies (Fig. 5). The azimuth vector approach of Grace and Newberry (1990) yields the same result, and plotting the dip azimuth vector of the lower channel-fill subfacies against the tail of the dip azimuth of the middle channel-fill subfacies produces an acute angle for a downstream location. In addition, the dip azimuth vector plot suggests that the thalweg evolved by lateral shifting. Therefore, the geometry should be a pod elongated in a northwest direction, as it is mapped (Fig. 3B).

SUMMARY

The Bartlesville zone and middle and upper Skinner zone were studied using facies architectural approach. Discrete genetic intervals (DGIs) are the elements mapped in the subsurface using core-calibrated well logs and a borehole image. Two DGIs are recognized in the Bartlesville and five in the Skinner. Facies typical of a meandering fluvial system with tidal influence dominate the section. Minor carbonate facies, which represent minor marine inundations, are less important.

The approach used in this study should be of value to those seeking to more efficiently exploit petroleum resources from the Bartlesville and Skinner, as well as similar Cherokee Group reservoirs.

ACKNOWLEDGMENTS

We gratefully acknowledge the support and cooperation received from the former Amoco Production Research Center and Core Facility in Tulsa. The staff provided access to core, conventional logs, borehole image, and computational resources. BP America and Schlumberger Well Logging Services granted permission to publish core and borehole image data.

We also thank Anton Pangabean for assistance during the early phases of this study. The manuscript has benefited from reviews by Dan Boyd, Thomas W. Henry, and Neil Suneson.

REFERENCES CITED

Andrews, R. D., 1996, Fluvial-dominated deltaic (FDD) oil reservoirs in Oklahoma: the Skinner and Prue plays: Oklahoma Geological Survey Special Publication 96-2, 106 p.

Andrews, R. D.; and Northcutt, R. A., 1997, Fluvial-dominated deltaic (FDD) oil reservoirs in Oklahoma: the Bartlesville play: Oklahoma Geological Survey Special Publication 97-6, 93 p.

Blum, M. D., 1994, Genesis and architecture of incised valley fill sequences: a late Quaternary example from the Colorado River, gulf coastal plain of Texas, *in* Weimer, P.; and Posamentier, H. W. (eds.), Siliciclastic sequences stratigraphy: recent developments and applications: American Association of Petroleum Geologists Memoir 58, p. 259–283.

Dalrymple, R. W.; Zaitlin; B. A.; and Boyd, R., 1992, Estuarine facies models: conceptual basis and stratigraphic implications: Journal of Sedimentary Petrology, v. 62, p. 1130–1146.

Ebanks, W. J., Jr., 1979, Correlation of Cherokee (Desmoinesian) sandstones of the Missouri–Kansas–Oklahoma tri-state area, *in* Hyne, N. J. (ed.), Pennsylvanian sandstones of the Mid-Continent: Tulsa Geological Society Special Publication 1, p. 295–312.

Farrell, K. M., 1987, Sedimentology and facies architecture of overbank deposits of the Mississippi River, False River region, Louisiana, *in* Ethridge, F. G.; Flores, R. M.; and Harvey, M. D. (eds.), Recent developments in fluvial sedimentology: Society of Economic Paleontologists and Mineralogists Special Publication 39, p. 111–131.

Grace, M.; and Newberry, B. M., 1990, Geologic applications of borehole electrical images and dipmeter: Schlumberger Educational Services, Houston, Texas, 724 p.

Hemish, L. A., 1986, Coal geology of Craig County and eastern Nowata County, Oklahoma: Oklahoma Geological Survey Bulletin 140, 131 p.

_____ 1988, Report of core-drilling by the Oklahoma Geological Survey in Pennsylvanian rocks of the northeastern Oklahoma coal belt, 1983–86: Oklahoma Geological Survey Special Publication 88-2, 174 p.

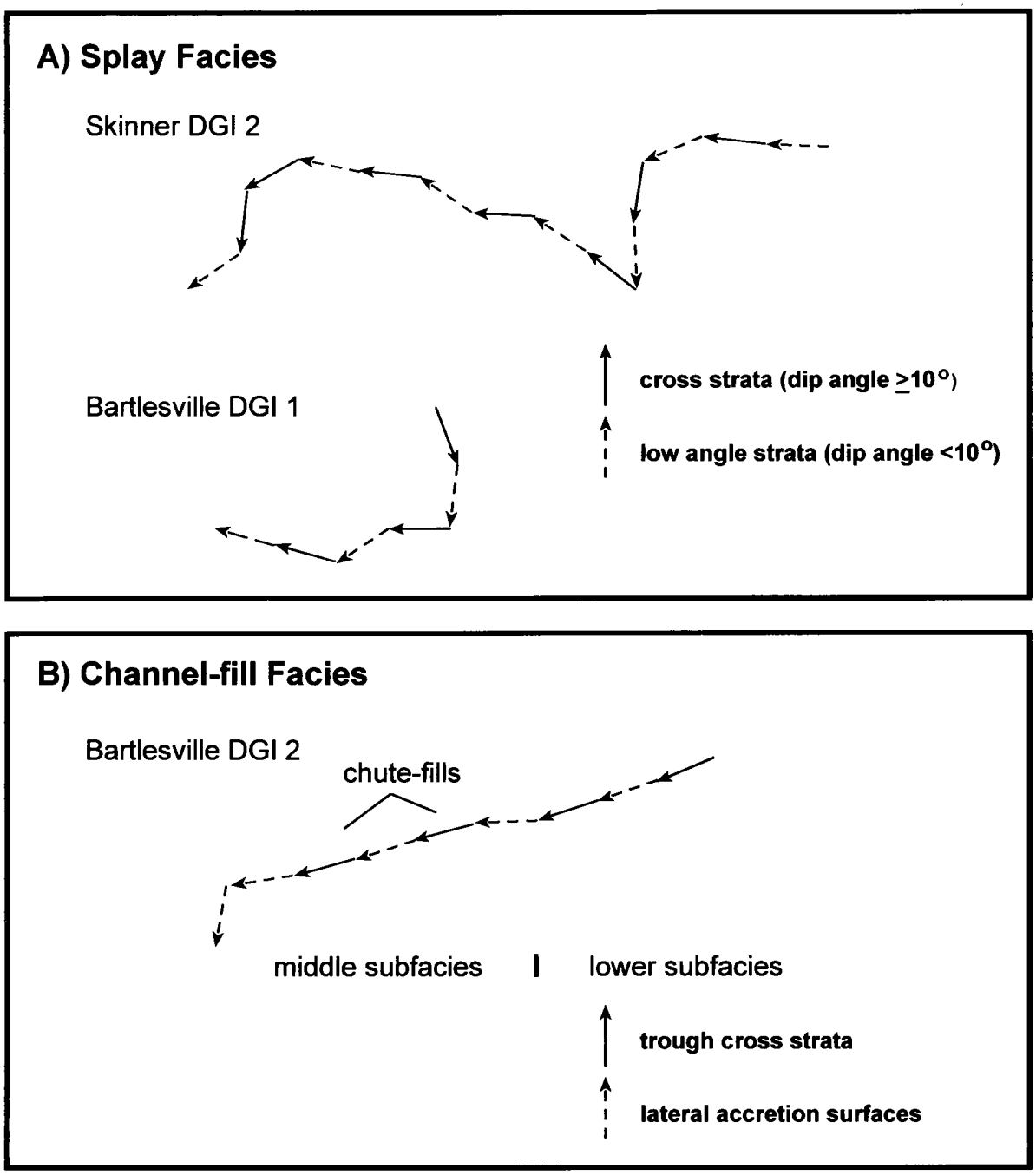

Figure 5. Examples of dip azimuth vectors for splay and channel-fill facies. Each vector is given unit length and comes from analysis of Amoco DM21A borehole image. Vector plots are arranged to preserve stratigraphic position in ascending order as viewed in the direction of the arrowhead. (A) Splay facies dip azimuth vectors rotate upwards finally pointing away from the direction of the inferred crevasse break. (B) Channel-fill facies dip azimuth vectors record a down-channel location and an evolution of thalweg amplitude increase by lateral shifting. See Figure 2 for depth range of each discrete genetic interval (DGI).

_____ 1989, Goal geology of Rogers County and western Mayes County, Oklahoma: Oklahoma Geological Survey Bulletin 144, 118 p.

_____ 1990a, Inola Limestone Member of the Boggy Formation (Pennsylvanian) in its type area: Oklahoma Geology Notes, v. 50, p. 4–23.

_____ 1990b, Tiawah Limestone Member of the Senora Formation (Pennsylvanian) in its type area: Oklahoma Geology Notes, v. 50, p. 40–53.

_____ 1997, Lithologic descriptions of Pennsylvanian strata north and east of Tulsa, Oklahoma: Oklahoma Geological Survey Special Publication 97-2, 44 p.

Johnson, K. S.; Amsden, T. W.; Denison, R. E.; Dutton, S. P.; Goldstein, A. G.; Rascoe, Bailey, Jr.; Sutherland, P. K.; and Thompson, D. M., 1988, Southern Midcontinent region, *in* Sloss, L. L. (ed.), Sedimentary cover—North American craton: Geological Society of America, The Geology of North America, v. D-2, p. 307–359.

Jordan, Louise, 1957, Subsurface stratigraphic names of Oklahoma: Oklahoma Geological Survey Guidebook 6, 220 p.

Kerr, D. R., 1990, Reservoir heterogeneity in the middle Frio Formation: case studies in Stratton and Agua Dulce fields, Nueces County, Texas: Gulf Coast Association of Geological Societies Transactions, v. 40, p. 363–372.

Kerr, D. R.; and Jirik, L. A., 1990, Fluvial architecture and reservoir compartmentalization in the Oligocene middle Frio Formation, south Texas: Gulf Coast Association of Geological Societies Transactions, v. 40, p. 373–380.

Kerr, D. R.; Ye, L.; Bahar, A.; Kelkar, B. G.; and Montgomery, S., 1999, Glenn Pool field, Oklahoma: a case of improved production from a mature reservoir: American Association of Petroleum Geologists Bulletin, v. 83, p. 1–18.

Martinez, G., 1993, Reservoir heterogeneity in a portion of the Bartlesville sandstone (Desmoinsian), Mayes County, northeastern Oklahoma: University of Tulsa unpublished M.S. thesis, 147 p.

Miall, A. D., 1996, The geology of fluvial deposits: Springer-Verlag, New York, 582 p.

Reineck, H. E.; and Singh, I. B., 1980, Depositional sedimentary environments [2nd edition]: Springer-Verlag, New York, 549 p.

Shanley, K. W.; and McCabe, P. J., 1994, Perspectives on the sequence stratigraphy of continental strata: American Association of Petroleum Geologists Bulletin, v. 78, p. 544–568.

Smith, D. G., 1987, Meandering river point bar lithofacies models: modern and ancient examples compared, *in* Ethridge, F. G.; Flores, R. M.; and Harvey, M. D. (eds.), Recent developments in fluvial sedimentology: Society of Economic Paleontologists and Mineralogists Special Publication 39, p. 83–92.

Van Wagoner, J. C.; Mitchum, R. M.; Campion, K. M.; and Rahmanian, V. D., 1990, Siliciclastic sequence stratigraphy in well logs, cores, and outcrops: American Association of Petroleum Geologists Methods in Exploration Series 7, 55 p.

Visher, G. S.; Saitta, S.; and Phares, R. S., 1971, Pennsylvanian delta patterns and petroleum occurrences in eastern Oklahoma: American Association of Petroleum Geologists Bulletin, v. 55, p. 1206–1230.

Ye, L.; and Kerr, D. R., 2000, Sequence stratigraphy of the Middle Pennsylvanian Bartlesville sandstone, northeastern Oklahoma: a case of an underfilled incised valley: American Association of Petroleum Geologists Bulletin, v. 84, p. 1185–1204.

Ye, L.; Kerr, D. R.; and Yang, K., 1999, Facies architecture of the Bluejacket Sandstone in the Eufaula Lake area Oklahoma: implications for the reservoir characterization of the subsurface Bartlesville sandstone, *in* Jordan, J. F.; and Schatzinger, R. (eds.), Reservoir characterization—recent advances: American Association of Petroleum Geologists Memoir 72, p. 29–44.

Accurate Geological Model for Enhanced Oil Recovery in Fluvial Bartlesville Channel Sand, Delaware–Childers Field, Nowata County, Oklahoma

Mohamed A. Eissa
Tanta University
Tanta, Egypt, and
University of Oklahoma
Norman, Oklahoma

John P. Castagna and Roy M. Knapp
University of Oklahoma
Norman, Oklahoma

ABSTRACT.—A detailed geological model was constructed using well-log data for the fluvial, oil-producing Pennsylvanian Bartlesville Sand located in the NW¼ sec. 36 and the NE¼ sec. 35, T. 27 N., R. 16 E. of the Delaware–Childers Field, Nowata County, Oklahoma. The high density of wells in the study area (2.5-acre spacing) made it possible to construct a geological model for the sand that is believed to be sufficiently accurate to capture its vertical and lateral heterogeneity and to serve as input for reservoir simulation.

The Bartlesville Sand is shallow in the area of study. Its measured depth is about 600 ft, and it has average gross- and net-sand thicknesses of 44 ft and 35 ft, respectively. The southeast-trending Bartlesville channel sand gently dips to the northwest. The Bartlesville sand has good porosity and permeability with average values of 20% and 90 millidarcies (md), respectively.

The importance of a detailed geological model for enhanced oil recovery in the Bartlesville is because of the inherent lateral and vertical heterogeneity of the reservoir. Many secondary-recovery programs have been tested and some used in the area of study since the field's discovery in 1906. In 1988 through 1990, all of the old wells that could be found were plugged, and new wells were drilled on 2.5-acre spacing. For ease of completion, injection wells were completed with a 1-ft slot cut into the casing at the bottom of the pay zone and producers had a similar 1-ft slot cut at the top of the pay zone. Most wells were then given large sand-fracture treatments. The plan was for water to be injected into the horizontal fractures at the bottom of formation and then "pancake" flood upward through the sand to the producers. Because it was assumed that the sand was homogenous, both laterally and vertically, this plan was unsuccessful.

A detailed stratigraphic correlation from well-log data shows that the Bartlesville channel sand consists of four main units. In some places, shale interbeds separate these sand units, whereas, in other locations, they form a stacked package of continuous sand. The two middle sand units (S2 and S3) have good lateral continuity in the area of study. The top and bottom units (S1 and S4) have limited lateral distribution and grade rapidly into shale. It was the variability of these sand units that caused the failure of the "pancake"-flooding process.

The results of this study have identified previously unrecognized drilling opportunities. Of note is the F. R. Grimmett-739, which was selected based on an expected thickness of 38 net ft of sand and which proved to contain 36 ft of sand. This geological model is now being used to study the use of surfactants in a tertiary-recovery project.

Eissa, M. A.; Castagna, J. P.; and Knapp, R. M., 2002, Accurate geological model for enhanced oil recovery in fluvial Bartlesville channel sand, Delaware–Childers Field, Nowata County, Oklahoma, *in* Boyd, D. T. (ed.), Finding and producing Cherokee reservoirs in the southern Midcontinent, 2002 symposium: Oklahoma Geological Survey Circular 108, p. 175–192.

INTRODUCTION

An accurate geological model is a first step in applying successful enhanced oil-recovery methods, especially in heterogeneous reservoirs like the Bartlesville Sand. There have been several episodes of secondary/enhanced–oil-recovery operations in Delaware–Childers Field. In terms of recovery volumes, Johnston and Riggs (1946) stated that the application of modern secondary-recovery methods has made possible the recovery of more than 13 million barrels of crude from the eastern part of the field alone. However, because none of the previous work was performed with the aid of a detailed geological model, it was decided that another generation of enhanced recovery work was in order. A pilot area in an eastern portion of the field was chosen as the area to test this work.

AREA OF STUDY

The Delaware–Childers Field is located in Nowata County on the Cherokee Platform in northeastern Oklahoma. The pilot area itself is situated in NW¼ sec. 36 and NE¼ sec. 35, T. 27 N., R. 16 E. (Fig. 1). This area of study is part of a regional southeast-trending Bartlesville channel system in which the 2.5-acre well spacing made it possible to construct a very detailed geological model (Fig. 2). Thirty-seven wells were used in mapping the study area, and these led to the drilling of one additional well.

PURPOSE OF STUDY

The Bartlesville reservoir has produced oil in Delaware–Childers Field since its discovery in 1906. Recent core measurements indicate that the sand currently contains about 36% of residual heavy oil with API gravity ranging between 34° and 37°. This high percentage of residual oil, combined with the shallowness of the reservoir, makes this area attractive for additional enhanced oil-recovery work. Many secondary/enhanced-recovery projects have been implemented since the field's discovery. However, by the 1988 through 1990 timeframe, no active wells were left. This led to a renewed development program in which the area was drilled on 2.5-acre spacing. During this program, injection wells were completed with a 1-ft slot cut into the casing at the bottom of the pay zone, and producers had similar slot cut into the casing at the top of the pay zone. Most of the wells were then given a large sand-fracture treatment. This was done to enable water to enter the artificial horizontal fractures at the bottom of formation and then "pancake" flood upward through the sand to the producers. The assumption was that the sand was homogenous both laterally and vertically was false, leading to the failure of this project. The purpose of this study was to determine if it would be possible to achieve an economically successful project using surfactants when both the detailed structure and reservoir heterogeneities were factored into the geologic model.

STRATIGRAPHY

The Middle Pennsylvanian (Desmoinesian) Bartlesville Sand is an informal subsurface subdivision of the Cherokee Group, occurring below the Inola Limestone and above the Brown Limestone (Fig. 3). Named for the city of Bartlesville, Oklahoma, it has also been called the Glenn Sand (for the Ada Glenn farm at Glennpool Field) and the Salt Sand in the Okmulgee area (Jordan, 1957). The Bartlesville Sand is also correlative with the outcropping Bluejacket Sandstone (Boggy Formation, Krebs Group), named by Ohern (1914) for the town of Bluejacket in Craig County, Oklahoma (Northcutt and others, 1997). Figure 3 is a stratigraphic-nomenclature/type-log chart for the study area showing all of the rock units discussed and their typical log character.

REGIONAL GEOLOGY

The area of study is located on the Cherokee Platform, which is bounded by the Ozark Uplift to the east, Nemaha Uplift to the west, and Arkoma Basin to the south (Fig. 1). Early Pennsylvanian uplift and erosion removed much of the Mississippian strata in central and northeastern Oklahoma, exposing these and older rocks on the emergent Ozark Uplift. A large, north-trending, faulted arch extended from central Oklahoma into Kansas. This incipient Nemaha Uplift (or fault zone) separated the Anadarko Basin to the west from the Cherokee Platform to the east. During the Early Pennsylvanian, Atoka and Morrow sediments, which are now largely absent on the Cherokee Platform, were deposited in the Arkoma Basin located to the southeast (Johnson, 1971).

At the beginning of the Desmoinesian in the Arkoma Basin, sands of the Hartshorne Formation prograded from Arkansas westward into Oklahoma, forming a deltaic system along the axis of the basin (Houseknecht, 1984). Following Hartshorne deposition, the McAlester Formation was deposited as a series of deltaic sequences prograding southward across the Cherokee Platform into the Arkoma Basin.

The Brown Limestone of the Savanna Formation was deposited as a series of transgressive marine shales and thin limestones that lap onto the McAlester Formation and older underlying strata on the platform. It was on this surface that the Bartlesville equivalents—including the Bluejacket Sandstone—of the Boggy Formation were deposited. Bartlesville deposition and production are situated primarily on the Cherokee Platform (Northcutt and others, 1997).

GEOLOGICAL MODEL

Bartlesville Sand Log Character

The Bartlesville Sand typically shows a low gamma-ray reading ranging from 35° to 60° API. It also exhibits neutron and density porosity values that average approximately 20%. The Bartlesville Sand, where oil

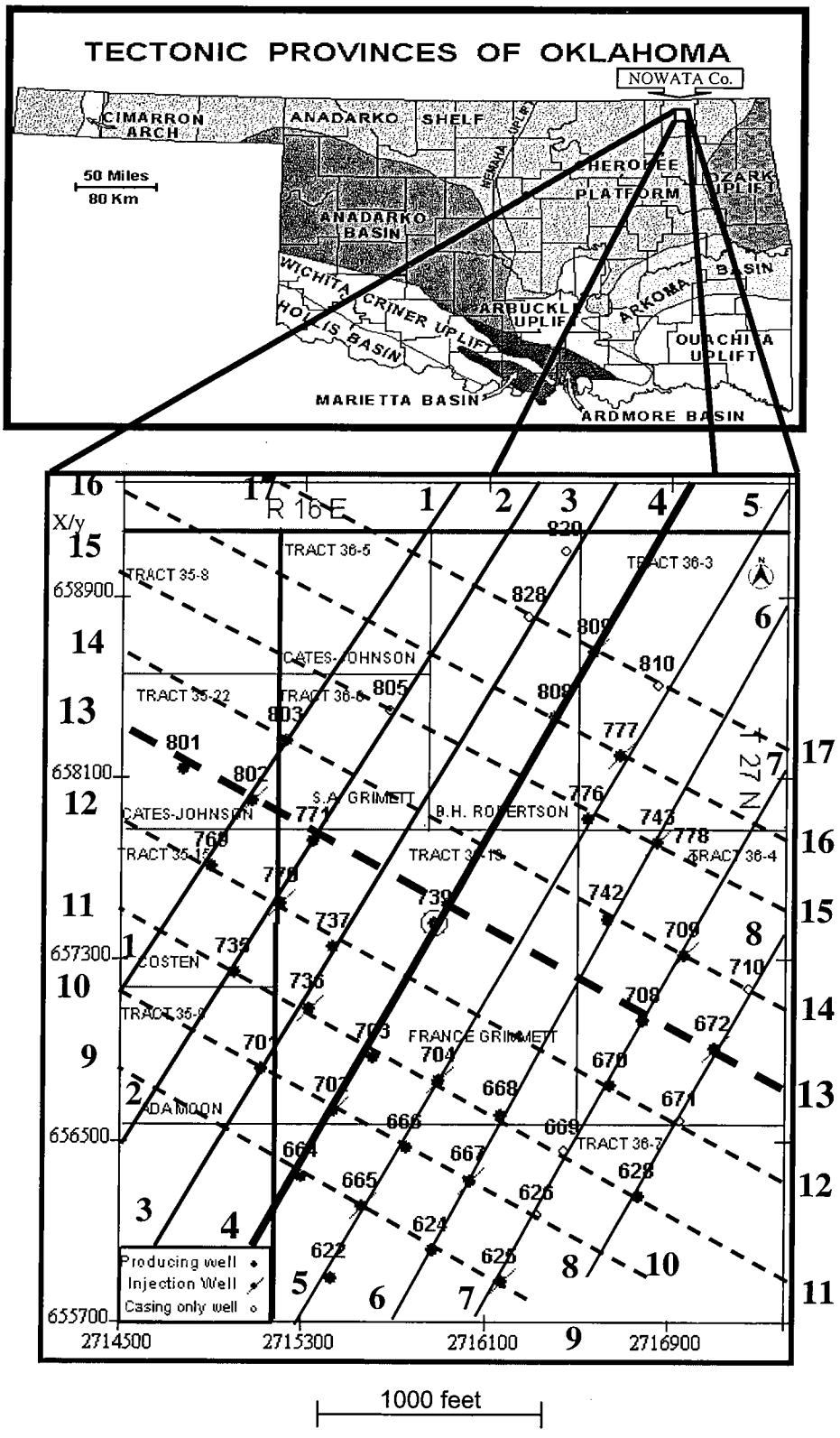

Figure 1. Map of tectonic provinces of Oklahoma, showing study area, location of wells, and lines of cross sections. Cross sections 13 and 4 (bolder lines) are shown in detail in Figures 6 and 7, respectively.

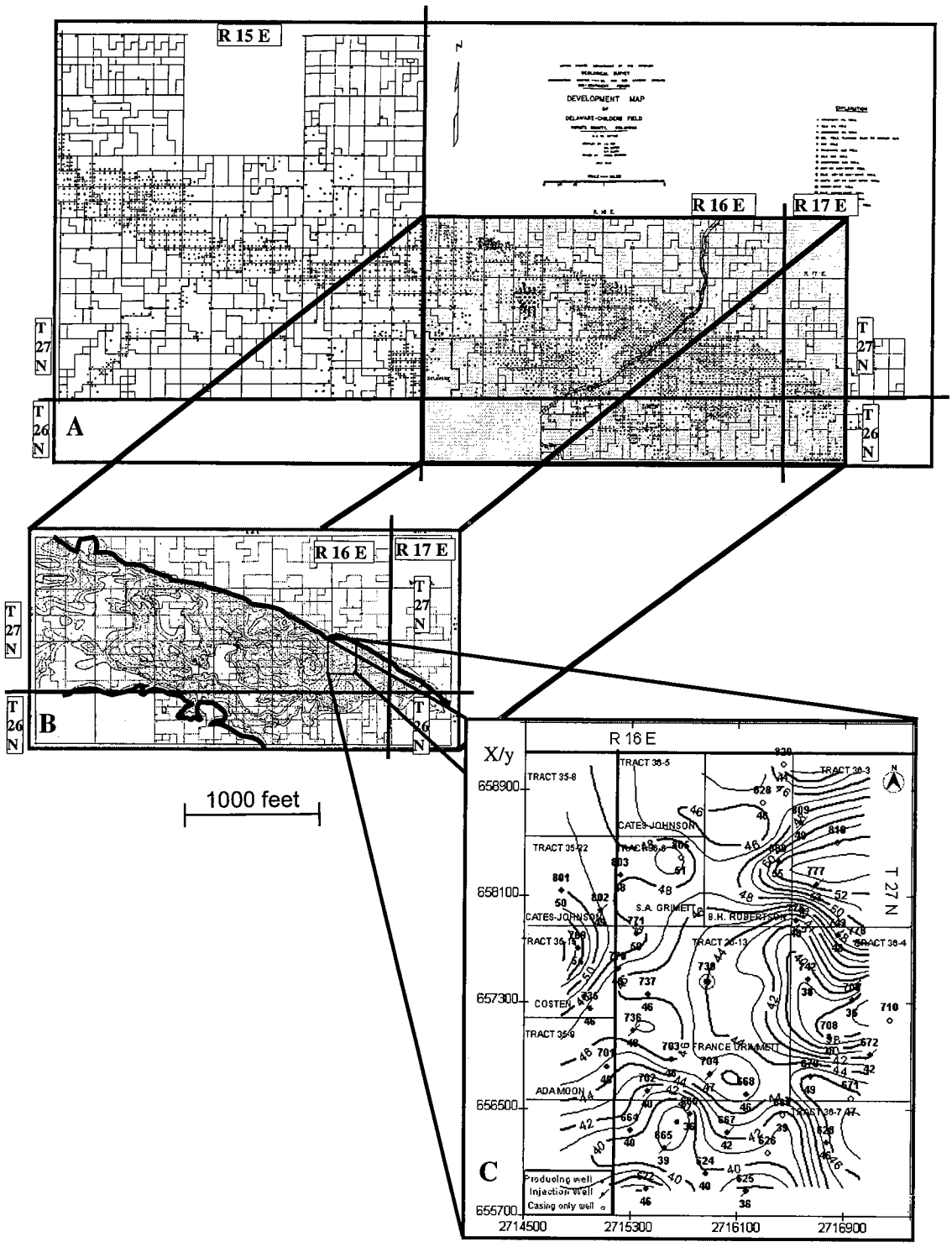

Figure 2. Maps of Delaware–Childers Field. (A) Regional development map showing location of oil-producing wells from Bartlesville Sand. (B) Map showing regional gross thickness of Bartlesville Sand, highlighting channel orientation. (C) Detailed gross-sand thickness map for the Bartlesville channel in feet (contour interval 1 ft) in study area.

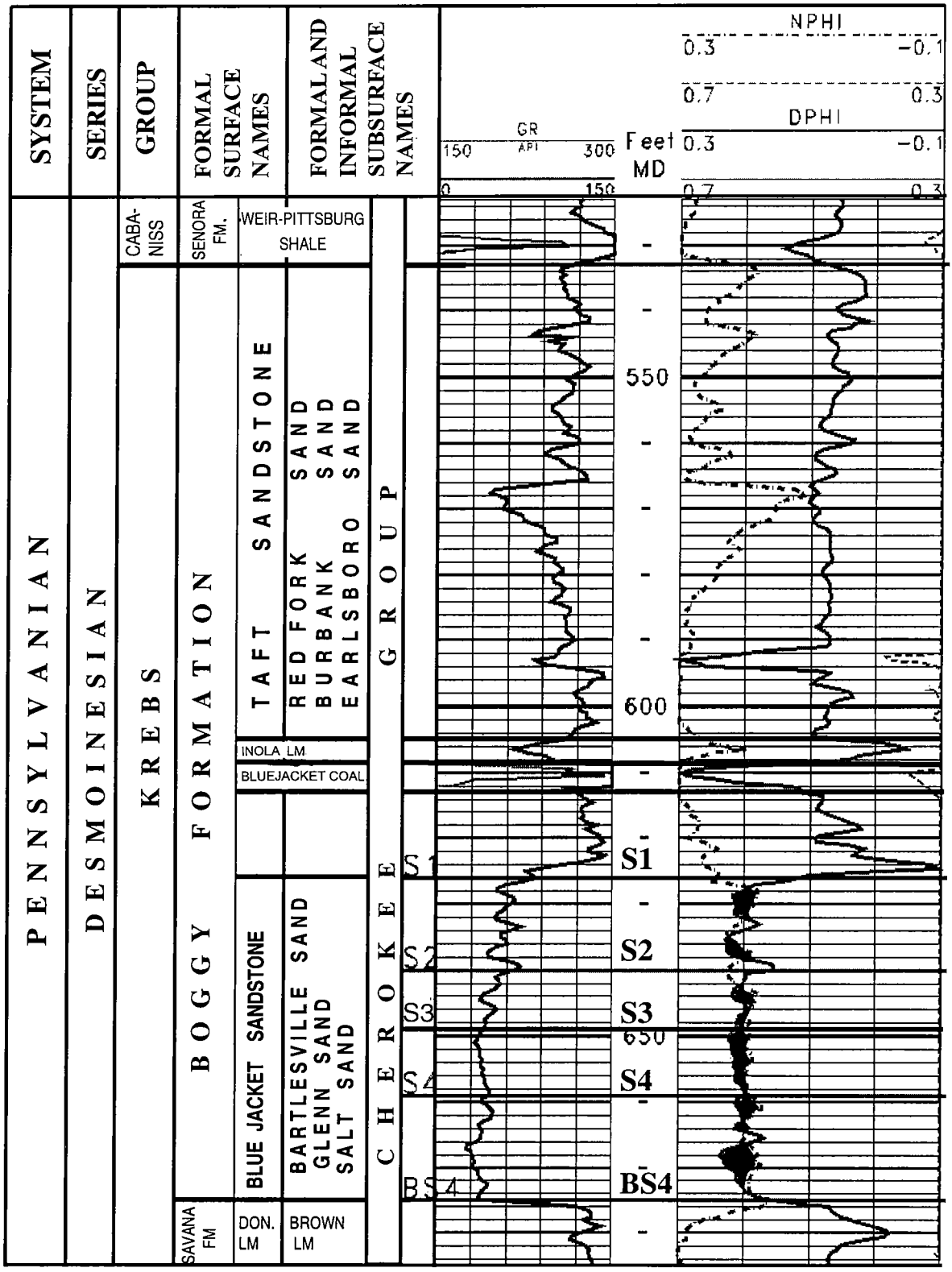

Figure 3. Type log showing stratigraphic column, subdivisions, and well-log characteristics of Bartlesville Sand in the Cates Johnson 802 well.

saturated, has a deep resistivity reading that ranges from 30 to 100 ohm-m.

Bartlesville Sand Core Analysis

Core-analysis reports were available for most of the cored wells in the study area. Figure 4 shows a typical core photograph for the Bartlesville Sand in the Cates Johnson 802 well with the contacts for all of the subunits of the sand that will be discussed here. The dark-brown color of the sand is probably due to residual-oil staining, which is supported by the lighter color in the lower part of the core where the oil/water-transition zone occurs. Although visible in the core, thin-shale or impermeable-sand streaks cannot be resolved on well logs. The four subdivisions of the Bartlesville Sand utilized here are not as easy to recognize in core as they are on well logs. Examination of the core itself was not carried out.

Porosity, permeability, water saturation, and capillary pressure were measured for the F. R. Grimmett 739 well at the University of Oklahoma Core Characterization Center in Tulsa (Table 1). Figure 5A is a graphic display of the permeability, water-saturation, and porosity measurements, whereas Figure 5B shows capillary pressure versus mercury saturation for selected core plugs. These measurements show that the Bartlesville Sand in this well has an average water saturation of about 64% (residual-oil saturation of 36%), permeability of about 90 millidarcies (md), and porosity of about 20%.

Stratigraphic Correlation

Well data from the 38 wells in Table 2 were used to build the geological model. The lower Weir-Pittsburg shale marker, about 100 ft above the Bartlesville Sand, was used as a stratigraphic datum for well-log correlation. Seventeen stratigraphic cross sections were constructed, nine of which are directed northeast–southwest and eight directed northwest–southeast (Fig. 1). Based on log character, the Bartlesville Sand was divided into four sand units: S1, S2, S3, and S4, from top to bottom. These are stacked as continuous sand in some places and are separated by shale streaks in others. The two middle sand units (S2 and S3) have good lateral continuity. The top sand unit (S1) and the bottom sand unit (S4) have limited lateral distribution and change rapidly laterally to shale. These sand units are not homogenous vertically or horizontally.

Two stratigraphic cross sections have been selected as figures in this paper. Figure 6 is a northwest–southeast stratigraphic cross section parallel to the transport direction of the Bartlesville channel sand. The four sand units are quite continuous in this cross section, with only S1 shaling out to the southeast. Figure 7 is a northeast–southwest stratigraphic cross section perpendicular to the channel. It shows that the upper three units (S1, S2, and S3) are absent in the Ida Mae Brown 809 well, which is close to the channel edge.

STRUCTURE

Structure maps were constructed on top of all four sand units (Fig. 8A–D), with each exhibiting similar structural features. All depths are above sea level. These maps show gentle northwest dip with a structural high located in the area of the B. H. Robertson 672 well. At this micro-structural scale, two small ridges parallel the channel with an intervening saddle.

Reservoir Distribution

Gross- and net-sand thickness maps also were constructed for individual sand members and for the complete sand package. The gamma-ray log was used as a shale indicator, with a cutoff halfway between the clean sand and shale baselines.

Gross Thickness

The S1 unit shows an increase in gross thickness to the southwest, with an elongated sand "thick" coincident with the established structural low. This unit's gross thickness ranges from 8 to 17 ft (Fig. 9A).

The S2 unit shows an increase in gross thickness to the north and northeast, with a thick lenticular sand body developed around the Ida Mae Brown 777, B. H. Robertson 808, and Ida Mae Brown 809 wells (Fig. 9B). Like Unit 1, the area of thickest sand in S2 is in the structural low. This unit has a maximum gross thickness of 17 ft in the B. H. Robertson 808 well and a minimum of 6 ft in the area of the southeastern structural high.

The gross-sand map for the S3 unit shows several elongated sand "thicks," with the thickest (16 ft) located in the B. H. Robertson 808 well. A parallel "thin" is present in the southwestern portion of the study area, with minimum thickness of 6 ft in the F. R. Grimmett 736 well (Fig. 9C).

The S4 gross-sand map shows a number of disconnected sand "thicks" in the study area. These range in thickness from 5 to 17 ft (Fig. 9D).

Net-Sand Thickness

The net-sand thickness map for S1 shows lenses of thick sand in the southwestern and northwestern corners of the area of study (Fig. 10A). The edge of the Bartlesville channel sand can be seen to the northeast where the net sand is zero. Net-sand thickness for this unit ranges from 0 to 16 ft.

Figure 10B shows the net-sand thickness map for unit S2. There, a thick, elongated sand body is present to the northeast, around the B. H. Robertson 808 well, near the edge of the channel. Net-sand thickness ranges from 0 to 17 ft.

Figure 10C exhibits the net-sand thickness for unit S3. It also shows a thick, elongated sand body to the northeast around the B. H. Robertson 808 well. Its thickness ranges from 0 to 16 ft.

The net-sand–thickness map for unit S4 shows elongated sands bodies thickening to the northeast, north-

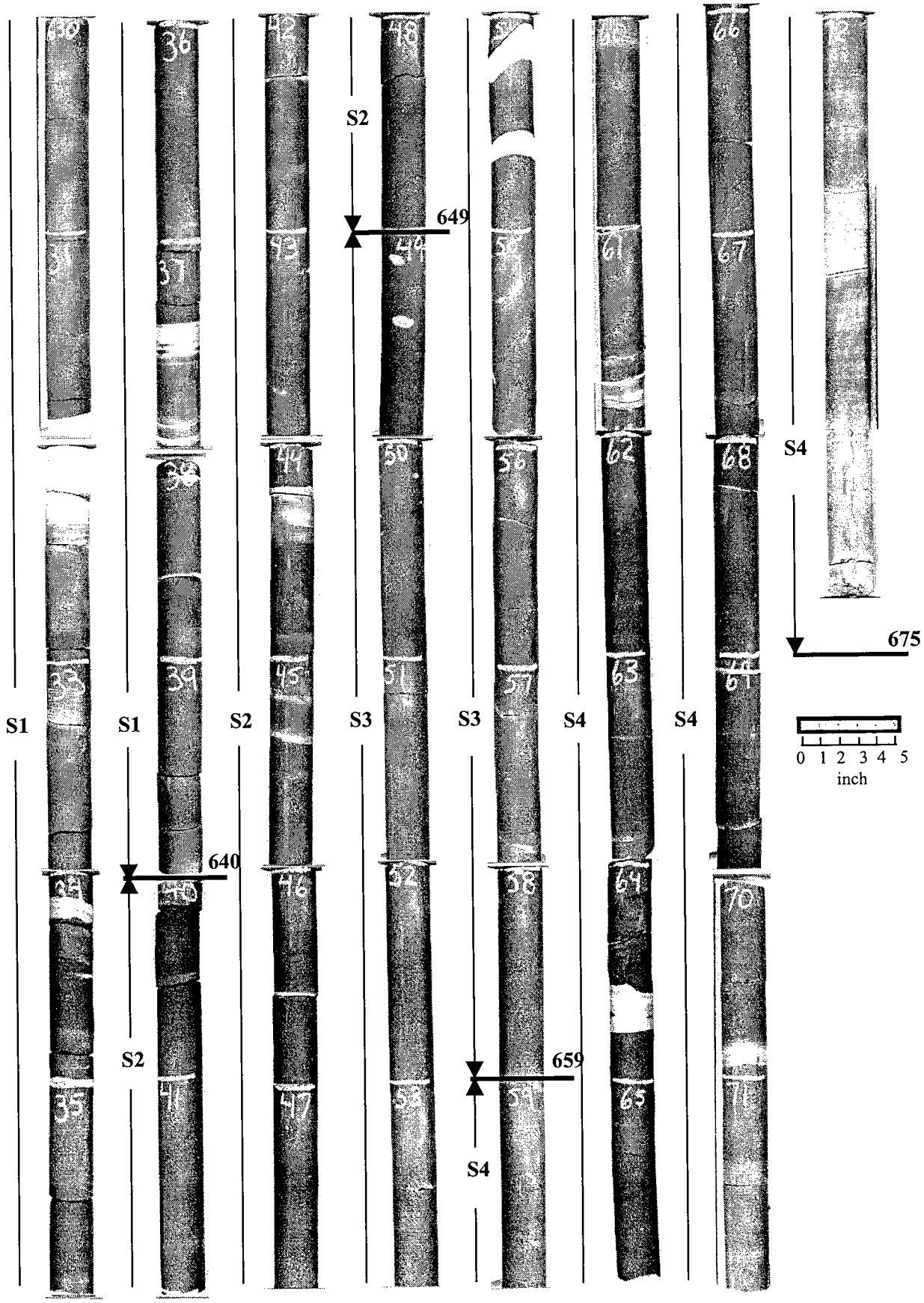

Figure 4. Photograph of core of Bartlesville Sand from Cates Johnson 802 well, from depth 630 ft (4 ft below top of unit S1) to 675 ft (base of unit S4), showing different sand units. Depth is marked every 1 ft.

TABLE 1.—Core Analysis for the F. R. Grimmett 739 Well

Depth (ft)	Porosity (%)	Permeability (md)	Water saturation (Sw)
613.0	18.06	18.840	66.72
614.0	15.12	3.496	
615.0	9.08	0.029	100.00
616.0	9.38	0.041	
617.2	7.72	0.022	100.00
618.0	8.83	0.030	
619.0	9.17	0.028	100.00
619.4	7.82	0.014	100.00
620.0	6.85	0.005	
621.0	7.42	0.014	100.00
622.0	5.59	0.002	
623.0	9.27	0.024	71.68
623.2	11.38	0.380	37.47
624.0	3.04	0.000	
625.0	6.73	0.011	100.00
626.0	18.33	39.984	
627.0	20.37	156.289	65.49
628.0	20.37	86.764	
629.0	20.43	226.606	85.19
630.0	12.62	1.203	
631.0	20.06	146.526	73.96
632.0	19.49	114.327	
633.0	19.27	174.070	71.93
634.0	19.88	174.180	
635.0	20.33	150.410	78.72
635.5	17.90	26.020	50.61
636.0	19.24	53.349	
637.0	16.87	26.596	61.24
638.0	19.03	16.506	
639.0	20.50	102.473	59.69
640.0	11.96	2.434	
641.0	18.96	43.050	67.41
642.0	19.29	51.931	
643.0	20.26	93.420	72.89
644.0	16.76	41.862	
645.0	19.92	75.19	62.04
646.0	18.15	47.50	
647.0	19.95	91.65	61.49
648.0	19.43	74.64	
649.0	19.55	84.12	69.33
650.0	21.94	170.87	
651.0	20.28	90.81	63.36
652.0	21.37	116.32	
653.0	17.83	15.32	60.74
654.0	21.03	113.26	
655.0	22.19	211.99	66.08
656.0	20.40	197.50	
657.0	18.59	60.59	77.20
658.0	21.33	146.58	
659.0	12.89	6.24	78.49
660.0	21.55	107.04	
661.0	19.81	262.85	47.85
662.0	8.49	0.99	

west, and southeast. Net thickness ranges from 5 to 17 ft (Fig. 10D).

Net-to-Gross Maps

Net-to-gross maps for each sand unit and for the complete sand package also were constructed (Fig. 11). The net-to-gross thickness for unit S1 decreases to the north and becomes zero at the north edge of the Bartlesville channel. In S2, most of the wells have net-to-gross value of 1, showing its low shale content and good horizontal and vertical continuity. Net-to-gross values for unit S3 decrease to the northeast but show good vertical and horizontal continuity in the southwest. S4 values are also quite high, ranging from 0.55 to 1.

Composite-Sand Package

The structure map at the base of the Bartlesville sand package shows gentle dip to the northwest with two small-scale anticlines trending in the same direction (Fig. 12A). The areas of thickest net sand (>40 ft) show a possible connection with structural lows.

Figure 12B shows the total-gross thickness of the Bartlesville sand package from the top of S1 to the base of S4, which varies from 36 ft to 55 ft. The corresponding net-sand thickness for the composite Bartlesville sand is shown in Figure 12C, and it shows elongate sand "thicks." One of these sand "thicks" is present around the B. H. Robertson 808 well and another around the F. R. Grimmett 737, 736, 703, and 704 wells. Based on this map, a well was proposed northeast of this area of thick sand, at a location on the 38-ft contour line. The F. R. Grimmett 739 well was drilled on May 2, 2001, and encountered 36 ft of net sand.

Figure 12D maps the net-to-gross ratio for the sand package. It shows a similar distribution as that seen in the net-sand map, with a decrease in the ratio to the north, in the direction of the channel margin.

ESTIMATE OF POSSIBLE TERTIARY OIL RECOVERY

An estimate of possible tertiary oil recovery can be derived using the parameters shown in Table 3. These estimates suggest that a surfactant-based, tertiary-oil–recovery pilot project can recover from 20% to as much as 80% of the residual-oil saturation in this pilot area. The higher recovery values can be obtained using a higher concentration of surfactant. If the efficiency of the tertiary recovery process is at least 25%, then about 4,750 stock-tank barrels per acre (stb/ac) is an attainable target for this field. Because the field is on a 2.5-acre spacing, per well recoveries would be 11,875 stb. If this process could be expanded to all 38 wells, it could mean that the entire tertiary recovery target could be about 450,000 stb.

CONCLUSIONS

Seven significant conclusions have been reached as a result of this study. (1) An accurate geological model is critical for enhanced oil recovery projects. (2) The heterogeneity of the fluvial Bartlesville Sand was

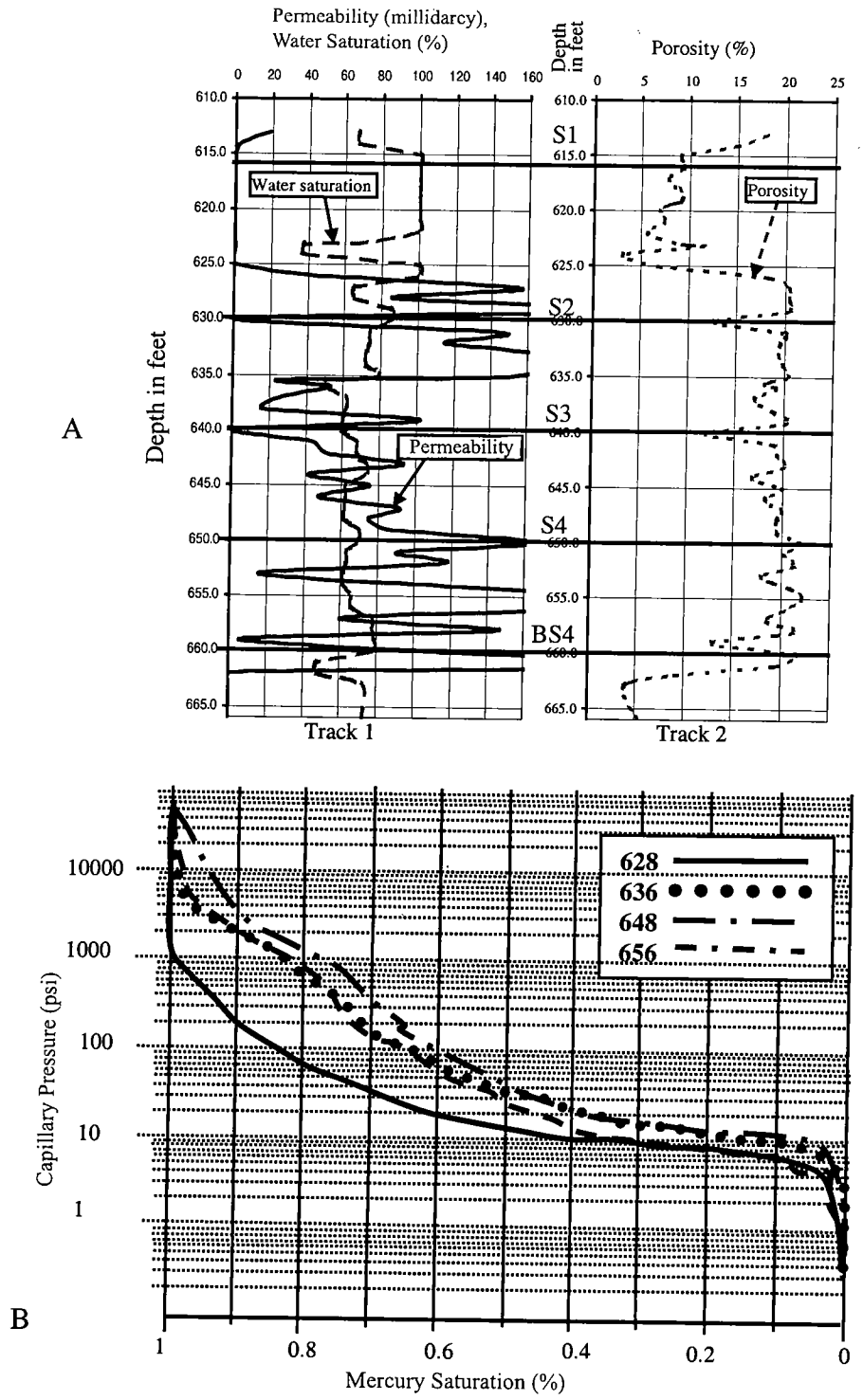

Figure 5. Core-derived petrophysical measurements in the Bartlesville Sand from the F. R. Grimmett 739 well. (A) Permeability and water saturation in track 1 and porosity in track 2 versus depth in feet. (B) Capillary pressure versus saturation for core plugs at depths of 628, 636, 648, and 656 ft.

addressed by dividing it into four separate sand units. (3) The S2 and S3 units show better lateral continuity than the S1 and S4. (4) Bartlesville Sand deposition may be influenced by structure. (5) The Bartlesville Sand has good porosity and permeability. (6) The geological model shown herein led to an accurate prediction of the F. R. Grimmett 739 well sand thickness. (7) By using an accurate geological model, 450,000 stb could be recovered easily from the area of study.

TABLE 2.—Well Log Data Sheet

Well name	KB (ft)	Measured depth (ft)					Subsea depth (ft)					Gross thickness (ft)					Net sand thickness (ft)					Net to gross				
		S1	S2	S3	S4	BS4	S1	S2	S3	S4	S1-BS4	S1	S2	S3	S4	S1-BS4	S1	S2	S3	S4	S1-BS4	S1	S2	S3	S4	S1-BS4
1) Cates Johnson 801	735	650	665	675	684	700	85	70	60	51	35	15	10	9	16	50	15	10	9	16	50	1	1	1	1	1
2) S. A. Grimmett 803	709	618	632	642	649	666	91	77	67	60	43	14	10	7	17	48	0	0	4	17	21	0	0	0.57	1	0.43
3) Costen 769	718	634	648	660	674	688	84	70	58	44	30	14	12	14	14	54	3	12	14	9	38	0.21	1	1	0.64	0.70
4) F. R. Grimmett 771	707	620	633	645	654	670	87	74	62	53	37	13	12	9	16	50	2	12	9	16	39	0.15	1	1	1	0.78
5) Costen 735	709	626	641	654	660	672	83	68	55	49	37	15	13	6	12	46	2	13	6	12	33	0.13	1	1	1	0.71
6) F. R. Grimmett 737	703	618	634	644	654	664	85	69	59	49	39	16	10	10	10	46	16	10	10	10	46	1	1	1	1	1
7) Ada Moon 701	698	619	634	644	656	664	79	64	54	42	34	15	10	12	8	45	0	10	12	5	27	0	1	1	0.62	0.6
8) F. R. Grimmett 703	702	615	630	640	647	663	87	72	62	55	39	15	10	7	16	48	15	10	7	16	48	1	1	1	1	1
9) Lillie Tanner 664	695	615	630	642	650	655	80	65	53	45	40	15	12	8	5	40	15	12	8	5	40	1	1	1	1	1
10) Lillie Tanner 666	702	620	631	639	647	656	82	71	63	55	46	11	8	8	9	36	6	8	8	5	27	0.54	1	1	0.55	0.75
11) Lillie Tanner 668	707	608	621	629	642	654	99	86	78	65	53	13	8	13	12	46	13	8	13	12	46	1	1	1	1	1
12) Cates Johnson 802 I	714	626	640	649	659	675	88	74	65	55	39	14	9	10	16	49	14	9	10	16	49	1	1	1	1	1
13) Costen 770 I	707	630	647	655	665	676	77	60	52	42	31	17	8	10	11	46	2	8	10	7	27	0.12	1	1	0.64	0.57
14) F. R. Grimmett 736 I	700.6	617	633	645	651	665	83.6	67.6	55.6	49.6	35.6	16	12	6	14	48	16	12	6	14	48	1	1	1	1	1
15) F. R. Grimmett 702 I	699.5	618	634	644	652	658	81.5	65.5	55.5	47.5	41.5	16	10	8	6	40	16	10	8	6	40	1	1	1	1	1
16) F. R. Grimmett 704 I	708	615	629	640	648	662	93	79	68	60	46	14	11	8	14	47	14	11	8	14	47	1	1	1	1	1
17) Lillie Tanner 665 I	697	614	629	639	648	653	83	68	58	49	44	15	10	9	5	39	15	10	9	5	39	1	1	1	1	1
18) Lillie Tanner 667 I	700	604	619	627	635	646	96	81	73	65	54	15	8	8	11	42	15	2	8	11	36	1	0.25	1	1	0.86
19) Lillie Tanner 622	691.5	606	618	632	643	652	85.5	73.5	59.5	48.5	39.5	12	14	11	9	46	3	14	11	9	37	0.25	1	1	1	0.80
20) Lillie Tanner 624	697	608	622	630	638	648	89	75	67	59	49	14	8	8	10	40	14	8	8	8	38	1	1	1	0.8	0.95
21) Lillie Tanner 625 I	699	610	622	632	640	646	89	77	67	59	53	12	10	8	6	36	12	10	8	6	36	1	1	1	1	1
22) Lillie Tanner 628	710.5	602	616	622	634	648	108.5	94.5	88.5	76.5	62.5	14	6	12	14	46	14	0	12	14	40	1	0	1	1	0.87
23) Lillie Tanner 669I	710	610	622	634	644	649	100	88	76	66	61	12	12	10	5	39	10	12	10	5	37	0.83	1	1	1	0.95
24) Lillie Tanner 671	716	602	613	620	633	649	114	103	96	83	67	11	7	13	16	47	11	7	10	12	40	1	1	0.77	0.75	0.85
25) B. H. Robertson 670	707	611	625	636	644	660	96	82	71	63	47	14	11	8	16	49	12	11	8	16	47	0.86	1	1	1	0.96
26) B. H. Robertson 672	710	589	600	611	621	631	121	110	99	89	79	11	11	10	10	42	0	11	10	10	31	0	1	1	1	0.74
27) B. H. Robertson 708 I	711	603	614	622	632	639	108	97	89	79	72	11	8	10	7	36	7	8	10	5	30	0.64	1	1	0.71	0.83
28) B. H. Robertson 709	702	596	606	616	624	632	106	96	86	78	70	10	10	8	8	36	0	10	8	8	26	0	1	1	1	0.72
29) B. H. Robertson 742	705	607	618	628	636	645	98	87	77	69	60	11	10	8	9	38	0	10	5	9	24	0	1	0.62	1	0.63
30) B. H. Robertson 743	700	596	606	618	632	644	104	94	82	68	56	10	12	14	12	48	8	12	10	12	42	0.8	1	0.71	1	0.87
31) B. H. Robertson 808	701	609	617	634	650	664	92	84	67	51	37	8	17	16	14	55	0	17	16	14	47	0	1	1	1	0.85
32) B. H. Robertson 828	692	610	617	629	640	656	82	75	63	52	36	7	12	11	16	46	0	0	0	16	16	0	0	0	1	0.35
33) B. H. Robertson 829	686	602	614	625	632	643	84	72	61	54	43	12	11	7	11	41	0	0	5	8	13	0	0	0.71	0.73	0.32
34) Ida Mae Brown 776	711	614	626	639	650	654	97	85	72	61	57	12	13	11	4	40	12	13	3	4	32	1	1	0.27	1	0.8
35) Ida Mae Brown 777	705	611	620	636	650	664	94	85	69	55	41	9	16	14	14	53	0	16	14	14	44	0	1	1	1	0.83
36) Ida Mae Brown 805	702.5	612	622	638	649	663	90.5	80.5	64.5	53.5	39.5	10	16	11	14	51	7	16	0	14	37	0.7	1	0	1	0.73
37) Ida Mae Brown 809	701	615	623	639	647	664	86	78	62	54	37	8	16	8	17	49	0	0	0	17	17	0	0	0	1	0.35
38) F. R. Grimmett 739	703	616	630	640	650	660	87	73	63	53	43	14	10	10	10	44	6	10	10	10	36	0.43	1	1	1	0.81

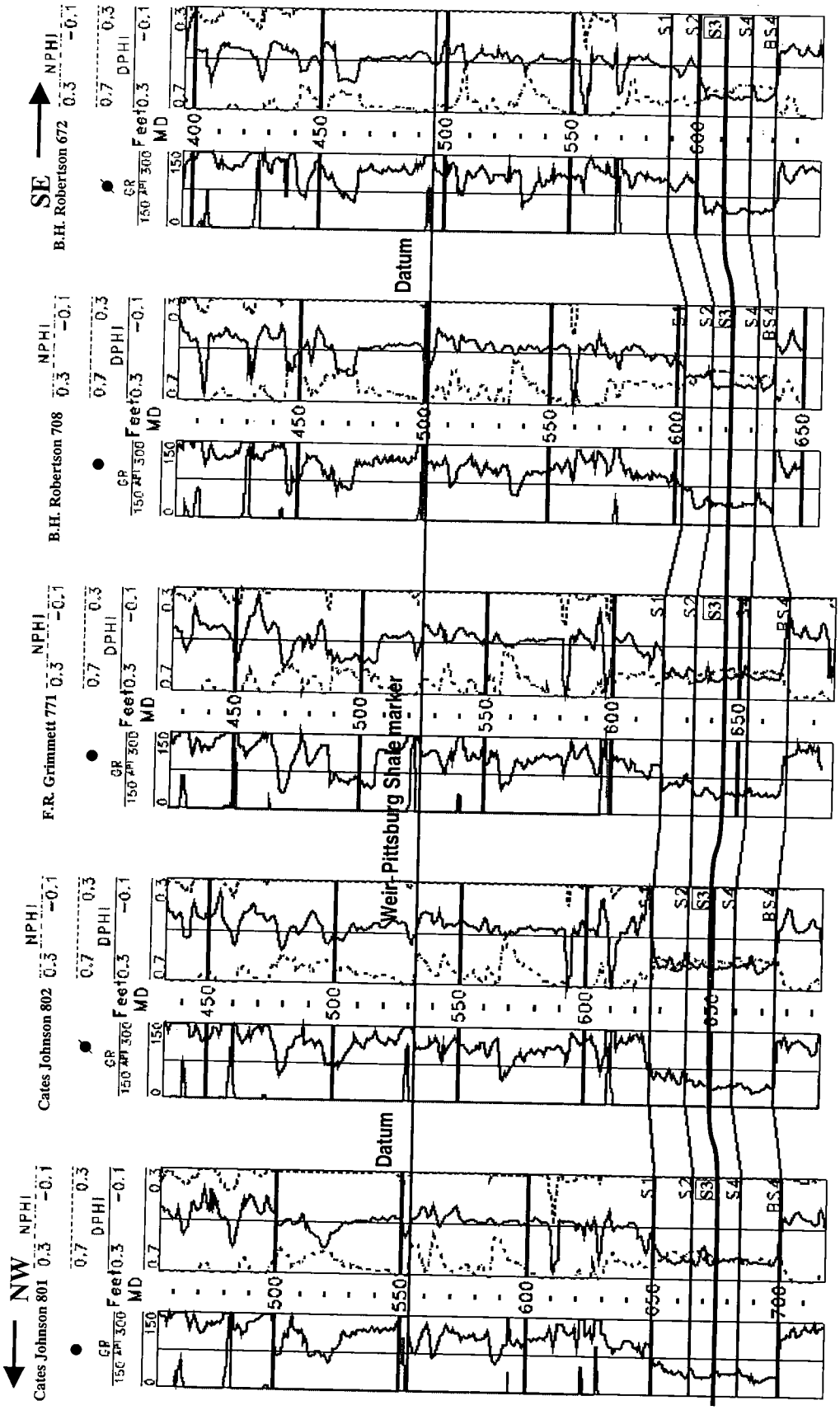

Figure 6. Northwest–southeast stratigraphic cross section (#13 on Fig. 1).

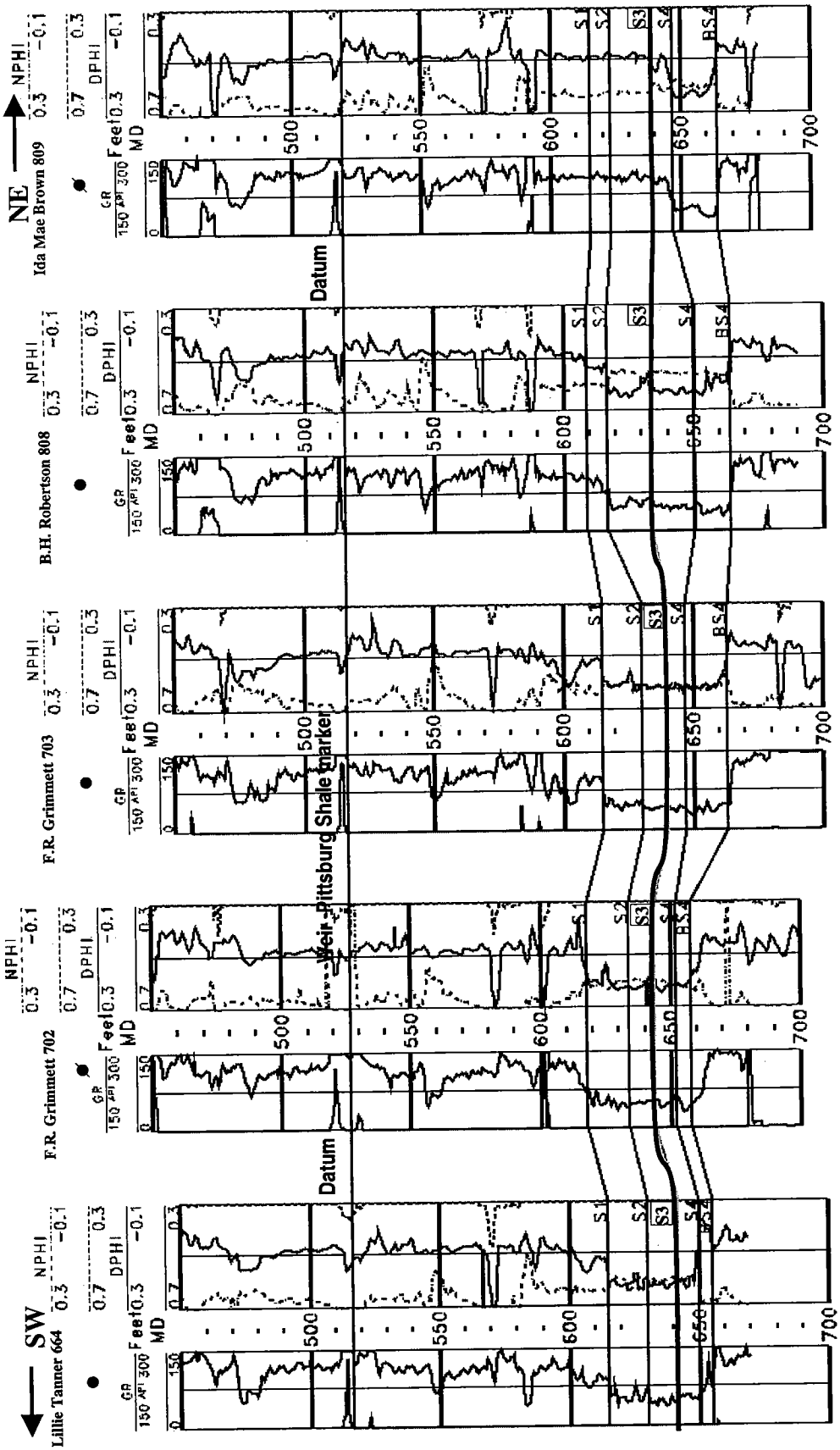

Figure 7. Northeast–southwest stratigraphic cross section (#4 on Fig. 1).

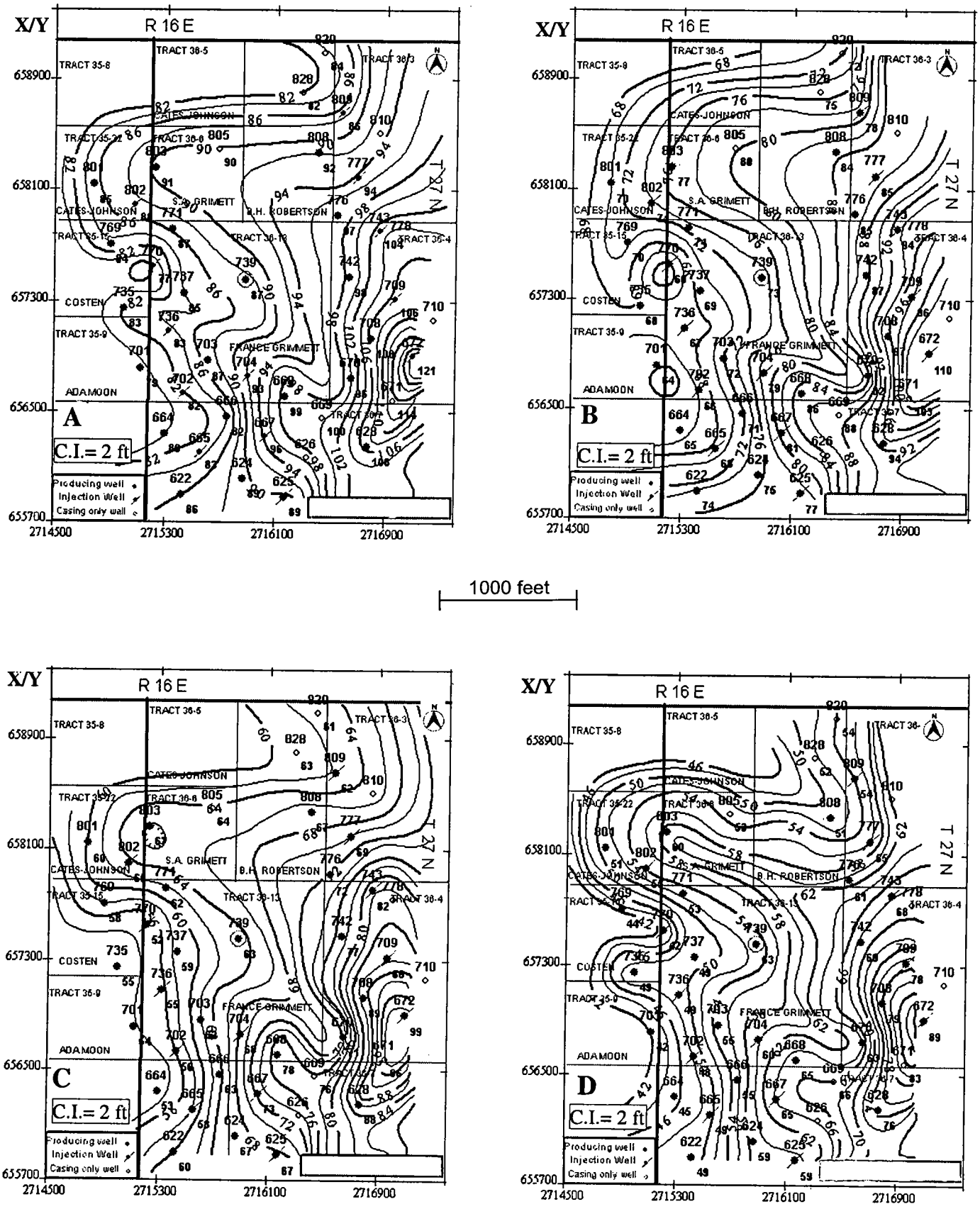

Figure 8. Subsurface structure-contour maps on top of the Bartlesville Sand units, with contour interval 2 ft. (A) S1, (B) S2, (C) S3, and (D) S4.

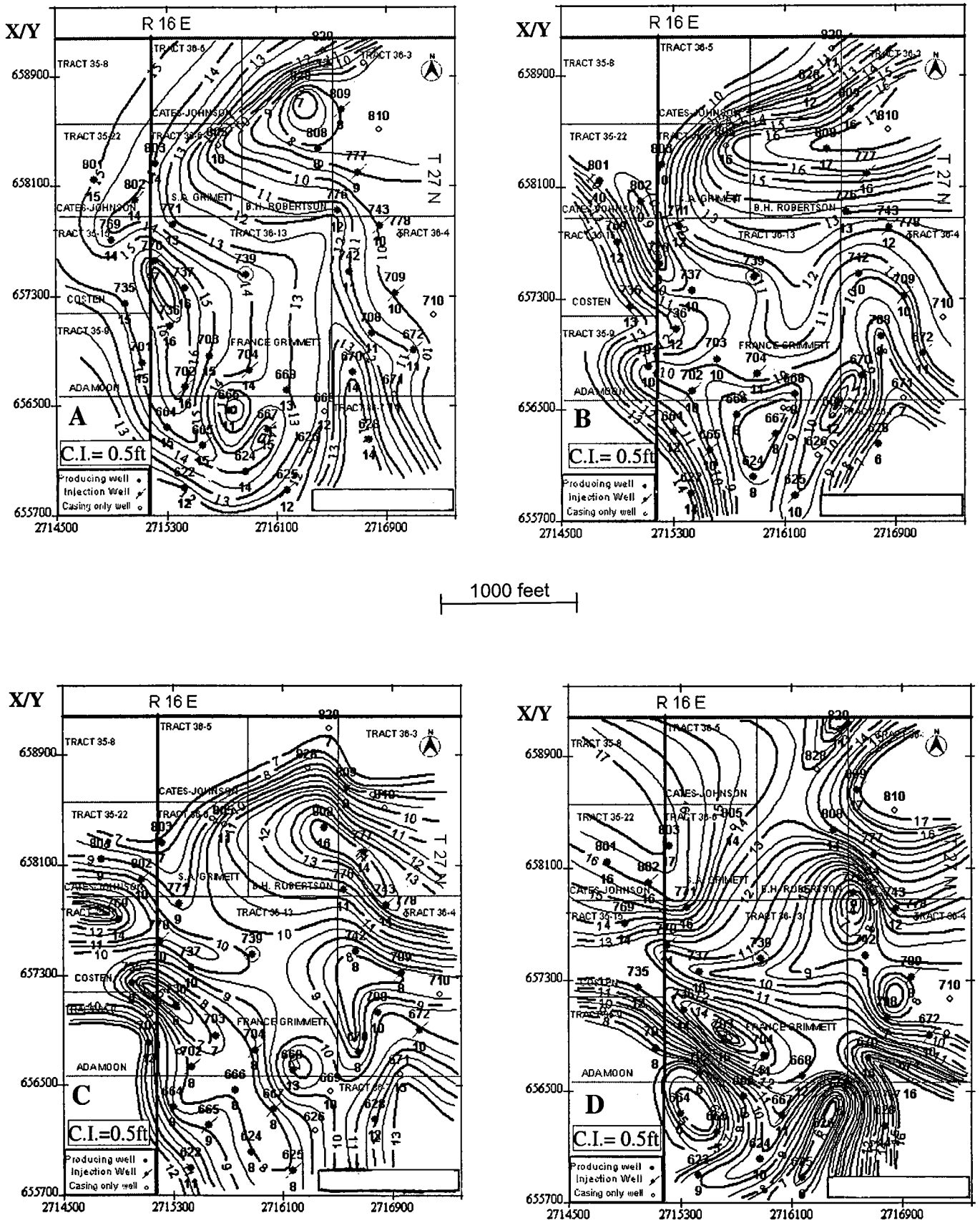

Figure 9. Gross-interval isopach maps for the Bartlesville Sand units, with contour interval 0.5 ft. (A) S1, (B) S2, (C) S3, and (D) S4.

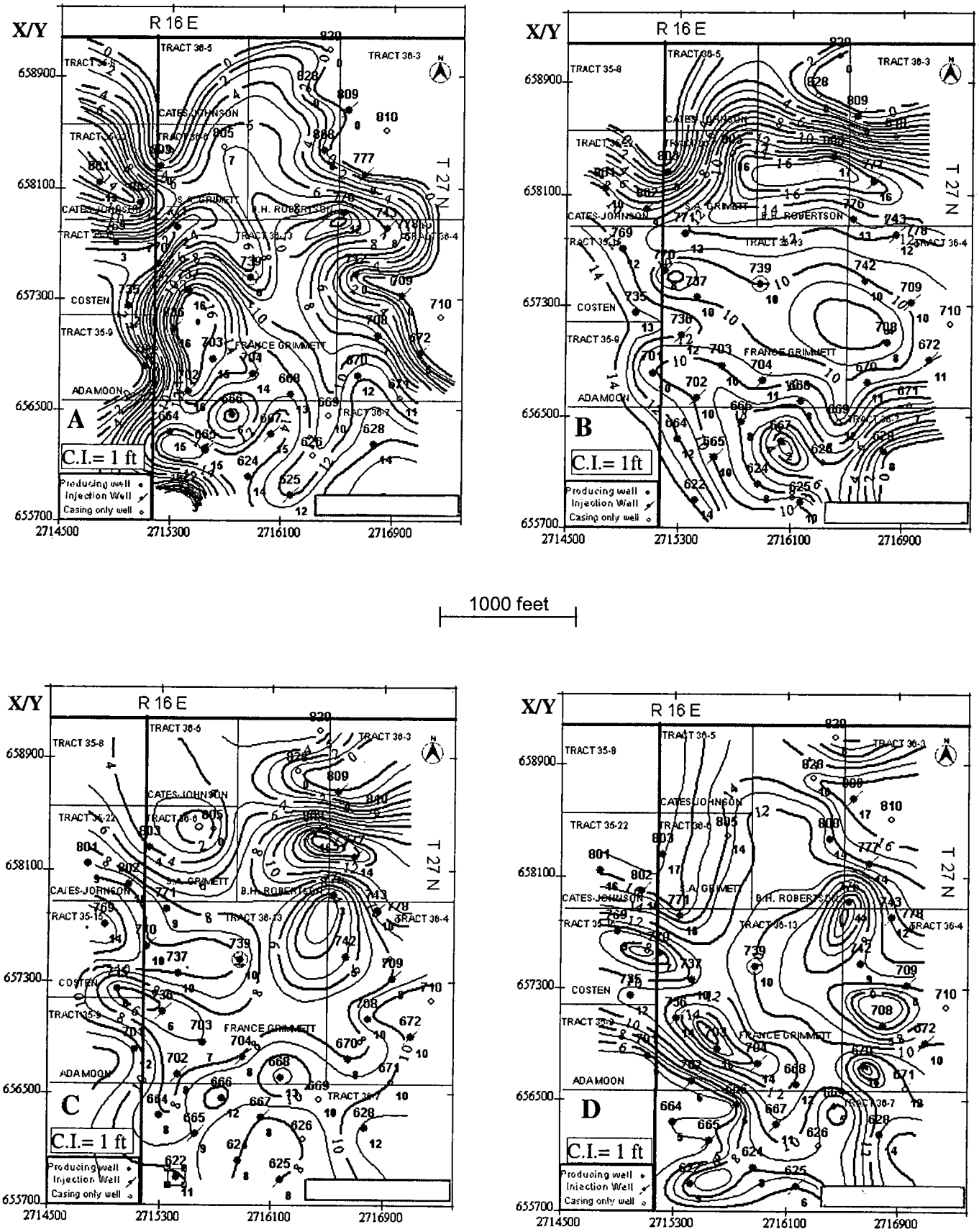

Figure 10. Net-sand isopach maps for the Bartlesville Sand units, with contour interval 1 ft. (A) S1, (B) S2, (C) S3, and (D) S4.

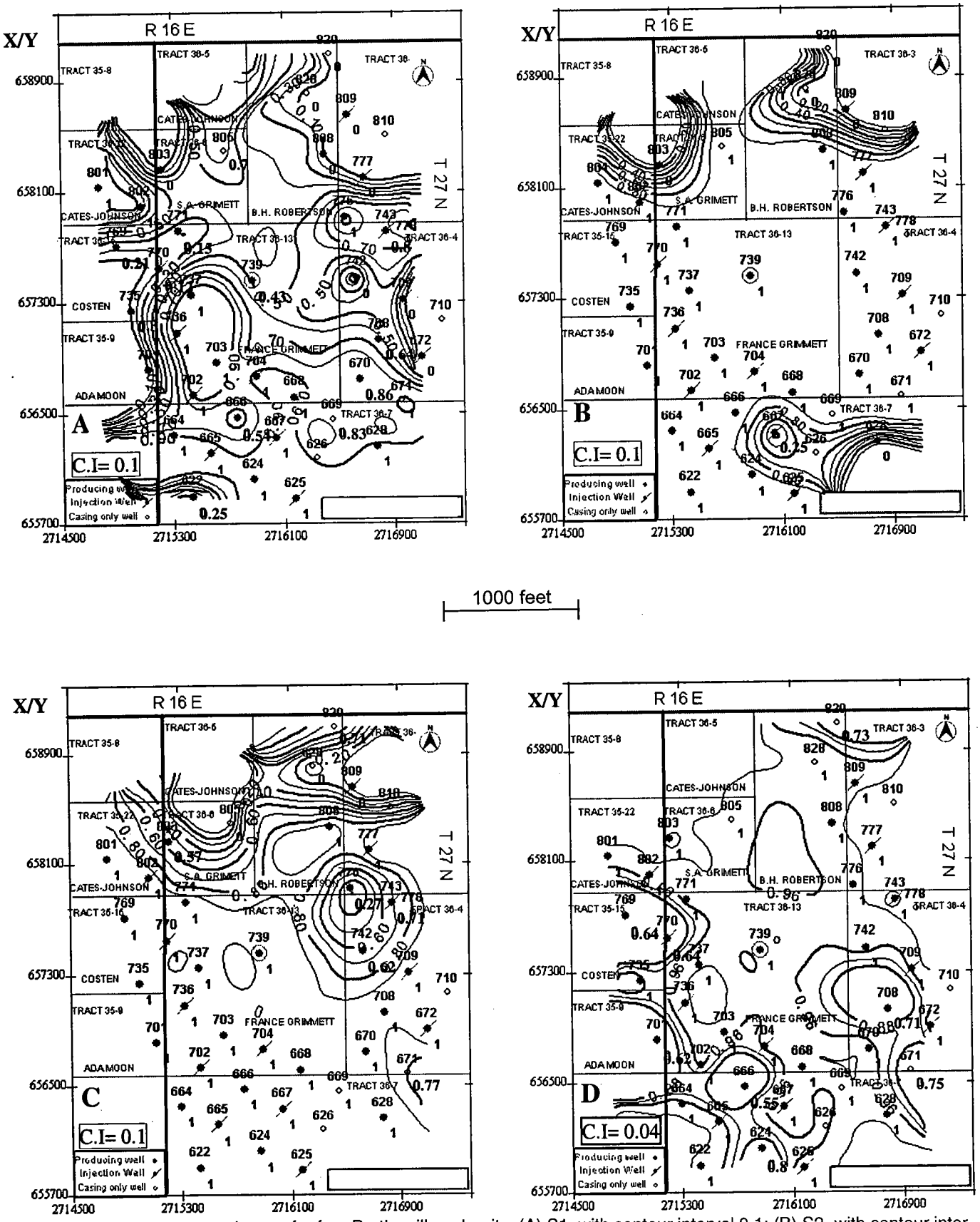

Figure 11. Net-to gross-sand maps for four Bartlesville subunits. (A) S1, with contour interval 0.1; (B) S2, with contour interval 0.1; (C) S3, with contour interval 0.1; (D) S4, with contour interval 0.04.

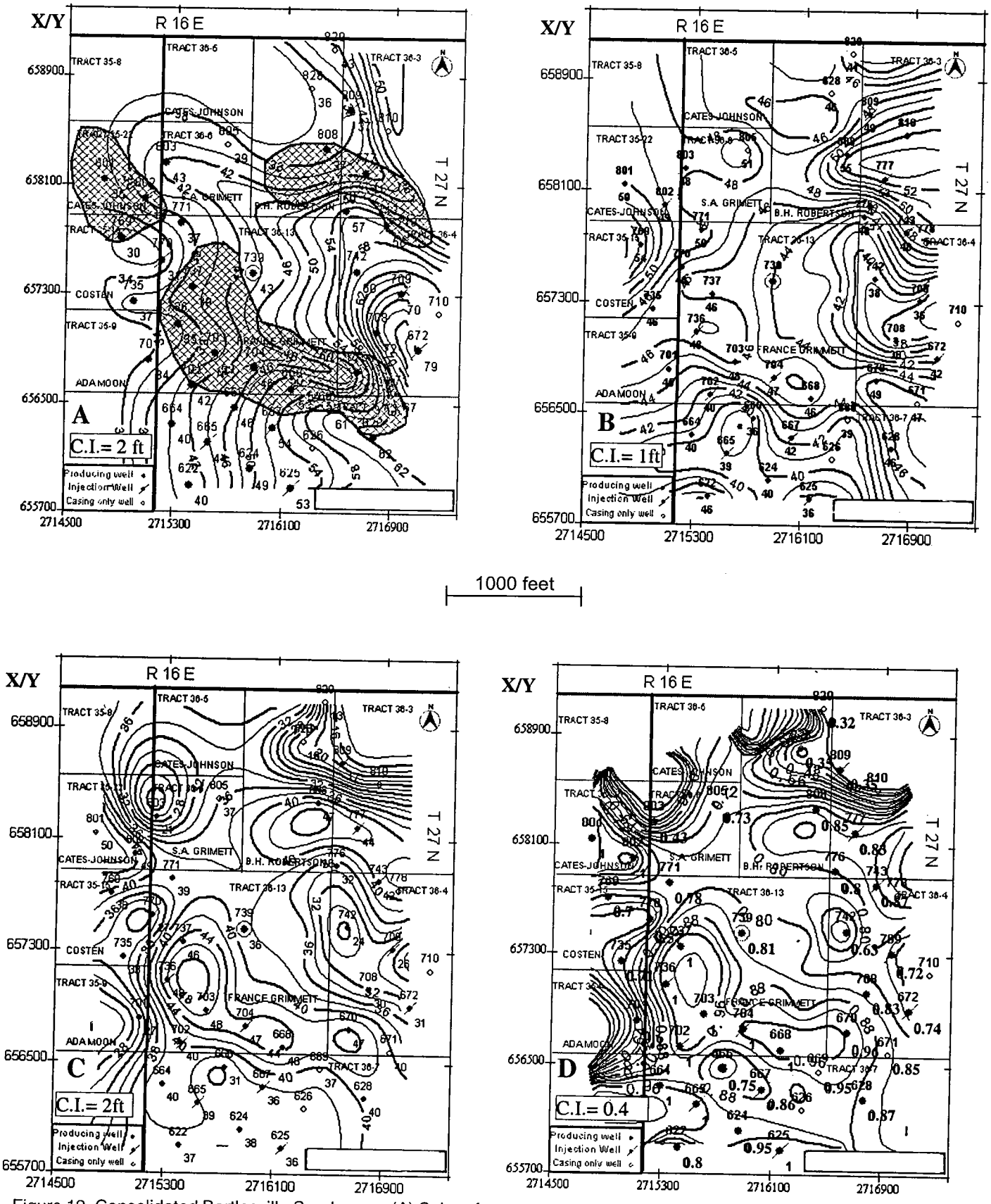

Figure 12. Consolidated Bartlesville Sand maps. (A) Subsurface structure-contour map to base of Bartlesville channel sand, with contour interval 2 ft (shaded areas represent net-sand thickness of 40–50 ft). (B) Map of gross thickness for sands S1 to S4, with contour interval 1 ft. (C) Map of net-sand thickness for sands S1 to S4, with contour interval 2 ft. (D) Map of net-to-gross sands for units S1 to S4, with contour interval 0.4.

TABLE 3.—Parameters Used to Estimate Tertiary Oil Recovery for Delaware–Childers Field

Parameter	Value or Calculation	Symbol
Average net-sand thickness	= 35 ft	h
Average porosity	= 20 %	ϕ
Average residual-oil saturation	= 36 %	S_{hr}
Estimated oil formation volume factor	= 1.05 (rb/stb)	B_o
Oil remaining / acre	$= 7758 \times h \times \phi \times S_{hr} / B_o$ [stb/ac]	
Oil remaining / acre	= 7758 (rb/ac-ft) × 35 (ft) × 0.20 × (0.36/1.05)†	
Oil remaining / acre	$= 18.6 \times 10^3$ (stb/ac) ~ 19×10^3 (stb/ac)	

ac = acre; ac-ft = acre-feet; stb = stock-tank barrels; rb = reservoir barrels
† ratio based on rb/stb

ACKNOWLEDGMENTS

The authors would like to thank Mr. Marshall Brackin, the manager of Arrow Oil & Gas, Inc., for providing the data and permitting the publication of this paper.

REFERENCES CITED

Johnson, K. S., 1971, Introduction, guidelines, and geological history of Oklahoma, *Book 1 of* Guidebook for geological field trips in Oklahoma: Oklahoma Geological Survey Educational Publication 2, p. 8–15.

Johnston, K. H.; and Riggs, C. H., 1946, Secondary-recovery practices and oil reserves in the eastern part of the Delaware–Childers Field, Nowata County, Oklahoma: Reprinted from Bureau of Mine Report of Investigation 4019, 50 p.

Jordan, Louise, 1957, Subsurface stratigraphic names of Oklahoma: Oklahoma Geological Survey Guidebook 6, 220 p.

Houseknecht, D. W.; and others, 1984, High-constructive, tidally influenced deltaic sedimentation in the Arkoma Basin: the Desmoinesian Hartshorne Sandstone, *in* Borger, J. G., II (ed.), Technical Proceedings of the 1981 American Association of Petroleum Geologists Mid-Continent Regional Meeting: Oklahoma City Geological Society, p. 26–41.

Northcutt, R. A.; and others, 1997, Fluvial-dominated deltaic (FDD) oil reservoirs in Oklahoma: the Bartlesville play: Oklahoma Geological Survey Special Publication 97-6, 98 p.

Ohern, D. W., 1914, Geology of the Nowata and Vinita Quadrangles: Unpublished manuscript, on file in the offices of the Oklahoma Geological Survey, p. 28–29.

Development of Microbially Enhanced Oil-Recovery Process: Delaware–Childers Field, Nowata County, Oklahoma

Saikrishna Maudgalya, Roy M. Knapp, Michael J. McInerney, David P. Nagle, and Martha M. Folmsbee
University of Oklahoma
Norman, Oklahoma

ABSTRACT.—The Delaware–Childers Field, T. 26 and 27 N., R. 14 and 17 E., is located in Nowata County in northeastern Oklahoma. Oil is produced mainly from a zone located in a channel deposit in the Bartlesville Sandstone with some production from stray sands above this deposit. This field is operated by the Arrow Oil Company and is currently under an active water flood with injectors and producers arranged in a line-drive pattern. The current water cut is approximately 97%. However, a recent core obtained from the central part of the field had an average residual-oil saturation of 36% after 60 years of water flooding. Thus, the field is an attractive target for tertiary oil recovery. One option is a chemical surfactant-based recovery process. An alternative is a microbial process to generate a bio-surfactant in the reservoir. Microbially enhanced oil recovery (MEOR) is an economically viable alternative to injecting chemical surfactants into reservoirs. In MEOR, nutrients are injected into the reservoir, where they are metabolized by microbes and form bio-surfactants and other products that are useful in mobilizing oil.

Laboratory flooding experiments with sand packs at residual-oil saturation showed that a bio-surfactant generated by the microbe, *Bacillus mojavensis JF-2*, was able to recover residual oil. Sand packs saturated with 34–37° API crude oil were water flooded to residual oil saturation. The packs were then flooded with surfactant solution made of *Bacillus mojavensis JF-2* bio-surfactant, a co-surfactant, 2,3-butanediol, and partially hydrolyzed polyacrylamide (PHPA) polymer as a viscosifying agent. Recoveries from these sand packs ranged from 20% to 80% of residual oil. Deletion of one of the above ingredients resulted in much lower residual-oil recoveries, ranging from 0% to 15%. These data show that the combination of bio-surfactant, co-surfactant, and polymer is needed for significant recovery of residual oil. The absence of one of these key ingredients may explain why residual oil recoveries by MEOR have been unpredictable and low in the past. Calculations indicate that MEOR would be relatively inexpensive to implement in the field. This suggests that MEOR provides a cheap and efficient alternative to expensive chemicals and may result in a successful tertiary-recovery project in the Delaware–Childers Field.

FIELD LOCATION AND GEOLOGY

Delaware–Childers Field is in Nowata County in northeastern Oklahoma (Fig. 1). This field is on the Cherokee Platform with a pay zone in the Bartlesville Sandstone (Fig. 2). This study concentrates on a method of oil recovery from the eastern part of this field, which is located in T. 26 and 27 N., R. 16 and 17 E. (Fig. 3). The field, discovered in 1906, produced under solution-gas drive until 1911 when secondary-recovery techniques started. Since the 1960s the field has been under an active water flood and currently produces oil at an average 95–98% water cut.

The pay zone is at a depth of approximately 630–650 ft with the thickness varying from 30 to 60 ft. Shale streaks divide this pay into thinner zones. The horizontal permeability is between 90 and 110 millidarcies and the porosity in the oil producing sand varies from 19% to 26%. A core recently extracted from the central part of the area of interest had a residual-oil saturation of 36%. Despite the water flood, the presence of such high residual-oil saturations and high permeabilities makes this field a good target for tertiary oil recovery. One of the possible methods of oil recovery being investigated is surfactant-based recovery where chemicals that lower the interfacial tension between oil and water to

Maudgalya, Saikrishna; Knapp, R. M.; McInerney, M. J.; Nagle, D. P.; and Folmsbee, M. M., 2002, Development of microbially enhanced oil-recovery process: Delaware–Childers Field, Nowata County, Oklahoma, *in* Boyd, D. T. (ed.), Finding and producing Cherokee reservoirs in the southern Midcontinent, 2002 symposium: Oklahoma Geological Survey Circular 108, p. 193–200.

mobilize oil are flooded through the reservoir. An alternative to a recovery method based on chemical surfactants is bio-surfactant–based, microbial-enhanced oil recovery (MEOR).

MICROBIAL-ENHANCED OIL RECOVERY

In MEOR, microbial metabolic products are used to recover oil from reservoirs. Byproducts useful for oil recovery include bio-surfactants, alcohols, acids, gases, and biopolymers. However, MEOR has not developed into a commercial field technology because of a lack of understanding of microbial process involved in oil recovery. Studies show that *Bacillus mojavensis JF-2* (Collins, 1961; Javaheri and others, 1985; Han and others, 2001) generates a bio-surfactant in the absence of oxygen that reduces the interfacial tension between water and hydrocarbons by two to three orders of magnitude under saline conditions (McInerney and others, 1990), making it useful for oil recovery.

EXPERIMENTAL PROCEDURE

Three separate sand-pack flooding experiments were conducted to investigate the ability of *Bacillus mojavensis JF-2* bio-surfactant to recover water-flood residual oil. Sand packs were prepared by uniformly packing 20/40-mesh sand into polycarbonate cores. Air was removed from them by applying a vacuum. Deareated 2.5% NaCl brine was flooded first through the packs to saturate them with brine. The brine was reduced to residual-water saturation by flooding the packs with 34–37° API crude oil. These oil-saturated packs were then water flooded to residual-oil saturation with 2.5% NaCl brine. Volumes of displaced brine and oil were measured after each stage to calculate residual phase saturations. The packs were then flooded with a surfactant solution of *Bacillus mojavensis JF-2* bio-surfactant, partially hydrolyzed polyacrylamide (PHPA) polymer, and 2,3-butanediol that was called co-surfactant. PHPA polymer was added to increase the surfactant-solution viscosity and 10.0 millimoles (mM) 2,3-butanediol was added to replicate the bio-product composition found in nature.

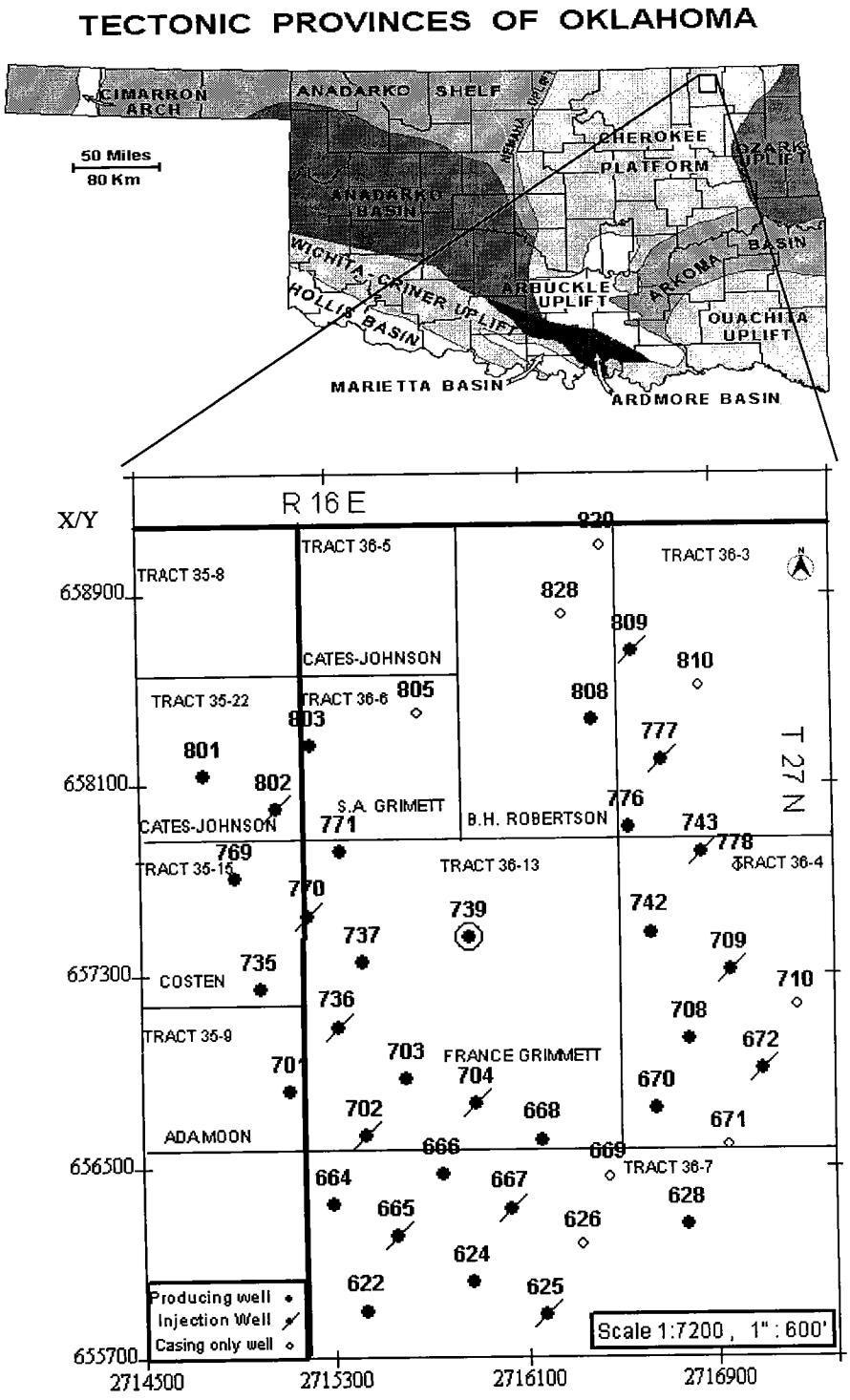

Figure 1. Generalized map of Oklahoma, showing structural provinces and location of study area, the Delaware–Childers Field, Nowata County, Oklahoma.

Surfactant and polymer solutions with 1,000 ppm of PHPA were prepared by dissolving 0.1 gm of PHPA polymer for every 100.0 cc of surfactant solution or water. The solutions were left undisturbed for 24 hours to allow the polymer molecules to hydrolyze.

SYSTEM	SERIES	GROUP	FORMAL SURFACE NAMES OF FORMATIONS OR MEMBERS			FORMAL & INFORMAL SUBSURFACE NAMES	
PENNSYLVANIAN	DESMOINESIAN	Marmaton	Ft. Scott Limestone	Higginsville Limestone		Oswego lime	"Wheeler sand"
				Little Osage Shale			
				Blackjack Creek Ls.			
		Cabaniss	Senora Formation	Excello Shale			
				Breezy Hill Ls.			
				Lagonda Sandstone		Cherokee group	Prue sand
				Verdigris Limestone			Verdigris Limestone
				Croweburg coal			Henryetta coal
				Oowala Sandstone			Upper Skinner sand
				Mineral coal			Morris coal
				Chelsea Sandstone			Middle Skinner sand Lower Skinner sand
				Tiawah Limestone			Pink lime
		Krebs	Boggy Formation	Taft Sandstone			Red Fork sand Burbank sand Earlsboro sand
				Inola Limestone			Inola Limestone
				Bluejacket Sandstone			Bartlesville sand Glenn sand Salt sand
			Savanna Fm.	Doneley Limestone			Brown lime
				Sam Creek Ls.			
				Spaniard Limestone			
			McAlester Formation	Keota Sandstone			Upper Booch sand
				Tamaha Sandstone			Taneha sand
				Cameron Sandstone			Tucker sand
				Lequire Sandstone			
				Warner Sandstone			Lower Booch sand
				McCurtain Shale			
			Hartshorne Formation	Hartshorne Sandstone			Hartshorne sand

Figure 2. Stratigraphic nomenclature for the Krebs, Cabaniss, and lower part of Marmaton Groups (Desmoinesian Series), showing the formal surface names and the commonly accepted subsurface names used in northeastern Oklahoma. Modified from Scruton (1950), Oakes, (1953), Jordan (1957), Cole (1967, 1970), Berg (1966, 1969), Branson (1968), Chandler (1977), Bennison (1979), Bissell (1984), Lojek (1984), Tulsa Geological Society (1984–1989), and Hemish (1989, 1993, 1997).

Experiment 1

In the first experiment, residual-oil recovery was tested using *Bacillus mojavensis JF-2* bio-surfactant, 2,3-butaediol, and partially hydrolyzed polyacrylamide polymer. Viscous-preflush and gravity effects also were investigated.

Procedure

Bacillus mojavensis JF-2 (Javaheri and others, 1985) was grown aerobically. The cells were removed by centrifugation at 10,000 g for 10.0 minutes at 4°C and the concentration of bio-surfactant in the supernatant was 910 ppm as determined by high-pressure liquid chromatography. The alcohol, 2,3-butanediol, 10.0 mM was added to this bio-surfactant solution. PHPA, at a concentration of 1,000 ppm, was mixed with this surfactant solution. Eight sand packs, numbered 1.1 to 1.8 at water-flood residual-oil saturation were used in this experiment. Residual oil volumes and saturations are tabulated in Table 1. The oil was a 34° API oil with a viscosity of 10.0 cp. The pore volume of all sand packs was approximately 100.0 cc. To flood a pore volume of surfactant through each pack, 100.0 cc of surfactant solution was used.

Packs 1.1 and 1.2 were flooded vertically. Five cc of the 1,000 ppm PHPA solution first was injected as preflush ahead of the surfactant solution and 25.0 cc of PHPA solution as mobility buffer was injected behind the surfactant solution. The flooding was continued with 2.5% NaCl brine until no more oil was recovered. A total of 200.0 cc of fluids was flooded through every pack. Packs 1.3 and 1.4 were injected using a protocol similar to Packs 1.1 and 1.2, except that no preflush was used before the surfactant. Packs 1.5 and 1.6 were injected with a protocol identical to Packs 1.1 and 1.2, except that these packs were flooded horizontally. Pack 1.7 and 1.8 were the controls for the experiment. In these two packs, instead of flooding the packs with surfactant, 100.0 cc of a mixture of PHPA and 10.0 mM of 2,3-butanediol dissolved in uninoculated medium was injected. This was done to study whether 2,3-butanediol by itself could mobilize oil. The pressure across each pack was kept constant at 8.0 psig during the surfactant flood. The effluent from the packs was collected in 50.0 cc samples.

Discussion

Observations and results are presented in Table 1. Packs 1.1 and 1.2 that received a preflush and were flooded vertically had the highest recovery of nearly 80.0% residual oil. Nearly 70% of residual oil was recovered from Packs 1.3 and 1.4 that did not receive a preflush. About 63% of residual oil was recovered from Packs 1.5 and 1.6 that were flooded horizontally and only 1% of residual oil was recovered from the control packs 1.7 and 1.8.

Oil produced with the first 50.0-cc sample of effluent was excluded from the recovery calculations because this was oil trapped in the pack head space at the end of water flooding and was produced at the instant the preflush of solution flooding began. A higher recovery of oil from Packs 1.1 and 1.2 compared with recovery from Packs 1.3 and 1.4 suggested that the viscous preflush improved oil recovery. In Figure 4, oil production versus the cumulative volume flooded showed an improvement in oil recovery when a preflush was used. In the figure, a peak in oil production followed by a decline was the point at which the mobilized oil bank was produced. The figure showed smaller peaks for Packs 1.3 and 1.4 contrasted to the peaks for Packs 1.1 and 1.2. This suggested that the preflush in Packs 1.1 and 1.2 helped mobilize more oil. Because the sand packs had

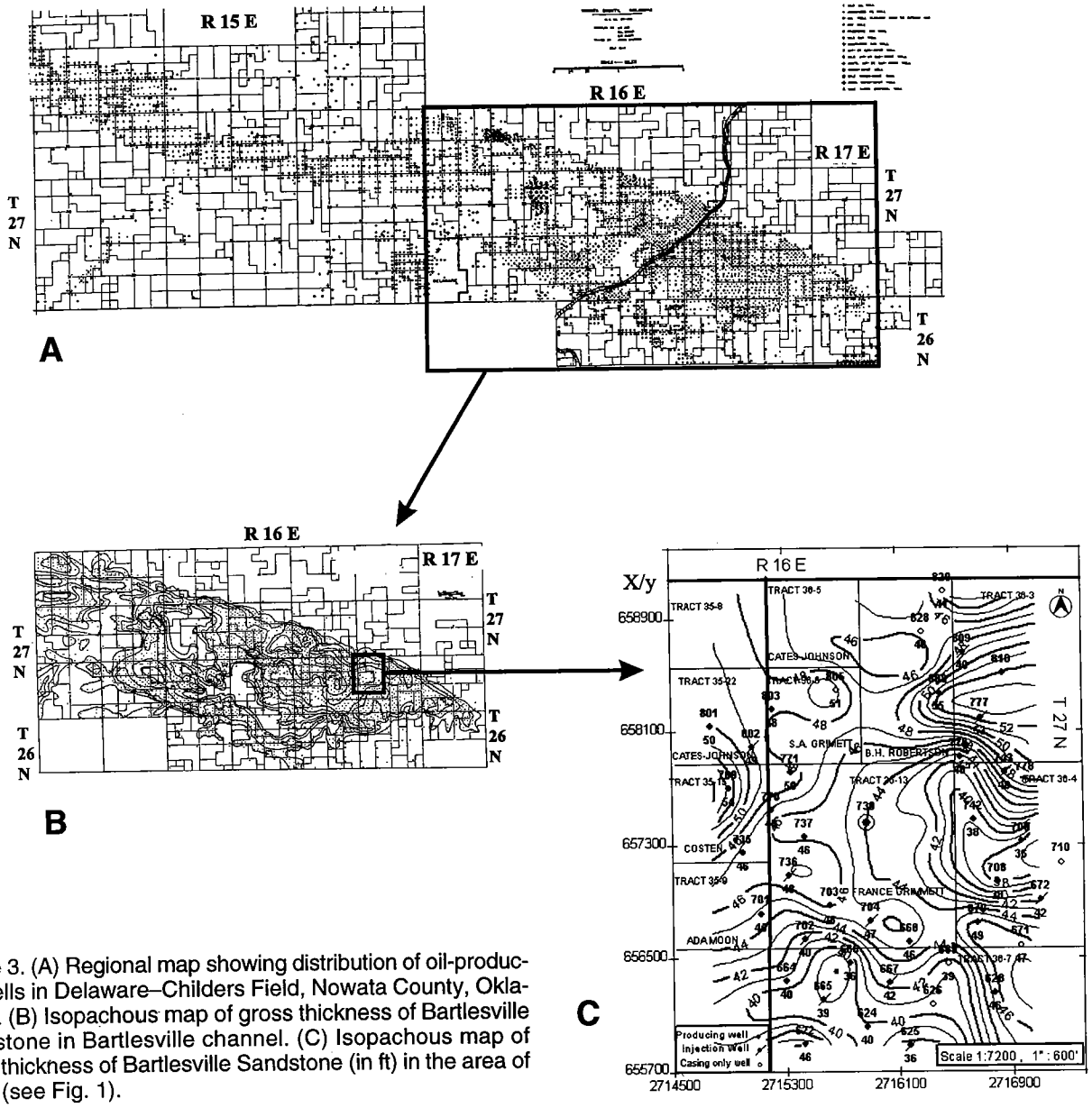

Figure 3. (A) Regional map showing distribution of oil-producing wells in Delaware–Childers Field, Nowata County, Oklahoma. (B) Isopachous map of gross thickness of Bartlesville Sandstone in Bartlesville channel. (C) Isopachous map of gross thickness of Bartlesville Sandstone (in ft) in the area of study (see Fig. 1).

an approximate pore volume of 100.0 cc, a complete pore volume of surfactant solution was flooded through when 200.0 cc of fluid was produced. This was why oil production continued up to 200.0 cc of fluid production (Fig. 4).

A 12.5% decrease in oil recovery from packs 1.5 and 1.6 compared with the recovery from Packs 1.1 and 1.2 confirmed that surfactant flooding against gravity improved oil recovery. Gravity maintained a stable flood front and improved the surfactant sweep efficiency. The production of oil in packs 1.5 and 1.6 through the 200.0 cc mark is a combination of flooding a pore volume of surfactant solution and the rarefaction curve. The negligible recoveries from the control packs, 1.7 and 1.8 confirmed that 2,3-butanediol and polymer alone do not recover residual oil.

Experiment 2

Experiment 2 was designed to analyze the relation between oil recovery and volume of *Bacillus mojavensis JF-2* surfactant solution flooded through the sand packs.

Procedure

In this experiment, the bio-surfactant concentration was 283 ppm, and the polymer and 2,3-butanediol concentrations were the same as Experiment 1. Eight sand packs, numbered 2.1 to 2.8 were water flooded to residual oil saturation using 2.5% NaCl brine. Residual oils saturations are shown in Table 2. The oil was 34.5° API oil with a viscosity of 11.5 cp. Two packs each were flooded with 100.0, 80.0, 60.0, and 40.0 cc of surfactant

solution, respectively. All packs were flooded vertically and were first injected with 5.00 cc of a 1,000 ppm PHPA solution as preflush, followed by surfactant-solution injection and 50.0 cc of PHPA concentration graded-mobility buffer. The buffer consisted of 25.0 cc of 1000 ppm PHPA solution followed by 25.0 cc of a 700 ppm PHPA solution. Injection continued with 2.5% NaCl brine. A larger volume mobility-buffer solution was used to prevent viscous fingering of chase water through the buffer and into the surfactant solution. Concentration grading was performed to reduce the consumption of the polymer PHPA. The total volume of injected fluids was 200.0 cc. Oil production is plotted against cumulative volume flooded in Figure 5.

TABLE 1.—Summary of Results from Experiment 1

Pack	Direction of flooding	$S_{OR,wf}$ (%)	Volume pre-flush (cc)	Volume surfactant (cc)	Recovery (%)
1.1	Vertical	20.6	5	100+PO+CS	77.5
1.2	Vertical	19.2	5	100+PO+CS	85.6
1.3	Vertical	21.0	0	100+PO+CS	67.9
1.4	Vertical	19.8	0	100+PO+CS	73.9
1.5	Horizontal	25.4	5	100+PO+CS	64.1
1.6	Horizontal	21.9	5	100+PO+CS	63.5
1.7	Vertical	26.7	0	PO+CS	1.2
1.8	Vertical	21.7	0	PO+CS	1.1

$S_{OR,wf}$: residual-oil saturation in packs after water flooding.
PO: 1,000 ppm PHPA dissolved in 100.0 cc of bio-surfactant solution.
CS: 2,3-butanediol, 10.0 mM dissolved in 100.0 cc of bio-surfactant solution.
Concentration of bio-surfactant: 910 ppm.
NaCl concentration in brine: 2.5% by wt.
Polymer solution: 1,000 ppm Partially Hydrolyzed Polyacrylamide in 2.5% NaCl brine.

Discussion

Table 2 summarizes the experiment and its results. Oil produced with the first 50.0 cc of effluent was excluded from the recovery calculations. Distinct oil banks formed in all packs. Packs 2.1 and 2.2 were flooded with 100.0 cc of surfactant solution and had the highest recovery of nearly 50% additional oil. Packs 2.7 and 2.8 were flooded with 40.0 cc of surfactant solution and recovered 30% of additional residual oil. Because every sand pack had a pore volume of approximately 100.0 cc, oil recovery from Packs 2.7 and 2.8 was significant because nearly 30% of additional residual oil was recovered using less than half a pore volume of surfactant solution.

Figure 5 shows a peak in oil production followed by a decline for Packs 2.5 and 2.6 that were flooded with 60.0 cc of surfactant solution and Packs 2.7 and 2.8 that were flooded with 40.0 cc of surfactant solution. This peak in production occurred when the mobilized oil bank was produced. Behind the oil surfactant solution was displaced from the packs by the mobility buffer solution. No additional oil could be mobilized after the surfactant was removed and oil production declined.

Figure 5 also shows that Packs 2.1 to 2.4 had an anomalous oil-recovery profile. The figure does not show a peak in oil production followed by a slow decline in production for these four packs. Because of a large time gap between the water flooding of these packs and surfactant flooding, oil and water segregated inside the packs creating a bank of mobile oil at the pack's outlet. This oil was produced at the instant the preflush was injected. Oil that should have been produced as mobilized oil in a bank and that would have shown as a peak on the production plot was produced prematurely;

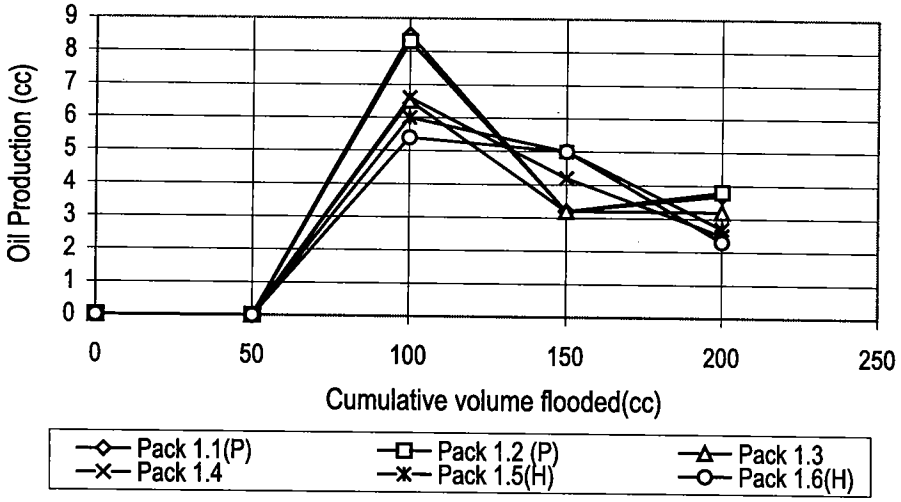

Figure 4. Plot of oil production versus cumulative volume flooded through each pack in Experiment 1. *Abbreviations:* (P) = packs flooded with a preflush of polymer ahead of the surfactant solution; (H) = packs flooded horizontally (to check effect of gravity).

hence, there were no observed peaks in oil production. This may have also resulted in lower oil recoveries from Packs 2.3 and 2.4 as compared to recoveries from Packs 2.5 and 2.6 that were flooded with a smaller volume of surfactant solution. Segregation of oil and water was corrected in Packs 2.5 to 2.8.

TABLE 2.—Summary of Results from Experiment 2

Pack	$S_{OR,wf}$ (%)	Volume surfactant (cc) 283 ppm	Volume post-flush (cc) 1,000 ppm	Volume post-flush (cc) 700 ppm	Recovery (%)
2.1	15.8	100+PO+CS	25.0	25.0	52.7
2.2	16.7	100+PO+CS	25.0	25.0	48.1
2.3	19.4	80+PO+CS	25.0	25.0	33.1
2.4	22.8	80+PO+CS	25.0	25.0	32.7
2.5	20.8	60+PO+CS	25.0	25.0	36.1
2.6	20.7	60+PO+CS	25.0	25.0	40.6
2.7	26.5	40+PO+CS	25.0	25.0	30.4
2.8	22.6	40+PO+CS	25.0	25.0	30.1

See Table 1 for explanation of $S_{OR,wf}$, PO, and CS.
Concentration of bio-surfactant: 283 ppm.
NaCl concentration in brine: 2.5% by wt.
Polymer solution: 1,000 ppm Partially Hydrolyzed Polyacrylamide in demineralized water.

Experiment 3

This experiment was designed to confirm that the *Bacillus mojavensis JF-2* bio-surfactant requires the 2,3-butanediol and PHPA to recover oil efficiently.

Procedure

Eight sand packs, numbered 3.1 to 3.8 at water-flood residual-oil saturation were used in this experiment. The oil was 34.5° API oil with a viscosity of 11.5 cp. Packs 3.1 and 3.2 were first injected with 5.0 cc of 1,000 ppm PHPA solution as viscous preflush. This was followed by 100.0 cc solution of 10.0 mM 2,3-butanediol and 1000 ppm dissolved in uninoculated medium and 50.0 cc of a concentration-graded mobility-buffer solution as used in Experiment 2. Flooding was continued with 2.5% NaCl brine until 200.0 cc of fluid was flooded through each pack. In packs 3.3 and 3.4, the flooding protocol was similar as the first two packs, except that a 100.0 cc solution of 10.0 mM 2,3-butanediol dissolved in bio-surfactant solution was injected behind the preflush followed by the mobility-buffer solution. In Packs 3.5 and 3.6, a 100.0 cc solution of 1,000 ppm PHPA dissolved in bio-surfactant solution was used, and, in packs 3.7 and 3.8, a 100.0 cc solution of bio-surfactant solution with 10.0 mM of 2,3-butanediol and 1000 ppm PHPA was injected behind the preflush. All the packs were flooded vertically from the bottom up. The bio-surfactant concentration was 43 ppm. Cumulative-percentage oil recovery was plotted against cumulative-volume flooded for each pack in Figure 6.

Discussion

Table 3 shows the experimental summary and results. About 1% of additional residual oil was recovered from Packs 3.1 and 3.2. Approximately 12% of the residual oil was recovered from Packs 3.3 and 3.4, 17% from Packs 3.5 and 3.6, and 22.0% from Packs 3.7 and 3.8.

Negligible oil recovery from Packs 3.1 and 3.2 confirmed that 2,3-butanediol and PHPA only assisted *Bacillus mojavensis JF-2* in recovering oil. In Packs 3.3 and 3.4 the less viscous bio-surfactant and co-surfactant solution without any polymer managed to finger through the polymer preflush and mobilize some oil.

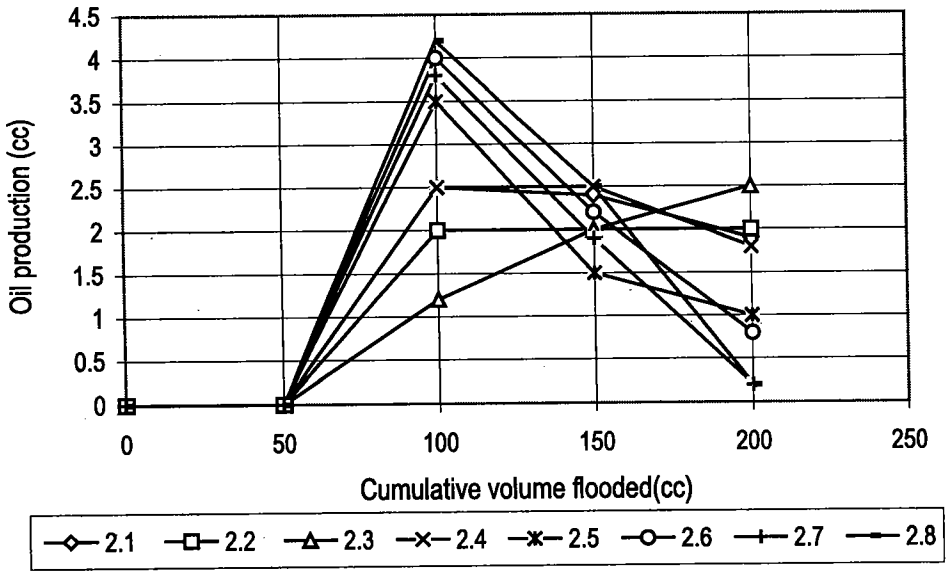

Figure 5. Plot of oil production versus cumulative volume flooded through each pack in Experiment 2.

On injecting the mobility-buffer solution, this oil was seen as an increase in oil recovery between the 100.0 and 150.0 cc injection points in Figure 6. For Packs 3.5 and 3.6, through which a solution of bio-surfactant and 1,000 ppm PHPA was flooded, an oil bank formed. The breakthrough of this bank shows an increase in cumulative recovery in Figure 6. Oil production declined behind the oil bank as indicated by the flattening of the cumulative-recovery curves for the two packs. Packs 3.7 and 3.8 produced nearly 22% of the oil and had the highest recoveries. This confirms that the bio-surfactant worked best when combined with 2,3-butanediol and a viscosity-modifying polymer. The cumulative recovery increased until the 200.0 cc flooding point. Because a complete pore volume was flooded through the packs, mobilized oil was produced until the 200.0 cc flooding point. Significantly, 22% of the oil was recovered with a bio-surfactant concentration as low as 0.0043%.

TABLE 3.—Summary of Results from Experiment 3

Pack	Volume of flooded solution (100.0 cc flooded in each pack)	$S_{OR,wf}$ (%)	Recovery (%)
3.1	PHPA + 2,3-butanediol	26.7	1.20
3.2	PHPA + 2,3-butanediol	21.7	1.05
3.3	Bio-surfactant + 2,3-butanediol	19.8	11.1
3.4	Bio-surfactant + 2,3-butanediol	18.2	13.0
3.5	Bio-surfactant + PHPA	23.4	15.5
3.6	Bio-surfactant + PHPA	23.4	18.8
3.7	Bio-surfactant + PHPA + 2,3-butanediol	24.7	21.9
3.8	Bio-surfactant + PHPA + 2,3-butanediol	25.3	21.8

$S_{OR,wf}$: residual-oil saturation in packs after waterflooding.
Concentration of bio-surfactant: 43 ppm.
NaCl concentration in brine: 2.5% by wt.
Polymer solution: 1,000 ppm Partially Hydrolyzed Polyacrylamide in demineralized water.

CONCLUSIONS

The results of these experiments using *Bacillus mojavensis JF-2* bio-surfactant with a co-surfactant and a viscosity-modifying agent have demonstrated the potential in tertiary recovery of residual oil in certain types of oil fields. The Delaware–Childers Field seems to be an ideal candidate for a pilot recovery study. Our conclusions are summarized below.

1. *Bacillus mojavensis JF-2* bio-surfactant can be developed into an effective surfactant when combined with co-surfactant 2,3-butanediol and a viscosity-modifying agent such as partially hydrolyzed polyacrylamide (PHPA) polymer.
2. A viscous preflush ahead of the surfactant solution improved oil recoveries.
3. About 30% of residual oil could be recovered with less than half a pore volume of surfactant-solution injection.
4. About 22% of the residual oil could be recovered by a solution having a bio-surfactant concentration as low as 43 ppm or 0.0043% by weight.
5. The surfactant-solution–flooding protocol was designed and tested on sand packs, but testing must be extended to cores and ultimately a field pilot study.

REFERENCES CITED

Bennison, A. P., 1979, Mobile basin and shelf border area in northeast Oklahoma during Desmoinesian cyclic sedimentation, *in* Hyne, N. J. (ed.), Pennsylvanian sandstones of the Mid-Continent: Tulsa Geological Society Special Publication 1, p. 283–294.

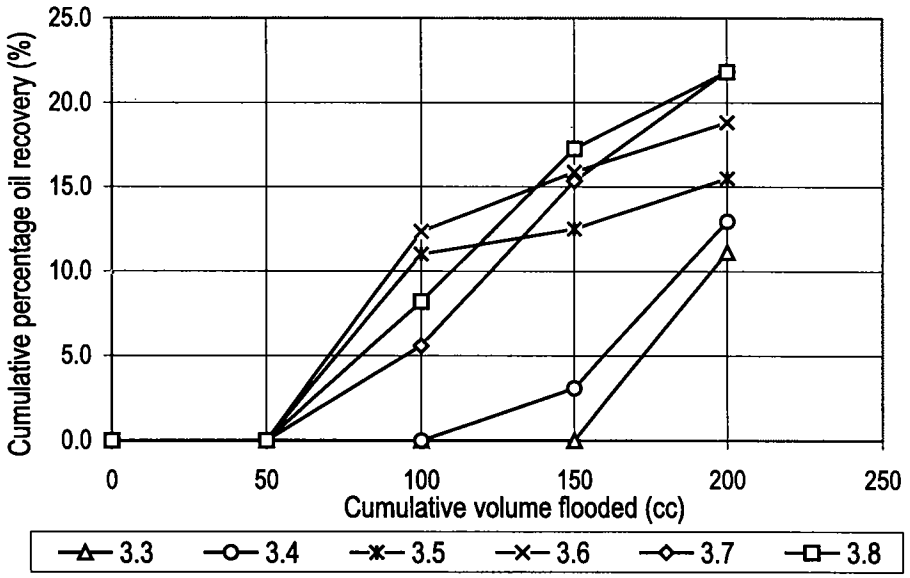

Figure 6. Plot of cumulative-percentage recovery versus cumulative volume flooded through each pack in Experiment 3.

Berg, O. R., 1966, Depositional environment of a portion of the Bluejacket Sandstone, Mayes County, Oklahoma: Shale Shaker, v. 17, no. 3, p. 50–54.

_____ 1969, Cherokee Group, west flank of the Nemaha Ridge, north-central Oklahoma: Shale Shaker, v. 19, no. 6, p. 94–109.

Bissell, C. R., 1984, Stratigraphy of the McAlester Formation (Booch sandstones) in the Eufaula Reservoir area, east-central Oklahoma: Oklahoma State University unpublished M.S. thesis, 120 p.

Branson, C. C., 1968, The Cherokee Group, *in* Visher, G. S. (ed.), A guidebook to the geology of the Bluejacket–Bartlesville Sandstone of Oklahoma: Oklahoma City Geological Society, p. 26–31.

Chandler, C. E., 1977, Subsurface stratigraphic analysis of selected sandstones of the "Cherokee" Group, southern Noble County, Oklahoma: Shale Shaker, v. 28, no. 3, p. 5659 [part 1]; v. 28, no. 4, p. 72–83 [part 2].

Cole, J. G., 1967, Regional stratigraphy of the Marmaton Group in northeastern Oklahoma: Shale Shaker, v. 17, no. 5, p. 86–97.

_____ 1970, Marmaton Group, east flank of the Nemaha Ridge, north-central Oklahoma: Shale Shaker, v. 21, no. 3, p. 52–66.

Collins, R. E., 1961, Flow of fluids through porous media: PennWell Publishing Co., Tulsa, Oklahoma, 196 p.

Donaldson, E. C.; Chilingarian, G. V.; and Yen, T. F. (eds.), 1989, Microbial enhanced oil recovery: Elsevier Science Publishing Company Inc., New York, 227 p.

Gogarty, W. B.; Meabon, H. P.; and Milton, H. W., Jr., 1970, Mobility control design for miscible-type water floods using micellar solutions: Journal of Petroleum Technology, v. 22, p. 141–147.

Hemish, L. A.,1989, Bluejacket (Bartlesville) Sandstone Member of the Boggy Formation (Pennsylvanian) in its type area: Oklahoma Geology Notes, v. 49, p.72–89.

_____ 1993, Spaniard(?) and Sam Creek(?) limestones in Le Flore County, Oklahoma: Oklahoma Geology Notes, v. 53, p. 84–111.

_____ 1997, Lithologic descriptions of Pennsylvanian strata north and east of Tulsa, Oklahoma: Oklahoma Geological Survey Special Publication 97-2, 44 p.

Jenneman, G. E.; McInerney, M. J.; Knapp, R. M.; Clark, J. B.; Feero, J. M.; Revus, D. E.; and Menzie, D. E., 1983, A halotolerant, bio-surfactant–producing *Bacillus* species potentially useful for enhanced oil recovery: Developments in Industrial Microbiology [a publication of the Society of Industrial Microbiology], v. 24, p. 485–492.

Han, S. O.; Nagle, D. P.; and McInerney, M. J., 2001, Identification and analysis of bio-surfactant genes in *Bacillus mojavensis*: Abstracts of the 101st meeting of the American Society of Microbiology, Washington, D.C., p. 626.

Javaheri, M.; Jenneman, G. E.; McInerney, M. J.; and Knapp, R. M., 1985, Anaerobic production of bio-surfactant by *Bacillus licheniformis JF- 2*: Applied and Environmental Microbiology, American Society of Microbiology, v. 51, p. 698–700.

Jordan, Louise, 1957, Subsurface stratigraphic names of Oklahoma: Oklahoma Geological Survey Guidebook 6, 220 p.

Krug, J. A.; and Sayers, R. R., 1946, Secondary recovery practices and oil reserves in the eastern part of the Delaware–Childers field, Nowata County, Oklahoma: U.S. Department of the Interior, Report of Investigations 4019, p. 1–11.

Lojek, C. A., 1984, Petrology, diagenesis, and depositional environment of the Skinner sandstone, Desmoinesian, northeastern Oklahoma platform: Shale Shaker, v. 34, no. 7, p. 82–92 [part 1]; v. 34, no. 8, p. 95–103 [part 2].

McInerney, M. J.; Javaheri, M.; and Nagle, D. P., 1990, Properties of the bio-surfactant produced by *Bacillus licheniformis strain JF-2*: Journal of Industrial Microbiology, v. 5, p. 95–102.

Oakes, M. C., 1953, Krebs and Cabaniss Groups of Pennsylvanian age in Oklahoma: American Association of Petroleum Geologists Bulletin, v. 37, p. 1523–1526.

Salter, S. J., 1977, The influence of type and amount of alcohol on surfactant-oil–brine phase behavior and properties: Paper 6843, presented at the Society of Petroleum Engineers of AIME Annual Fall Technical Conference and Exhibition, Denver, Colorado, October 9–12, 1977, p. 1–12.

Scruton, P. C., 1950, The petrography and environment of deposition of the Warner, Little Cabin and Hartshorne sandstones in northeastern Oklahoma: American Journal of Science, v. 248, p. 408–426.

Tulsa Geological Society, Stratigraphic Committee, 1984–89, Type logs of Oklahoma: Available from Riley's Electric Log, Inc., Oklahoma City.

Cherokee-Equivalent Formations of the Ardmore Basin: A New Look at Old Data

Robert E. Harmon
C. E. Harmon Oil, Inc.
Tulsa, Oklahoma

ABSTRACT.—Nine informal Middle Pennsylvanian (Desmoinesian) formations that form a sequence of strata equivalent to the "Cherokee Group" of northern Oklahoma are found in the Ardmore Basin of southern Oklahoma. From uppermost to lowermost, these are the Culberson, Upper and Lower Fusulina, Tussy, Edwards, Carpenter, Pickens, Morris, and Hefner formations. These subsurface "Cherokee equivalent" formations were identified from Chenoweth (1979) and researched as to both their stratigraphic position and the location of the well from which they were defined (Jordan, 1957). These wells are randomly scattered across Sho-Vel-Tum Field.

Sho-Vel-Tum is an irregularly shaped field in the Ardmore Basin that covers about 75,000 acres in Carter, Garvin, and Stephens Counties in south-central Oklahoma. Sho-Vel-Tum had the highest production rate and largest proven reserves for Oklahoma in 1999. The Cherokee "Group" makes up most of the greater Deese Group in this field and carries the bulk of its remaining oil.

Sho-Vel-Tum consists of more than 30 separate, smaller fields. Eight of these are evaluated as individual field studies. The stratigraphy and relative quality of the reservoirs in Cherokee formations in this area are studied using electric logs, production data, and cross sections. Based on this work, operators can assess the need for further evaluation of individual areas and reservoirs in the Sho-Vel-Tum Field.

INTRODUCTION

In the determination of Cherokee-equivalent formations in the Ardmore Basin, three references were identified that contained somewhat similar Cherokee formations. These three references and their formation ranges, from upper to lower Cherokee equivalents, are: (1) Chenowith (1979), who starts with the Culberson and ends with the Hefner sand; (2) Kennedy (1982), who starts with the Upper Fusulinia (or Fusulinid or Fusulina) and ends with the combined grouping of Morris, Griffen (or Griffin) and Hefner; and (3) Fay (1997), who starts with the Fusulina and goes to the lower Griffin sand. Actually, all three of these references present an applicable picture, and that is what makes this area particularly difficult to understand in regard to stratigraphic nomenclature.

The next step was to take the formations that each reference presented and look them up according to both their stratigraphic location in the "Cherokee Group" and identify their type log locations by section, township, and range. Both stratigraphic and type log locations were obtained from the book, *Subsurface Stratigraphic Names of Oklahoma* (Jordan, 1957). It was discovered that the type log locations for formations from each of the three sources are all situated in the giant Sho-Vel-Tum Field (Fig. 1). Data were then acquired to evaluate individual formations of the Cherokee "Group" from the smaller fields that now make up Sho-Vel-Tum.

ARDMORE BASIN

The Ardmore Basin is about 330 mi long and 60 mi wide and lies in a structural trough known as the southern Oklahoma Aulacogen (Billingsley, 1992). This foreland basin is located in Marshall, northeast Love, southwest Johnston, Carter, eastern Stephens, and southwest Garvin Counties. (Parish, 1991)

The Ardmore Basin is complex both structurally and stratigraphically and has produced oil and gas since the early 1900s. Most of the hydrocarbon traps are located on regional highs within the basin or on the basin margins. Hydrocarbon migration in the basin is both lateral and vertical, with the vertical component facilitated by faults and angular unconformities (Brown and Corrigan, 1997).

The structural style of the Ardmore Basin is closely tied to structures in the Arbuckle Mountain region, where a wide variety of deformation types have

Harmon, R. E., 2002, Cherokee-equivalent formations of the Ardmore Basin: a new look at old data, *in* Boyd, D. T. (ed.), Finding and producing Cherokee reservoirs in the southern Midcontinent, 2002 symposium: Oklahoma Geological Survey Circular 108, p. 201–211.

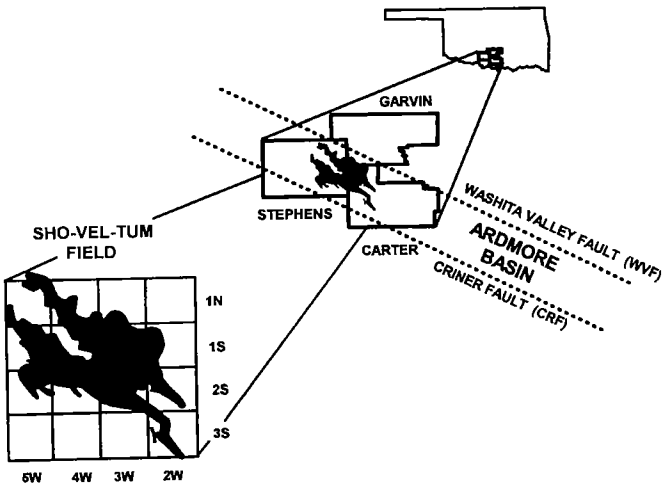

Figure 1. Location map of Sho-Vel-Tum Field in the Ardmore Basin of southern Oklahoma. Modified after Johnson and others (1987).

posed many interpretational challenges. The most widely accepted model proposes that the region is a complex half-graben in which inversion occurred due to left-lateral transpression (Tapp, 1995). Inversion is the reversal of direction of movement along basin controlling faults. According to Tapp (1995), evidence for inversion in the Arbuckle region includes the presence of backthrusts that formed as a result of rollover anticlines. Gold (1997) also noted that inversion-produced backthrusts are common in the region.

Deformation in the Ardmore Basin created two types of uplifts. These were caused by strike-slip deformation. Known as "flower structures," these uplifts are called squeeze-up and pop-up structures. Squeeze-up structures developed as steep-sided folds with internal faults that converged downward into a single strike-slip fault, and pop-up structures developed as uplifts bounded by downward-converging, through-going faults (McBee, 1995). Both types are common in the Ardmore Basin.

STRATIGRAPHY

The Deese Group of the Ardmore Basin consists of up to 7,500 ft of sedimentary rock consisting dominantly of sandstone and shale with interbedded limestone and conglomerate. The Desmoinesian sedimentary section in the basin is equivalent to both the "Cherokee" and Marmaton Groups of northern Oklahoma (Raymer, 1987), and it consists mainly of material reworked from the Springer rocks (Jacobsen, 1959). Johnson and others (2001) break the Deese Group into the Marmaton, Cabaniss, and Krebs Sub-Groups, with the Cabaniss and Krebs being stratigraphically equivalent to the "Cherokee."

A review of literature dealing with detailed Cherokee-equivalent stratigraphy in the Ardmore Basin shows that Chenowith (1979) is the most internally consistent and agrees best with industry terminology. His list of nine formations from youngest to oldest (top to bottom) are: (1) Culberson, (2) Upper Fusulina, (3) Lower Fusulina, (4) Tussy, (5) Edwards, (6) Carpenter, (7) Pickens, (8) Morris, and (9) Hefner (Fig. 2). In areas where the stratigraphy is more generalized, only the Culberson, Fusulina, and Tussy appear, with the Tussy including all sands through the Hefner.

When the Culberson, Fusulina, and Tussy formations are compared with the formations recognized in north-central and northeast Oklahoma, the Culberson is seen to be roughly equivalent to the Skinner, the Fusulina to the Red Fork, and the Tussy to the Bartlesville (Fig. 2). Although these units are stratigraphic equivalents, the environments of deposition obviously vary between these areas of the State.

A base map (Fig. 3) was constructed showing where the nine type well logs and the fields in which they are found are located. All of these fields have since been combined into the greater Sho-Vel-Tum Field. Located in the northwestern part of this field complex, the combined fields on the base map (Billingsley, 1956) include Camp, Doyle, Fox-Graham, Milroy, North Alma, Sholem Alechem, Tatums-Tussy, and Velma.

GREATER SHO-VEL-TUM FIELD

Sho-Vel-Tum is an irregularly shaped field that encompasses about 75,000 net acres, or 117 mi^2 in Carter, Garvin, and Stephens Counties (Fig. 1). First producing oil in 1905, the name Sho-Vel-Tum, was not adopted until 1956. The field was initially consolidated from three older fields: Sholem Alechem, Velma, and Tatums. Today, Sho-Vel-Tum has grown to include 42 smaller fields (Lacina, 1979).

The western Ardmore Basin—especially the Stephens County area—underwent more intense faulting than did the eastern side of the basin. Because of this, most of the oil in the Stephens County area is focused more along the basin axis than the basin margins (Brown and Corrigan, 1997). In addition to the anticlinal (four-way dip closure) traps at the Velma, Sholem Alechem, and Fox-Graham Fields, the trap types in other areas of the greater Sho-Vel-Tum include structural noses (three-way dip closure), fault truncations, and unconformities (Clemons, 1984).

The formations equivalent to the Cherokee in greater Sho-Vel-Tum are in the Deese Group and are located stratigraphically between the overlying Marmaton and the underlying Dornick Hills Group. Reservoirs in the Cherokee-equivalent formations represent the largest remaining reserve volume for the field. Johnson and others (1987) showed that, at the time of their report, the Deese Group in Sho-Vel-Tum had 634 million stock tank barrels (MMSTB) of remaining oil-in-place (ROIP) and 278 MMSTB of unswept mobile oil (UMO). In 1999, the greater Sho-Vel-Tum Field had the largest remaining oil reserves in Oklahoma and also the highest production rate (U.S. Department of Energy Information Administration, 2000).

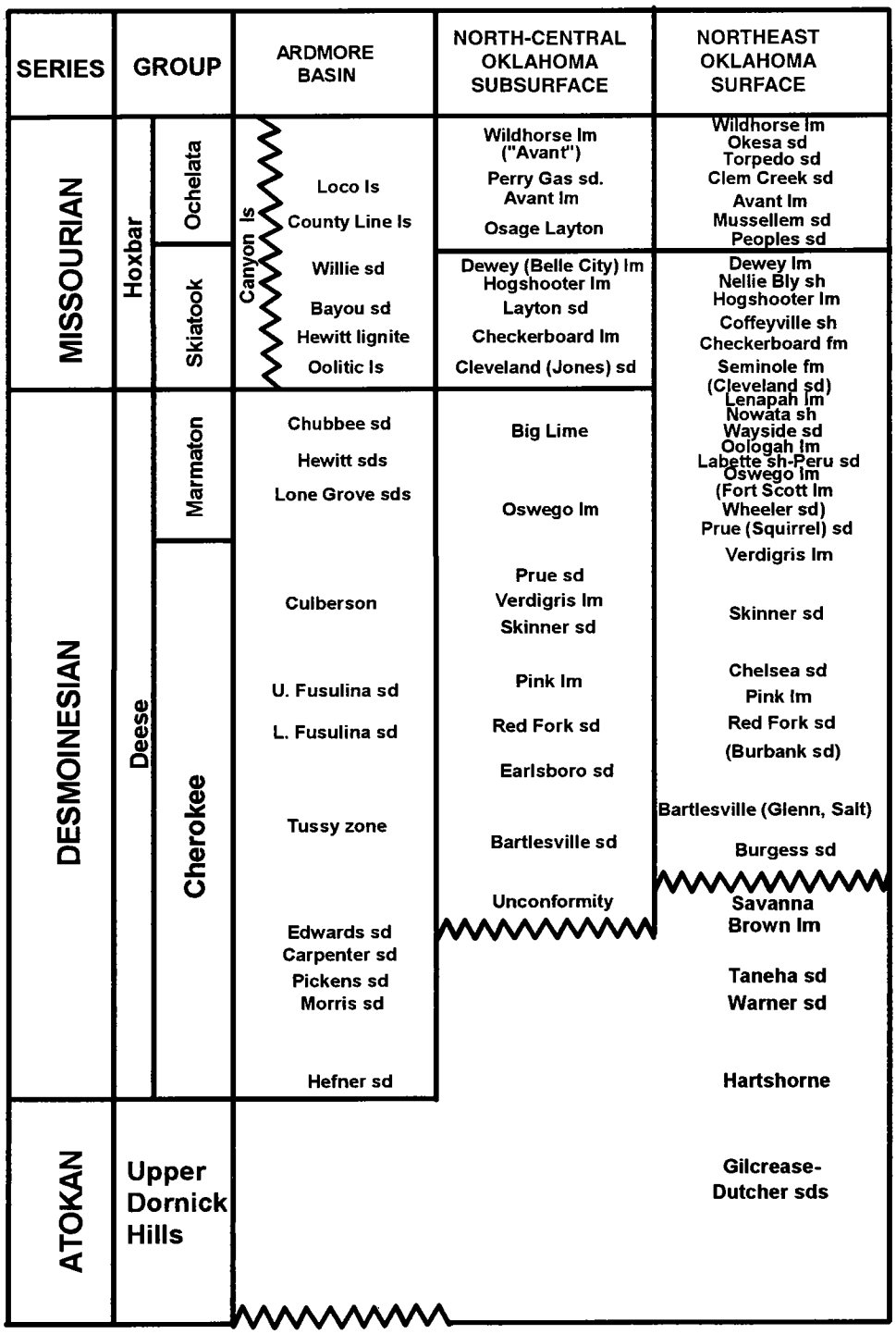

Figure 2. Stratigraphic chart of the "Cherokee-equivalent" formations in the Ardmore Basin (left column) correlated with the predominantly subsurface terminology in north-central Oklahoma and surface terminology in northeast Oklahoma. Adapted from Chenowith (1979).

COMPOSITE TYPE ELECTRICAL LOG FOR SHO-VEL-TUM FIELD

The construction of a "Cherokee" Group type log for all of Sho-Vel-Tum Field was aimed at producing a composite that was representative of all nine constituent type logs in which individual sands were developed (Fig. 4). It is apparent from Table 1 that all nine formations (sands) never appear together in any one location. However, those used in the greater Sho-Vel-Tum composite were selected based on their mutual proximity.

The local type logs chosen to build the composite log (Fig. 5) are all in an area just northwest of North Alma Field, between Velma and Sholem Alechem, which is

TABLE 1.—Field Coverage of "Cherokee Equivalent" Formations of the Ardmore Basin

Formation name	Name and operator of "type log well"	Type log location	Camp	Doyle	Fox-Graham	Milroy	North Alma	Sholem Alechem	Tatums-Tussy	Velma
1. Culberson	No. 1 Hitchcock Phillips	18, T. 1 N., R. 4 W.	F, (F)	Type log, (F)	EF					EF, (F)
2. U. Fusulina	No. A-8 Humphreys Skelly	13, T. 1 S., R. 5 W.	F, (F)	(F)	EF		(F)	(F)	F, (F)	Type log, (F)
3. L. Fusulina	No. A-8 Humphreys Skelly	13, T. 1 S., R. 5 W.	F, (F)	(F)	EF	(F)	(F)	(F)	F, (F)	Type log, (F)
4. Tussy	No. 1 Ledbetter Eason	6, T. 1 S., R. 3 W.	F, (F)	(F)	F	(F)	(F)	(F)	Type log, (F)	(F)
5. Edwards	No. 1 Edwards Van Grisso and Norville	9, T. 1 S., R. 4 W.	EF		EF		Type log, (F)		EF	
6. Carpenter	No. 1 Carpenter Nichols and Duncan	15, T. 2 S., R. 3 W.	EF	(F)	Type log		EF, (EF)		EF	
7. Pickens	No. 1 Pickens Crosbie, Inc.	9, T. 1 S., R. 4 W.		EF	EF		Type log, (F)	F, (F)		EF
8. Morris	No. 1 M. Morris Morgan and Pray	29, T. 2 S., R. 3 W.	EF	EF	Type log		EF	EF	EF	
9. Hefner	No. 4 Hefner Sunray	12, T. 1 N., R. 5 W.		Type log, (F)						

Abbreviations: F = formation; EF = equal formation.
Notes: Parentheses ( ) around F or EF indicate reference other than Jordan (1957). Camp data in parentheses are from Parker (1956). Doyle data in parentheses are from Bochneak (1982). Milroy data in parentheses are from Schweers (1959). North Alma data in parentheses are from Norville (1956). Sholem Alechem data in parentheses are from Billingsley (1956). Tatums-Tussy data in parentheses are from Hoard (1956). Velma data in parentheses are from Mallory (1948) and Rutledge (1956).

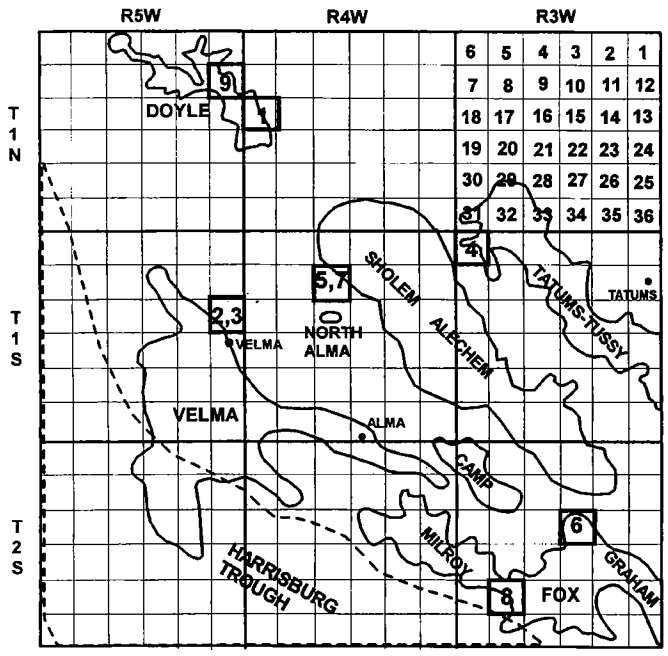

Figure 3. Sho-Vel-Tum Field base map showing the locations of the eight smaller fields studied: Camp, Doyle, Fox-Graham, Milroy, North Alma, Sholem Alechem, Tatums-Tussy, and Velma. The Harrisburg Trough helps highlight the northwest–southeast trend of the fields. Numbers in bold boxes represent type wells of "Cherokee-equivalent" formations in the greater Sho-Vel-Tum Field, which are, in descending order, 1 = Culberson, 2 = Upper Fusulina; 3 = Lower Fusulina; 4 = Tussy; 5 = Edwards; 6 = Carpenter; 7 = Pickens; 8 = Morris; and 9 = Hefner. Adapted from Billingsley (1956) and Jacobson (1981).

fortuitously near the middle of greater Sho-Vel-Tum. The four wells used in the construction of the composite type log for the equivalents of the "Cherokee" Group in the Ardmore Basin are listed in Table 2.

TYPE LOGS FOR CHEROKEE-EQUIVALENT FORMATIONS

Cherokee-equivalent formations in the Ardmore Basin are primarily marine units, and the reservoirs are dominantly sandstones, although some production is from limestones. In the following discussion of these formations, the upper and lower Fusulina are combined. Information concerning the current status of each formation is taken directly from the IHS (2002) database (Table 3).

Culberson Formation

The type log for this formation is the Phillips No. 1 Hitchcock, located in sec. 18, T. 1 N., R. 4 W., in the Doyle Field (Fig. 4). In addition, the Culberson formation is identified in Camp and Velma Fields and has an equivalent that is found in the Fox-Graham Field (Table 1). IHS data show Culberson-productive leases in Doyle and Fox-Graham Fields. This formation forms the uppermost unit of the Deese Group Cherokee equivalents in the Ardmore Basin and is not continuous across the area.

Fusulina Formation

The type log for this formation (Fig. 4), which includes both the upper and lower Fusulina, is the Skelly No. A-8 Humphreys, located in sec. 13, T. 1 S., R. 5 W.,

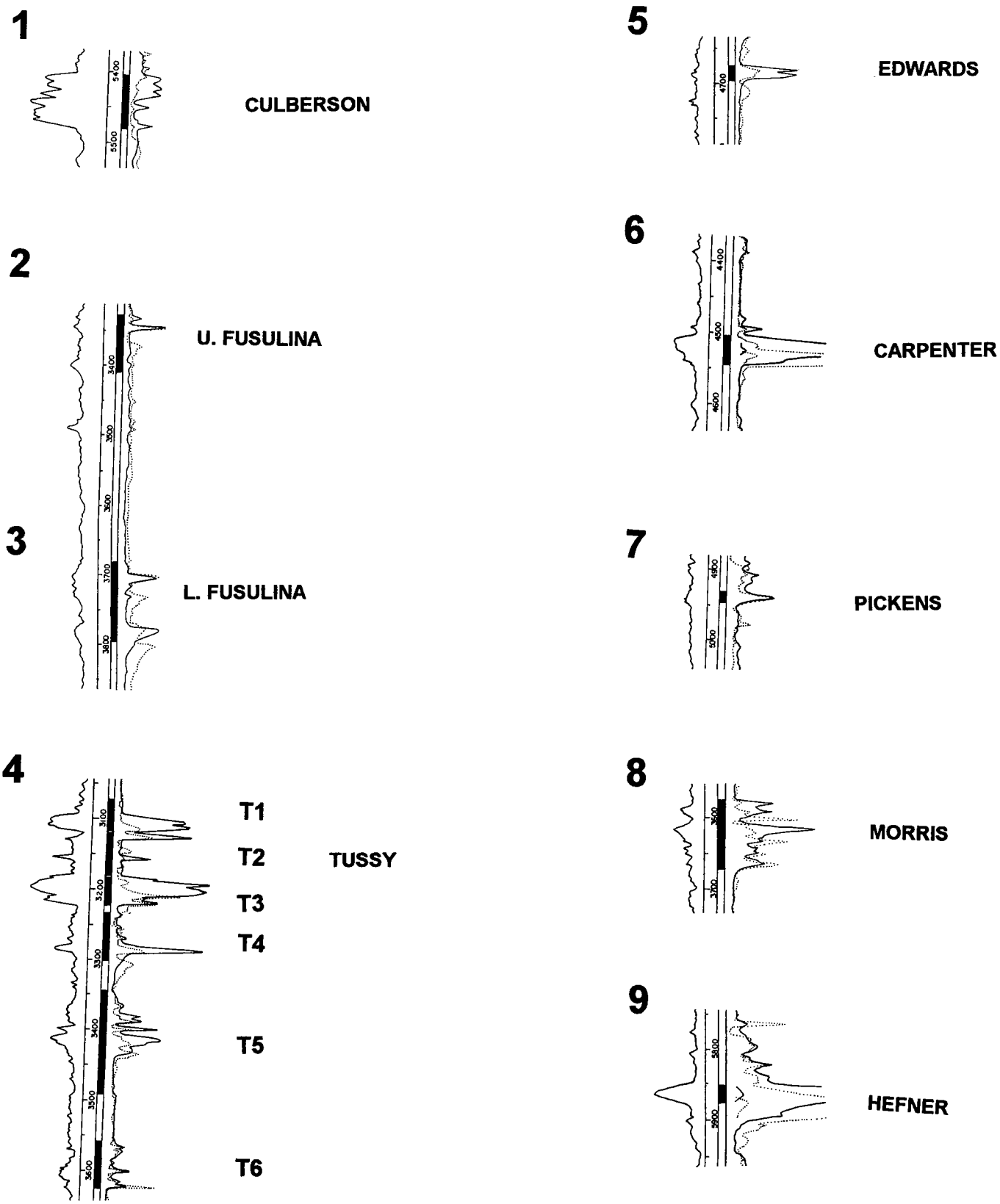

Figure 4. Type logs of the nine "Cherokee-equivalent" formations of the Ardmore Basin. See Figure 3 for map showing locations. From Jordan (1957).

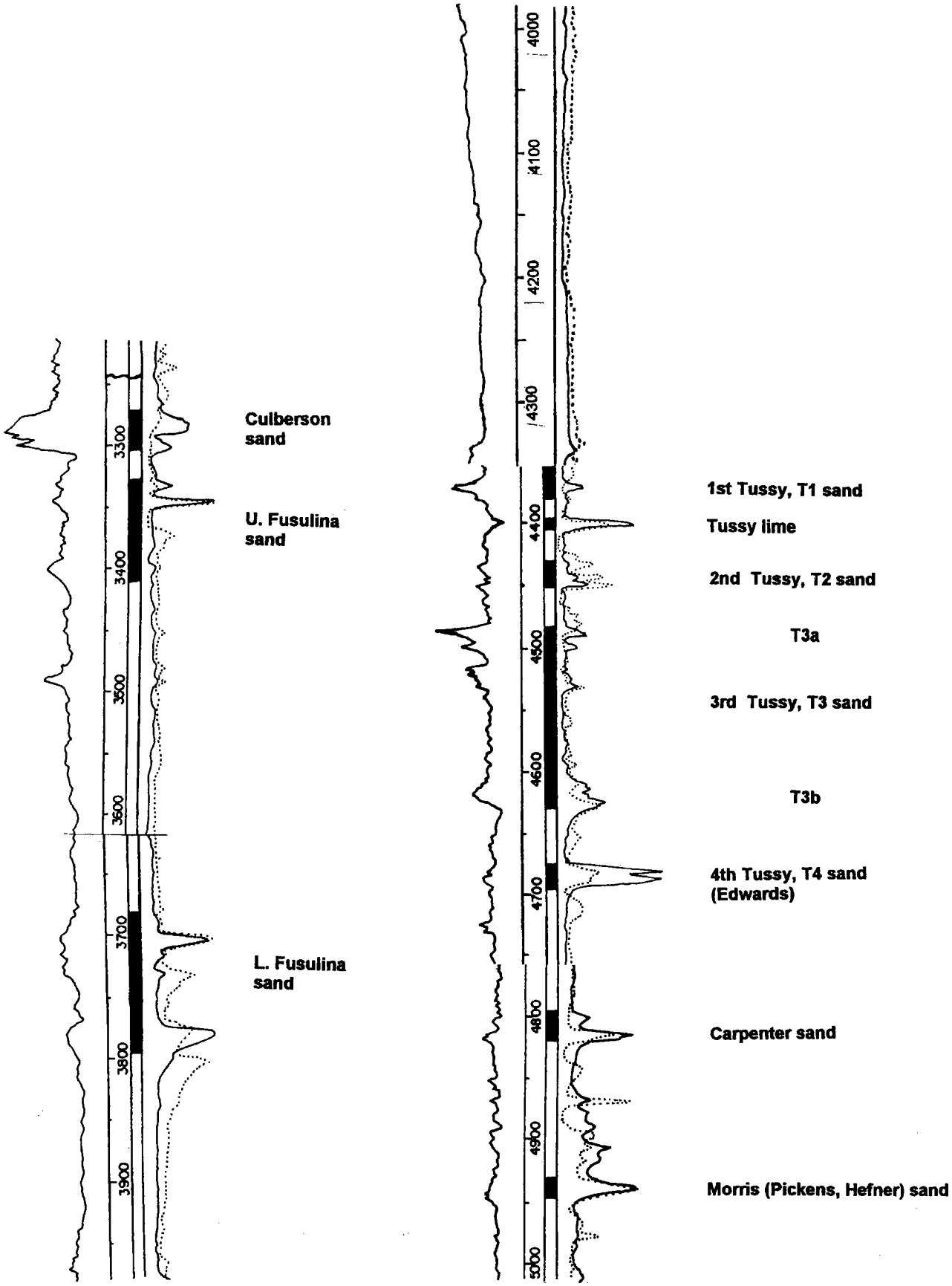

Figure 5. Composite type electrical log of the nine "Cherokee-equivalent" formations of the Ardmore Basin. Depths in feet. Adapted primarily from Jordan (1957).

TABLE 2.—Wells Used in Construction of Composite Type Log for "Cherokee-Equivalent" Formations of the Ardmore Basin

Operator	Well	Location	Depth (ft)	Formations
Skelly Oil Co	Humphrey No. A-8	SW¼SE¼SW¼ sec. 13, T. 1 S., R. 5 W.	3,220–3,980	Culberson, Upper Fusulina, & Lower Fusulina
Sinclair-Prairie Oil Co.	Fitzhugh No. 1	NW¼SW¼SW¼ sec. 19, T. 1 S., R. 4 W.	3,980–4,350	None
Van-Grisso Oil and Glen S. Norville	Edwards No. 1	NW¼NE¼NE¼ sec. 9, T. 1 S., R. 4 W.	4,350–4,770	Tussy & Edwards
J. E. Crosbie, Inc.	Pickens No. 1	NW¼SE¼NE¼ sec 9, T. 1 S., R. 4 W.	4,770–5,030	Carpenter, Pickens, Morris, & Hefner

Note: The composite type log for the basin is shown as Figure 5.

TABLE 3.—Table of the Nine "Cherokee Equivalent" Formations of the Ardmore Basin

Formation name	Total no. of leases	Oil cum.	Gas cum.	Ave. oil cum. per lease	Ave. gas cum. per lease	Oil only leases	Gas only leases	Oil & gas leases	Inactive leases	Active leases	First lease prod.
1. Culberson	9	1,112,366	7,694,671	123,596	854,963	1	4	4	6	3	1943
2,3. U & L Fusulina	37	4,841,356	4,521,895	130,847	122,213	20	7	10	18	19	1928
4. Tussy	161	34,322,962	11,696,541	213,186	72,649	124	2	35	89	72	1943
5. Edwards	4	544,237	15,878	136,059	3,970	3	0	1	3	1	1950
6. Carpenter	22	2,288,635	1,338,373	104,029	60,835	16	0	6	12	10	1951
7. Pickens	17	3,298,362	217,271	194,021	12,781	13	1	3	7	10	1949
8. Morris	14	3,222,067	1,258,278	230,148	89,877	7	0	7	9	5	1951
9. Hefner	11	908,942	360,113	82,631	32,738	7	1	3	4	7	1954
Totals of all nine formations	275	50,538,927	27,103,020			191	15	69	148	127	

Note: The data are current through December 2001 and show how the formations compare regarding total leases, cumulatives, averages, active and inactive leases, and first-lease production. The Table includes data supplied by Petroleum Information/Dwights LLC; Copyright 2002 Petroleum Information/Dwights LLC (IHS, 2002).

in the Velma Field. The Fusulina is found in Camp, Doyle, Milroy, North Alma, Sholem Alechem, Tatums-Tussy, and Velma Fields and has an equivalent formation found in the Fox-Graham Field (Table 1). The Fusulina formation is continuous across the base map area and produces in Camp, Fox-Graham, Milroy, North Alma, Sholem Alechem, Tatums-Tussy, and Velma Fields.

Tussy Formation

The type log for the Tussy formation is the Eason No. 1 Ledbetter, located in sec. 6, T. 1 S., R. 3 W., in the Tatums-Tussy Field. The Tussy formation is found and, according to IHS (2002), produces in all eight fields found on the base map. The Tussy limestone is about 10 ft thick and lies immediately below the uppermost Tussy sandstone (T1 of Fig. 4). This limestone is a key stratigraphic marker used throughout the Ardmore Basin (Hoard, 1956). Note that the Tussy consists of a number of sandstone beds, the nomenclature for which is shown in Figure 5.

Edwards Formation

The type log for the Edwards formation is the Van Grisso and Norville No. 1 Edwards, located in sec. 9, T. 1 S., R. 4 W., of North Alma Field (Fig. 4). The Edwards

is sometimes called the 4th Tussy (see Fig. 5). The Edwards formation is found only in North Alma Field, but has an equivalent formation found in Camp, Fox-Graham, and Tatums-Tussy Fields. Leases that produce from this formation are located in Doyle and Sholem Alechem Fields.

Carpenter Formation

The type log for the Carpenter formation is the Nichols and Duncan No. 1 Carpenter, located in sec. 15, T. 2 S., R. 3 W., in the Fox-Graham Field (Fig. 4). The Carpenter is found only in the Fox-Graham and Doyle Fields, but has an equivalent formation in Camp, North Alma, and Tatums-Tussy Fields. IHS (2002) data show leases that produce from this formation in the area of Fox-Graham, North Alma, and Sholem Alechem Fields.

Pickens Formation

The type log (Fig. 4) for the Pickens is the Crosbie, Inc. No. 1 Pickens, located in sec. 9, T. 1 S., R. 4 W., of North Alma Field. The Pickens formation is found only in the North Alma and Sholem Alechem Fields, but has an equivalent in Doyle, Fox-Graham, and Velma Fields. Leases that produce from this formation are located in and around Sholem Alechem, and between Sholem Alechem and Doyle Field.

Morris Formation

Figure 4 shows the type log for the Morris formation, which is the Morgan and Pray No. 1 M. Morris, located in sec. 29, T. 2 S., R. 3 W., of Fox-Graham Field. The Morris is found only in the Fox-Graham Field, but has an equivalent formation found in Camp, Doyle, Sholem Alechem, and Tatums-Tussy Fields. IHS (2002) data show productive leases in the area of Camp, Fox-Graham, and Sholem Alechem Fields.

Hefner Formation

The basal-most Cherokee-equivalent formation in the Ardmore Basin is the Hefner formation. The type log for the Hefner formation (Fig. 4) is the Sunray No. 4 Hefner, located in sec. 12, T. 1 N., R. 5 W. of Doyle Field. The Hefner formation is found only in the Doyle Field, and it has no equivalents. IHS (2002) data show leases that produce from this formation are located in and around Doyle Field.

STUDIES OF THE GREATER SHO-VEL-TUM FIELD

The following eight fields were evaluated in this study of the greater Sho-Vel-Tum Field: Camp, Doyle, Fox-Graham, Milroy, North Alma, Sholem Alechem, Tatums-Tussy, and Velma (Fig. 6) Fields in the region cluster around northwest–southeast-trending faults (Schweers, 1959). The base map is centered on the Harrisburg Trough to outline production trends. The Harrisburg Trough lies just southwest of Milroy Field and it crosses parts of the Fox-Graham and Velma Fields. The Fox-Graham, Milroy and Velma

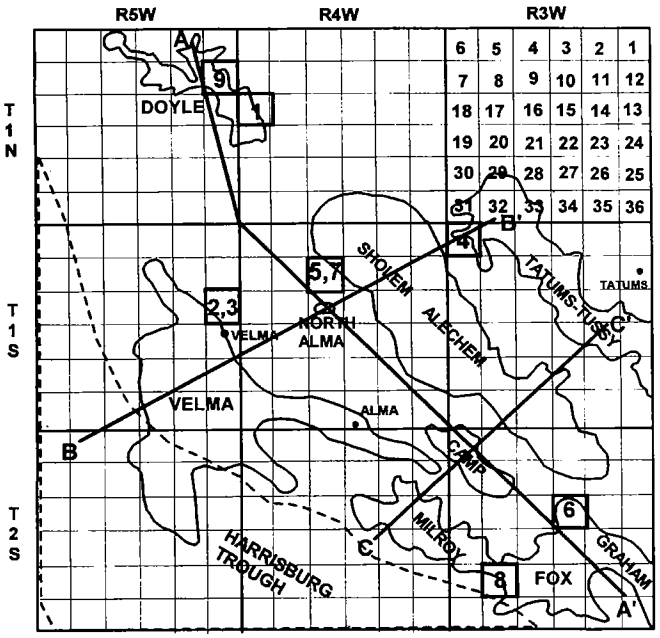

Figure 6. Base map of Sho-Vel-Tum Field; locations of three cross sections , A–A′, B–B′, and C–C′ (Fig. 7) shown.

Fields lie along a single, 30-mi-long uplift (Tomlinson, 1952) with the Milroy Field on the southwest side approaching the axis of the trough (Harmon and others, 2002).

Camp Field

Camp Field is located on a faulted northwest–southeast-trending anticline with 1,500 ft of closure at the Springer level (Clemons, 1984). From a regional perspective, the Camp Field is on a relatively minor anticline between the major uplifts of Milroy and Sholem Alechem (Parker, 1959).

Doyle Field

Doyle Field Cherokee-equivalent reservoirs produce from five lenticular sands. Hydrocarbons are trapped in anticlinal structures or stratigraphic traps created by either truncation or sandstone pinchout. The structural component to the Doyle trap is a plunging anticline with a northwest–southeast axis (Bochneak, 1982).

Fox-Graham Field

Fox-Graham is much like the adjacent Milroy Field in that both lie in areas of extreme compression. These stresses were so great at Fox-Graham that seven major anticlinal folds were produced in the single township. The Graham part of the structure is a sharp, faulted anticline with a steep northeastern limb and a normal fault along its southwestern flank (Shaw, 1954).

Milroy Field

The Milroy structure is a result of reactivation and reversal of the major faults, forming a steep anticline. Computer modeling of Milroy suggests that the basal

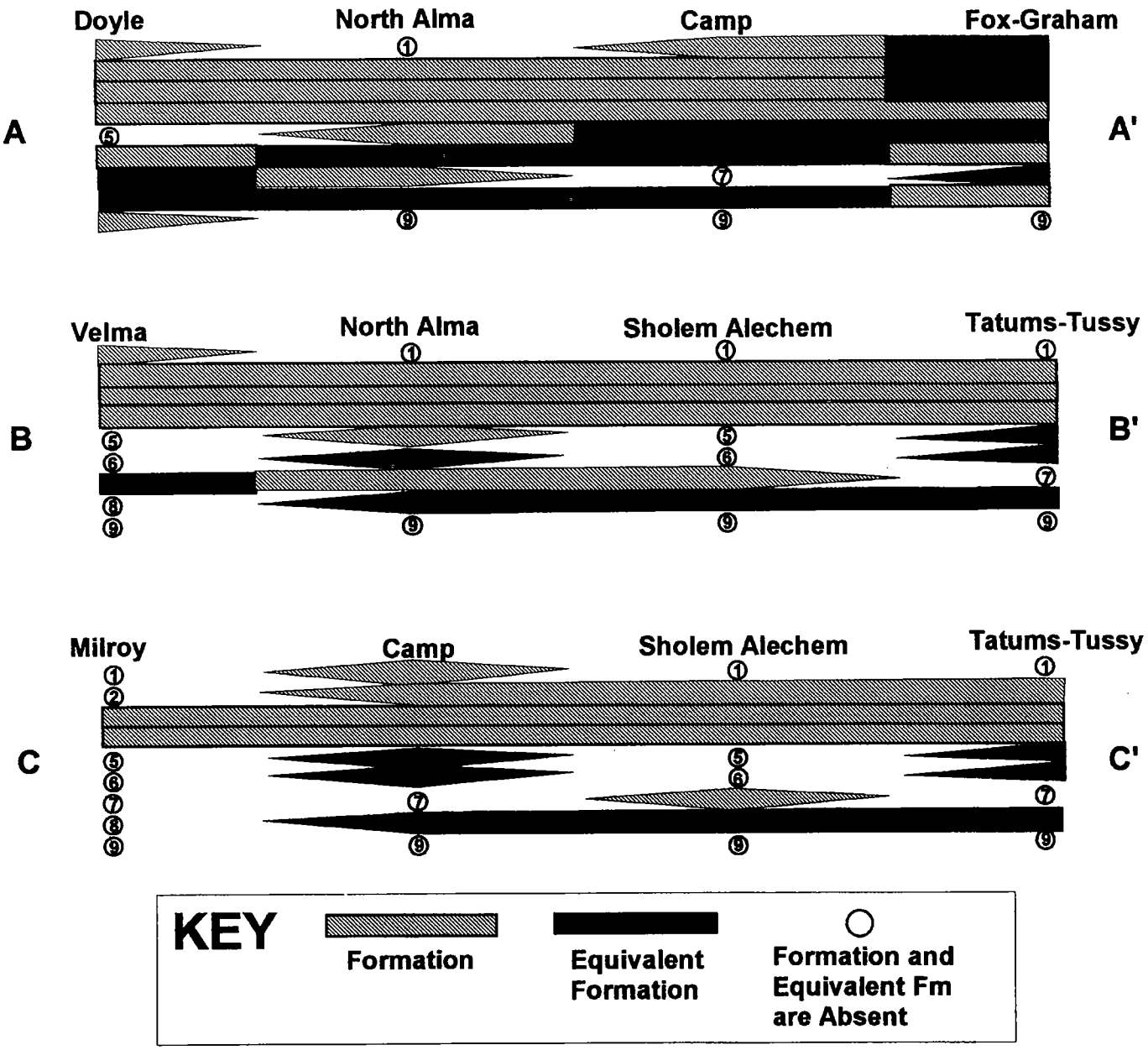

Figure 7. Three cross sections (A–A′, B–B′, and C–C′) showing "Cherokee-equivalent" formation, equivalent formation, and absent formation coverage across the eight fields of the Sho-Vel-Tum base map. See Figure 6 for locations of cross sections.

Morrowan unconformity, which separates the Dornick Hills and Tussy formations from the Springer and older formations (Harmon and others, 2002), is continuous beneath either the Upper Dornick Hills or, in its absence, the Tussy limestone.

North Alma Field

Contrasted to most other structures in the Ardmore Basin, the North Alma Field is a relatively flat structure. There is no evidence of any large scale faulting in North Alma (Vanbuskirk, 1960), and the structure is that of a northwest-plunging anticline with a scant 50 ft of closure (Norville, 1956).

Sholem Alechem Field

Sholem Alechem is formed by a sharp anticlinal fold with about 1,500 ft of closure. Reservoirs consist of several lenticular sands, making the traps a combination of stratigraphy and structure (Billingsley, 1956).

Tatums-Tussy Field

The Tatums-Tussy Field is composed of four small anticlines that concentrate hydrocarbons into structural traps (Hoard, 1956). Dominated by four-way and faulted three-way closures, some production is also stratigraphically controlled (Clemons, 1984).

Velma Field

The Velma Field is in an area of severely faulted folds with displacements of >1,600 ft (Clemons, 1984). Post-Deese erosion has removed much of the upper Deese, occasionally cutting below the Culberson, and causing the Hoxbar to lie disconformably on middle Deese in much of the Velma Field (Mallory, 1948).

CROSS SECTIONS

The Cherokee equivalent formations present in the eight fields studied vary widely from field to field. To illustrate this fact three cross sections were constructed. Their location is shown on Figure 6. Cross section A–A′ runs northwest–southeast from the Doyle to the Fox-Graham Field, B–B′ runs southwest–northeast from Velma to Tatums-Tussy Field, and C–C′ trends southwest–northeast from Milroy to the Tatums-Tussy Field.

In Figure 7, a formation is shown by gray shading, an equivalent formation by black shading, and a circle drawn around the formation number shows a missing formation or missing equivalent formation. Each cross section has nine lines representing the nine formations from the Culberson (1), at the top of the sequence, to the Hefner (9), at the bottom. The data are from Table 1. The absence of a formation is invariably due to paleostructural position that caused either nondeposition or subsequent erosion.

SUGGESTIONS FOR FUTURE RESEARCH

It is hoped that this report will stimulate others to do more detailed work on Cherokee-equivalent formations in the Ardmore Basin and the fields in which they produce. IHS data sometimes showed producing formations in fields previously thought of as not having a particular formation present. For example, the Edwards formation is not supposed to be in Doyle or Sholem Alechem Fields, yet IHS data show it produces in those fields. Could the formation be wrongly identified or does it extend to other fields, and where are field boundaries? Cross sections, computer modeling, and core data could do much to help resolve these problems. In 1947, Ardmore Basin expert Frank Gouin pointed out that no field in southern Oklahoma had ever been completely defined either laterally or vertically. As Oklahoma's oil supplies continue to dwindle, perhaps a renewed look at field development in this area may identify previously overlooked hydrocarbons.

CONCLUSIONS

This project was an attempt to provide an updated study of the formations that make up the Cherokee Group in the Ardmore Basin. Many references to formations equivalent to Cherokee strata in the Ardmore Basin, unless mentioned in theses or dissertations, generally were found in papers dedicated to non-Cherokee formations.

This paper, as far as is known, provides the first composite electrical type log for Cherokee-equivalent formations in the Ardmore Basin. Reference tables of formation coverage and lease production statistics are also shown.

Not only is Sho-Vel-Tum the oil field that has had the highest production rate and largest proven reserves in Oklahoma in recent years, but Cherokee-equivalent formations contain the largest remaining oil reserves in the field. This fact is perhaps the most important conclusion reached in this paper.

ACKNOWLEDGMENTS

I wish to recognize those who have been so helpful to this project. Thanks go to Dan Boyd, of the Oklahoma Geological Survey, who provided direction and assistance in the early stages of this project. I also wish to express my thanks to my father, Charles E. Harmon of C. E. Harmon Oil, Inc., for allowing me the time and opportunity to work on this project. My sincere thanks also go to my wife, Angela, and our daughters, Katie and Anna, for their patience and prayers on this project.

This paper includes data, referenced as IHS (2002), supplied by Petroleum Information/Dwights LLC, copyright 2002. I appreciate the release of this confidential data for this paper by Jeffrey S. Kay and the IHS Energy Group. Other sources of data for this project include: The Tulsa City-County Library System and the various theses, dissertations, and books from libraries across the United States, the American Association of Petroleum Geologists Library in Tulsa, and the Oklahoma Well Log Library in Tulsa.

REFERENCES CITED

Billingsley, H. R., 1956, Sholem Alechem oil field, Stephens and Carter Counties, Oklahoma, *in* Hicks, I. C.; Westheimer, J.; Tomlinson, C. W.; Putman, D. M.; and Selk, E. L. (eds.), Petroleum geology of southern Oklahoma, v. 1: American Association of Petroleum Geologists, Tulsa, Oklahoma, p. 244–259.

Billingsley, P. C., 1992, Facies patterns in the lower Deese group (Desmoinesian) of the Ardmore Basin, southern Oklahoma: University of Oklahoma M.S. thesis, 104 p.

Bochneak, D. L., 1982, A subsurface study of the Doyle field, Stephens County, Oklahoma: Baylor University M.S. thesis, 157 p.

Brown, Alton; and Corrigan, Jeff, 1997, Petroleum systems, Ardmore Basin and Arbuckle Mountains, Oklahoma: Guidebook for Field Trip 2, Dallas Geological Society, for American Association of Petroleum Geologists 1997 Annual Convention, 88 p.

Chenowith, P. A., 1979, Geological prospecting for Mid-Continent sandstones, *in* Hyne, N. J. (ed.), Pennsylvanian sandstones of the Mid-Continent: Tulsa Geological Society Special Publication 1, p. 13–18.

Clemons, R. R., 1984, The remote sensor exploration of the Ardmore and Marietta Basins of Oklahoma: Texas Tech University Ph.D. dissertation, 134 p.

Fay, R. O., 1997, Stratigraphic units in Oklahoma, Texas, Arkansas, and adjacent areas: Oklahoma Geological Survey Open-File Report 2-97, 4 charts, 229 p.

Gold, J., 1997, Inversion tectonics: applications in the southern Oklahoma aulacogen, Criner Hills region,

Carter and Love Counties, Oklahoma: University of Tulsa thesis, 63 p.

Gouin, Frank, 1947, Southern Oklahoma oil: The Oil Weekly, v. 126, no. 4, p. 34–41.

Harmon, R. E.; Banks, Richard; and Suhm, R. W., 2002, Computer modeling of a small-scale inversion feature: Milroy field, southern Oklahoma, *in* Cardott, B. J. (ed.), Revisiting old and assessing new petroleum plays in the southern Midcontinent, 2001 symposium: Oklahoma Geological Survey Circular 107, p. 21–38.

Hoard, J. L., 1956, Tussy sector of the Tatums field, Carter and Garvin Counties, Oklahoma, *in* Hicks, I. C.; Westheimer, J.; Tomlinson, C. W.; Putman, D. M.; and Selk, E. L. (eds.), Petroleum geology of southern Oklahoma, v. 1: American Association of Petroleum Geologists, Tulsa, Oklahoma, p. 174–185.

[IHS] Information Handling Services, 2002, Petroleum Information/Dwights LLC [Restricted database for petroleum production, leasing, etc.], copyright Petroleum Information/Dwights LLC (2002), Dallas, Texas. [Data released by IHS Energy Group.]

Jacobsen, L., 1959, Petrology of Pennsylvanian sandstones and conglomerates of the Ardmore Basin: Oklahoma Geological Survey Bulletin 79, 144 p.

Jacobson, M. I., 1981, The Harrisburg trough, Stephens County, Oklahoma—an update, *in* Borger, J. G. II (ed.), Technical proceedings of the 1981 American Association of Petroleum Geologists Mid-continent regional meeting: Oklahoma City Geological Society, p. 127–137.

Johnson, H. R.; Biglarbigi, K.; Schmidt, L.; Ray, R. M.; and S. C. Kyser, 1987, Primary and secondary recovery in the Sho-Vel-Tum oilfield, Oklahoma: U.S. Department of Energy Topical Report, DOE/BC/14000-1, 26 p.

Johnson, K. S.; Northcutt, R. A.; Hinshaw, G. C.; and Hines, K. E., 2001, Geology and petroleum reservoirs in Pennsylvanian and Permian rocks of Oklahoma, *in* Johnson, K. S. (ed.), Pennsylvanian and Permian geology and petroleum in the southern Midcontinent, 1998 symposium: Oklahoma Geological Survey Circular 104, p. 1–19.

Jordan, Louise, 1957, Subsurface stratigraphic names of Oklahoma: Oklahoma Geological Survey Guidebook 6, 220 p.

Kennedy, C. L. (ed.), 1982, The deep Anadarko Basin: Petroleum Information Corporation, Denver, Colorado, 359 p.

Lacina, J. L., 1979, Index to names of oil and gas fields in Oklahoma, 1978: Bartlesville Energy Technology Center, U.S. Department of Energy, 250 p.

Mallory, W. W., 1948, Pennsylvanian stratigraphy and structure, Velma pool, Stephens County, Oklahoma: American Association of Petroleum Geologists Bulletin, v. 32, p. 1948–1979.

McBee, William, Jr., 1995, Tectonic and stratigraphic synthesis of events in the region of the intersection of the Arbuckle and Ouachita structural systems, *in* Johnson, K. S. (ed.), Structural styles in the southern Midcontinent, 1992 symposium: Oklahoma Geological Survey Circular 97, p. 45–81.

Norville, G. C., 1956, North Alma field, *in* Hicks, I. C.; Westheimer, J.; Tomlinson, C. W.; Putman, D. M.; and Selk, E. L. (eds.), Petroleum geology of southern Oklahoma, v. 1: American Association of Petroleum Geologists, Tulsa, Oklahoma, p. 282–293.

Parker, E. C., 1956, Camp field, Carter County, Oklahoma, *in* Hicks, I. C.; Westheimer, J.; Tomlinson, C. W.; Putman, D. M.; and Selk, E. L. (eds.), Petroleum geology of southern Oklahoma, v. 1: American Association of Petroleum Geologists, Tulsa, Oklahoma, p. 174–185.

_____ 1959, Structure and lithology of the Springer in southeast Velma-Camp area, *in* Hicks, I. C.; Westheimer, J.; Tomlinson, C. W.; Putman, D. M.; and Selk, E. L. (eds.), Petroleum geology of southern Oklahoma, v. 2: American Association of Petroleum Geologists, Tulsa, Oklahoma, p. 227–248.

Parish, D. T., 1991, Geohistory of the Ardmore Basin, Carter County, Oklahoma: Baylor University B.S. thesis, 84 p.

Raymer, J. H., 1987, The Deese Group (Middle Pennsylvanian) of the Ardmore Basin, southern Oklahoma: University of Oklahoma M.S. thesis, 289 p.

Rutledge, R. B., 1956, The Velma oil field, Stephens County, Oklahoma, *in* Hicks, I. C.; Westheimer, J.; Tomlinson, C. W.; Putman, D. M.; and Selk, E. L. (eds.), Petroleum geology of southern Oklahoma, v. 1: American Association of Petroleum Geologists, Tulsa, Oklahoma, p. 260–281.

Schweers, F. P., 1959, Milroy field, Stephens and Carter Counties, Oklahoma, *in* Mayes, J. W.; Westheimer, J.; Tomlinson, C. W.; and Putman, D. M. (eds.), Petroleum geology of southern Oklahoma, v. 2: American Association of Petroleum Geologists, Tulsa, Oklahoma, p. 220–226.

Shaw, R. F., Jr., 1954, A subsurface study of the Post-Morrowan series of the Pennsylvanian system of township 2 south, range 3 west, Carter County, Oklahoma: University of Oklahoma M.S. thesis, 77 p.

Tapp, Bryan, 1995, Inversion model for the structural style of the Arbuckle region, *in* Johnston, K. S. (ed.), Structural styles in the southern Midcontinent, 1992 symposium: Oklahoma Geological Survey Circular 97, p. 113–118.

Tomlinson, C. W., 1952, Odd geologic structures of southern Oklahoma: American Association of Petroleum Geologists Bulletin, v. 36, no. 9, p. 1820–1840.

U.S. Department of Energy Information Administration, 2000, U.S. crude oil, natural gas, and natural gas liquids reserves—1999 annual report: Available online at: http://www.eia.doe.gov/pub/oil_gas/natural_gas/data_publications/crude_oil_natural_gas_reserves/historical/1999/html/cr.html (accessed March 2, 2001).

Vanbuskirk, J. R., 1960, Investigation of reservoir conditions of lower Deese sandstones (Pennsylvanian) for a flood project in the North Alma pool, Stephens County, Oklahoma: University of Oklahoma M.G.E. thesis, 165 p.

Bluejacket to Bartlesville, Oklahoma: Surface to Subsurface

G. Carlyle Hinshaw
Consulting Geologist
Norman, Oklahoma

ABSTRACT.—Outcropping Pennsylvanian formations in northeastern Oklahoma, especially those of the informal "Cherokee" group, have been providing natural resources since before statehood. The ability to harvest these resources on a large scale was provided by the introduction of railroads into Indian Territory after the Civil War. Concurrently, Indian land sovereignty began to change, and white entrepreneurs zeroed in on the fallow resources. Coal usage was started by the railroads as they switched from wood engine fuel. The "Cherokee" coals were and still are, a vast surface resource. As these rocks entered the subsurface from their outcrop area, the sandstones subsequently became oil and gas producers. The coal beds in the last 20 years became an important gas resource.

This paper describes the political history of resource usage of the "Cherokee" group, gives an overview of its geological history, and discusses current activity in the harvesting of "Cherokee" resources in northeastern Oklahoma

INTRODUCTION

Outcropping Pennsylvanian formations in northeastern Oklahoma, especially those of the informal "Cherokee" group, have provided energy resources since before statehood, and their subsurface equivalents continue to do so today. This research project focused on the "Cherokee" group, and a geologic profile was constructed across its outcrop from the area of Bluejacket, Craig County, Oklahoma, and extended westward in the subsurface to the town of Bartlesville, Washington County (Fig. 1).

The ability to pursue "Cherokee" resources en masse was kicked off on June 6, 1870, when the Missouri–Kansas–Texas (Katy) Railroad laid the first rail into Indian Territory at the northern end of the Cherokee Nation (Fig. 1). To make a short story long, the Katy and another rail line were in a race to win approval from the tribes in Indian Territory to build across their lands to Texas. The Katy was building south from Junction City, Kansas, and the other line was building southwest from Kansas City, Missouri. The Katy was behind schedule, and its construction superintendent, George Stevens, contacted Cherokee General Stand Watie and his nephew, Colonel Elias Boudineau, to put in a fix. As the other line approached Baxter Springs, Kansas, the Cherokees loaded up two wagons with whiskey at the Katy railhead well north of Chetopa, drove over to Baxter Springs, and told the other superintendent that the Missouri boys had already crossed the line into Indian Territory. They broke out the whiskey to celebrate and kept everyone drunk for two days and the Katy built on through. The race exhausted the Katy's means to finance another foot of rail, so they spent the better part of a year raising enough money to continue. Thus, it was almost a year later before the Katy completed the rail line southward across the Cherokee Nation toward the Red River, which forms the boundary between Oklahoma and Texas. At that time, Baxter Springs, Chetopa, and Coffeyville were centers for trade with the Cherokee Nation (Campbell, 1969, p. 19).

CATTLE THEN COAL

As construction picked up in Indian Territory, the Katy installed a cattle-loading spur 12 mi south of the Kansas State Line. The immediate reason for building the line was to move cattle to market. In 1871, it was estimated that 600,000 head forded the Red River from Texas and rumbled across Indian Territory to railroad pens in Kansas. A calf could be bought for $1 to $2, and beef sold for $10 a hundredweight in the northern markets.

The spur immediately attracted the tents of rail-construction followers. The surrounding area had been settled by Shawnee Indians, who merged with the Cherokee Nation as a result of a treaty between the two tribes in 1869. The Shawnee leader, Rev. Charles Bluejacket, lived near the spur and lent his name to the motley tent town, which became Bluejacket Station (Fig. 1). Called "Big Charles" by his relatives and "Uncle Charley" by almost everyone, he was an ordained Methodist minister, outlasted three wives, and

Hinshaw, G. C., 2002, Bluejacket to Bartlesville, Oklahoma: surface to subsurface, *in* Boyd, D. T. (ed.), Finding and producing Cherokee reservoirs in the southern Midcontinent, 2002 symposium: Oklahoma Geological Survey Circular 108, p. 213–225.

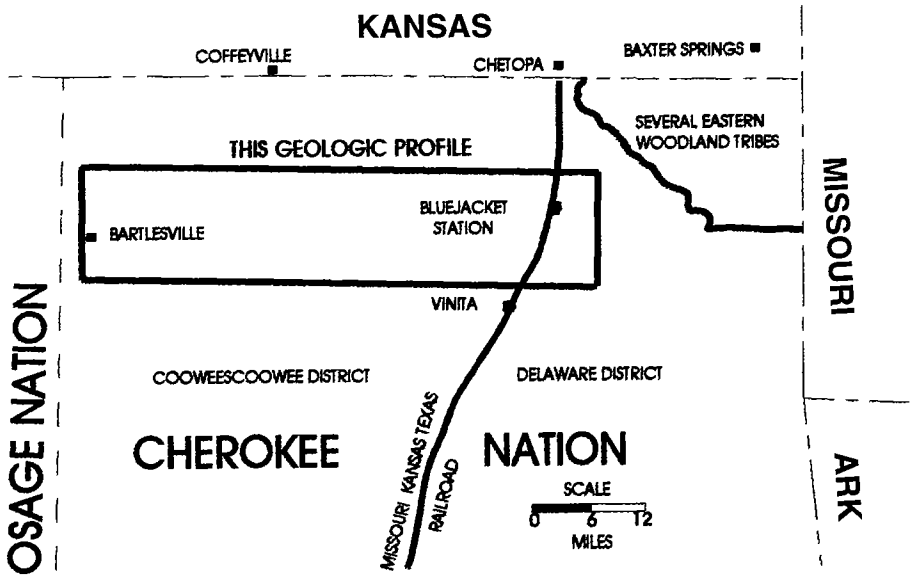

Figure 1. Map of Indian Territory in 1871, showing route of the Missouri-Kansas-Texas (Katy) Railroad from the Kansas State Line southward.

sired 23 children. In 1884, the first post office was established in Bluejacket, and the Rev. Charles was the first postmaster (Craig County Heritage Association, 1981, p. 9). This community is the anchor of the eastern part of this study.

In 1867, Nelson Carr established a small trading post on the banks of the Caney River at Black Dog Ford, at the north edge of present-day downtown Bartlesville (Fig. 1). He cut a millrace across a narrow neck of land in a horseshoe bend of the Caney and built a corn gristmill. Jacob Bartles purchased the operation in 1875, converted it to a flourmill, and started the Bartlesville post office in 1879.

With the founding of Bluejacket and Bartlesville, the cradle of Oklahoma's fossil-fuel industry was ready to develop in the "Cherokee" group of rocks.

Prehistoric, Native American, and European settlers utilized the country's vast coal reserves, and Indian Territory's share put a gleam in many a Pennsylvania miner's eye. Miners began to trickle into Indian Territory as soon as the Katy drove its last spike on the banks of the Red River preparatory to crossing into Texas. The first engines to enter the Territory burned wood but quickly converted to "Cherokee" coal. The first-known mining operation began in 1872 in the Choctaw Nation (southeastern Indian Territory) to fuel the burgeoning railroads. The Cherokee Nation "nationalized" its coal resources when individual members were doled out their own tracts leading to Oklahoma statehood.

THE "CHEROKEE" GROUP

The "Cherokee" outcrop extends from the Forest City Basin in Iowa southwest to the Arkoma Basin in southeastern Oklahoma and western Arkansas (Fig. 2). This paper describes a geological profile across the northern Cherokee Nation (Fig. 1). It is two townships high (T. 26 N. and T. 27 N.) and extends from the Craig-Ottawa County Line (R. 21 E.) west to the west line of R. 13 E. This strip of land is 12 mi high and 54 mi long. The profile crosses the Prairie Plains Physiographic Province near its southern terminus.

The formations grouped by the term "Cherokee group" were named for exposures in Cherokee County, Kansas (Fig. 2), in the early 1890s (Branson, 1968, p. 26). In Oklahoma, the Krebs and Cabaniss Groups formally contain the "Cherokee." The "Cherokee" group just south of the study area normally extends from the base of the Hartshorne Formation of the Krebs Group (Desmoinesian Series) upward to the base of the Fort Scott Limestone in the Marmaton Group (Desmoinesian) (Fig. 3). In the geological profile under discussion, the Hartshorne, however, is not present; The Hartshorne Sandstone extends northward from the Arkoma Basin only to the northern edge of Okmulgee County (T. 16 N.) (Andrews and others, 1998). Thus, in the study area, the "Cherokee" extends from the base of the McCurtain Shale of the McAlester Formation to the base of the Fort Scott Limestone (Fig. 3).

The "Cherokee" outcrop is about three townships wide, and nearly all exposures in the area under study are in Craig County, as shown in Figure 4. Mississippian rocks form the surface on which the "Cherokee" was deposited over most of the study area (Figs. 3, 4).

The major surface members or units of the "Cherokee" for the study area are listed in the right column of Figure 3, and equivalent subsurface terms used by the oil and gas industry are shown in the left column. It is common for all sands above the Bartlesville and below the Oswego to be called Squirrel.

COAL OCCURRENCE AND PRODUCTION

The cyclical sequence of the "Cherokee" group contains a number of named coal beds in all four formations that make up the "group"—i.e., the McAlester, Savanna, Boggy, and Senora Formations, in ascending order (Fig. 3). Historically and currently, several of those have been mined in the study area both as subsurface mines and as strip-mining operations. These are discussed below

The type locality of the Bluejacket Sandstone Member is about 2 mi west of the town of Bluejacket, the unit having been named by Ohern in 1914. The type locality now consists of a type section and two core holes drilled by the Oklahoma Geological Survey (Hemish, 1989a). A prominent topographic feature called Timber Hill contains the locality. Timber Hill was formed by resistant beds of riverine deposits of

Bluejacket sand being flanked by softer alluvial silts and muds. As erosion ensued, the fluvial point bars remained, leaving a hill covered with timber. The hill contains several adits and shafts into the Drywood coal, which underlies the Bluejacket Sandstone (Fig. 3).

The eastern edge of coal mining is an abandoned stripping operation in sec. 32, T. 27 N., R. 21 E., just south of the town of Bluejacket, from the Rowe coal. Additionally and westward, strip mining has been extensive in the Weir-Pittsburg, Mineral, Croweburg, and Iron Post coal beds. In the Nowata portion of this profile, only the Iron Post coal has produced from the "Cherokee." The 1999 Annual Report of the Oklahoma Department of Mines (Pritchard, 1999) lists coal-mining figures dating back to 1930. In 1999, in descending order of tonnage, the Iron Post, Croweburg, and Mineral coals were the Craig County producers. In the year 2000, production for all of Craig County was 73,000 short tons. No coal is being mined currently in Nowata County.

Today, coal is shipped on the old Katy Railroad, now the Union Pacific, from the Powder River Basin in eastern Wyoming to eastern Oklahoma electrical plants. Each day, 23 120-car coal trains cross the Kansas-Oklahoma line and pass over the "Cherokee" coals on the way. The quality of Oklahoma coals is insufficient to meet today's environmental and economic standards as fuel for utility manufacturing.

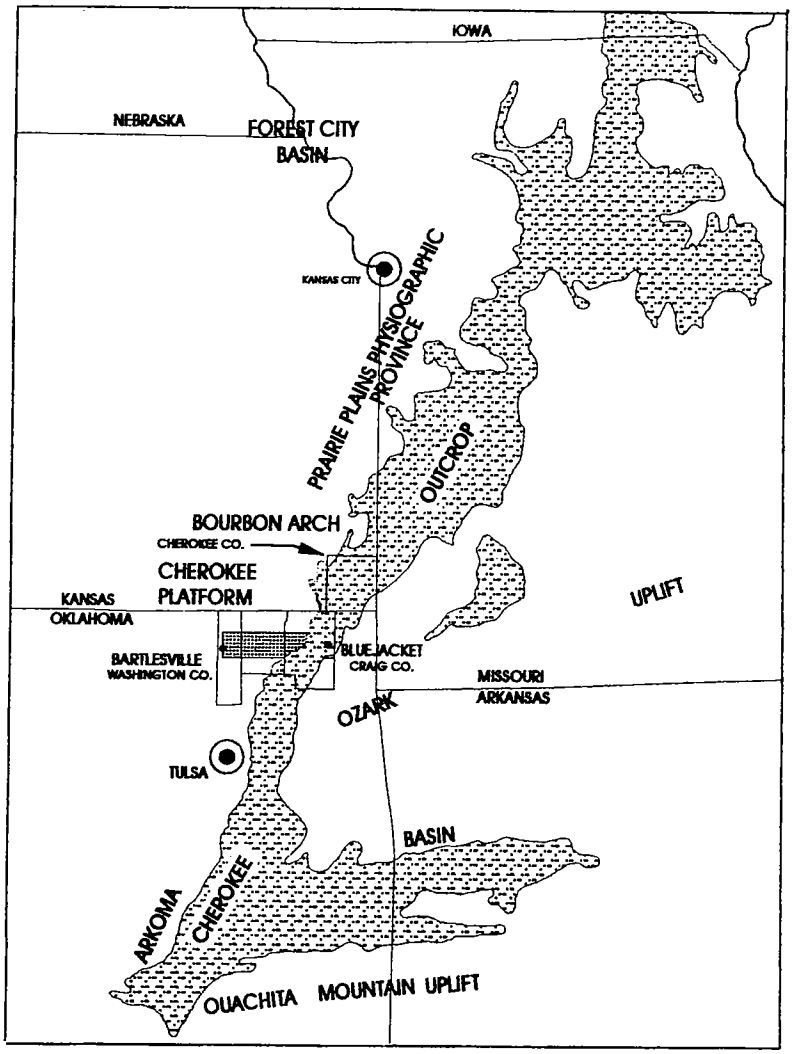

Figure 2. Outcrop map of the "Cherokee" group; location of geologic profile shown in dark stippled pattern. Map modified from Branson (1968, p. 27).

OIL AND GAS RESERVOIRS

The profile from Bluejacket to Bartlesville is an oil-rich province with most of the gas present being from the Chat and Mississippi lime. Most of the production is from the "Cherokee" group and is stratigraphic in nature, being related to depositional environments in complexes of fluvial deltaic systems. Mississippian reservoirs and the Lower Ordovician Arbuckle dolomite produce from paleogeomorphic traps. Marmaton Group sands and limes produce in Nowata and Washington Counties. Pennsylvanian structure is simple. The beds exhibit a slight regional dip toward the west with a few low-amplitude anticlinal and synclinal features with sparse, small-throw normal faults. In this two-township strip, about 15,000 wells have been drilled. Currently, drilling activity is primarily targeted to the Mississippi lime, and Nowata County is where most of the drill sites are located.

Five zones of "Cherokee" oil reservoirs are developed in the study area. These are the Burgess, Bartlesville, Red Fork, Skinner, and Prue. Figures 5–9 are examples of gamma-ray–compensated-neutron logs of sands in each group.

The Burgess sands (Warner) are about 10 ft thick and, as indicated by the coarsening-upward gamma-ray profile, tend to be marginal marine in character (Fig. 5). Rarely are there more than one sand in a borehole. Aerially, the Burgess produces over most of the profile but pools are small in size and the amount of production is low. The term Booch (Fig. 3) is the subsurface name for the outcropping Warner sandstone in the Arkoma Basin to the south. There, the terms lower, middle and upper are commonly used.

The Bartlesville sand (Fig. 6) is by far the most prolific producer in the area. The interval contains numerous systems of anastomosing fluvial courses. Consequently, in Nowata and Washington Counties, the Bartlesville sand zones may account for 75% or more of the oil production. In Figure 6 the thickness of the reservoir is 34 ft. The Bartlesville can cut out the underlying Drywood coal.

The Red Fork (Fig. 7) illustrates a "multi-story" sand quite well. As stream channels migrated laterally, ad-

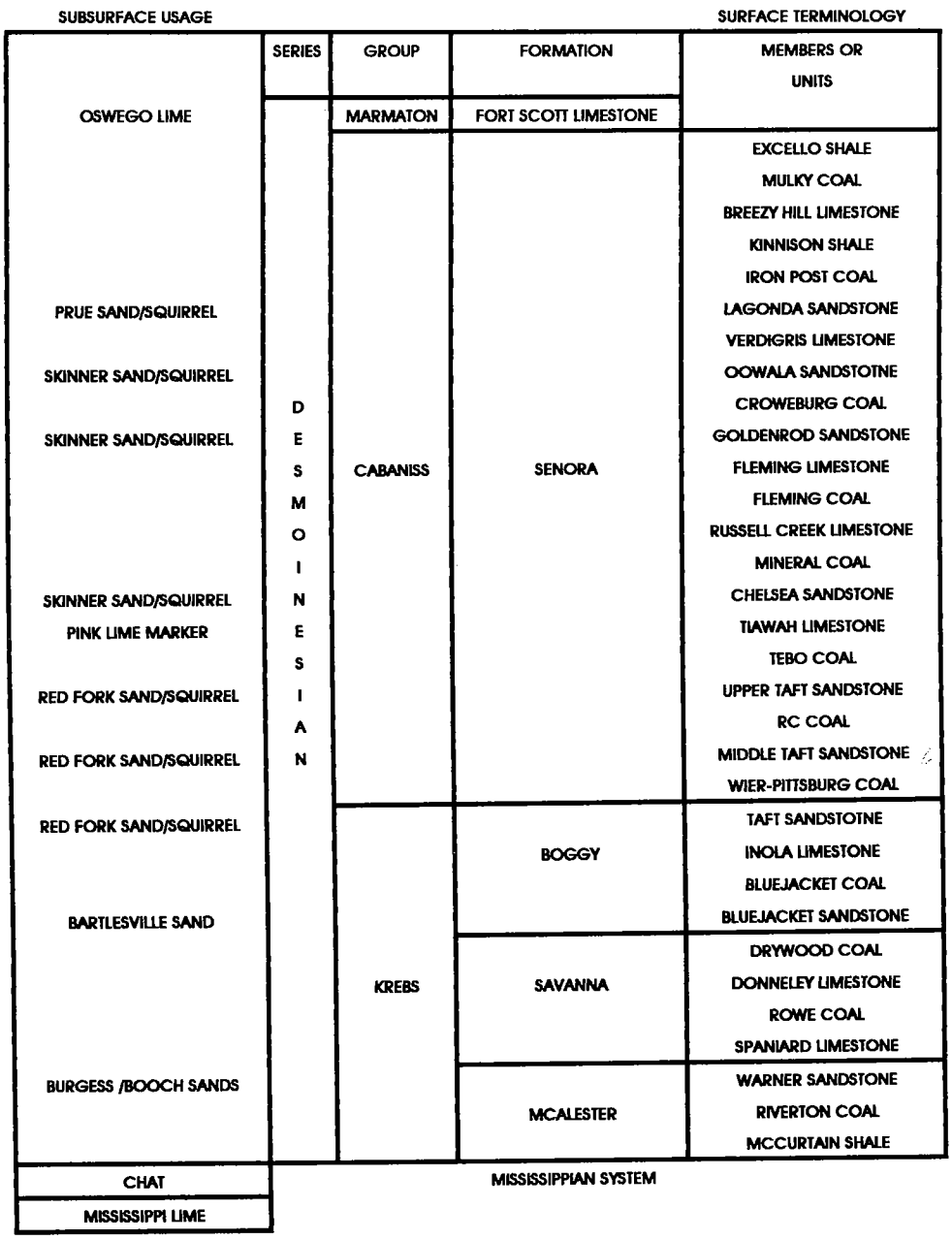

Figure 3. "Cherokee" group stratigraphic chart

jacent alluvial plains were placed over the sands, resulting in distinct shale breaks between reservoirs. Compartmentalization is well developed as a result. Figure 3 reflects the problems with surface and subsurface terminology of this interval. The Taft Sandstone Member is in the Boggy Formation. However, two sandstone beds in the overlying Senora Formation have been called the middle Taft member and the upper Taft member (Hemish, 1989b, p. 9). Renaming these would benefit the literature. The Red Fork sands probably are named Squirrel in this area more than any of the Skinner or Prue zones.

The Skinner sands lie between the Red Fork and the Prue and are equivalent to the Chelsea, Goldenrod, and Oowala Sandstone Members of the Senora Formation at the surface. Production has been found in less than a handful of wells. A few wells are listed as producing from the Skinner but have been improperly identified. The Skinner sands are sparse in occurrence, quite thin, and tend to be marine or marginal marine as shown in the coarsening-upward sequence in Figure 8.

The Verdigris Limestone Member of the Senora Formation was deposited across the entire profile; however, as shown in Figure 9, it has been eroded out in places. This example shows where a 60-ft–thick riverine system has eroded downward and the void filled with sand. Thus, of the five sand groupings of the "Cherokee," three exhibit fluvial-deltaic deposi-

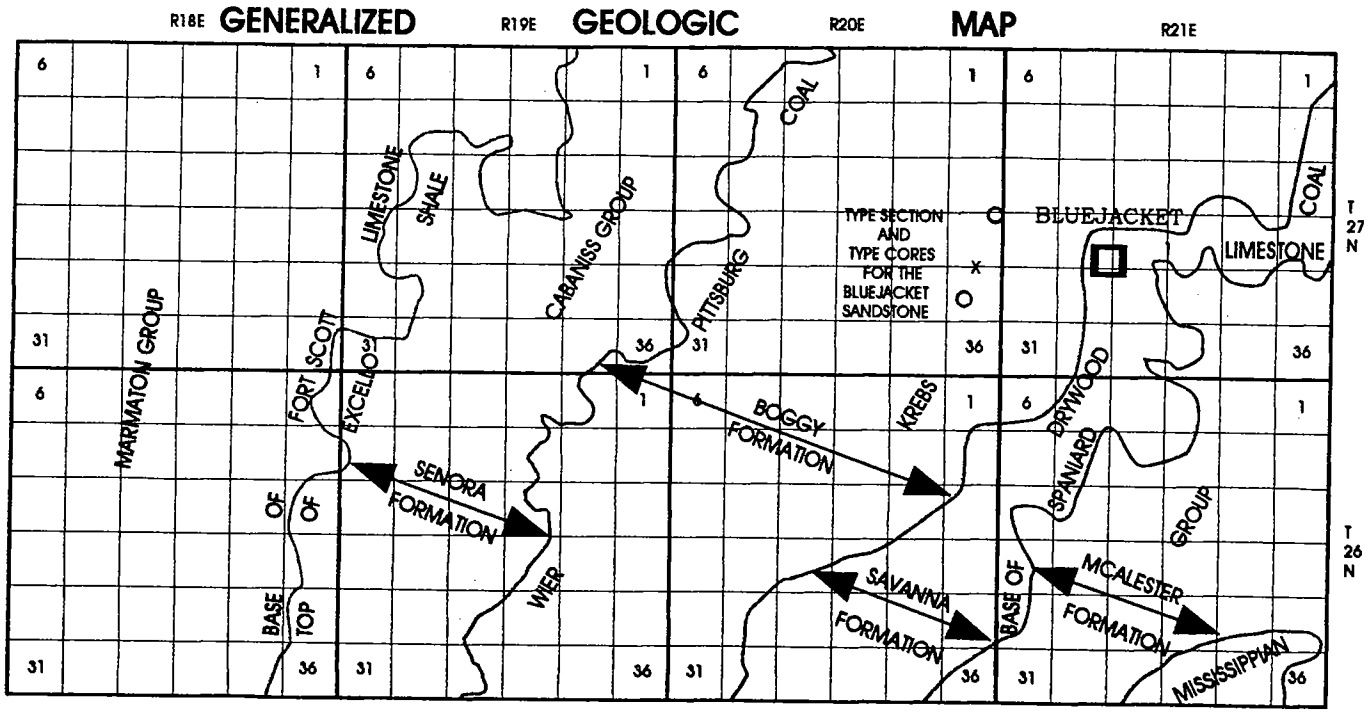

Figure 4. Generalized geologic map of study area showing area of "Cherokee"group outcrops, extending from top of Mississippian System to base of Fort Scott Limestone (Marmaton Group).

tional environments where abundant amounts of sand crossed or came to rest on the "Cherokee" shelf area.

OIL AND GAS FIELDS

Almost all "Cherokee " sands are oil productive from stratigraphic traps in the study area. As previously stated, minor contributing zones are the Arbuckle dolomite, Mississippi lime, Chat and Marmaton Group sandstones and limestones. Coal-gas–methane beds will be treated separately below.

The Oklahoma Tax Commission provides production information to industry. The reported amounts are given by lease, not by well. The entire history of production figures is not available, but current production is provided on a monthly basis. No attempt was made to tabulate individual fields because little effort has been made to define fields, only random labeling by operators. For the entire area, the Tax Commission reports 1,373 leases. The earliest figures in the list go back to 1925. Cumulative oil production for the 18-township area is stated as nearly 24,000,00 barrels. Current monthly production is about 37,000 barrels. Cumulative gas is about 22,000,000 MCF (thousand cubic feet) and monthly is about 350,000 MCF. Estimated coalbed figures will be stated later.

Well data for this project were garnered from the Oklahoma Geological Society Log Library in Oklahoma City and from the log library of the Oklahoma Geological Survey in Norman. Between the two, enough material has been archived to provide a reliable history of the "Cherokee" group. The following five illustrations (Figs. 10–14) show productive areas and the general location and depth of producing reservoirs. Patterned fills inside field outlines on ensuing maps show gas production. With the exception of Craig County, where small fields are found, production outlines can only be regarded as a guide. At this writing, the Oklahoma Geological Survey is in the process of compiling a new state field map (Boyd, 2002).

Eastern Craig County

The beginning of "Cherokee" sand production was in the Bluejacket S Field located mainly in sec. 4, T. 26 N., R. 21 E., at a depth of 76 ft from the Burgess (Fig. 9). Several of the fields on this map (Fig. 10) in the Bluejacket area have produced from Burgess sands, and its oil gravities are in the middle to low 30s. Reservoir energy, however, is quite low as production was generally less than one barrel per day.

Western Craig County

The Bartlesville sand began producing at a depth of 290 ft in an unnamed field in sec. 20, T. 26 N., R. 18 E., found in 1920 (Fig. 11). In the Centralia NE Field in sec. 1, T. 27 N., R. 18 E., production from the Burgess was found at 550 ft, from the Bartlesville at 325 ft, and from the Squirrel at 75 ft, this latter zone being a Skinner sand.

Eastern Nowata County

The area of intensive production begins in eastern Nowata County. As indicated by Figure 12 and the pre-

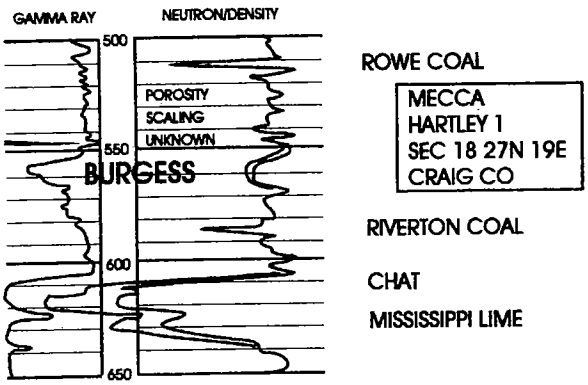

Figure 5. Typical log of the Burgess sand interval.

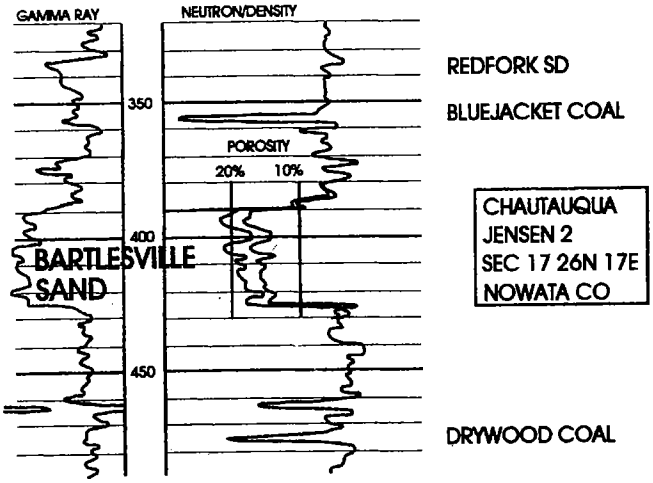

Figure 6. Typical log of the Bartlesville sand interval.

vious maps, field nomenclature in the cradle of Oklahoma oil is chaotic. The Coodys Bluff Field, for instance, includes a number of small pools extending across the north part of T. 26 N., R. 16 E., and down the west and south halves of T. 26 N., R. 17 E. The Delaware-Childers Field includes the extensive Bartlesville sand production across the south half of T. 27 N., R. 16 E., and the Chat and Mississippi lime gas production trending from the northwest corner of T. 27 N., R. 16 E., to the northeast corner of T. 26 N., R. 17 E. Of all the fields in the profile, the Nowata-Claggett in T. 26 N., R. 16 E contains the most individual producing reservoirs.

Western Nowata County

Westward, the productive area continues to increase. To repeat, nearly all of the oil is derived from the Bartlesville sands. Labels indicate the depths and scattered areas where other zones produce (Fig. 13).

Washington County

Finally, every section of the profile in Washington County has production. This area is where commercial

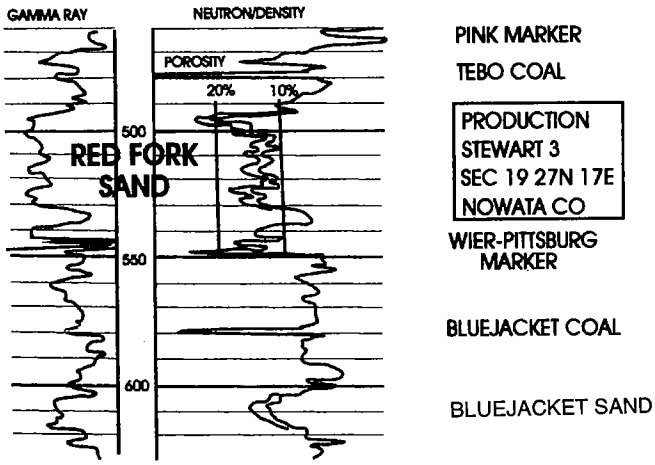

Figure 7. Typical log of the Red Fork sand interval.

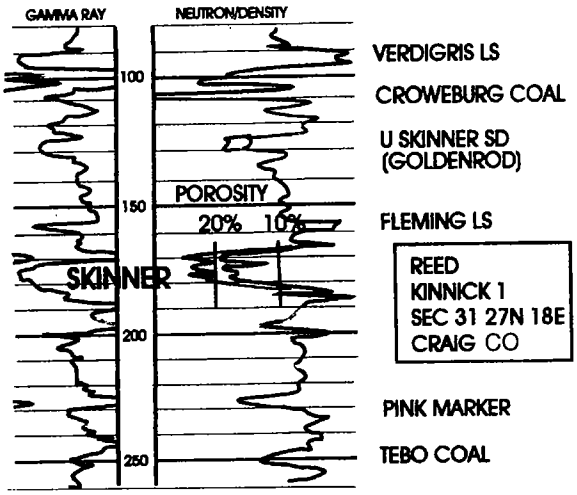

Figure 8. Typical log of the Skinner sandstone.

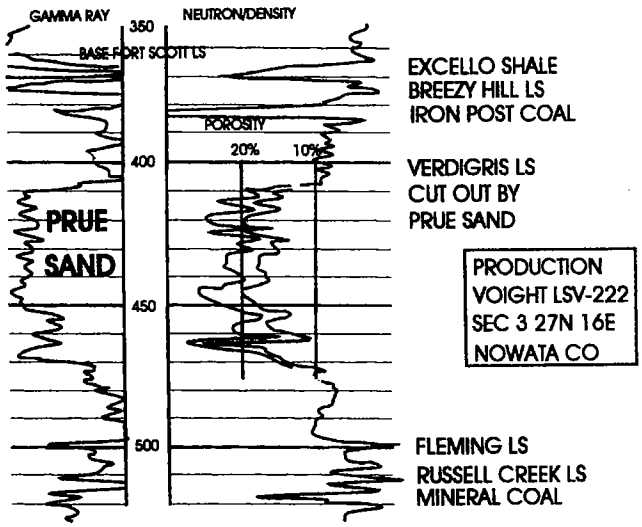

Figure 9. Typical log of the Prue sandstone.

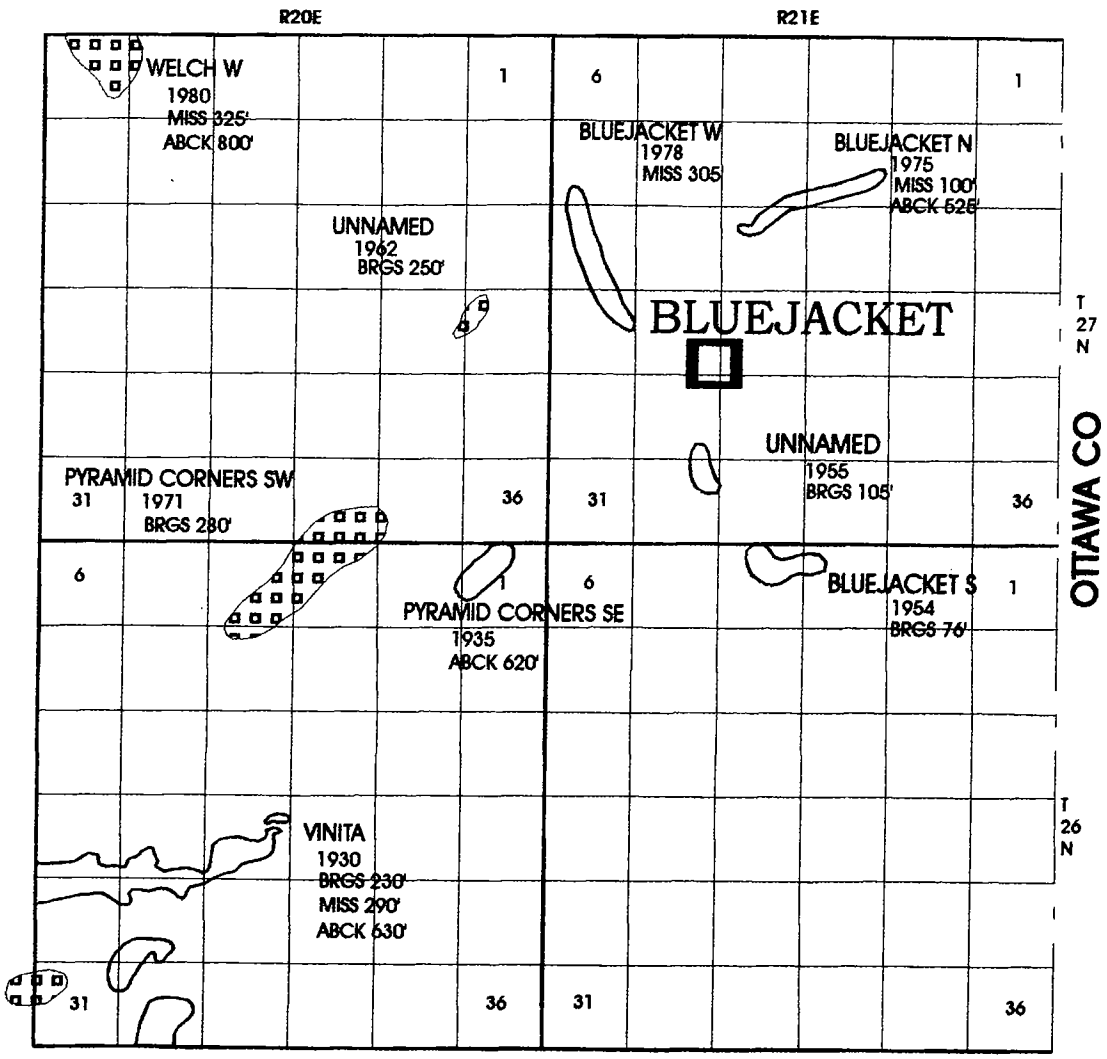

Figure 10. Oil and gas fields in eastern Craig County. Areas of gas production shown by pattern of small squares. *Abbreviations:* ABCK = Arbuckle; BRGS = Burgess; MISS = Mississippian.

production began in Indian Territory with the drilling of the Cudahy No. 1 Nellie Johnstone in the NE¼ of sec. 12, T. 26 N., R. 12 E. at the northern edge of Bartlesville (Fig. 14). The discovery well reached a total depth of 1,327 ft and was completed on April 15, 1897, in the Bartlesville sand. Actual production began several years later because of unclear land title and low oil prices. The well produced until 1946 when it was plugged due to a casing leak. Its cumulative was about 100,000 barrels (Visher, 1968, p. 69).

COAL-BED METHANE

Today, activity for coal-bed methane occurs in seven northeastern Oklahoma counties and in eastern Kansas (Hemish, 2002). Along the current study area, production has been found in R. 13–16. "Cherokee" group coal-gas beds are the Riverton, Rowe, Weir-Pittsburg, Mineral, Croweburg, and Iron Post coals (Fig. 3). The Excello Shale produces gas and is called Mulky coal, but Hemish (1989b, p. 18) found that the Mulky coal is not developed south of the Kansas line except in three boreholes in secs. 13 and 22, T. 28 N., R. 19 E. The shallowest production is found 2 mi north of Nowata at a depth of 435 ft in the Mulky (Excello Shale) (Fig. 15), and the deepest, 3 mi southeast of Bartlesville at 1,407 ft in the Riverton (Fig. 16).

Distribution of production reflects the irregularity of coal-bed deposition. The Rowe gas production is the most extensively developed, followed at a distant second by the Mulky (Excello Shale).

Economics of coal-bed drilling obviously controls the level of activity, but the fact that much of this area is held by production probably retards ventures into coal-bed methane. As long as Bartlesville production remains economical, reworking of the older wells into coal seams will be a slow process. At the end of 2001, cumulative production of coal gas for the 18-township study area was 7,400,000 MCF. The monthly production was 260,000 MCF. One hundred leases in the area are currently producing coal-bed gas.

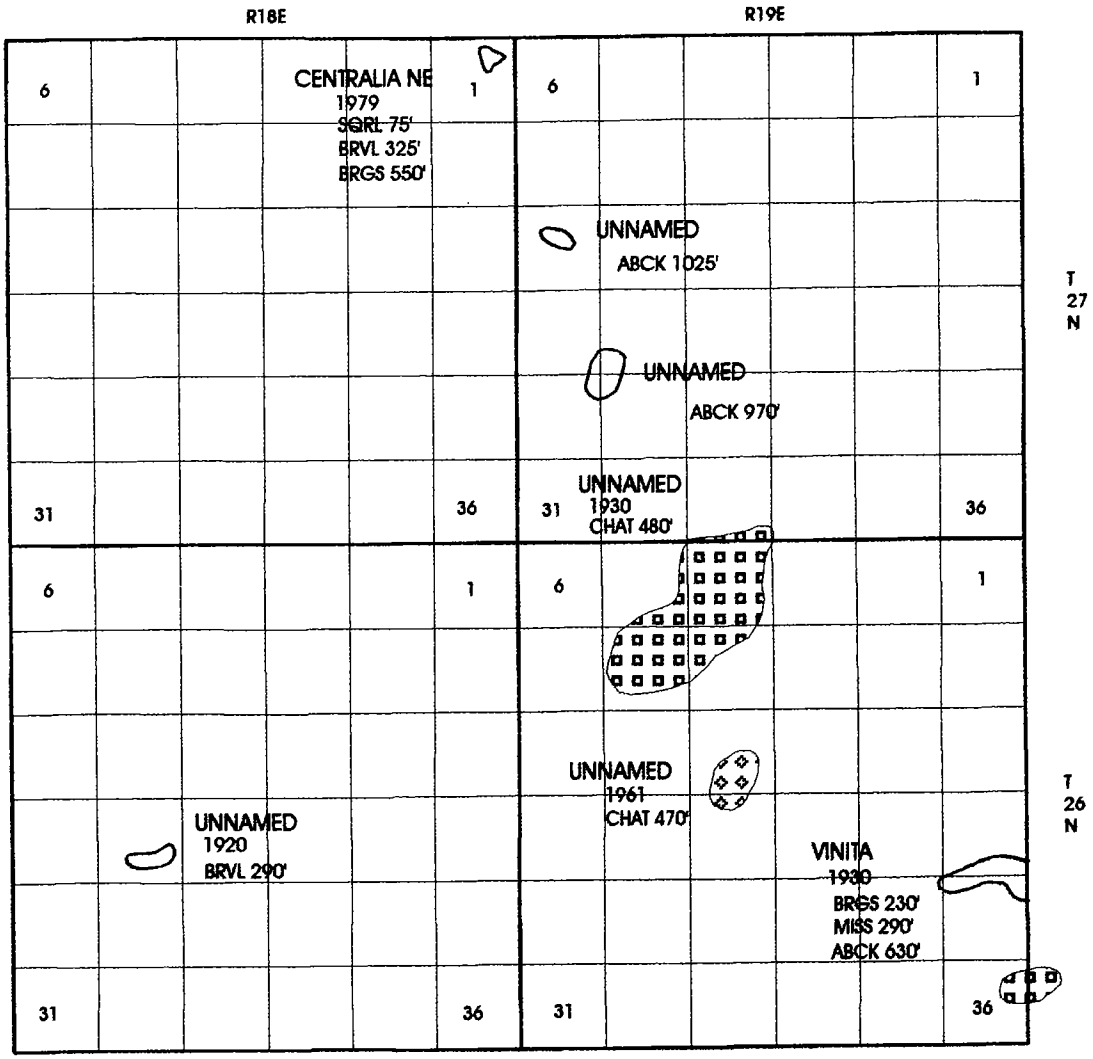

Figure 11. Oil and gas fields in western Craig County. *Abbreviations:* ABCK = Arbuckle; BRGS = Burgess; BRVL = Bartlesville; CHAT = Mississippian chat; MISS = Mississippian; SQRL = Squirrel.

EPILOGUE

This project lies across the Cooweescoowee Judicial District of the Cherokee Nation (Fig. 1). Adopted Shawnee and Delaware members of the Cherokee Nation abound here, as do members of the Shawnee Tribe. Congress reconstituted the Shawnee as a tribe on December 28, 2000, after they languished in the Cherokee Nation since 1869. Many Shawnees have relinquished their membership in the Cherokee Nation to return to their tribal heritage. Both the Shawnees and the Katy Railroad came to Indian Territory from Kansas at about the same time. The destiny of both has undergone vast changes in the last 133 years, but the resources of this "Cherokee" land remain and continue to provide significant amounts of energy resources to American industry.

SELECTED REFERENCES

Andrews, R. D., 1997, Fluvial-dominated deltaic (FDD) oil reservoirs in Oklahoma: the Red Fork play: Oklahoma Geological Survey Special Publication 97-1, 90 p.

Andrews, R. D.; and Northcutt, R. A., 1996, Fluvial-dominated deltaic (FDD) oil reservoirs in Oklahoma: the Prue and Skinner plays: Oklahoma Geological Survey Special Publication 96-2, 106 p.

Andrews, R. D.; Cardott, B. J.; and Storm, Taylor, 1998, The Hartshorne play in southeastern Oklahoma: Oklahoma Geological Survey Special Publication 98-7, 90 p.

Bloesch, Edward, 1928, Nowata and Craig Counties, *in* Oil and gas in Oklahoma: Oklahoma Geological Survey Bulletin 40-EE, p. 353–376.

Boyd, D. T., 2002, Oil and gas fields of Oklahoma: Oklahoma Geological Survey Geologic Map 36, scale 1:500,000.

Branson, C. C., 1968, The Cherokee Group, *in* Visher, G. S. (ed.), Geology of the Bluejacket-Bartlesville Sandstone, Oklahoma: Oklahoma City Geological Society Guidebook, p. 26–31.

Branson, C. C.; Huffman, G. G.; Strong, D. M.; and others, 1965, Geology and oil and gas resources of Craig County, Oklahoma: Oklahoma Geological Survey Bulletin 99, 109 p.

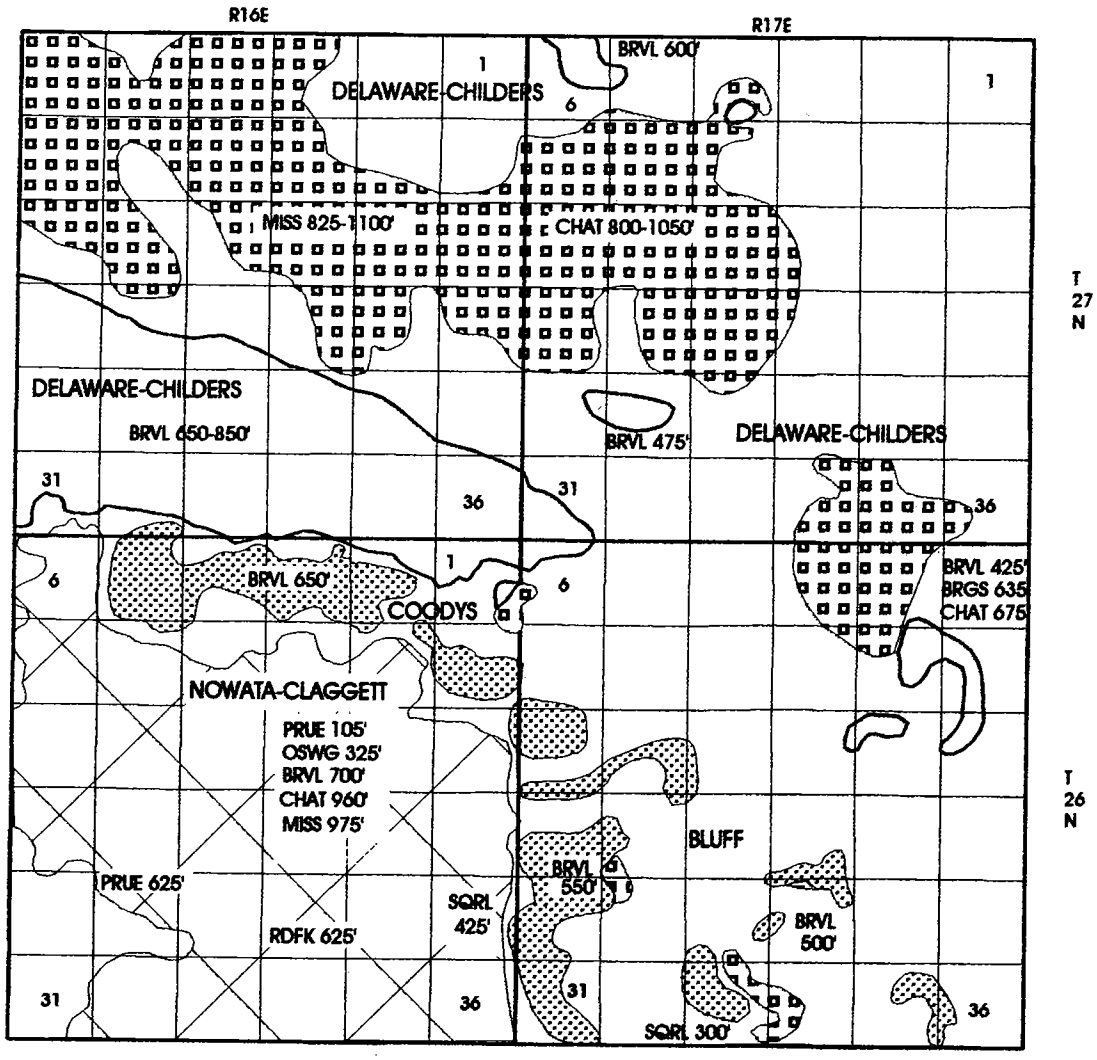

Figure 12. Oil and gas fields in eastern Nowata County. *Abbreviations:* ABCK = Arbuckle; BRGS = Burgess; BRVL = Bartlesville; CHAT = Mississippian chat; MISS = Mississippian; PRUE = Prue; RDFK = Red Fork; SQRL = Squirrel.

Campbell, O. B., 1969, Vinita, I.T.: Colorgraphics, Oklahoma City, 171 p., LCCN: 73-78788.

Craig County Heritage Association, 1981, The story of Craig County, its people and places: Curtis Media, Dallas, LCC: 85-115473.

Hemish, L. A., 1986, Coal geology of Craig County and eastern Nowata County, Oklahoma: Oklahoma Geological Survey Bulletin 140, 131 p.

_____ 1989a, Bluejacket (Bartlesville) Sandstone Member of the Boggy Formation (Pennsylvanian) in its type locality: Oklahoma Geology Notes, v. 49, p. 72–89.

_____ 1989b, Coal geology of Rogers County and western Mayes County, Oklahoma: Oklahoma Geological Survey Bulletin 144, 118 p.

_____ 2002, Surface to subsurface correlation of methane-producing coal beds, northeast Oklahoma shelf: Oklahoma Geological Survey Special Publication 2002-2, 22 p.

Johnson, K. S.; Northcutt, R. A.; Hinshaw, G. C.; and Hines, K. E., 2001, Geology and petroleum reservoirs in Pennsylvanian and Permian rocks of Oklahoma, *in* Johnson, K. S. (ed.), Pennsylvanian and Permian geology and in the southern Midcontinent, 1998 Symposium: Oklahoma Geological Survey Circular 104, p. 1–19.

Northcutt, R. A., 1995, Fluvial-dominated deltaic (FDD) oil reservoirs in Oklahoma: the Booch play: Oklahoma Geological Survey Special Publication 95-3, 67 p.

_____ 1997, Fluvial-dominated deltaic (FDD) oil reservoirs in Oklahoma: the Bartlesville play: Oklahoma Geological Survey Special Publication 97-6, 98 p.

Ohern, D. W., 1914, Geology of the Nowata and Vinita Quadrangles: Unpublished manuscript on file at the offices of the Oklahoma Geological Survey, p. 28–29.

Pritchard, Mary Ann, 1999, Annual Report: Oklahoma Department of Mines, Oklahoma City, 52 p.

Visher, G. S., 1968, History of the Bartlesville oil sand, *in* Visher, G. S. (ed.), Geology of the Bluejacket–Bartlesville Sandstone, Oklahoma: Oklahoma City Geological Society Guidebook.

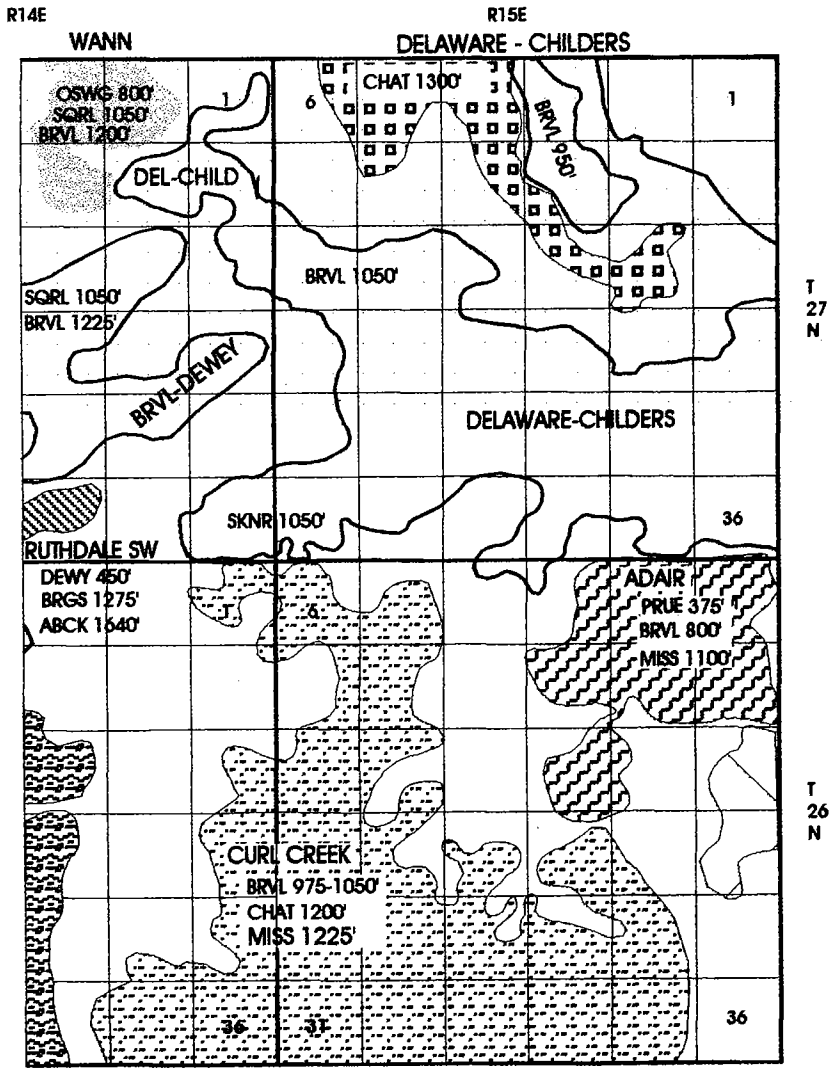

Figure 13. Oil and gas fields in western Nowata County. *Abbreviations:* ABCK = Arbuckle; BRGS = Burgess; BRVL = Bartlesville; CHAT = Mississippian chat; DEWY = Dewey; MISS = Mississippian; OSWG = Oswego; PRUE = Prue; RDFK = Red Fork; SKNR = Skinner; SQRL = Squirrel.

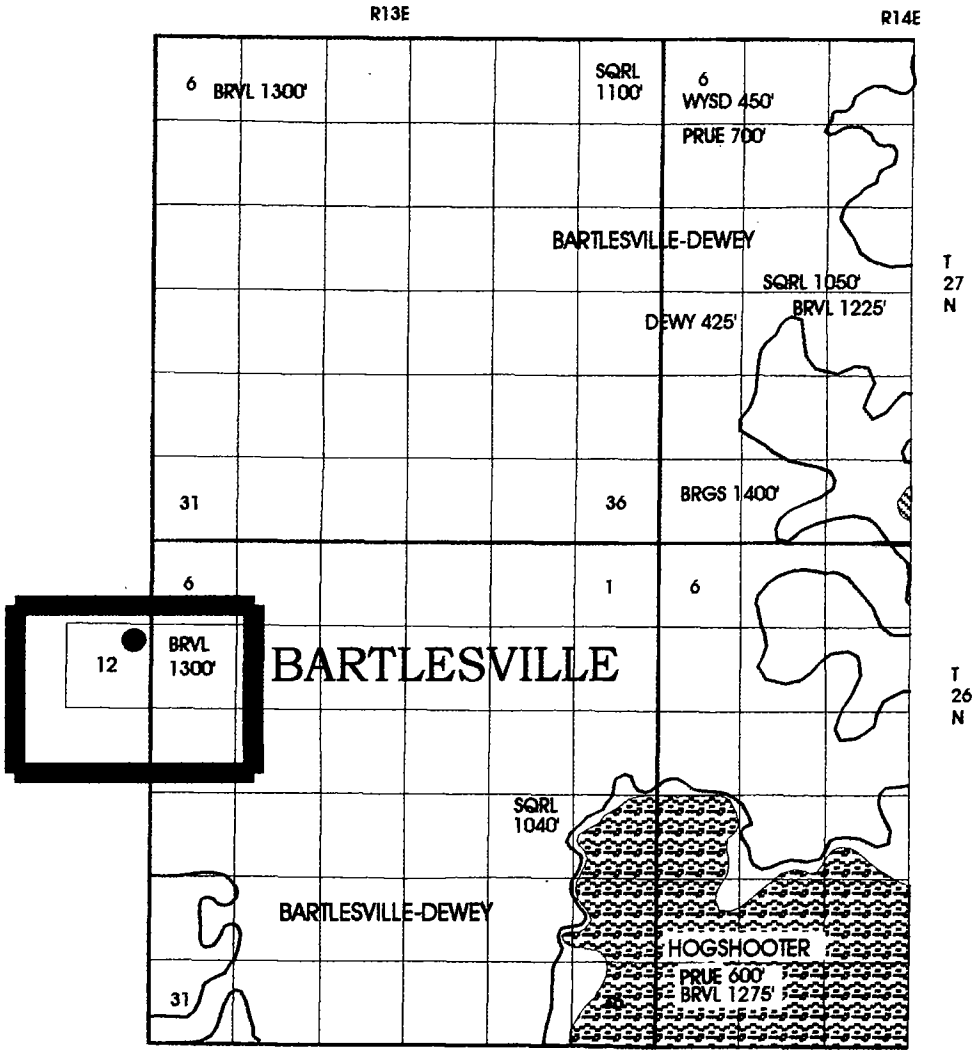

Figure 14. Oil and gas fields in Washington County. *Abbreviations:* ABCK = Arbuckle; BRGS = Burgess; BRVL = Bartlesville; CHAT = Mississippian chat; DEWY = Dewey; MISS = Mississippian; OSWG = Oswego; PRUE = Prue; RDFK = Red Fork; SKNR = Skinner; SQRL = Squirrel; WYSD = Wayside.

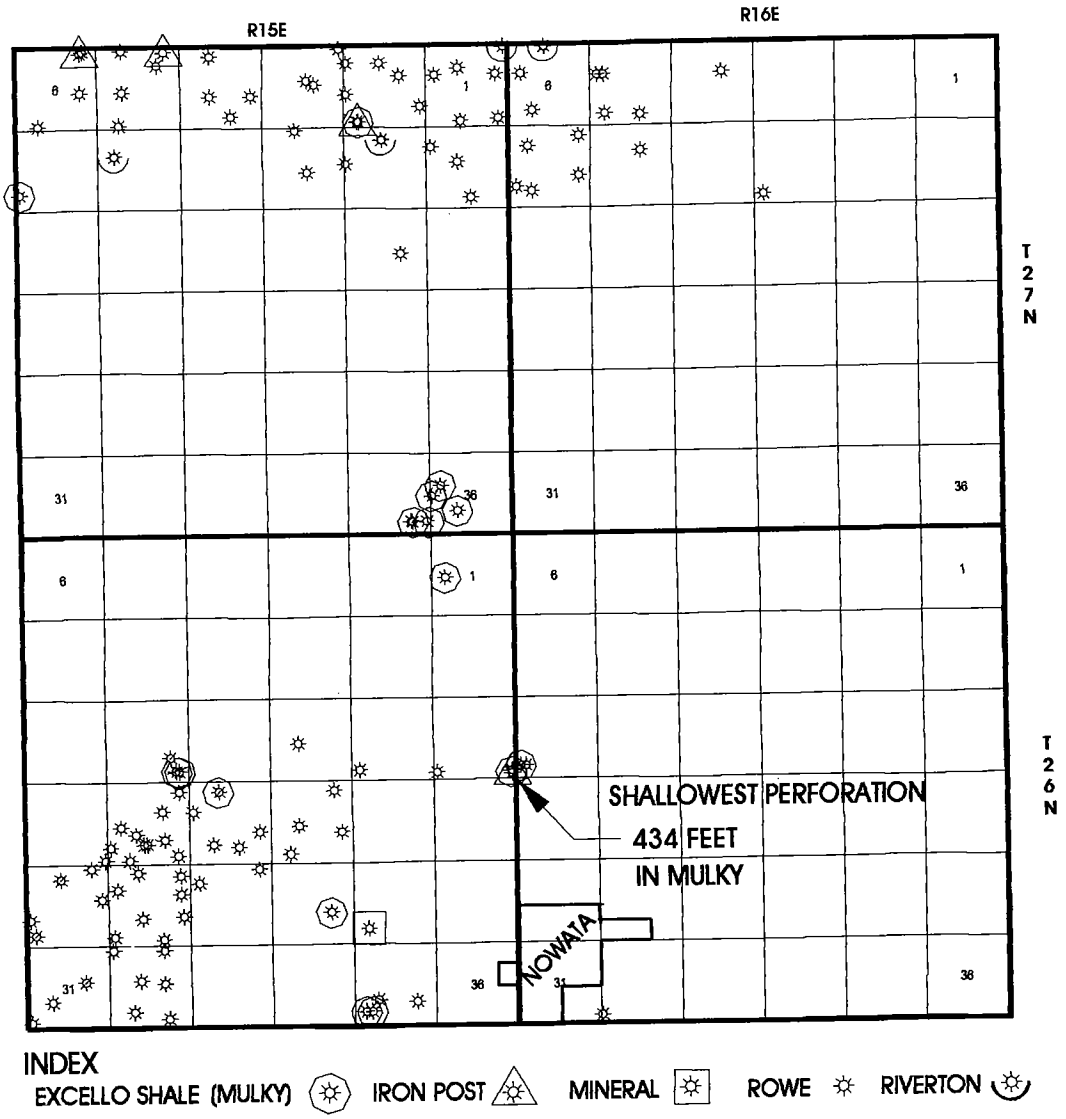

Figure 15. Coal-bed–methane wells in Nowata County.

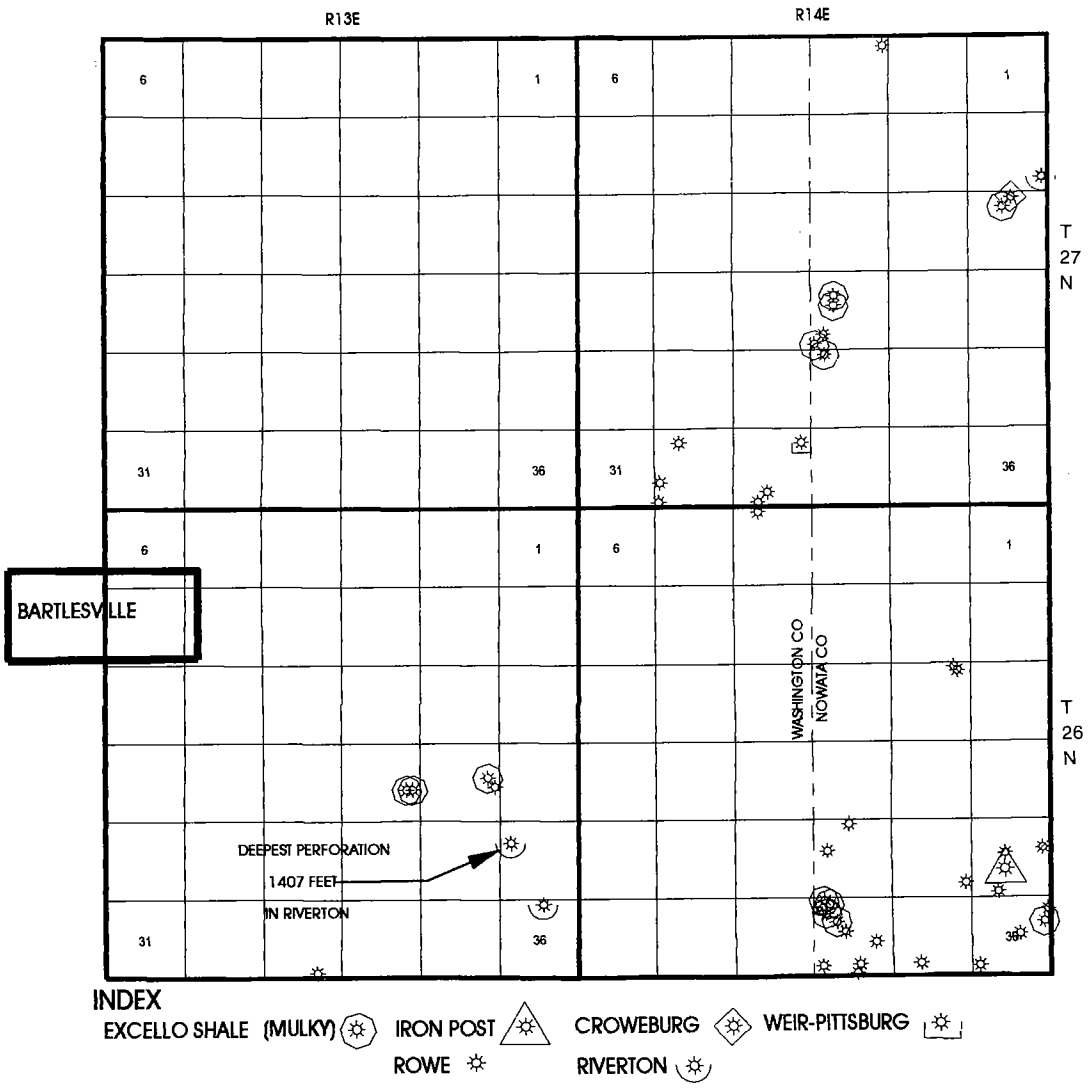

Figure 16. Coal-bed–methane wells in Washington County.

Opportunity Identification Using Integrated-Modeling Techniques—Cherokee Hydrocarbon Reservoirs

Bob Shelley
Halliburton
Houston, Texas

Bill Grieser
Halliburton
Oklahoma City, Oklahoma

ABSTRACT.—State-of-the art completion/stimulation well design uses results and interpretations from a variety of independent models. Information used in the design process is obtained by interpreting open-hole logs, reservoir simulators, and geologic models. During the completion/stimulation design process, numerous assumptions are made about formation mechanical properties, fracture mechanics, fluid loss, conductivity, perforating effects, and more. Is it appropriate to assume that such a fragmented approach to completion design will result in the optimum well completion?

This paper describes the incorporation of a holistic and pragmatic perspective to the completion design process. This high-level aspect is obtained with the use of artificial-neural–network (ANN) technology to simultaneously model the reservoir, geology, completion, and production results for a field of wells. This process, when applied to a granite-wash field in the Texas Panhandle and Redfork well completions in Roger Mills and Custer Counties, Oklahoma, identified significant opportunities for production and economic improvement.

ARTIFICIAL-NEURAL–NETWORK MODELING

Many technical papers have been written about the development of artificial-neural–network (ANN) models (McCulloch and Pitts, 1943; Nelson and Illingworth, 1991; McVey and Mohaghegh, 1994; Boomer, 1995; White and others, 1995; Gurney, 1996; Mohaghegh and others, 1996; Grieser and Stark, 1998; Shelley and others, 1998a,b). The ANN models contained in this article were developed by back-propagation–training a feed-forward neural network that allowed the ANN to predict production for a well using reservoir and completion information from wells in a field. In effect, an ANN model is developed without any previous knowledge that a relationship may exist among the input parameters that are used to train the network. These models are not restricted, confined, or limited by incorrect assumptions associated with theory-based methods. Important aspects of developing an ANN for an application include data preparation, determining the significance of variables, training a network, and evaluating network suitability. Figures 1 and 2 show a summary of the integrated-modeling process and important aspects of ANN-model development. The integrated-modeling process facilitated by ANN technology played a key role in justifying additional expenditures and/or using nonstandard procedures necessary to improve well economics for the case histories presented in this paper.

GRANITE-WASH COMPLETIONS

The following sections detail the background, model development, model application, case histories, and economic analysis for the granite-wash completions.

Background

An operator acquired the Red Deer Creek Field in 1995 in the Texas Panhandle with the intent to develop the granite-wash and shallower zones. The first two wells in the development program were drilled back-to-back in different areas of the field to define the limits of economic production. These wells were completed in a manner that conformed to the contemporary completion/stimulation school of thought. The first well performed below expectations because of unexpected water production, even though this well was structurally high to wells producing water-free gas. The second well resulted in an above-average producer for the field with a 60-day cumulative of 82 million standard cubic feet

Shelley, Bob; and Grieser, Bill, 2002, Opportunity identification using integrated-modeling techniques—Cherokee hydrocarbon reservoirs, *in* Boyd, D. T. (ed.), Finding and producing Cherokee reservoirs in the southern Midcontinent, 2002 symposium: Oklahoma Geological Survey Circular 108, p. 227–235.

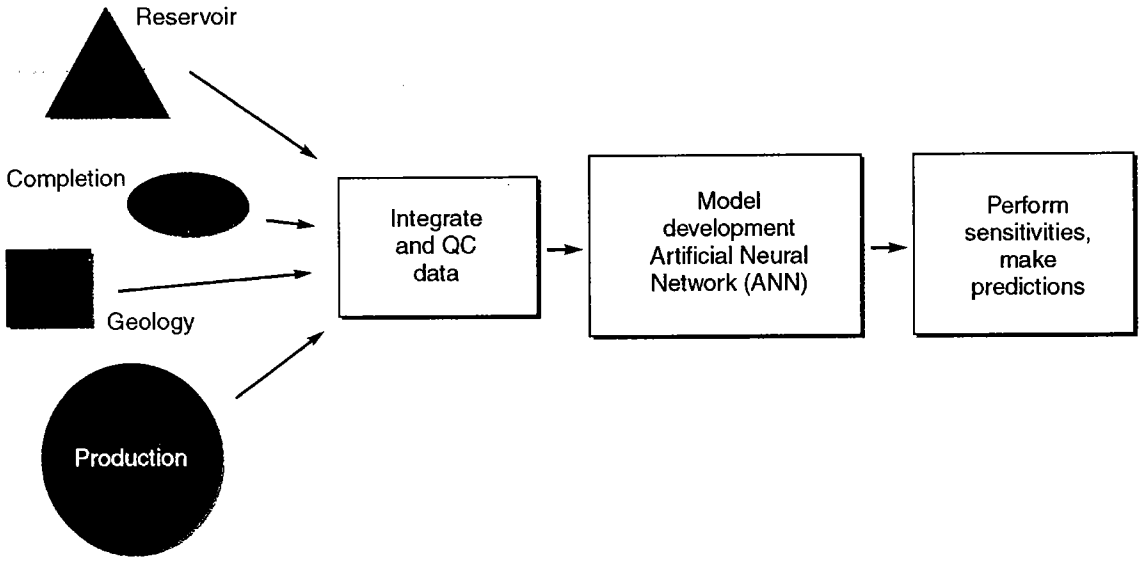

Figure 1. Integrated-modeling process. *Abbreviation*: QC = quality control.

(MMscf) versus a field average of 48 MMscf. The operator drilled and completed three more wells, which resulted in cumulative production values below the field average. The 60-day cumulative values were 34, 35, and 31 MMscf. Further field development could not be justified based on these lower-production levels. A study to determine if low production could be attributed to either reservoir quality or the completion method was attempted.

ANN Model Development

- **Evaluate data**
  - Visualization, statistics
- **Date preprocessing and enhancement**
  - Spatial sampling, clustering, fuzzy logic
  - Split data (train, test, validation)
- **Develop predictive model**
  - Back-propagation training
  - Selection of predctors
  - Selection of neural topology
- **Model evaluation**
  - Examination and comparisons
  - Engineering scrutiny

Figure 2. Important aspects of development of artificial-neural–network (ANN) model.

Conventional engineering approaches to reservoir and completion analysis were inconclusive. Some issues included confusion about how to interpret field data and uncertainty about reservoir pressure and permeability. Consequently, differentiation of native permeability from stimulation permeability proved difficult. In other words, the estimated effectiveness of a stimulation treatment is directly related to the interpreted values of permeability and reservoir pressure.

Granite-Wash–Model Development

A production-predictive ANN was developed from 15 granite-wash completions in the Red Deer Creek Field in the Texas Panhandle. A complete data set for all wells was required for development of the neural network. Nine wells were used to train the neural-network models and six wells were held back for test purposes. A 2-month cumulative production value was set as the outcome to train the ANN because limited-production data were available for recently completed wells. Engineering analysis indicated that the 2-month value was a good indicator of both stimulation effectiveness and long-term–production potential.

The ANN model predicts two outcomes simultaneously: (1) a 2-month cumulative gas equivalent and (2) a 2-month water cumulative. The ANN was a back-propagation network consisting of a single hidden layer with six multifunction neurons. The average absolute error between the predicted and actual production values was 7% for cumulative gas-equivalent production and 25% for cumulative water production.

Granite-Wash–Model Application

The source of the water production on recent completions could not be determined. A difference of opinion existed as to whether the pay zone contained movable

TABLE 1.—Completion–Method Evaluation

Application	ANN-enhanced completions	Conventional completions
Completion type	Cased, cemented, single-stage hydraulic-fracture stimulation	Cased, cemented, multiple-stage hydraulic-fracture stimulaiton
Perforations	Selectively perforate on permeability highs identified by MRIL*	Use a point-source perforating technique to encourage a dominant fracture
Treatment fluids	Less-viscous treatment fluids	High-viscosity, borate-crosslinked fluids
Proppant placement	200,000 to 370,000 lb at concentrations up to 3 or 4 lb/gal	500,000 to 600,000 lb at concentrations in excess of 6 lb/gal
Pump rate	Maximized pump rate to at least 45 bbl/min	Moderate pump rate of 30 to 40 bbl/min
Stimulation pressure response	Controlled design limits placed on pressure increase	Limited only by tubular burst
Breaker loadings	Maximized breaker loadings	Maximized early-time viscosity to minimize tortuosity

*MRIL = magnetic-resonance-imaigng logs.

water that would be produced with hydrocarbon production. An analysis by an independent consultant indicated a correlation between water production and pay-zone water saturation. However, magnetic-resonance–imaging logs (MRIL) indicated no movable water within the pay zones. ANN sensitivity studies for this field indicated that both structural position and completion method were responsible for water production and low gas production. The ANN model also supported the MRIL conclusion that the water production on recent completions was not coming from the pay zones. Table 1 contains a comparison of the operator's current completion objectives and new objectives defined by the ANN model.

The ANN model was used to evaluate the operator's completions. Figure 3 compares the actual, model-predicted, and potential gas production for these completions. The model predicted twice the amount of gas could have been produced with a different completion/fracture-stimulation philosophy.

Granite-Wash Case Histories

Log analysis of Well A showed that the A, B, and C zones had a total 207 ft of pay thickness with an average effective porosity of 5.4%. The sub-sea depth of the B zone was 7,205 ft, which was slightly above average for the field. The reservoir volume penetrated by the well bore was estimated at 6.31 hydrocarbon-ft, which was below average for the field. Based on these estimates, the Red Deer Creek ANN predicted an optimized completion could result in a potential 2-month cumulative gas-equivalent production of 97 MMscf. Although the magnitude of production falls below the production rate of the best well in the field, the production rate is well above the field average. The neural network also predicted that a completion procedure similar to the procedure used on the first four completions would result in a 2-month cumulative gas-equivalent production of only 45 MMscf with significant water.

Well evaluation was assisted by the use of rotary sidewall cores, MRIL, electrical micro-imaging, and full-wave sonic logging. The well results were incorporated into an integrated log to facilitate completion design. Three-dimensional (3-D) fracture-design simulators indicated the absence of barriers that could effectively contain vertical hydraulic-fracture growth, which posed a significant stimulation design constraint.

ANN analysis of the formation characteristics of Well A indicated that significant gas production could be achieved with a different perforating scheme, lower viscosity fluids, and lower propping-agent (proppant) concentrations and volume. The ANN analysis also supported the MRIL conclusion that the B zone had most of the permeability and that significant water would not be produced from the pay zone.

The fracture design was forced to conform to guidelines established by the Red Deer Creek ANN. This design was simulated using a 3-D fracture model. The service company completed the well using a limited-entry/biased perforating technique and stimulated with 360,000 lb of 20/40 sand placed with 145,000 g of linear/zirconate crosslinked carboxymethylhydroxypropyl guar energized with 30% CO_2. Onsite diagnostic procedures confirmed the validity of the 3-D–design assumptions. The actual 60-day cumulative gas-equivalent production value for this well was 90 MMscf.

Granite-Wash Economic Analysis

Figure 4 is a bubble map of the Red Deer Creek Field. Three well groups are shown: the existing wells in the field, the operator's first completions, and the ANN-enhanced completions. The radius of the bubble is proportional to the first 2-month cumulative gas pro-

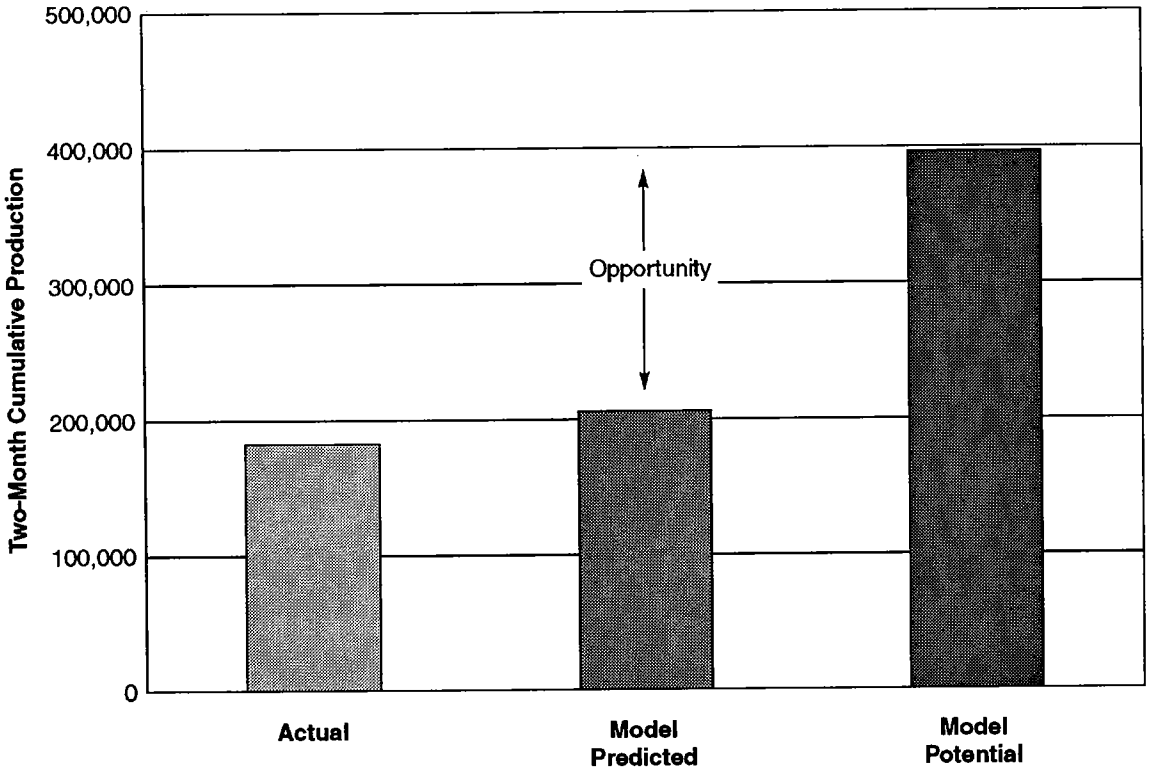

Figure 3. Granite-wash artificial-neural–network (ANN) completions for four recent completions. Cumulative production in thousand cubic feet (mcf).

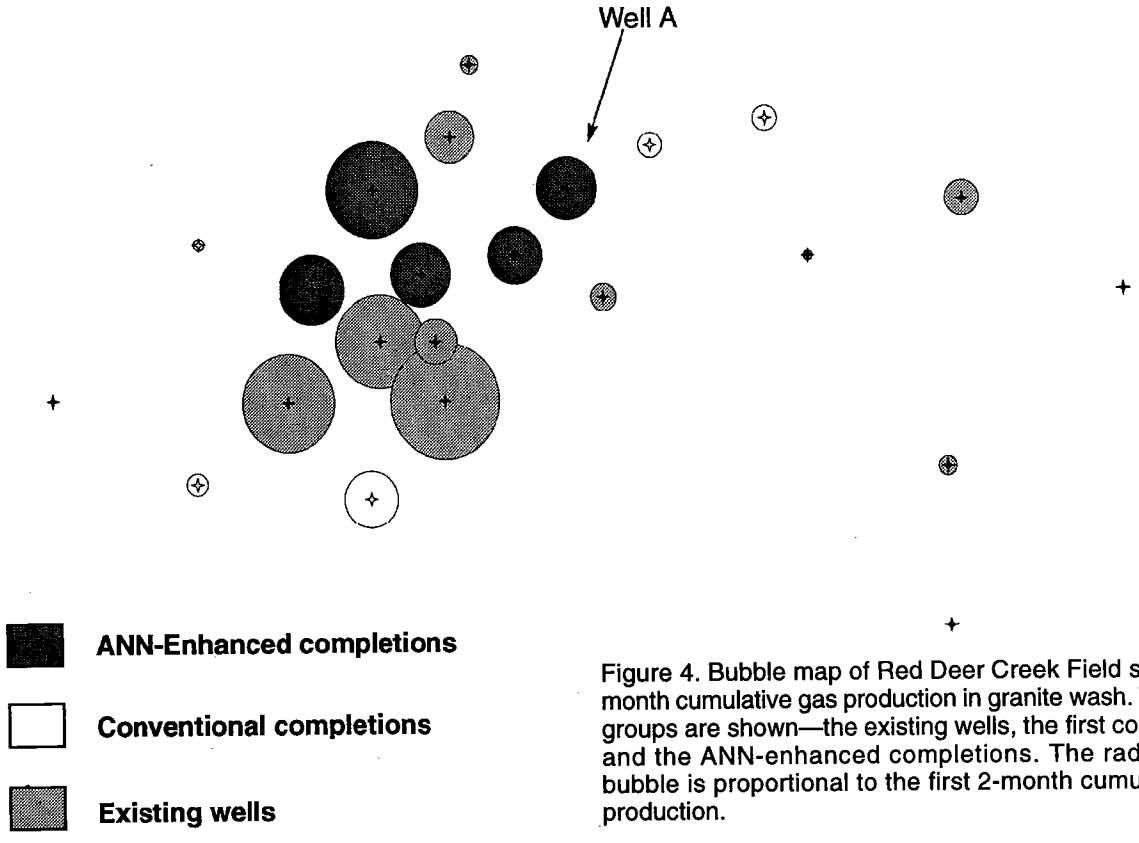

Figure 4. Bubble map of Red Deer Creek Field showing 2-month cumulative gas production in granite wash. Three well groups are shown—the existing wells, the first completions, and the ANN-enhanced completions. The radius of the bubble is proportional to the first 2-month cumulative gas production.

duction. The location of Well A is also shown. The average pay thickness for the two well groups was similar. The conventional completions were performed on better-quality reservoir rock, with an average effective porosity of 6.8% versus 5%. The conventional completions employed techniques intended to facilitate placement of large proppant volumes. These techniques included the use of high-viscosity borate fluids and point-source perforating techniques.

Figure 5 shows a comparison of the average net present values (NPV) based for the conventional and ANN-enhanced well groups. The NPV calculation is based upon actual production and includes all completion costs, including open-hole logging. Discount rate and net gas price were assumed to be 10% and $2.00, respectively. The ANN-enhanced completions cost less than the conventional completions. Although the open-hole logging for the ANN-enhanced completion cost approximately four times the amount for the conventional case, this increased cost was more than offset by cost savings on the stimulation treatment. During the first 24 months of production, the average ANN-enhanced completed well performed as the model predicted and generated an NPV of approximately $600,000 additional value than the average conventional completion. In addition, the incremental difference in NPV with time between the two well groups is on an increasing trend.

REDFORK COMPLETIONS

The following sections detail the background, model development, model application, case histories, and economic analysis for the Redfork completions.

Background

The Redfork Sandstone in Custer and Roger Mills Counties in Oklahoma consists of very fine to fine-grained sand deposited in a deltaic/marine complex. The formation consists of successions of shales and siltstones up to 700 ft thick, as well as thinly interbedded sandstones and shales. The channels of fine, sandy shales consist of feldspathic sandstones with interstitial clay materials. Differences in depositional environments cause reservoir characteristics to vary from area to area or even well to well. The depth of the Redfork ranges from 10,600 ft to as deep as 14,600 ft at its base. These extreme depths limit coring efforts, consequently limiting detailed depositional analysis. Engineers generally rely on well logs and mud-log data to determine sand thickness and reservoir quality.

Historically, much controversy has existed concerning Redfork well completions, and much has been written on the subject (Brunette, 1983; Harris and others, 1984; Cornell, 1991; Hentz, 1993; Shelley and Stacy, 1997). More recently, a statistical approach has concluded that stimulation/completion methods do have a

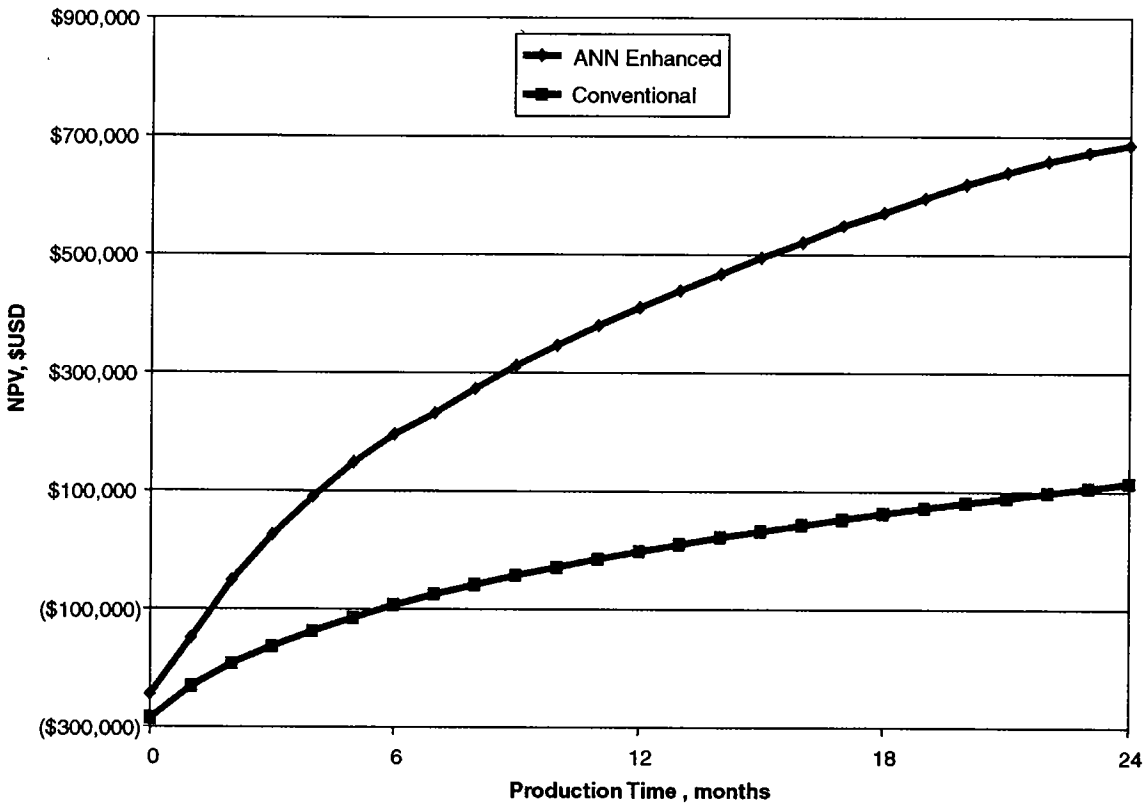

Figure 5. Comparison of average net-present-completion values (NPV), in U.S. dollars, versus production time, in months, for granite-wash formations. Negative values are enclosed in parentheses.

significant effect on production (Shelley and Stacy, 1997). Stimulation-fluid selection alone was estimated to have a two-fold impact on the one- and two-year cumulative production for the average Redfork well. General completion guidelines were determined. However, the absence of reservoir quantification complicated the application of these guidelines on an individual well basis.

Redfork Model Development

A database containing reservoir, geology, completion, production, and well information for 105 fracture-stimulated wells was assembled. For purposes of well-performance comparison, a 2-month and 12-month cumulative-production oil and gas volume associated with each well was determined and compiled into the database. An ANN model was selected to predict production for wells in the database. This model is a back-propagation neural network that uses one hidden layer with seven neurons. The network was trained to predict the cumulative gas equivalent production values. The prediction of cumulative gas-equivalent production values had an average absolute error of approximately 14%.

Redfork Model Application

In the real world, a comparison of actual production from two different completion types on the same well can never occur. Even in cases where restimulation is performed, the well and reservoir conditions have been altered by the initial completion. In other words, a restimulation cannot provide a useful comparative-production result. However, analysis of various stimulation/completion scenarios can be facilitated by the virtual reality of an ANN model. Using exactly the same well and reservoir attributes, the ANN model can be used to predict production for different completion/fracture types on the same well.

Considering the unresolved controversy concerning stimulation-fluid selection, the Redfork ANN model was used to evaluate the effect of stimulation-fluid selection on production results for wells in the database. Would it be important to know how non-foamed stimulated wells would perform if they had been foam fractured? Figure 6 summarizes the change in production assuming that all non-foamed, stimulated wells in the database were stimulated with foam-type fluids. The ANN model predicts that approximately 70% of the wells would perform better, whereas 30% would experience a production decrease. Approximately 20% of the wells would produce significantly better, an incremental production of more than a 400,000 thousand cubic feet (mcf). Further examination of the model indicates that reservoirs with relatively lower bottom-hole pressure, high porosity, and a high degree of lamination offer the greatest potential for production enhancement through the use of foam-stimulation fluids.

Redfork Case Histories

A new well located in Custer County was to be completed in the lower and upper Redfork intervals. This well was the sixth in a drilling program to be evaluated by the ANN model. Analysis of open-hole logs showed

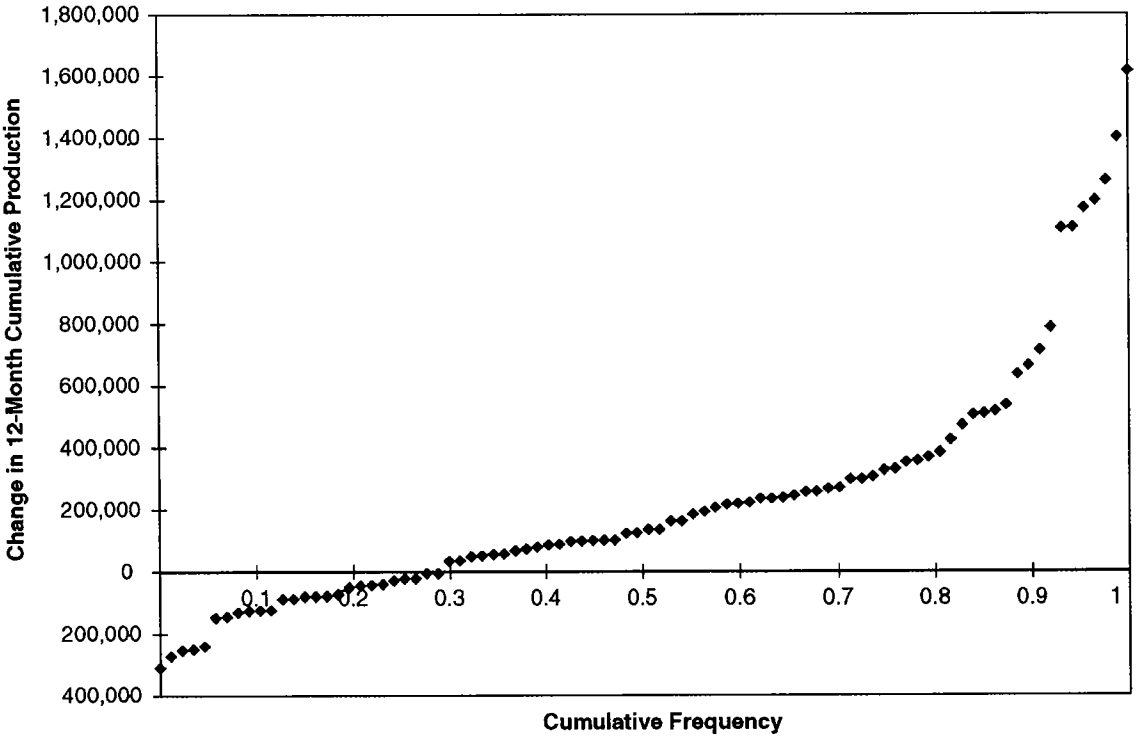

Figure 6. Plot of cumulative frequency versus change in 12-month cumulative production (in thousand cubic feet) for Redfork wells, showing what would have happened if the wells were foam-fractured. See text for explanation.

that the well had a gross interval thickness of 60 ft with about 28 ft capable of producing gas. Average porosity was estimated at 11.4%. The sand development in this well correlated to offset producers; however, significant depletion in the reservoirs penetrated by this well bore was not indicated. Reservoir pressure was estimated at 6,000 psi. Based on analysis and a comparison with other wells in this field, the operator anticipated this well to be one of the better producers in this field. The operator expected a productive potential of about 2 MMscfd for the first 60 days of production, or a 60-day cumulative of 120 MMscf.

Analysis using ANN indicated significant additional productive potential from this well. This analysis indicated that almost twice the productive potential could be achieved if a foamed stimulation fluid was used. This completion technology had not been used previously in this field because the associated costs were too high. However, in this case, the value of the incremental production predicted by the model was many times the cost of the foamed stimulation. Based on this analysis, a foamed stimulation treatment that conformed to the guidelines determined from the ANN model was proposed. A fracturing procedure was designed with a 3-D simulator, and the operator and service company came to a procedural and financial agreement on the well completion. The well was completed using a biased perforating scheme and stimulated with 96,500 lbs of resin-coated sand placed within 40,000 g of 65 q CO_2 foam. Onsite diagnostic procedures confirmed the validity of 3-D–design assumptions. The ANN model predicted a 2-month cumulative production from this well of 185 MMscf for the ANN-optimized completion. The actual 2-month cumulative production for the ANN-optimized completion is 173 MMscf. Figure 7 shows a comparison of the actual and model-predicted production for the well.

Redfork Well Economic Analysis

A production benchmark was needed for comparison to establish an economic value for the ANN-optimized completion on the new well. Because the operator's production expectations were reasonably close to the ANN-predicted production volume for the standard completion, the ANN-estimated production was used for the non-foam–completion case. The NPV for the two completion scenarios was calculated using completion costs including open-hole logging, a discount rate of 10%, and a $2.00/mcf net gas price. Figure 8 shows a comparison of NPV for the two completion scenarios on the new well. Although the foam stimulation cost $45,000 more than the standard completion, it has generated $265,000 increased value after 11 months of production.

The Redfork ANN model has been used to predict production and evaluate other new Redfork well completions. In general, the model has been a reasonably good predictor of a well's production potential. A comparison of model-predicted production versus actual production is shown in Figure 9. It has been our experience that the model is subject to prediction error

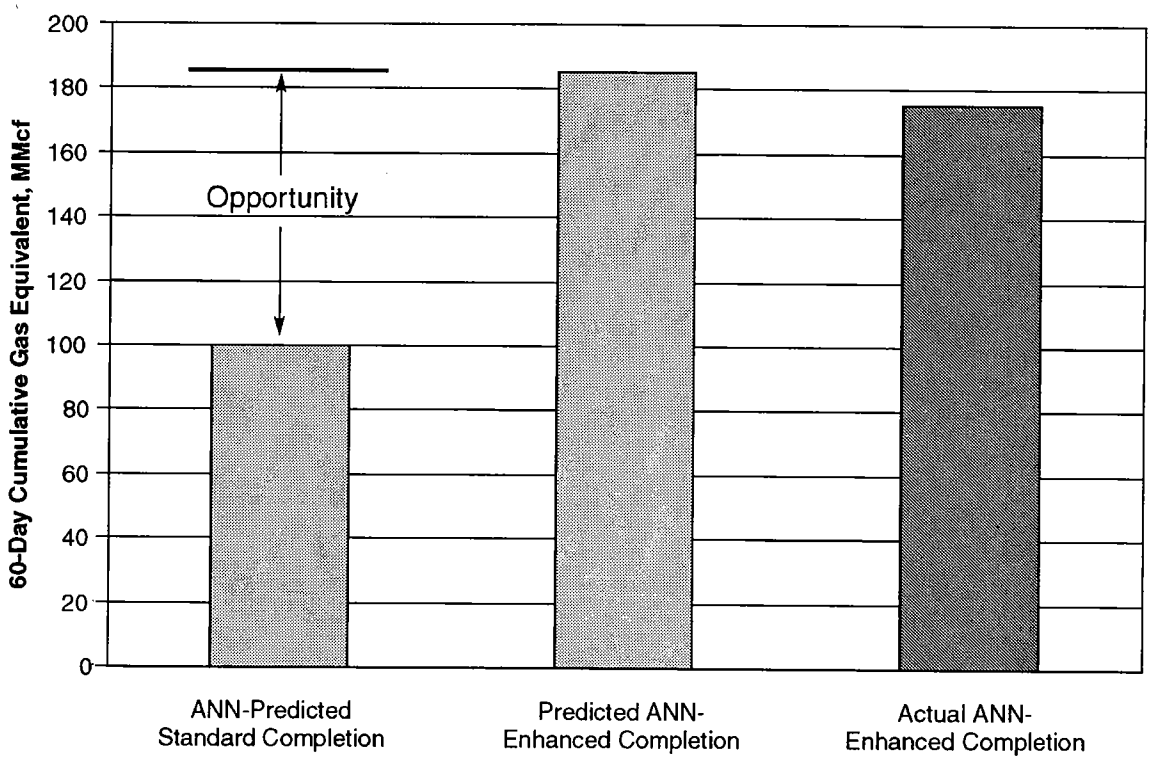

Figure 7. Comparison of artificial-neural–network- (ANN-) predicted standard completion, ANN-predicted enhanced completion, and ANN-enhanced actual completion in Redfork wells; 60-day completion values in million cubic feet.

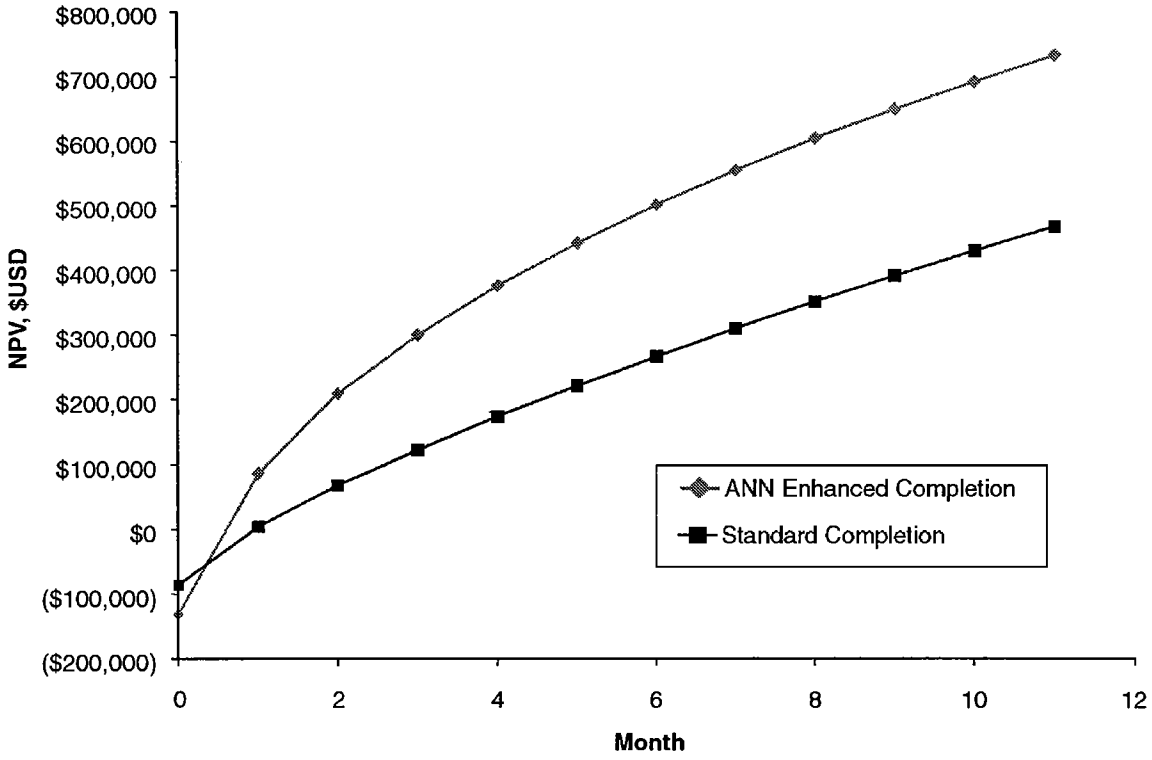

Figure 8. Comparison of net-present–completion values (NPV) for Redfork completions over a 12-month period.

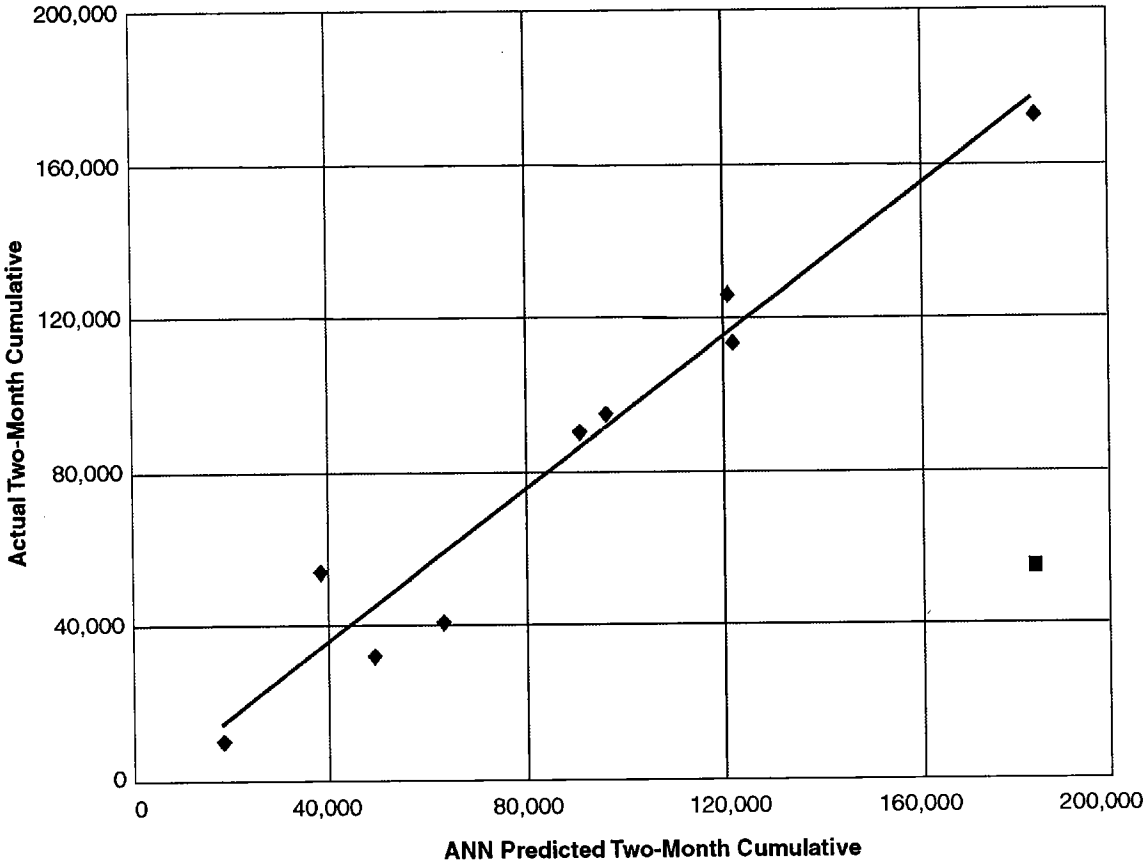

Figure 9. Plot of actual 2-month cumulative production in the Redfork, in thousand cubic feet, versus the 2-month cumulative production predicted by the artificial-neural–network- (ANN-) model.

when poor quality or inconsistent predictor values are used. The model is also subject to error due to extrapolation when making predictions from data outside the range of values from which the model was developed.

REFERENCES CITED

Boomer, R., 1995, Predicting production using a neural network: Society of Petroleum Engineers Paper 30202, presented at the Petroleum Computer Conference, Houston, Texas, June 11–14, 1995, 10 p.

Brunette, P. T., 1983, Stimulation techniques in the Redfork Formation in the Anadarko Basin: Society of Petroleum Engineers Paper 11574, presented at the Production Operations Symposium, Oklahoma City, Oklahoma, February 27–March 1, 1983, 10 p.

Cornell, F. L., 1991, Engineering improvements for Redfork fracturing: Journal of Petroleum Technology, v. 43, p. 132–137.

Grieser, B.; and Stark, J., 1998, Identifying high impact parameters in stimulation treatments using a trend empirical analysis model: Society of Petroleum Engineers Paper 39966, presented at the Rocky Mountain Regional Meeting/Low-Permeability Reservoir Symposium, Denver, Colorado, April 5–8, 1998, 10 p.

Gurney, K., 1996, Computers and symbols vs. nets and neurons; University College of London [UCL] Press Limited, London, England, 234 p.

Harris, P. C.; Haynes, R. J.; and Eggar, L. P., 1984, The use of CO_2-based fracturing fluids in the Redfork Formation in the Anadarko Basin, Oklahoma: Journal of Petroleum Technology, v. 36, p. 1003–1017.

Hentz, T. F., 1993, Geologic challenges and opportunities of the Cherokee Group play (Pennsylvanian), Anadarko Basin, Oklahoma: Gas Research Institute Topical Report, Contract No. 5082-211-0708, 38 p.

McCulloch, W. S.; and Pitts, W., 1943, A logical calculus of the ideas immanent in nervous activity: Bulletin of Mathematical Biophysics, v. 5, p. 115–133.

McVey, D.; and Mohaghegh, S., 1994, Identification of parameters influencing the response of gas storage wells to hydraulic fracturing with the aid of a neural network: Society of Petroleum Engineers Paper 29159, presented at the Eastern Regional Conference and Exhibition, Charleston, West Virginia, November 8–10, 1994, 4 p.

Mohaghegh, S.; Balan, B.; Ameri, S.; and McVey, D., 1996, A hybrid, neuro-genetic approach to hydraulic fracture treatment design and optimization: Society of Petroleum Engineers Paper 36602, presented at the Annual Technical Conference and Exhibition, Denver, Colorado, October 6–9, 1996, 6 p.

Nelson, M. M.; and Illingworth, W. T., 1991, A practical guide to neural nets: Addison-Wesley Publishing Company, Inc., Reading, Massachusetts, p. 352 p.

Shelley, R. F.; and Stacy, A., 1997, Production data analysis aids fracture treatment design/Cherokee Group in western Oklahoma: Society of Petroleum Engineers Paper 37433, presented at the Production Operations Symposium, Oklahoma City, Oklahoma, March 9–12, 1997, 14 p.

Shelley, R.; Massengill, D. R.; Scheuerman, P.; McRill, P. E.; and Hamilton, R., 1998a, Granite wash completion optimization with the aid of artificial neural networks: Society of Petroleum Engineers Paper 39814, presented at the Gas Technology Symposium, Calgary, Alberta, Canada, March 15–18, 1998, 7 p.

Shelley, R.; Stephenson, S.; Haley, W.; and Craig, E., 1998b, Redfork completion analysis with the aid of artificial neural networks: Society of Petroleum Engineers Paper 39963, presented at the Rocky Mountain Regional Meeting/Low-Permeability Reservoir Symposium, Denver, Colorado, April 5–8, 1998, 8 p.

White, A. C.; Molnar, D.; Aminian, K.; and Mohaghegh, S., 1995, The application of ANN for zone identification in a complex reservoir: Society of Petroleum Engineers Paper 30977, presented at the Eastern Regional Conference and Exhibition, Morgantown, West Virginia, September 17–21, 1995, 6 p.

The Red Fork Sandstone: An Overview of Fluvio-Deltaic Platform and Shelf Reservoirs

Zuhair Al-Shaieb and Jim Puckette
Oklahoma State University
Stillwater, Oklahoma

ABSTRACT.—The Red Fork Sandstone (Middle Pennsylvanian, Desmoinesian) is one of the primary oil- and gas-producing rock units in Oklahoma. Red Fork sediments were distributed by a large fluvial-deltaic and submarine dispersal system. Most sediment was transported southward from the northern Midcontinent across the Cherokee Platform toward the evolving Anadarko and Arkoma depocenters.

Red Fork sands were deposited as channel fills within alluvial and deltaic settings on the Cherokee Platform and northern shelf of the Anadarko Basin. Some Red Fork sandstone trends fill valleys that incised older deltaic and marine units. Depositional setting profoundly influenced sandstone geometry and distribution. Platform valleys are less than 1 mi to several miles wide and contain multiple episodes of filling. Sandstone thickness commonly exceeds 100 ft but can vary greatly within the valley. Individual sandstone trends can be difficult to isolate on wireline logs, and reservoir heterogeneity is a major concern. Trapping is controlled by structural attitude and facies. Traps form where: (1) sandstone trends cross structural noses and anticlinal folds; (2) valley trends are subparallel to strike, and reservoir facies (channel-fill sandstone) terminate updip against shaley rock; and (3) differential sandstone thickness creates "pseudo-highs." Trapping is commonly complicated by active migration of oil along major valley trends. As a result, separation of oil and water phases is incomplete, and thick sandstone intervals are commonly composed of multiple layers with differing oil/gas saturations. These reservoirs are not amenable to conventional completion and production practices but can be produced using high-water–volume production techniques.

The Red Fork Sandstone on the northern shelf of the Anadarko Basin is characteristic of a deltaic distributary system. Channel fill is located along linear trends (typically less than 2 mi wide) that show evidence of southerly bifurcation and anastamosing distribution patterns. Sandstone thickness in these trends rarely exceeds 60 ft. Trapping is almost entirely stratigraphic, and reservoirs produce little water. Locating porous sandstone within channel trends is the most critical factor in establishing production.

Detrital composition is an essential element in reservoir evolution. Metastable grains, including schistose metamorphic rock fragments and plagioclase feldspar, are common to all Cherokee sandstones. Porosity in Red Fork reservoirs is overwhelmingly secondary and a result of the dissolution of these metastable detrital grains and matrix.

Al-Shaieb, Zuhair; and Puckette, Jim, 2002, The Red Fork Sandstone: an overview of fluvio-deltaic platform and shelf reservoirs, *in* Boyd, D. T. (ed.), Finding and producing Cherokee reservoirs in the southern Midcontinent, 2002 symposium: Oklahoma Geological Survey Circular 108, p. 237.

Preliminary Conodont Biostratigraphy of the Cherokee Group (Lower Desmoinesian) of Oklahoma and Southern Kansas

D. R. Boardman II and T. R. Marshall
Oklahoma State University
Stillwater, Oklahoma

ABSTRACT.—The Desmoinesian (Upper Moscovian) of the North American Midcontinent arguably represents the most complete and fossiliferous stratigraphic section by which to characterize this time interval in the world. Conodonts provide the best potential for intrabasinal as well as interbasinal correlations due to the inherent endemism of Carboniferous fusulinaceans and the facies restrictions of ammonoids. Prior to this study, only the top of the Cherokee Group and Marmaton Group has been collected systematically for conodonts. Analysis presented herein reveal that 16 conodont-bearing depositional sequences are present within the Cherokee Group, 13 of which are reported for the first time.

The Krebs Group consists of the Hartshorne, McAlester, Savannah, and Boggy Formations, in ascending order. Conodonts have been recovered from two levels within the basal McAlester McCurtain Shale and unnamed shale above thin limestones above the Tamaha coal bed in the upper McAlester. Four conodont faunas have been recovered from the Savanna Formation including the Spaniard Limestone, Sam Creek Limestone, the shale above the Doneley Limestone and from shale above the Drywood coal bed. The Boggy Formation contains two conodont-bearing units the Inola Limestone and associated black shale along with black shale above the Wainwright coal bed.

The Cabaniss Group contains the Senora Formation. Conodonts have been recovered from eight horizons from the Senora Formation. The lowest interval within the Senora that yields conodonts is the Tiawah Limestone and black shales stratigraphically below as well as above the Tiawah. Conodonts are also present in the carbonate and dark shales above the Mineral, Fleming, Croweberg, and Bevier coal beds as well as in the Breezy Hill Limestone and Excello Shale.

Based on preliminary evaluation a number of conodont zones are represented by these new findings. Current taxonomic work is under way in order to establish a taxonomic framework for a refined *Idiognathodus* and *Neognathodus*-based zonation.

Boardman, D. R. II; and Marshall, T. R., 2002, Preliminary conodont biostratigraphy of the Cherokee Group (Lower Desmoinesian) of Oklahoma and southern Kansas, *in* Boyd, D. T. (ed.), Finding and producing Cherokee reservoirs in the southern Midcontinent, 2002 symposium: Oklahoma Geological Survey Circular 108, p. 238.

Oklahoma Oil and Gas: Three Moments in Time

Dan T. Boyd
Oklahoma Geological Survey
Norman, Oklahoma

ABSTRACT.—The evolution of Oklahoma's oil and gas industry can be traced with remarkable clarity utilizing field maps constructed by the U.S. Geological Survey (Richardson, 1939) and the Oklahoma Geological Survey (Burchfield, 1985; Boyd, 2002). These maps reflect both technological advances that permitted ever-deeper exploration and changes in the nation's hydrocarbon appetite. This demand has progressed from being dominated by oil, to oil and gas, and finally to oil and conventional gas augmented by coalbed methane.

The first exploration success in Oklahoma, the Bartlesville-Dewey Field, came in 1897 and was also the State's largest oil discovery. The time frame between 1897 and 1939 shows a dominance of relatively shallow oil production from the Cherokee Platform, the Seminole Structure, and the Ardmore-Marietta Basins. This period saw the discovery of 20 of the 26 major oil fields in the State (recovery of >100 million barrels of oil through January 2000) and surprisingly also four of the 10 major gas fields (recovery of >1 trillion cubic feet of gas through January 2000). Although oil was generally produced as rapidly as possible during this time, gas was not the primary objective and was still mainly seen as a drilling hazard.

This was not the situation during the period from 1939 through 1985. Although continued exploration identified the remaining major oil fields, it was during this time that gas production became a key component of the State's energy mix. More important than the fact that all of the remaining major gas fields were found during this period, a massive program of gas (and oil) exploration and field extension largely defined the major productive regions that are known today. Chief among these were wide areas within the Arkoma Basin and the Anadarko Basin and Shelf.

The last period, from 1985 to the present, has been dominated by oil and gas infill drilling and field extension that has taken place in virtually all regions of the State. Although many new fields were identified during this time, these were generally small and commonly have been combined with the now interlocking mega-fields that we know today. Of note is the advent of coalbed methane exploration and production on the Cherokee Platform and Arkoma Basin. This activity began slowly in 1988 and gained momentum through the 1990s. Because it is treated as distinct from conventional gas, it has accounted for the bulk of new field discoveries in Oklahoma since 1997.

References Cited

Boyd, D. T., 2002, Map of Oklahoma oil and gas fields (distinguished by GOR and conventional gas vs. coalbed methane): Oklahoma Geological Survey Geologic Map 36, scale 1:500,000.

Burchfield, M. R., 1985, Map of Oklahoma oil and gas fields: Oklahoma Geological Survey Geologic Map 28, scale 1:500,000.

Richardson, G. B., 1939, Oil and gas fields of the State of Oklahoma: U.S. Geological Survey, scale 1: 500,000.

Boyd, D. T., 2002, Oklahoma oil and gas: three moments in time, *in* Boyd, D. T. (ed.), Finding and producing Cherokee reservoirs in the southern Midcontinent, 2002 symposium: Oklahoma Geological Survey Circular 108, p. 239.

Red Fork Sandstone of Oklahoma: Depositional History, Sequence Stratigraphy, and Reservoir Distribution

Richard D. Fritz
American Association of Petroleum Geologists
Tulsa, Oklahoma

Edward A. Beaumont
Consultant
Tulsa, Oklahoma

ABSTRACT.—The Middle Pennsylvanian Red Fork Sandstone formed as a result of progradation across eastern Kansas and most of Oklahoma. It is one of several transgressive-regressive sequences (cyclothems) developed within the Desmoinesian "Cherokee" Group. Sea-level changes together with varying subsidence were dominant factors controlling the general stratigraphic (correlative) characteristics of the Red Fork interval. Progradation was episodic with sand deposition in the more active part of the basin during lower sea-level stands and valley-fill deposition in the more stable areas during sea-level rises.

The Red Fork was correlated, subdivided, and mapped using data from more than 27,000 wells. Maps of Red Fork sand trends reveal a fluvial-deltaic complex covering most of Oklahoma. The Red Fork consists primarily of undifferentiated alluvial-valley and plain (fluvial) bodies in the northernmost part of Oklahoma, fluvial-deltaic bodies in most of the remaining parts of shelf area, and off-shelf, submarine-fan complexes and slope–basinal-floor deposits within the deeper part of the Anadarko Basin. The basinal facies can also be interpreted as low-stand deltaic deposits.

The Red Fork appears to represent one Vail-type third-order sequence. It can be divided into at least three parasequences that, for the purpose of this study, are called upper, middle and lower. Each parasequence represents a transgressive-regressive episode commonly separated by thin regional limestones or shale markers. Correlation of these parasequences is relatively easy from the lower shelf to the basin and more difficult on the upper shelf.

The provenance for the Red Fork was most likely an extensive drainage system to the north and northeast of Oklahoma. This drainage system probably extended as far as the Canadian Shield or even Greenland and appears to be subparallel to the Midcontinent Rift. A secondary source for the Red Fork was the Wichita–Amarillo Mountains in the south.

Much of the oil and gas has been trapped in stratigraphic traps, and a significant amount of oil is in channel sandstones and trends at high angles to the structural grain. The Cherokita–Wakita Trend, South Thomas Field, East Clinton Field, and Strong City Field represent excellent examples of facies and reservoir development controlled by facies distribution and related diagenesis.

Fritz, R. D.; and Beaumont, E. A., 2002, Red Fork Sandstone of Oklahoma: depositional history, sequence stratigraphy, and reservoir distribution, *in* Boyd, D. T. (ed.), Finding and producing Cherokee reservoirs in the southern Midcontinent, 2002 symposium: Oklahoma Geological Survey Circular 108, p. 240.

Subsurface Correlation of Methane-Producing Coal Beds, Northeast Oklahoma Shelf

LeRoy A. Hemish
Oklahoma Geological Survey
Norman, Oklahoma

ABSTRACT.—Coalbed-methane production has been reported by operators from ten named Pennsylvanian (Desmoinesian) coals in the northeast Oklahoma shelf area. They are (from oldest to youngest): the Riverton (McAlester Formation); Rowe, Drywood (Savanna Formation); Bluejacket (Boggy Formation); Weir-Pittsburg, Croweburg, Bevier, Iron Post, Mulky (Senora Formation); and Dawson (Holdenville Formation). Most of the production is from wells located in Nowata, Osage, Rogers, Tulsa, and Washington Counties.

A subsurface stratigraphic framework, based primarily on gamma, density, and neutron well logs and core-hole logs, is established to assist operators in correctly identifying methane-producing coal beds. About 65 high-quality well logs (from the more than 200 examined) were used to construct six cross sections. Three east–west cross sections are oriented approximately parallel to present-day dip and extend about 60 mi west from the coal outcrop belt across T. 22, 25, and 28 N. Three north–south cross sections are oriented approximately parallel to present-day strike and extend about 50 mi from the Kansas–Oklahoma state line south to T. 20 N. Persistent markers such as the Oologah Limestone (Big lime), the Fort Scott Limestone (Oswego lime), the Verdigris Limestone, the Tiawah Limestone (Pink lime), and others, were used as reference strata to correlate the coal beds. Two composite type logs are designated in the methane-producing shelf area—one in the northern part, and one in the southern part. They show the important marker beds (limestones, black shales, and persistent sandstones), as well as the stratigraphic positions of named coals.

Hemish, L. A., 2002, Subsurface correlation of methane-producing coal beds, northeast Oklahoma shelf, *in* Boyd, D. T. (ed.), Finding and producing Cherokee reservoirs in the southern Midcontinent, 2002 symposium: Oklahoma Geological Survey Circular 108, p. 241.

Middle Desmoinesian Subsurface Sequence Stratigraphy, Creek and Okfuskee Counties and Adjacent Areas, Oklahoma

Dennis R. Kerr, Yosi Hirosiadi, and Dwi K. Hustiara
University of Tulsa
Tulsa, Oklahoma

ABSTRACT.—Sequence stratigraphic analysis was conducted using logs from 37 wells arrayed in one long northwest–southeast and five southeast–northwest cross sections. The lithostratigraphic interval encompasses the Krebs and Cabaniss Groups. Eight stratigraphic sequences were correlated across the study area.

Condensed—or, more appropriately, compressed—sections are placed at thin anomalously low resistivity and high gamma-ray–log responses. These sections are the most lateral continuous sequence stratigraphic elements.

Carbonate units are associated with condensed sections. They are included in either the transgressive systems tract and/or the highstand systems tract depending on their position relative to the condensed section and parasequence stacking patterns.

Incised-valley fills are readily recognizable at the base of the Bartlesville and Booch sandstones. In these cases, thick, blocky-profile sandstones with limited lateral continuity rest above thinner sandstones and mudstone successions with greater lateral continuity. Less obvious incised-valley fills have been identified with the Red Oak and upper and lower Skinner intervals. Other sequence boundaries are identified by the termination parasequences and/or vertical change in parasequence stacking patterns. Lowstand, transgressive and to a lesser extend highstand systems tracts constitute the incised-valley fills.

Kerr, D. R.; Hirosiadi, Yosi; and Hustiara, D. R., 2002, Middle Desmoinesian subsurface sequence stratigraphy, Creek and Okfuskee Counties and adjacent areas, Oklahoma, *in* Boyd, D. T. (ed.), Finding and producing Cherokee reservoirs in the southern Midcontinent, 2002 symposium: Oklahoma Geological Survey Circular 108, p. 242.

Depositional Analysis of the Lower Skinner Sandstone on "Cherokee" Platform, Payne County, Oklahoma

James Reece Kinser
Kansas State University
Manhattan, Kansas

ABSTRACT.—Middle Pennsylvanian, Desmoinesian sandstones are well known for their hydrocarbon production in the Midcontinent of the United States. The lower Skinner sandstone is an oil- and gas-producing member of the Senora Formation ("Cherokee" Group), in north-central Oklahoma. This study examines the sandstone, as well as the mud-rich facies of the lower Skinner sandstone sequence. Although the sandstone sequences are of primary interest because of their hydrocarbon production, the mud-rich sequences function as seals of hydrocarbon reservoirs and inhibitors to permeability. In addition, the mud-rich sequences are potentially more sensitive indica-tors of depositional environment than are the sandstones.

The lower Skinner sandstone has been interpreted commonly as a fluvial-dominated deltaic reservoir sand. However, other researchers assert that some facies commonly interpreted as deltaic or prodeltaic in the Midcontinent should be reinterpreted as fluvial-estuarine sequences. Furthermore, they also indicate that estuary-mouth marine sands potentially have been misinterpreted as offshore bars or barrier islands. Thus, much of the older interpretations as fluvial-deltaic, should be re-examined with estuarine models in mind.

Kinser, J. R., 2002, Depositional analysis of the lower Skinner sandstone on "Cherokee" platform, Payne County, Oklahoma, *in* Boyd, D. T. (ed.), Finding and producing Cherokee reservoirs in the southern Midcontinent, 2002 symposium: Oklahoma Geological Survey Circular 108, p. 243.

Outcrop-Based Cyclic Stratigraphy of the Cherokee Group

T. R. Marshall and D. R. Boardman II
Oklahoma State University
Stillwater, Oklahoma

ABSTRACT.—There has been a remarkable lack of sequence stratigraphic studies on the strata of the lower Desmoinesian Cherokee Group despite the fact that Cherokee reservoirs account for a large percentage of hydrocarbons produced within the North American Midcontinent. Detailed basinwide correlation has not been completed for any of the productive depositional sequences within the Cherokee Group. This study is a first attempt to identify outcrop marine-nonmarine cycles (fourth-order depositional sequences) that can be the cornerstone for more detailed sequence stratigraphic studies that will integrate both surface and subsurface data.

Cherokee marine–nonmarine cycles consist of nonmarine deposits consisting of fluvial channel, incised valley fills, and paleosols that are typically overlain by a regional coal bed, followed by marine shale or limestone, a black fissile shale and typically with deltaic highstand deposits in the case of a major cycle. Intermediate and minor cycles are similar but lack black, fissile shales and have weakly developed marine bands.

The Krebs Subgroup (Cherokee Group) comprises the Hartshorne, McAlester, Savanna, and Boggy Formations. The stratigraphically lowest major marine cycle within the Cherokee Group occurs with the upper Hartshorne coal that is overlain by black, fissile, phosphatic shale within the basal McCurtain Shale that represents a marine condensed section of the cycle. Overall, the McAlester contains three major marine–nonmarine cycles as well as three small to intermediate cycles. The Savanna Formation contains four intermediate to major marine–nonmarine cycles, two of which contain black fissile shales. The Boggy Formation contains two major cycles along with three minor cycles.

The Cabaniss Subgroup (Cherokee Group) is represented by the Senora Formation. The Senora Formation includes five major cycles along with two minor scale cycles.

Marshall, T. R.; and Boardman, D. R. II, 2002, Outcrop-based cyclic stratigraphy of the Cherokee Group, *in* Boyd, D. T. (ed.), Finding and producing Cherokee reservoirs in the southern Midcontinent, 2002 symposium: Oklahoma Geological Survey Circular 108, p. 244.

Development of a Microbially Enhanced Oil Recovery Process for the Delaware–Childers Field, Nowata County, Oklahoma

Michael J. McInerney, Roy M. Knapp, David Nagle, Martha Folmsbee, and Saikrishna Maudgalya
University of Oklahoma
Norman, Oklahoma

ABSTRACT.—The Delaware–Childers field, T. 26 and 27 N., R. 16 and 17 E., is located in Nowata County in northeastern Oklahoma. The oil is produced mainly from a zone located in a Bartlesville sandstone channel deposit with some production from stray sands above this deposit. This field is operated by the Arrow Oil Company and currently is under an active water flood with injectors and producers arranged in a line-drive manner. The current water cut is approximately 99%. However, a recent core obtained from the central part of the field had an average residual-oil saturation of 48% even after 60 years of water flooding. Thus, the field is an attractive target for tertiary oil recovery. One option is a chemical surfactant-based recovery process. An alternative is a microbial process to generate a bio-surfactant in the reservoir. Microbially enhanced oil recovery (MEOR) is an economically viable alternative to injecting chemical surfactants into reservoirs. In MEOR, nutrients are injected into the reservoir, where they metabolize by resident microbes to bio-surfactants and other useful products that can mobilize oil.

Laboratory flooding experiments with sand packs at residual-oil saturation showed that a bio-surfactant generated by the microbe, *Bacillus mojavensis JF-2,* was able to mobilize and displace residual oil. Sand packs saturated with 37° API crude oil were water flooded to residual-oil saturation. The packs were then flooded with fluid that contained the microbially generated bio-surfactant and co-surfactant, 2,3-butanediol, and partially hydrolyzed polyacrylamide as a viscosifying agent. Residual-oil recoveries from these sand packs ranged from 65% to 80% of residual oil. Deletion of one of the above ingredients resulted in much lower residual-oil recoveries, ranging from 0% to 10%. Our data show that a combination of bio-surfactant, co-surfactant, and polymer is needed for significant recovery of residual oil. The absence of one of these key ingredients may explain why residual-oil recoveries by MEOR have been unpredictable in the past. Our calculations indicate that MEOR would be relatively inexpensive to implement in the field. This study suggests that MEOR provides a cheap and highly efficient alternative to expensive chemicals and may result in a successful tertiary recovery project in the Delaware–Childers field.

McInerney, M. J.; Knapp, R. M.; Nagle, David; Folmsbee, Martha; and Maudgalya, Saikrishna, 2002, Development of a microbially enhanced oil recovery process for the Delaware–Childers field, Nowata County, Oklahoma, *in* Boyd, D. T. (ed.), Finding and producing Cherokee reservoirs in the southern Midcontinent, 2002 symposium: Oklahoma Geological Survey Circular 108, p. 245.